12 October 2007 | $10

Science

NEW HORIZONS at Jupiter

AAAS

Volume 318, Issue 5848

COVER

A montage of images of Jupiter and its volcanic moon Io, taken from the spacecraft New Horizons. On Jupiter, high-altitude clouds are shown in blue and deeper clouds in red. The bluish-white oval is the Great Red Spot. Just visible in the Io image is an ongoing volcanic eruption on its nightside, in which incandescent lava glows red beneath a high volcanic plume lit by sunlight. See the special section beginning on page 215.

Images: Jupiter, infrared color composite from the Linear Etalon Imaging Spectral Array (LEISA) reprojected onto a crescent to compensate for rotational distortion; Io, approximate true-color composite from the Long-Range Reconnaissance Imager (LORRI) with color information from the Multispectral Visible Imaging Camera (MVIC); NASA/APL/SwRI/GSFC

DEPARTMENTS

EDITORIAL

SPECIAL SECTION

New Horizons at Jupiter

INTRODUCTION

PERSPECTIVE

REPORTS

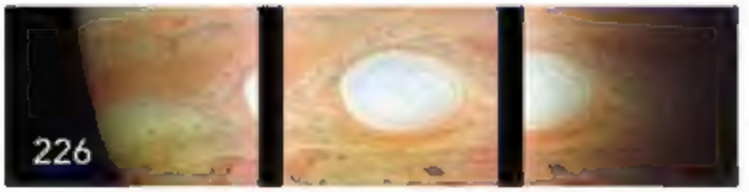

NEWS OF THE WEEK

NEWS FOCUS

CONTENTS continued >>

Science

SCIENCE EXPRESS

www.sciencexpress.org

PLANETARY SCIENCE

Widespread Morning Drizzle on Titan
M. Ádámkovics, M. H. Wong, C. Laver, I. de Pater
Infrared mapping of the atmosphere of Saturn's moon Titan suggests that small methane droplets that form each morning help to cycle methane between the atmosphere and surface.
10.1126/science.1146244

APPLIED PHYSICS

Orbital Reconstruction and Covalent Bonding at an Oxide Interface
J. Chakhalian et al.
A charge transfer from Mn atoms in an oxide layer to Cu atoms in a superconductor layer changes the orbital configuration of the Cu atoms and the properties of the layered structure.
10.1126/science.1149338

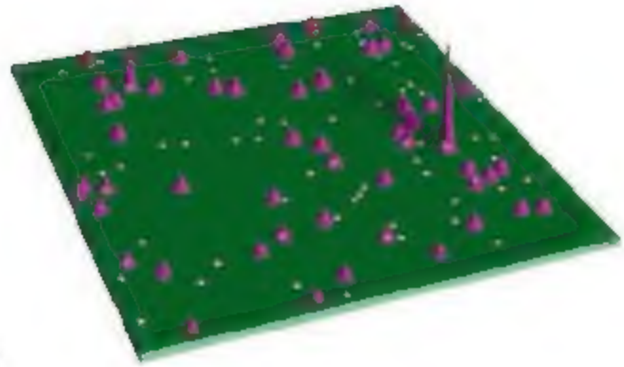

MEDICINE

The Genomic Landscapes of Human Breast and Colorectal Cancers
L. D. Wood et al.
Tumor growth seems to be driven by many genes mutated at low frequencies, most of which act through well-known signaling pathways.
10.1126/science.1145720

LETTERS

BOOKS ET AL

POLICY FORUM

PERSPECTIVES

TECHNICAL COMMENT ABSTRACTS

NEUROSCIENCE

REVIEW

ASTRONOMY

BREVIA

PLANETARY SCIENCE

CONTENTS continued >>

Science

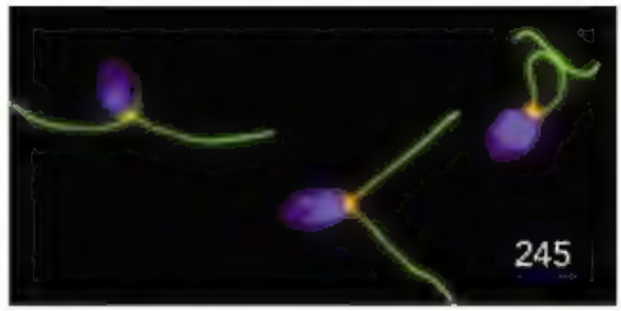

RESEARCH ARTICLE

REPORTS

AAAS
ADVANCING SCIENCE, SERVING SOCIETY

SCIENCE (ISSN 0036-8075) is published weekly on Friday, except the last week in December, by the American Association for the Advancement of Science, 1200 New York Avenue, NW, Washington, DC 20005. Periodicals Mail postage (publication No. 484460) paid at Washington, DC, and additional mailing offices. Domestic individual membership and subscription ($$ invest: $142 ($134 allocated to subscription). Domestic institutional subscription ($$ issues): $710. Foreign postage extra: Mexico, Caribbean (surface mail) $45; other countries (air assist delivery) $85. First class, airmail, student, and electronic rates on request. Canadian rates with GST available upon request, GST #125488122. Publications Mail Agreement Number 1069424. SCIENCE is printed on 30 percent post-consumer recycled paper. **Printed in the U.S.A.**

Change of address: Allow 4 weeks, giving old and new address and 8-digit account number. **Postmaster:** Send change of address to AAAS, PO. Box 96178, Washington, DC 20090-6178. **Single-copy sales:** $10.00 current issue, $15.00 back issue prepaid includes surface postage; bulk rates on request.

CONTENTS continued >>

Quarterly Author Index www.sciencemag.org/feature/data/aindex.dtl

SCIENCENOW

www.sciencenow.org DAILY NEWS COVERAGE

Something in the Way She Moves?
Lap dancers earn more when ovulating, suggesting that a woman gives off subliminal cues to her fertility.

Ig Nobel Prizes Stranger Than Fiction
Ceremony honors dubious uses of Viagra, a gay bomb, and other duds from the world of research.

Lungs to Brain: Don't Panic!
Anxiety may stem from the brain's mistaken activation of its carbon dioxide sensor.

Clustering of glutamate receptors.

SCIENCE'S STKE

www.stke.org SIGNAL TRANSDUCTION KNOWLEDGE ENVIRONMENT

PERSPECTIVE: Receptors Look Outward—Revealing Signals That Bring Excitation to Synapses
K. Gerrow and A. El-Husseini
Proteins derived from both sides of the synapse contribute to glutamate receptor clustering.

PERSPECTIVE: P.S. to PS (Phosphatidylserine)–Pertinent Proteins in Apoptotic Cell Clearance
R. A. Schlegel and P. Williamson
The receptor on phagocytes that recognizes phosphatidylserine on apoptotic cells remains elusive.

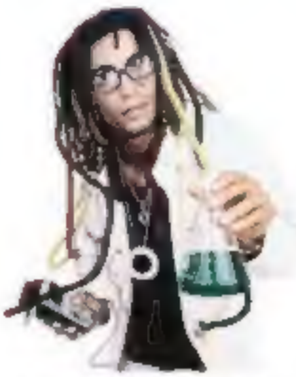

Obstacles and opportunities facing minorities.

SCIENCE CAREERS

www.sciencecareers.org CAREER RESOURCES FOR SCIENTISTS

GLOBAL: Special Feature—Experiences of Ethnic Minorities in Science
E. Pain
Differences of origin, cultural identity, and appearance can mean additional difficulties for early-career scientists.

US: Turning Obstacles Into Stepping-Stones
A. Sasso
Rita Thornton's success demonstrates that age, race, and disability need not be barriers to success in science.

EUROPE: Bouncing Back in a New Country
E. Pain
Ahcène Bounceur left Algeria to pursue a career in operations research and microelectronics in France.

EUROPE: In the Minority
H. Devlin
Three Oxford University scientists describe their experiences outside their native lands.

GLOBAL: Experiences of Ethnic Minorities in Science—Resources
E. Pain
Here's a roundup of support programs for ethnic minority scientists in the United States and Europe.

SCIENCE PODCAST

Download the 12 October *Science* Podcast to hear about polar lightning on Jupiter, experiences of ethnic minorities in science, the neurobiology of itch, politics influencing medicine, and more.
www.sciencemag.org/about/podcast.dtl

Separate individual or institutional subscriptions to these products may be required for full-text access.

EDITED BY STELLA HURTLEY AND PHIL SZUROMI

<< Almost in a Day's Work

Many plants coordinate their annual time of flowering with particular seasons of the year, and one indicator that they use to determine the change of seasons is day length. **Sawa *et al.*** (p. 261, published online 13 September; see the Perspective by **Rubio and Deng**) provide some insights into the molecular interactions that translate day length into flowering initiation. The day needs to be long enough for the blue-light–stimulated expression of proteins FKF1 (FLAVIN-BINDING, KELCH REPEAT, F-BOX1) and GIGANTEA (GI), to coordinate. The daily rise in expression of GI lags far enough behind the daily rise in expression of FKF1 that, in the shorter days of the year, daylight has waned by the time there is enough GI to form complexes with FKF1. With the longer days of spring and summer, there is enough time to form complexes and signal to the *CONSTANS* gene to trigger the flowering pathway.

Interior Design for Polymers

Separation systems need to achieve both high throughput and high selectivity. For polymer membranes, separations depend on the size of the cavities that lead to porosity on the Ångstrom scale (the free volume), but these cavities typically display a broad size distribution. Rodlike polymers with kinks can have more uniform cavitiy sizes but can also be difficult to process. **Park *et al.*** (p. 254) used processible forms of rigid polymers and a thermal postconversion process to create tailored free-volume elements with well-connected morphology in amorphous polymers. These materials formed membranes with outstanding transport and separation properties for small molecules and ions.

Sticky Is More Than Skin Deep

The feet of some climbing anthropoids and vertebrates can both strongly attach to surfaces as well as release, and attempts have been made to mimic patterned surfaces of adhesion pads. **Majumder *et al.*** (p. 258; see the Perspective by **Barnes**) have focused on the role of subsurface structures in altering adhesion. They show that fluid-filled micrometer-diameter channels in the subsurface region can significantly improve the adhesion of a soft elastomeric material. The fluid channels blunt the propagation of cracks that form as the film is peeled from the surface, and the fluid itself helps in the capillary adhesion of the material.

CREDITS (TOP TO BOTTOM): TAKATO IMAIZUMI, BRYAN DANIELS

Earth-Like Planets

The search for Earth-like planets is accelerating as detection technology and methodology improves. Current and proposed space missions should find many more in the next few years. **Gaidos *et al.*** (p. 210) review our understanding of how Earth-like planets form around stars, and how many we might expect to harbor water and orbit at just the right distance from their host star to be potentially habitable.

Disturbing Dislocations

In an avalanche, a formation that appears to be stable suddenly fails with a large movement of material. This phenomenon also occurs on the very small scale, such as the motion of defects in crystalline materials, where stress-strain jumps are observed during deformation. **Csikor *et al.*** (p. 251; see the Perspective by **Sethna**) have used simulations to measure dislocation avalanche bursts in microcrystals subjected to various modes of deformation at various orientations with respect to the crystal axes. Universal behavior is seen for the avalanche size distribution for all cases. The size of the bursts scales with the inverse of the sample length, which indicates that there may be a lower limit on the size of a material that can be shaped and formed.

The Animal Side of a Green Alga

Organisms at the base of the eukaryotic tree share features with both plants and animals. **Merchant *et al.*** (p. 245) present the sequence of the green alga *Chlamydomonas reinhardtii*, one of the most basal green plants. Their analysis of the genome demonstrate that, despite its closer relation to the land plants, this alga retains genes and features shared with animals, such as motile cilia that have nine outer doublet microtubules surrounding a central pair. In addition, the authors investigate the genes and evolution of photosynthesis in the plant lineage.

Maintaining Diversity Sans Sex

Some obligate asexual species, including the bdelloid rotifers, have survived for long time periods despite the absence of the benefits of

Continued on page 167

Fitzhugh Mullan is a professor of health policy and pediatrics at the George Washington University in Washington, DC, and a former Assistant Surgeon General.

Plight of the Surgeon General

ON 10 JULY 2007, THREE FORMER U.S. SURGEONS GENERAL SAT BEFORE THE HOUSE Committee on Oversight and Government Reform and detailed a rising tide of political interference in the conduct of the office in which they had served. Richard Carmona, who resigned the position last year, told of being blocked from speaking out on issues such as stem cell research and emergency contraception, and of instructions to reference President Bush three times on every page of any speech he gave. David Satcher of the Clinton Administration recounted interference with his report on sexuality and public health, in part because of the Monica Lewinsky affair. And C. Everett Koop described attempts of the Reagan political staff to thwart his AIDS campaign.

The hearing raised questions not just about political interference with science but about the Surgeon Generalship itself—a position that has had a mercurial ride through U.S. political history. Legislation in 1889 established the position of Surgeon General of the Marine Hospital Service, a minor government agency that evolved rapidly during the 20th century into the U.S. Public Health Service (PHS). By the 1960s, the Surgeon General, always an appointee from the ranks of PHS career officers, was in charge of a small empire of federal health programs, including the National Institutes of Health, the Food and Drug Administration, and the Indian Health Service. In 1967, a politically appointed Assistant Secretary for Health in the Department of Health, Education, and Welfare supplanted the Surgeon General as the line manager of the PHS, and the Surgeon Generalship became ceremonial. Nixon left the job empty from 1972 to 1976, and Carter designated his Assistant Secretary for Health as Surgeon General as an afterthought.

In 1981, President Reagan nominated C. Everett Koop for the job, a physician with little public health experience, who withstood a bruising confirmation marathon and then reinvented the position of Surgeon General. At a time when most public officials were distancing themselves from AIDS, he tackled the exploding epidemic. His willingness to speak frankly, embrace those suffering with the disease, and disregard the apparent preferences of his political overlords was welcomed by both scientists and the public. The president remained silent but supportive, according to Koop, while others in the Administration schemed to oust him. His name and his office gained wide recognition and helped propel his campaigns in other areas such as smoking, child health, and nutrition. Internally, he revitalized the PHS Commissioned Corps, generating a pride in the mission of public health that had been absent for many years.

The force of Koop's personality, the happenstance of the AIDS epidemic, and a hands-off president resulted in an extraordinary moment of power and effectiveness for the Surgeon General. But this alignment of events is rare, and Surgeons General since Koop have struggled to achieve the independence and visibility that he enjoyed. The Surgeon General remains a respected figure, but the job is ill-defined, budgetless, and subject to the whims of political appointees at the Department of Health and Human Services and the White House.

The Surgeon General is widely considered to be the doctor for the nation and an ombudsman for the public's health. But in reality, modern holders of the office are tightly constrained by the increasingly politicized environment of Washington. It is difficult to imagine a modern Congress creating the office of Surgeon General. Politics wouldn't allow it to happen. Fortunately, and to our nation's great benefit, the position and the tradition already exist. But the job needs help.

Legislation is needed to do three things: provide an independent budget for the currently mendicant position; mandate an annual Surgeon General's Report on the state of the nation's health; and, essential to all else, insulate the Surgeon General from political interference. Political shielding for key government officials (such as departmental inspectors general) has precedent, and similar measures should be adapted for the Surgeon General. It is Congress that needs to rescue the office of Surgeon General and give it, once and for all, the support and protection it needs to advance the public's health.

– Fitzhugh Mullan

10.1126/science.1149333

Illustration of *Vibrio cholerae*.

MICROBIOLOGY

Self-Puncturing Pathogens

To interact (often adversely) with the outside world, bacteria have several types of mechanism for transporting toxins and enzymes across complex cell envelopes. A recently described Type 6 secretion system (T6SS) has been added to the list, and its highly conserved gene clusters are found in numerous Gram-negative organisms, including strains of *Vibrio cholerae*. Pukatzki *et al.* used the social amoeba *Dictyostelium discoideum* as an experimental host in which to test T6SS mutants of this pathogen. Four proteins are needed to assemble a complete apparatus: The authors speculate that initially trimers of VgrG proteins penetrate the membrane to form a channel, and then units of a ringlike substrate, Hcp, are exported and stack up to form a hollow needle that facilitates its own transport. Remarkably, the components have homologs in the tail-spike membrane-puncturing device of the T4 bacteriophage. After export, the VgrG-1 component promotes pathogenesis by cross-linking host actin. — CA

Proc. Natl. Acad. Sci. U.S.A. **104**, 15508 (2007).

CHEMISTRY

Gently Excising Nitrogen

Removal of nitrogen from heterocyclic aromatic components of crude petroleum is performed at enormous scale through high-temperature catalytic hydrogenolysis, with the aim of minimizing generation of nitrogen oxides during combustion. However, the mechanistic details of this process are only loosely understood, and there has been little headway in finding well-characterized homogeneous systems that excise aromatic nitrogen directly. Fout *et al.* have now discovered that a titanium carbene complex cleanly and selectively swaps its carbon for the nitrogen in pyridine on treatment with trimethylsilyl chloride. The homogeneous reaction proceeds at 65°C to yield a substituted benzene and Ti imido complex as products. The authors propose a mechanism of electrocyclic rearrangements initiated by N-silylation; substituting a protic acid for the silyl reagent failed to drive the swap. The titanium reagent is recoverable by alkylation after donation of its imido group to high-valent molybdenum, which leads to an easily separable insoluble Mo nitride species. — JSY

J. Am. Chem. Soc. **129**, 10.1021/ja075326n (2007).

CROP SCIENCE

A Boost from Wild Wheat

Nitrification, a microbial process that generates nitrate in the rhizosphere through the biological oxidation of ammonia with oxygen, deleteriously affects the availability of soil nitrogen to plants and is a major agricultural concern, as approximately one-third of fertilizer nitrogen is lost in this manner. Subbarao *et al.* report a potentially powerful strategy to reduce nitrification in cultivated wheat. A wild relative of wheat, *Leymus racemosus*, releases biological nitrification inhibitors that dramatically reduce nitrification in the root rhizosphere in comparison to domesticated wheat. When a *Leymus* chromosome containing the relevant gene(s) was introduced into wheat, biological nitrification inhibitors were also produced, and productivity increased. New strains of wheat can now be bred to transfer this trait stably into the domesticated wheat genome. — LMZ

Plant Soil 10.1007/s11104-007-9360-z (2007).

CLIMATE SCIENCE

More Water in the Air

Anthropogenic influence on the climate system is manifest not only in the rise of near-surface tropospheric temperatures (the effect people experience most directly), but also in the hydrological cycle. Recent observational studies have shown that continental river runoff, zonal-mean rainfall, and surface humidity all display trends that can be ascribed to the results of human activity, primarily the temperature rise caused by increasing concentrations of atmospheric greenhouse gases. Another atmospheric attribute of great importance, the total amount of atmospheric water vapor, *W*, has been more difficult to study. Santer *et al.* use data from the satellite-based Special Sensor Microwave Imager (SSMI) to show that the total atmospheric moisture content over the oceans has increased by 0.41 kg/m^2 per decade since 1988. They then use results from 22 different climate models to show that the size of the observed increase in *W*, and the pattern of changes that it has displayed over that interval, can be explained only if the primary cause is the human-induced increases in greenhouse gases in the atmosphere. In this way, they show that the "fingerprint" of anthropogenic impact can be seen in the moisture content of Earth's atmosphere, and that the increase is consistent with theory, thereby strengthening confidence both in those models and in how well the mechanics of climate are understood. — HJS

Proc. Natl. Acad. Sci. U.S.A. **104**, 15248 (2007).

CHEMISTRY

Where Water Holds Still

When polar molecules dissolve in water, the solvent's accommodation of groups that resemble its own structure (such as hydroxyls and amines) is unsurprising. Less clear is how the network of hydrogen-bonded H_2O molecules accommodates

Continued on page 173

Continued from page 171

a solute's nonpolar alkyl components. Rezus and Bakker explored this question through ultrafast vibrational anisotropy measurements of nitrogen-based aqueous solutes with varying degrees of N-alkylation. After tagging water molecules in the solvation shell with low-level vibrational excitation, the authors used the femtosecond time resolution of a laser probe to monitor rotational mobilities of these molecules before diffusional exchange with the surrounding bulk region. The data revealed two distinct reorientation rates, and the population of more slowly rotating water molecules steadily increased as the number of hydrophobic methyl groups on the solute rose. A correlation of four immobilized OH groups with each methyl group suggests a strong disruption of the solvent dynamics in the hydrophobic vicinity, though the authors emphasize that the structure in which the waters are briefly locked remains disordered, rather than ice-like. — JSY

Phys. Rev. Lett. **99**, 148301 (2007).

MATERIALS SCIENCE

Wiry Approaches to Solar Harvesting

Silicon wire arrays could in principle provide a cost-effective alternative to high-performance single-crystal Si wafers. Wires grown via vapor-liquid-solid methods are also single crystals and avoid problems of recombination at grain boundaries. Moreover, the wire geometry facilitates carrier collection and fosters carrier generation in the space charge region deep within the array. Two studies have explored the use of Si wire arrays in photoelectrochemical cells. Goodey *et al.* grew p-type Si nanowire (NW) arrays either from a base of gold-capped cobalt NWs in anodic aluminum oxide membranes, or from a gold-coated p-type Si (111) substrate. On array immersion in dry acetonitrile solutions of $Ru(2,2'\text{-bipyridyl})_3^{2+}$ and Hg/Xe arc lamp illumination, cyclic voltammetry showed a shift in reduction wave peaks to more positive voltages relative to a Pt disk electrode. Photocurrent densities were about twice that of planar p-type Si. Maiolo *et al.* grew single-crystalline Si wires with diameters of ~1 μm using a gold catalyst on an n-type Si(111) substrate with a silicon oxide buffer layer. In a 1,1'-dimethylferrocene redox system in methanol, illumination with simulated sunlight produced a short-circuit photocurrent density of 2.2 mA/cm^2. In both systems, better protection of the wire surfaces may improve performance. — PDS

J. Am. Chem. Soc. **129**, 10.1021/ja073125d; 10.1021/ja074897c (2007).

Science STKE AAAS

www.stke.org

<< Serpins Save Cells

Biologically active proteases are held in check in part by a family of peptidase inhibitors known as serpins. Most serpins are secreted, but some are intracellular proteins implicated in regulating lysosomal proteases. Luke *et al.* found that in the worm *Caenorhabditis elegans*, loss of the intracellular serpin SRP-6 caused animals to become highly sensitive to hypo-osmotic stress and to die as a result of necrotic cell death. This effect appeared to require inhibition of cysteine peptidases because survival of the knockout worms was improved in mutant animals engineered to express wild-type SRP-6 but not in animals that expressed a mutant serpin that lacked inhibitory activity. Calcium mobilization appeared to be required for cell death because SRP-6 knockout animals lacking the ryanodine receptor, the inositol-1,4,5-trisphosphate receptor, or the Ca^{2+}-binding protein calreticulin showed suppression of cell death. Lysosome-like gut granules also appeared to be required, because death was suppressed in animals lacking a guanosine triphosphatase required for formation of these acidic granules. Animals lacking SRP-6 were also more susceptible than wild-type animals to heat shock, hypoxia, or hyperoxia. The authors argue that the common effects of serpins on these stimuli may indicate that there is a central necrotic death mechanism that can be regulated by serpins. If so, serpins could act as an antidote to cells undergoing, for example, hypoxic stress during heart attacks. Such a prosurvival function of intracellular serpins might also explain why increased expression of some serpin family members portends a poor prognosis in various human cancers. — LBR

Cell **130**, 1108 (2007).

CREDIT: JOHN FOXX/GETTY IMAGES

www.sciencemag.org

Science

1200 New York Avenue, NW
Washington, DC 20005
Editorial: 202-326-6550, FAX 202-289-7562
News: 202-326-6581, FAX 202-371-9227

Bateman House, 82-88 Hills Road
Cambridge, UK CB2 1LQ
+44 (0) 1223 326500, FAX +44 (0) 1223 326501

Subscription Services For change of address, missing issues, new orders and renewals, and payment questions: 866-434-AAAS (2227) or 202-326-6417, FAX 202-842-1065. Mailing addresses: AAAS, P.O. Box 96178, Washington, DC 20090-6178 or AAAS Member Services, 1200 New York Avenue, NW, Washington, DC 20005

Institutional Site Licenses please call 202-326-6755 for any questions or information

Reprints: Author inquiries 800-635-7181
Commercial Inquiries 803-359-4578

Permissions 202-326-7074, FAX 202-682-0816

Back Issues: AAAS Publication Sales, 1-800-[illegible] or http://www.aaas.org/pubs

AAAS Online Store http://www.apisource.com/aaas/ code MB84; AAAS Travels: Betchart Expeditions 800-252-4910; Apple Store www.apple/epptstore/aaas; Bank of America MasterCard 1-800-833-6262 priority code FAA3YU; Cold Spring Harbor Laboratory Press Publications www.cshlpress.com/affiliates/aaas.htm; GEICO Auto Insurance www.geico.com/landing/page/go51.htm?logo=17624; Hertz 800-654-2200 CDP#343457; Office Depot https://bsd.officedepot.com/portallogin.do; Seabury & Smith Life Insurance 800-424-9883; Subaru VIP Program 202-326-6417; VIP Moving Services http://www.vipmoyRoser.com/domestic/index.html; Other Benefits: AAAS Member Services 202-326-6417 or www.aaasmember.org

science_editors@aaas.org (for general editorial queries)
science_letters@aaas.org (for queries about letters)
science_reviews@aaas.org (for returning manuscript reviews)
science_bookrevs@aaas.org (for book review queries)

Published by the American Association for the Advancement of Science (AAAS), *Science* serves its readers as a forum for the presentation and discussion of important issues related to the advancement of science, including the presentation of minority or conflicting points of view, rather than by publishing only material on which a consensus has been reached. Accordingly, all articles published in *Science*—including editorials, news and comment, and book reviews—are signed and reflect the individual views of the authors and not official points of view adopted by the AAAS or the institutions with which the authors are affiliated.

AAAS was founded in 1848 and incorporated in 1874. Its mission is to advance science and innovation throughout the world for the benefit of all people. The goals of the association are to: foster communication among scientists, engineers and the public; enhance international cooperation in science and its applications; promote the responsible conduct and use of science and technology; foster education in science and technology for everyone; enhance the science and technology workforce and infrastructure; increase public understanding and appreciation of science and technology; and strengthen support for the science and technology enterprise.

Information for Authors

See pages 120 and 121 of the 5 January 2007 issue or access www.sciencemag.org/feature/contribinfo/home.shtml

EDITED BY CONSTANCE HOLDEN

PILEUP ON THE MOON

The moon is the hottest new destination in space. With a slew of moon missions coming up, scientists warned at a meeting in Hyderabad, India, last month that lunar junk poses a serious pollution threat.

A lot of one-way traffic is expected to crash on the moon in the next decade. The first, Japan's 3000-kilogram Kaguya remote-sensing satellite, will arrive this month. Next up is China's 1900-kilogram Chang'e 1, being sent to map lunar resources. In April 2008, India will launch Chandrayaan-I, an orbiter that will also send a 29-kilogram probe hurtling into the lunar surface. British and Italian vehicles will be adding to the pileup. Only China has a plan for disposing of its rubbish.

Bernard Foing, director of the International Lunar Exploration Working Group in the Netherlands, pointed out that the Apollo missions left behind several hundred kilograms of waste. Noting that it took 27 years for the post-Apollo lunar atmosphere to "stabilize back," physicist Roger-Maurice Bonnet, president of France's Committee on Space Research, called for a "conservation area" untouched by humans. Wu Ji, China's chief lunar exploration scientist, is plumping for a moon dump. Foing also suggested that satellites might be put to sleep in a long-term orbit. Without an "exit policy from the moon," said Bonnet, it "will be destroyed sooner [rather] than later."

Talking Turtle

"I am suggesting that we are only a few years away from the point at which the proposition that there are no cognitive differences between men and women will be as hard to sustain as the proposition that the Earth rides on the back of a turtle."

—*Political scientist Charles Murray, co-author of* The Bell Curve, *at a 2 October meeting at the American Enterprise Institute in Washington, D.C., to discuss why there aren't more women in some branches of science.*

It's Tapir Time

With their droopy noses and beefy bodies, tapirs look like a cross between an elephant, a pig, and a hippopotamus. You don't have to leave your chair to get close to these strangely engrossing tropical herbivores. Just click over to the Tapir Specialist Group Web site from the World Conservation Union (IUCN), which offers photos, videos, conservation news, and scientific information.

Fans of these creatures can wallow in background pages on the four existing species, including Baird's tapir (below), which ranges from Mexico to Colombia. For researchers working with tapirs in the wild, the field veterinary guide furnishes advice on everything from making captures—darting works well, although the crepuscular conditions tapirs prefer can make it hard to aim—to serological tests. And if you think the animals are oh-so-cute, check out the interview with the former Costa Rican environment minister, who was attacked and nearly killed by an enraged mother tapir. >> www.tapirs.org

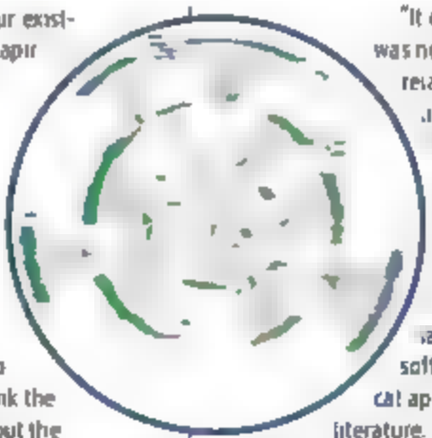

CREDITS (TOP TO BOTTOM): PAT LEWIS, MARIE HOLLIMAN, WILLIAM KONSTANT/TAPIR SPECIALIST GROUP

Sorting Through Astro-Chaff

The power of social networking is being extended to scientific papers. With the sheer volume of articles published nowadays, figuring out which are the key ones is a tricky problem. By showing how many "friends" articles have, a new tool called PaperScope is helping astronomers find the papers that really matter.

"It dawned on me that there was no easy way to identify key relationships between published papers," says Mark Holliman of the European Virtual Observatory Technology Project, who unveiled PaperScope at an astronomical data conference last month in London. The software provides a graphical approach to searching the literature. Users can create personalized charts with each paper drawn as a box connected by arrows pointing to the papers it cites and pointing from the papers that cite it. By revealing the papers with the most incoming arrowheads, PaperScope sorts out the seminal works from the academic chaff.

For example, searching for "solar radio bursts" brings up more than 2500 hits on an academic database. But a few clicks of the mouse reveal the handful of oft-cited papers—the yellow boxes in the screenshot above. "There's an 'aha' moment. As in, 'Aha, that's the paper I should read next,'" says Norman Gray, an astronomer at the University of Leicester, U.K.

PaperScope (paperscope.sourceforge.net) is currently compatible only with astrophysics papers, but Holliman hopes to extend it to other scientific databases.

EDITED BY YUDHIJIT BHATTACHARJEE

ON CAMPUS

MUZZLED. Two years after Lawrence Summers made the fateful remarks about women and science that got him pushed out of the Harvard University presidency, some still treat him like a pariah. A recent instance involved female faculty members at the University of California (UC) who led a successful petition to have Summers disinvited as a dinner speaker at the September meeting of the UC Board of Regents. But the controversy has earned Summers the sympathy of some of his erstwhile critics.

Among them is Harvard psychologist Howard Gardner, who says, "I don't know anyone at Harvard who favors what happened at UC Davis. ... The regents and faculty who opposed [Summers's] appearance look like ignorant fools." The petition that led the regents to rescind the invitation cited Summers's "poor relationships with both women and underrepresented minority faculty at Harvard." Summers says, "I was somewhat surprised that none of the [UC] chancellors spoke up publicly on the precedent set by rescinding speaking engagements because of controversy."

Regents' spokesperson Trey Davis dismisses the episode as "no big deal," adding that "you don't want to annoy people needlessly." Maureen Stanton, an evolutionary biologist at UC Davis who signed the petition, says what she and others were really objecting to was the decision by the university's governing body to grant a private audience to a controversial figure like Summers. "It wasn't a free-speech issue," she says. "Had Summers been invited to a public forum at the university on how to diversify science and engineering, we would have had no problems. We would simply have shown up with some tough questions."

CREDITS (TOP TO BOTTOM): SOURCE AP; ROSE LINCOLN/HARVARD NEWS OFFICE; U.S. DEPARTMENT OF COMMERCE; WORLD HEALTH ORGANIZATION

THEY SAID IT

"I am now a heavenly body. I found out about it yesterday ... I was blown away. It came out of the clear blue sky just like an asteroid."

—Actor George Takei, who played Sulu in the original *Star Trek* series, reacting to the International Astronomical Union's decision to name an asteroid in his honor. Discovered by Japanese astronomers in 1994, 7307 Takei is located between Mars and Jupiter

INSIDE GOVERNMENT

YOUNG BLOOD. The U.S. Commerce Department has picked a 32-year-old political operative with no scientific background or industrial experience to head a new office intended to foster innovation. Joel Harris, who has worked at the White House and for Republican former Colorado governor William Owens, will direct the Technology Council, which replaces the department's 19-year-old Technology Administration.

The Technology Administration, which once boasted a $10 million budget and 50-plus person staff, including an undersecretary for technology, was allowed to wither on the vine until Congress and the White House agreed this year to eliminate it. But experts don't hold out much hope for the new council, tucked within the secretary's office and lacking a budget. "It's definitely an opportunity lost," says Christopher Hill of George Mason University in Fairfax, Virginia, a veteran player in technology issues. "I can't imagine that it is a prescription for actually doing anything."

Harris hopes to prove the critics wrong. "Technology is a critical driver for our economy," he says, "and my job will be to identify and coordinate action on the most important issues."

Got a tip for this page? E-mail people@aaas.org

Movers >>

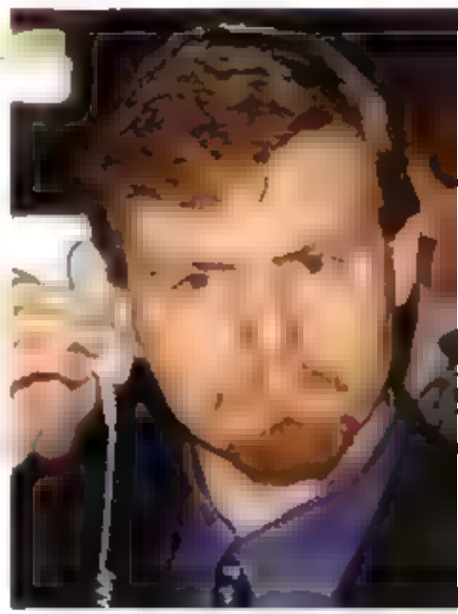

WORLDLY-WISE. Barring objections from the U.S. Senate, the controversial chief of global health at the Department of Health and Human Services (HHS) could soon be headed off to a new assignment. Last week, a Senate committee considered whether to approve William Steiger as U.S. ambassador to Mozambique. Steiger, 37, a Ph.D. in Latin American history and the son of a former Republican congressman, has been accused by HHS employees and outside researchers of micromanaging HHS scientists' international activities and pushing conservative, pro-industry positions (*Science*, 10 September 2004, p. 1551). Recently, he came under fire for allegedly suppressing a global health report from the U.S. Surgeon General.

At last week's hearing, Steiger deflected questions about some of these matters from the presiding member, Russ Feingold (D–WI), asserting that the Surgeon General's report "had serious flaws" and disputing the scientific value of an international AIDS meeting. He said he has "gained much experience" that has prepared him for dealing with Mozambique's problems with AIDS and malaria. The committee is expected to approve the nomination, as is the full Senate. HHS spokesperson Bill Hall said "no decisions have been made" about when Steiger might depart or who would take over his position. "His departure will be a relief for HHS scientists and professionals," says University of California, San Francisco, international health expert Thomas Novotny, a former HHS official.

Life at the bottom of the Bering Sea 181

Coring the San Andreas 183

NOBEL PRIZES

A Knockout Award in Medicine

The one-two research punch that allowed the creation of designer mice has earned the 2007 Nobel Prize in Physiology or Medicine. Mario Capecchi, a Howard Hughes Medical Institute investigator at the University of Utah in Salt Lake City, Oliver Smithies of the University of North Carolina, Chapel Hill and Martin Evans of Cardiff University, U.K., will share the prize for developing the techniques to make knockout mice, animals that lack a specific gene or genes. Such mice have allowed scientists to learn the roles of thousands of mammalian genes and provided laboratory models of human afflictions in which to test potential therapies.

Against the odds. Pursuing ideas that others said would never work, the three researchers who share this year's Nobel Prize in physiology or medicine set the stage for the creation of designer mouse strains in which specific genes are altered or disabled.

The techniques "truly provided a revolution in mammalian biology," says Raju Kucherlapati, a geneticist at Harvard University. "It is not an exaggeration to say that there is no mammalian biologist today who does not use these tools in one way or another."

Biologists have long studied mutant mice for insights into the mammalian body. But for decades, they were limited to rodents whose DNA had been disrupted in random places by natural mutations or the application of mutagenic chemicals. In fact, most of the time, biologists studying a mutant mouse strain didn't even know which gene was broken. The ability to mutate a specific gene at will seemed a distant dream.

Working independently in the 1980s, however, Capecchi and Smithies each crafted ways to slip foreign DNA into a specific place in the chromosomes of mammalian cells. A similar strategy exploiting a natural DNA-swapping process called homologous recombination, had been used to alter genes in yeast and other organisms, but most people assumed it wouldn't work in mammals. Indeed, in the early 1980s, Capecchi's grant application was rejected by the National Institutes of Health in Bethesda, Maryland, with the advice that he should forget the idea.

He persevered, using money cobbled together from other projects. And a few years later, both he and Smithies, then working at the University of Wisconsin, Madison, showed that targeting specific genes in mammalian cells via homologous recombination was indeed possible. But the work was in cells in culture dishes, and the technique seemed far too inefficient to be used to make whole animals with genetic alterations.

Enter Martin Evans, then at the University of Cambridge, U.K. He led a group that in 1981 reported growing embryonic stem (ES) cells from mouse embryos. Evans, too, had faced skepticism. Experts had doubted whether such cells, which can become any cell in the body, could be grown in the lab. Even Evans was confused when he first saw the cells in culture, says Elizabeth Robertson of the University of Oxford, U.K., who was a postdoc in the lab. "He came to us and said, 'Someone contaminated my media!' " because there were strange-looking cells growing in it. Lab members had to convince him that the cells were ES cells, she says.

A few years later, Evans and his colleagues showed that they could produce live mice by injecting cultured ES cells into a developing embryo. The result is a chimera, an animal whose tissues are a mix of the ES cells and those from the host embryo. In many of those chimeras, the added ES cells by chance produce the animal's sperm or eggs, and when these chimeras mate, some of their offspring carry the stem cells' genes in all their tissues.

Capecchi and Smithies both quickly saw that ES cells offered an opportunity to generate live animals with a desired mutation in every cell. Researchers could target genes in ES cells and then sort out the cells that carried the desired modification, using them to create chimeras. Some of the chimeras' offspring would have the altered gene in all their tissues, and by breeding these animals together, biologists could create mice that completely lack the two working copies of a given gene. Although they never formally collaborated, Evans "brought the ES cells to my lab in his own pocket," Smithies says, while Capecchi spent time in Evans's lab learning the technology.

Every biologist soon wanted a favorite gene punched out, and a handful of companies quickly began competing with places such as the Jackson Laboratory in Bar Harbor, Maine, to provide knockout strains to drug companies and academic labs. To date, researchers have knocked out at least 11,000 genes in mice, observing what goes wrong in development or adulthood and thereby gaining a sense of what the gene does. By deactivating ▶

CREDITS (LEFT TO RIGHT): TIM ROBERTS/PA NEWSWIRE; HYNE, JASON BYE/PA PHOTOS/LANDOV; UNIVERSITY OF NORTH CAROLINA AT CHAPEL HILL SCHOOL OF MEDICINE

specific genes this way, for example. Capecchi and his colleagues went on to identify ones that shape limbs, organs, and the overall mammalian body plan. Both Smithies and Evans developed mice lacking the cystic fibrosis gene, one of many knockout mouse strains created to mimic a human illness. Indeed, there is now a worldwide effort to knock out every mouse gene (*Science*, 30 June 2006, p. 1862).

Skeptical grant reviewers were not the only hurdle Capecchi overcame on his way to scientific stardom. As a child in war-torn Italy, he survived alone—often begging and stealing on the streets—between the ages of 4 and 9 while his mother, a poet, was imprisoned in the Dachau concentration camp for her anti-Fascist writings. After the war, she tracked down a very malnourished Mario in a hospital, and a few days later they were on a boat to the United States to live with her brother in Pennsylvania. The young Mario expected the streets to be literally paved with gold, he told a press conference in Salt Lake City on the day he won the prize. What he found instead, Capecchi says, "was opportunity." **–GRETCHEN VOGEL**

NOBEL PRIZES

Effect that Revolutionized Hard Drives Nets a Nobel

If you work at a computer, play video games, or listen to music on an iPod, you've benefited directly from the efforts of the winners of the 2007 Nobel Prize in Physics. Albert Fert of France's national research agency, CNRS, in Orsay, France, and Peter Grunberg of the Jülich Research Center in Germany independently discovered an effect known as giant magnetoresistance (GMR) that fueled a dramatic increase in the capacity of computer hard drives. The discovery also laid the cornerstone of a new field known as spintronics, in which researchers try to exploit the fact that electrons spin like little tops to make novel devices.

"It's a physics discovery that has had real consequences," says Robert Buhrman, an applied physicist at Cornell University. "Without GMR, we would not be able to carry our whole life around on a 3-inch hard drive."

Long before the discovery of GMR, researchers knew that applying a magnetic field to a material such as iron or nickel could change its conductivity. Electric current would flow less readily parallel to the direction in which the material was magnetized and more readily across it. Technologists harnessed that effect to make the "read heads" that sensed the setting of the magnetized bits in a computer hard drive. But the effect, known as anisotropic magnetoresistance, was small, the resistance varied by a few percent.

In 1988, Grünberg and Fert found that they could greatly increase the change in resistance if they made layer-cake films with layers of iron separated by layers of nonmagnetic chromium only a few atoms thick. If two adjacent iron layers are magnetized in the same direction, then electrons spinning in one direction will pass along the film readily, whereas electrons spinning in the other direction will not. If, however, the iron layers are magnetized in opposite directions, then all electrons run into greater resistance, regardless of how they are spinning. That makes a GMR film an extremely sensitive magnetic field detector. As a result, all the bits and hardware in a disk drive can be made much smaller.

The basic quantum mechanical concepts behind GMR were understood in the 1970s, but at the time technology was not available to exploit them, Fert says. "I put this idea in the fridge," he says. "Then in the 1980s, it became possible to fabricate these materials." Grünberg could not be reached for comment when *Science* went to press.

Although Fert and Grünberg discovered the effect, Stuart Parkin of IBM's Almaden Research Center in San Jose, California, did much of the work to make GMR technologically useful. Stuart Wolf, a physicist at the University of Virginia, Charlottesville, says he was surprised that Parkin was not honored as well. But Tony Bland of the University of Cambridge, U.K., says that the Nobel committee apparently distinguished between the discovery and its cultivation. "This is properly a physics prize for a truly extraordinary and novel effect."

The advent of GMR helped launch the emerging field of spintronics, Wolf says. "This particular discovery seemed to crystallize a lot of people's interest in working in this area," he says. Their efforts may someday lead to myriad other devices, such as computer memory that can hold information even when it loses power and microchips that exploit spin to perform computations.

–ADRIAN CHO

With reporting by Daniel Clery.

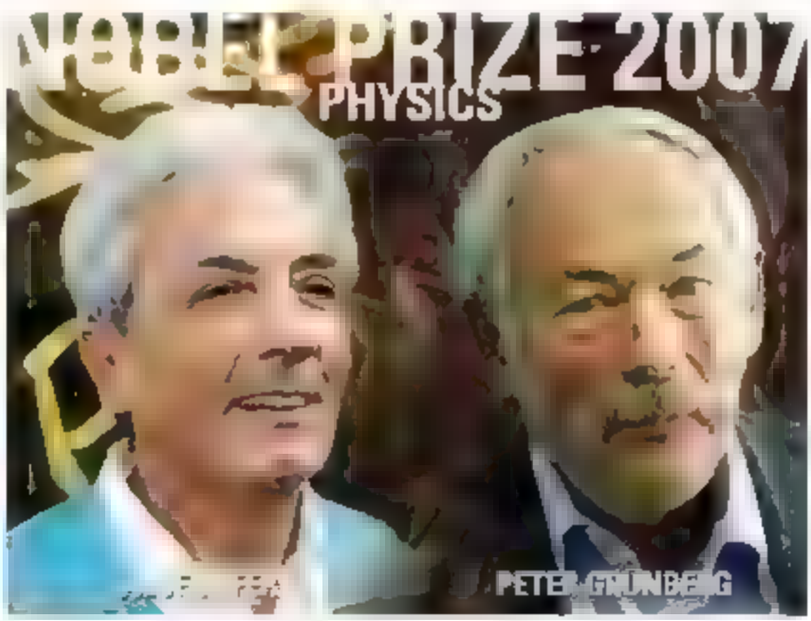

Thanks for the memories. Physicists Albert Fert (*left*) and Peter Grünberg independently discovered an effect that vastly increased the capacity of computer drives.

CREDITS (LEFT TO RIGHT): PHILIPPE WOJAZER/REUTERS; INA FASSBENDER/REUTERS; LANDOV

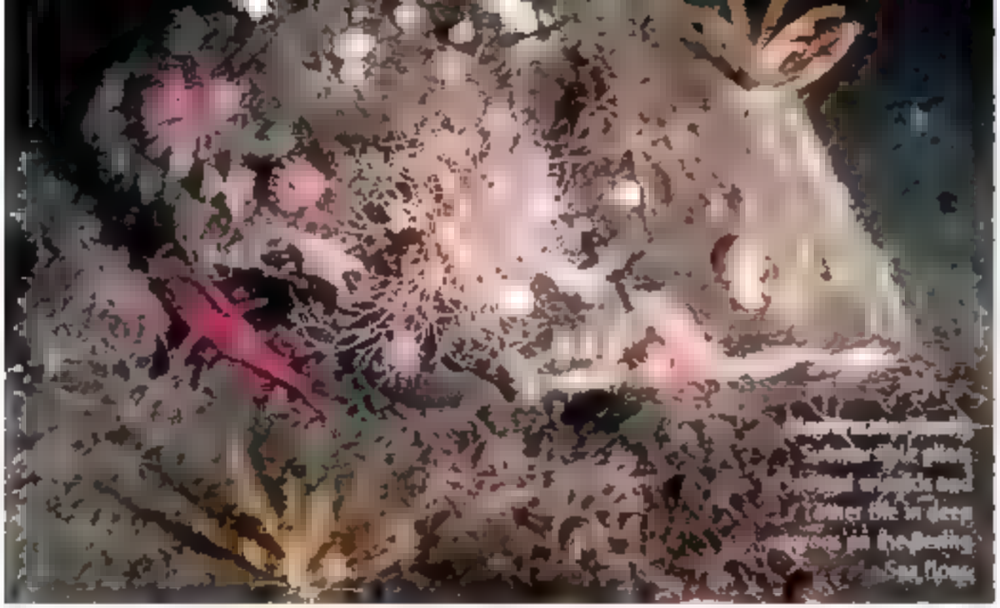

CREDIT: JOHN HOCEVAR/GREENPEACE

MARINE BIOLOGY

Into the Deep: First Glimpse of Bering Sea Canyons Heats Up Fisheries Battle

Marine biologists this summer peered for the first time into the depths of two massive canyons below Alaska's Bering Sea canyons that may be key to sustaining the world's largest food fishery. Their firsthand glimpse of life in Zhemchug and Pribilof canyons may set conservationists and the Alaskan fisheries industry on a collision course, with conservationists arguing that the canyons need protection from fishing, and fisheries managers countering that the canyons' ecosystems are not necessarily unique and are not heavily fished.

Last week in Anchorage, expedition members unveiled their preliminary findings in a packed but unofficial session of the North Pacific Fishery Management Council (NPFMC), the advisory board that works with the National Marine Fisheries Service (NMFS) to oversee the resources of the Bering Sea.

The canyons sit in the middle of one of the most heavily fished areas on Earth, the Bering Sea Shelf break, where nearly 2 million metric tons of fish, particularly pollock, are caught each year. But little was known about other life in the canyons, with data from only a handful of dives by remotely operated vehicles (ROVs) and from by-catch hauled up by trawlers. "The canyons are one of the places in the world where nobody has looked before," says Robert Stone, a benthic habitat ecologist at NMFS in Juneau, who helped design the survey. Last December, NPFMC ruled that it lacked sufficient data about the canyons to justify a closure. So John Hocevar, a marine biologist and Greenpeace representative who organized and led the more than $400,000 expedition, outfitted Greenpeace's vessel, *Esperanza*, with two human-piloted submersibles and one ROV. The team systematically surveyed parts of the canyons, one of which plunges 2730 meters down.

They found rocks and stony outcrops protruding through the muddy canyon floors. And on every such hard substrate, submersible pilots spotted the bright colors of life: fan-shaped corals as orange as a tropical sunset, magenta-hued rockfish, crystalline barrel sponges, and young golden king crabs. "It was absolutely amazing to see the colors below the gray sea, and to have such a close view of fine features of the ecosystem," says marine ecologist Michelle Ridgway, a consultant with Oceanus Alaska in Juneau, who piloted one of the submersibles.

Ridgway is also a member of NPFMC's advisory panel and says she has "taken plenty of shrapnel" from colleagues for her part in the expedition because of Greenpeace's advocacy role. She, Stone, and other NMFS and university scientists say that they joined the cruise because of the rare opportunity to explore the region.

The team has just started to analyze the collected specimens and videotape recorded during 25 dives. So far, Ridgway counts nine genera of coral, including red tree (*Primnoa sp.*) and black coral (*Lillipathes sp.*), dozens of sponge genera, and several unidentified sponges that Stone expects will prove to be new species. Similar coral habitat, which serves as a refuge for fish and crab, was recently protected near the Aleutians. The team also discovered swaths of sea whip coral (*Halipteris sp.*) as wide as "a freeway" that had been damaged by ▶

SCIENCESCOPE

Brechot Out at INSERM

PARIS—Christian Brechot, the head of French biomedical research agency INSERM, has resigned amid allegations of a conflict of interest involving a company he set up with his wife, INSERM oncologist Patrizia Paterlini. In a statement released on Monday, Brechot, 55, said he wanted to explore other career options and have his hands free to defend himself in the affair.

The duo is fighting a legal battle with Metagenex, a company they set up to commercialize a technique to detect cancer cells or diagnose fetal abnormalities using blood samples. Brechot says that the company—in which Paterlini and the couple's children own shares equaling 44%—is rushing the system to market without proper clinical validation. Metagenex director David Znaty says Brechot has improperly used his position to prevent the product from reaching the market (*Science*, 3 August, p. 585). Brechot's resignation comes as a joint inquiry by the research and health ministries is drawing to a close, although its findings have not been made public. Brechot denies that he was pressured but concedes in an interview that he had "strong discussions about the timing" of his departure. For more see www.sciencemag.org/cgi/content/full/2007/1009/3.

–MARTIN ENSERINK

Astronomy Still Hot in Chile

It's official: The first of a new generation of monster telescopes will be built in Chile. Sporting seven 8.4-meter mirrors, the Giant Magellan Telescope (GMT) will have the light-gathering power of a single 22-meter behemoth. Last week, the GMT consortium—eight American institutes and universities plus one Australian—selected Cerro Las Campanas in northern Chile as the future site for the record-shattering instrument, due to be completed in 2016. The mountaintop, at 2300 meter altitude, is already home to the twin 6.5-meter Magellan telescopes.

Only $30 million of the project's $550 million price tag has been raised as funding agencies wait for the results of the first mirror casting and polishing. But that hasn't dampened enthusiasm by Chilean astronomers. "This will keep Chilean astronomy at the [cutting] edge of science and development," says Leopoldo Infante of the Pontificia Universidad Catolica de Chile in Santiago.

–GOVERT SCHILLING

fishing lines dragged along the bottom, says submersible pilot David Guggenheim of the nonprofit Ipanet Ocean in Washington, D.C.

Hocevar notes that federal law requires the National Oceanic and Atmospheric Administration, of which NMFS is a part, to report new data about deep-sea corals to Congress and to outline steps that may be taken to protect these vulnerable, slow-growing organisms. "I think the council will have to consider a fishing closure in the canyons based on our findings," says Hocevar.

But council members aren't so sure. NPFMC "already took action on a Bering Sea conservation package," says Patricia Livingston, NMFS fisheries biologist and NPFMC's scientific committee chair; she was referring to protections extended to other sea floor areas on the Bering Sea Shelf. To close them, "the canyons would have to be designated as habitats of particular concern," which hasn't yet been proposed, she says. For now, the council is not taking any specific action in response to this unofficial presentation.

–VIRGINIA MORELL

Virginia Morell is a science writer in Ashland, Oregon.

BIODEFENSE

Lawmakers Worry that Lab Expansion Poses Risks

A congressional committee last week took a hard look at the explosion of U.S. biodefense research since the 2001 anthrax attacks and concluded that the number of labs is growing without adequate oversight. At a 5-hour hearing, federal officials acknowledged gaps in monitoring safety at biocontainment labs. But although scientists agree there's a problem, they worry that hasty reforms could do more harm than good.

The hearing by the House Energy and Commerce Committee oversight and investigations subcommittee was held to examine the growth in biosafety level 4 (BSL-4) labs, which study deadly pathogens for which there is no treatment, as well as BSL-3 labs, which study less risky bugs (*Science*, 28 September, p. 1852). The National Institute of Allergy and Infectious Diseases (NIAID) alone has spent more than $1 billion in the past 5 years on new BSL-3 and BSL-4 labs.

Meanwhile, a spate of accidents is stirring concerns about safety, including an unreported infection and other violations at Texas A&M University in College Station that led federal officials to suspend its biodefense work in June. The Texas incident came to light only after public records requests by the Sunshine Project, an activist group in Austin, Texas. At the hearing, subcommittee chair Bart Stupak (D-MI) asked, "Are so many labs doing this research that you actually increase the chances of a catastrophic release of a deadly disease?"

According to an analysis presented at the hearing, the risks are rising. In a preliminary report, Keith Rhodes of the Government Accountability Office (GAO) found that by its count there are five existing BSL-4 labs and 10 more under construction or planned by various funders (including separate labs at the same institution). GAO was unable to tally BSL-3 labs, which could number in the thousands. These labs mean more new workers and more dangerous pathogens in labs, Rhodes noted. Without any central oversight, "I would say we are at greater risk" for accidents and misuse, he said, adding that the FBI and intelligence agencies told GAO investigators that they share those concerns.

Other federal officials acknowledged gaps in oversight of labs handling select agents, pathogens that could be used as bioweapons. A 2003 regulation requires that these labs register with the Centers for Disease Control and Prevention (CDC) in Atlanta, Georgia, and undergo inspections. But inspectors apparently missed serious problems at Texas A&M in 2006. Richard Besser, director of CDC's terrorism preparedness office, conceded a need to improve what he calls a "young program." He said CDC now plans to conduct more in-depth inspections, including unannounced visits. Besser also endorsed creating an accident-reporting system, like those run by NASA and the aviation industry, that would enable labs to share experiences without being punished.

To date, 105 possible exposures and losses have been reported to CDC under the existing rules. The oversight subcommittee last week disclosed details of those incidents, which included animal bites, needle sticks, and possible lost samples. Three releases were detected when five workers became ill from working with a select agent. None of the incidents posed a public health threat, Besser said. Another case involving two shipments of leaky vials of anthrax resulted in a $450,000 fine last month for the shipper, the Lawrence Livermore Berkeley Laboratory in California.

Another gap highlighted at the hearing is that, unless the work involves recombinant DNA, no agency oversees labs working on pathogens not on the select-agent list, such as SARS and dengue. NIAID Deputy Director Hugh Auchincloss Jr. said agencies plan to form an interagency task force to improve biosafety oversight.

Rhodes suggested that a single agency should oversee all BSL-3 and BSL-4 labs. But one lawmaker cautioned against stifling research. Michael Burgess (R-TX) noted the research community's success at identifying the SARS coronavirus and stopping its spread in 2003. "I don't want to see us do anything that would rob us of that ability," he said. That concern is shared by the American Society for Microbiology (ASM) in Washington, D.C. "We need to be careful that whatever legislation emerges doesn't create such a burden that it actually interferes with public health measures and research," says ASM's public affairs director Janet Shoemaker.

The panel expects to hold more hearings on similar labs in other countries, and on the implications of closing the Plum Island Animal Disease Center, located off Long Island, New York, the U.S. laboratory where the most dangerous animal pathogens are studied.

–JOCELYN KAISER

Under scrutiny. Congress is concerned about safety at the rising number of biodefense labs, including those like this Army BSL-4.

CREDIT: SAM YU/THE FREDERICK NEWS-POST/AP PHOTO

SEISMOLOGY

Piercing the San Andreas's Heart, But Missing a Vital Target

For the first time, drillers have retrieved rock from deep within an active fault where earthquakes can get a start, researchers announced last week. With a ton of rock core to take to the lab, excited scientists will be dissecting their haul for clues to how and why faults rupture in quakes. But the uncooperative San Andreas fault has frustrated drillers targeting their ultimate goal: a small patch of the fault that regularly breaks in tiny quakes.

One hit. Drillers cored a creeping part of the fault but couldn't get to a quake.

CREDITS: CLAY HAMILTON/STANFORD SCHOOL OF EARTH SCIENCES. (INSET) ICDP

Drilling for the San Andreas Fault Observatory at Depth (SAFOD) began in 2004 just west of the fault near the tiny central California town of Parkfield and culminated early this past September, when drillers retrieved the last of 44 meters of rock core. In two summers, the drillers had bored the hole straight down before angling it off to the east to grind through the fault at a depth of 3 kilometers. This past summer, they bored out 10-centimeter-thick side cores across two active strands of the fault.

"It was a challenging summer," says seismologist William Ellsworth of the U.S. Geological Survey in Menlo Park, California, one of three co–principal investigators in the $24.6 million project funded by the National Science Foundation. The "damage zone" of hundreds of meters of contorted, broken rock created by millions of years of faulting "is a very unstable piece of rock," says Ellsworth. Again and again, the hole's walls collapsed, and drill pipes got stuck.

Despite the obstacles, SAFOD drillers retrieved cores across two "creeping" fault segments: active strands of the San Andreas where rock on opposing faces of a fault strand slips smoothly by without generating quakes of any size. Seismologists have long thought that something about creeping segments—perhaps the presence of particularly soft and slippery rock—in effect lubricates the fault and short-circuits quakes (*Science*, 11 October 1991, p. 197). Indeed, researchers found the slippery mineral talc, of baby-bottom fame, in debris from the initial SAFOD drilling of the fault. And cores through the ground rock at the heart of the creeping fault contain bits of serpentine (inset, greenish), which can give rise to talc.

But mounting costs have pulled the research up short. "Because of a lack of funds, we were unable this year to drill into the repeating earthquake," Ellsworth tells *Science*. The ultimate target of SAFOD drilling had always been a 100-meter-wide patch embedded in the creeping fault. Rather than creeping, that patch breaks every couple of years in a magnitude-2 earthquake (*Science*, 23 December 2005, p. 1898). Researchers hoped to learn how that part of the fault can accumulate enough stress to produce quakes even though the surrounding fault can't.

Team members still want to drill the quake target, but they can't afford to do it now. Drilling through the rotten rock of the fault zone added unplanned costs. And the frenzied search for $80-a-barrel oil boosted costs across the drilling industry. Before researchers could target the quake patch, SAFOD funding for drilling ran out. They will soon install several kinds of sensors in the borehole just 100 meters from the patch, which should fail again in a year or two, but drilling into it will require new funding beyond SAFOD. Researchers outside the project strongly support more drilling. "I think it would be a crime if in the next few years we don't go back in and drill into" the rupturing patch, says rock mechanicist Terry Tullis, a professor emeritus at Brown University. "It's really worth it."

—RICHARD A. KERR

SCIENCESCOPE

Few Clues in Rice Mystery

After a 14-month investigation to find out how unapproved varieties of genetically engineered rice got into U.S. and European food, the U.S. Department of Agriculture (USDA) has come up with no insights into exactly what went wrong. Bayer CropScience discovered one of its experimental herbicide-tolerant long-grain rice varieties in commercial samples last year (*Science* 22 September 2006, p. 1714) and another this year. USDA last week admitted that it wasn't able to figure out how the experimental rice got into the food supply. But as part of a broader review of its biotech regulations, the agency says it is thinking about ways to keep a tighter lid on experimental plants, such as requiring more isolation of seed-breeding fields. And to aid subsequent investigations, it may also require companies to keep better records.

—ERIK STOKSTAD

Bill and Melinda Play Risk

The Bill and Melinda Gates Foundation has announced a $100 million program to fund 1000 high-risk research projects. Tadataka "Tachi" Yamada, head of the Seattle foundation's global health program, says the focus will be in areas the charity already supports: infectious disease, maternal and newborn health, and nutrition, with the hopes that the research will complement the $436 million the philanthropy spread to 43 grant winners in its Grand Challenges in Global Health program. Proposals can run no more than two pages, and decisions will be made within 3 months, with the first grants going out in the second half of 2008. Yamada says the relatively small, roughly $100,000 awards should allow scientists to test novel ideas and reveal "Is this really wacko or does it have life?"

—JON COHEN

California's Heavy Hitter: Bonds

State bonds for stem-cell work flew off the shelves in a 2-day sale last week in California in what supporters say illustrates popular interest in the state's nascent research effort. Individual investors snatched up more than 40% of the $250 million worth of bonds designed to finance Proposition 71, the initiative voters passed in November 2004 to authorize a $3 billion institute. "We were thinking we'd get about $30 million" in sales to individuals, but "we wound up with almost $103 million," says California treasury spokesperson Tom Dresslar. Lawsuits that were finally resolved this spring delayed the sales of the bonds for more than 2 years.

—CONSTANCE HOLDEN

A Culture Under Siege

Myanmar's military rulers have eroded the country's education system and damaged its heritage. Scientific cooperation might offer a lifeline to beleaguered academics

YANGON, MYANMAR—When saffron-robed monks took to the streets last month in a rare display of public protest in Myanmar's cities, one familiar element in uprisings around the world was largely missing: university students. There's a good reason, say Burmese academics. The junta that has ruled Myanmar, formerly Burma, for the past 19 years has stultified and splintered the universities. "The military has a deliberate policy to not educate the people," alleges a Western diplomat in Yangon. "They are afraid people will learn to think critically." Burmese dissident Aung Zaw, editor of *The Irrawaddy* magazine, agrees. "The military leaders think it is easier to control an uneducated population," he asserts.

The protests have prompted a bloody crackdown. United Nations special envoy Ibrahim Gambari was in Myanmar last week to try to open a dialogue between the junta and opposition leaders, including Aung San Suu Kyi, the Nobel Peace laureate who has spent 11 of the past 18 years under house arrest. But as *Science* went to press, soldiers had embarked on a door-to-door campaign to round up activists and put the country in lockdown. This is discouraging news for those who hoped Myanmar's academic life might be revitalized soon. "The country has suffered catastrophic losses of human capacity," says a United Nations Educational, Scientific, and Cultural Organization (UNESCO) official who requested anonymity.

The turmoil has rekindled a debate about how to assist Myanmar's fading academic community. Sanctions and approbation have failed to sway the junta, which gets vital economic support and political cover from its neighbors, especially China. In the diplomat's view, attempts to engage the government haven't paid dividends either. Others argue for bolder outreach: "The best way to support our colleagues in Myanmar is to maintain and strengthen our professional ties with them, and to continue to provide them with opportunities to do their work and interact with the world beyond their country," says Miriam Stark, an expert on Southeast Asian archaeology at the University of Hawaii, Manoa.

Shortly before the recent protests, *Science* met informally with two dozen researchers* in Bagan, Pyay, and Yangon. Academic freedom is virtually nonexistent, they say. Even scientists in North Korea were freer to speak with a journalist from *Science*. Forging lasting bonds with skittish colleagues in the shadow of one of the world's most repressive regimes will not be easy. "Burma is a moral minefield," says Aung Zaw. "There is no black and white."

Venting frustration. Buddhist monk leaders speak at Yangon's Shwedagon Pagoda during a protest on 23 September.

CREDITS (TOP TO BOTTOM): MUTSUMI STONE/AP

* All the people in Myanmar interviewed for this article are anonymous, to protect them from retribution for speaking to a foreign journalist without government authorization.

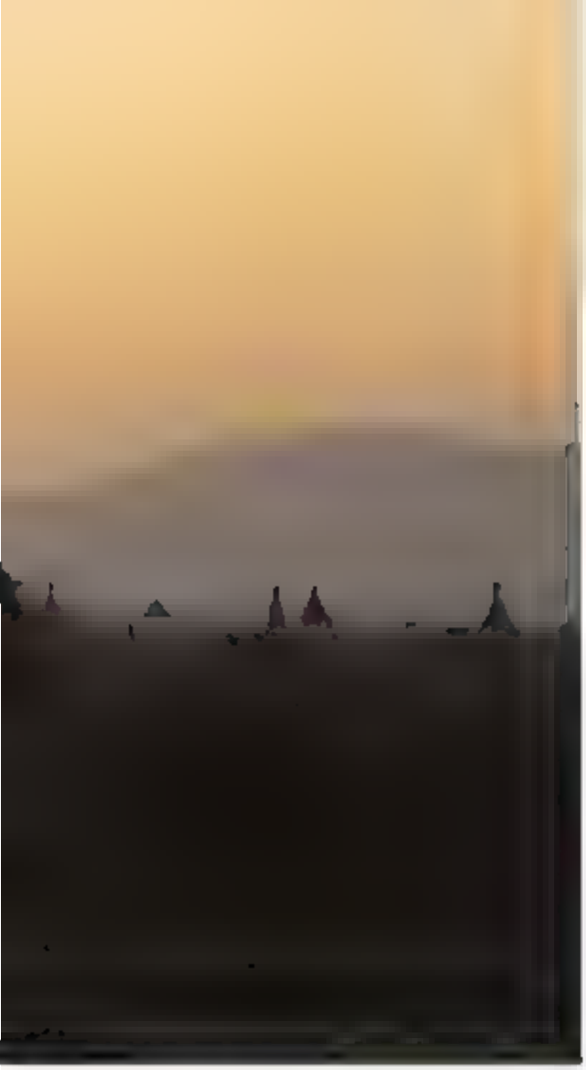

CREDIT: MITSUMI/STONE

A benighted populace

After crushing demonstrations fomented by university students in 1988, the omnipresent military, or Tatmadaw, closed the country's premier higher education institution, the University of Rangoon. The university partially reopened—but only for graduate study and research. *Science* was not permitted to enter the campus. According to news reports, university facilities are being used to jail dissidents.

The abolition of undergraduate programs at the University of Rangoon may have eliminated the problem of enlightened young men and women congregating in large numbers, but the country still required competent workers. As a solution, the Tatmadaw government, which in an Orwellian touch 10 years ago renamed itself the State Peace and Development Council, claims to have established 156 universities and colleges throughout the country, up from 38 in 1988. In a recent speech, the junta's leader, Than Shwe, cited the "promotion of the education standard of the nation" as one of three requirements to "practice democracy effectively."

"Than Shwe is living in a fantasy world," fumes the Western diplomat in Yangon. She and other critics say that education levels have declined precipitously. "The tragedy is that the country is further behind than it was in the

MYANMAR'S MAGIC KINGDOM

BAGAN, MYANMAR—Its skyline is studded with more than 3200 temples and bell-shaped stupas: Bagan, a sprawling ancient city on the bank of the Ayeyarwady River in central Myanmar, is the largest assemblage of Buddhist monuments in the world. But its breathtaking vista is riddled with impostors.

In the past decade, some 1100 monuments have been rebuilt from the ground up. At the construction site of a nearly finished temple, the foreman retreats into the building's shadow to escape the midday sun. This is the 231st temple his team has built, but he's in no mood to brag. "I'm losing out on this job," he says, mopping his brow with a rag as masons use a rope pulley to haul cheap red bricks to the roof. They are behind schedule, having worked on the building for more than half a year, and the foreman has spent more on materials and labor than he received up front from the local administration.

Over the centuries, bandits, floods, and earthquakes, including a devastating temblor in 1975, have eroded many of Bagan's medieval wonders. Not content with safeguarding a fragile heritage, in 1998 the government of Myanmar, formerly known as Burma, ordered a sweeping restoration. The result is what one prominent Burmese scholar has dubbed "blitzkrieg archaeology": the quick and cheap erection of cookie-cutter temples and stupas. The shoddy structures, along with a 50-meter-tall, corn-silo-shaped viewing tower and a garish new museum built in a style from another region and period, are meant to attract more tourists—and cash. Cultural integrity is an afterthought, and many archaeologists are appalled.

"So many sites have been pillaged or destroyed by misguided attempts at restoration and tourism development," says John Miksic, an archaeologist at the National University of Singapore who has studied Bagan's murals, "that our chances of reconstructing an accurate picture of the evolution of civilization along the Ayeyarwady have been seriously compromised."

Miksic and others acknowledge that Bagan is a living monument, and as such, the Burmese have a right to restore temples for worship. "In Asia, to let your heritage go into a state of disrepair is not acceptable," says a UNESCO official. The problem, he says, is that "nobody there now is professionally trained." After the 1975 earthquake, Myanmar invited UNESCO to take the lead in shoring up weakened structures, a program that ran until money dried up in 1995. Since then, poor restoration work has rendered ancient structures more vulnerable to future earthquakes, says Pierre Pichard of the French Research School of the Far East in Bangkok. "It's quite dangerous," he says.

Ironically, the rapid rebuilding of the Bagan temples may be repeating history. Recent evidence suggests that some 2500 temples rose in Bagan over a 70-year period in the 13th century, a staggering rate of one temple every 10 days. "Perhaps your modern, harried, budget-cut artisans, pressured by donors and contractors, are actually continuing an ancient tradition," says Robert Hudson, an archaeologist at the University of Sydney, Australia, who has excavated at Bagan. To Pichard, Nouveau Bagan's simple designs and bright colors have "spoiled" the site. "Officials there," he says, "call it beautification." Hudson puts it differently: The restoration at times "verges on Disneyfication."

—R.S.

All the more special. A research station rises in Myanmar's Special Region Four.

EXPLORING ALTERNATIVES IN MYANMAR'S WILD NORTH

BEIJING—Ask Burmese how they feel about China, and you're likely to get an earful about the hunger of their northern neighbor for Myanmar's timber, gas, and other natural resources. But an unusual new venture in sustainable development in the Shan State of northeastern Myanmar, just across the border from China, could be a small step in improving China's image—and a leap in both local living standards and access for scientists to a biodiversity hot spot.

In January 2008, the private Research and Education Center for Alternative Development (RECAD) will open for business in Special Region Four (SR-4), a district of Shan that shares a stretch of the Mekong River with China's Yunnan Province, in the Golden Triangle. These verdant highlands where China, Laos, Myanmar, and Thailand converge are notorious for opium poppies. In SR-4, the illicit crop was eradicated in 1998. But poppies thrive in other corners of Myanmar, which is second only to Afghanistan in opium production. "They grow poppies not from desire. It's because they are starving," says Wang Yingming, a Chinese entrepreneur with a Ph.D. in environmental sciences who is spearheading RECAD's establishment.

Rubber and research. Wang Yingming is hoping to help cure Myanmar of its opium habit.

Experts are concerned that SR-4 is poised to regain its addiction to opium. In the 1990s, casinos sprang up in the region, catering to moneyed Chinese tourists. Two years ago, as part of an antigambling campaign, Chinese authorities forced dozens of casinos to close and cut off power to the region, which is on the Chinese grid. "Without alternative development, there is a likelihood of excessive deforestation for the resumption of opium cultivation," says Guofan Shao, a forest ecologist at Purdue University in West Lafayette, Indiana, who visited SR-4 in 2004 and 2005. This, he says, "would directly threaten biodiversity conservation."

Hoping to avert that prospect—while creating a sustainable business venture—RECAD, bankrolled by Pudu Co., a private investment firm in Beijing, will test plants such as *Jatropha* that can be used to produce biofuels for the Chinese market. The $5 million center will manage a 6500-hectare rubber plantation that hopes to break even within a decade, says Wang, Pudu's president.

RECAD could also act as a brake on unbridled development. The center is "a good starting point" for helping SR-4 authorities with sustainable land-use planning, says Shao. He hopes that with an understanding of biodiversity and the value of preserving forest alongside plantations, SR-4 can avoid the fate of Xishuangbanna Prefecture in Yunnan, where rubber plantations have run riot. "It will be a total disaster if the same rubber-tree landscape model is repeated in SR-4," Shao says.

In a departure from the usual Chinese business model, Wang has put scientific concerns at the forefront. "No organization in Myanmar has done research to guide development," Wang says. RECAD has dormitories for visiting scientists, who will pursue everything from applied projects in biofuels and sustainable development to basic forest ecology. Wang has established links with the Chinese Academy of Sciences, which plans to dispatch four to six teams of researchers to the SR-4 facility early next year. Foreign scientists will be warmly welcomed, says Wang. "I intend to turn it into a real international research center."

Wang concedes that launching the center in SR-4, which enjoys significant autonomy from Myanmar's central government, is a gamble. "Only high-risk investors come here," he says. But Wang has won the hearts of locals with the promise of employment for as many as 1500 people and a pledge to build a school and a hospital with help from the Chinese government. Scientists, too, are eager to participate in the experiment. "SR-4 is a unique site for promoting alternative development and protecting forest biodiversity in Southeast Asia," says Shao. An initial project, he says, could be a biodiversity inventory of the region.

—R.S.

CREDITS (TOP TO BOTTOM): COURTESY OF WANG YINGMING

1950s." The University of Rangoon's closure to undergrads was a crippling blow, she says: "It was considered one of the finest universities in Southeast Asia." Now, most Burmese undergraduates attend classes a month at a time at one of the campuses outside Yangon and take correspondence courses. Children of the Tatmadaw elite are sent abroad for study, says the diplomat. Apart from them, she says, "young people with good education are growing scarcer and scarcer."

This, combined with a dire shortage of funding, has made it harder for older researchers, many of whom received training in China or the Soviet Union, to recruit fresh talent. "University laboratories are in terrible condition. They are like ghost towns," says one chemist. "That's why the government doesn't want foreigners to see the university," he says. "Chemistry students can only read about experiments; they can't do them," adds the Western diplomat. And scientific literature is scarce.

Only a handful of science and technology projects receive significant government resources. One is the revival of plans to build a nuclear research facility. Five years ago, the government inked a deal to buy a 10-megawatt research reactor from Russia. The agreement stalled until Myanmar announced its intention earlier this year to follow through with the purchase. Projects can fall out of fashion abruptly, however. In Bagan, an ancient city in central Myanmar (see sidebar, p. 185), the excavation site of a royal palace is now fenced off by barbed wire. The dig has been dormant since its patron, former Prime Minister Khin Nyunt, was ousted 3 years ago.

Any collaboration with foreign scientists is vulnerable to the Tatmadaw's whims. According to Burmese scientists, each ministry has a "Foreign Affairs Committee," including representatives of the defense and security bureaus, that evaluates proposals; the minister must sign off on approved projects. That process got more complicated when the government relocated up country to Myanmar's remote new capital, Naypyidaw, in February.

Yet there are a few bright spots in the landscape. Over the past 2 years, for example, the International Rice Research Institute's Irrigated Rice Research Consortium has run workshops and training in Myanmar on topics such as integrated weed control, nutrient management, and laser land leveling. "There is a great need to support the livelihoods of the poor farmers and to strengthen scientific capacity," says Grant Singleton, the consortium's coordinator. These efforts will continue in 2008, he says.

Other success stories include bird-flu monitoring with help from the United Nations Food and Agriculture Organization, the creation of the Hukaung Valley Tiger Reserve with the Wildlife Conservation Society in New York City, and the establishment of two facilities, a conservation center in northern Myanmar (see sidebar, p. 186) and an archaeological field school in Pyay.

Throwing a lifeline

Founded 20 centuries ago, the circular walled city of Sri Ksetra on the banks of the Ayeyarwady River was a key outpost of the Pyu civilization. Today, Sri Ksetra, near the city of Pyay, 270 kilometers northwest of Yangon, is a rarity in Myanmar: an active excavation site involving foreign researchers. Even more surprising is a cluster of whitewashed buildings just inside Sri Ksetra's overgrown brick and earthen walls: It's the Field School of Archaeology, Pyay.

Getting their hands dirty. Students learn artifact preservation at the Archaeological Field School in Pyay.

CREDIT: MITSUMI STONE

Opened in 2005, the school now has three dozen students in a 1-year diploma course in applied archaeology that emphasizes preservation. Easy access to Sri Ksetra provides hands-on learning. "It is a great site" because the huge ancient town offers lots of space for practical work, says Elizabeth Moore, an archaeologist at the University of London who has worked in Myanmar. Several field school instructors have completed the well-respected Archaeological Survey of India graduate diploma program.

Crucially, Myanmar authorities have allowed foreign researchers, including Robert Hudson, an archaeologist at the University of Sydney, Australia, to lecture at the school. "A common and very heartening comment from the students is that the work here is much harder than at university," says Hudson. With colleagues in Pyay, Hudson conducted a ground and satellite survey of Sri Ksetra in 2005 and 2006 that revealed an extensive system of waterworks for irrigation and flood control. The survey, building on excavations carried out sporadically since 1907, also revealed new features, including the remains of a vast brick complex of Pyu burials and iron furnaces outside Sri Ksetra's walls.

Promising as these interactions are, their impact is limited. The archaeologists in Pyay have virtually no budget beyond their meager salaries. Restoration of Sri Ksetra's 1500-year-old Baw Baw Gyi pagoda has been frozen for 2 years due to lack of funds. Working farther afield is largely out of the question—for archaeologists anywhere in Myanmar—especially after the hefty increases in fuel prices that sparked the recent demonstrations.

Now is the time to redouble efforts to reach out to Myanmar scholars, says John Miksic, an archaeologist at the National University of Singapore—and archaeology is a good place to start. Hawaii's Stark agrees. Foreign archaeologists, she says, "are now the lifeline for scientists in Myanmar." She and others hope that unspecified sanctions announced last month by U.S. President George W. Bush will not target scholarly exchange. "Banning foreign scientists from working in the country will primarily isolate and weaken our colleagues in-country who will train the next generation," Stark says.

Nurturing young minds won't be easy, as the deterioration of the education system has taken a heavy toll. "Even if there is an overnight change in the country's openness," says the UNESCO official, "it will take a long time to recover." —RICHARD STONE

BIOMEDICINE

Grasping for Clues to The Biology of Itch

Chronic itch afflicts millions of people, but little is known about the underlying mechanisms

SAN FRANCISCO, CALIFORNIA—For most people, itch is an occasional, short-lived annoyance, provoked by a run-in with bloodthirsty insects or poisonous plants. But for Mary Ellen Nilsen, itchiness became a life-altering experience. In 1998, at age 38, Nilsen had a shingles outbreak, a resurgence of the chickenpox virus. Antiviral drugs cleared up the painful shingles rash on her face and scalp, but a ferocious itch took its place. "It was relentless," Nilsen says. Over a 13-month period, Nilsen scratched and scratched, despite her best efforts not to and despite her horror at the growing lesions she saw in the mirror. At the time, Nilsen says, she had no idea that the damage she was doing to herself was more than skin deep, but she ended up in a Boston emergency room with brain tissue protruding through a hole she'd scratched in her skull.

"She gave herself frontal-lobe brain damage," says Anne Louise Oaklander, a neuroscientist and neurologist at Harvard Medical School in Boston, who treated Nilsen and described her case at a recent meeting* here. Oaklander blames the infuriating itch on severe nerve damage caused by the virus—damage that also left Nilsen unable to feel pain from her scratching-induced wounds. Although Nilsen's experience is extreme, to say the least, chronic itch is far from rare. Millions of people worldwide suffer from incessant and largely unexplained itchiness brought on by kidney or liver disease, HIV, or various other ailments. Chronic itch disrupts sleep, reduces the quality of life, and undermines the health of those who suffer from it—yet there is little doctors can do to help.

At the meeting, a diverse group of clinicians and researchers tried to scratch beneath the surface of recent findings for clues about the biology of itch. "Itch remains one of the greatest puzzles in sensory physiology," says Hermann Handwerker, a pioneering itch researcher at the University of Erlangen-Nuremberg in Germany.

Once thought to be a lesser form of pain, itch does share some neural wetware with that other unpleasant sensation. But recent research points to receptors and nerves that may selectively signal itch. Drugs that turn the volume down on such signaling pathways could vastly improve the lives of many people who desperately need help, clinicians say. "Itch is absolutely a neglected area of medicine," says Oaklander. "It's extremely disabling."

And chronic itch is surprisingly widespread. At the meeting, Gil Yosipovitch, a dermatologist at Wake Forest University School of Medicine in Winston-Salem, North Carolina, reeled off a long list of scratch-inducing statistics. A 2006 study in *The Lancet Infectious Diseases* estimated that 300 million people worldwide suffer from scabies, an itchy skin disorder caused by biting mites. A report published online in *Dermatitis* in August estimated that 31.6 million Americans suffer from the itchy, inflamed skin of eczema, and a 2006 study in *Nephrology Dialysis Transplantation* found moderate to severe itch in 42% of nearly 19,000 kidney-dialysis patients surveyed in 12 countries. Other studies have associated intense itchiness with bile duct obstructions, infectious diseases, and drug reactions. For reasons that are poorly understood, some conditions cause itch over large swaths of the body, whereas others tend to affect only the face, back, or other region, Yosipovitch says.

Wherever it strikes, chronic itch isn't good for your health, Yosipovitch adds. The study of kidney-dialysis patients, for example, found a 17% higher mortality rate in those with chronic itch, a finding the researchers attributed to loss of sleep. In a literature review published in the July issue of *Acta Dermato-Venereologica*, Yosipovitch concludes that itch is often worse at night. He suspects that circadian fluctuations in compounds that aggravate or dampen itch may be the reason. Levels of the itch-suppressing hormone corticosterone, for example, wane in the evening.

* 4th International Workshop for the Study of Itch, 9–11 September.

CREDIT: GRAHAM DEAN/CORBIS

Biological roots

If itch is so problematic, why do we have it in the first place? Many researchers think it evolved as a defense mechanism against insects. Unlike pain, which elicits a withdrawal response, itch draws attention to a particular area of the skin and elicits scratching, so it may serve to remove insects and any stingers, eggs, or other deposits they leave behind, says Handwerker. "It may have been more important for early man to protect himself against insects than against tigers or other large animals," he says.

Although itch and pain are different sensations tied to different behaviors, their biology appears to be inextricably intertwined. In fact, itch was once considered pain's little brother. Both sensations are conveyed from the periphery to the spinal cord by nerves called C fibers, and the thinking was that a little bit of C-fiber stimulation caused itch, whereas more stimulation caused pain. In this view, pain and itch share a communication link to the brain, and only one of them can talk at a time. This would explain why pain tends to quell itch and why certain painkilling drugs facilitate it.

But in 1997, a research team led by Martin Schmelz, now at the University of Mannheim in Germany, reported the discovery in healthy human subjects of C fibers that respond vigorously to an itch-inducing injection of histamine under the skin but not to painful heat or pinching. The findings suggested that itch and pain may talk independently to the brain after all.

A more recent strike for itch independence comes from geneticists at Washington University in St. Louis, Missouri. Yan-Gang Sun and Zhou-Feng Chen used DNA microarrays to search for itch-related genes in the spinal cords of mice. Based on its high levels in spinal neurons thought to convey itch, one candidate stood out: the gene for gastrin-releasing peptide receptor (GRPR). When the researchers created mice lacking the GRPR gene, the rodents scratched much less than normal mice when both sets of animals were injected with several itchy substances. Yet the mutant mice responded normally to painful poking, heat, and noxious chemical injections, Chen reported at the conference and in the 9 August issue of *Nature*.

The findings offer an important insight into the biology of itch, other researchers say, and they may point to possible treatments. Part of the reason chronic itch conditions have been so hard to treat is that, unlike acute itchy reactions caused by mosquito bites and poison ivy, most of them are not mediated by histamine, and so they do not respond to antihistamine drugs. There must be molecular players in itch transmission besides histamine, but their identity is a mystery. Even so, when Sun and Chen gave genetically normal mice a drug that blocks GRPR, the rodents scratched less in response to subsequent injections of three itch-provoking compounds—including two that don't work through histamine. That's a good sign, Chen says: "Our results suggest that GRPR [blockers] could be particularly promising for treating chronic itch."

Other researchers reported on a variety of possible treatments for chronic itch including medications more commonly used to treat depression (selective serotonin reuptake inhibitors) and epilepsy (such as gabapentin) that may quiet hyperactive itch-transmitting neurons. One of the most promising leads, say several researchers, are drugs that stimulate so-called κ opioid receptors. Opioid receptors are best known as the site of action for powerful painkillers like morphine, which activates μ opioid receptors, dulling pain but often producing itch as a side effect. Drugs that stimulate κ receptors seem to have nearly opposite effects, reducing itch without dulling pain in a handful of recently published studies with patients suffering chronic itch related to kidney disease. (Pain does serve a purpose, after all, as Nalsen's case illustrates.) And at the meeting, researchers from the pharmaceutical branch of a Japanese chemical company reported encouraging findings from a small pilot study in cirrhosis patients with chronic itch.

Itchy nightmare. Bandages protect Mary Ellen Nalsen's head after a chronic itch drove her to scratch through her skull (CT scan, *inset*).

CREDITS (TOP TO BOTTOM): A. L. OAKLANDER ET AL. PAIN 114 (2005); ANNE LOUISE OAKLANDER

Scratch, scratch

Some researchers are also studying the oldest itch remedy of all: scratching. Neuroscientists Steve Davidson and Glenn Giesler and colleagues at the University of Minnesota, Minneapolis, recently investigated the effects of scratching on the activity of neurons in the spinal cords of anesthetized monkeys. These neurons rev up when researchers inject histamine or other itchy compounds under the skin, firing impulses at an elevated rate. But when Davidson used a saw blade to gently scratch the site of the injection, the neurons interrupted their barrage of impulses for a few seconds. This inhibition only happened when the spinal neurons were signaling an itch: scratching in the absence of itch made them more excited, Davidson reported in a poster presentation at the meeting. The findings suggest that scratching inhibits itch in the spinal cord, before it even reaches the brain, he says.

That's not to say the message never makes it through. Several recent studies have used functional magnetic resonance imaging to investigate how the brain responds to itch. In a study with 16 people, half with chronic itch caused by atopic dermatitis, Yosipovitch's group found hearty responses to itch in the anterior cingulate cortex, a brain area that, among other things, may attach emotional significance to sensory experience. Neural activity in the anterior cingulate ramped up when the researchers injected histamine into the skin of the subjects' forearms, Yosipovitch reported. This increase was greater in the dermatitis subjects and varied in proportion to the severity of their itch. In another study, Yosipovitch and colleagues found that scratching, even in the absence of itch, decreases activity in the anterior cingulate.

Such studies may eventually shed light on why scratching is so addictive. "There is definitely a rewarding effect to the scratch itself," Yosipovitch says. Perhaps that helps explain why people often scratch when they see others in an itchy state. A few years ago, German researchers videotaped people watching a public lecture about itch and caught them scratching more than usual. The effects of reading articles about itch have yet to be rigorously tested. **–GREG MILLER**

Identities revealed. Some taxonomists thought these two types of ginger were the same species, but DNA barcoding proved otherwise.

TAXONOMY

Wanted: A Barcode for Plants

Quick-and-easy DNA identification of animals is under way, but plants are proving harder to pigeonhole

Four years ago, Paul Hebert wowed researchers at the Smithsonian Institution's National Museum of Natural History (NMNH) in Washington, D.C., with the results of a pilot study that he said demonstrated a way to distinguish any animal species from any other, using only a short piece of variable DNA. Hebert, an evolutionary biologist at the University of Guelph in Canada, called it an organism's "barcode." He appealed for a similar effort to find a unique identifier in plants. "He was staring right at me," recalls W. John Kress, a botanist at NMNH. "I took it as a challenge." Kress and his colleagues began what has become a controversial quest for a botanical barcode.

At a meeting in Taipei last month,* hundreds of researchers described their successes in barcoding birds, moths, fish, and other animals, demonstrating rapid progress for this high-tech approach to cataloging biodiversity. Representatives from regulatory agencies outlined plans to use barcodes to track water quality, as well as invasive and endangered species. But despite a strong effort by Kress and dozens of other botanists and systematists, barcoding for plants has yet to gel. "We did not reach consensus" about a few issues, says Ki-Joong Kim, a botanist at Korea University in Seoul, who has come up with his own barcoding scheme.

Debates have been raging about how many and what pieces of DNA it takes to tell one plant from another. Some groups have forged ahead, gathering representative sequences from plants ranging from mosses to daisies, and several teams are developing DNA catalogs of medicinal plants or endangered trees. Yet, for the most part, these data are of little use until everyone can agree on a standard. "Botanists around the world are champing at the bit to get involved in barcoding," says Kenneth Cameron, a plant systematist at the New York Botanical Garden in New York City. "People are very frustrated" by the lack of consensus. And the potential for confusion is rising, as groups pursue selected DNA sequences and different cataloging strategies.

Proposed Plant Barcodes

GROUP	GENE	SPACER
Kress *et al.*	*rbcL*	*trnH-psbA*
Chase *et al.*	*matK, rpoC1, rpoB*	
Chase *et al.*	*matK, rpoC1*	*trnH-psbA*
Kim *et al.*	*matK, atpF/H*	*trnH-psbA*
Kim *et al.*	*matK, atpF/H*	*psbK/I*

On the table. Over the past 6 months, researchers have proposed several combinations of DNA regions for barcoding plants.

No simple solution

Barcodes on groceries instantly reveal the identity and cost of an item in just a few black and white stripes. In animals, a mitochondrial gene called *CO1* seems to work in a similar way, as a kind of species tag. Its sequence varies enough to distinguish most animal lineages but is conserved enough that a single DNA probe works for most organisms. This simplicity has sparked plans to make hand-held sequencers that can provide quick readouts in the field (*Science*, 18 February 2005, p. 1037).

From the start, Kress and others knew that plants would need a different tag. Mitochondrial genes wouldn't work because they evolve more slowly in plants than in animals; too few differences exist between, say, a potato and a tomato to tell them apart. Nuclear genes weren't very appealing either because plant cells often have many copies of a mitochondrial gene but relatively little nuclear DNA. So plant experts turned to a genome not found in animals—that of the chloroplast, the organelle that converts sunlight to chemicals.

As a first pass, Kress and his colleagues scanned the two chloroplast genomes that researchers had already sequenced, picking out nine stretches that varied the most. "The sequences have to be similar enough to be [probed] easily but different enough to distinguish plant species," explains Chang Liu of the University of Hong Kong. Kress's group evaluated these regions. In 2005, at the first international barcode meeting, they nominated about 450 bases, part of a "spacer" sequence between two genes for the plants' barcode, *trnH-psbA*. Spacers tend to be more variable than genes themselves and therefore better identifiers. "So far it seems to work the best" of all barcodes, Kress insists.

At that meeting, however, "a lot of the botany community said, 'Whoa, there's problems with this,'" recalls Cameron. He and others thought more comprehensive, systematic studies were needed. Representatives from the Alfred P. Sloan and Gordon and Betty Moore foundations—which had financed work in the area—responded with $900,000 to support further evaluation of barcode candidates. Mark Chase and Robyn Cowan of the Royal Botanic Gardens, Kew, in Richmond, U.K., and researchers from about 10 institutions screened 100 gene and spacer regions in the chloroplast to see which could be pulled out by a single probe. They also checked 96 pairs of species representing

CREDITS (TOP TO BOTTOM): W. JOHN KRESS

*The Second International Barcode of Life Conference was held 16 to 21 September 2007 in Taipei, Taiwan.

the plant kingdom to see which were variable. And they evaluated the most promising half-dozen in specific plant groups. Kress's Smithsonian group declined to participate; they continued refining the spacer strategy they had proposed.

In the 6 June issue of *PloS One*, Kress and his colleagues reported their results: They adopted a more complex strategy to conduct a survey of 50 plant species. "We all wanted the ideal—a single region," Kress recalls. But as his team looked beyond flowering plants to mosses, liverworts, and other distant kin, they ran into too much variation. Although researchers could line up and compare sequences in closely related plants, those in unrelated plants such as ginger and tomato were too different. The remedy they suggest is a "two-locus barcode," says Kress: both the *trnH-psbA* spacer and part of a gene called *rbcL*. Adding the gene, which has changed much more slowly over evolutionary time, is useful for distinguishing distantly related plants.

"It's a concept that I actually like," says Cameron. But Chase and Cowan haven't been eager to buy into the strategy. Earlier, their team turned away from *rbcL*, which codes for a key enzyme involved in capturing carbon dioxide for photosynthesis, because they couldn't come up with a universal probe for pulling out short, easy-to-sequence pieces. As for the *trnH-psbA* spacer, Chase says their results suggest that its variability limits its utility as a universal barcode.

In the May issue of *Taxon*, Chase's team instead proposed a barcode using three DNA regions. A triple probe is needed, Chase explains, because "no one of them works universally." His group had not quite settled on which probes work the best; different ones help distinguish certain groups of plants (see table).

Meanwhile, Kim had struck out on his own in search of the best plant barcode. His group sequenced the chloroplasts from nine plants, including seven ginseng species, discovering several regions that provided unique species signatures. Kim's group also decided on a three-region barcode—a gene and two spacers—and could discriminate flowering plants belonging to 10 other genera, including dandelions, lilacs, and *Cardamine*. The gene they chose is *matK*, one of Chase and Cowan's choices. Using this method, Kim has already barcoded 500 Korean species.

In all, about a half-dozen proposals came up during the Taipei meeting; discussions were intense. The Korean strategy bubbled up as quite promising, says plant systematist Sean Graham of the University of British Columbia in Vancouver, Canada. But "a final set of markers was not quite decided on," he notes. Most of the researchers agree that Kim and Chase's *matK* and Kress's spacer should be used. And most are calling for a third region, likely one of the two other spacers proposed by Kim. Graham and his colleagues are going to evaluate these four candidates and report back later this fall on how well they work.

Kress, however, left frustrated. He points out that several papers presented at the meeting supported his choices for a barcode, whereas there's little published data supporting other scenarios. He's hesitant about any three-gene scenario because it would create "an order of magnitude more work." Anyway, he says, "we're moving ahead" for now using his two-barcode regions.

Intense debate. In Taipei, plant researchers wrangled over potential barcode regions, making headway but not reaching full agreement.

CREDIT: YUN-CHIH JAO

Conflicting needs

Part of the problem is that plant researchers have different needs. For example, a unique barcode may not be all that critical for cataloging the plants in a given habitat, where typically the species aren't closely related. "Less than three, and often one, gene will work quite well" in a local survey, Graham points out. Indeed, last year, Pierre Taberlet of Joseph Fourier University in Grenoble, France, and colleagues found they could use just one DNA snippet—a noncoding part of a gene—to distinguish half of 132 Arctic species studied and the onion, potato, and leek ingredients in a dried soup mix. The snippet also worked on plant matter extracted from a 20,000-year-old frozen human fecal sample, the group reported online 14 December 2006 in *Nucleic Acids Research*. They suggest that this limited barcode would suffice for tracking plants used in the food and cosmetic industries.

In contrast, taxonomists need more depth within a genus—enough DNA to reveal the degree of relatedness. Introns and spacer regions don't always do that; multiple genes are needed. And some systematists argue that nuclear genes will eventually have to be part of the barcode mix. "It's a Catch-22 situation," says Graham. "The criteria to pick these markers are somewhat contradictory."

But there's a growing need to come up with a solution. Right now, the Barcode of Life Data Systems (BOLD) provides one-stop shopping for anyone seeking animal barcodes. But neither BOLD nor public databases that archive DNA sequences will accept plant barcodes until there is a single agreed-upon standard. Furthermore, BOLD will need to develop new bioinformatics to accommodate barcodes that include multiple DNA regions. "I am worried that if we don't start thinking about this database [problem], suddenly we will have thousands of sequences and no place to put them," Kress says.

The potential chaos is reflected in barcoding for medicinal plants. The Smithsonian group has developed a barcode library for 750 medicinal plants. But until recently, Kress wasn't aware that Liu has been using yet another barcode combination to catalog Chinese medicinal plants.

And some researchers aren't waiting for the standard to be decided upon. Kress and his collaborators are barcoding the 300 tree species in a long-term study site in Panama, and they plan to do the same at 16 other study sites around the world. Chase's group is developing a barcode database of endangered tropical trees for the United Kingdom to use in detecting illegal timber imports. The Sloan Foundation has asked Cameron to draft a plan to coordinate the barcoding of the world's tree species. And Genome Canada is 500 plants into a scheme to develop barcodes for the country's 5000 plant species.

Yet despite all this activity, David Schindel, executive secretary for the Consortium for the Barcode of Life based in Washington, D.C., argues for patience. "This process has taken longer than anticipated and certainly longer than what we hoped," he points out. "But, at the end of the day, the data will reveal which are the most effective high-performing regions."

–ELIZABETH PENNISI

ASTRONOMY

Tooled-Up Amateurs Are Joining Forces With the Professionals

Hobbyists who love the night sky are finding that their skills, and telescopes, are in demand with academic astronomers

BARCELONA, SPAIN—By day, Antonio Garrigós-Sánchez seems like an ordinary guy. The proud 46-year-old father of two girls works as a technician at a printing firm. But by night, he transforms. After sundown, Garrigós-Sánchez retreats to his underground lair, a basement office that would not be out of place at NASA headquarters. The walls are lined with shelves of instruments, journals, astronomical reference books, and stacks of data backup disks. And with a few clicks at the computer on his desk, Garrigós-Sánchez is staring into deep space.

Behind the Garrigós-Sánchez domicile stands an observatory he built from off-the-shelf components. Through the open dome of the cottage-sized building points a telescope as big as a torpedo. Night after night, guided by his computer, it collects light from a zoo of strange celestial objects and records its data on disk. Garrigós-Sánchez doesn't do this only for the joy of watching the night sky. His data are vital for several ongoing academic research projects, and his name appears as co-author on a string of peer-reviewed papers.

Among scientific fields, astronomy may be the last one in which amateurs can stand shoulder to shoulder with professionals and expand the envelope of knowledge. In some cases, they are even outcompeting professionals for research grants. The past decade has seen a renaissance in amateur astronomy due to technological innovations and cheaper components. Basic research can only benefit by tapping into this resource, says Joseph Patterson, a professional astronomer at Columbia University. "The sum total of ingenuity and energy among the world's amateur astronomers vastly exceeds that of professionals."

Cheap tools, long nights

Amateur astronomers are quick to point out that their research has a long pedigree. Many astronomical pioneers were rich men who liked to play with telescopes. William Herschel was an organist and composer in the English town of Bath when, in 1781, he discovered Uranus. In North America, amateurs began exchanging observations and theory with professionals as early as 1868 with the founding of the Royal Astronomical Society of Canada. But things really got cooking in 1911 when the American Association of Variable Star Observers (AAVSO) started pooling data in what has become the world's largest database of amateur astronomical observations. It was founded at Harvard University to ensure that the observations made by amateurs would not be lost.

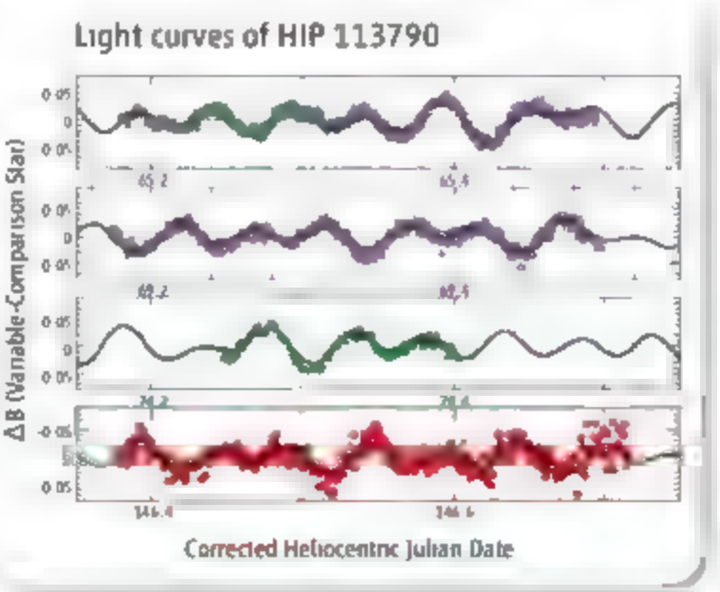

Top quality. Data like these observations of a variable star from amateurs are bread and butter for professional astronomers.

AAVSO now logs about 1 million observations per year from amateurs in 45 countries.

The scale of such amateur scientific efforts is unknown in other fields. (Imagine 2500 volunteer biologists studying fruit fly development with state-of-the-art equipment in their own homes.) The AAVSO amateurs co-authored 30 peer-reviewed papers last year alone, and the association usually holds several active research grants at any one time. Dozens of other networks have sprouted up in the past decade. Garrigós-Sánchez is part of a Barcelona-based group called AstroGea that links amateurs with professional astronomy projects throughout Europe. The quality of these backyard observatories is such that professional astronomers are regular users.

There are several reasons for this blossoming, says Richard Fienberg, editor of *Sky & Telescope* magazine. "But the biggest breakthrough was the CCD camera," he says. "It immediately allowed us to see objects 10 times fainter with the same telescopes."

The CCD, or charge-coupled device, camera has become the sine qua non of astronomical data collection since its invention 3 decades ago, as well as making possible cheap video cameras and digital photography. CCD cameras allow astronomers to convert photons into data much more efficiently. In traditional photography, photons trigger a chemical reaction in the film that, after several steps of development, produces metallic grains that add up to an image. But in a CCD camera, incident photons directly create an electrical pulse in a circuit that can be recorded on a computer as a pixel. The boost in efficiency—CCD cameras detect 70% of photons compared with film's 2%—suddenly turned humble backyard telescopes into "very powerful tools," says Fienberg, who was finishing his astrophysics Ph.D. at Harvard in the 1980s when CCD cameras were first coming into mainstream use among professional astronomers. Cheap mass-production put CCD photography in the hands of amateur astronomers by the early 1990s.

The new bounty of digital data has required heavy-duty computing, and amateurs have played a role here as well. An amateur-scripted program called MaxIm DL controls telescope positioning and the CCD camera and processes the data. "The quality of this software is superb," says AAVSO director Arne Henden, "and it is heavily used by professionals." The program is one among many, he says.

The other key breakthrough was online communication, because it enables observers to react quickly to fast-changing events. "The Internet is key to the blurring of the amateur-professional dividing line," says Henden. A recent example is the observation of an extremely rare pair of stars, known as V455 And (for "Andromedae"), in which a white dwarf is sucking matter from its partner, a brown dwarf. Professionals have been waiting for the white dwarf to gather enough nuclear fuel to become "cataclysmic," releasing a

CREDIT: PATRICIA LAMPENS/ROYAL OBSERVATORY OF BELGIUM

sudden explosion of light that provides valuable data on stellar evolution. The outburst was not expected for decades, but it happened on 5 September. A Japanese amateur spotted it and sent out a notice online, and amateur telescopes around the world swiveled to capture the brief event. "Amateurs are leading the observational studies," says Henden, and "there will be many important papers that will come from this event."

For the love of it. Antonio Garrigós-Sánchez (*right*) in a homemade observatory. Backyard facilities such as these are luring professional astronomers into research collaborations.

CREDIT: J. BOHANNON/SCIENCE

Redefining amateur

But are amateur astronomers aware of how their observations translate into real science? They are, says Fienberg. "It's amazing how well some of them follow the field."

Take Brian D. Warner, for example. (The initial distinguishes him from a professional astronomer in South Africa.) "I got my first CCD in 1992," says Warner, who was working as a computer programmer and television reporter in Colorado Springs, Colorado, at the time. He is part of a network of more than 4,000 international amateurs scrutinizing our solar system's minor planets—the asteroids and their ilk, most of which orbit beyond Mars. Many are as big as mountains, but just finding them in the inky blackness was a feat. Mapping the distribution of these bodies is needed to constrain models of how the solar system evolved. Armed with CCD cameras, amateurs became latter-day Galileos, reporting hundreds of previously unidentified astronomical bodies.

That bonanza came to an end when the professionals caught up in 1997 with the first full-sky digital surveys. "But that just changed the game," says Warner. Instead of identifying new minor planets, amateurs focused their efforts on characterizing them, making repeated observations to reveal their size and rotational speed and whether they are orbited by their own tiny moons. And this is where Warner and others got deep into the science.

A burning question is how minor planets acquire their own satellites. The prevailing theory in the 1990s held that if a minor planet swings close to an enormous body like Mars, the pull of its gravity can break a chunk free from the small body's surface. To test that theory, Warner searched for dancing pairs of bodies far beyond the reach of the major planets. Over the past 3 years, he has identified five pairs. The discovery helped rule out the tug-of-gravity theory, and a new explanation that solar heating causes rotational acceleration that flings chunks off—made the cover of *Science* last year (24 November 2006).

Warner is sheepish about calling himself an amateur these days, because he has earned a master's degree in astronomy from James Cook University in Townsville, Australia, and is a full member of the American Astronomical Society (AAS), an organization generally open only to professional astronomers, granted on the basis of his published work. But he still considers himself the amateur half of a collaboration that began at a minor planet conference in 1999 when he met Alan Harris, a planetary astronomer at the Space Science Institute in Boulder, Colorado. Warner himself won grants from the U.S. National Science Foundation and NASA this year. One of his missions is to catalog the spin properties of all known near-Earth objects, based on his observations and those in the literature. Aside from the value to basic science, the project "does have that extra Hollywood aspect of helping to prevent a global catastrophe," says Warner. Any one of thousands of nearby asteroids could devastate the planet on impact.

Warner's achievements in the field make him stand out, but he's not unique. The number of amateur-professional research collaborations has exploded simply because "professional astronomers need them," says Patricia Lampens, an astronomer at the Royal Observatory of Belgium in Brussels. Her own field of research, variable stars, is a case in point. This class of stars is mysterious because they grow brighter and fainter periodically. To tease apart the many causes of variability, data must be collected continuously throughout a star's cycle, which can range from minutes to years in duration, to obtain a "light curve." Getting just a single night at one of the major professional telescopes is like winning the lottery, but amateurs have the "luxury" of observing whenever they want, she says. Amateurs such as Garrigós-Sánchez "deliver very high-quality data" on the same target over "many weeks or even months" for free. The stellar light curves cataloged by AAVSO are of similar quality.

For professionals to take full advantage of this free resource, some sort of dating agency is required. "What's needed is an efficient system to connect professional astronomers one-to-one with well-equipped amateurs," says Fienberg. He is now helping to set up a "pro-amateur registry" through AAS. Profiles of international amateurs will include their telescope specifications, observing experience, and e-mail addresses. And professional astronomers will post details about their research projects and what kinds of observations they seek.

The registry is bound to blur the amateur-professional line further. When it comes to astronomy, says Donald Kurtz, an astronomer at the University of Central Lancashire in Preston, U.K., "the term 'amateur' should be taken in its original French meaning": a "lover" of astronomy, not necessarily lacking in skill.

—JOHN BOHANNON

LETTERS

edited by Jennifer Sills

The Fire Retardant Dilemma

ALTHOUGH SMOKING AND FIRE DEATHS ARE RAPIDLY DECREASING IN THE United States (*1*), proposed new flammability regulations could add tens of millions of additional pounds of potentially toxic fire-retardant chemicals to bed clothing, pillows, and foam within upholstered furniture (*2*). In the 1970s, the flame retardants brominated tris [tris (2,3-dibromopropyl) phosphate] and chlorinated tris [tris (1,3-dichloro-2-propyl) phosphate] were removed from use in children's sleepwear after being found to be mutagens (*3*, *4*) that could be absorbed into children's bodies (*5*). They are also probable human carcinogens (*6*, *7*). Today, chlorinated tris is the second most used fire retardant in furniture, found in amounts up to 5% of the foam's weight. How did this happen?

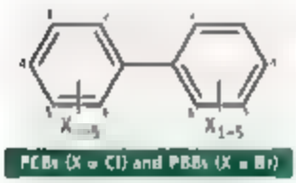

PCBs (X = Cl) and PBBs (X = Br)

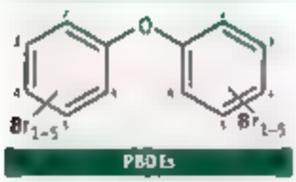

PBDEs

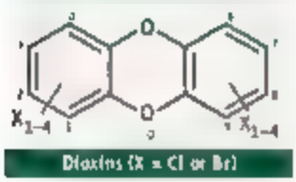

Dioxins (X = Cl or Br)

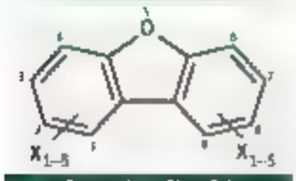

Furans (X = Cl or Br)

Related structures. PBDEs, used as fire retardants in furniture, are structurally similar to the known human toxicants PBBs, PCBs, dioxins, and furans. In addition to having similar mechanisms of toxicity in animal studies, they also bioaccumulate and persist in both humans and animals.

In the 1980s, the fire retardant pentabromodiphenyl ether (pentaBDE) was added to polyurethane foam to meet California's Technical Bulletin 117, to date, no other states have similar regulations. PentaBDE disassociates from foam and migrates into the indoor environment [especially household dust (*8*)]; studies show that pentaBDE is bioaccumulating and has the potential to adversely affect health (*9*) and the environment. In 2003 California banned pentaBDE, eight other states and the European Union (EU) followed suit. In 2004, the U.S. manufacturer voluntarily ceased production.

PentaBDE was replaced by chlorinated tris and unknown proprietary mixtures containing chemicals such as chloroalkyl phosphates, halogenated aryl esters, and tetrabromophthalate diol diester, which may be no safer. An EPA study of these chemicals shows areas of concern, as well as large data gaps for human health and environmental safety information for all of them (*10*).

While we continue to risk our health through exposure to these retardants, they do not appear to provide measurable fire protection. From 1980 to 1999, states that did not regulate furniture flammability experienced declines in fire death rates similar to that seen in California (*1*). Other causes of fire death reductions nationwide include a 50% decrease in per capita cigarette consumption since 1980, enforcement of improved building, fire, and electrical code and increased use of smoke detectors and sprinklers. Recent legislation mandating fire-safe cigarettes in 22 states, including California, should bring further reductions in deaths due to fire, without adding questionable chemicals to home furnishings.

Detection. Biophysical chemist Arlene Blum, using an x-ray fluorescence analyzer, measures 5% bromine from the fire retardant in her couch foam.

New European regulations for the Registration, Evaluation, and Authorization of Chemicals (REACH) require industry to provide data to establish the safety of new and existing chemicals. The United States should follow suit. In California, Assemblyman Mark Leno introduced AB 706, a bill that authorizes the state to consider human health and environmental impacts, as well as fire safety, when regulating flammability. This bill would prohibit the most toxic classes of chemicals in furniture, mattresses, and bed clothing (unless the manufacturer can establish their safety) and stop the cycle of replacing one toxic fire retardant with another.

Fire-retardant chemicals in our homes should not pose a greater hazard to our health and environment than the risk of the fires they are supposed to prevent. Equivalent or greater fire safety can be achieved with new technologies and materials, furniture design, and green chemistry.

ARLENE BLUM

Center for Institutions and Governance, University of California, Berkeley, CA 94720, USA.

References and Notes

1. J. R. Hall Jr., "U.S. unintentional fire death rates by state" (Fire Analysis and Research Division, National Fire Protection Association, Quincy, MA, 2006).
2. There are four types of new regulations and legislation under consideration. (i) federal regulation by the CPSC ("CPSC staff draft standard for upholstered furniture flammability, May 2005"); (ii) U.S. Senate CPSC Reform Act of 2007 (S.2045) (U.S. Senate Bill 3616); (iii) pending California state regulation 604 to require bedding and pillows to be fire retardant (*Tech. Bull. 604* (State of California, Department of Consumer Affairs, DRAFT, 2006)); and (iv) bills in four states (Illinois House Bill 1610, New Jersey Assembly Bill 2299, New York Assembly Bill 1417 and Pennsylvania Senate Bill SB 173) to adopt California TB117 for furniture flammability.
3. A. Blum, B. N. Ames, *Science* **195**, 17 (1977).
4. M. D. Gold, A. Blum, B. N. Ames, *Science* **200**, 785 (1978).
5. A. Blum *et al.*, *Science* **201**, 1020 (1978).
6. *Report on Carcinogens, Eleventh Edition* (U.S. Department of Health and Human Services, National Toxicology Program, Research Triangle Park, NC, 2005); http://ntp.niehs.nih.gov/ntp/roc/eleventh/profiles/s061firs.pdf.
7. M. Babich, "CPSC staff preliminary risk assessment of flame retardant (FR) chemicals in upholstered furniture foam" (U.S. Consumer Product Safety Commission, Bethesda, MD,

PHOTO CREDIT: CONTRA COSTA TIMES/NEWSCOM

2006), p. 5, available at www.cpsc.gov/library/foia/foia07/brief/tulum2.pdf.
8. M. Lorber, *J. Exposure Sci. Environ. Epidemiol.*, published online 11 Apr. 2007 (PMID: 17426733).
9. T. A. McDonald, *Integrated Environ. Assess. Manage.* **1**, 343 (2005).
10. EPA, *Furniture Flame Retardancy Partnership: Environmental Profiles of Chemical Flame-Retardant Alternatives for Low-Density Polyurethane Foam* (EPA 742-R-05-002A, September 2005), pp. 4-2 to 4-5.

Addressing Cumulative Selection

IN HIS UNFAVORABLE REVIEW ("GOD AS GENETIC engineer," Books *et al.*, 8 June, p. 1427) of my book, *The Edge of Evolution* (*1*), Sean Carroll writes that "Behe's chief error is minimizing the power of natural selection to act cumulatively," and implies that I fail to discuss "pyrimethamine resistance in malarial parasites ... a notable omission given Behe's extensive discussion of malarial drug resistance." The insinuation is that I included only what fit my purposes. Yet I explicitly discuss multiple mutations of pyrimethamine resistance: "Although the first mutation (at position 108 of the protein, as it happens) grants some resistance to the drug, the malaria is still vulnerable to larger doses. Adding more mutations (at positions 51, 59, and a few others) can increase the level of resistance" [(*1*), p. 79]. In the same section, I also discuss the development of insecticide resistance in mosquitoes by "tiny, incremental steps—amino acid by amino acid—leading from one biological level to another." Furthermore, in other sections, I describe a cumulative Darwinian route to antifreeze proteins and extensively address hemoglobin C-Harlem to illustrate the crucial difference between beneficial intermediate mutations and deleterious intermediate ones.

MICHAEL J. BEHE

Department of Biological Sciences, Lehigh University, Bethlehem, PA 18015, USA.

Reference

1. M. J. Behe, *The Edge of Evolution: The Search for the Limits of Darwinism* (Free Press, New York, 2007).

Response

BEHE DID INDEED DISCUSS PYRIMETHAMINE resistance on pages 75 and 76 of his book (*1*). My criticism is that Behe omitted the clear evidence for the cumulative selection of multiple changes in the drug target protein in nature and that he invoked an altogether different and unsupported explanation in an attempt to bolster his main premise. In his Letter, Behe has misrepresented the thrust of the actual text of his book.

With respect to the latter, the passage he quotes in his Letter about how "[a]dding more mutations ... can increase the level of resistance" is immediately followed in his book by the disclaimer that "[h]owever, as usual there's a hitch. Some of those extra mutations (but not the first one) seem to interfere with the normal work of the protein" (p. 75). Behe is clearly seeking to convey the message that there is some impediment to Darwinian evolution via multiple intermediates, both in this specific case and in general (hence the phrase "as usual").

However, this is not the case. Careful inspection of the data in the reference I cited (*2*) reveals that, in fact, certain mutations (e.g., Cys^{59}→Arg) increase specific parameters of the enzyme's performance. Structural studies suggest that this mutation, found at very high frequency in drug-resistant parasites in nature, improves enzyme binding to substrates in the context of otherwise adverse mutations (*3*). Furthermore, pyrimethamine-resistant dihydrofolate reductase enzymes actually have activities equal to or better than the wild-type enzyme (*4*). Behe also neglects to note the fact that such triple and quadruple mutant enzymes have been found in isolates from India, Southeast Asia, Eastern Africa, and South America, including areas where pyrimethamine use has been limited. The latter suggests that mutant parasites may be as fit as wild-type parasites.

Instead of enlightening his readers with an explanation of how sequential mutation and cumulative selection has operated in this example, Behe changes the direction of the discussion back to the main (and erroneous) argument of his book—the necessity for two or more simultaneous mutations for changes in function. He speculates that "two further, simultaneous mutations seem to be necessary" for the evolution of pyrimethamine resistance, despite the fact that the authors I cited (*2*) explicitly demonstrated two different pathways to triple and quadruple mutants via stepwise processes. Behe does not cite this work and he obfuscates the clear but inconvenient message in this body of data.

If, as Behe now seems to imply in his Letter, he is a greater proponent of cumulative selection than I gave him credit for, why would he, with so many available examples, characterize it as "rare"? It is because cumulative selection is fully capable of producing what he claims Darwinian evolution cannot do. The minimization of cumulative selection and the complete disregard of a massive literature surrounding protein interactions are crucial to Behe's entirely unfounded conclusion that "complex interactive machinery ... can't be put together gradually" (p. 81) and must therefore be designed.

SEAN B. CARROLL

Laboratory of Molecular Biology, Howard Hughes Medical Institute, University of Wisconsin, Madison, WI 53706, USA.

References

1. M. J. Behe, *The Edge of Evolution: The Search for the Limits of Darwinism* (Free Press, New York, 2007).
2. W. Sirawaraporn *et al.*, *Proc. Natl. Acad. Sci. U.S.A.* **94**, 1124 (1997).
3. J. Yuvaniyama *et al.*, *Nat. Struct. Biol.* **10**, 357 (2003).
4. C. J. Sandefur, J. M. Wooden, I. K. Quaye, W. Sirawaraporn, C. H. Sibley, *Mol. Biochem. Parasitol.* **154**, 1 (2007).

TECHNICAL COMMENT ABSTRACTS

COMMENT ON "Emergence of Novel Color Vision in Mice Engineered to Express a Human Cone Photopigment"

Walter Makous

Jacobs *et al.* (Reports, 23 March 2007, p. 1723) reported that plasticity in the mammalian visual system permitted the emergence of "a new dimension of sensory experience" in mice genetically engineered to express a human long-wavelength–sensitive cone photopigment. However, neither neural plasticity nor a new dimension of sensory experience is required to explain their results.

Full text at www.sciencemag.org/cgi/content/full/318/5848/196b

RESPONSE TO COMMENT ON "Emergence of Novel Color Vision in Mice Engineered to Express a Human Cone Photopigment"

Gerald H. Jacobs and Jeremy Nathans

Makous suggests that the novel color vision documented in knock-in mice neither requires visual system plasticity nor implies the emergence of a new dimension of sensory experience. We explain why we disagree.

Full text at www.sciencemag.org/cgi/content/full/318/5848/196c

EVOLUTION

... and a Partridge in Allopatry

Loren H. Rieseberg

Trevor Price is a brave man. In writing a book on speciation in birds, Price faces inevitable comparisons with larger-than-life evolutionary biologist Ernst Mayr, who was "first and foremost an ornithologist" (*1*). Mayr's studies of bird species formed the basis for many of his ideas about speciation and provided the foundation for his influential monographs on animal speciation (*2*, *3*). *Speciation in Birds* also has the misfortune of appearing shortly after comprehensive and critically acclaimed treatments of speciation (*4*) and speciation theory (*5*). These are hard acts to follow.

So how does *Speciation in Birds* compare with these earlier volumes? In my view, it fares well. Price (an evolutionary biologist at the University of Chicago) has an advantage relative to Mayr in that most bird species and their geographic ranges have now been described. Also, for many bird species, an enormous quantity of information now exists about their behaviors, phylogeography, phylogenetic relationships, age, cross-compatibility, and past instances of hybridization. This has allowed Price to conduct a wide array of meta-analyses, which lead to quantitative and statistically supported conclusions about speciation that were not possible in Mayr's day. This exhaustive compilation of relevant data and the subsequent analyses give Price's book value beyond any conclusions about speciation that are made.

Speciation in Birds is largely complementary to Jerry Coyne and Allen Orr's *Speciation* (*4*) and Sergey Gavrilets's *Fitness Landscapes and the Origin of Species* (*5*). Birds have been favorite subjects of ecological, behavioral, and biogeographic study for more than a century, and *Speciation in Birds* makes its most valuable contribution in these areas. Birds are less amenable to genetic study, an area in which *Speciation* excels. Likewise, despite Price's cogent explanations of speciation theory, more comprehensive discussion and evaluation of mathematical models of speciation can be found in *Speciation* and in *Fitness Landscapes*. Lastly, if one cares about speciation in more diverse organismal groups, such as beetles or flowering plants, one must understandably turn to other sources.

Price's conclusions about species and speciation are mostly in line with those of Mayr, Gavrilets, and Coyne and Orr. Like these authors, Price adheres to Mayr's biological species concept and its focus on the evolution of reproductive barriers. However, Price is more willing than Mayr to recognize its operational difficulties when classifying allopatric taxa. Price uses a combination of phylogenetic and biogeographic data to assess and validate Mayr's claim that geographic separation (allopatry) contributes to nearly all speciation events in birds. Whether this conclusion can be applied to other less vagile organisms remains unclear.

In contrast to his support for the biological species concept and allopatric speciation theory, Price finds little evidence for Mayr's founder effect speciation model, in which colonization of an empty habitat by a few individuals increases the probability of speciation. On the basis of comparative ecological data, he concludes that selection pressures imposed by variation in the biotic environment on small islands are responsible for phenotypic differences that Mayr attributed to drift. In this conclusion, Price is supported by theoretical and experimental studies, which indicate that genetic drift is less efficient than selection in the generation of population differences (*4*, *5*). However, these data do not rule out a pluralistic explanation for the evolution of reproductive isolation involving both selection and drift across high fitness ridges (*5*, *6*).

Of perhaps greater interest are Price's conclusions about the roles of ecology and social selection in speciation; these remain relatively unexplored subjects about which birds have much to offer (*6*). Closely related species of birds often differ in ecologically important traits—such as body size, habitat preferences, and feeding and migratory behaviors—that are also likely to contribute to both premating and postmating reproductive isolation. These observations, combined with classic studies of ecologically driven speciation in Darwin's finches (*7*) and crossbills (*8*), imply that ecological selection likely contributes to most speciation events in birds. However, Price cautions that divergence of most co-occurring bird species is too ancient to make inferences about the causes of speciation and that studies of recently diverged species, such as Darwin's finches, highlight the fragility of ecological reproductive barriers. He concludes that "it is unclear if ecological causes are sufficient or even important in many speciation events." This somewhat negative assessment of the role of ecology in speciation is tempered by speculation in later chapters that rapid ecological speciation may account for short branch lengths detected early in the evolution of many bird genera.

Price is more confident about the importance of social selection in speciation, concluding that "divergence in socially selected traits is an essential component of most (perhaps all) speciation events." The main support for this conclusion is that socially selected traits such as differences in song and plumage are used in species recognition by both birds and their taxonomists. Interestingly, social selection appears to be more generally important in speciation in birds than sexual selection, despite the emphasis in the literature on the latter. Price also argues that ecological factors are a major cause of divergence in socially selected traits, an assertion that, while strongly supported, seemingly is at odds with his earlier pessimistic assessment of the importance of ecology in speciation.

Students of speciation are fortunate to have three important books on the topic appear in the past three years, particularly given that during the previous century, books of this quality on speciation appeared once every one or two decades. *Speciation in Birds* also demonstrates the influential contributions, indeed special role, that studies of birds continue to make to our understanding of speciation.

The reviewer is at the Department of Biology, University of British Columbia, 3529-6270 University Boulevard, Vancouver, BC V6T 1Z4, Canada. E-mail: rieseber@interchange.ubc.ca

References

1. E. Mayr, *Systematics and the Origin of Species* (Columbia Univ. Press, New York, 1942).
2. E. Mayr, in *The Evolutionary Synthesis*, E. Mayr, J. Diamond, Eds. (Harvard Univ. Press, Cambridge, MA, 1980).
3. E. Mayr, *Animal Species and Evolution* (Harvard Univ. Press, Cambridge, MA, 1963).
4. J. A. Coyne, H. A. Orr, *Speciation* (Sinauer, Sunderland, MA, 2004); reviewed by B. K. Blackmon, L. H. Rieseberg, *Science* **305**, 612 (2004).
5. S. Gavrilets, *Fitness Landscapes and the Origin of Species* (Princeton Univ. Press, Princeton, NJ, 2004).
6. D. Futuyma, *PLoS Biol.* **3** (2), e62 (2005).
7. D. Schluter, T. D. Price, P. R. Grant, *Science* **227**, 1056 (1985).
8. C. W. Benkman, *Evolution* **57**, 1176 (2003).

10.1126/science.1147892

SYMPOSIUM PSYCHOLOGY

Matters of the Heart

A. J. Wells

Cardiology tells us that the heart is a pump, a complex but unfeeling piece of machinery that sustains and regulates the circulation of the blood. Cultural traditions from around the world, by contrast, suggest that the heart is the seat of the emotions. Language, both mundane and poetic, has many terms that link the heart and the emotions, not least the English adjective "heartfelt." A heartfelt emotion is sincere, impassioned, and deeply rooted in the psyche of one who experiences it. The word heartfelt has positive emotional connotations, while heartless has negative ones.

Is there any truth in the long-standing association of emotions with the heart, or is it merely the stuff of superstition and myth? "Heartfelt Emotions," a symposium that brought to a close a program of events supporting *The Heart* exhibition at the Wellcome Collection's recently refurbished building in London, explored this question. The symposium included contributions from the exhibition's curators, heart scientists, poets, writers, historians, psychologists, and a keenly interested audience. (Some participants also contributed to the volume edited by James Peto, which accompanied the exhibition.) It was a fascinating meeting that included readings of poems and discussion of a wide range of emotion-related topics. The current scientific consensus does not endorse the view that the heart is the seat of the emotions. However, we learned, this does not imply that the heart has no role in emotional experience. Accumulating evidence is building a complex and intriguing picture of the emotions as elements of a sophisticated and highly reactive behavioral control system involving the heart, among other organs, and both central and autonomic nervous systems. Broadly speaking, the autonomic nervous system provides, in Walter Cannon's wonderful phrase, "the wisdom of the body," the central nervous system exercises a degree of conscious control over behavior, and the heart powers the musculoskeletal system for fight and flight responses.

Our Lady of the Seven Sorrows (polychromed wood, 18th century, Italy)

CREDIT: © ROYAL MUSEUMS OF ART AND HISTORY, BRUSSELS

The reviewer is at the Institute of Social Psychology, London School of Economics, Houghton Street, London WC2A 2AE, UK. E-mail: A.J.Wells@lse.ac.uk

Heartfelt Emotions
A Symposium
Presented by the Wellcome Collection, London, 7–8 September 2007. www.wellcomecollection.org/...

The Heart
James Peto, Ed.
Yale University Press, New Haven, CT, and Wellcome Collection, London, 2007.
272 pp. $35, £19.95.
ISBN 9780300126198

The conscious mind and the heart are interdependent parts of this complex emotion system. Evidence presented at the symposium suggests that people who are more aware of their bodily responses (including their heartbeat) may experience emotions more strongly than others. Also discussed was evidence for the "broken heart" syndrome: Involvement in traffic accidents increases after bereavement, and the age-related probability of dying increases for a period after the death of a spouse.

Neuroscientific, clinical, behavioral, social, epidemiological, historical, and literary expertise were all in evidence at the symposium. Each of these sources feeds information into the contemporary study of emotions. The confluence of such diverse streams prompts questions, also suggested by the organization of the symposium, about the nature of emotions and the best ways to study them. It was heartening to see practitioners of so many different disciplines coming together in the same auditorium, but the symposium was multidisciplinary rather than interdisciplinary because the arts and the sciences remained sundered. The poets and the cardiologists, for example, never shared the platform. Although a cross-disciplinary panel involving all the disciplines represented in the symposium might have mixed even the highly skilled organizer and the session chairs, it would have been a worthwhile exercise.

It is clear from the symposium that the emotion system is highly complex, but the continuing separation of the disciplines studying it suggests that we have yet to achieve an overarching framework within which it could be understood as a unified whole. The eminent mathematician and computer pioneer John von Neumann, in a prescient 1948 paper (*1*), distinguished "special phases" from "general syndromes" of behavior. The distinction is, essentially, one between parts and wholes. Von Neumann's view was that the individual parts of complex systems would be amenable to standard, scientific methods of investigation but that the functioning of highly complex wholes was likely to require new insights and methods.

Evolutionary biology has made enormous progress in recent decades, and evolutionary theory has begun to make its presence felt in other life and social sciences, including psychology. It may well be that evolutionary theory will also provide the core concepts for the study of the emotion system. Darwinian thinking was in evidence during this most enjoyable symposium but more in the background than as a unifying framework.

The Wellcome Collection is part of the Wellcome Trust, one of whose founding principles is the idea that science is part of culture. When the broader culture of a society nurtures science, the innovative thinking on which scientific progress depends is fostered. "Heartfelt Emotions" was a fine example of the principle in practice. Following the model of *The Heart* and "Heartfelt Emotions," the Wellcome Collection plans future exhibitions with related symposia. The chances seem excellent that those events will set the pulses racing as this one did.

Reference

1. J. von Neumann, in *Cerebral Mechanisms in Behavior: The Hixon Symposium*, L. A. Jeffress, Ed. (Wiley, New York, 1951), pp. 1–31.

10.1126/science.1150005

SUSTAINABILITY

USGS Goals for the Coming Decade

M. D. Myers,†* M. A. Ayers,* J. S. Baron,* P. R. Beauchemin,* K. T. Gallagher,* M. B. Goldhaber,* † D. R. Hutchinson,* J. W. LaBaugh,* R. G. Sayre,* S. E. Schwarzbach,*† E. S. Schweig,* J. Thormodsgard,* C. van Riper III,* W. Wilde*

The U.S. Geological Survey (USGS) proposes six strategic directions for managing ecosystems along with modernization of observation networks of land, water, and biological resources.

The United States and the world today face formidable challenges that have major implications for priorities in the conduct and direction of natural science, particularly government-sponsored science. With these challenges in mind, the U.S. Geological Survey (USGS) proposes six integrated multiscale strategic directions that will help the United States address complex environmental problems (*1*).

What sets this plan apart from previous efforts is a vision of integration across and among each of the science directions. For each, we will take a systems approach to evaluate broad causes and consequences of the use and management of natural resources and earth processes. This vision will be fostered by the integration of the talents of the USGS workforce of biologists, hydrologists, geologists, and geographers. The six directions described below are mutually reinforcing and ecosystem-based. They build upon, rather than supplant, existing areas of expertise within the USGS.

Understanding ecosystems and predicting ecosystem change. USGS will develop and convey a fundamental understanding of ecosystem distributions and their components and dynamics. In addition to forming a scientific basis for managing ecosystems, the information, understanding, methods, and approaches will serve as a critical underpinning for all other USGS science directions. To make these measurements, we will expand and modernize observing networks by colocating biological, biophysical, and biogeochemical measurements. USGS will systematically characterize the distribution, interactions, condition, and conservation requirements of organisms in terrestrial, freshwater, and coastal marine environments. We plan to provide a variety of services including maps, regular updates on the status and trends of species and resources, and plausible forecasts of potential shifts in environmental conditions. Data holdings indexed by subject, place, and time will be made available through Internet portals.

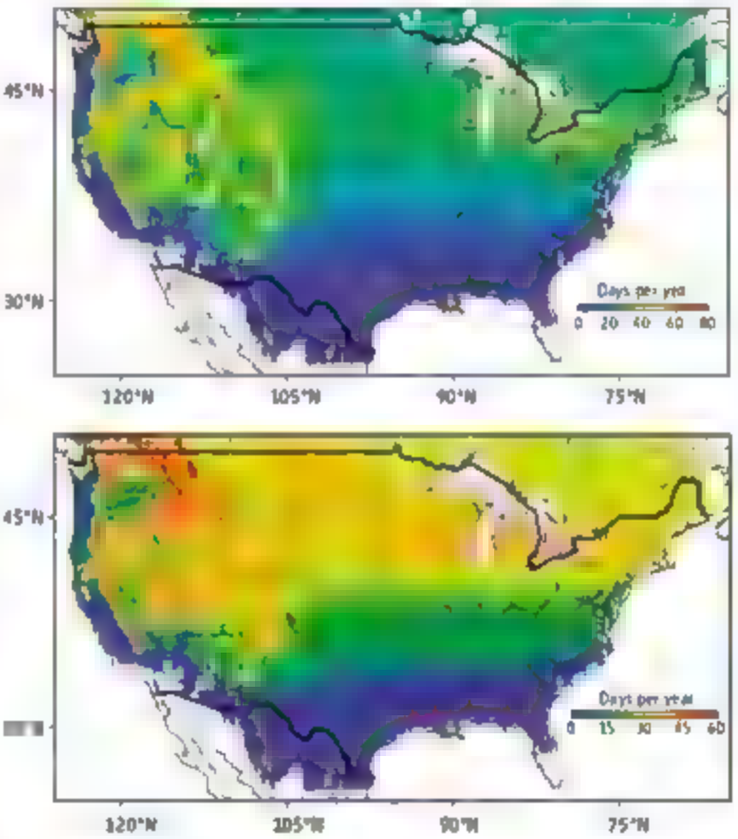

By documenting the number of days historically close to freezing, USGS has begun mapping vulnerability to warming. (**Top**) Number of days per year with mean temperatures between 0°C and −3°C (1950–1999) (*3*). (**Bottom**) Number of new days above freezing projected to occur at different degrees of warming, with probability-weighted distribution as determined from an ensemble using 18 projections in various climate models (*4*). Knowledge about how climate change affects seasonal snowpacks is used to forecast future changes in timing and amount of river flow and other ecological responses by vegetation and wildlife that rely on snow for moisture and habitat.

Climate variability and change. The USGS will build on its strengths in paleoclimatology and past interactions of climate with landscapes and ecosystems and apply the knowledge gained to understanding potential future states and processes. Expanded and modernized USGS observing networks of land, water, and biological resources will be crucial to rigorous analyses of future responses of biological organisms, hydrological conditions, and ecosystem conditions to climate change. The USGS will increase its capability to provide output from predictive and empirical models for managers to test adaptive strategies, to reduce risk, and to increase the potential for hydrological and ecological systems to be self-sustaining, resilient, or adaptable to climate change and related disturbances. Coupled modeling and long-term monitoring in the western United States already show strong responses of ecosystems, streamflow dynamics, and sea level to climate change and variability; results that have been put to use for setting climate-change policy in California. Although some findings have been applied in the past, the expanded effort will extend capabilities across the United States in response to the need of management agencies.

Energy and minerals for America's future. USGS will move beyond documenting the origin and occurrence of today's dominant mineral and hydrocarbon resources to a global-scale interdisciplinary research approach. We will expand the portfolio of commodities addressed and will assess the flow of materials through our economy, as well as their impacts on the environment. The result will be an enhanced understanding and evaluation of how the complex "life cycle" of occurrence, genesis, extraction, use, and waste influence, are influenced by landscape, hydrology, climate, ecosystems, and human health. USGS will integrate assessments of energy resources such as geothermal, gas hydrates, and oil shale with the consequences of developing and using fossil and alternative fuels, including

Director, U.S. Geological Survey, USGS National Center, Reston, VA, 20192, USA; *Science Strategy Team Authors in alphabetical order

†Author for correspondence. E-mail: mgold@usgs.gov

CREDIT: (FIGURES AND ANALYSIS) M. D. DETTINGER, USGS

changes in atmospheric carbon dioxide levels, land-use change, and climate change. USGS will expand existing research efforts on the carbon cycle and carbon sequestration in geological and biological reservoirs.

A national hazards risk and resilience assessment program. The risk to society and environment of the combined effects of such natural hazards as coastal erosion, earthquakes, floods, geomagnetic storms, landslides, tsunamis, volcanoes, wildfires, and zoonotic diseases will be assessed and communicated. USGS will also address the influence of climate variability and change on the frequency and intensity of natural-hazard events. Accurate forecasts and predictions of hazard losses depend on a thorough understanding of the processes controlling hazard occurrence, distribution, timing, and severity, as well as the effects of the hazard on the landscape, built environment, and human safety. USGS will expand its present strength in hazard process research to advance improvements in forecasting probabilities of hazards, as well as to improve understanding of societal vulnerabilities to hazards. Reduction of losses from natural hazards requires the best information about hazards themselves, as well as an understanding of risk and the cost effectiveness of mitigation and response strategies. It also requires commitment and involvement with communities. USGS will increase efforts to communicate how communities are at risk from natural hazards, about what makes communities more resilient to extreme events, and about ongoing changes in the environment that relate to natural hazard vulnerability.

The role of environment and wildlife in human health. USGS scientists have a long-standing multidisciplinary focus on environmental aspects of human health. USGS scientists are among the world's experts on wild-animal disease transmission to humans, drinking water contaminants, air-dust-soil-sediment-rock contaminants, pathogens in recreational water, and the use of wild animals as sentinels for human health. USGS is the primary governmental agency responsible for wildlife research and has, for example, been heavily involved in tracking bird deaths from West Nile virus. It has worked in close collaboration with the U.S. Department of Agriculture to monitor and assess the potential for Avian Influenza introduction to the United States by migratory birds. USGS scientists also conducted the first national reconnaissance of emerging contaminants such as pharmaceuticals, hormones, and other organic wastewater contaminants in our streams. What has been lacking is a systematic organization and communication of these data in a human health context. USGS proposes to develop an online data atlas of potential environmental health threats and to develop a periodic reporting of how conditions are changing at the national and regional level.

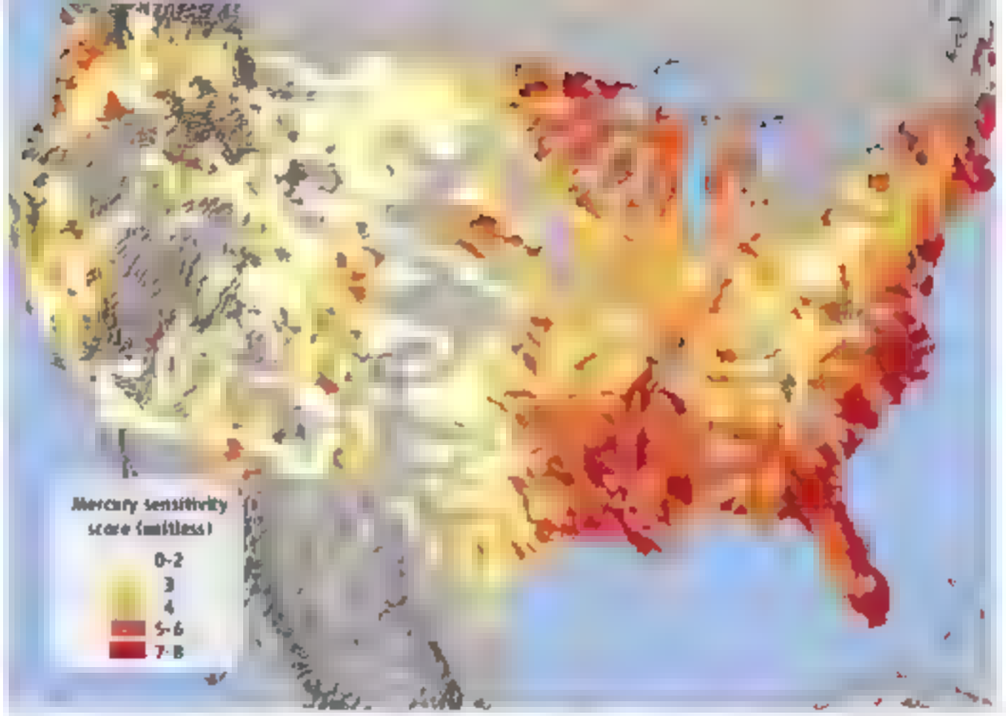

A nationwide mercury-sensitivity map is being developed at USGS for aquatic ecosystems in the contiguous 48 states. On this map, greater scores represent more sensitive ecosystems. The primary route of methylmercury exposure for both people and fish-eating wildlife is mercury in fish. This map is derived from more than 55,000 water-quality sites and 2500 watersheds. [USGS mercury information (5)]

A water census for the United States. The USGS will develop a National Water Census for the first time in 25 years to meet the need for a comprehensive, scientific accounting of the status and trends in freshwater quantity and quality for human and ecological needs of the nation.

The USGS water census will focus on the 21 water-resource regions of the United States, including their watersheds and associated aquifers (*2*), as well as offshore extents. Each region has local and regional aspects of water supply and demand that must be considered in determining where the water is located, how much fresh water is present, the quality of that water, the amount of water used, and if that supply of fresh water is stable, increasing, or decreasing. New research will better define the characteristics of watersheds and aquifers that constrain how much water can be stored, transmitted, and used for societal or environmental purposes. New directions will include estimates of water use and water availability, as well as quantification of the dynamic freshwater resource needs of aquatic ecosystems and their biota. The water census will inform the public and decision-makers about forecasts of likely outcomes for water availability, water quality, and aquatic ecosystem health caused by changes in land use and land cover, natural and engineered infrastructure, water use, and climate change.

Conclusions. Initial steps toward implementing the six strategic directions can be made with existing funding, but the realization of the full benefits to the nation will require an infusion of new resources. The benefits to the nation will be substantial. Sustainability not only requires that scientists document the condition and trends of Earth's resources, but also implies that scientists effectively inform nonscientists on the drivers of change so that society may effectively manage natural resources and can avoid crossing thresholds leading to disasters. The USGS chooses the above science directions because they are critically important and will require the best of the organization to fulfill, and because we believe these are the science directions that can and must provide information for resolving some of the most critical natural resource challenges facing the nation and the world.

References

1. USGS, "Facing tomorrow's challenges: U.S. Geological Survey science in the decade 2007–2017" (Circular 1309, USGS, Reston, VA, version 1.0, April 2007); available at http://pubs.usgs.gov/circ/2007/1309/
2. USGS, "A U.S. Geological Survey data standard: codes for the identification of hydrologic units in the United States and the Caribbean outlying areas" (Circular 878-A, USGS, Reston, VA, 1982); available at http://pubs.usgs.gov/circ/circ878-A/pdf/circ_878-a.pdf
3. R. C. Bales *et al.*, *Water Resour. Res.* **42**, W08432 (2006).
4. M. D. Dettinger, *Clim. Change* **76**, 149 (2006).
5. USGS Mercury Study Team, http://infotrek.er.usgs.gov/mercury.

10.1126/science.1147228

CREDIT: D. KRABBENHOFT/USGS

EVOLUTION

Stable Heterozygosity?

Evolutionary change in organisms that reproduce asexually may be driven in part by the divergent function of genes that were formerly alleles.

Matthew Meselson and David Mark Welch

Bdelloid rotifers (see the figure), comprising some 380 described species, are common aquatic invertebrates with highly unusual properties, most famously their putatively ancient asexuality and ability to survive desiccation at any life stage. If truly asexual, their evolutionary success may hold the answer to why nearly all higher eukaryotes reproduce sexually and why asexual eukaryotes, arising occasionally from sexual ones, are almost always evolutionarily short-lived. On page 268 of this issue, Pouchkina-Stantcheva *et al.* (*1*) present evidence of functional divergence between two copies of a gene expressed in bdelloids during desiccation. Such genes encode proteins involved in desiccation resistance in plants, invertebrates, and microorganisms. The authors argue that such divergence could provide bdelloid rotifers with greater phenotypic variation and a potential advantage from asexual reproduction.

The most sturdy evidence for bdelloid asexuality is that despite much observation and study in the field and in laboratory culture since bdelloids were described by van Leeuwenhoek more than 300 years ago, males, hermaphrodites, vestigial male structures, and meiosis (the reductional cell division process that gives rise to gametes in sexually reproducing organisms) have never been documented. Instead, bdelloid eggs are produced from primary oocytes by mitosis (the cell division process by which most cells divide).

Another sort of evidence for asexuality has been sought in the form of high divergence between gene copies that were alleles—that is, alternative forms of a gene that occupy the same position on a chromosome—before sex was abandoned (*2*). In sexual species, meiosis separates alleles, and not all alleles in the parental gene pool are transmitted to the next generation, thus limiting the divergence that can accumulate within a species. But if sex, and therefore meiotic segregation of alleles, is abandoned (so the argument goes), former alleles should diverge, with only occasional homogenization by molecular recombination processes such as gene conversion or mitotic crossing-over. Under such conditions, in which former alleles are allowed to evolve more or less independently for sufficiently long intervals, alleles at some loci might be imagined to diverge in function. This is how Pouchkina-Stantcheva *et al.* interpret their findings.

In a screen for genes involved in desiccation resistance, Pouchkina-Stantcheva *et al.* identified two copies of a late embryogenesis abundant (*lea*) gene from a complementary DNA (cDNA) library of the bdelloid rotifer *Adineta ricciae*. Although differing at only 12 of 376 aligned amino acid positions, the two proteins encoded by the genes are found, when tested in vitro, to have putative desiccation-protective activities that are distinct. Analyses of bdelloid nuclei with a *lea* probe indicate that the two *lea* genes are likely located on two different chromosomes. The authors interpret this to mean that the two *lea* genes descended from former alleles that had not segregated for a very long time—long enough to accumulate 13.5% divergence at those sites that do not change the amino acid sequence of the LEA protein. By contrast, a broad survey of invertebrate species found an average of only 2.7% divergence between alleles at sites that do not change the amino acid sequence (*3*). Arguably, the ~5-kb region of homology that the authors identify as containing the *lea* copies could represent a duplication of the *lea* gene rather than allelic segments. Nevertheless, their results are consistent with indications of divergent function between gene copies on characterized allelic segments of the bdelloid *Philodina roseola* (*4*, *5*).

Assuming that the two *lea* genes are located in allelic segments of different chromosomes, as Pouchkina-Stantcheva *et al.* conclude, could they represent an extremely polymorphic locus in a sexual population? Or, if bdelloids really are ancient asexual organisms, are the *lea* genes descendants of former alleles that have escaped homogenization? It would be evidence for the latter if the divergent *lea* copies were found on separate chromosomes in bdelloid species other than *A. ricciae*. Although it could be argued that selection against homozygotes (identical alleles at a particular locus) could have maintained heterozygosity even in a sexual population, it is striking that, other than the textbook case of excess heterozygosity at the human β-hemoglobin locus (in populations in malarial regions), compelling evidence for other

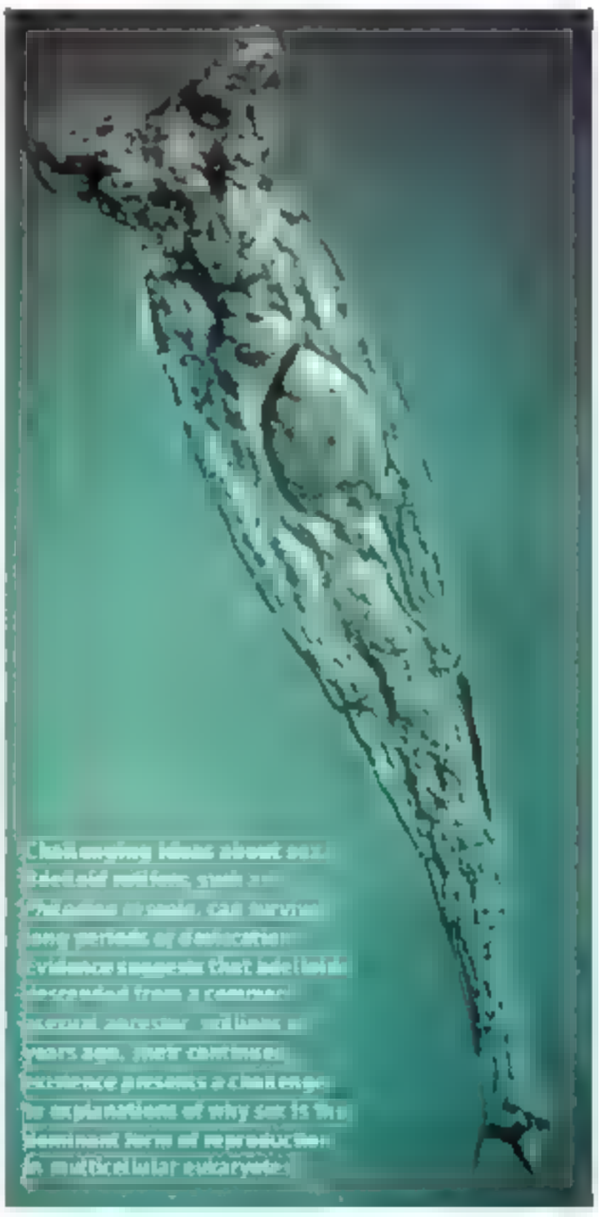

CREDIT: D. MARK WELCH

M. Meselson is in the Department of Molecular and Cellular Biology, Harvard University, Cambridge, MA 02138, and Josephine Bay Paul Center for Comparative Molecular Biology and Evolution, Marine Biology Laboratory, Woods Hole, MA 02543, USA. D. Mark Welch is at the Josephine Bay Paul Center for Comparative Molecular Biology and Evolution, Marine Biological Laboratory, Woods Hole, MA 02543, USA. E-mail: msm@mcb.harvard.edu

examples is almost entirely lacking (*6*).

If bdelloids are asexual, such divergence might be quite stable if the lethality of homozygosis from occasional homogenizing events is offset by the benefit of having two gene copies with divergent function. In that case, heterozygosity might persist even across species and higher taxonomic groups. In addition to firming up the evidence that the two *lea* genes are indeed on allelic segments of separate chromosomes, it could therefore be most informative to study their population genetics. The persistence of both gene copies on separate chromosomes would constitute independent evidence for bdelloid asexuality and, as Pouchkina-Stantcheva *et al.* suggest, such stable heterozygosity may have contributed to the fitness of bdelloid rotifers.

References

1. N. N. Pouchkina-Stantcheva *et al.*, *Science* **318**, 268 (2007).
2. D. B. Mark Welch, M. Meselson, *Science* **288**, 1211 (2000).
3. M. Lynch, *Mol. Biol. Evol.* **23**, 450 (2006).
4. D. B. Mark Welch *et al.*, www.sil2007.org.
5. D. B. Mark Welch, www.moo.knaw.nl/networks/partners.
6. N. Gemmell, J. Slate, *PLoS ONE* **1**, e125 (2006).

10.1126/science.1150197

MATERIALS SCIENCE

Biomimetic Solutions to Sticky Problems

In a smart adhesive inspired by biological adhesive structures, subsurface structures dramatically increase adhesive strength.

W. Jon P. Barnes

Many biological surfaces have remarkable properties, some of which have inspired materials science. For example, Velcro was developed from the interlocking mechanism of the seeds of burdock that readily attach to one's clothes as one walks through the countryside. Similarly, self-cleaning materials have been developed based on the "Lotus effect" (the way in which water drops roll off the superhydrophobic leaves of lotus plants, taking dirt particles away with them).

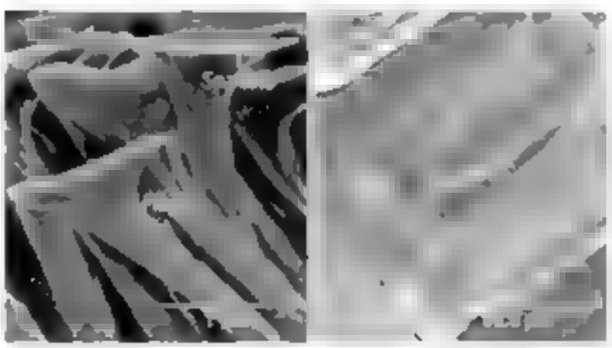

Of lizards and robots. The spatula-tipped adhesive setae in an anoline lizard (*Anolis*) (**left**) inspired the structured adhesive used by Daltorio *et al.* (*7*) in the development of climbing robots (**right**).

The adhesive mechanisms of climbing animals have also guided materials scientists. An excellent example is provided by Majumder *et al.* (*1*) on page 258 of this issue. Inspired by the complex subsurface structure of the smooth adhesive pads of tree frogs and insects such as grasshoppers and ants, they show that adhesive force can be increased by up to a factor of 30 by subsurface structures such as air- or fluid-filled pockets.

Climbing animals have many abilities that are the envy of materials scientists. First, they have remarkable powers of adhesion. Even a large gecko can run across a ceiling; a tree frog jumping from branch to branch does not fall so long as a single toe pad makes good contact with the tree; ants can carry more than 100 times their own weight while walking upside-down. Second, the adhesive mechanisms are reversible (geckos can walk at more than 10 steps a second), and detachment is effortless. Third, animal adhesive pads can have self-cleaning properties and thus do not get fouled. Finally, the adhesive pads of geckos only stick when required.

How different these abilities are from the properties of parcel tape! Following contact and mild pressure, parcel tape will adhere quite well, but it does not detach easily and is seldom reusable, because its tacky nature means that it is quickly fouled by adhering material. It also has an uncanny knack of sticking to anything it comes into contact with, making the wrapping of presents a lot less pleasurable than it ought to be.

So how do climbing animals stick? In addition to claws, present in many species but not tree frogs, two rather different adhesive structures have evolved: hairy and smooth adhesive pads. The toe pads of geckos and other lizards are covered with millions of tiny branching hairs, which can get so close to the substrate that intermolecular forces provide excellent adhesion (*2*). In contrast, the smooth adhesive pads of tree frogs, arboreal salamanders, and insects such as ants secrete a fluid so that they adhere by wet adhesion (*3*, *4*). In tree frogs at least, the main force appears to be capillarity, but viscosity and direct molecular contact may also play a role because of the thinness (0 to 35 nm) of the intervening fluid layer (*5*). (The hairy pads of insects also carry tiny amounts of fluid; adhesion is thus also likely to be mainly by capillarity.)

Such mechanisms have inspired materials scientists in a number of ways (*6*). For example, both Daltorio *et al.* (*7*) and Santos and colleagues (*8*) have used microstructured polymer adhesive feet based on the hairy pads of geckos (see the first figure) in the development of robots that can successfully climb a vertical glass sheet. Another particularly successful biomimetic structure—reusable tape that adheres equally well in wet and dry conditions—combines the microstructure of gecko pads with a thin layer of synthetic polymer that mimics the protein glue of mussels (*9*). Also, car tires are in production with a honeycomb tread pattern that closely resembles the surface structure of tree frog toe pads (see the second figure).

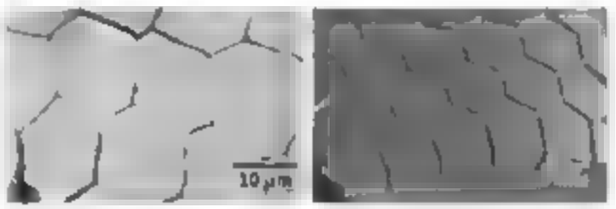

From toe pads to tires. Hexagonal toe pad epithelial cells surrounded by mucus-filled channels in the tree frog, *Litoria* (**left**). A similar hexagonal tread pattern is used in a Continental winter tire (**right**).

The author is at the Centre for Cell Engineering, Institute of Biomedical and Life Sciences, University of Glasgow, Glasgow G12 8QQ, UK. E-mail: j.barnes@bio.gla.ac.uk

Majumder *et al.* started from the discovery that micropatterned structures resembling the toe pads of tree frogs and crickets can enhance adhesion (see the third figure). Normal adhesive tape detaches when cracks spread into the adhesive from the point of peeling. When all the energy is concentrated at a single crack, peeling occurs readily, but micropatterning can increase the force required to produce peeling by up to a factor of three. Cracks form wherever there is a groove in the pattern, when the energy is spread between many cracks—as is the case in a micropatterned tape—more force is required to produce separation (*10*, *11*).

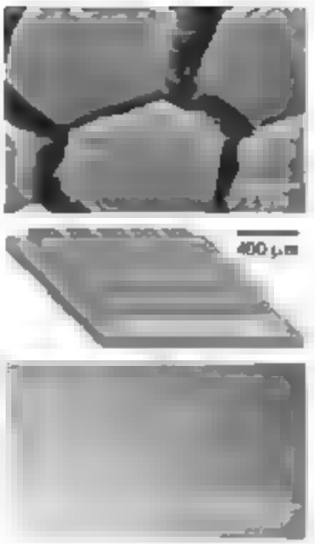

The power of ridges. The adhesive surface of the smooth adhesive pad of the cricket *Tettigonia* contains a hexagonal pattern of grooves (**top**) (*12*). On an elastic film incised with a related pattern (**middle**), cracks spread differently during peeling (**bottom**) than they would on an unpatterned surface (*10*).

The authors take this principle a step further. They have investigated the role of subsurface structures such as air- and oil-filled microchannels. The channels have similar crack-arresting properties as some of the patterned surfaces studied in (*10*, *11*), but the effect is much more dramatic. Depending on several factors such as the thickness of the adhesive layer, the channel diameter, the interchannel spacing, and whether the channel is filled with air or oil, adhesion can be increased by up to a factor of 30. Under different conditions, the adhesive can act as a quick-release coating so that the tape, while sticking well, can be peeled off easily. The adhesive remains elastic and can thus be used again with no reduction in adhesive efficiency.

Future smart adhesives like that reported by Majumder *et al.*, designed to do particular tasks, are also likely to be inspired by the remarkable mechanisms developed by climbing animals over millions of years of evolution. In this area of materials science, biomimetics is certainly coming of age.

References

1. A. Majumder, A. Ghatak, A. Sharma, *Science* **318**, 258 (2007).
2. K. Autumn *et al.*, *Proc. Natl. Acad. Sci. U.S.A.* **99**, 12252 (2002).
3. W. J. P. Barnes, C. Oines, J. M. Smith, *J. Comp. Physiol. A* **192**, 1179 (2006).
4. W. Federle *et al.*, *Integr. Comp. Physiol.* **42**, 1100 (2002).
5. W. Federle *et al.*, *J. R. Soc. Interface* **3**, 689 (2006).
6. C. Creton, S. Gorb, Eds., *MRS Bull.* **32**(6) (2007).
7. K. A. Daltorio *et al.*, *MRS Bull.* **32**, 504 (2007).
8. D. Santos *et al.*, *Proceedings of the IEEE International Conference on Robotics and Automation*, Rome, Italy, 10 to 14 April 2007, pp. 1262–1267.
9. H. Lee, B. P. Lee, P. B. Messersmith, *Nature* **448**, 338 (2007).
10. A. Ghatak *et al.*, *Proc. R. Soc. Lond. A* **460**, 2725 (2004).
11. J. Y. Chung, M. K. Chaudhury, *J. R. Soc. Interface* **2**, 55 (2005).
12. S. N. Gorb, M. Scherge, *Proc. R. Soc. Lond. B* **267**, 1239 (2000).

10.1126/science.1149994

ATMOSPHERE

Monsoon Mysteries

Today's climate models cannot adequately predict the mean intensity and the seasonal variations of the Asian summer monsoon

Jagadish Shukla

The Asian summer monsoon, manifested in all its glory and fury over the Indian subcontinent, is the largest seasonal abnormality of the global climate system. During the monsoon, the equatorial region is colder than the regions to the north. The summer monsoon rains that result are critical for food production, water supply, and the economic well-being of the Asian society. There is thus great interest in predicting the waxing and waning of the Asian monsoon.

What are the prospects for predicting monsoon rainfall over India and the surrounding regions? Why has the accuracy (or "skill") of monsoon forecasts been so low? What are the projected impacts of global warming on the Asian summer monsoon? In July of this year, a conference at the Indian Institute of Sciences, in Bangalore, addressed some of these questions (*1*).

A review of the current status of short-range (1 to 10 days) forecasting presented at the conference shows that the weather prediction centers in the world have made steady progress in improving the skill of 5-day forecasts. But India somehow missed the revolution in numerical weather prediction. According to A. K. Bohra and S. C. Kar (*1*), there has been no improvement in the accuracy of the 5-day forecasts over India for many years.

Monsoon forecasting has a long history in India. After the subcontinent had experienced a devastating drought and famine in 1877, the British Government asked the recently established India Meteorological Department (IMD) to forecast monsoon rainfall. The earliest methods of forecasting the summer monsoon were based on the snowfall in the preceding winter in the Himalayan region (*2*). In the early 20th century, Sir Gilbert Walker—an applied mathematician at the University of Cambridge who became director-general of observatories in India in 1904—identified empirical relationships between the monsoon rainfall and global circulation features in data from other British colonies around the world. He devised a forecasting methodology using a linear regression model with past data (*3*).

Normand showed over 50 years ago that the forecasts made by Walker had no skill (*4*). (A forecast has no skill if it is no better than forecasting each year's rainfall to be the same as the long-term average rainfall.) Yet, the IMD continues to forecast monsoon rainfall over India using the same basic methodology as Walker did. Verification of forecasts for seasonal mean rainfall over India for the recent 1990 to 2006 period also shows that there is no skill (*5*). The problem is that the IMD uses too many nonindependent predictors, giving artificial skill in explaining the past data and poor skill in actual forecasts (*6*).

What determines the predictability of monsoon rainfall? More than 25 years ago, Charney and I proposed (*7*) that seasonal mean monsoon rainfall is influenced by the slowly varying boundary conditions of sea surface temperature (SST), soil wetness, and snow cover. Many global climate models have since been used to test the validity of this hypothesis, but none have been successful in making skillful predictions of Indian monsoon rainfall. It remains an open question

The author is at George Mason University and the Institute of Global Environment and Society, Calverton, MD 20705, USA. E-mail: shukla@cola.iges.org

whether the problem is with the hypothesis or the models. At present, the biggest stumbling block in predicting monsoon rainfall appears to be the deficiency of models. In particular, the models fail to capture the detailed spatial structure of monsoon rainfall (see the figure).

The lack of success in predicting Indian monsoon rainfall with climate models can be attributed to two major causes. First, the models have large errors in simulating the seasonal mean rainfall. The year-to-year standard deviation of Indian monsoon rainfall is less than 10% of the mean rainfall, yet the errors in simulating the mean rainfall are larger than these observed year-to-year changes. It is therefore not surprising that models cannot predict the departures from the mean that are relevant for societal applications and policy. Second, the climate models cannot simulate monsoon rainfall variations within seasons, and therefore perform very poorly in predicting fluctuations in the mean rainfall.

There is considerable debate in the research community whether mean monsoon rainfall is indeed determined by the slowly varying SSTs. If so—and if we had better models that capture crucial couplings between ocean, atmosphere, and land processes (*8*)—then we could make skillful predictions of monsoon rainfall. However, if the intraseasonal variations are fundamentally unpredictable, then seasonal mean rainfall is also not predictable (*9*).

At the Bangalore conference, presentations by S. Gadgil and S. Nigam (*1*) reaffirmed that there are statistically significant relationships between SST changes over the Pacific and the Indian Ocean and monsoon rainfall averaged over India, and that the combined effects of the SST anomalies over both of the ocean basins are most important for predictions of summer monsoon rainfall over India.

The prediction of the seasonal mean rainfall averaged over all of India, although of great value to the national policy-makers, is of limited value to the farmers and water managers in any of the individual states. It is therefore important to develop methods of predicting fluctuations of rainfall within the season over different regions of India. Several papers at the conference showed real progress in understanding the structure and the mechanisms of intraseasonal variations. Although the current climate models remain quite deficient in simulating the structure and life cycle of intraseasonal variations, the prospects of empirical prediction of intraseasonal variations look promising, because intraseasonal variations have a well-defined structure and tend to propagate from south to north.

Nearly half of the world's population is affected by the Asian monsoon. How reliable are the projections of changes in monsoon in a changing climate? What if the Asian monsoon rainfall, which has not changed by more than 10% in hundreds of years, decreases abruptly and substantially because of increased rainfall over warmer oceans due to global warming? These questions affect the future of global societies, and yet there are no adequate climate models to investigate them. None of the climate models assessed by the Intergovernmental Panel on Climate Change can simulate the observed monsoon rainfall and its interannual and decadal variability. If it is not possible to simulate the mean monsoon rainfall and its variability nor to make skillful seasonal predictions with existing climate models, one cannot expect the projections of regional climate changes to be reliable. What adaptation and mitigation strategies should monsoon countries adopt in the face of such large uncertainties?

Climate models can now describe and predict extratropical cyclones, but not the tropical cloud systems. To simulate the monsoon and its variability at intraseasonal, interannual, and decadal time scales, the next generation of climate models must be able to resolve the cloud systems with embedded deep convection, and to simulate mean rainfall and its variability in space and time. The stakes are high, involving food production and water availability for billions of people. Every effort should be made to produce reliable projections of monsoons and regional predictions of rainfall.

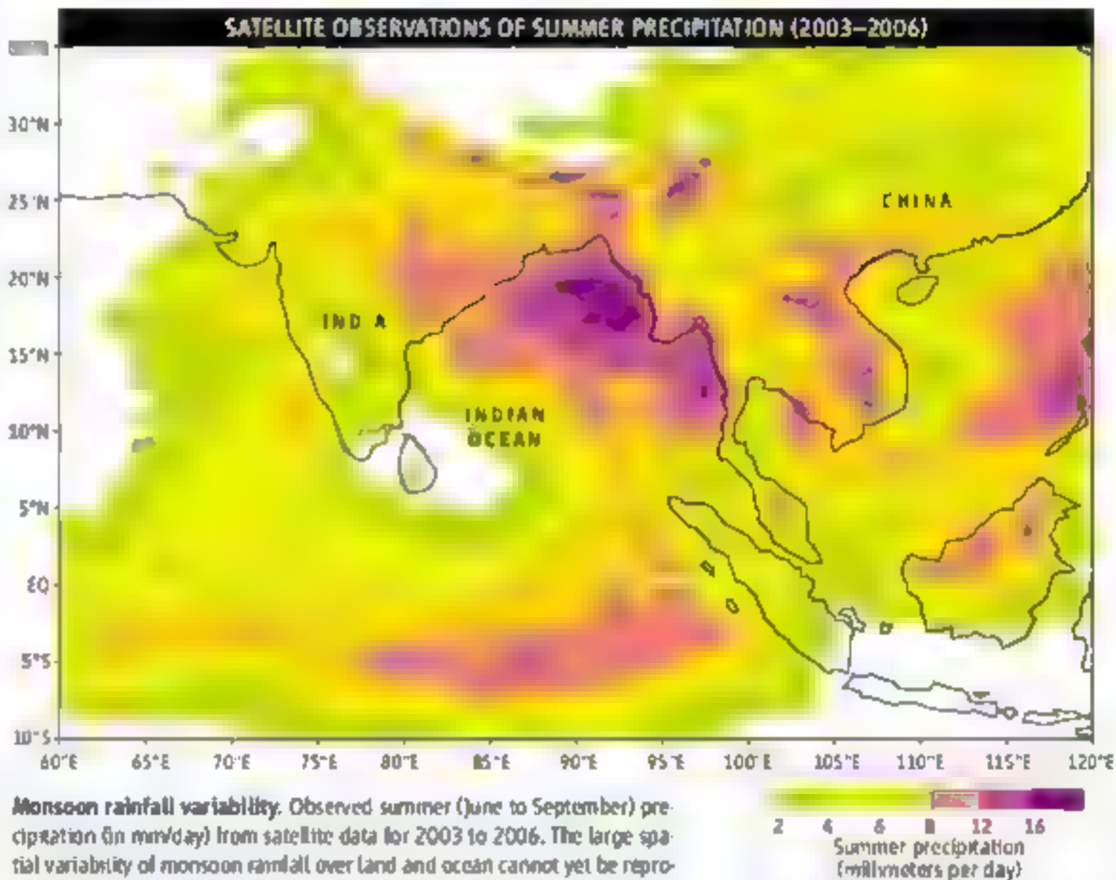

Monsoon rainfall variability. Observed summer (June to September) precipitation (in mm/day) from satellite data for 2003 to 2006. The large spatial variability of monsoon rainfall over land and ocean cannot yet be reproduced by models, and forecasts lack accuracy. Figure generated with the NOAA CPC Morphing Technique, see www.cpc.ncep.noaa.gov/products/janowiak/cmorph_description.html.

CREDIT: MIKE FENNESSY/COLA

References

1. The conference *Celebrating the Monsoon* was held in Bangalore, India, from 24 to 28 July 2007; see http://caos.iisc.ernet.in/monsoon2007/program.html.
2. H. F. Blanford, *Proc. R. Soc. London* **37**, 3 (1884).
3. G. T. Walker, *Mem. Indian Meteorol. Dept.* **24**, 333 (1924).
4. C. Normand, *Q. J. R. Meteorol. Soc.* **79**, 463 (1953).
5. S. Gadgil, M. Rajeevan, R. Nanjundiah, *Curr. Sci.* **88**, 1389 (2005).
6. T. DelSole, J. Shukla, *J. Climate* **15**, 3645 (2002).
7. J. G. Charney, J. Shukla, in *Monsoon Dynamics*, J. Lighthill, R. P. Pearce, Eds. (Cambridge Univ. Press, Cambridge, 1981), pp. 99–110.
8. B. Wang *et al.*, *Geophys. Res. Lett.* **32**, L15711 (2005).
9. P. J. Webster *et al.*, *J. Geophys. Res.* **103**, 14451 (1998).

10.1126/science.1150045

PLANT SCIENCE

Standing on the Shoulders of GIGANTEA

Plants translate the sensation of light into the regulation of protein interactions that directly control their internal molecular clock mechanism and the time of flowering.

Vicente Rubio and Xing Wang Deng

Recognizing seasonal change allows many plant species to select the most favorable time of the year to flower, thereby increasing the chances of their reproductive success. To recognize these transitions, a plant measures variations in day length and compares them with its circadian clock, an internal molecular oscillator that controls daily biological rhythms, such as leaf movements and the opening of stomata, pores in the plant's leaves (*1*). However, the molecular mechanisms underlying this coordination are still largely missing. Now, Sawa *et al.* on page 261 of this issue (*2*) and a recent study by Kim *et al.* (*3*) bring us a big step closer toward characterizing such mechanisms by identifying two light-sensing molecular switches that directly control flowering and clock oscillation.

Molecular genetic studies performed in the plant *Arabidopsis thaliana* have shown that photoperiodic flowering and regulation of the circadian clock share common elements, including light receptors and proteins comprising the circadian timekeeper (*1*). The light receptors include the phytochromes and cryptochromes, which control both clock resetting and flowering in response to different wavelengths of light (*4*). Members of the ZTL-FKF1-LKP2 protein family [consisting of ZEITLUPE (ZTL), FLAVIN-BINDING, KELCH REPEAT, F-BOX 1 (FKF1), and LOV KELCH PROTEIN 2 (LKP2)] are also proposed to act as receptors that mediate light input to the clock (*5*–*7*).

The ZTL-FKF1-LKP2 proteins contain a light, oxygen, or voltage (LOV) domain, which likely functions as a blue light–sensing motif, and an F-box domain (*8*). F-box containing proteins are usually part of complexes that attach ubiquitin molecules to protein targets to promote their destruction in a structure called the proteasome. The presence of LOV and F-box domains suggests roles for this protein family in transducing light into intracellular signals through the degradation of key proteins. Indeed, FKF1 and ZTL regulate flowering time and circadian rhythms by controlling the protein stability of CYCLING OF DOF FACTOR 1 (CDF1), a transcriptional repressor of flowering, and the oscillator component TIMING OF CAB 1 (TOC1), respectively (*9*, *10*). Accordingly, mutations in the *FKF1* and *ZTL* genes delay flowering under favorable conditions (long days) and alter expression of genes controlled by the circadian clock. Similar effects are caused by lack of GIGANTEA (GI), a protein that controls clock oscillations and photoperiodic flowering, but whose precise biochemical activity in these processes has remained unknown (*11*).

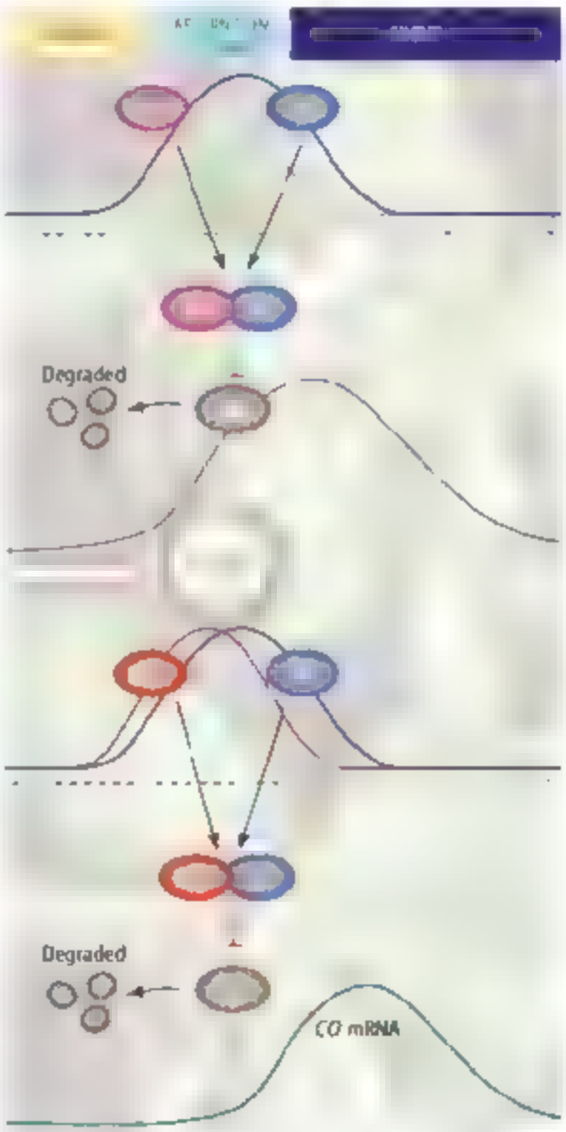

When to flower? (Upper panel) The plant circadian clock controls rhythmic expression of the GI protein, whose interaction with ZTL is stabilized by blue light. ZTL-GI interaction controls accumulation of the clock component TOC1, thus allowing robust circadian oscillations in gene expression. **(Lower panel)** Blue light also induces formation of an FKF1-GI protein complex, which in turn targets CDF1, a transcriptional repressor of flowering, for degradation. CDF1 proteolysis releases transcriptional repression of the *CO* gene, which allows CO protein expression and long day–dependent accumulation to promote flowering.

Similarities in the function and rhythmical expression of FKF1 and GI prompted Sawa *et al.* to analyze possible regulatory relationships between these two proteins by looking for their physical interactions in plants. To do so, they used *Arabidopsis* transgenic plants that expressed epitope-tagged versions of GI and FKF1. Such tagging allowed them to use epitope-specific antibodies to detect the tagged proteins in plant extracts. The authors found that both proteins precipitated together, indicating that FKF1 and GI associate in a complex in vivo. The interesting thing is that their interaction occurred differentially throughout the day, peaking in the afternoon during both long and short days, and diminishing at night. Moreover, they found that the FKF1-GI interaction was induced by blue but not red light, and that the LOV domain in FKF1 was responsible for blue light absorption, demonstrating that FKF1 functions as a blue light receptor.

In accordance with light requirement, FKF1-GI association was disrupted in the dark and was very rapidly induced upon light exposure. The latter response coincided with quick induction of the expression of *CONSTANS* (*CO*), a gene encoding a positive regulator of flowering, whose transcription is impaired by the flowering repressor CDF1. An FKF1-GI-CDF1 complex was detected on the promoter region of the *CO* gene, which suggests that the association of FKF1 and GI causes CDF1 to release its repression of *CO* expression, thus promoting flowering. These results unveil the molecular basis

PHOTO CREDIT: JEREMY BURGESS/PHOTO RESEARCHERS INC.

V. Rubio is in the Department of Plant Molecular Genetics, Centro Nacional de Biotecnología-CSIC, Madrid 28049, Spain. X. W. Deng is in the Department of Molecular, Cellular and Developmental Biology, Yale University, New Haven, CT 06520, USA. E-mail: vrubio@cnb.uam.es, xingwang.deng@yale.edu

of how photoperiodic flowering is controlled by the coincidence of light with circadian timing [the so-called external coincidence model (*1*)].

By analyzing the phenotype of plants with mutations in *FKF1* and *GI*, Sawa *et al.* determined that GI function in photoperiodic flowering does not completely depend on FKF1. Thus, GI may regulate the activity of other ZTL-FKF1-LKP2 family members or that of additional proteins controlling circadian clock functions. The demonstration of such a possibility comes from a complementary study by Kim *et al.* (*3*) describing the relationship between GI and ZTL. Kim *et al.* show that GI interacts with ZTL in plants and that ZTL-GI complex formation is, as in the case of FKF1, triggered by blue light. Interaction between GI and ZTL cooperatively stabilized both proteins, thereby increasing their accumulation. This increase consequently amplified and sharpened the rhythmic expression profile of the clock protein TOC1, thus providing the clock oscillator with the robustness necessary to maintain proper circadian rhythms.

Both Sawa *et al.* and Kim *et al.* provide mechanistic views on how day-night cycles shape circadian clock oscillations and how light is integrated into the clock to precisely regulate expression of a gene (*CO*) that controls flowering. The studies raise many questions. What factors control ZTL, FKF1, and GI stability? What role(s) do other light receptors (phytochromes and cryptochromes) play in controlling light signaling to the clock? Are there more targets for the GI-containing complexes? These insights will help us to better understand why plants see changes in seasons by standing on the shoulders of GIGANTEA.

References

1. M. J. Yanovsky, S. A. Kay, *Nat. Rev. Mol. Cell Biol.* **4**, 265 (2003)
2. M. Sawa, D. A. Nusinow, S. A. Kay, T. Imaizumi, *Science* **318**, 261 (2007); published online 13 September 2007 (10.1126/science.1146994)
3. W. Y. Kim *et al.*, *Nature*, 10.1038/nature06132 (2007)
4. D. E. Somers *et al.*, *Science* **282**, 1488 (1998)
5. D. C. Nelson *et al.*, *Cell* **101**, 331 (2000)
6. D. E. Somers *et al.*, *Cell* **101**, 319 (2000)
7. T. F. Schultz *et al.*, *Plant Cell* **13**, 2659 (2001)
8. T. Imaizumi *et al.*, *Nature* **426**, 302 (2003)
9. T. Imaizumi *et al.*, *Science* **309**, 293 (2005).
10. P. Más *et al.*, *Nature* **426**, 567 (2003)
11. D. H. Park *et al.*, *Science* **285**, 1579 (1999)

10.1126/science.1150213

MATERIALS SCIENCE

Crackling Wires

Wires bend through a series of tiny avalanches as defects move through the material.

James P Sethna

Take a paper clip, and pull one of the ends sideways. If you pull gently and release, it will elastically rebound to its original shape like a spring. If you pull harder, it deforms permanently into a new shape, a process called yielding. On page 251 of this issue, Csikor *et al.* (*1*) provide convincing theoretical evidence that, rather than a smooth process, yielding is like a phase transition that consists of a series of small avalanches. These avalanches not only provide the microscopic underpinnings we need to build theories of how ordinary-sized objects bend, but Csikor *et al.* further argue that the avalanches become crucial problems for controlling bending on micrometer and nanometer scales (see the figure).

Phase transitions are either abrupt or continuous. For example, the melting transition (solid to liquid) and the boiling transition (liquid to gas) are usually abrupt; water is water until at 0°C it turns to ice. Brittle materials respond to external stress in a similarly abrupt fashion, a piece of glass will bend elastically until abruptly it breaks in two. In contrast, magnets gradually reduce their magnetization as they are heated, with the magnetization smoothly going to zero at the critical temperature. Superconductors, superfluids, and some liquid crystals also change phases in a continuous fashion. Near continuous phase transitions there are dramatic fluctuations, the material doesn't know which phase to choose, so it wanders in space and time among its options.

In the past few decades, physicists found that the characteristic features of continuous thermodynamic (temperature-driven) phase transitions are also found at so-called depinning (force-driven) transitions—continuous transitions between a stuck ("pinned") and moving phase as an external force is increased. Depinning has been studied in many systems (*2*, *3*): charge-density waves in electric fields, fluids invading porous media (milk being poured into breakfast cereal), tearing of paper, superconductors with large currents, and domain walls in magnets. Here the fluctuations near the transition take the form of avalanche-like motions, resulting in crackling noise (*4*). A good example is provided by the response of the Earth's crust to the motion of the tectonic plates—earthquakes are avalanches driven by the forces across fault lines. If you speed up the seismic recordings of earthquakes from 1 year to occupy a single second, they sound like crackling noise (*5*). The characteristic power-law distribution of earthquakes, with many small ones and few large ones, has analogs in all of these other depinning systems.

What about paper clips? The yielding of crystals can be viewed as the depinning of tangles of dislocation lines (flaws in the crystalline lattice structure). But rather than concentrating on deformation of materials, physicists have focused on relatively obscure cases

Miniature avalanches. Csikor *et al.* predict that bending a 0.1-μm-wide aluminum wire will be an irregular, jerky process, dominated by a few large dislocation avalanches that span the width of the wire. The different images show the progression of bending. The color scale shows the local amount of deformation (blue is low, red is high). Note that the red regions are introduced one by one (individual avalanches).

CREDIT: IMAGE BY BRYAN DANIELS/CORNELL UNIVERSITY, BASED ON DATA FROM CSIKOR *ET AL.*

The author is in the Laboratory of Atomic and Solid State Physics, Cornell University, Ithaca, NY 14853, USA. E-mail: sethna@lassp.cornell.edu

like magnetic vortex motion in superconductors and sliding of charge-density waves. Why is this? Surely the deformation of metals would rank just below earthquakes in the list of important depinning problems to study.

First, deformation of crystals seemed complicated. Yielding in solids is microscopically more complicated than in these other systems; studying avalanches of dislocation lines (each with a Burgers vector indicating the direction and magnitude of the dislocation, a slip plane, and a long-range interaction with all of the others) is daunting both analytically and numerically. Second, deformation seemed different from other phase transitions. The yield stress (the force per unit area at which the material begins to deform) depends on the deformation history. Roughly speaking, it grows to equal the previous peak stress, because the yielding leads to tighter dislocation tangles, resisting further deformation (a phenomenon called work hardening). In contrast, the freezing point for water doesn't rise as the water heats. We should have understood work hardening as an example of self-organized criticality (*6*), the dislocations moved as far as they could under the previous stress, so they start moving again (the new yield stress) at the historical stress maximum. And finally, physicists were ignorant of the fluctuations. Textbooks treat the yielding of solids as a smooth process—oozing, not crackling.

Recent experiments in ice and recent simulations in two dimensions (*7*) show clear evidence for avalanches and crackling noise during yielding—completely analogous to that seen in earthquakes, magnets, and other depinning systems, and in complete contrast to textbook discussions. But why don't we hear crackling noise every time we bend a paper clip? Is yielding in three dimensions different from that in two? Are metals different in some crucial way from ice? (Indeed, ice has a different crystal structure and different allowed dislocations than most structural metals.)

Csikor *et al.* address precisely these last questions, using a large-scale numerical simulation of the dislocation motion, designed to describe yielding in aluminum. Is aluminum different from ice? No, they find an excellent power-law distribution of avalanches; aluminum crackles just like ice. Are there enormous crackles, which should be visible in any experiment? No, they find a cutoff in their avalanche size distribution, and provide a theoretical explanation for their cutoff.

Why are there no large dislocation avalanches? The key observation of Csikor *et al.* is that the avalanches are not three-dimensional objects. They find that the avalanches have a fractal dimension of roughly two (see their figure 2); indeed, their avalanches are fractal versions of the pancake-like lamellar slip models long used by materials engineers. A two-dimensional slipped region of thickness δ extending entirely across a sample of length L can only relieve the strain in a fraction δ/L of the sample. Their theoretical explanation for the cutoff (involving work hardening and the limitations of the measuring device) gives a thickness δ that varies between one and a thousand atomic spacings. The largest avalanches in a centimeter-scale experimental sample (10^8 atomic spacings) will thus have strains of 10 parts in a million—easily ignored in textbooks.

On geological length and time scales, continental drift is smooth; the fact that the motion of South America away from Africa is mediated by earthquakes may not be crucial for theories of plate tectonics, even though it is important to those living near fault lines. Similarly, dislocation avalanches cause jerky bending fluctuations that can be ignored on the scale of automobile fenders and beer cans. But as we bend metals on the micrometer and nanometer scales (such as the wires attaching to computer chips), the irregular, jerky microscopic deformation will become a serious (and interesting) problem.

References

1. F. F. Csikor, C. Motz, D. Weygand, M. Zaiser, S. Zapperi, *Science* **318**, 251 (2007).
2. M. Kardar, *Phys. Rep.* **301**, 85 (1998).
3. D. S. Fisher, *Phys. Rep.* **301**, 113 (1998).
4. J. P. Sethna, K. A. Dahmen, C. R. Myers, *Nature* **410**, 242 (2001).
5. M. C. Kuntz, J. P. Sethna, http://simscience.org/cracking/Advanced/Earthquakes/TheEarthC alkles.html.
6. P. Bak, C. Tang, K. Wiesenfeld, *Phys. Rev. Lett.* **59**, 381 (1987).
7. M.-C. Miguel, A. Vespignani, S. Zapperi, J. Weiss, J.-R. Grasso, *Nature* **410**, 667 (2001).

10.1126/science.1148507

MATERIALS SCIENCE

Printing Cells

Paul Calvert

Inkjet printing technology offers a way to create three-dimensional biological structures for studying cell interactions and artificial organs.

Materials scientists and biotechnologists are eager to build three-dimensional structures of cells held together in a tissue matrix. With such structures, researchers could study how cells interact and perhaps fabricate implantable organs. Inkjet printing—essentially the same technology used in desktop printers—is a promising method because it is simple and versatile and avoids contact with the substrate. A number of groups have recently developed inkjet printing of various cell types, so this is a good time to consider what can be done and what remains to be resolved.

There are two main types of inkjet printer. In thermal printers, a pulse of energy boils liquid at the surface of a small heater, and the expanding bubble drives a drop of ink through the nozzle. In piezoelectric printers, an applied voltage pulse causes a glass tube or a bending plate to eject the droplet from the nozzle. Inkjet printers for the low-cost consumer market can use either type of drive, whereas most high-end commercial printers are piezoelectric. A number of researchers, including my colleagues and me, have simply rebuilt consumer printers to replace the paper-feed system with a computer-driven platform to move the sample under the nozzle (*1*).

As might be expected, bacteria and yeast can be readily printed, whereas animal cells vary in their ability to survive the process. In addition to selecting the right cell type, one can use a concentrated buffer solution to shrink the cells and so reduce the possibility of damage in the nozzle. Often a more complex growth medium may be necessary to protect the cells during printing, in which case viscosity may be a limiting factor. Sterility is of course also a major concern in cell viability. Consumer cartridges probably cannot be autoclaved and must be cleaned and washed with alcohol. In addition, the printing equipment must be sterilized and used in a laminar flow hood to avoid airborne contamination.

Recently, for example, Chinese hamster ovary (CHO) cells and motor neuron cells have been printed from 3× concentrated phosphate buffer with a thermal printer (*2*). For the CHO cells, about 20% were damaged during "ink" preparation and a few percent during the printing step. In our work with

The author is in the Department of Materials and Textiles, University of Massachusetts Dartmouth, North Dartmouth, MA 02747 USA. E-mail: pcalvert@umassd.edu

human stem cells, we found that viability dropped rapidly when the buffer concentration increased from 1× to 3×. However, the cells were viable and printable in a medium that included glucose, glutamine, and pyruvate. Human fibroblasts printed with a piezoelectrically driven glass tube printhead showed 95 to 98% viability, which went even higher at lower drive voltages. Cells did tend to agglomerate and print less well as the "ink" aged over 20 min (*3*, *4*). The bottom line, though, is that damage during printing is not a major issue, and cell printing could become routine as equipment is adapted and techniques are improved (see the figure).

Cells on demand (**Left**) Three-dimensional tube structure made from bioprinted cells. This composite image shows an inner layer of human umbilical endothelial cells (green) and an outer layer of human aortic smooth muscle cells (red). (**Right**) Printed and cultured yeast patterns after 3 days of culture. The patterns were printed at 75, 150, and 300 drops per second, from top to bottom.

In many cases, cells are printed as a stream of drops into the well of a tissue culture plate. The cells will thus be in a puddle of medium and so will survive until further medium is added (*3*). In printing CHO cells, Xu *et al.* used a gel substrate with added liquid medium to keep the surface wet (*2*). If this liquid layer is too thick, the cells will float and printing resolution will be lost. At present, there is no established method to print a single line of cells with any precision, but Nakamura *et al.* have addressed this question of printing patterns of single drops, each containing one or two cells (*5*). With this method, they were able to write lines about 50 μm wide by printing cells suspended in sodium alginate onto a thin film of calcium chloride, which gels the alginate (*6*). Recent work has also shown that yeast cells modify a surrounding organic-inorganic hybrid matrix (*7*), implying that we must always consider changes in matrix structure surrounding embedded cells.

Cell printing is a tool still in development, and its final applications are not yet clear. As with the example of the polymerase chain reaction for copying and amplifying DNA, it may well be that the ultimate use of the tool can really not be foreseen at the development stage. Although there are other ways of depositing patterns of cells (*8*, *9*), inkjet printing offers a convenient noncontact method. That is, one cycle of printing need not redissolve or redisperse that material from previous cycles. Similar structures can be built by depositing cells and matrix through fine nozzles, but it can be very difficult to maintain the necessary precise height control of the nozzles above the surface (*10*). It is also possible to print patterns of materials that show preferential cell binding and then allow cells in suspension to migrate onto these patterns (*11*), but this is less versatile. The core question for cell printing is then "what can be done with inkjet printing that cannot be done already?" There are two obvious directions: (i) the fabrication of structures to explore cell-to-cell communication and (ii) building organs for implant.

For cell interaction studies, one simple experimental approach is to build simple layered structures. Inkjet-printed polymers can be used to form coherent films about 100 nm in thickness. Usually these are porous, but pore-free layers should be possible. Layers of cells and biopolymer could be printed into multilayer sandwiches to study the effect of proximity of different cell types on tissue development or on the development of disease.

Next, but more difficult, would be to accurately position cells in patterns with controlled densities. This would let us study the effect of spacing between different cell types on tissue development over distances comparable to printed line widths of 100 μm. Patterns of stem cells could also be used to explore the effects of cell distribution on matrix-mediated differentiation. Such coupled patterns of cells could be the basis for new types of cell-based chemical sensors.

The power of inkjet printing lies in the ability to print patterns, to provide submicrometer depth resolution combined with lateral resolution of tens of micrometers, and to deliver timed sequences of active substances to a developing structure. If we envisage the inkjet printhead moving over a layer of cells, we should be able to build complex three-dimensional tissues by printing the right precursors and enzymes in sequence. Given the right sources of the precursor proteins or compatible substitutes, we can build many passive structures such as bone, ligament, cartilage, and cornea.

To this is now added the ability to incorporate cells. A small cell population could undertake the rebuilding of the structural tissue after implantation. To build a functioning organ, one can envisage printing a geometrically correct matrix with a few cells that will grow to complete the structure or correctly distributed populations of cells that will then create their own matrix. To do either of these will require a more detailed understanding of the communication between cells and of the response of cells to their matrix (*12*, *13*).

CREDITS: (LEFT) M. NAKAMURA/BIOPRINTING PROJECT, KANAGAWA ACADEMY OF SCIENCE AND TECHNOLOGY; (RIGHT) SANDER LAB/UNIVERSITY OF MASSACHUSETTS DARTMOUTH

References

1. T. Boland *et al.*, *Mat. Sci. Eng. C* **27**, 372 (2007).
2. T. Xu, J. Jin, C. Gregory, J. J. Hickman, T. Boland, *Biomaterials* **26**, 93 (2005).
3. R. Saunders, J. Gough, B. Derby, in *Nanoscale Materials Science in Biology and Medicine. MRS Proceedings Volume 845*, C. T. Laurencin, E. A. Botchwey, Eds. (Materials Research Society, Warrendale, PA, 2005), pp. 57–62.
4. R. Saunders, B. Derby, J. Gough, N. Reis, in *Architecture and Application of Biomaterials and Biomolecular Materials, MRS Extended Summary Volume EXS-1*, J. Y. Wong *et al.*, Eds. (Materials Research Society, Warrendale, PA, 2004), pp. 95–97.
5. M. Nakamura *et al.*, *Tissue Eng.* **11**, 1658 (2005).
6. M. Nakamura *et al.*, in *Digital Fabrication 2006* (Society for Imaging Science and Technology, Springfield, VA, 2006), pp. 89–92.
7. H. K. Bose *et al.*, *Science* **313**, 337 (2006).
8. T. Boland *et al.*, *Adv. Mater. Processes* **165**, 51 (2007).
9. B. R. Ringeisen, C. M. Othon, J. A. Barron, D. Young, B. J. Spargo, *Biotechnol. J.* **1**, 930 (2006).
10. C. M. Smith *et al.*, *Tissue Eng.* **10**, 1566 (2004).
11. E. A. Roth *et al.*, *Biomaterials* **25**, 3707 (2004).
12. V. Mironov, G. Prestwich, G. Forgacs, *J. Mat. Chemistry* **17**, 2054 (2007).
13. C. M. Nelson, M. M. VanDuijn, J. L. Inman, D. A. Fletcher, M. J. Bissell, *Science* **314**, 298 (2006).

10.1126/science.1144212

New Worlds on the Horizon: Earth-Sized Planets Close to Other Stars

Eric Gaidos,[1,2]* Nader Haghighipour,[2,3] Eric Agol,[4] David Latham,[5] Sean Raymond,[2,6] John Rayner[3]

The search for habitable planets like Earth around other stars fulfills an ancient imperative to understand our origins and place in the cosmos. The past decade has seen the discovery of hundreds of planets, but nearly all are gas giants like Jupiter and Saturn. Recent advances in instrumentation and new missions are extending searches to planets the size of Earth but closer to their host stars. There are several possible ways such planets could form, and future observations will soon test those theories. Many of these planets we discover may be quite unlike Earth in their surface temperature and composition, but their study will nonetheless inform us about the process of planet formation and the frequency of Earth-like planets around other stars.

The ancients looked at the night sky and wondered what the lights wandering among the fixed stars were. After the Copernican revolution, humanity asked whether any of them—the planets of the solar system—are worlds like ours and support life. The search for habitable worlds now extends to the other stars, around which more than 200 planets have been discovered. Until recently, all discoveries were of planets far more massive than Earth, that is, like Jupiter or Saturn. This is because most of them were discovered by Doppler velocimetry, a technique that measures the motion of the star around the system's center of mass by detecting the alternating Doppler shift of starlight toward red or blue wavelengths (Fig. 1). The shift is proportional to a planet's mass, and thus more-massive planets are easier to detect. The orbits of a few such planets are observed edge-on, and the planets periodically pass in front of (transit) their host star (Fig. 1). The masses of planets on such orbits are known unambiguously, and their diameters and mean densities can be calculated from the small (~1%) fraction of starlight that is occulted as well as knowledge of their stars' diameters. These planets turn out to have densities similar to those of the gas giants in our solar system and are presumed to be made mostly of hydrogen and helium gas.

Such objects fascinate astronomers, but our quest to find Earth-like planets with solid surfaces and conditions suitable for life continues. One condition is the presence of liquid water, and orbits on which a planet's surface temperature permits stable liquid water describe a circumstellar "habitable zone" (*1*). The detection of a planet like Earth in the habitable zone of even the nearest Sun-like stars is an enormous challenge because its Doppler signature is only 0.3% of a Jupiter-mass planet, it can occult only 0.01% of the star, and its distant orbit means the likelihood of a transit is less than 1 in 200. But the discovery of planets not too unlike the Earth may not be far off. Doppler velocimetry with more stable instruments has recently discovered several objects much less massive than Saturn and as small as five times larger than Earth (*2*–*4*); one of these has now been observed to transit its star (*5*). Like many of the giant planets detected by this method, they are much closer to their host stars than Earth is to the Sun (1 astronomical unit or AU), and so the Doppler shift they induce is larger and more detectable. New instruments, on the ground and in space, will discover still smaller planets. These worlds will also be on close orbits, many will be much hotter than the Earth, and some may have very different compositions. All will help us understand how planets form and the propensity for that process to yield planets like Earth.

Recipes for Earths

Mercury orbits only 0.38 AU from the Sun, but Earth-mass planets could exist on even closer orbits around other stars. The theory of in situ formation begins with a disk of gas and km-sized bodies (planetesimals); the latter accrete into ~100 Moon- to Mars-sized protoplanets in about 1 million years; these in turn collide and coalesce to form planets in 10 to 100 million years (*6*). Planets are unlikely to form very close to their host stars because accretion will occur over a narrow range of orbits and will include little material. Disks that contain much more mass than the one that formed the solar system could form close-in planets, but observations of young stars showed massive disks to be relatively uncommon (*7*). Numerical simulations of planet formation in such disks produced several closely spaced planets (*8*).

Alternatively, Earth-sized planets form farther out in the disk and spiral inward toward the star as they exchange angular momentum with a residual disk of gas and planetesimals. Orbital migration is one explanation for the origin of close-in or "hot" giant planets, and Earth-sized planets have been predicted to migrate inward in the space of about a million years (*9*). Migration can be halted at the disk's inner edge (*10*) or where there is a change in the disk's ability to dissipate heat by radiation (*11*). Several planets migrating together can become trapped in "mean-motion" resonances, at which their orbital periods are integer ratios (*12*, *13*). The system will stop evolving when inward-directed torques acting on the outer planets balance the outward-directed torques on the innermost planets (*14*).

Fig. 1. A schematic view illustrating how an Earth-sized planet orbiting close to its host star can be discovered and studied. The planet orbits inside the orbit of a giant planet. Nothing is to scale, and both planets are shown at multiple positions in their orbits. The presence of the unseen planets can be inferred from the periodic Doppler shift of starlight (represented by the blue and red dashed circles) as the star moves toward and away from the observer on different parts of its orbit around the system's center of mass. The Earth-sized planet transits the star and occults a small fraction of the light, allowing the planet's diameter to be estimated. At the opposite phase, the planet will be eclipsed by the star, and its infrared flux can be measured by comparing the total flux outside of and during eclipse. The inner planet perturbs the outer giant planet on its orbit (dashed lines), causing times of transit of the latter to deviate from simple periodicity by a measurable amount.

[1]Department of Geology and Geophysics, University of Hawai'i at Mānoa, Honolulu, HI 96822, USA. [2]NASA Astrobiology Institute, Ames Research Center, Moffett Field, CA 94035–1000, USA. [3]Institute for Astronomy, University of Hawai'i at Mānoa, Honolulu, HI 96822, USA. [4]Astronomy Department, Box 351580, University of Washington, Seattle, WA 98195, USA. [5]Harvard-Smithsonian Center for Astrophysics, 60 Garden Street, MS 20, Cambridge, MA 02138, USA. [6]Center for Astrophysics and Space Astronomy, University of Colorado Boulder, CO 80309–0389, USA.

*To whom correspondence should be addressed. E-mail: gaidos@hawaii.edu

Earth-sized planets might also form from planetesimals shepherded interior to an inwardly migrating giant planet (Fig. 2). The giant planet perturbs an interior protoplanet into an elliptical orbit; circularization of that orbit by gas drag and gravitational scattering of smaller planetesimals leaves the planet on a slightly smaller orbit, and the process repeats as the giant planet moves further inward (*15*). Planets grow rapidly in the dense annulus of shepherded planetesimals interior to the giant's orbit (*16*–*19*). In numerical simulations, about half of the growing planets were scattered onto exterior orbits by a close encounter with the giant planet, depending on the mass of the giant planet and its rate of migration (Fig. 2). Planetesimals can also be shepherded interior to the locations of "secular" resonances, where orbits in the gravitational field of a primordial gas disk precess (wobble) at a resonant frequency of the planetary system. Eventual dispersal of the gas causes the inward "sweeping" of these resonances, stimulating the growth of planets (*20*). However, this mechanism ceases to be effective close to the star, where general relativistic effects dominate orbital precession.

Each of these models makes testable, although not necessarily unique, predictions. The in situ formation model predicts that close-in Earths are not isolated; if there is sufficient mass to form one, then several should form. They will be preferentially found around stars with a relatively high abundance of the heavy elements that make up such planets; it is already known that such stars are more to likely host giant planets. The migration model also predicts that multiple planets will be found in a series of near-resonant orbits, although isolated planets could exist if migration halts. The gas giant shepherding model predicts that Earth-sized planets will be found near the interior mean-motion resonances of close-in gas giants (Fig. 2). On the other hand, the disk dispersal model predicts that planets will be well removed from such resonances. For example, Zhou *et al.* (*16*) invoked a combination of gas giant shepherding and disk dispersal to explain the close-in, ~7.5 Earth-masses planet orbiting star GJ 876, which also hosts two more-distant giant planets. In their model, the two gas giants co-migrated inward to their final orbits, shepherding planetesimals near mean-motion resonances along the way. As the gas disk disappeared, secular resonances moved the material further inward, causing a planet to grow. Another example is the Gliese 581 system, which contains three close-in planets with masses between 5 and 15 times that of Earth (*4*) but as yet no discovered giants. These planets either formed in situ from a very massive disk or migrated inward to their present positions.

These simulations highlight the possibility that Earth-sized planets exist close to many stars. Nevertheless, confidence in such predictions must be tempered by the facts that none of the models includes the physics of collisions between planetesimals (which may result in disruption rather than accretion) and that current computing power can simulate the dynamics of only a meager number of planetesimals (no more than 10^5) compared with reality (10^{12}). Furthermore, close-in planets may undergo further orbital evolution because of tides raised on both the host star and planet or the gravitational influence of two or more giant planets. Ultimately, such predictions must be tested by observations.

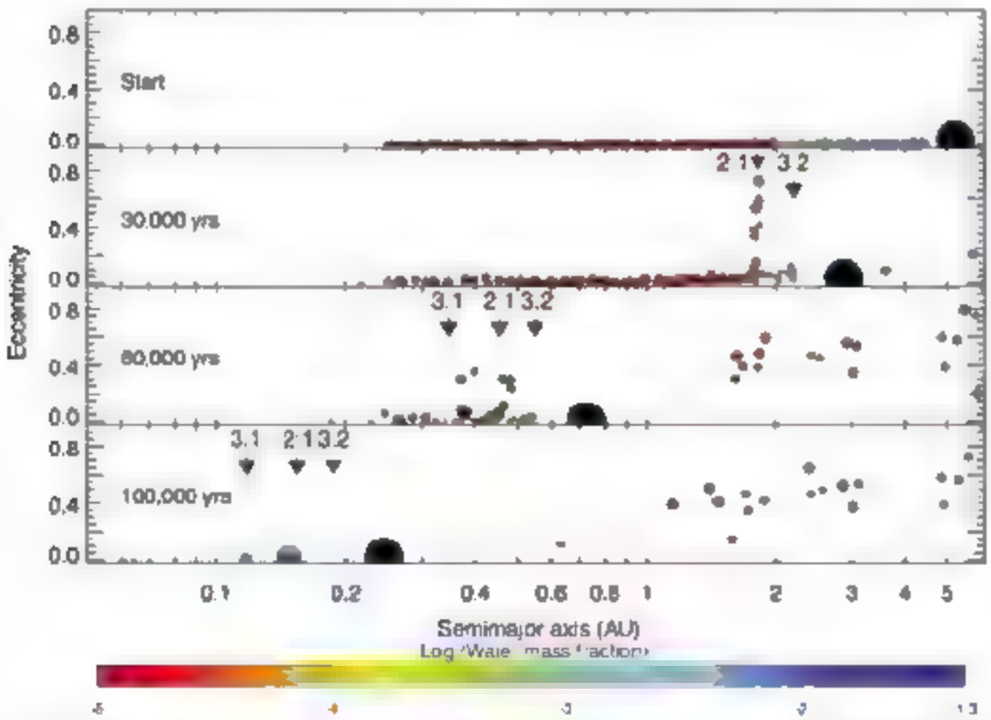

Fig. 2. Numerical simulation of the formation of close-in Earth-sized planets via inward shepherding of material by a migrating giant planet (large black circle). The four panels are snapshots in time of the orbital eccentricity (deviation from circularity) versus semimajor axis (orbit size) of each surviving body during the migration of a Jupiter-mass planet from 5.2 to 0.25 AU in 10^5 years (*18*, *19*). The size of each body is proportional to the cube root of its mass but is not to scale with the giant planet or the *x* axis. The color of each body corresponds to its water content as shown on the color bar. The dark inner region of each body shows the approximate size of the planet's iron core [for details, see Raymond *et al.* (*8*)]. The 2:1, 3:1, and 3:2 mean-motion resonances with the giant planet are labeled; the 2:1 mean-motion resonance is responsible for the bulk of the inward shepherding, and simulations often produce an Earth-sized planet near that resonance.

Doppler Detection of Earths

Confronting theoretical expectations with observations, however, will require extraordinary feats of observation. For Doppler detection, a velocity precision better than 1 m/s, less than the average walking speed of a human, can now be achieved by comparing the position of thousands of features in the spectrum of a star with a fiducial spectrum of an absorbing gas cell, lamp, or laser. Sensitivity is now limited by the noise or "jitter" produced by turbulence, spots, and acoustic oscillations in stellar atmospheres. Better sensitivity may eventually be achieved by understanding the precise characteristics of such noise or averaging over many orbits. Meanwhile, meter-per-second accuracy is not sufficient to find a "twin" to the Earth-Sun system, but it is enough to detect somewhat more massive planets on closer orbits. Earth-mass planets could be detected around the lowest-mass (M dwarf) stars, whose motion will be more affected by an unseen companion. M dwarfs are numerous, and planets have already been found around the most massive representatives of this type. However, the relative propensity of less-massive M dwarf stars to host planets (of any type) is not yet known. If the mass of the planet-forming disk scales with that of the star, fewer planets and/or smaller planets might be found.

The atmospheres of M dwarf stars do not appear to be especially "jittery" compared to those of higher mass stars (*21*). However, M dwarfs are cooler and much less luminous; their flux peaks at near-infrared (1 to 3 μm) wavelengths, and the coolest ones are very difficult targets for visible-wavelength spectrographs on current telescopes. One solution is to build a much larger telescope than the current record-holders, the 10-m Keck telescopes on Mauna Kea. An economical alternative is to carry out high-precision spectroscopy at near-infrared wavelengths. Doppler velocity precision is proportional to the number of features in a stellar spectrum and the square root of the number of detected photons. Although the former is higher at visible wavelengths, for stars less massive than about 30% of the Sun this is outweighed by the higher number of detectable photons in the near infrared. Furthermore, star spot contrast in the near infrared is reduced by a factor of two compared with the visible, and its contribution to Doppler noise may be less. One

potential problem of near-infrared spectroscopy is contamination by numerous terrestrial atmospheric absorption lines compared with the optical. The depth and central wavelength of these lines varies with the water vapor content and high-altitude wind pattern of the atmosphere. However, simulations suggest that this problem can be reduced by masking out the deepest such lines, still leaving sufficient wavelength coverage to achieve the required Doppler precision.

Several projects to develop precision near-infrared spectrographs are under way. These include the precision radial velocity spectrograph (PRVS) for one of the two Gemini 8-m telescopes, a collaboration between the Astronomy Technology Centre in the United Kingdom, the University of Hertfordshire, the University of Hawai'i, and Pennsylvania State University; a PRVS pathfinder at Penn State; and TripleSpec Externally Dispersed Interferometer for the Palomar 5-m telescope, a collaboration between Cornell University and the University of California, Berkeley. A PRVS-like instrument on Gemini could survey 300 M dwarfs over the course of 5 years for close-in Earth-sized planets, a sufficiently large sample to test theories of their origin.

Detecting Earths with Transits

In the small fraction of systems whose orbits happen to appear edge-on, planets can be detected as they transit the disk of the host star. Planets on closer orbits are statistically more likely to transit and will transit more frequently. A giant planet like Jupiter occults ~1% of the disk of a Sun-like star, an effect that can be detected by ground-based instruments. It is not known which stars have planets with favorable orbital geometries, and a large number must be monitored, but searches for giant planet transits are beginning to pay off (*22*). However, an Earth-sized planet occults only 0.01% of the starlight, and this level of precision is not possible with telescopes on the ground because of scintillation by the atmosphere ("twinkling"). Another approach is to search for transits of the smallest M dwarfs for which an Earth-sized planet would occult a detectable fraction (0.1 to 1%) of the stellar disk. However, such stars are extremely faint, and only the nearest are suitable targets. These will be widely distributed over the sky, and monitoring them with the appropriate cadence will require robotic telescopes. A prototype of one such observatory, Panoramic Survey Telescope and Rapid Response System (Pan-STARRS), has already seen "first light" from the summit of Haleakala in Hawai'i.

An alternative method for finding smaller planets exists in systems with a transiting giant planet. The existence and position of Neptune was correctly inferred from observations of the departure of Uranus from its predicted orbit. Likewise, an otherwise invisible planet can be detected by its gravitational effect on the orbit of a second planet that transits the host star. Those perturbations will cause the transit times to deviate from simple periodicity. When the two planets are in or near a mean-motion resonance, their mutual gravitational perturbations are amplified, and the deviations are larger. The variation of the times of transit is proportional to the ratio of the planets' masses, and for an Earth-mass planet affecting a transiting Jupiter-mass planet the signal can be as large as a few minutes over a period of a few months to years. The transits of giant planets can be timed to a precision of a few tens of seconds with ground-based telescopes, and Earth-mass or smaller planets are detectable (*23*, *24*). The shepherding theory of formation predicts objects near resonant orbits interior to close-in giant planets (Fig. 2), and the transit timing technique has already been used to rule out the existence of Earth-sized planets in one system (*25*). One unpleasant possibility is that those planets nearest to mean-motion resonances, and therefore the most detectable, will also have the most unstable orbits.

The most direct approach to find transiting Earth-sized planets is to observe from space. CoRoT (Convection, Rotation, and Planetary Transits), a joint mission of the Centre National d'Études Spatiales and the European Space Agency (ESA), was launched last December and should be capable of finding transiting planets as small as a few Earth masses on close orbits around any of ~120,000 stars (*26*). NASA's Kepler mission, scheduled for launch in early 2009, will push the limit to planets the size of the Earth around about 100,000 stars (*27*) (Fig. 3). Both CoRoT and Kepler will perform more-precise transit timing of giant planets and thus make more-sensitive searches of Earth-like planets on resonant orbits within these systems. Radial velocity measurements of stars with transiting planets can then give orbits, masses, and mean densities.

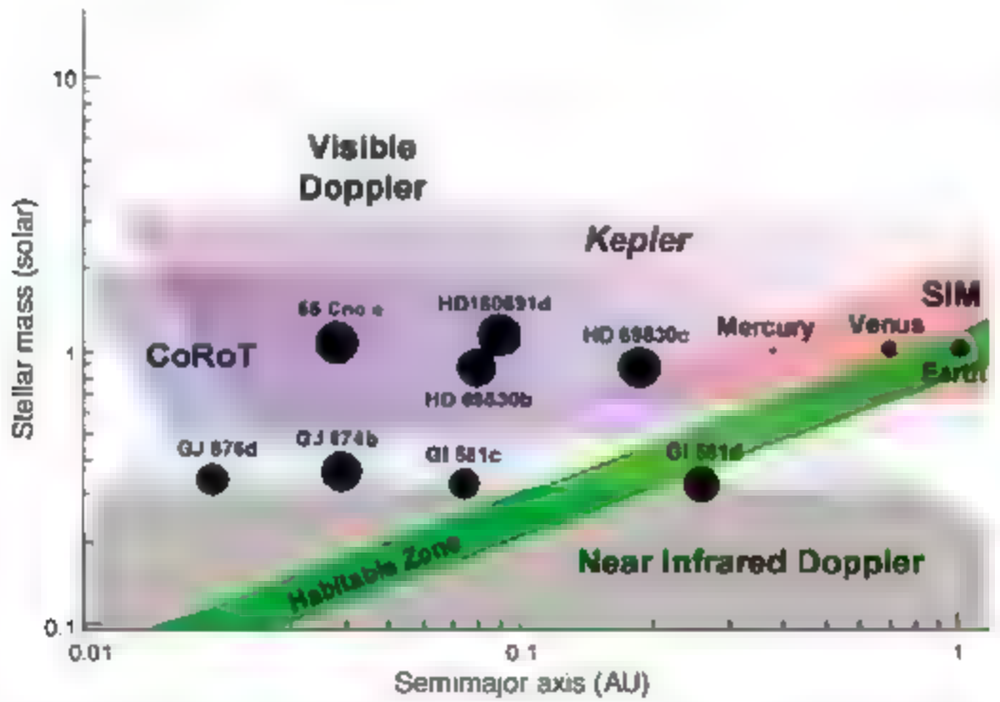

Fig. 3. Potential for different techniques, instruments, and missions to detect Earth-sized planets on close-in orbits around stars of different masses. The inner solar system and all reported extrasolar planets with minimum masses less than 15 times that of the Earth are shown as black circles. The diameter of each circle is proportional to the cube root of the (minimum) mass. The green zone is the habitable zone in which liquid water is stable on an Earth-like planet (*1*). The upper-right boundary for Doppler velocity detection corresponds to the orbits of five Earth-mass planets that produce a maximum Doppler shift of 1 m/s, and upper left-hand boundary corresponds to orbits with a 1-day period. CoRoT and Kepler can detect only those planets that transit their host star. Also, the actual boundaries are not as distinct as presented here, and the applicability of each method may in fact extend beyond the zones depicted.

Habitability

Our prospects for finding Earth-sized planets close to their host stars and even learning something about them seem promising. But will any of such planets have surface conditions that could support life as we understand it? Close-in planets around low-luminosity M dwarfs can orbit within the habitable zone (Fig. 3). However, charged particles in flares from the nearby host star or impacts at the high velocities of these orbits may remove such planets' atmospheres, rendering their surfaces inhospitable (*28*). Composition and mass are also important, and not all planets are created equal in this regard (*29*). For example, Venus was originally in the habitable zone of a fainter early Sun, but we do not know whether it ever had water. On the other hand, Mars is now just inside the habitable zone of the Sun, but it lacks a substantial greenhouse atmo-

sphere because it is too small to have prevented its atmosphere from escaping or to maintain the volcanic activity to replenish it.

Theory provides some guidance for our expectations. Planets that formed close to their host stars are less likely to have water because the primordial disks of gas and dust are thought to have hot and dry inner regions. Water is also more likely to be lost because the speed of impacts during accretion is higher (*30*), and the high orbital angular momentum of any water-rich planetesimals from further out in the system would prevent them from reaching the planet (*31*).

Conversely, planets that formed in the outer, water-rich regions of a disk and migrated inward are more likely to have abundant water (*13*, *19*). In a system with a chemical composition like that of our solar system, such planets could be composed of as much as 20 to 50% ice. These would be "ocean worlds," with ~100-km-deep oceans overlying thicker mantles of high-pressure phases of water ice (*32*, *33*). However, if the planet's surface temperature is above the critical point of water (374°C), there will be no liquid phase; this structure has been suggested for the Neptune-mass planet Gliese 436b (*5*).

Planet-forming disks around other stars may also have different chemistries, spawning a greater diversity of planets than is represented in our solar system. For example, the initial ratio of carbon to oxygen can vary between planet-forming disks and with it the amount of water that can be incorporated into planets (*34*). In the extreme case of a carbon-rich disk, water is completely absent, and silicate minerals are replaced by silicon carbides such as carborundum. Such a disk would produce "carbide worlds" covered with oceans and atmospheres of hydrocarbons and more closely resemble the satellite Titan than Earth. Other planets may have had their rocky mantles removed by high-speed collisions during their formation and, like Mercury, be composed mostly of iron.

By combining space-based transit detection with ground-based Doppler velocimetry to calculate mean densities, it should be possible to distinguish between worlds composed mostly of rock, water ice, or iron (*35*, *36*). Spectra of starlight during and outside a transit can be compared to search for absorption by gases in any planetary atmosphere (Fig. 1). The planet's emission at infrared wavelengths can also be recovered by measuring the change in flux as the planet moves behind the star (Fig. 1). Both of these techniques have been successfully used with transiting giant planets. The James Webb Space Telescope (JWST), an infrared space telescope scheduled to be launched in 2013, should be capable of detecting the emission from a "hot" Earth-sized planet close to a Sun-like star. The total emission is related to the amount of starlight absorbed by the planet, which, because the planet's diameter is known, can be related to the average reflectivity of the planet. That quantity contains information about the scattering properties of the atmosphere and the presence or absence of clouds. Much more could be discovered about planets in or interior to the habitable zone of M dwarfs. In such cases, the day-night temperature difference on the planet can be measured, indicating the presence or absence of an atmosphere to redistribute heat, and it may be possible to extract a low-resolution spectrum and search for absorption by gases such as carbon dioxide, water vapor, and methane in any such atmosphere.

NASA's proposed Space Interferometer Mission (SIM), designed to detect the minute motions of stars on the plane of the sky, might also be pressed into service to search for Earth-sized planets (*39*) (Fig. 3). In the more distant future, the ambitious Terrestrial Planet Finder (NASA) and Darwin (ESA) space observatories would spatially separate light from planets from that of their host stars, allowing direct spectroscopy of Earth-sized planets. Because of the great technical and fiscal challenges to that approach, alternatives need to be considered. Some investigators argue that the temporal techniques successfully used to isolate signal from transiting gas giants should be pursued for smaller planets, with use of ground-based campaigns to find Earth-sized planets in the habitable zone of M dwarfs and new observations, beginning with JWST, to observe them (*40*). But do Earth-sized planets exist close to low-mass stars, and are any of them Earth-like and possibly habitable? Astronomers are beginning to look, and answers may soon be on the horizon.

References and Notes

1. J. F. Kasting, D. P. Whitmire, R. T. Reynolds, *Icarus* **101**, 108 (1993).
2. E. J. Rivera *et al.*, *Astrophys. J.* **634**, 625 (2005).
3. C. Lovis *et al.*, *Nature* **441**, 305 (2006).
4. S. Udry *et al.*, *Astron. Astrophys. Lett.* **469**, L43 (2007).
5. M. Gillon *et al.*, *Astron. Astrophys. Lett.*, in press, preprint available at http://arxiv.org/abs/0705.2219v3.
6. J. J. Lissauer, *Annu. Rev. Astron. Astrophys.* **31**, 129 (1993).
7. J. A. Eisner, J. M. Carpenter, *Astrophys. J.* **641**, 1162 (2006).
8. S. N. Raymond, T. Quinn, J. I. Lunine, *Astrophys. J.* **632**, 670 (2005).
9. W. R. Ward, *Icarus* **126**, 261 (1997).
10. F. S. Masset, G. D'Angelo, W. Kley, *Astrophys. J.* **652**, 730 [illegible].
11. S. J. Paardekooper, G. Mellema, *Astron. Astrophys.* **459**, L17 (2006).
12. M. H. Lee, S. J. Peale, *Astrophys. J.* **567**, 596 (2002).
13. V. Alibert *et al.*, *Astron. Astrophys.* **455**, L25 (2006).
14. C. Terquem, J. C. B. Papaloizou, *Astrophys. J.* **654**, 1110 (2007).
15. H. Tanaka, S. Ida, *Icarus* **139**, 350 (1999).
16. J.-L. Zhou, S. J. Aarseth, D. N. C. Lin, M. Nagasawa, *Astrophys. J.* **631**, L85 (2005).
17. M. J. Fogg, R. P. Nelson, *Astron. Astrophys.* **441**, 791 (2005).
18. S. N. Raymond, A. M. Mandell, S. Sigurdsson, *Science* **313**, 1413 (2006).
19. A. M. Mandell, S. N. Raymond, S. Sigurdsson, *Astrophys. J.* **660**, 823 (2007).
20. M. Nagasawa, D. N. C. Lin, E. Thommes, *Astrophys. J.* **635**, 578 (2005).
21. J. T. Wright, *Publ. Astron. Soc. Pac.* **117**, 657 (2005).
22. F. Pont, in *Tenth Anniversary of 51 Peg-b: Status of and Prospects for Hot Jupiter Studies*, L. Arnold, F. Bouchy, C. Moutou, Eds. (Frontier Group, Observatoir de Haute Provence, France, 2006), pp. 153–164.
23. M. J. Holman, N. W. Murray, *Science* **307**, 1288 (2005).
24. E. Agol, J. H. Steffen, R. Sari, W. Clarkson, *Mon. Not. R. Astron. Soc.* **359**, 567 (2005).
25. E. Agol, J. H. Steffen, *Mon. Not. R. Astron. Soc.* **374**, 941 (2007).
26. P. Bordé, O. Rouan, A. Léger, *Astron. Astrophys.* **405**, 1137 (2003).
27. M. Gillon, F. Courbin, P. Magain, B. Borguet, *Astron. Astrophys.* **442**, 731 (2005).
28. J. Scalo *et al.*, *Astrobiology* **7**, 85 (2007).
29. E. Gaidos *et al.*, *Astrobiology* **5**, 100 (2005).
30. J. J. Lissauer, *Astrophys. J.* **660**, L149 (2007).
31. S. N. Raymond, T. Quinn, J. I. Lunine, *Icarus* **168**, 1 (2004).
32. M. J. Kuchner, *Astrophys. J.* **596**, L105 (2003).
33. A. Léger *et al.*, *Icarus* **169**, 499 (2004).
34. E. J. Gaidos, *Icarus* **145**, 637 (2000).
35. J. J. Fortney, M. S. Marley, J. W. Barnes, *Astrophys. J.* **659**, 1661 (2007).
36. F. Selsis *et al.*, *Icarus*, in press, preprint available at http://arxiv.org/abs/astro-ph/0701608.
37. D. Valencia, D. D. Sasselov, R. J. O'Connell, *Astrophys. J.*, in press; preprint available at http://arxiv.org/abs/0704.3454.
38. S. Sasaki, M. J. Kuchner, C. Hier-Majumder, B. Militzer, *Astrophys. J.*, in press, preprint available at http://arxiv.org/abs/0707.2895.
39. J. Catanzarite, M. Shao, A. Tanner, S. Unwin, J. Yu, *Publ. Astron. Soc. Pac.* **118**, 1322 (2006).
40. O. Charbonneau, D. Deming, http://arxiv.org/abs/0706.1047.

41. This manuscript is a result of discussions at a session of the 210th Meeting of the American Astronomical Society sponsored by the NASA Astrobiology Institute. E.G. acknowledges support by the NASA Terrestrial Planet Finder Foundation Science Program. N.H. is supported by the NASA Astrobiology Institute under cooperative agreement no. NNA04CC08A. S.R. is supported by the NASA Postdoctoral Program at the University of Colorado Astrobiology Center, administered by Oak Ridge Associated Universities through a contract with NASA. The contribution by J.R. is on behalf of the PRVS team.

10.1126/science.1144358

INTRODUCTION

Grand Tour

TRAVELING OUT TO THE FARTHEST REACHES OF THE SOLAR SYSTEM, TO PLUTO AND the Kuiper belt where it will arrive in 2015, the New Horizons probe has to endure a long and mostly uneventful journey. But luckily there are some spectacular sights along the way. On 28 February 2007, New Horizons flew past Jupiter, where it used the gas giant's gravity to slingshot it to even greater speeds and also test its instruments in flight. New Horizons' transit took it to unvisited areas of the planet's spacescape. The papers in this special issue record how the probe witnessed lightning and aurorae in Jupiter's atmosphere, volcanic eruptions on the moon Io, and the pulsing of Jupiter's magnetosphere, a cocoon of charged particles that swathes the entire system.

On Earth, although seen planetwide, the most powerful thunderstorms concentrate near the equator and in the tropics. Not so on Jupiter. Lightning flashed near both poles as well as elsewhere, suggesting that convective electrical storms bubble up everywhere in Jupiter's atmosphere because of global heat imbalances. Nighttime auroral glows, on the other hand, were not as widespread as expected.

Skirting the giant planet, New Horizons also flew by Jupiter's rings and attendant moons, big and small. Surprisingly, no moonlets smaller than a kilometer in size were seen in Jupiter's faint rings, a puzzle if they are built from the debris of shattered moons. Rubble also clumps together in locations favored by gravity resonances with larger moons.

An eruption of the Tvashtar volcano on the satellite Io was caught in the act, allowing the mechanics of the sulfurous plume and the lava temperature to be measured. Pollution from Io's volcanoes has even reached the shores of Europa, an icy moon that may harbor oceans beneath its frozen surface. Io's volcanic emissions feed extra sulfur and oxygen ions into a vast particle cloud that circles the entire Jupiter system, held in place by the planet's strong magnetic field. Behind the planet, it is pulled into a magnetic shadow billions of kilometers long, streaming away from the Sun as the solar wind deflects around Jupiter. Acting like a giant pipe, this magnetic tail drains half a metric ton of charged particles out of the jovian system each second. New Horizons' route took it down the magnetotail, to regions unexplored by earlier Galileo or Voyager missions (see the Perspective on p. 216). Pulses of energetic particles flow along the tail in synchrony with Jupiter's 10-hour rotation rate and also every few days as plasma blobs are fed down the tube.

With Pluto still in its sights, New Horizons' snapshots show that Jupiter inhabits an active landscape, experiencing storms, the pumping of the magnetosphere, and volcanic ash falls. A pity then that it is the last time we will visit Jupiter until the Juno mission in 2016. So sit back, enjoy these views, and think of New Horizons as it races along the solar system's back roads to an even stranger destination.

– JOANNE BAKER

CREDIT: PAM ENGEBRETSON AND JEFF MOORE (MONTAGE)

New Horizons at Jupiter

CONTENTS

Perspective

Reports

Science

PERSPECTIVE

New Surprises in the Largest Magnetosphere of Our Solar System

Norbert Krupp

En route to its ultimate rendezvous with Pluto, the New Horizons spacecraft passed through the magnetic and plasma environment of Jupiter in February 2007. Onboard instruments collected high-resolution images, spectroscopic data, and information about charged particles. The results have revealed unusual structure and variation in Jupiter's plasma and large plasmoids that travel down the magnetotail. Data on Jupiter's aurora provide details of the interaction with the solar wind, and a major volcanic eruption from the moon Io was observed during the encounter.

A planet with a magnetic field deflects the solar wind (a stream of ionized particles continuously leaving the Sun), forming a cavity that protects the planet against this harsh environment by excluding particle radiation. This outermost region where the internal magnetic field of a planet dominates is called the magnetosphere. Besides Earth and Mercury, each of the four gas giants (Jupiter, Saturn, Uranus, and Neptune) have magnetospheres. The only moon known to have its own magnetosphere is Ganymede, one of the four so called Galilean moons of Jupiter. Although the magnetosphere of a planet is compressed on the side facing the sun, it is enormously stretched on the opposite side (Fig. 1), forming a region called the magnetotail. Jupiter's magnetosphere is the largest in our solar system (with a diameter ~200 times that of Jupiter itself), and its magnetotail is at least 10,000 jovian radii R_J (1 R_J = 71,400 km).

This immense magnetospheric system has now given up some of its secrets. The previously unexplored deep magnetotail of Jupiter was traversed for the first time by the New Horizons spacecraft in February 2007 on its way toward Pluto. Before that encounter, Jupiter had been visited by seven other spacecraft, including the first jovian orbiter mission, Galileo, and six flyby missions (Pioneer 10 and 11, Voyager 1 and 2, Ulysses, and Cassini). The trajectories of each of the previous missions covered only regions of the magnetosphere near the planet, or the spacecraft departed the magnetosphere along the dawn, dusk, or noon flanks. These previous measurements, especially in the magnetotail, penetrated only about 150 R_J.

Data from all of the previous missions have shown that Jupiter's moon Io is the most important player in the configuration and dynamics of the jovian magnetosphere. Io is the most volcanically active body in our solar system, and its volcanoes produce about 1 metric ton of SO_2 per second. This huge amount of material is partly being ionized and partly being transported into the magnetosphere of Jupiter. As a result, the magnetic field lines are loaded with heavy ions (S and O) and are even further stretched, forming a so-called plasma disk around Jupiter's equatorial plane. This "pancake" is filled with charged particles and wobbles during each rotation of the planet. As the mass loading and the stretching of the field lines reach a limit, the plasma is released into the magnetotail in the form of a magnetic bubble called a plasmoid. The mass released in plasmoids is a large part of the mass of the entire system. Analysis of the data from the particles and field instruments onboard the spacecraft can be used as a tool to observe plasmoid structures in magnetospheres.

New Horizons, with its unique trajectory through the jovian magnetotail, yielded a series of surprises. McComas *et al.* (*1*) report low-energy ion measurements at distances between 200 and 2500 R_J. They point out that the observations show a tremendous amount of structure, including sharp discontinuities and variations of several days. The surprise is that, even at those distances, the plasma has imprinted the rapid rotation of the jovian system, which is "visible" in a 10-hour modulation of particle parameters. Another key result is the identification of large-scale plasmoids filled with O and S ions from the moon Io and H_3^+ and H^+ from the jovian ionosphere. The surprise here is that the plasmoids seem to reoccur every 3 to 4 days, even at those distances. This observation confirms the earlier Galileo observations at ~100 R_J and can help to address the remaining question of mass-loading rates and mass release down the tail.

The results of McNutt *et al.* (*2*) also address the plasmoid observations in terms of velocity dispersions, directional anisotropies, and ion-composition variations. It seems plausible that the observed reconnection events (collisions between magnetic field lines that are followed by a plasmoid release) seen in Galileo data at 100 R_J expanded and survived down the tail and were observed by the New Horizons instrumentation. Evidence for that scenario is the S:O ratio, which is only comparable inside the events in the Galileo data and inside the plasmoids in the New Horizons data.

The investigation of auroral emissions (Fig. 2) is also a useful tool to "see" the dynamics of the invisible magnetosphere and to understand the influence of the solar wind at Jupiter. Gladstone *et al.* (*3*) discuss the jovian aurora measurements in the ultraviolet wavelength range during the New Horizons flyby. They also found surprises in their data implying a major change in the night-glow emissions since the Voyager era, as well as an unusual local-time dependence of precipitating-electron fluxes that is consistent with a possible source region in the dusk side of the magnetosphere. Those results can be used to gain a better understanding of the influence of

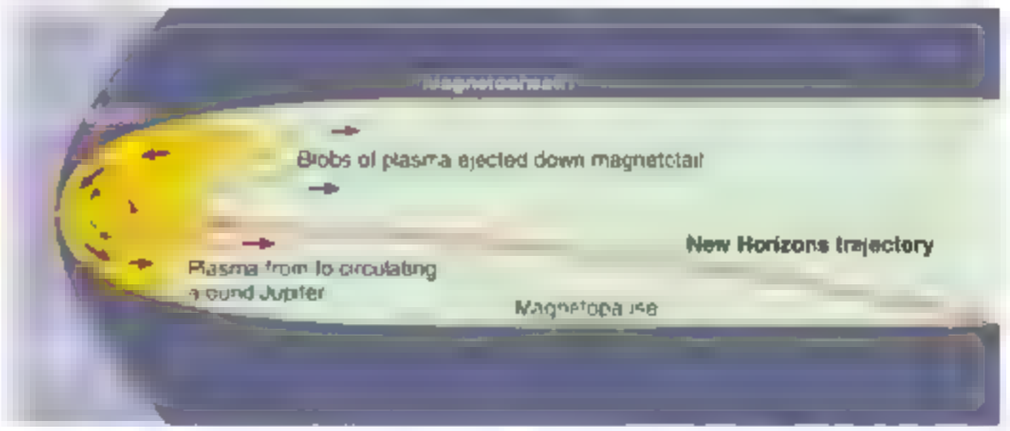

Fig. 1. Schematic diagram of Jupiter's plasma environment and the trajectory of the New Horizons spacecraft. The solar wind hits the magnetic field of Jupiter (red dot) to create a bow shock and flows around the planet in a magnetosheath and an extended magnetotail. Plasma from the moon Io (orbit shown as purple arrows) and from other sources is ejected down the magnetotail. The magnetic boundary between the planet's magnetic field and the solar wind is called the magnetopause. [Adapted by K. Sutliff from a NASA image]

Max-Planck-Institut für Sonnensystemforschung, Max-Planck-Straße 2, 37191 Katlenburg-Lindau, Germany.

*To whom correspondence should be addressed. E-mail: krupp@mps.mpg.de

Fig. 2. Hubble Space Telescope image of Jupiter's aurora taken at ultraviolet wavelengths in November 1998. The planetary magnetic field funnels charged particles onto the atmosphere, causing the molecules to glow. Besides the main auroral oval, additional glowing lines with a bright spot on one end result from the magnetic flux tubes that connect Jupiter with its moons Io, Ganymede, and Europa. (Photo credit: NASA/ESA/University of Michigan)

energetic electrons on the brightness of the various regions of jovian aurora. They may also provide evidence for dynamic changes in the auroral emissions with the solar cycle. In addition, the extended and structured auroral emissions associated with the interaction between Jupiter and its satellite Io seen in the New Horizons data will help to shed light on the magnetosphere-moon coupling system.

New Horizons has also observed a major volcano eruption during the flyby. Spencer *et al.* (*4*) report details of a very large volcanic plume (320 to 360 km in height) above the surface where the material condenses in the plume rather than being ejected from the source. By analyzing this material and modeling the eruption, another question could be tackled: How variable is the mass provided by Io and how does this affect the mass loading of the magnetosphere with all its implications? The New Horizons measurements will provide crucial data for resolving that puzzle.

The investigation and knowledge of the jovian system is important for understanding the origin and formation of our planetary system. As the largest and most massive planet, Jupiter played a critical role in that process. The data from New Horizons will also help to focus future missions to the jovian system, several of which are being discussed among the international science community for the next decade. Additionally, if we understand "our" Jupiter better, we will be able to further understand the extrasolar "hot Jupiters" of other stars. Those massive gas giants with 10s of Jupiter masses most probably have strong internal magnetic fields with huge and powerful magnetospheres. Our understanding of the jovian magnetosphere will also help us to comprehend our own terrestrial magnetosphere, this shield protects us and all terrestrial life against the harsh interplanetary environment.

References

1. D. J. McComas *et al.*, *Science* **318**, 217 (2007).
2. R. L. McNutt Jr. *et al.*, *Science* **318**, 220 (2007).
3. G. R. Gladstone *et al.*, *Science* **318**, 229 (2007).
4. J. R. Spencer *et al.*, *Science* **318**, 240 (2007).

10.1126/science.1150448

REPORT

Diverse Plasma Populations and Structures in Jupiter's Magnetotail

D. J. McComas,[1,2]* F. Allegrini,[1,2] F. Bagenal,[3] F. Crary,[1] R. W. Ebert,[1,2] H. Elliott,[1] A. Stern,[4] P. Valek[1,2]

Jupiter's magnetotail is the largest cohesive structure in the solar system and marks the loss of vast numbers of heavy ions from the Jupiter system. The New Horizons spacecraft traversed the magnetotail to distances exceeding 2500 jovian radii (R_J) and revealed a remarkable diversity of plasma populations and structures throughout its length. Ions evolve from a hot plasma disk distribution at ~100 R_J to slower, persistent flows down the tail that become increasingly variable in flux and mean energy. The plasma is highly structured—exhibiting sharp breaks, smooth variations, and apparent plasmoids—and contains ions from both Io and Jupiter's ionosphere with intense bursts of H^+ and H_3^+. Quasi-periodic changes were seen in flux at ~450 and ~1500 R_J with a 10-hour period. Other variations in flow speed at ~600 to 1000 R_J with a 3- to 4-day period may be attributable to plasmoids moving down the tail.

The jovian magnetotail is created by the interaction of the supersonic solar wind with Jupiter's magnetic field and plasmas. This structure stretches at least 500 million km antisunward from Jupiter, as evidenced by several transient encounters 5000 to 9000 R_J behind the planet when Voyager 2 was approaching Saturn (*1*).

[1]Southwest Research Institute, 6220 Culebra Road, San Antonio, TX 78238, USA. [2]Department of Physics and Astronomy, University of Texas, San Antonio, TX 78249, USA. [3]Laboratory for Atmospheric and Space Physics, University of Colorado, Campus Box 392, Boulder, CO 80309, USA. [4]Science Mission Directorate, NASA Headquarters, Washington, DC 20546, USA.

*To whom correspondence should be addressed. E-mail: dmccomas@swri.edu

Jupiter's moon Io spews out volcanic gases, roughly 1000 kg s^{-1} of which (mostly S and O) become ionized and are trapped in the planet's strong magnetic field, forming the Io torus (*2*). Roughly half of the torus ions are lost via charge exchange; the other half are transported radially outward and ultimately escape down the tail (*3*). In addition, Jupiter's ionosphere provides a roughly comparable number of light ions, primarily H^+ and H_3^+, to the magnetosphere (*4*–*6*). This mixture of ions, along with Jupiter's fast rotation rate (~10 hours), creates a dense rotating plasma disk that dominates the inner magnetosphere (*7*). A key issue for the jovian magnetosphere is how more than 500 kg s^{-1} of heavy ions from Io and a comparable number of light ionospheric ions are lost from the system down the magnetotail (*7*).

Jupiter's magnetosphere and near tail were previously explored by seven spacecraft, including extensive observations from Galileo, which was in orbit there from 1995 to 2003 (*8*, *9*). However, other than the brief Voyager 2 intervals at very great distances, no previous spacecraft had made observations more than ~200 R_J from Jupiter. Then, on 28 February 2007 the New Horizons (NH) spacecraft flew past Jupiter en route to its primary mission at Pluto, following nearly an ideal trajectory for magnetotail observations. The observations reported here sample the low-energy plasma ions and their properties from ~200 to ~2500 R_J deep in the magnetotail (Fig. 1).

NH's Solar Wind Around Pluto (SWAP) instrument makes coincidence measurements of ions with energy per charge (E/q) ranging from 35 eV/q to 7.5 keV/q within a 276° × 10° field of view (FOV) centered on NH's high-gain antenna pointing direction. Other than a few data gaps, SWAP observed the magnetotail continuously back to >1700 R_J. From there back to >2500 R_J when observations were terminated, NH repeatedly crossed back and forth between the deep magnetotail and the surrounding magnetosheath.

Near closest approach, we observed narrow energy distributions of low-energy ions (tens of eV/q). These ions are almost certainly an even lower-energy population (few eV) that was subsequently accelerated into SWAP by spacecraft charging, as is sometimes observed in the terrestrial magnetosphere [e.g., (*10*)]. Inside of ~130 R_J, SWAP observed the low-energy tail of the hot plasma disk ion population (*9*, *11*). These

fluxes peaked nearer to closest approach and displayed periodicities associated with Jupiter's plasma disk rotation.

Beginning on day of year (DOY) 62 at ~75 R_J, we intermittently observed both the low-energy tail of the hot plasma population and

energy distributions that show peak fluxes within SWAP's energy range (<7.5 keV/q). Around the middle of DOY 64 at ~125 R_J, the higher-

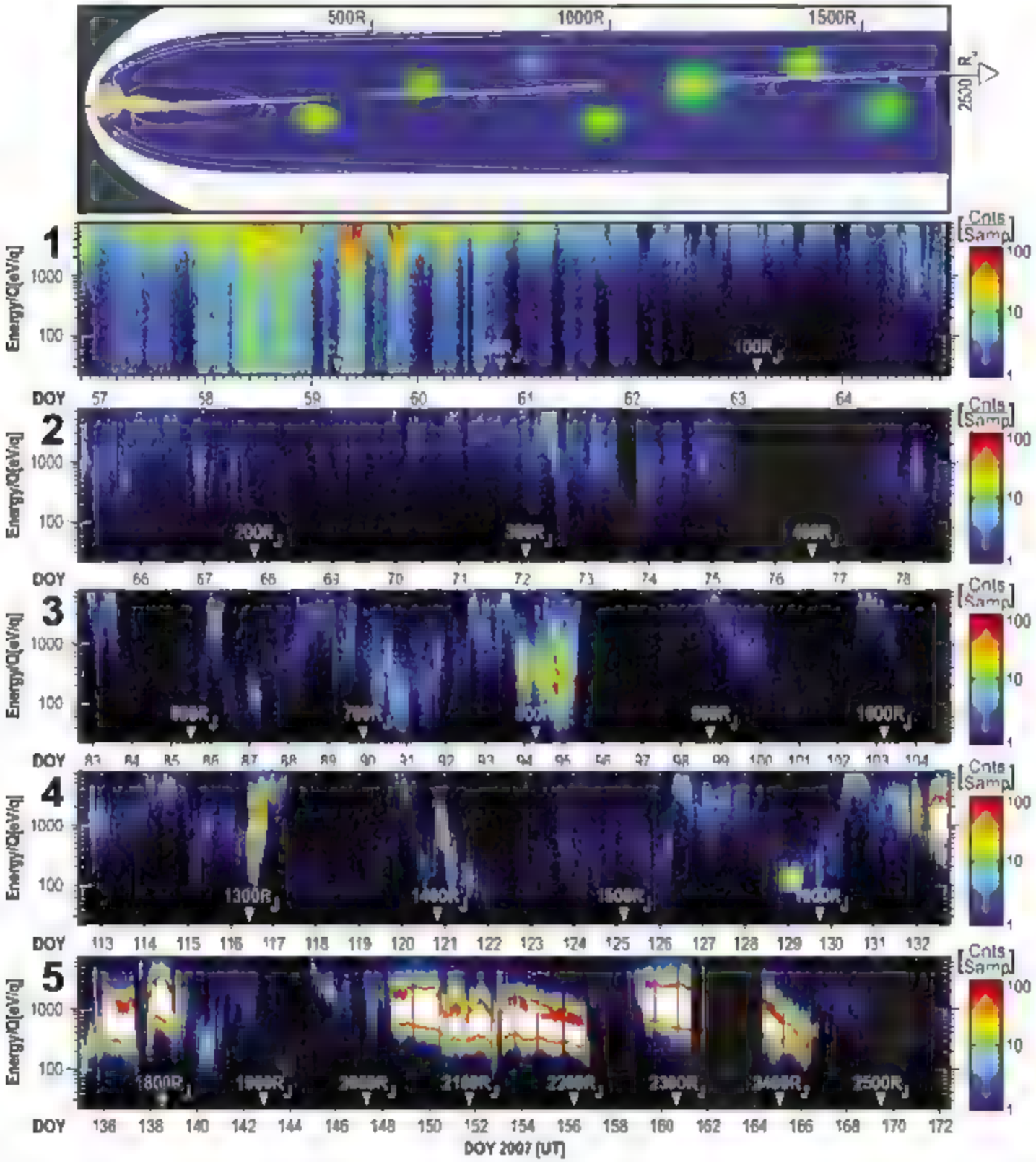

Fig. 1. Plasma observations from just after NH's inbound crossing of Jupiter's magnetopause late on DOY 56, through closest approach (CA) at ~32 R_J, and back down the magnetotail to >2500 R_J. The schematic diagram of a meridional cut through Jupiter's magnetotail (top) shows the plasma disk near Jupiter and notional large plasmoids (colored) moving down the tail, past NH. The five E/q spectrograms of the log of coincidence count rates per 0.5-s sample cover the five intervals numbered in the schematic. In general, the tail becomes more disturbed with increasing variability in ion flux and flow speed with greater distances down the tail. Finally, starting on DOY 132, NH crosses back and forth between the magnetotail and deep magnetosheath (intense white intervals in bottom panel).

energy tails ended and thereafter we only observed the lower-energy populations. These distributions became increasingly variable in both intensity and E/q with distance down the tail (and simultaneously away from its central axis). We found that the tail is very highly structured, with both gradual variations in the plasma and many sharp boundaries (discontinuities) between plasma regimes. Further, we observed both energy-dispersed and nondispersed plasma boundaries.

The SWAP observations display several interesting periodicities. The 10-hour jovian rotation period is clearly present in the count rates seen on DOY 77 and 78 at ~450 R_J, far tailward of the plasma disk. These observations suggest a process where plasma is shed preferentially for one orientation of the disk, possibly when the corotating convective outflow is directed tailward (*12*). Although the 10-hour periodicity was then absent for most of the rest of the tail passage, it appeared to return again on DOY 123 to 128, at 1500 to 1600 R_J, just inside the magnetopause (first encountered on DOY 132). A possible explanation for the return of this periodicity is that this region may be on open field lines inside the magnetopause that connect to relatively low latitudes, close to the plasma disk, back at Jupiter.

An even more surprising 3- to 4-day quasi-periodicity, especially noticeable over distances from ~600 to 1000 R_J, is seen in the mean energy, which varies from ~0.1 to 3 keV/q. Galileo observations had indicated a 2- to 3-day periodicity in bursts of radial energetic particle flows (*13*) and the release of plasma from the edge of the plasma disk, especially in the predawn sector (*14*, *15*). Here, the variations in the mean energy indicate variations in the plasma speed with this energy range, corresponding to ~140 to 760 km s^{-1} for H^+, ~80 to 440 km s^{-1} for H_3^+, and 35 to 190 km s^{-1} for O^+ or S^{2+}. Although we do not have a definitive explanation, these observations could represent the passage of a series of plasmoids or discrete magnetic and plasma structures. For each expanding plasmoid, the material near the front would move faster (sum of the flow and expansion speeds) than the material near the back (difference of these speeds), for a speed difference of only 150 km s^{-1}, 3 days corresponds to ~4×10^7 km (~500 R_J).

After DOY 81, NH was spinning at 5 RPM with its high-gain antenna pointing back toward Earth (<10° from sunward). Under these conditions, SWAP's FOV samples ~87% of 4π sr, including all look directions except a 42° half-angle hole along the antisunward spin direction. The spacecraft spin produces a beat pattern between the rotation rate and the observation cadence ("herringbone" pattern, Fig. 2A) for times when the plasma has a substantial nontailward flow. When this pattern is not present, the plasma is very hot relative to the bulk flow energy and/or the flows are nearly tailward and fall within SWAP's FOV for all spin angles. The distributions of E/q as a function of spin angle on DOY 86 (Fig. 2B) are beam-like, being relatively narrow in both angle (~30°) and E/q (~50%). This ion beam has a substantial cross-tail (east-west) and small north-south flow components. Many similar intervals observed after NH was spinning indicate both narrower and broader distributions. Although most of the tail observations indicate primarily tailward flow, cross-tail and north-south flows are not uncommon, hence the magnetotail is variable and structured in all three dimensions.

As NH moved deeper into the magnetotail, it observed more frequent and more intense ion bursts. The most intense, ~10^3 times that of tenuous ion distributions seen in the tail, occurred on DOY 116 at ~1300 R_J (Fig. 3A). The onset of this burst, as well as other changes in flux and energy throughout this interval, are discontinuous between adjacent 5-min data samples; similar discontinuities and more gradual variations are observed throughout the tail passage. The ratio

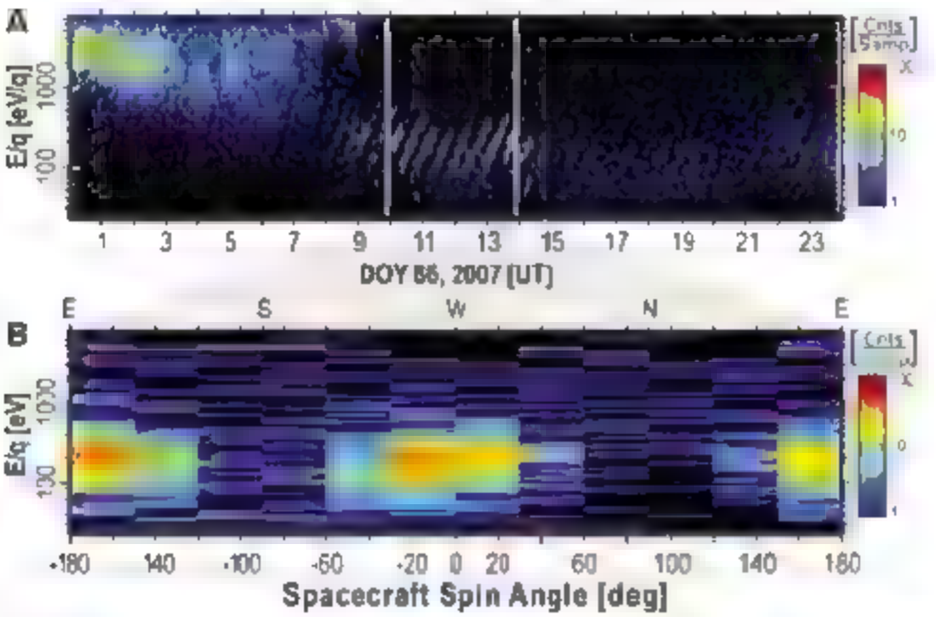

Fig. 2. (**A**) Coincidence count spectrogram for DOY 86. (**B**) Spacecraft spin phase spectrogram for the data from 1000 to 2400 UT. Angles indicate spacecraft rotation phase for the viewing of one side of SWAP's symmetric aperture.

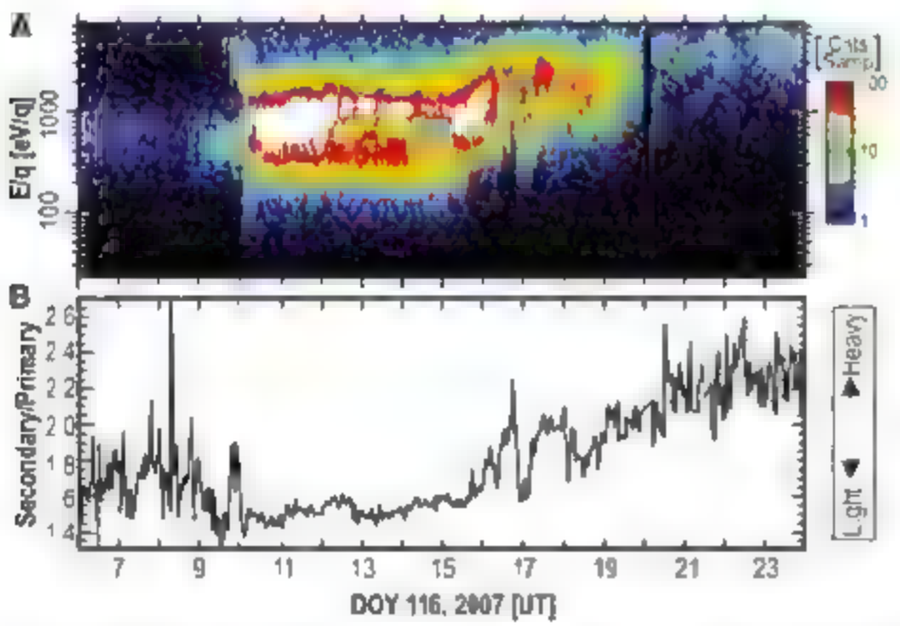

Fig. 3. (**A**) Coincidence count spectrogram for 0600 to 2400 UT on DOY 116. (**B**) Ratio of secondary to primary counts, an indicator of ion composition. Small ratios, such as during the intense burst, indicate predominantly light ions. From ~1200 to 1500 UT, the two separated E/q distributions indicate two species with m/q values of ~3, which we identify as H_3^+ and H^+ from Jupiter's ionosphere.

of counts detected in SWAP's secondary and primary detectors (Fig. 3B) provides an approximate measure of ion mass. Ground calibration results for a heavy ion (1 keV N^+) produced a ratio of ~2.7, whereas 1 keV H^+ had a ratio of ~1.3. In this interval, the higher-energy ions (hundreds of eV) were primarily lighter ions before and during the intense burst, but the higher-energy ions after the burst were increasingly dominated by heavy ions. These results, and similar ratios seen throughout the tail, show that the tail plasma is a variable mixture of heavy and light ions, as also seen at higher energies (*16*).

Another key aspect of the burst (Fig. 3) is that two separate E/q populations are present from ~1200 to 1500 UT. These relatively narrow distributions are likely created by two species moving at a common bulk speed such that the E/q spectrum provides a mass per charge (m/q) measurement. The two populations are both light ions, as shown above, and the m/q separation of ~3 identifies them as H^+ and H_3^+. Although H^+ could come from either the solar wind or the ionosphere, large fluxes of H_3^+ clearly indicate a primarily jovian origin for ions in this interval.

In addition to the quasi 10-hour periodicity seen for days inside of the first magnetopause crossing, this and other crossings (Fig. 1, bottom panel) display a clear boundary layer. The boundary layer contains lower fluxes of magnetosheath ions sometimes mixed with magnetotail ions, indicative of at least a partially open boundary and mixing of magnetosheath and tail plasmas.

Overall, our observations show a tremendous amount of structure, from sharp discontinuities up to multiday quasi-periodic variations. One key result is the identification of large plasmoids, containing magnetospheric plasma from both Io and the jovian ionosphere, that move down the magnetotail. Our observations are generally consistent with the theoretical pictures of Vasyliunas (*17*) and Kivelson and Southwood (*18*), where flux tubes carrying plasma sheet material expand as they rotate into the dusk side, stretch down the magnetotail, and eventually pinch off and become ejected. The ions predominantly from Io and Jupiter flow largely antisunward throughout the tail without any obvious evidence for a planetward return flow.

References and Notes

1. E. C. Sittler, R. P. Lepping, B. H. Mauk, S. M. Krimigis, *J. Geophys. Res.* **92**, 9943 (1987) and references therein.
2. N. Thomas, F. Bagenal, T. W. Hill, J. K. Wilson, in *Jupiter: The Planet, Satellites and Magnetosphere*, F. Bagenal, T. Dowling, W. McKinnon, Eds. (Cambridge Univ. Press, New York, 2004), pp. 561–592 and references therein.
3. P. A. Delamere, F. Bagenal, *J. Geophys. Res.* **108**, 1276 (2003).
4. S. M. Krimigis *et al.*, *J. Geophys. Res.* **86**, 8227 (1981).
5. A. F. Nagy, A. R. Barakat, R. W. Schunk, *J. Geophys. Res.* **91**, 351 (1986).
6. R. V. Yelle, S. Miller, in *Jupiter: The Planet, Satellites and Magnetosphere*, F. Bagenal, T. Dowling, W. McKinnon, Eds. (Cambridge Univ. Press, New York, 2004), pp. 185–219.
7. F. Bagenal, *J. Atmos. Sol. Terr. Phys.* **69**, 387 (2007) and references therein.
8. N. Krupp *et al.*, in *Jupiter: The Planet, Satellites and Magnetosphere*, F. Bagenal, T. Dowling, W. McKinnon, Eds. (Cambridge Univ. Press, New York, 2004), pp. 617–638 and references therein.
9. K. K. Khurana *et al.*, in *Jupiter: The Planet, Satellites and Magnetosphere*, F. Bagenal, T. Dowling, W. McKinnon, Eds. (Cambridge Univ. Press, New York, 2004), pp. 593–616, and references therein.
10. D. J. McComas *et al.*, *J. Geophys. Res.* **98**, 13453 (1993).
11. S. M. Krimigis, E. C. Roelof, in *Physics of the Jovian Magnetosphere*, A. J. Dessler, Ed. (Cambridge Univ. Press, New York, 1983), pp. 106–156.
12. T. W. Hill, A. J. Dessler, C. K. Goertz, in *Physics of the Jovian Magnetosphere*, A. J. Dessler, Ed. (Cambridge Univ. Press, New York, 1983), pp. 353–394.
13. N. Krupp *et al.*, *Geophys. Res. Lett.* **25**, 1249 (1998).
14. E. A. Kronberg *et al.*, *J. Geophys. Res.* **112**, A05203 (2007) and references therein.
15. K. Fukazawa, T. Ogino, R. Walker, *J. Geophys. Res.* **111**, A10207 (2006), and references therein.
16. R. L. McNutt Jr. *et al.*, *Science* **318**, 220 (2007).
17. V. M. Vasyliunas, in *Physics of the Jovian Magnetosphere*, A. J. Dessler, Ed. (Cambridge Univ. Press, New York, 1983), pp. 395–453.
18. M. G. Kivelson, D. J. Southwood, *J. Geophys. Res.* **110**, A12209 (2005).

19. We thank the entire New Horizons mission team and our colleagues on the New Horizons science team. New Horizons is funded by NASA, whose financial support we gratefully acknowledge.

5 July 2007; accepted 31 August 2007
10.1126/science.1147393

REPORT

Energetic Particles in the Jovian Magnetotail

R. L. McNutt Jr.,[1]* D. K. Haggerty,[2] M. E. Hill,[2] S. M. Krimigis,[1,2] S. Livi,[3] G. C. Ho,[3] R. S. Gurnee,[1] B. H. Mauk,[1] D. G. Mitchell,[1] E. C. Roelof,[1] D. J. McComas,[3] F. Bagenal,[4] H. A. Elliott,[3] L. E. Brown,[1] M. Kusterer,[1] J. Vandegriff,[1] S. A. Stern,[5] H. A. Weaver,[1] J. R. Spencer,[6] J. M. Moore[7]

When the solar wind hits Jupiter's magnetic field, it creates a long magnetotail trailing behind the planet that channels material out of the Jupiter system. The New Horizons spacecraft traversed the length of the jovian magnetotail to >2500 jovian radii (R_J, 1 R_J = 71,400 kilometers), observing a high-temperature, multispecies population of energetic particles. Velocity dispersions, anisotropies, and compositional variation seen in the deep-tail (≥ 500 R_J) with a ~3-day periodicity are similar to variations seen closer to Jupiter in Galileo data. The signatures suggest plasma streaming away from the planet and injection sites in the near-tail region (–200 to 400 R_J) that could be related to magnetic reconnection events. The tail structure remains coherent at least until it reaches the magnetosheath at 1655 R_J.

A magnetotail is produced by the interaction of a magnetized planet with the solar wind (*1*). Early observations suggested that Jupiter might have one as long as ~4.6 astronomical units (AU) (1 AU = 2095 R_J) (*2*). Voyager 2 encountered the jovian magnetotail in 1980–1981 at ~5000 to 9000 R_J (~2.4 to 4.3 AU) downstream from the planet (*3*–*5*), and Cassini encountered it as far as ~900 R_J (*6*). Key questions are: How does the magnetotail structure evolve with distance? What is the composition of the tail plasma and particles? To what extent does flowing plasma and a hot plasma component within the tail contribute to pressure balance across the tail? (*3*) The New Horizons flyby of Jupiter provided a unique opportunity to address these questions with the Pluto Energetic Particle Spectrometer Science Investigation (PEPSSI) and Solar Wind Around Pluto (SWAP) (*7*, *8*) instruments.

In 2007 PEPSSI operated from 6 January through closest approach (CA) to Jupiter (32.3 R_J) until 09:41 11 Universal Time Coordinated (UTC) on 21 June [day of year (DOY) 172] at 2565 R_J (1.22 AU). Magnetopause (MP) crossings are identified by the increase (~18:00 UTC on DOY 56, 67.4 R_J from Jupiter) and decline (beginning DOY 132 at 1655 R_J = 0.790 AU) of the energetic electrons (Fig. 1), as well as heavy oxygen (O) and sulfur (S) ions from Jupiter's moon Io. High fluxes in the proton and electron channels seen before crossing the magnetopause (beginning ~05:00 UTC on DOY 56) are associated with either crossing(s) of the jovian bow shock or upstream events as seen previously near Jupiter (*9*, *10*).

Anisotropies in the electron fluxes in the lowest (~25 to 190 keV) channel (Fig. 2) observed when the spacecraft was spinning are consistent with

[1]Applied Physics Laboratory, Johns Hopkins University, Laurel, MD 20723, USA. [2]Academy of Athens, 28 Panepistimiou, 10679 Athens, Greece. [3]Southwest Research Institute, San Antonio, TX 78228, USA. [4]Laboratory of Atmospheric and Space Physics, University of Colorado, Boulder, CO 80309–0392, USA. [5]NASA Headquarters, Washington, DC 20546–0001, USA. [6]Southwest Research Institute, Boulder, CO 80302, USA. [7]NASA Ames Research Center, Moffett Field, CA 94035, USA.

*To whom correspondence should be addressed. E-mail: ralph.mcnutt@jhuapl.edu

electrons streaming away from Jupiter (>400 R_J from the planet), presumably along a magnetic field distended away from the planet in the distant magnetotail. The return to near isotropy and decrease in intensity began on 12 May and was completed ~3 days later, consistent with the magnetopause signature seen by the SWAP instrument (*8*).

We analyzed the sulfur-to-oxygen ratio (see also Fig. 3B) with distance down the tail and found an average value of S/O ~0.8, consistent with determinations closer to Jupiter (*11*) but somewhat higher than the value obtained by Voyager 2 (~0.4) at higher (~500 keV/nucleon) energies (*12*). Large fluxes of protons are also present.

The spectrogram (Fig. 1) contains signatures of six events before the MP crossing that indicate dispersion: ions with higher energies and lighter masses seen sooner at the spacecraft (Fig. 3C). If we assume that the particles are guided by a magnetic field aligned with the Jupiter-Sun line, then the inferred injection sites (Table 1) correspond to ~200 to 500 R_J from Jupiter during the time period from 8 April (DOY 98) through 9 May (DOY 129). The simplest interpretation is that particle acceleration events are occurring in this near-tail region, sending particles in large bursts down the tail (Fig. 3D). A likely source is magnetic reconnection, part of the energy going into particle streaming and part into the pressure that maintains the tail against collapse.

The temporal separation of these events, as well as the velocity dispersion, provides evidence that they are the same phenomena observed by the Galileo Energetic Particle Detector (EPD) (*13*) at closer distances (~80 to 115 R_J) in the predawn region of the magnetosphere every ~2.6 days (*14*, *15*) (Fig. 3A). With the Lomb-Scargle algorithm (*16*–*20*), we sought periodicities in the varying PEPSSI particle fluxes. For the DOY 113 to 127 (1220 to 1540 R_J) interval, we found a periodicity of 3.0 ± 0.5 (mean ± SD) days, with a second periodicity at 2.3 ± 0.5 days, consistent with Galileo observations (*11*, *21*). Independently, the PEPSSI heavy-ion-to-proton ratio exhibits a 3.46 ± 0.10 day period. Anisotropies within the six events are consistent with strong tailward (anti-Jupiter) flow and are dominated by heavy ions (*11*, *22*, *23*).

Flow anisotropies were also seen at greater distances of ~170 R_J in the predawn magnetosphere by Voyager 1 and 2 (*24*). PEPSSI observed these events in the premidnight region, with later events observed when the spacecraft was further north and toward dusk of the presumed tail current sheet than during the Galileo observations. Given the similar periodicities observed by Galileo and New Horizons, this phenomenon appears to occur across the entire magnetotail, although the initiation sites may be farther from the planet before midnight than after.

To estimate the dynamical effect of these particle distributions, we fit PEPSSI data to a model from which density and pressure can be determined (supporting online material). The spatial variations of density and pressure are both well fit by a power-law in radial distance r from Jupiter, scaling (figs. S1 to S4) as $\sim r^{-3.4}$ and $\sim r^{-3.2}$, respectively. These fits do not account for the bulk of the particle density, which resides at energies below the PEPSSI energy threshold (*8*), however; this energetic population usually dominates the overall pressure (*24*, *25*). The derived proton pressure varies between ~500 and 2 eV cm^{-3}, with an average of ~40 eV cm^{-3} (electrons and O and S ions will increase this amount). At Jupiter's location, this is greater than typical interplanetary magnetic field pressures.

The picture emerging from the PEPSSI and SWAP data is that the jovian magnetotail exhibits a dynamic periodicity associated with ejection of plasma. The hot plasma component plays a major role in defining the configuration and extension of the jovian magnetotail, while simultaneously channeling sulfur and oxygen from Io into the outer heliosphere and beyond.

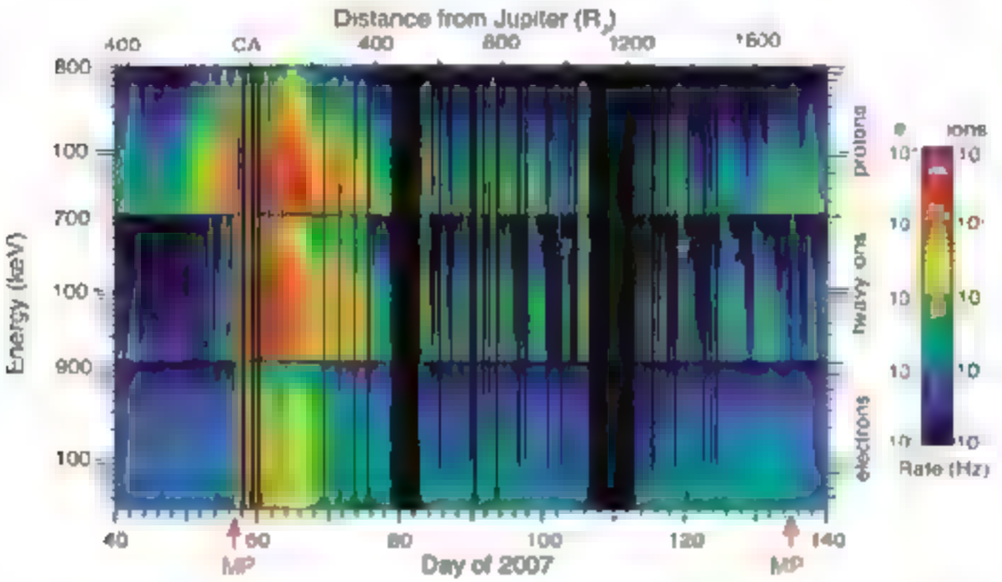

Fig. 1. PEPSSI energy-time spectrogram from DOY 40 through 139, showing hourly averaged count rates of protons, heavy ions (primarily O and S), and electrons (top to bottom, respectively) summed over all six angular segments. The vertical scales show energy deposited. The top scale indicates radial distance of the spacecraft in R_J. CA marks closest approach. Data gaps (2007/078 16:48 to 2007/082 20:35 and 2007/106 06:40 to 2007/112 22:05) result from spacecraft activities. Dark vertical lines indicate times the instrument was powered off, times when the PEPSSI high voltage was lowered are dark in the ion and higher-energy electron channels. MP crossings are indicated in red. White numbers label the six dispersion events in Fig. 3C and Table 1.

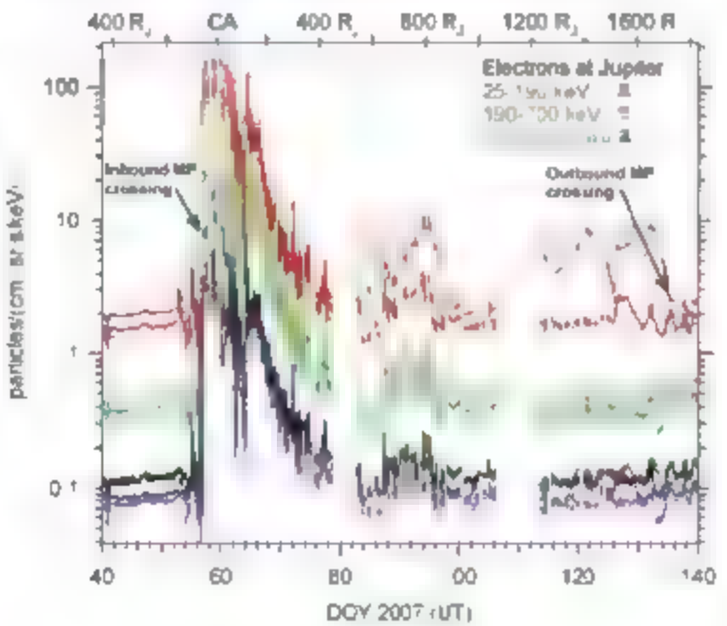

Fig. 2. Jovian electrons for the same period as in Fig. 1. After DOY 82, the spacecraft spun at 5 rpm. The sensor viewing electrons between 90° and 116° to the Jupiter direction is the third color trace at each energy. Viewing directions between the two other sensor boresights and the center of Jupiter varied between 12° and 38° and 21° and 47°, respectively, during each spin (top two color traces, respectively, at each energy). Distances, MP crossings, and CA are shown.

References and Notes

1. N. F. Ness, *Rev. Geophys.* 7, 97 (1969).
2. S. M. Krimigis, E. T. Sarris, T. P. Armstrong, *Geophys. Res. Lett.* 2, 561 (1975).
3. R. P. Lepping *et al.*, *J. Geophys. Res.* 88, 8801 (1983).

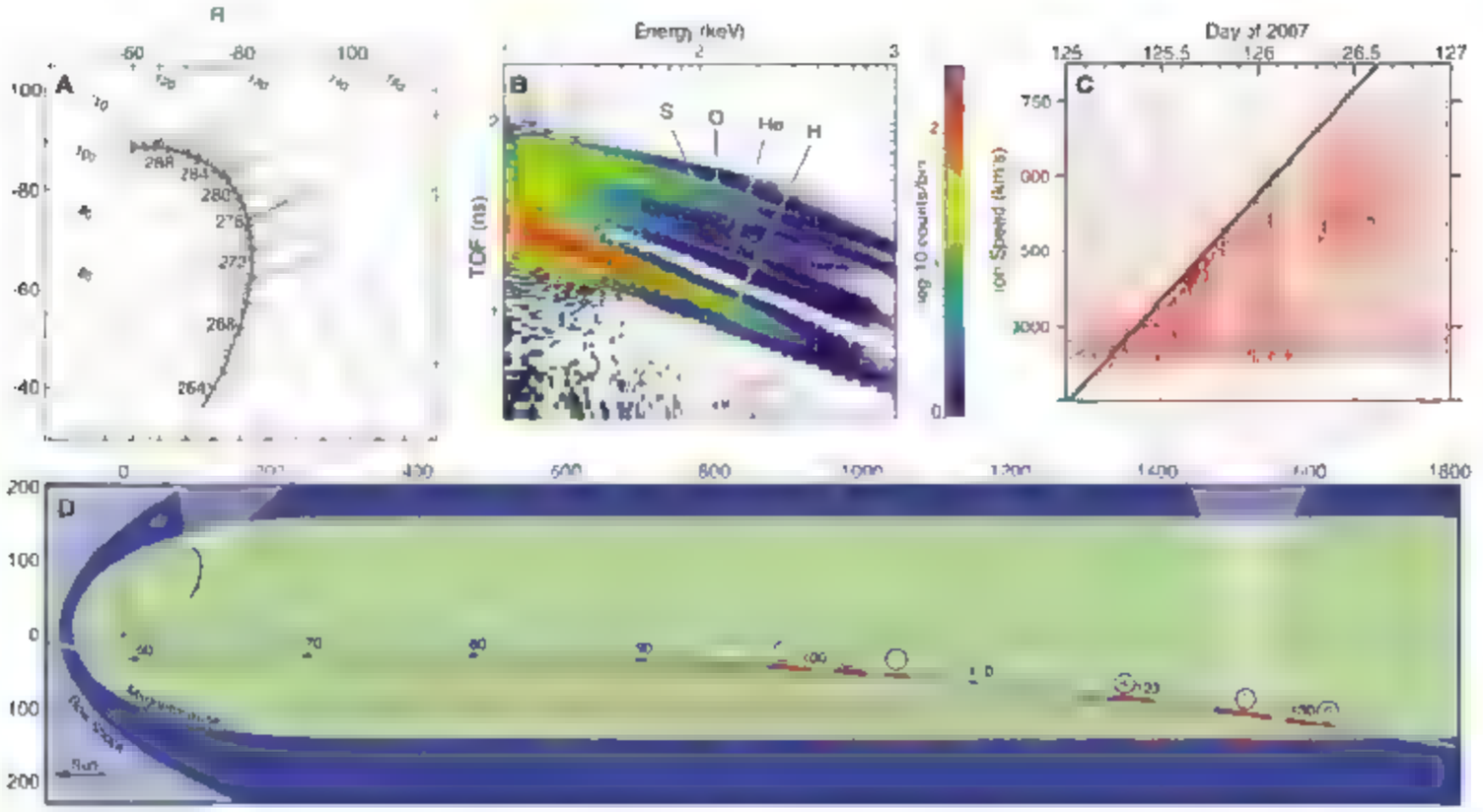

Fig. 3. (**A**) Anisotropies of energetic ions measured by the Galileo EPD showing tailward bursts at ~3-day intervals (*26*). (**B**) PEPSSI combined time-of-flight and energy deposition measurements of ions integrated throughout the magnetosphere (2007/056 18:00 to 2007/132 07:00); the color scale indicates how many particles were detected with a given TOF and energy. (**C**) Dispersion analysis of ion speeds during event 5 of Table 1; each point is a single detected particle; the black line shows the best fit. (**D**) Trajectory of New Horizons in Jupiter's equatorial plane showing a model of the magnetotail, black marks show 10-day intervals starting from DOY 60 near CA, and six red heavy bars on the trajectory indicate observed event durations; associated horizontal red lines indicate the approximate length of path traveled by the particles in the six dispersive events, assuming anti-sunward propagation. Units in (A) and (D) are R_J.

Table 1. Dispersive event fit parameters. The common initiation time of the particle acceleration is t_0. d is the derived distance from the spacecraft back to the common acceleration point, and d_{NH} is the radial distance of New Horizons from the center of Jupiter at the observation time t. These parameters are fit from the set of particle velocities v observed at times t, related by $v^{-1} = (t - t_0)/d$. The difference $d - d_{NH}$ gives the largest possible sunward distance. Cited errors are due to the deviations in the v^{-1} dispersion signature (compare to Fig. 3C).

Event	t_0	d (R_J)	Radial distance of New Horizons from Jupiter d_{NH} (R_J)	Most sunward distance possible $d - d_{NH}$ (R_J)
1	2007/098 01:10 ± 10	410 ± 30	882.97	470 ± 30
2	2007/102 00:20 ± 20	790 ± 20	972.20	180 ± 20
3	2007/104 23:10 ± 10	700 ± 20	1038.62	340 ± 20
4	2007/118 23:00 ± 30	1110 ± 90	1352.54	240 ± 90
5	2007/125 00:20 ± 30	1270 ± 40	1490.37	220 ± 40
6	2007/129 05:30 ± 40	1090 ± 50	1585.52	490 ± 50

4. F. L. Scarf, W. S. Kurth, D. A. Gurnett, H. S. Bridge, J. D. Sullivan, *Nature* **292**, 585 (1981).
5. R. P. Lepping, R. F. Burlaga, M. D. Desch, L. W. Klein, *Geophys. Res. Lett.* **9**, 845 (1982).
6. N. Krupp *et al.*, *J. Geophys. Res.* **109**, A09S10 (2004).
7. D. J. McComas *et al.*, *Space Sci. Rev.* in press, preprint available at http://arxiv.org/abs/0709.4505 (2007).
8. D. J. McComas *et al.*, *Science* **318**, 217 (2007).
9. S. M. Krimigis *et al.*, *Nature* **415**, 994 (2002).
10. D. Haggerty, T. P. Armstrong, *J. Geophys. Res.* **104**, 4629 (1999).
11. A. Radioti *et al.*, *J. Geophys. Res.* **112**, A06221 (2007).
12. D. C. Hamilton, G. Gloeckler, S. M. Krimigis, L. J. Lanzerotti, *J. Geophys. Res.* **86**, 8301 (1981).
13. D. J. Williams, R. W. McEntire, E. P. Keath, S. Jaskulek, B. Wilken, *Space Sci. Rev.* **60**, 385 (1992).
14. N. Krupp, J. Woch, A. Lagg, B. Wilken, S. A. Livi, *Geophys. Res. Lett.* **25**, 1249 (1998).
15. E. A. Kronberg *et al.*, *J. Geophys. Res.* **112**, A05203 (2007).
16. W. H. Press, G. B. Rybicki, *Astrophys. J.* **338**, 277 (1989).
17. J. D. Scargle, *Astrophys. J.* **263**, 835 (1982).
18. J. H. Horne, S. L. Baliunas, *Astrophys. J.* **302**, 757 (1986).
19. G. J. MacDonald, *Rev. Geophys.* **27**, 449 (1989).
20. M. E. Hill, D. C. Hamilton, S. M. Krimigis, *J. Geophys. Res.* **106**, 8315 (2001).
21. J. Woch, N. Krupp, A. Lagg, B. Wilken, S. A. Livi, *Geophys. Res. Lett.* **25**, 1253 (1998).
22. N. Krupp *et al.*, *J. Geophys. Res.* **106**, 26017 (2001).
23. J. Woch, N. Krupp, A. Lagg, *Geophys. Res. Lett.* **29**, 1138 (2002).
24. S. M. Krimigis *et al.*, *J. Geophys. Res.* **86**, 8227 (1981).
25. B. H. Mauk *et al.*, *J. Geophys. Res.* **109**, 24 (2004).
26. N. Krupp *et al.*, in *Jupiter: The Planet, Satellites and Magnetosphere*, F. Bagenal, T. E. Dowling, W. B. McKinnon, Eds. (Cambridge Univ. Press, Cambridge, 2004), pp. 617–638.

27. We acknowledge many useful discussions with colleagues, in particular C. P. Paranicas. The PEPSSI effort is part of the New Horizons mission managed at the Applied Physics Laboratory under NASA Contract NAS5-97271.

Supporting Online Material

www.sciencemag.org/cgi/content/full/318/5848/220/DC1
SOM Text
Figs. S1 to S4
References

19 July 2007; accepted 19 September 2007
10.1126/science.1148025

REPORT

Jupiter Cloud Composition, Stratification, Convection, and Wave Motion: A View from New Horizons

D. C. Reuter,[1]* A. A. Simon-Miller,[1] A. Lunsford,[1] K. H. Baines,[2] A. F. Cheng,[3,4] D. E. Jennings,[1] C. B. Olkin,[5] J. R. Spencer,[5] S. A. Stern,[4] H. A. Weaver,[3] L. A. Young[5]

Several observations of Jupiter's atmosphere made by instruments on the New Horizons spacecraft have implications for the stability and dynamics of Jupiter's weather layer. Mesoscale waves, first seen by Voyager, have been observed at a spatial resolution of 11 to 45 kilometers. These waves have a 300-kilometer wavelength and phase velocities greater than the local zonal flow by 100 meters per second, much higher than predicted by models. Additionally, infrared spectral measurements over five successive Jupiter rotations at spatial resolutions of 200 to 140 kilometers have shown the development of transient ammonia ice clouds (lifetimes of 40 hours or less) in regions of strong atmospheric upwelling. Both of these phenomena serve as probes of atmospheric dynamics below the visible cloud tops.

The New Horizons spacecraft observed Jupiter's atmosphere by means of the Multispectral Visible Imaging Camera (MVIC) and the Linear Etalon Imaging Spectral Array (LEISA) components of the Ralph imaging instrument (*1*, *2*) and the panchromatic Long-Range Reconnaissance Imager (LORRI) (*3*–*5*). These observations have expanded on results gained from previous in situ Jupiter exploration (e.g., Pioneer, Voyager, Galileo, and Cassini), as well as Hubble Space Telescope (HST) and ground-based observations. In particular, the observations have been used to quantify the phase velocity of a series of mesoscale waves similar to those initially discovered in Voyager images (*6*) and to study the evolution of ammonia clouds over several successive Jupiter rotations. Because the origins of the mesoscale gravity waves and the upwelling ammonia clouds lie below the upper cloud layer, these measurements provide a window into the structure and dynamics of a region of the atmosphere that is not directly accessible to remote sensing observations.

A series of scans using the MVIC color channels were taken from a mean distance of 2.3 million km over a 45-min period beginning at 05:58 UT on 28 February 2007. At this distance MVIC's spatial resolution is about 45 km, which is about a factor of 3 higher than HST resolution and is comparable to Galileo's resolution. The scans provided a pole-to-pole, terminator-to-limb image of Jupiter in the spectrally narrow MVIC methane channel, as well as pole-to-pole images of the terminator region in the other, spectrally broader, color channels.

Extended mesoscale wave trains occur over much of the region within about 5° of the equator (Fig. 1). The MVIC methane channel is sensitive to light from altitudes with pressures lower than about 600 mbar. Thus, the mesoscale waves correspond to the modulation of the cloud optical depth in a band somewhere above 600 mbar. There are additional clouds within this altitude range that are not modulated by gravity waves. The waves appear everywhere except for small cloudy regions, where the visual contrast is reduced, and in the region near the limb, where curvature reduces the apparent wave spacing and the scenes are more crowded. Both of these effects reduce contrast. It is possible, then, that there is one continuous wave pattern over the entire equator. When adjusted for the solar illumination angle, the contrast ratio of the mesoscale waves ranges from 1% to almost 10%. The mesoscale waves were also observed in the other

[1]NASA Goddard Space Flight Center, Code 693, Greenbelt, MD 20771, USA. [2]Jet Propulsion Laboratory, Pasadena, CA 91109, USA. [3]Johns Hopkins Applied Physics Laboratory, Laurel, MD 20723, USA. [4]NASA Science Mission Directorate, NASA Headquarters, Washington, DC 20546, USA. [5]Department of Space Studies, Southwest Research Institute, 1050 Walnut Street, Suite 300, Boulder, CO 80302, USA.

*To whom correspondence should be addressed. E-mail: dennis.c.reuter@nasa.gov

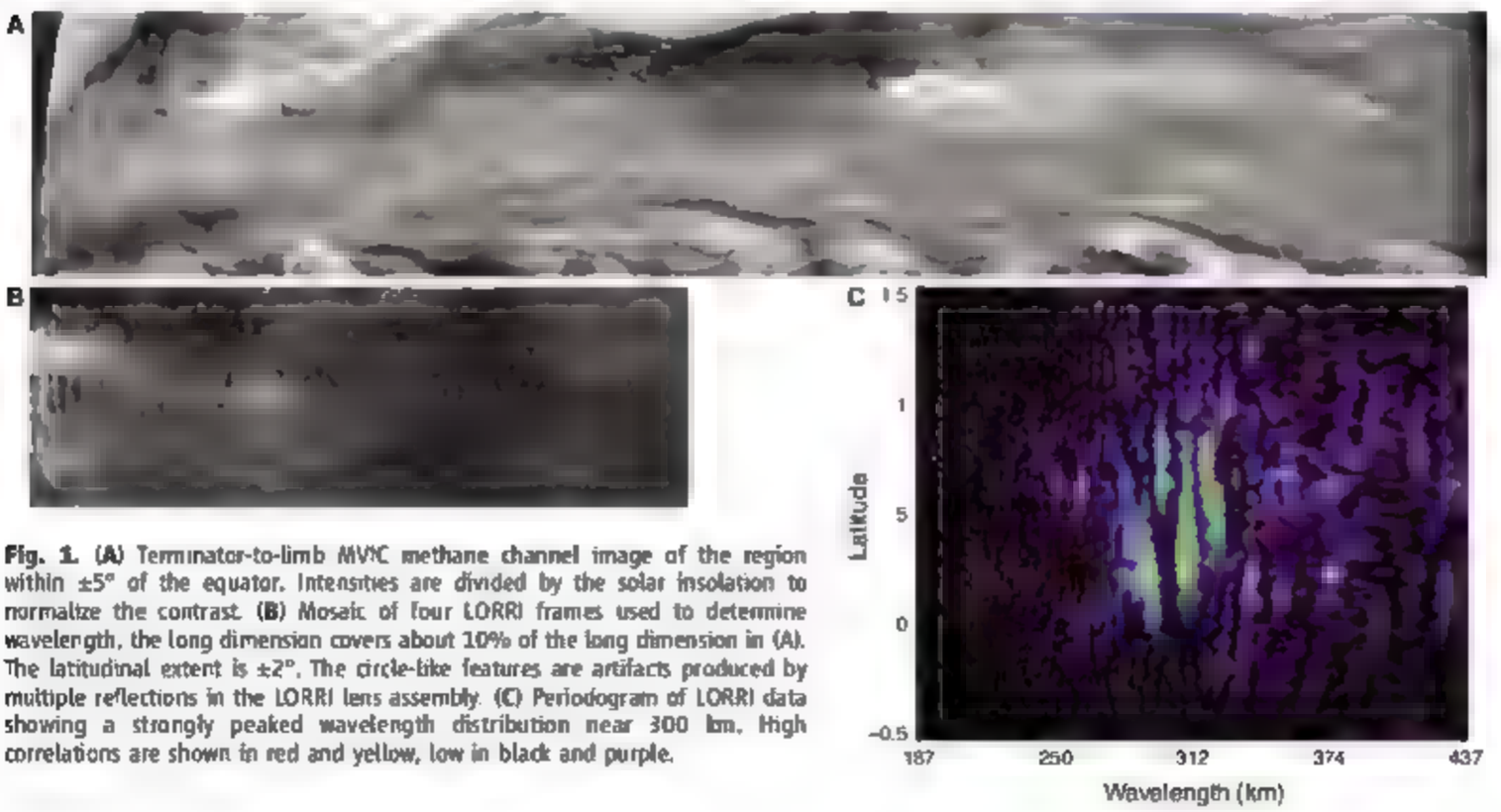

Fig. 1. (**A**) Terminator-to-limb MVIC methane channel image of the region within ±5° of the equator. Intensities are divided by the solar insolation to normalize the contrast. (**B**) Mosaic of four LORRI frames used to determine wavelength; the long dimension covers about 10% of the long dimension in (A). The latitudinal extent is ±2°. The circle-like features are artifacts produced by multiple reflections in the LORRI lens assembly. (**C**) Periodogram of LORRI data showing a strongly peaked wavelength distribution near 300 km. High correlations are shown in red and yellow, low in black and purple.

MVIC color channels near the terminator, to the extent allowed before saturation occurred.

Transient mesoscale waves such as these have been observed previously in Voyager (*6*) and Galileo (*7*) images, although their longitudinal extent appeared more limited during these previous encounters. The equatorial region of Jupiter was unusually free of clouds during the New Horizons encounter (*8*), and this may have made the waves more visible than they were previously, the region was brownish but had more visible clouds during Voyager, and was filled with opaque white clouds during Galileo. Alternatively, the absence of clouds may indicate that the equatorial region was less turbulent than in the previous epochs, and this may have allowed longer gravity wave trains to develop. An analysis of the MVIC methane channel image indicated a narrow distribution of mesoscale wave train wavelengths with a peak near 300 km.

A better measure of wavelength can be obtained from an analysis of a mosaic of four LORRI images taken at nearly the same time as the MVIC images (Fig. 1B). The LORRI images have a spatial resolution of about 11 km, the same as the highest resolution obtained by Voyager. Figure 1B covers about 10% of the longitudinal range of Fig. 1A. As shown in a periodogram analysis of the LORRI data (Fig. 1C), high spectral power occurs for wavelengths near 300 km with a greater than 99% probability that the wavelength is between 280 and 330 km. This is similar to the wavelength of 300 ± 60 km determined for the Voyager and Galileo mesoscale waves (*6*, *7*). Mesoscale waves have not been identified in HST observations of Jupiter, presumably because averaging over its spatial resolution limit (>150 km) reduces the amplitude of the signal.

The MVIC data were also used to determine a phase velocity for the waves. Three scans were made over a 41-min period, and identifiable localized wave structure persisted over that time scale. Only one scan extended from terminator to limb. Planetary navigation of the scans was done by rectifying from the scan with the full limb present, with an uncertainty of 1 pixel or less. The 41-min separation resulted in a 1-pixel velocity uncertainty of 16.9 m/s. Individual wave crests can be identified because unique structures and splits appear in some of the wave fronts, and it is possible to determine their displacement (and thus the wave speed) by a lagged correlation analysis (movie S1). As shown in Fig. 2B, the resulting absolute eastward velocity is between 204 and 276 m/s (±3σ). The correlations show a second peak near 100 m/s, whose source is sparse clouds moving at the zonal average velocity, as confirmed by manual measurements of these cloud features. A velocity of 100 m/s is consistent with measured values for the equatorial wind velocity from nearly simultaneous HST images, lending credence to the correlation results.

When determining wave velocities, care must be taken to ensure that the solution is unique and does not correspond to an integer wavelength shift. In particular, in the case of the 41-min lag, if the wave fronts were not identifiable, then, given a background velocity of 100 m/s and a wavelength of 300 km, one would expect to see solutions corresponding to 100 ± 122*n* m/s, where *n* is an integer. The identified solution of 204 to 276 m/s encompasses this for $n = 1$, but it is important to note that because the wave fronts have identifiable structure, the other solutions do not correspond to correlation maxima, and the solution is unique. This was verified by manually tracking the wave front identified by the line in Fig. 2A to calculate the velocity independent of the correlation analysis. Allowing for potential remapping uncertainty, the phase speed of the mesoscale waves is at least 100 m/s faster than the equatorial zonal wind speed.

This result has implications for the source of the mesoscale waves and atmospheric stability. Flasar and Gierasch (*6*) developed a three-layer model of the relevant portion of Jupiter's atmosphere in which the bottom layer acts as a leaky cavity (analogous to an optical etalon), generating a resonant gravity wave that excites another gravity wave in the wave guide–like second layer, where it is trapped, producing the observed mesoscale waves. Bosak and Ingersoll (*9*) posited a model in which, similar to processes occurring on Earth, Kelvin-Helmholtz instability produced the waves. Their model included the shear layer thickness measured by the Galileo probe, which entered near 7°N latitude. Both models were successful in reproducing the observed 300-km wavelength with reasonable assumptions about the state of the atmosphere, but both models also predicted that the phase speed of the waves would be near the zonal wind speed, contrary to our findings. The wind speeds measured by New Horizons lie outside the realm of either theory, although it is possible that one or both models might be corrected by a new set of atmospheric parameters. Therefore, the mesoscale waves serve as probes of lower atmospheric levels (about 2 to 10 bar) not directly observable by passive remote sensing methods because of the opaque cloud decks.

A different probe of the dynamics of Jupiter's lower atmosphere is provided by measurements of the distribution and temporal evolution of spectrally identifiable ammonia clouds (SIACs). Jupiter is covered in clouds, and thermochemical models (*10*) imply that the uppermost cloud layer (near 600 mbar) must be composed primarily of ammonia ice. Only recently, however, was ammonia ice detected spectrally by Infrared Space Observatory observations in the 2.7- to 3-μm spectral region (*11*). This implies that the background ammonia ice is in some way altered, and that it does not display the expected spectral characteristics. Baines *et al.* (*12*) used Galileo Near-Infrared Mapping Spectrometer (NIMS) spectral maps to determine that these SIACs were relatively short-lived (on the order of hours to days) and covered less than 1% of the planet. The latter conclusion was supported by 10-μm spectral measurements made by the Composite Infrared Spectrometer instrument on Cassini (*13*). SIACs were found in regions such as storm areas,

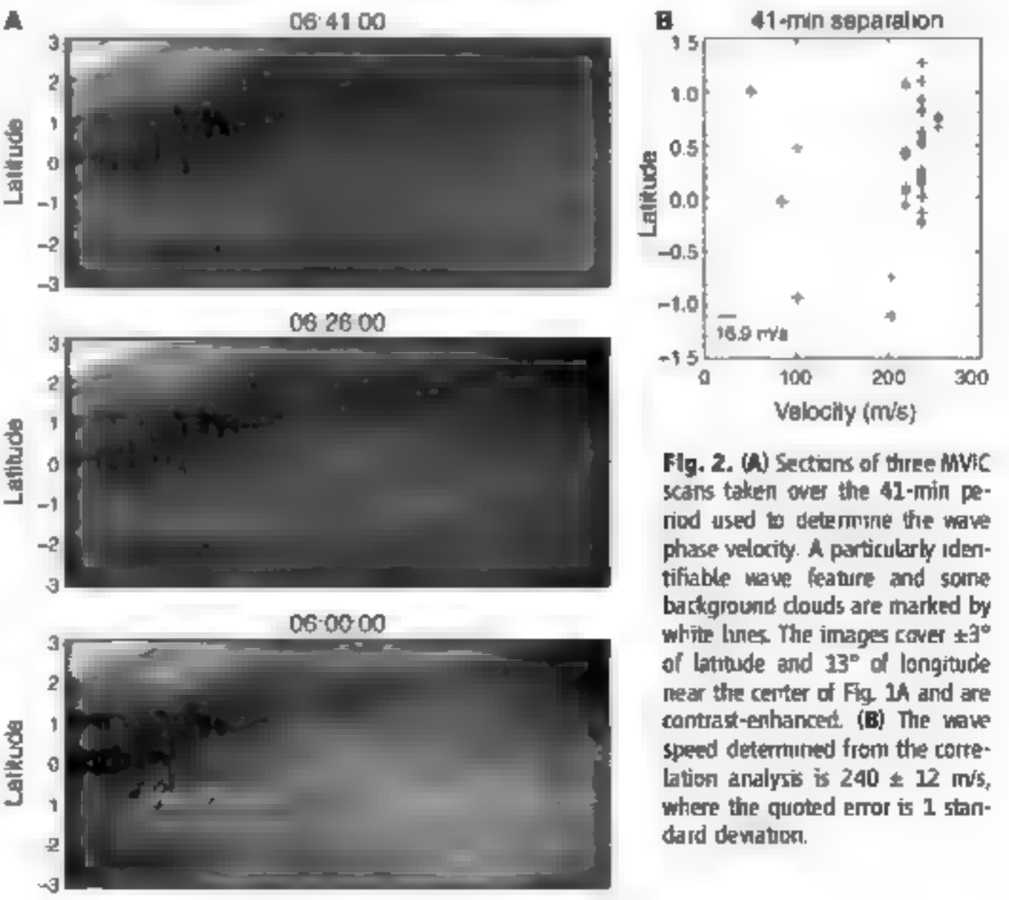

Fig. 2. (**A**) Sections of three MVIC scans taken over the 41-min period used to determine the wave phase velocity. A particularly identifiable wave feature and some background clouds are marked by white lines. The images cover ±3° of latitude and 13° of longitude near the center of Fig. 1A and are contrast-enhanced. (**B**) The wave speed determined from the correlation analysis is 240 ± 12 m/s, where the quoted error is 1 standard deviation.

where ammonia gas upwelled from deeper in the atmosphere and condensed in the upper cloud regions. Thus, SIACs are freshly condensed ammonia clouds and serve as tracers for localized dynamically active events. One suggested reason for the lack of SIACs over most of the globe is that soon after ammonia clouds form in the upper atmosphere, they are modified by a continual rain of hydrocarbon material in an upper atmospheric haze and lose their spectral character (*14*).

New Horizons made several observations of Jupiter with its LEISA infrared spectral imager, including scans of the full illuminated disk and smaller scans of the area near the Great Red Spot. The measurements with highest spatial resolution (200 to 140 km) were carried out from 26 to 28 February 2007 as the distance to Jupiter decreased from 3.4 million to 2.3 million km. Fresh ammonia ice was detected in several localized regions in these scans via the 1.99-μm absorption band. LEISA's spectral resolution is a factor of ~3 better than that of the Galileo NIMS for wavelength near 2 μm, which improves the spectral selectivity. As in the Galileo observations, the areas where fresh ammonia ice is found correspond to active storms or upwelling regions (Fig. 3A), and they tend to occur in areas of high clouds (Fig. 3B).

Maps of a region centered at −35° latitude and 8° longitude on five successive Jupiter days, starting on 26 February 2007 at 19:35 UT, reveal the evolution of the ammonia cloud (Fig. 3C). Appearing as a localized source on day 1, it intensified and broadened on day 2, became more diffuse on days 3 and 4, and disappeared on day 5. The diffusion seemed to follow the movement of a dark spot along the boundary of the oval region. Whether the dark spot was associated with the source of the fresh ammonia cloud or simply traveled with it along the oval boundary is not clear. There are, however, other ammonia features that disappear by day 3, perhaps indicating the cessation of a local upwelling source.

These observations show that the source of the SIACs can be quite transient, in this case appearing to last less than 24 hours. Atmospheric transport, followed by either precipitation of large particles or chemical alterations (*14*) or both, rapidly eliminated the spectral signature of the ammonia ice particles. This result supports the conclusion (*12*) that these optically thick clouds are young (less than a few days old) and represent areas of unusually strong vertical dynamics, such as that produced by convection, as likely occurred in this instance. These clouds therefore serve as tracers of the energetics and small-scale dynamics of Jupiter's atmosphere at pressures of up to a few bars. New Horizons detected very few ammonia clouds northwest and west of the Great Red Spot, where the largest clouds had previously been observed (*11*). Such a finding is consistent with imaging observations and indicates that active convection is not now occurring in this region. This, along with changes in cloud cover of other regions, indicates that at the time of the New Horizons encounter there was a temporary change in the state of Jupiter's atmosphere relative to that observed throughout the 1990s and during the Cassini flyby in 2000 (*7*, *8*, *15*, *16*).

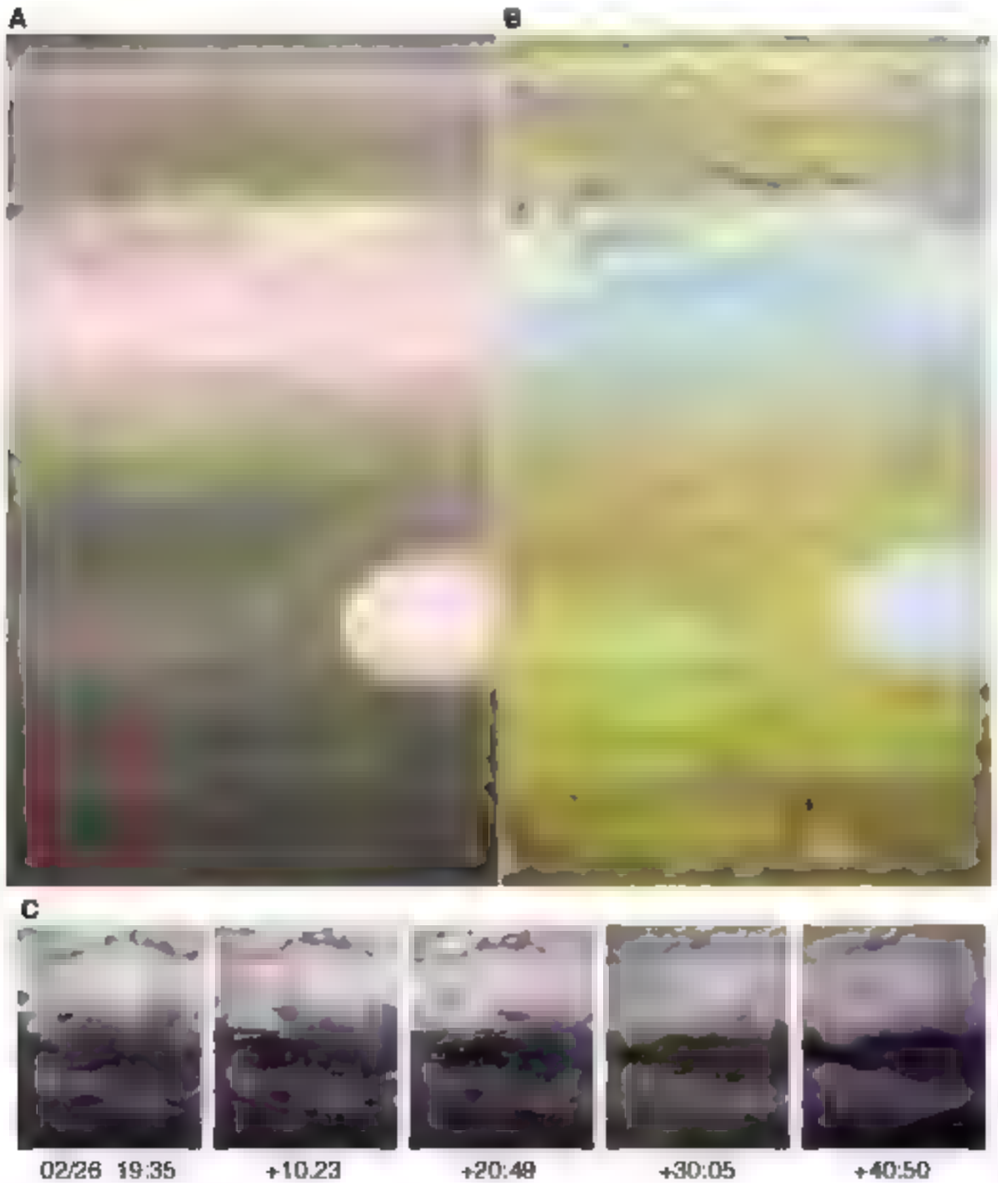

Fig. 3. (**A**) False-color image of the region around the Great Red Spot (red, 1.99 μm; green, 1.94 μm; blue, 2.04 μm). SIACs appear as bright blue. (**B**) False-color image of the same region shown in (A), but with wavelengths chosen to measure cloud height (red, 1.60 μm; green, 1.89 μm; blue, 2.04 μm). Blue and white regions are high clouds. (**C**) Map of SIACs on five successive rotations of Jupiter in the region near −35° latitude and 8° longitude outlined in red in (A).

References and Notes

1. D. C. Reuter *et al.*, *Space Sci. Rev.* in press (http://arxiv.org/abs/0709.4281)
2. D. Reuter *et al.*, *Proc. SPIE* **5906**, 433 (2005).
3. A. F. Cheng *et al.*, *Space Sci. Rev.* in press (http://arxiv.org/abs/0709.4278)
4. S. Jaskulek *et al.*, *Proc. SPIE* **5906**, 409 (2005).
5. See supporting material on *Science* Online.
6. F. M. Flasar, P. J. Gierasch, *J. Atmos. Sci.* **43**, 2683 (1986).
7. M. J. S. Belton *et al.*, *Science* **274**, 377 (1996).
8. K. H. Baines *et al.*, *Science* **318**, 226 (2007).
9. T. Bosak, A. P. Ingersoll, *Icarus* **158**, 401 (2002).
10. S. J. Weidenschilling, J. S. Lewis, *Icarus* **20**, 465 (1973).
11. T. Y. Brooke, R. F. Knacke, Th. Encrenaz, P. Drossart, D. Crisp, *Icarus* **136**, 1 (1998).
12. K. H. Baines, R. W. Carlson, L. W. Kamp, *Icarus* **159**, 74 (2002).
13. M. H. Wong, G. L. Bjoraker, M. D. Smith, F. M. Flasar, C. A. Nixon, *Planet. Space Sci.* **52**, 385 (2004).
14. S. K. Atreya, A. S. Wong, K. H. Baines, M. H. Wong, T. C. Owen, *Planet. Space Sci.* **53**, 498 (2005).
15. C. C. Porco *et al.*, *Science* **299**, 1541 (2003).
16. See the Hubble Space Telescope press release, 28 June 2007, showing Jupiter's changing clouds at http://hubblesite.org/newscenter/archive/releases/solar-system/2007/25.

17. We thank the New Horizons mission team and our colleagues on the New Horizons science team. New Horizons is funded by NASA.

Supporting Online Material

www.sciencemag.org/cgi/content/full/318/5848/223/DC1
Materials and Methods
References

10 July 2007; accepted 19 September 2007
10.1126/science.1147618

REPORT

Polar Lightning and Decadal-Scale Cloud Variability on Jupiter

Kevin H. Baines,[1] Amy A. Simon-Miller,[2] Glenn S. Orton,[1] Harold A. Weaver,[3] Allen Lunsford,[2] Thomas W. Momary,[1] John Spencer,[4] Andrew F. Cheng,[3] Dennis C. Reuter,[2] Donald E. Jennings,[2] G. R. Gladstone,[5] Jeffrey Moore,[6] S. Alan Stern,[7] Leslie A. Young,[4] Henry Throop,[4] Padma Yanamandra-Fisher,[1] Brendan M. Fisher,[1] Joseph Hora,[8] Michael E. Ressler[3]

Although lightning has been seen on other planets, including Jupiter, polar lightning has been known only on Earth. Optical observations from the New Horizons spacecraft have identified lightning at high latitudes above Jupiter up to 80°N and 74°S. Lightning rates and optical powers were similar at each pole, and the mean optical flux is comparable to that at nonpolar latitudes, which is consistent with the notion that internal heat is the main driver of convection. Both near-infrared and ground-based 5-micrometer thermal imagery reveal that cloud cover has thinned substantially since the 2000 Cassini flyby, particularly in the turbulent wake of the Great Red Spot and in the southern half of the equatorial region, demonstrating that vertical dynamical processes are time-varying on seasonal scales at mid- and low latitudes on Jupiter.

Although lightning has been well documented on the gas giants Jupiter and Saturn at middle and low latitudes (*1*–*13*), it has never been observed in the polar regions. Here we report images of jovian lightning in both hemispheres poleward of 60° latitude obtained with the broadband (0.35- to 0.85-μm bandpass) New Horizons LORRI (Long Range Reconnaissance Imager) camera (*14*). On 3 March 2007, 16 observations were made of the planet's nightside, eight each of the north and south polar regions, consisting of 40 s of total exposure time for each pole. Thirteen lightning strike events were observed poleward of 60° (planetographic) latitude: six in the north polar region and seven in the south polar region (Table 1). The most poleward strikes were at 80°N and 74°S; three separate flashes observed were within 0.5° of 80°N.

Five other lightning strikes were seen near 52°N in 15 s of total exposure time during the three most equatorward observations, which covered latitudes southward to 45°N. Earlier spacecraft (*1*, *7*) had found that the most active lightning region was at latitudes near 50°N. Multiple strikes were seen during a 10-s period within a localized region covering less than 0.7° of longitude in a field of view greater than 35° of longitude. Here, one flash event in a 5-s exposure was followed immediately by at least three spatially separated events in the next 5-s interval (Fig. 1, top row). This corresponds to an average flash rate of 0.4/s (or greater) over 10 s and 0.6/s (or greater) over the single high-activity observation. These rates are greater than the 0.2/s rate previously observed during 60-s scanning exposures by Galileo (*6*, *8*).

Polar lightning flashes integrated over our 5-s exposure times are comparable in brightness to aurorae or the Io Flux Tube in the north polar region (Fig. 1) (*15*). Lightning flashes extend spatially over many pixels in our images (representative lightning flashes are seen in the lower row of images in Fig. 1); each pixel subtends about 28 km at the subspacecraft point on Jupiter (corresponding to 56 km latitudinally at 60°N latitude on the central meridian). This extent indicates that lightning emissions propagated through overlying scattering aerosols or that multiple flashes extended over a large area (typically >10,000 km²) during the exposure.

The average optical energies per strike in the north and south polar regions were nearly identical, 2.90×10^9 and 2.87×10^9 J for the north and south polar regions, respectively (Table 1) (*16*), despite the large (factor of 5) variability of lightning strength. These values agree well with the mean optical energy of strikes found in nonpolar storms: $2.5 \pm 1.9 \times 10^9$ J (*3*). The largest bolts observed were 9.3×10^9 J in the north and 15.7×10^9 J in the south, which is also in agreement with the largest flashes observed in nonpolar storms by Galileo (*6*). These largest

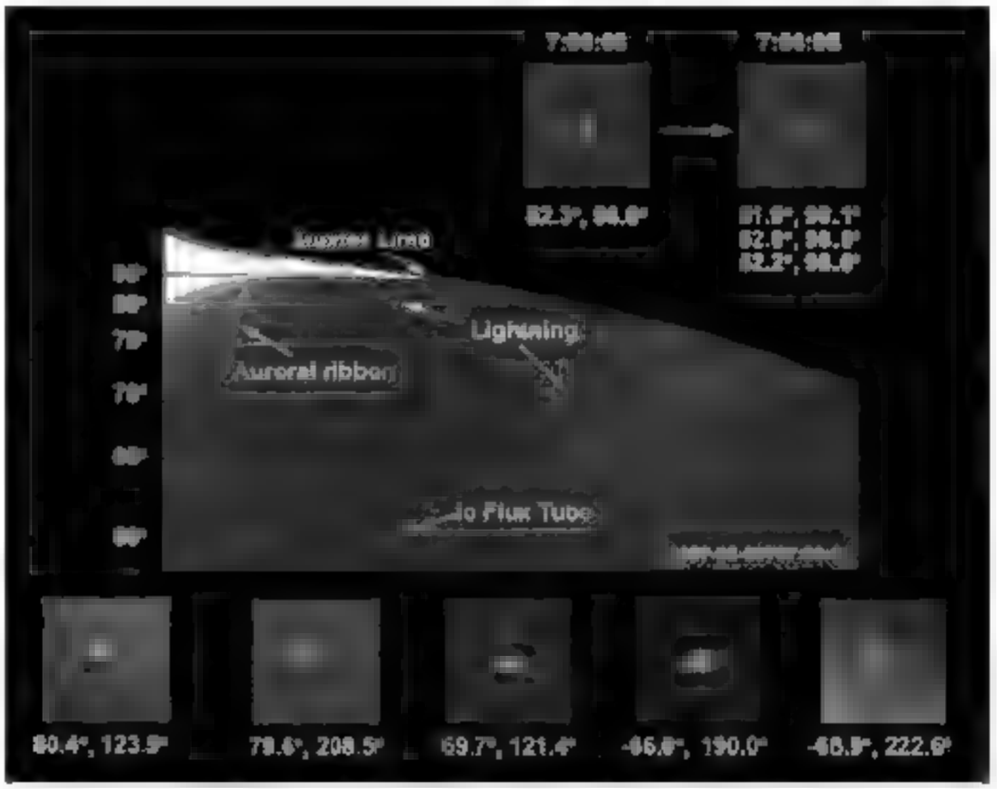

Fig. 1. Representative lightning flashes imaged by LORRI (*14*). (**Top row**) Multiple flashes are observed in consecutive 5-s exposures near 52°N latitude (planetographic). (**Middle**) Two north polar flashes observed simultaneously in a single 5-s exposure. (**Bottom row**) Flashes in both the north and south polar regions show substantial spatial extension, which is indicative of diffusive aerosol scattering of upwelling emission from near the 5-bar water condensation level.

[1]Jet Propulsion Laboratory, California Institute of Technology, 4800 Oak Grove Drive, Pasadena, CA 91109, USA. [2]NASA/Goddard Space Flight Center, Code 693, Greenbelt, MD 20771, USA. [3]The Johns Hopkins University Applied Physics Laboratory, 1110 Johns Hopkins Road, Laurel, MD 20723, USA. [4]Southwest Research Institute, 1050 Walnut Street, Suite 300, Boulder, CO 80302, USA. [5]Southwest Research Institute, 6220 Culebra Road, San Antonio, TX 78238, USA. [6]NASA/Ames Research Center, MS 245-3, Moffett Field, CA 94035-1000, USA. [7]NASA Science Mission Directorate, NASA Headquarters, Washington, DC 20546, USA. [8]Harvard-Smithsonian Center for Astrophysics, 60 Garden Street, Cambridge, MA 02138, USA.

bolts, located near 66° latitude in both hemispheres, were four to five times the mean size and >18 times the smallest strike energies observed in the respective polar regions.

The half-width half-maximum (HWHM) of a lightning flash (the distance over which the lightning radiance falls to half of its peak value) is a measure of the depth of the flash. The New Horizons values (a mean of 92 km) are comparable to those seen in previous investigations (*6*, *8*, *17*) in which flash depths were near the 5- to 8-bar level of water condensation (*18*). Thus, the source of the lightning in our observations was probably also within the deep water-rich regions of Jupiter.

Previous observations found lightning predominantly near 14°N and 50°N (planetographic) and less often at 33°N and 60°N. These appear to mark the southern edges of westward-moving jets (*2*, *4*, *6*) and are regions with notable cyclonic shear. Similarly, the three lightning strikes we saw at the highest latitudes (69° to 71°N, planetographic) coincided with the southern edge of the most northerly westward jet near 72°N discovered by Cassini (*19*).

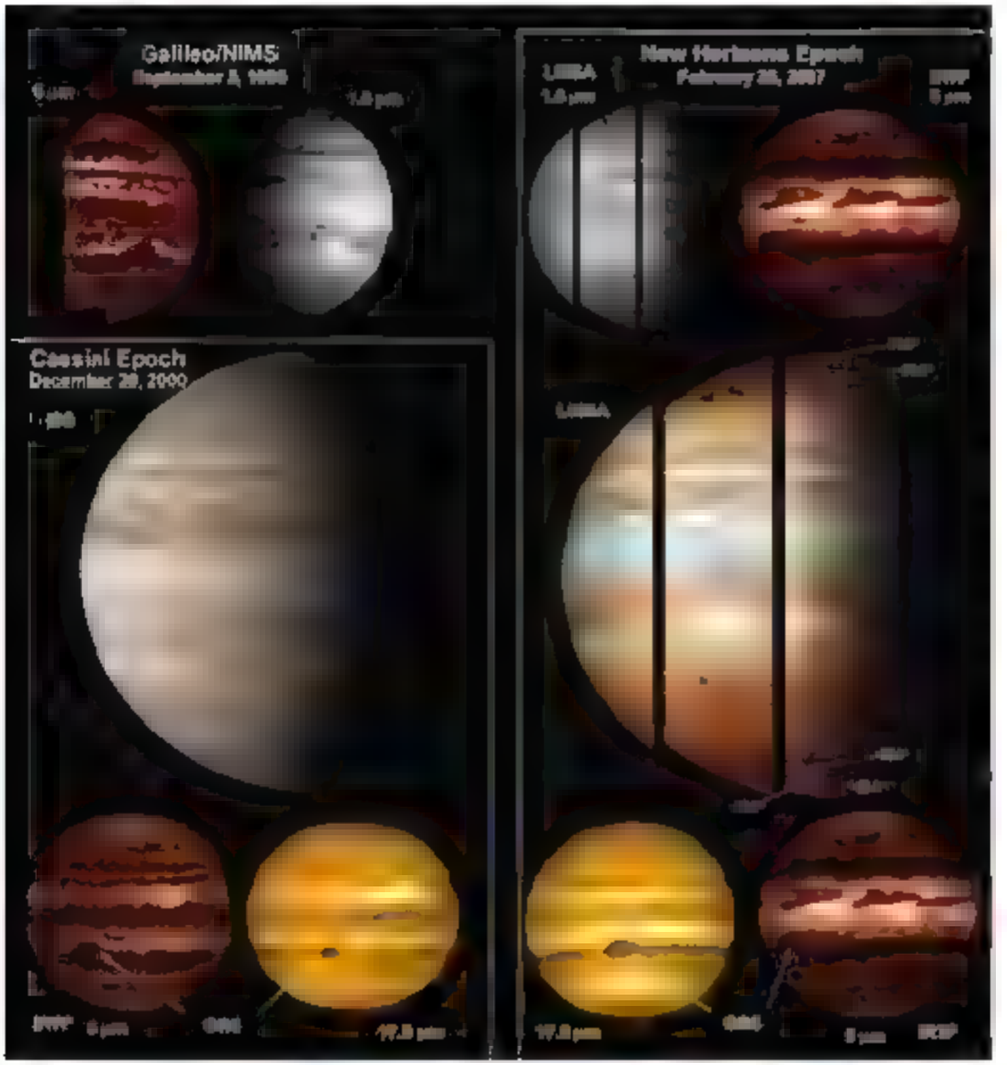

Fig. 2. Global changes in Jupiter's structure: September 1996 (top left) and December 2000 (lower left) versus February 2007 (right). (**Top row**) Near-infrared views of Jupiter from Galileo NIMS in 1996 at 5 μm (red image) and 1.6 μm (gray image) are compared to similar 2007 New Horizons images. Substantial differences in cloud cover are seen in the south equatorial region and northwest of the Great Red Spot (GRS). Similar differences are seen in comparing the 2000 Cassini view (lower left) with the 2007 New Horizons view (right). Here, three global views are shown: three-color images in reflected sunlight (large images), 5-μm thermal imagery (red images, bottom row), and 17.9-μm thermal imagery (orange images, bottom row). The near-natural–color Cassini image is compared to a New Horizons image composed of 1.59-μm (red), 1.90-μm (green), and 1.85-μm (blue) images, emphasizing cloud altitudes and cloud opacities (*28*). The near-uniform thick equatorial cloud structure in 2000 is more complex in 2007, with distinct latitudinal variability in cloud opacity. The increased brightness of the 2007 5-μm images (red images, bottom row) confirms cloud thinning. Little change is seen in the 17.9-μm images (orange), which map 200-mbar-level temperatures. Arrows with labels show several latitudes where polar lightning has been discovered.

These locations are characterized by vigorous upper-level convective clouds and potentially large instabilities (*6*, *20*, *21*). Lightning generally appears near the 5- to 6-bar level (*6*, *8*, *17*), where upwelling water can condense, triggering strong convection and thunderstorms (*2*, *5*, *6*). Vertical transport may be aided by three-dimensional planetary waves, such as have been observed near the equator (*22*, *23*), and by colliding air masses as in the turbulent region to the northwest of the Great Red Spot. Both mechanisms have been observed to produce rapid formation of optically thick ammonia condensation clouds (*23*) and in the latter case, lightning at depth (*24*).

In the southern polar region, only half of the lightning strikes occurred in the cyclonic shear or maximum westward-moving jet regions. In particular, the strikes at 60.2°S and 66°S were on the anticyclonic sides of the two most southerly eastward jets observed by Cassini (*19*). The most polar strikes near 80°N and 74°S were located in regions of weak winds (<10 m/s) and thus also may not be consistent with the westward wind paradigm. The remaining strikes at 68.4°S, 68.9°S, and 71.2°S are consistent with it.

The distribution and power of jovian lightning are different from those on Earth (*5*, *6*). Rather than being concentrated within tens of degrees of the equator, on Jupiter lightning is most optically active near 50°N as observed by every investigating spacecraft (*1*–*7*), now including New Horizons. The distribution of Jovian lightning to high latitudes is probably a consequence of the relative strength of internal heat as compared to solar heating over latitude (*2*, *5*): As one proceeds poleward, solar heating of the atmosphere decreases, allowing the internal heat of Jupiter to power strong vertical dynamics near the 5-bar condensation level of water (*25*, *26*).

Before the New Horizons observations, more and stronger flashes were seen in the northern hemisphere than in the southern at nonpolar latitudes (*5*, *6*). Voyager 2 saw no southern lightning, despite an intense observational campaign (*5*). Such hemispherical differences may be a consequence of slight differences in solar insolation or atmospheric stability. In contrast, New Horizons observed nearly identical rates of lightning strikes in the polar regions (0.15 strikes/s in the north versus 0.18 strikes/s in the south). In each case, about one-fifth of the polar region was viewed at any one time. The mean optical flash energies of the individual northern and southern lightning strikes agree to within 2%. If these average values are representative of all longitudes, the average lightning power per area was about 0.6×10^{-6} and 0.5×10^{-6} W m^{-2} poleward of 60° latitude for the south and north polar regions, respectively. These values are comparable to the optical power measured previously for the nonpolar regions: $0.3\ 10^{-6}$ W m^{-2} (*6*) and $0.32\ 10^{-6}$ W m^{-2} (*3*).

Thus, over our small sampling of time and longitude, the lightning frequency and optical

power in the south and north polar regions agree to within 20%. This similarity suggests that mechanisms that lead to large mid-latitude differences in lightning activity are not important in the polar regions. This view is supported by the Galileo observation (*6*) that, averaged over 5° latitude bins, the greatest number of storms per unit area is observed in the southern hemisphere near 55° latitude (planetographic), but for the broader 45° to 60° latitude region, the northern and southern hemisphere values are comparable. Together, the New Horizons and Galileo high-latitude observations give additional support to the notion that internal heat drives convection and dynamics more effectively in sunlit-poor polar and high-latitude regions than in sunlit-rich equatorial latitudes.

Additional insight into the nature of convection and vertical dynamics on Jupiter is provided by New Horizons global images. These show that vertical dynamics is variable on decadal scales at low and middle latitudes when compared to similar imagery obtained in September 1996 by the Galileo Orbiter and in December 2000 by Cassini-Huygens. The Linear Etalon Infrared Spectral Imager (LEISA) (*27*) on New Horizons obtained a high spatial-resolution near-infrared global-scale map of Jupiter, timed to provide nearly the same observational and lighting geometry of the Great Red Spot as in the best Galileo near-infrared and Cassini visual imagery (Fig. 2) (*28*).

Distinct differences in cloud cover are seen when directly comparing 1.6-μm images obtained by the Near-Infrared Mapping Spectrometer (NIMS) on Galileo in 1996 (*23*) and the 2007 New Horizons images. This pseudo-continuum wavelength accentuates views of tropospheric clouds found near the 0.5- to 2-bar level. In the 2007 image, these clouds are notably scarcer than in the 1996 image in both the south equatorial region and in the "turbulent wake" region northwest of the Great Red Spot. In 5-μm thermal imagery, the 2007 ground-based images show increased flux, similarly due to the thinning of tropospheric clouds, which allows Jupiter's 5-μm thermal emissions, generated at depth near the 8-bar level, to readily escape out of the atmosphere.

Similar differences in cloud cover are seen between the 2000 Cassini images and the 2007 New Horizons images. The equatorial region is uniformally cloudy in the 2000 Cassini three-color image, whereas the three-color Cassini image shows few clouds in the southern half of this region. Again, the turbulent wake region to the northwest and west of the Great Red Spot is remarkably quiescent in the 2007 image, in stark contrast to the turbulent region of swirling clouds seen in the 2000 image by Cassini and observed consistently for more than 20 years by Voyager, Galileo, and Cassini-Huygens (*1*, *19*, *23*, *29*). This region has been observed to produce the largest spectroscopically identifiable ammonia clouds on Jupiter (*23*), indicative of powerful vertical transport delivering relatively large quantities of ammonia gas to the upper atmosphere. There, large-particle thick clouds are produced on a time scale of a day or less. Yet the 2007 LEISA images show this area almost clear of clouds. Spectroscopic searches for ammonia in this region, such as were successfully conducted with the Galileo NIMS instrument (*23*), show no spectroscopic evidence of ammonia clouds, although such clouds were seen in other regions by LEISA (*30*). The latitudinal region to the west was also clear of thick convective clouds, out to the western limb.

The 5-μm ground-based observations of Jupiter, taken contemporaneously with the Cassini and New Horizons images (Fig. 2, bottom row), confirm the changes in cloud cover. In contrast, the 17.9-μm images of Jupiter, which are indicative of temperatures near the 200-mbar level just below the tropopause, shows few changes between 2000 and 2007.

Thus, the changes seen in 2007 are indicative of changes restricted to tropospheric depths underneath the 200-mbar level. The observed regional changes in mid- and low-latitude cloud properties suggest changes in vertical dynamics and transport, including convection, between ~400 mbar and perhaps several bars. The cause of such changes in vertical dynamics is unclear, but they may be due to variations in atmospheric stability at depth, perhaps due to variations in water content and/or the emission of internal heat. Because the primary driver of Jupiter's global circulation at depth is Jupiter's own internal heat, we suspect that the atypically quiescent view of Jupiter observed by New Horizons and ground-based observations in early 2007 will be relatively short-lived as the planet reverts to its typically dynamic state.

Table 1. Record of lightning strikes observed by New Horizons.

Planetographic latitude	W. longitude (system III)	Image SOC root name	Time on 3 March 2007 (UTC)	Energy (10^9 J)	HWHM of flash (pixels)	(km)
80.4°N	123.5	lor_0035211303_0x630_sci_1	07:03:02.886	1.46	1.84	81.0
80.1°N	132.5	lor_0035211308_0x630_sci_1	07:03:07.886	0.79	2.75	121.1
79.6°N	208.5	lor_0035219108_0x630_sci_1	09:13:07.886	2.67	2.17	95.6
70.3°N	89.0	lor_0035211663_0x630_sci_1	07:09:02.886	2.64	1.89	83.3
70.1°N	118.3	lor_0035211303_0x630_sci_1	07:03:02.886	0.50	1.51	66.3
69.7°N	121.4	lor_0035211483_0x630_sci_1	07:06:02.886	9.31	2.25	99.1
52.3°N	98.0	lor_0035211483_0x630_sci_1	07:06:02.886	3.06	2.00	88.3
52.2°N	98.6	lor_0035211488_0x630_sci_1	07:06:07.886	0.34	1.97	86.8
52.0°N	98.5	lor_0035211488_0x630_sci_1	07:06:07.886	1.10	1.79	78.8
51.9°N	98.1	lor_0035211488_0x630_sci_1	07:06:07.886	1.93	1.87	82.6
51.3°N	188.8	lor_0035219288_0x630_sci_1	09:16:07.886	2.23	2.19	99.1
60.2°S	116.7	lor_0035211843_0x630_sci_1	07:12:03.000	0.99*	1.55	68.3
66.0°S	190.0	lor_0035219643_0x630_sci_1	09:22:02.886	15.66	2.76	125.0
68.4°S	118.8	lor_0035211848_0x630_sci_1	07:12:07.885	0.64	2.23	100.8
68.9°S	222.6	lor_0035219648_0x630_sci_1	09:22:07.886	0.93	2.34	105.7
71.2°S	203.1	lor_0035219463_0x630_sci_1	09:19:02.885	0.60	1.77	79.9
73.7°S	207.1	lor_0035219648_0x630_sci_1	09:22:07.886	1.28	2.34	105.7

*Sum of double flash.

References and Notes

1. B. A. Smith *et al.*, *Science* **204**, 951 (1979).
2. A. F. Cook, T. C. Duxbury, G. E. Hunt, *Nature* **280**, 794 (1979).
3. W. J. Borucki, A. Bar-Nun, F. L. Scarf, A. F. Cook II, G. E. Hunt, *Icarus* **52**, 492 (1982).
4. J. A. Magalhães, W. J. Borucki, *Nature* **349**, 311 (1991).
5. W. J. Borucki, J. A. Magalhães, *Icarus* **96**, 1 (1992).
6. B. Little *et al.*, *Icarus* **142**, 306 (1999).
7. U. A. Dyudina *et al.*, *Icarus* **172**, 24 (2004).
8. U. A. Dyudina *et al.*, *Icarus* **160**, 336 (2002).
9. J. W. Warwick *et al.*, *Science* **212**, 239 (1981).
10. J. W. Warwick *et al.*, *Science* **215**, 582 (1982).
11. D. A. Gurnett *et al.*, *Science* **307**, 1255 (2005).
12. G. Fischer *et al.*, *Icarus* **190**, 528 (2007).
13. U. A. Dyudina *et al.*, *Icarus* **190**, 545 (2007).
14. A. F. Cheng *et al.*, *Space Sci. Rev.*, in press (available at http://arxiv.org/abs/0709.4216v1).
15. Nighttime polar images were obtained with LORRI from 5.6 × 10^6 to 5.8 × 10^6 km over a 2.3-hour period on 3 March 2007 with 5.0-s exposure times. Pixel resolution is 28 km/pixel on the sky, corresponding to 50 km in latitude at 60°N.
16. Lightning strikes could be distinguished from cosmic ray hits and auroral features by their distinctive shapes. Because of slight spacecraft nodding motions, constant-brightness point sources such as stars produce curtate features in our 5-s exposures, unlike our short-lived lightning strikes. Lightning flashes produce a bright central flash surrounded by a halo of light due to diffuse scattering by the overlying atmosphere. Lightning energies were calculated using the spectral irradiance of jovian lightning determined by Borucki *et al.* (*31*). The latitudes and longitudes of lightning flashes are determined by a limb/terminator fitting program that generates the planetary ellipse based on the range, camera focal length, and pixel scale. With sufficient contrast between the sky and the planet, the ellipse center is located with an iterative least-squares fit, typically with a precision of 0.1 pixel or better. For low-contrast images, the ellipse is placed manually with an uncertainty of a few pixels.

17. W. J. Borucki, M. A. Williams, *J. Geophys. Res.* **91**, 9893 (1986).
18. S. J. Weidenschilling, J. S. Lewis, *Icarus* **20**, 465 (1973).
19. C. P. Porco *et al.*, *Science* **299**, 1541 (2003).
20. A. P. Ingersoll *et al.*, *J. Geophys. Res.* **86**, 8733 (1981).
21. S. S. Limaye, *Icarus* **65**, 335 (1986).
22. M. Allison, *Icarus* **83**, 282 (1990).
23. K. H. Baines, R. W. Carlson, L. W. Kamp, *Icarus* **159**, 74 (2002).
24. P. J. Gierasch *et al.*, *Nature* **403**, 628 (2000).
25. A. P. Ingersoll, C. C. Porco, *Icarus* **35**, 27 (1978).
26. L. A. Pirraglia, *Icarus* **59**, 169 (1984).
27. D. C. Reuter *et al.*, *Space Sci. Rev.*, in press (available at http://arxiv.org/abs/0709.4281v1).
28. Galileo NIMS global maps were acquired on 5 September 1996 from a distance of 3.98×10^6 km, a phase angle of 64.3°, a subsolar latitude near 2°S, and a subspacecraft latitude near 0°. A Cassini Imaging Science Subsystem global image was acquired on 29 December 2000 from a distance of approximately 1.0×10^6 km, a phase angle near 90°, a subsolar latitude near 2.9°N, and a subspacecraft latitude near 3.5°N. A New Horizons LEISA global map was acquired on 28 February 2007 in three north/south scans over a 47-min period beginning at 01:40 universal time (UT) on 28 February from an altitude of 2.32×10^6 km, a phase angle of 76°, a subsolar latitude near 2.9°S, and a subspacecraft latitude of 8.4°S. The three-color image (middle right of Fig. 2) is composed of a 3.59-μm continuum wavelength image (red), a 3.90-μm wavelength image of moderate atmospheric gas absorption (green), and a 3.85-μm wavelength image of relatively strong absorption gas (blue). Blue accentuates high-altitude clouds and hazes above the 300 mbar level, green depicts clouds most prominently near and above the 600-mbar level, and red shows clouds down to several bars. The 4.8-μm pseudo-color images were acquired at NASA's Infrared Telescope Facility (IRTF) at 10:08 UT on 30 December 2000 by the National Science Foundation camera (NSFCam) camera and on 18 March 2007 at 14:53 UT by the NSFCam2 camera. The 17.9-μm images were acquired by the Jet Propulsion Laboratory's MIRLIN (Mid-Infrared Large-well Imager) camera (*37*) at 5:50 UT on 29 December 2000 and by the MIRSI (Mid-Infrared Spectrometer and Imager) camera/spectrometer (*33*) at 16:12 UT on 18 March 2007.
29. A. R. Vasavada *et al.*, *Icarus* **135**, 265 (1998).
30. D. C. Reuter *et al.*, *Science* **318**, 223 (2007).
31. W. J. Borucki, C. P. McKay, D. Jebens, H. S. Lakkaraju, C. T. Vanajakshi, *Icarus* **123**, 336 (1996).
32. M. E. Ressler *et al.*, *Exp. Astron.* **3**, 277 (1994).
33. L. Deutsch, *et al.*, *SPIE* **4841**, 106 (2002).
34. We thank the New Horizons mission and science teams. New Horizons is funded by NASA. G.S.O., P.Y.F., and B.M.F. were visiting astronomers at the IRTF, which is operated by the University of Hawaii under Cooperative Agreement no. NCC 5-538 with NASA, Science Mission Directorate, Planetary Astronomy Program. Thanks to E. Tollestrup and M. Connelley for IRTF instrument orientation and J. Kemerer and J. Yang for assistance in reducing the observations. Much of the work described in this paper was carried out at the Jet Propulsion Laboratory, Pasadena, CA, under contract with NASA.

17 July 2007; accepted 19 September 2007
10.1126/science.1147912

REPORT

Jupiter's Nightside Airglow and Aurora

G. Randall Gladstone,[1]* S. Alan Stern,[2] David C. Slater,[1] Maarten Versteeg,[1] Michael W. Davis,[1] Kurt D. Retherford,[1] Leslie A. Young,[3] Andrew J. Steffl,[1] Henry Throop,[1] Joel Wm. Parker,[3] Harold A. Weaver,[4] Andrew F. Cheng,[2] Glenn S. Orton,[5] John T. Clarke,[6] Jonathan D. Nichols[6]

Observations of Jupiter's nightside airglow (nightglow) and aurora obtained during the flyby of the New Horizons spacecraft show an unexpected lack of ultraviolet nightglow emissions, in contrast to the case during the Voyager flybys in 1979. The flux and average energy of precipitating electrons generally decrease with increasing local time across the nightside, consistent with a possible source region along the dusk flank of Jupiter's magnetosphere. Visible emissions associated with the interaction of Jupiter and its satellite Io extend to a surprisingly high altitude, indicating localized low-energy electron precipitation. These results indicate that the interaction between Jupiter's upper atmosphere and near-space environment is variable and poorly understood; extensive observations of the day side are no guide to what goes on at night.

Jovian dayside airglow and aurora have been extensively observed from Earth orbit since their initial detection during the Voyager flybys in 1979 (*1*–*8*). On 3 March 2007 between 06:28 and 09:58 universal time (UT) (about 3 days after closest approach on 28 February at 05:43 UT) during the flyby of Jupiter, the New Horizons spacecraft made several high phase-angle observations of nightside airglow (nightglow) and auroral emissions. Because the night side has not been well observed, long-standing questions remain, including the nature of Jupiter's 121.6-nm (Lyα) nightglow (for example, is it similar to the tropical arcs of Earth?), how the nightside auroras are different from those on the day side, and what the smallest structures in satellite footprint auroras are and what governs their size.

Jupiter's nightside hydrogen Lyα airglow was seen by Voyager 2 in 1979. Data from its ultraviolet (UV) spectrometer showed substantial non-auroral emissions well past the terminator, which were interpreted to result from low-latitude particle precipitation (*1*, *2*). Low-latitude particle precipitation was also suggested as a way to maintain Jupiter's large exospheric temperature (*9*) and to account for low-latitude x-ray emission (*10*). In contrast, several nightside east-west scans by the Alice UV spectrograph on New Horizons (*11*, *12*) indicate that the Lyα nightglow is faint, and there was no evidence of emission from high solar zenith angle regions on the night side that are far from the auroral regions (Fig. 1). Instead, the emissions are well fit by scattered solar Lyα radiation from the bright limb (*13*). This finding implies that no substantial low-latitude particle precipitation is currently occurring and suggests that either the Voyager results were spurious or Jupiter has changed between the two epochs (the Voyager flybys were during solar maximum, whereas the New Horizons flyby occurred during solar minimum).

Observations of Jupiter's night side also provide a way to search for the presence of tropical arcs, which at Earth are bands of emission on either side of the magnetic equator resulting from the recombination of ions and are useful tracers of ionospheric dynamics (*14*, *15*). The Lyα dayglow of Jupiter is known from Voyager Ultraviolet Spectrometer results to have a bulge of brightness that follows the magnetic dip equator (*16*). A possible explanation for the Lyα bulge is extra scattering of solar Lyα radiation from a hot hydrogen population resulting from H_3^+ recombination on either side of the magnetic equator; that is, the bulge might resolve into tropical arcs if seen at higher spatial resolution (*17*). Although no large-scale Lyα nightglow was seen by New Horizons, there are indications of excess brightening near the terminator, especially in regions where tropical arcs might be expected (such as near the end points of the low-latitude magnetic field line traces in Fig. 1).

Most of Jupiter's UV aurora results from collisions of energetic magnetospheric electrons with atmospheric hydrogen, leading to emissions at wavelengths from 80 to 165 nm. However, the more energetic electrons penetrate deeper into the atmosphere, where the resulting shorter-wavelength UV auroral emissions can be partially absorbed by atmospheric methane. The color ratio is defined as the ratio of the integrated auroral brightness from 155.7 to 161.9 nm over that from 123.0 to 130.0 nm (*18*, *19*) and is used as a proxy for the mean energy of auroral electrons. A larger color ratio results from preferential absorption of shorter-wavelength UV photons by hydrocarbons (primarily CH_4) overlying a deeper layer of auroral emissions. Data from the Space Telescope Imaging Spectrograph (STIS) on the Hubble Space Telescope (HST) (*20*) and the Ultraviolet Imaging Spectrograph on Cassini (*21*) show that typical color ratios were 3.5 to 6.0 and that the largest ratios (and presumably

[1]Southwest Research Institute, San Antonio, TX 78238, USA. [2]NASA Headquarters, Washington, DC 20546, USA. [3]Southwest Research Institute, Boulder, CO 80302, USA. [4]The Johns Hopkins University Applied Physics Laboratory, Laurel, MD 20723, USA. [5]Jet Propulsion Laboratory, Pasadena, CA 91109, USA. [6]Boston University, Boston, MA 02215, USA.

*To whom correspondence should be addressed. E-mail: rgladstone@swri.edu

the most energetic precipitating electrons) occurred over the morning or dawn side of the northern main auroral oval (as seen from Earth). In contrast, both the total UV brightness and the color ratios inferred from the Alice nightside scans (Fig. 2) are largest on the dusk side of the northern main auroral oval (regardless of the orientation of the oval in system III longitude). The implication is that variations in the mean energy of the precipitating electrons do not rotate with the planet in system III (along with the pattern of the main oval), but instead are controlled by solar local time, with the post-dawn daytime (*20*, *21*) and post-dusk nighttime (Fig. 2) regions experiencing the hardest auroral electrons. The electrons responsible for the post-dusk nighttime emissions seen by Alice are most likely connected to the dusk flank of the magnetosphere, which is likewise approximately fixed in

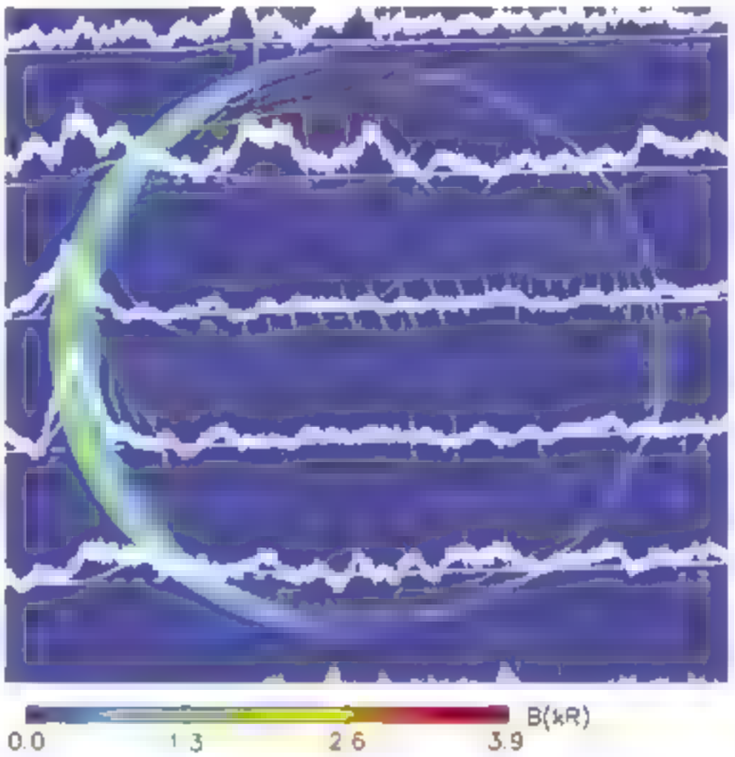

Fig. 1. East-west disk scans of the atomic hydrogen Lyα nightglow brightness across Jupiter obtained by the New Horizons Alice UV spectrograph on 3 March 2007. The long axis of the Alice 0.1° × 4° slit was aligned north-south, and the scan proceeded from the night side (right) toward the daylit crescent (left). The tracks (dashed white lines) and model-simulated Lyα brightnesses (solid white lines) for specific 0.1° × 0.3° pixels (row numbers are given at the right; the Alice boresight is located in the row-16 pixel) along the Alice slit and examples of their footprints (white boxes) are indicated on a simulated Lyα image (as would be seen from the spacecraft range, latitude, and system III longitude of 78.9 Jovian radii, 2.1°N, and 133.0°, respectively). Alice-measured Lyα brightnesses (starting at 06:28 UT at the spacecraft, at a phase angle of 153.6°) are shown (vertical white lines, representing measured values ±1σ during 10-s intervals); both model and measured brightnesses use their associated tracks (dashed white lines) as abscissas. The color bar at the bottom provides model image brightnesses in kilorayleighs (kR). The ovals of the main UV aurora and Io's orbit footprint are shown in red and orange, respectively. Also shown are VIP4 model (*31*) surface magnetic field strengths in Gauss (green contours) and model traces of low-latitude magnetic field lines having peak altitudes of 1500 km above the 1-bar pressure level along the magnetic dip equator, plotted every 5° of longitude (green vertical lines). The white dotted lines are planetographic latitude and longitude at 30° intervals.

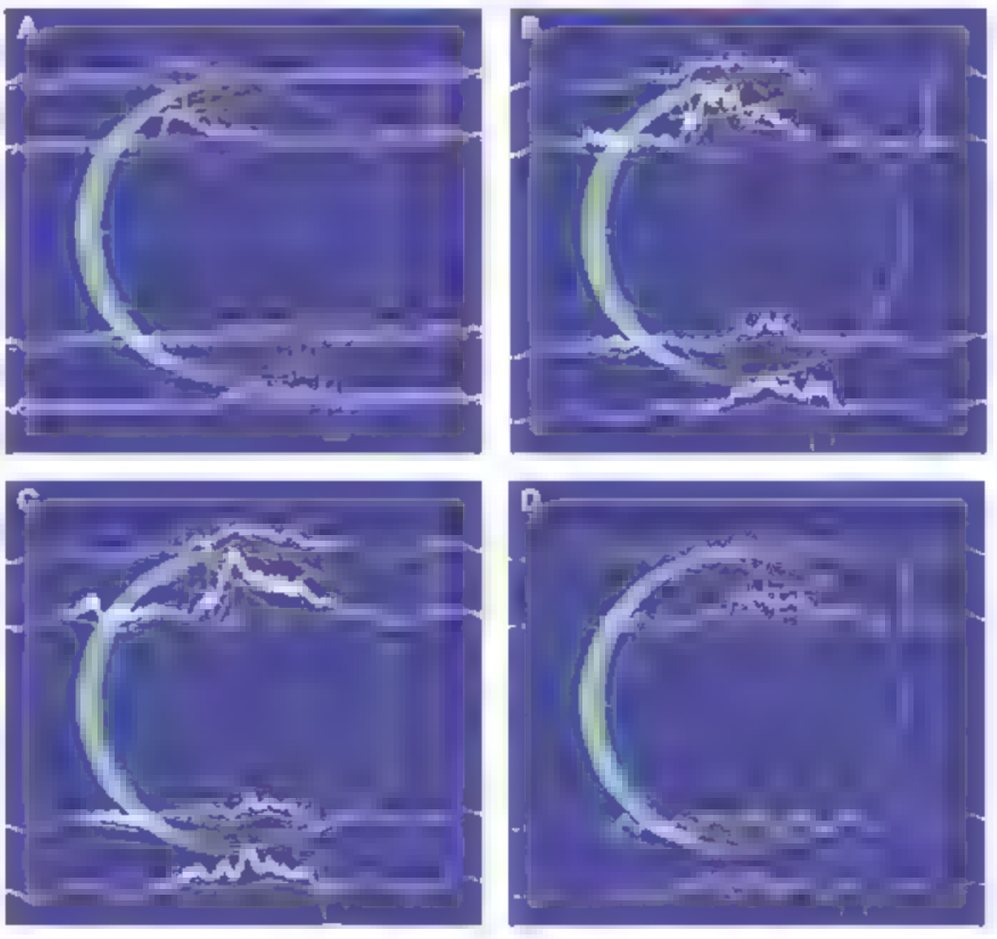

Fig. 2. Four east-west nightside auroral scans obtained by the New Horizons Alice UV spectrograph on 3 March 2007, starting at 06:28 UT (**A**), 07:28 UT (**B**), 08:38 UT (**C**), and 09:28 UT (**D**) (at the spacecraft). Auroral brightnesses in two wavelength bands are shown superposed on simulated Lyα images (Fig. 1). The ±1σ measured brightnesses are shown for emissions with wavelengths in the range from 155.7 to 161.9 nm (green lines) and in the range from 123.0 to 130.0 nm (rust-colored lines). The ratio of these two brightnesses gives the "color ratio" (*18*, *19*): a common proxy for auroral electron energy. The ±1σ derived color ratios along each scan are shown (solid white lines), and a numbered grid on the second scan from the top provides the scale (measured from the scan tracks shown by the white dashed lines; non-uniform tracks result from spacecraft attitude corrections). A white asterisk marks the location of maximum color ratio along each track. Other features are as described for Fig. 1. The peak color ratios observed in Alice row 16 (the second row from the top in each panel) are 4.5 (A), 8.5 (B), 8.1 (C), and 4.1 (D).

solar local time (22). This observation is surprising; however, other features of the main oval are also modified by local time, such as the bright dawn storms, which are always seen near the dawn limb (23). Likewise, the width of the main oval seems to always be narrower in the morning than the evening, irrespective of longitude (24). The Alice data imply that the mean energy of precipitating electrons varies with local time across the night side of Jupiter.

The Io Flux Tube (IFT) comprises Jovian magnetic field lines that are transiently interacting with the atmosphere of the satellite Io. At the footprint of the IFT in Jupiter's upper atmosphere, a spot and associated downstream tail of emission are seen in UV (and near-infrared) wavelengths (25, 26). The limb profile of the southern IFT footprint was observed (Fig. 3) by the New Horizons Long Range Reconnaissance Imager (LORRI) high-resolution visible imager during a series of 16 5-s exposures meant to establish peak auroral emission altitudes where the ovals cross the limb. Although the signal-to-noise ratio of the images is low, at ~28 km per pixel, this resolution is comparable to images obtained by Galileo (24). The visible emissions, which are probably mostly due to the Balmer series of atomic H lines and low-level H_2 bands, extend to high altitudes (>1000 km) above the limb. The integrated signal in the IFT profile measured at the spacecraft is 5×10^{-10} to 7×10^{-10} erg/cm^2/s; the emitted power is ~0.1 to 0.15 GW. The high altitudes indicate that either the electron precipitation was relatively soft or the atmosphere was highly disturbed, or both. Indeed, substantial soft electron precipitation would be expected to greatly disturb the high-altitude atmosphere (because of its low heat capacity), if the region affected weren't so localized (27). In contrast, previous HST STIS measurements of the IFT footprint color ratio are in the range from 1.7 to 2.3, showing the effects of absorption by methane and indicating that most of the precipitating electrons in the IFT penetrate to much lower altitudes, between ~200 and 300 km (28). The width of the IFT flux tube emission seen in Fig. 3 has an overall value of about 400 km, which maps to about three Io diameters at the satellite (that is, localized near Io). In addition, there appears to be a parallel substructure to the emission, consistent with the expected current loop connecting to the sub-Jupiter and anti-Jupiter points on Io (29, 30). However, it is also possible that the substructure results from the projection of a secondary spot located farther downstream (at lower longitude). A spot of emission noticeable on the limb to the left of the main emissions could be a precursor spot (in which case it is produced by electrons that are substantially more energetic than those responsible for the main IFT emissions), or it could be the highest-altitude emissions of a spot farther downstream just peaking above the limb, although that seems unlikely. UV images obtained by the Advanced Camera for Surveys (ACS) on the HST during the time of the New Horizons observations also show the IFT emissions at high altitude. The HST ACS data (100-s exposures, 125 km per pixel) do not exhibit multiple spots, although the observing geometry is poor (supporting online material). It may be that the IFT auroral electrons are generally less energetic when Io is on the night side of Jupiter. Further analysis of the IFT footprint morphology (for example, using the extensive data set of HST ACS observations) may be useful for determining whether there is a local time dependence in the vertical extent of the emissions.

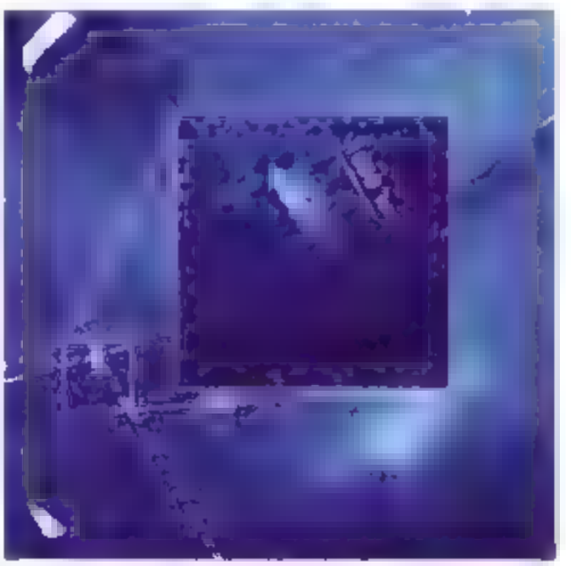

Fig. 3. IFT footprint limb profile as imaged by the New Horizons LORRI panchromatic camera in a 5-s exposure of Jupiter's nightside south auroral region on 3 March 2007, centered at 09:19:07.9 UT. Scattered sunlight from the nearby bright limb (the solar elongation was −26°) results in many artifacts at this stretch of the image, many of which have been removed (and several are covered by the inset image). The IFT profile (highlighted in the inset) shows up near its expected location in four separate images, of which this is the sharpest. The predicted location of the IFT footprint is just beyond the limb, as indicated by the white cross (at a planetographic latitude of 74.1°S and a system II longitude of 135.9°; the spacecraft was at a range of 5,810,940 km, a latitude of 2.2°N, and a system III longitude of 229.6°). Projected IFT magnetic field lines are shown (dashed lines); the right line connects to a location separated from the center of Io by 3642 km; that is, one Io diameter, toward Jupiter; the left line to a location the same separation from the center of Io away from Jupiter. A 10° graticule of Jupiter is overplotted with planetographic latitudes and longitudes at 1° spacing; the 180° meridian is highlighted and the limb of Jupiter is indicated (long-dashed line). The inset includes a scale bar that shows that the IFT emissions extend vertically over 1000 km above the limb of Jupiter. The inset is smoothed over 3 × 3 pixels; the brighter parts of the IFT footprint have a signal-to-noise ratio (SNR) of ~3.9, whereas the entire feature is detected at a SNR of ~33.

References and Notes

1. A. L. Broadfoot *et al.*, *J. Geophys. Res.* **86**, 8259 (1981).
2. J. C. McConnell, B. R. Sandel, A. L. Broadfoot, *Icarus* **43**, 128 (1980).
3. A. Bhardwaj, G. R. Gladstone, *Rev. Geophys.* **38**, 295 (2000).
4. T. G. Slanger, B. C. Wolven, in *Atmospheres in the Solar System: Comparative Aeronomy*, M. Mendillo, A. Nagy, J. H. Waite Jr., Eds. (American Geophysical Union, Washington, DC, 2002), pp. 77–93.
5. D. Grodent *et al.*, *J. Geophys. Res.* **108**, 1366 (2003).
6. D. Grodent *et al.*, *J. Geophys. Res.* **108**, 1389 (2003).
7. J. T. Clarke *et al.*, in *Jupiter: The Planet, Satellites and Magnetosphere*, F. Bagenal, T. E. Dowling, W. B. McKinnon, Eds. (Cambridge Univ. Press, Cambridge, 2004), pp. 639–670.
8. R. V. Yelle, S. Miller, in *Jupiter: The Planet, Satellites and Magnetosphere*, F. Bagenal, T. E. Dowling, W. B. McKinnon, Eds. (Cambridge Univ. Press, Cambridge, 2004), pp. 185–218.
9. D. M. Hunten, A. J. Dessler, *Planet. Space Sci.* **25**, 817 (1977).
10. J. H. Waite Jr. *et al.*, *Science* **276**, 104 (1997).
11. S. A. Stern *et al.*, *Proc. SPIE* **5906**, 358 (2005).
12. O. C. Slater *et al.*, *Proc. SPIE* **5906**, 368 (2005).
13. The data reduction uses an effective area for Lyα of 0.007 cm^2 as determined from comparison of International Ultraviolet Explorer and Alice cruise-phase observations of the bright UV stars γ Gru (HD 209771) and ρ Leo (HD 91316). The model used is described in (*27*) and calculates resonantly scattered sunlight, for a Jupiter atmosphere with 0.1% hot hydrogen, which provided the best fit to Galileo data. The solar Lyα flux (~3.8 × 10^{11} photons/cm^2/s at Earth), corrected for the distance to Jupiter and the angle between Earth and Jupiter as seen from the Sun, is from Solar Radiation and Climate Experiment data at http://lasp.colorado.edu/sorce/data/data_product_summary.htm.
14. E. V. Appleton, *Nature* **157**, 691 (1946).
15. A. B. Christensen *et al.*, *J. Geophys. Res.* **108**, 1451 (2003).
16. A. J. Dessler, B. R. Sandel, S. K. Atreya, *Planet. Space Sci.* **29**, 215 (1981).
17. G. R. Gladstone *et al.*, *Planet. Space Sci.* **52**, 415 (2004).
18. Y. L. Yung *et al.*, *Astrophys. J.* **254**, 165 (1982).
19. T. A. Livengood, H. W. Moos, G. E. Ballester, R. M. Prangé, *Icarus* **97**, 26 (1992).
20. J. Gustin, D. Grodent, J. C. Gérard, J. T. Clarke, *Icarus* **157**, 91 (2002).
21. J. M. Ajello *et al.*, *Icarus* **178**, 327 (2005).
22. K. K. Khurana *et al.*, in *Jupiter: The Planet, Satellites and Magnetosphere*, F. Bagenal, T. E. Dowling, W. B. McKinnon, Eds. (Cambridge Univ. Press, Cambridge, 2004), pp. 593–616.
23. J. T. Clarke *et al.*, *J. Geophys. Res.* **103**, 20217 (1998).
24. A. R. Vasavada *et al.*, *J. Geophys. Res.* **104**, 27133 (1999).
25. J. E. P. Connerney, R. L. Baron, T. Satoh, T. Owen, *Science* **262**, 1035 (1993).
26. R. Prangé *et al.*, *Nature* **379**, 323 (1996).
27. Even if there were no high-altitude winds to disperse the heat from the IFT footprint aurora, because of Io's orbital motion, the IFT footprint moves westward through the local atmosphere at ~5 km/s and so traverses its ~400-km width in about 80 s.
28. J.-C. Gérard *et al.*, *J. Geophys. Res.* **107**, 1394 (2002).
29. J. Saur *et al.*, *J. Geophys. Res.* **104**, 25105 (1999).
30. D. H. Pontius, *J. Geophys. Res.* **107**, 1165 (2002).
31. J. E. P. Connerney, M. H. Acuña, N. F. Ness, T. Satoh, *J. Geophys. Res.* **103**, 11929 (1998).

32. We thank the New Horizons mission team and the New Horizons science team. New Horizons is funded by NASA, whose financial support we gratefully acknowledge. G.R.G. thanks H. Waite, W. Lewis, D. Pontius, D. Grodent, and J.-C. Gérard for comments and D. Grodent for providing locations of the main auroral and Io ovals.

Supporting Online Material

Movie S1

10 July 2007; accepted 19 September 2007
10.1126/science.1147613

REPORT

Clump Detections and Limits on Moons in Jupiter's Ring System

Mark R. Showalter,[1]* Andrew F. Cheng,[2,3] Harold A. Weaver,[3] S. Alan Stern,[2] John R. Spencer,[4] Henry B. Throop,[4] Emma M. Birath,[4] Debi Rose,[5] Jeffrey M. Moore[6]

The dusty jovian ring system must be replenished continuously from embedded source bodies. The New Horizons spacecraft has performed a comprehensive search for kilometer-sized moons within the system, which might have revealed the larger members of this population. No new moons were found, however, indicating a sharp cutoff in the population of jovian bodies smaller than 8-kilometer-radius Adrastea. However, the search revealed two families of clumps in the main ring: one close pair and one cluster of three to five. All orbit within a brighter ringlet just interior to Adrastea. Their properties are very different from those of the few other clumpy rings known; the origin and nonrandom distribution of these features remain unexplained, but resonant confinement by Metis may play a role.

Planetary rings fall into two general categories: dense systems (exemplified by the main rings of Saturn) and faint, dusty rings (such as Jupiter's). The effects of plasma, electromagnetic perturbations, and solar radiation pressure limit the lifetimes of orbiting dust particles, so Jupiter's rings must be replenished continuously from a population of embedded "parent" bodies (*1*–*3*). Jupiter's moons Adrastea and Metis orbit within the main ring and are probably major sources of dust. However, spacecraft and Earth-based images have revealed a band of material ~1000 km wide between the orbits of the two moons (*3*–*5*); this is likely the primary source population.

[1]Search for Extraterrestrial Intelligence (SETI) Institute, Mountain View, CA 94043, USA. [2]NASA Headquarters, Washington, DC 20546, USA. [3]Applied Physics Laboratory, Johns Hopkins University, 11100 Johns Hopkins Road, Laurel, MD 20723, USA. [4]Southwest Research Institute, 1050 Walnut Street, Suite 300, Boulder CO 80302 USA. [5]Synthys-D, 1200 South Riverbend Court, Superior CO 80027, USA. [6]NASA Ames Research Center, Moffett Field, CA 94035, USA.

*To whom correspondence should be addressed. E-mail: mshowalter@seti.org

We used the New Horizons spacecraft to search for small moons in the main ring during its Jupiter approach, to better understand the relationship between the parent population and the prevalent dust. Adrastea (mean radius r = 8 km, semimajor axis a = 128,981 km) and Metis (r = 22 km, a = 127,980 km) are the smallest known inner moons, but the Long-Range Reconnaissance Imager (LORRI) was capable of detecting bodies just 0.5 km in radius. A comprehensive search was accomplished via two image sequences or "movies," in which LORRI targeted one lip of the ring and snapped an image every 8 to 10 min for a full orbital period (7.2 hours). The two movies comprised 49 images (designated 34600923 to 34629723) and 63 images (34742163 to 34779663), respectively, and were separated by 1.3 days. Exposure times were 3 s; pointing instability contributed a few pixels of smear to most images.

A co-added image (Fig. 1A) clearly shows the 1000-km-wide ring between the orbits of the two moons. Peaks in brightness are visible interior to Adrastea and exterior to Metis. A third enhancement appears just outside the orbit of Adrastea. The moons themselves occupy local minima in ring density, but these regions are not empty. This same triple-peaked pattern was first imaged by the Galileo spacecraft (*3*) but with lower signal-to-noise ratio (SNR). This pattern describes the locations of parent bodies; the ring looks radically different at high phase angles (Sun-ring-observer angles) (Fig. 1, B and C), which emphasize the tiny dust particles in the system. Here, the finer structure disappears, and the main ring extends inward ~6000 km (*6*, *7*), indicating that the dust grains are dispersed primarily inward from their point of origin.

To search for new moons, we extracted a sequence of thin strips from each frame, in which polar coordinates in the ring plane were reprojected into a rectangular grid. Strips were generally 4000 km wide radially and were generated at overlapping 2000-km steps. Pixel resampling was 0.1° to 0.2° in longitude (horizontally) and 100 to 200 km radially (vertically). Strips from the same radial range of each movie frame were then stacked vertically into a single image. At this step, we rotated longitudes to a common epoch.

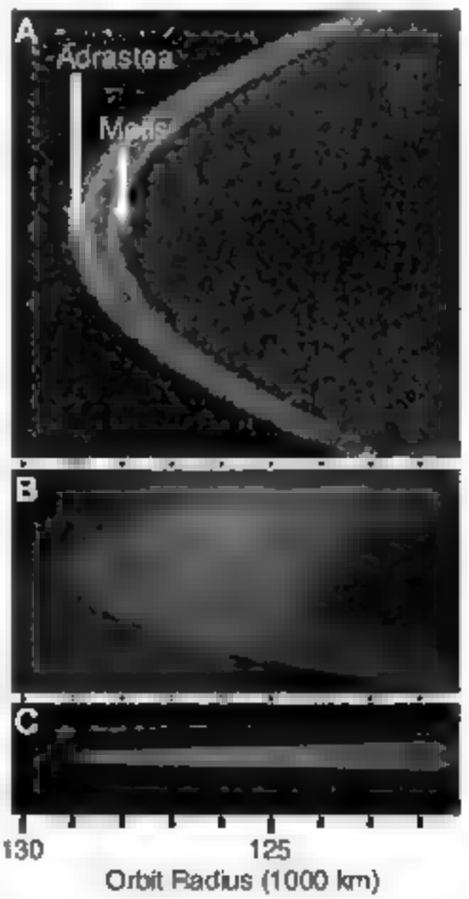

Fig. 1. The radial structure of the jovian ring in backscattered light (**A**) and forward-scattered light (**B** and **C**). Images are aligned vertically and shown at the same scale, as indicated by the horizontal axis. Solar phase angles are 21° (A), 120° (B), and 140° (C). The dust interior to the main ring becomes progressively brighter as the phase angle increases. Some scattered light appears in the middle of (B).

Table 1. Clump and body orbits and photometry.

Clump or body	Longitude at epoch* (°)	Mean motion (°/day)	a (km)	Equivalent radius† (km)
Family α		1210.547 ± 0.017	128737.7 ± 1.2	
α1	124.004 ± 0.035	1210.571 ± 0.039	128736.0 ± 2.8	0.86
α3	120.340 ± 0.021	1210.532 ± 0.020	128738.8 ± 1.4	0.79
α4	118.550 ± 0.066	1210.631 ± 0.063	128731.8 ± 4.5	
Family β		1210.471 ± 0.032	128743.0 ± 2.2	
β1	305.937 ± 0.219	1210.148 ± 0.224	128765.9 ± 15.9	
β2	303.957 ± 0.030	1210.478 ± 0.032	128742.6 ± 2.3	0.95
Adrastea‡	135.0	1207.001 ± 0.001	128980.5 ± 0.1	8.2
Metis‡	250.1	1221.252 ± 0.001	127979.8 ± 0.1	21.7

*Epoch is Julian ephemeris date 2454156.5 (25 February 2007). Longitudes are measured from the ascending node of the ring plane on Earth's J2000 equator. †Defined as the radius of a solid body equal in brightness, assuming properties similar to those of Adrastea. ‡Longitude from this work; mean motion, a, and size from earlier data (*14*).

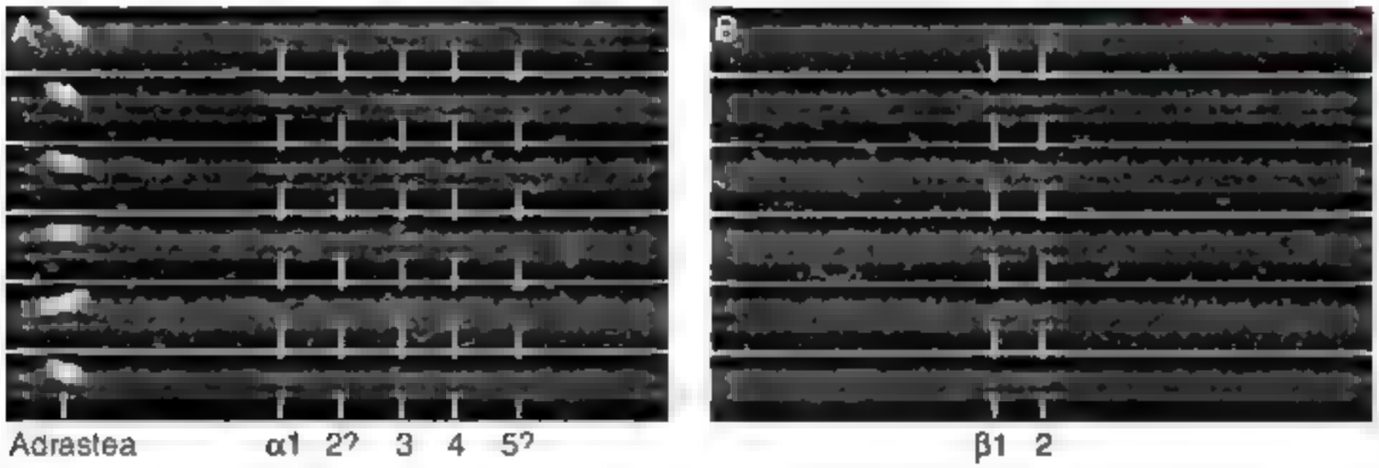

Fig. 2. Aligned image strips show the set of clumps identified as α (**A**) and β (**B**). Each strip has radial limits from 127,500 to 129,500 km. Longitudes are rotated to a common epoch, assuming the mean motion of a body at a = 129,000 km. Time steps increase upward. The bottom strip in each panel is an average of the strips above, which is used to show the clumps more clearly. Two of the five α features, numbered 2 and 5, are very marginal detections but seem to reveal an internal periodicity within this family.

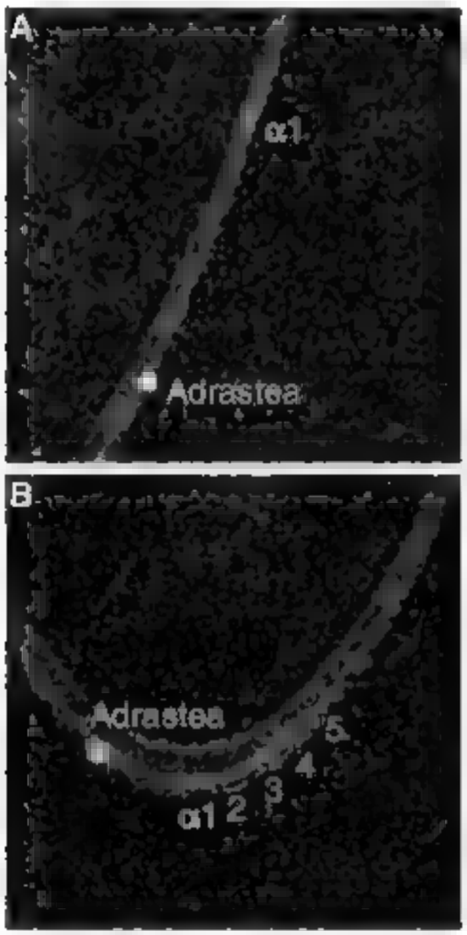

Fig. 3. Close-ups of feature α1 from images 34772943 (**A**) and 34774383 (**B**). The latter shows what appears to be a pointlike object near the tip of the ring, along with associated clumps α2 to α5. However, the longitude scale is less compressed as α1 approaches the tip (**A**), and it appears as an extended arc ~ 0.1° long.

using the mean motion for a body orbiting at the central radius of each strip. Thus, any object on a circular, equatorial orbit should appear aligned vertically at the same "rotating longitude" in adjacent strips and can be distinguished from the prevalent but randomly located background stars.

A set of unexpected features appeared (Fig. 2): two families of clumps within the main ring. Family "α" comprises three distinct features plus two more marginal ones; family "β" comprises two features separated by 2° in longitude. Both families are surrounded by a general brightening within several degrees of longitude. The clumps can be distinguished from moons because they have longitudinal extents ~ 0.1° to 0.3° (Fig. 3), which is larger than can be accounted for by image smear or resolution limits.

The brightest clumps are seen clearly in both ring movies, providing a time baseline sufficient to determine their orbits with reasonable precision (Table 1). The brightest features, designated α1, α3, and β2, are two to three times as bright as the local ring, with integrated intensities ~1% that of Adrastea. If they are composed of material with similar albedo (5%), then each has a cross section that is equivalent to a moon ~1 km in radius. Based on the orbits, the clump families should have appeared repeatedly in outbound images taken a few days later, with phase angles 130° to 160°. The clumps are undetectable in these images, at sensitivity levels ~10% that of the main ring. Because the clumps are substantially less forward-scattering than the main ring, they must be primarily concentrations of larger bodies, not dust.

No other moons or clumps were detected. The first ring movie was longitudinally complete between radial limits 104,000 to 185,000 km and was sensitive to moons 1 km in radius and larger. The second movie had narrower limits of 108,000 to 154,000 km and was sensitive to moons with r = 0.5 km. Our results reveal a marked truncation of the size distribution of moons in the inner jovian system. For comparison, until 2005, the smallest known regular satellite of Saturn was Calypso at r = 11 km. The Cassini mission has now revealed Daphnis at r = 6 to 8 km (*8*); Polydeuces, Pallene, and Methone each at r = 3 to 4 km (*9*); and Anthe (S/2007 S 4) at r ~ 1 km (*10*). Clearly, the population of saturnian moons shows no abrupt cutoff.

The large gap between 8-km Adrastea and our 0.5- to 1-km radius limit is therefore unexpected; it certainly violates our experience that astrophysical ensembles should follow power-law size distributions, with increasing numbers at smaller sizes. Two interpretations can be proposed. First, some models suggest that smaller bodies in planetary systems may have briefer lifetimes than larger ones against collisional disruption (*11*), although this assumes a steep size distribution of the incoming impactors. Alternatively, if micrometeoroid erosion plays an important role in the jovian ring (*2*), then this

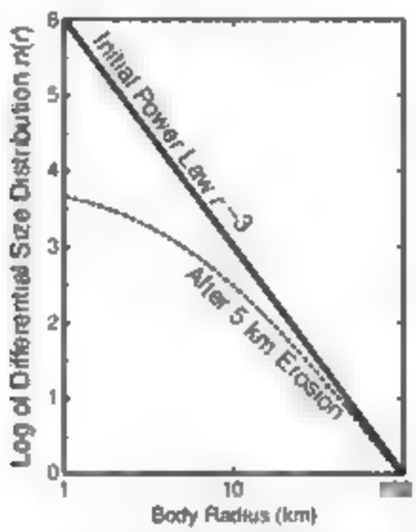

Fig. 4. An illustration of the effects of erosion on a power-law size distribution. Initially, bodies obey a differential size distribution $\propto r^{-3}$ (solid line). After erosion reduces all radii by 5 km, the population of smaller bodies (dashed line) is substantially reduced.

process can act to truncate the size distribution. In erosive processes, *dr/dt* is a constant, independent of *r*. Hence, at the same time that Metis shrinks from *r* = 27 to 22 km, all 5-km bodies in the system would vanish (Fig. 4). This explanation requires that reaccretion be negligible, which is reasonable so deep inside Jupiter's Roche limit.

Earlier images from Voyager and Galileo showed longitudinal asymmetries on a scale much larger than the tiny clumps found by New Horizons (*6*, *7*, *12*). The absence such large features in the recent data is puzzling; perhaps seasonal or other time-scale variations play a role. Cassini images found one hint of smaller-scale clumping in the jovian ring (*13*). An arc ~8° in length appeared near the outer edge of the rings in three low-phase images, leading Adrastea at the time by ~4°. The epoch was ~0:00 UTC on 13 December 2000. We can extrapolate our clump motions backward for the intervening 2265 days to determine that features α and β fell 232° ± 39° and 226° ± 72° ahead of Adrastea (*14*). Unless unknown orbital perturbations are at work, these families can both be ruled out as the feature imaged by Cassini; apparently, that feature no longer exists. Cassini's images had lower resolution and SNR, however, so we cannot rule out α and β as long-lived features that were too small for Cassini to detect.

The presence of these clumps challenges our theoretical understanding. By Kepler shear, a 1-km-wide clump at α's orbit will spread 5.1° in 1 year; this distance is far larger than the few tenths of a degree of individual clumps. This leaves two alternatives: either the clump families are young or they are actively confined. Transient features could be explained by impacts from meteoroids or by collisions among the ring members. If the clumps are spreading, then this would provide an unambiguous indicator of their youth. Of the two clumps with best-determined orbits, α1 and α3 (Table 1), the leading clump appears to be moving slightly faster, suggesting that they might have emerged from a single point ~90 days before the flyby. However, the mean motions are too uncertain to rule out a much longer lifetime. Of course, a recent impact should generate substantial dust, such as is widely seen in Saturn's F ring (*15*–*18*), but Jupiter's clumps are not dusty. Also, an impact would be expected to produce one broad arc rather than the multiple, seemingly uniformly spaced clumps seen in the α family.

Alternatively, the 1.8° periodicity of clumps in group α is suggestive of a resonant confinement mechanism, perhaps comparable to Galatea's effects on the Adams ring of Neptune (*19*, *20*). Metis' resonances probably dominate; although it orbits three times as far away from the clumps as Adrastea, Metis is ~20 times more massive. Notably, Metis' 115:116 corotation inclination resonance falls at 128736.9 km, just 0.8 km from the orbit of the α family. Also, its adjacent 114:115 resonance falls at 128743.6 km, which is 0.6 km from the orbit of the β family. With 6.7 km between resonances, the probability that both families would fall so close to resonant locations by random chance is 4% (although the orbits have relatively larger uncertainties). However, these resonances are expected to confine material at intervals of ~180°/115 = 1.56°, which does not match the observed clump spacings. Nevertheless, the clumps in Neptune's Adams ring also do not show the predicted periodicities, suggesting that our understanding of resonant confinement remains incomplete.

The jovian ring's large-scale asymmetries have now vanished, but different, much smaller structures have been revealed. This follows upon observations that the radial structure of Saturn's equally faint D ring has changed radically in the past 25 years; some features have faded and spread, whereas other regions show entirely new structure (*21*). Similarly, the uranian ζ ring has recently been found to have shifted radially since the 1986 Voyager flyby (*22*). We conclude that the general class of dusty rings may be much more dynamic and time-variable than was previously supposed, with variations on 10- to 20-year time scales not the exception but the norm.

References and Notes

1. J. A. Burns, M. R. Showalter, J. N. Cuzzi, J. B. Pollack, *Icarus* **44**, 339 (1980).
2. J. A. Burns, M. R. Showalter, G. Morfill, in *Planetary Rings*, R. Greenberg, A. Brahic, Eds. (Univ. Arizona Press, Tucson, 1984), pp. 200–272.
3. J. A. Burns *et al.*, in *Jupiter: The Planet, Satellites and Magnetosphere*, F. Bagenal, T. E. Dowling, W. B. McKinnon, Eds. (Cambridge Univ. Press, Cambridge, 2004), pp. 241–262.
4. M. R. Showalter, J. A. Burns, J. de Pater, D. P. Hamilton, M. Horanyi, *Bull. Am. Astron. Soc.* **35**, #11.08 (2003).
5. I. de Pater *et al.*, *Icarus* **138**, 214 (1999).
6. M. R. Showalter, J. A. Burns, J. N. Cuzzi, J. B. Pollack, *Icarus* **69**, 458 (1987).
7. M. Ockert-Bell *et al.*, *Icarus* **138**, 188 (1999).
8. C. C. Porco, Cassini Imaging Team, *Int. Astron. Union Circ.* #8242 (2005).
9. J. N. Spitale, R. A. Jacobson, C. C. Porco, J. W. M. Owen, *Astron. J.* **132**, 692 (2006).
10. C. C. Porco, Cassini Imaging Team, *Int. Astron. Union Circ.* #8857 (2007).
11. R. M. Canup, L. W. Esposito, *Icarus* **113**, 331 (1995).
12. S. M. Brooks, L. W. Esposito, M. R. Showalter, H. B. Throop, *Icarus* **170**, 35 (2004).
13. H. B. Throop *et al.*, *Icarus* **172**, 59 (2004).
14. C. C. Porco *et al.*, *Science* **299**, 1541 (2003).
15. M. R. Showalter, *Science* **282**, 1099 (1998).
16. M. R. Showalter, *Icarus* **171**, 356 (2004).
17. J. M. Barbara, L. W. Esposito, *Icarus* **160**, 161 (2002).
18. S. Charnoz *et al.*, *Science* **310**, 1300 (2005).
19. C. C. Porco, *Bull. Am. Astron. Soc.* **22**, #1043 (1990).
20. F. Namouni, C. C. Porco, *Nature* **417**, 45 (2002).
21. M. M. Hedman *et al.*, *Icarus* **188**, 89 (2007).
22. I. de Pater, H. B. Hammel, M. R. Showalter, M. A. van Dam, *Science* **317**, 1888 (2007).

23. We thank the entire New Horizons mission team and our colleagues on the New Horizons science team. New Horizons is funded by NASA, whose financial support we acknowledge.

11 July 2007; accepted 19 September 2007
10.1126/science.1147647

REPORT

New Horizons Mapping of Europa and Ganymede

W. M. Grundy,[1]* B. J. Buratti,[2] A. F. Cheng,[3] J. P. Emery,[4] A. Lunsford,[5] W. B. McKinnon,[6] J. M. Moore,[7] S. F. Newman,[2] C. B. Olkin,[8] D. C. Reuter,[5] P. M. Schenk,[9] J. R. Spencer,[8] S. A. Stern,[10] H. B. Throop,[8] H. A. Weaver,[3] and the New Horizons team

The New Horizons spacecraft observed Jupiter's icy satellites Europa and Ganymede during its flyby in February and March 2007 at visible and infrared wavelengths. Infrared spectral images map H_2O ice absorption and hydrated contaminants, bolstering the case for an exogenous source of Europa's "non-ice" surface material and filling large gaps in compositional maps of Ganymede's Jupiter-facing hemisphere. Visual wavelength images of Europa extend knowledge of its global pattern of arcuate troughs and show that its surface scatters light more isotropically than other icy satellites.

NASA's Voyager and Galileo space probes revealed the icy Galilean satellites to be distinct, complex worlds with surfaces geologically and chemically sculpted by diverse endogenic and exogenic processes (*1*, *2*). Many outstanding questions remain regarding the composition and biological potential of Europa's interior ocean and the nature of its icy crust, the existence of possible oceans within Ganymede and Callisto, and the composition of enigmatic "non-ice" material on Europa and Ganymede that distorts their H_2O ice absorption bands (*3*–*5*).

During its 2007 flyby of Jupiter, New Horizons (*6*) observed Europa, Ganymede, and Callisto (table S1) with its infrared (1.25 to 2.5 μm) Linear Etalon Imaging Spectral Array (LEISA) (*7*) and its panchromatic (0.35 to 0.85 μm) LOng-Range Reconnaissance Imager (LORRI) charge-coupled device camera (*8*). LEISA observations used spacecraft motion to slew the field of view across

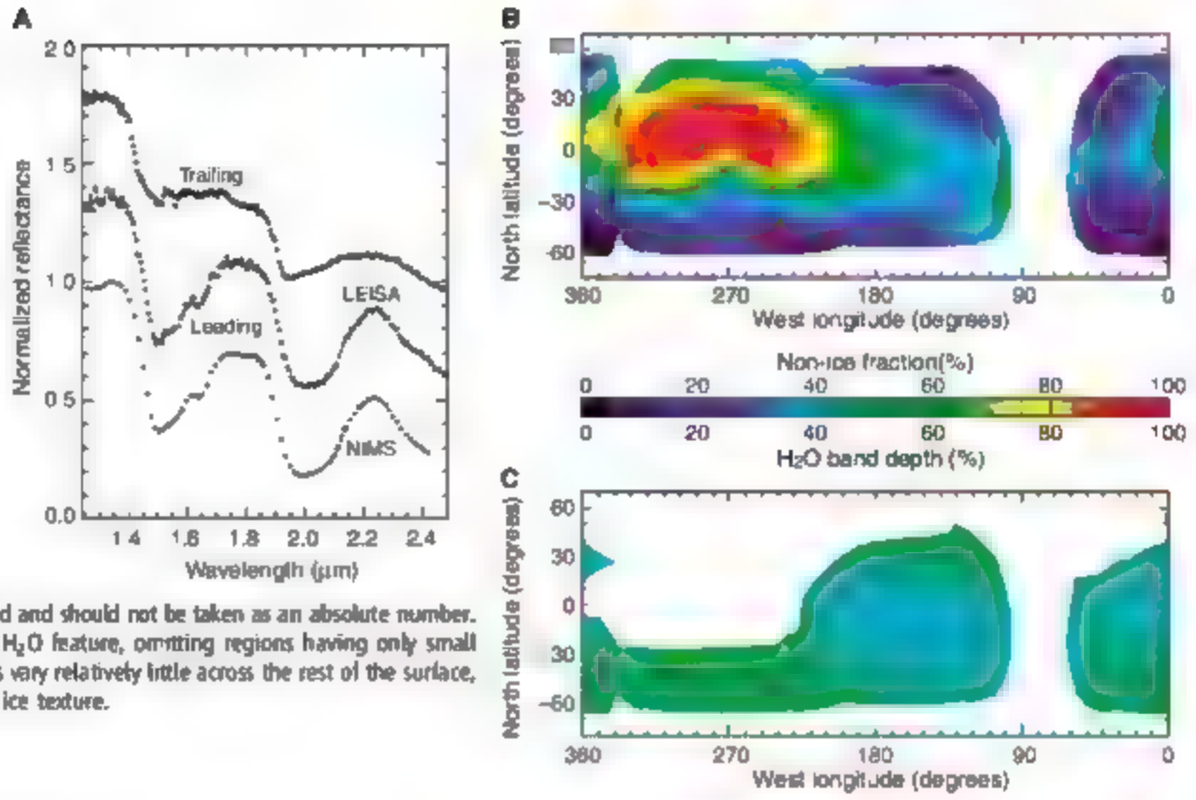

Fig. 1. LEISA compositional mapping of Europa. **(A)** Example spectra, top to bottom: LEISA trailing hemisphere spectrum showing distorted H_2O bands, then LEISA and NIMS (*5*) leading hemisphere spectra showing cleaner H_2O ice. These examples illustrate LEISA data quality and the spectral variability of Europa's surface. Upper spectra are offset by +0.4 and +0.8. Uncertainties are indicated by the scatter. **(B)** Spatial distribution of the "non-ice" material that distorts Europa's H_2O bands. Highest concentrations (in red, as indicated by the shared color bar) occur near the trailing apex (270°W, 0°N). The fraction depends on the specific end-members selected and should not be taken as an absolute number. **(C)** Depth of the 2-μm residual H_2O feature, omitting regions having only small fractions of pure ice. Band depths vary relatively little across the rest of the surface, indicative of homogeneous H_2O ice texture.

the target to build up spectral image cubes. LORRI observations consist of single images or pairs of images with bracketing exposure times made in a point-and-stare framing mode. During the several-day close approach phase, Ganymede and Callisto remained on the far side of Jupiter from New Horizons, limiting the spatial resolution achievable but allowing study of their Jupiter-facing hemispheres, including regions of Ganymede poorly mapped by Galileo's Near-Infrared Mapping Spectrometer (NIMS). Europa's more rapid orbital motion enabled compositional mapping of most of its surface.

Europa's distorted H_2O vibrational absorption band shapes are attributed to water of hydration, but the composition and origin of the hydrated material are unresolved. Association with lineae, chaos regions, and possible erup-

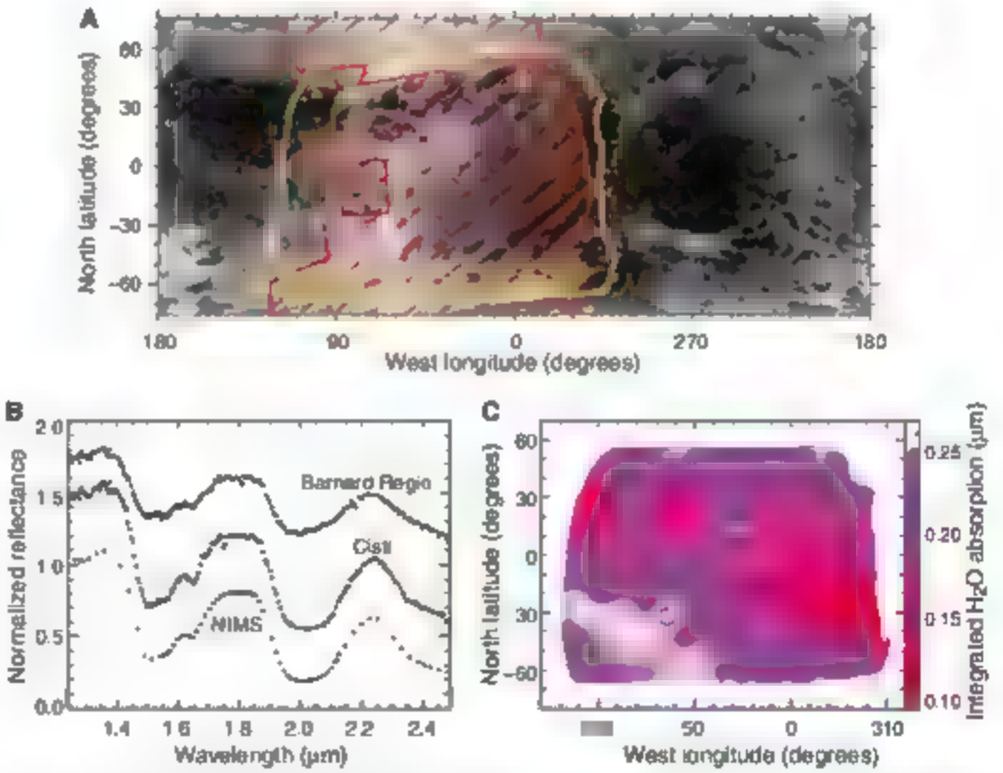

Fig. 2. LEISA compositional mapping of Ganymede. **(A)** Regions of Ganymede not mapped by NIMS (red hatches) and mapped by LEISA (yellow outline). **(B)** Example spectra, top to bottom: LEISA spectra of Barnard Regio (10°W, 2°S) and of the bright, rayed crater Cisti (64°W, 32°S) compared with NIMS spectrum of an ice-rich region (*27*). The spectra are normalized at 1.8 μm and offset by +0.6, +0.2, and −0.2, respectively. **(C)** Map of integrated absorption by the 1.5- and 2-μm H_2O ice bands. Regions around Cisti (black circle) and Barnard Regio (white circle) contributed to the LEISA average spectra in (B).

[1]Lowell Observatory, 1400 West Mars Hill Road, Flagstaff, AZ 86001, USA. [2]Jet Propulsion Laboratory, 4800 Oak Grove Drive, Pasadena, CA 91109, USA. [3]Johns Hopkins University Applied Physics Laboratory, 11100 Johns Hopkins Road, Laurel, MD 20723, USA. [4]SETI Institute/NASA Ames Research Center, 515 North Whisman Road, Mountain View, CA 94043, USA. [5]NASA Goddard Space Flight Center, Code 693, Greenbelt, MD 20771, USA. [6]Department of Earth and Planetary Science, Washington University, Campus Box 1169, 1 Brookings Drive, St. Louis, MO 63130, USA. [7]NASA Ames Research Center, MS 245-3, Moffett Field, CA 94035, USA. [8]Department of Space Studies, Southwest Research Institute, 1050 Walnut Street, Suite 300, Boulder, CO 80302, USA. [9]Lunar and Planetary Institute, 3600 Bay Area Boulevard, Houston, TX 77058, USA. [10]NASA Science Mission Directorate, NASA Headquarters, Washington, DC 20546, USA.

*To whom correspondence should be addressed. E-mail: w.grundy@lowell.edu

tions raise the possibility that the hydrated material came from Europa's interior ocean (*3*–*5*). Compositional interpretations favoring hydrated magnesium and/or sodium sulfate or sulfide salts might then constrain ocean chemistry and potential to host life (*9*, *10*). However, exogenic sulfur from Io (or from endogenic salts) was shown to be rapidly modified on Europa's surface by charged particles from the jovian magnetosphere, leading to a radiolytic sulfur cycle on thousand-year time scales between elemental sulfur, sulfur dioxide, and sulfuric acid, which is also a good spectral match for the "non-ice" material (*11*–*14*).

New Horizons made three LEISA observations of Europa with subspacecraft pixel scales from 250 to 180 km, corresponding to 120 to 230 pixels on the disk of Europa. The observations included the trailing hemisphere where the "non-ice" material was known to be more abundant (*13*). The spectral resolution of LEISA ($\lambda/\Delta\lambda \approx 240$) is potentially high enough to distinguish contending hydrated salt and acid species (*14*), but calibration procedures for LEISA data are still being refined, so we will concentrate on the two strong H_2O ice absorption complexes at ~1.5 and 2.0 μm that dominate the spectra (Fig. 1A).

We mapped the distribution of distorted H_2O bands by using a simple mixing model with two components derived by averaging several distorted spectra for one end-member and several clean ice-like spectra for the other. The resulting map (Fig. 1B) confirms previous results (*4*, *13*) and extends coverage substantially, showing that the band-distorting material is distributed symmetrically about the apex of the trailing hemisphere (270°W, 0°N). This pattern is consistent with implantation of sulfur from Io and of bombardment by magnetospheric charged particles (*15*). Our "non-ice" map also matches the distribution of an ultraviolet absorber, possibly sulfur, mapped from Voyager data (*16*). The main deviation from this symmetry in both maps is an area of cleaner ice south of the trailing apex associated with ejecta from the young, bright, rayed crater Pwyll (271°W, 25°S). That Pwyll ejecta contains less "non-ice" is consistent with an exogenic source for that material. However, instances of local geographical control of the "non-ice" material (*4*, *13*) imply at least some endogenic influence on its formation or preservation.

Removing appropriate fractions of distorted-band material from each pixel leaves residual H_2O spectra. The residual absorption bands measure the mean optical path length traversed within H_2O ice. A band depth map (Fig. 1C) shows little regional variation, implying relatively consistent ice textures across the surface of Europa. Processes governing ice texture evidently lack the strong hemispheric asymmetry of the processes responsible for the distribution of "non-ice" material.

New Horizons targeted Ganymede's subjovian hemisphere (Fig. 2A), including bright, rayed craters Cisti (64°W, 32°S), Tros (27°W, 11°N), and Shu (3°E, 43°N), as well as darker Nicholson Regio (50°W to 40°E, 10°S to 50°S), Barnard Regio (20°W to 10°E, 10°S to 10°N), and Perrine Regio (70°W to 0°W, 10°N to 50°N). The 1.65-μm H_2O ice band, characteristic of low-temperature crystalline ice (*17*), is well resolved by LEISA (Fig. 2B). Some regions of Ganymede's trailing hemisphere were reported to exhibit H_2O band asymmetries like Europa's "non-ice" (*5*). Asymmetric bands are also apparent in LEISA spectra, especially of darker areas. Subtle dips suggestive of hydrates appear around 1.4, 1.7, and 1.8 μm (*14*), but their interpretation awaits improved calibration. Comparison of an H_2O absorption map (Fig. 2C) with the context map (Fig. 2A) shows greater H_2O ice absorption associated with brighter regions and with recent impacts and their ejecta. The bright, heavily cratered, leading-hemisphere region south of 20°S and west of 40°W shows particularly strong H_2O absorption. This correlation is consistent with accumulation at the surface of a globally distributed dark material except where relatively recent impacts have excavated cleaner ice from below the surface.

LORRI panchromatic images of the satellites with spatial resolutions of 15 to 30 km/pixel reveal no changes since Galileo images ~5 years earlier. Processes that modify surfaces at large spatial scales, such as impacts of kilometer-sized bodies, are highly unlikely during that interval [$<10^{-3}$ probability (*18*)].

LORRI images surveyed Europa's large-scale arcuate troughs, which are notable for their scale and their symmetry. They form two sets of concentric small circles with centers at antipodal points 300°W, 10°N and 120°W, 10°S. From Galileo imaging and image-derived digital terrain models, they are up to ~50 km wide and from several hundred meters to more than a kilometer deep (*19*). They do not distort or displace other, intersecting surface albedo and tectonic features and are not obviously related to other tectonic patterns identified on Europa (*20*).

The New Horizons trajectory provided low Sun elevation, near-normal views of Europa's trailing hemisphere terminator, enabling us to target gaps in comparable Galileo coverage. LORRI images reveal a predicted northward extension (*19*) of the trough segment near 340°W longitude (Fig. 3), confirming

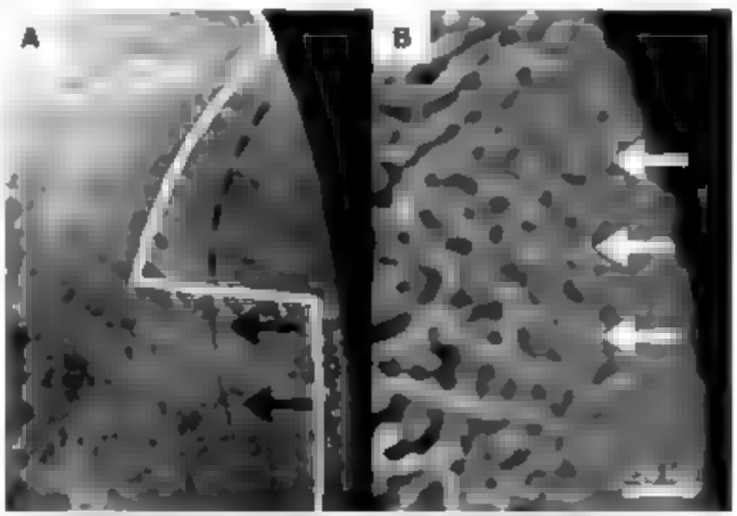

Fig. 3. Large-scale arcuate troughs on Europa. (**A**) Arrows mark the 340°W trough segment detected in Galileo images. Galileo only observed the region to the left of the white curve at suitable illumination geometry to reveal these features. Dashes indicate the predicted continuation of the trough (*19*). (**B**) A highly stretched New Horizons LORRI image of the same region (roughly 10°W to 30°E, 10°S to 45°N, with north up) reveals the continuation of the trough (white arrows).

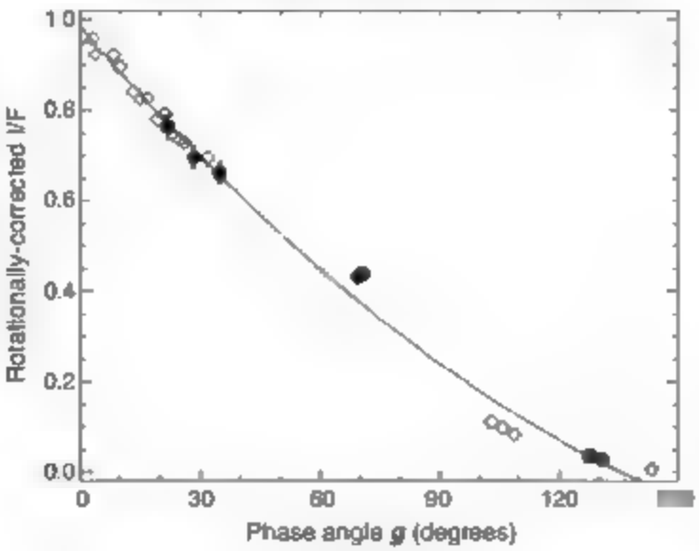

Fig. 4. LORRI disk-integrated photometry of Europa. New Horizons observations (filled circles, with 1-σ error bars) are consistent with Voyager measurements (open diamonds). A second-order polynomial $y(g) = c + bg + ag^2$ (smooth curve) approximates the data with $b = -0.01$ and $a = 2.2 \times 10^{-5}$.

that the troughs are a truly global phenomenon. No trough was seen near longitude 270°W, but that region is geologically complex, with numerous cross-cutting dark lineaments. The north-south offset of the antipodal centers of symmetry, maintained in the New Horizons images, hints at true polar wander of Europa's ice shell (*21*–*23*).

From Earth, the solar phase angle g for the Jupiter system is ≤12°, limiting Earth-based measurement of directional scattering by jovian satellites. Only spacecraft can access higher phase angles. LORRI observed the Galilean satellites at a range of phase angles (table S1), filling gaps in Europa's solar phase curve between 32° and 103° and between 109° and 143°. The photometric data, corrected for longitudinal variations and normalized to Voyager data (*24*), are shown in Fig. 4. Europa's brightness at $g = 70°$ is more than 40% of its fully illuminated brightness, underscoring the unique texture of its surface produced by active resurfacing. The comparable number for Earth's Moon is only 20%.

Our observations improve measurement of Europa's phase integral q, which describes the directional scattering properties of light reflected from its surface. The new q value is 1.01 ± 0.04, compared with 1.1 ± 0.1 from previous Voyager data (*24*). Compared with other actively resurfaced icy satellites, Europa's q is marginally higher than that of Enceladus (0.89 ± 0.10) (*25*) but lower than that of Triton (1.14 ± 0.03) (*26*). Using a geometric albedo of 0.67 ± 0.03 for LORRI wavelengths (*8*, *24*), we find a new Bond albedo of 0.68 ± 0.05, compared with a previous value of 0.6 ± 0.1 (*24*), meaning that Europa absorbs less sunlight than previously thought.

References and Notes

1. T. V. Johnson, C. M. Yeats, R. Young, *Space Sci. Rev.* **60**, 3 (1992).
2. F. Bagenal, T. E. Dowling, W. B. McKinnon, Eds., *Jupiter: The Planet, Satellites, and Magnetosphere* (Cambridge Univ. Press, New York, 2004).
3. T. B. McCord *et al.*, *Science* **280**, 1242 (1998).
4. T. B. McCord *et al.*, *J. Geophys. Res.* **104**, 11827 (1999).
5. T. B. McCord, G. B. Hansen, C. A. Hibbitts, *Science* **292**, 1523 (2001).
6. S. A. Stern, *Space Sci. Rev.*, in press, preprint available at http://arxiv.org/abs/0709.4411.
7. D. C. Reuter *et al.*, *Space Sci. Rev.*, in press, preprint available at http://arxiv.org/abs/0709.4281.
8. A. F. Cheng *et al.*, *Space Sci. Rev.*, in press, preprint available at http://arxiv.org/abs/0709.4278.
9. F. P. Fanale *et al.*, *J. Geophys. Res.* **106**, 14595 (2001).
10. K. P. Hand, C. F. Chyba, *Icarus* **189**, 424 (2007).
11. R. W. Carlson, R. E. Johnson, M. S. Anderson, *Science* **286**, 97 (1999).
12. R. W. Carlson, M. S. Anderson, R. E. Johnson, M. B. Schulman, A. H. Yavrouian, *Icarus* **157**, 456 (2002).
13. R. W. Carlson, M. S. Anderson, R. Mehlman, R. E. Johnson, *Icarus* **177**, 461 (2005).
14. J. B. Dalton *et al.*, *Icarus* **177**, 472 (2005).
15. R. E. Johnson *et al.*, in *Jupiter: The Planet, Satellites, and Magnetosphere*, F. Bagenal, T. E. Dowling, W. B. McKinnon, Eds. (Cambridge Univ. Press, New York, 2004), pp. 485–512.
16. A. S. McEwen, *J. Geophys. Res.* **91**, 8077 (1986).
17. W. M. Grundy, B. Schmitt, *J. Geophys. Res.* **103**, 25809 (1998).
18. P. M. Schenk, C. R. Chapman, K. Zahnle, J. M. Moore, in *Jupiter: The Planet, Satellites, and Magnetosphere*, F. Bagenal, T. E. Dowling, W. B. McKinnon, Eds. (Cambridge Univ. Press, New York, 2004), pp. 427–456.
19. P. M. Schenk, *Lunar Planet. Sci. Conf.* **36**, 2081 (2005).
20. R. Greeley *et al.*, in *Jupiter: The Planet, Satellites, and Magnetosphere*, F. Bagenal, T. E. Dowling, W. B. McKinnon, Eds. (Cambridge Univ. Press, New York, 2004), pp. 329–362.
21. A. C. Leith, W. B. McKinnon, *Icarus* **120**, 387 (1996).
22. A. R. Sarid *et al.*, *Icarus* **158**, 24 (2002).
23. P. M. Schenk, I. Matsuyama, F. Nimmo, Lunar and Planetary Institute's "Ices, Oceans, and Fire: Satellites of the Outer Solar System" meeting, Boulder CO, 3 to 15 August 2007, abstract 6090 (2007), available at www.lpi.usra.edu/meetings/icysat2007/pdf/6090.pdf.
24. B. J. Buratti, J. Veverka, *Icarus* **55**, 93 (1983).
25. B. J. Buratti, J. Veverka, *Icarus* **58**, 254 (1984).
26. J. Hillier *et al.*, *Science* **250**, 419 (1990).
27. G. B. Hansen, T. B. McCord, *J. Geophys. Res.* **109**, E01012 (2004).

28. We thank the entire New Horizons mission team and our colleagues on the New Horizons science team. New Horizons is funded by NASA, whose financial support we gratefully acknowledge. We also thank C. A. Hibbitts, J. B. Dalton III, G. B. Hansen, and K. Stephan for valuable scientific discussions as well as providing examples of NIMS data.

Supporting Online Material

www.sciencemag.org/cgi/content/full/318/5848/234/DC1
Table S1

10 July 2007; accepted 21 September 2007
10.1126/science.1147623

REPORT

Io's Atmospheric Response to Eclipse: UV Aurorae Observations

K. D. Retherford,[1*] J. R. Spencer,[2] S. A. Stern,[3] J. Saur,[4] D. F. Strobel,[5] A. J. Steffl,[2] G. R. Gladstone,[1] H. A. Weaver,[6] A. F. Cheng,[3] J. Wm. Parker,[2] D. C. Slater,[1] M. H. Versteeg,[1] M. W. Davis,[1] F. Bagenal,[7] H. B. Throop,[2] R. M. C. Lopes,[8] D. C. Reuter,[9] A. Lunsford,[9] S. J. Conard,[8] L. A. Young,[2] J. M. Moore[10]

The New Horizons (NH) spacecraft observed Io's aurora in eclipse on four occasions during spring 2007. NH Alice ultraviolet spectroscopy and concurrent Hubble Space Telescope ultraviolet imaging in eclipse investigate the relative contribution of volcanoes to Io's atmosphere and its interaction with Jupiter's magnetosphere. Auroral brightness and morphology variations after eclipse ingress and egress reveal changes in the relative contribution of sublimation and volcanic sources to the atmosphere. Brightnesses viewed at different geometries are best explained by a dramatic difference between the dayside and nightside atmospheric density. Far-ultraviolet aurora morphology reveals the influence of plumes on Io's electrodynamic interaction with Jupiter's magnetosphere. Comparisons to detailed simulations of Io's aurora indicate that volcanoes supply 1 to 3% of the dayside atmosphere.

Io is a volcanically active moon of Jupiter, and its volcanism is the ultimate source of material for Io's sulfur-dioxide atmosphere. The interaction between Io's atmosphere and the Io plasma torus produces displays of auroral emissions on Io, supplies plasma to Jupiter's magnetosphere, and physically links Io to Jupiter (*1*). The relative importance of the volcanoes as a direct, immediate source of the atmosphere, versus sublimation of frosts deposited around these volcanoes, has remained uncertain since the atmosphere's discovery in 1979 (*2*, *3*). Io's average dayside surface temperature rapidly drops after eclipse ingress or at night [likely from ~120 K to ~90 K, (*4*, *5*)], which is sufficient to diminish the sublimation component of the atmosphere across most of the surface and possibly results in an atmosphere mostly supplied directly from volcanoes.

Aurora observations, particularly while Io is in solar eclipse by Jupiter, can provide information on both Io's atmosphere and its interaction with Jupiter (*6*–*14*). The New Horizons (NH) spacecraft was able to observe Io in eclipse four times during its flyby of Jupiter in late February and early March 2007 (Table 1).

We report NH Alice ultraviolet (UV) spectrometer (*15*) observations of Io eclipse ingress and egress. Io eclipse observations by other NH instruments are reported separately (*16*, *17*). Alice provides spectral images in the extreme- and far-UV (EUV and FUV) pass-bands from 52 nm to 187 nm with 0.3- to 0.4-nm resolution for point sources and 1.0- to 1.2-nm resolution for extended sources, as Io was for our observations (*18*), and a spatial resolution of 0.1° by 0.3° along the 4° long narrow part of its slit.

Supporting observations were also made with the Advanced Camera for Surveys Solar Blind Channel (ACS/SBC) (*19*) on the Hubble Space Telescope (HST). Angular plate scales of 0.034 arc sec/pixel and 0.030 arc sec/pixel on the detector result in slightly rectangular pixels. Use of the SBC's F125LP filter excludes sky background signal from geocoronal Lyman-α emissions while passing through the atomic oxygen (OI) 130.4 nm and longer FUV emissions of interest for Io.

Auroral emission features include a global limb glow around the disk of the satellite, sub-Jupiter and anti-Jupiter equatorial spots (or glows), and a wake region (on the orbital leading hemisphere, down-

stream relative to the magnetospheric plasma flow). These large-scale features are known to change brightness and location with Jupiter's changing magnetic field orientation at Io and are diagnostic of the local flow of the Io plasma torus past the satellite and into its atmosphere (*10*, *11*, *20*–*23*). Dramatic visible auroral glows have been seen from numerous volcanic plumes, including the large Tvashtar plume that was active at this time (*17*).

The question of how much of the dayside atmosphere comes from SO_2 frost sublimation versus volcanoes remains difficult to resolve. Previous theoretical work demonstrated that aurora brightness variations with time after Io enters eclipse ingress provide a means to investigate the relative contributions of volcanic and sublimation sources to Io's dayside atmosphere (*14*). A relative contribution from volcanoes of 1 to 10% was suggested based on only a few data points with inadequate time coverage.

We observed the time series of Io's FUV emissions in shadow using Alice (Fig. 1) and the HST/SBC (Fig. 2). The last Alice exposure in IEclipse05 (red points in Fig. 3, A to C) is ~40% brighter than it is in earlier measurements (Table 2) and likely represents predicted posteclipse aurora brightening (*14*). In IEclipse01, the view is of the dayside, similar to that for HST (Fig. 2). This view includes Io's wake emissions. The high initial brightnesses and the decrease in brightness after ingress in IEclipse01 (Fig. 3) may be because the amount of sublimation is particularly sensitive to changes after eclipse ingress on the dayside atmosphere. There was little change in volcanic activity observed during the encounter period (*17*); thus, any changes in Io's neutral atmospheric density must be attributed to other sources. The plasma torus density is thought to be relatively stable on the time scale of days. The trend of brighter aurora with Io's location in denser regions of the plasma torus (*21*) would exacerbate the difference in measured OI 135.6-nm brightnesses between IEclipse01 and IEclipse04 (fig. S3B). Viewing geometry of the asymmetric atmosphere regions and the large-scale auroral features viewed (e.g., wake viewed in IEclipse01 but not IEclipse04) could explain the differences, but the FUV equatorial spots are consistently brighter than the wake in the IEclipse04 view is favored. Also, measurements of SO_2 longitudinal distribution (*24*) suggest that the dayside equatorial densities in the region viewed in IEclipse01 (at 344°) are a few times less dense than IEclipse04 (at 241°). The two Alice ingress series are best explained by a dramatic difference between the densities of Io's dayside and nightside atmospheres.

The HST/SBC data (Fig. 3D) show that Io's FUV brightness decreased between the first and last exposures by roughly factors of 1.5 and 1.3 for square regions of widths 0.55 R_{Io} and 4 R_{Io} (Io radii), respectively, centered on Io. The most prominent FUV emission lines that contribute to this image are the same neutral OI 130.4 nm, OI 135.6 nm, and SI 147.9 nm lines observed with Alice (Fig. 1B). However, the first SBC exposure occurred 12 min after umbral ingress, which is after the time expected for the most dramatic variations. Alice observed the key periods for IEclipse01 and IEclipse04, but only two points at ~90 min after ingress for the IEclipse03 event. Cassini visible aurora imaging (*11*) showed similarly moderate variations in brightness over a period starting ~20 min after ingress.

A comparison between aurora simulations and the auroral brightness time series shown in Fig. 3 enables a higher fidelity assessment of Io's atmospheric sources. Volcanic column densities of 2×10^{14} cm^{-2}, 4×10^{14} cm^{-2}, and 8×10^{14} cm^{-2} out of 1.5×10^{16} cm^{-2} were used in Fig. 3 (1%, 3%, and 5% cases, respectively). The data are best described by a volcanic contribution of 1 to 3% to a primarily sublimation-supplied dayside atmosphere. Volcanic contributions of >5% are rejected for the epoch of these observations.

Other methods for characterizing the atmospheric sources face the predicament of collocated volcanic plumes and SO_2 frost deposits, potentially confusing spatial associations of higher density near volcanoes with the respective sources. Recent reports using these other methods are in general agreement with the results of 1 to 3% reported here (*25*, *26*), but SO_2 maps derived from Lyman-α absorption images show more gas near the equatorial terminator than expected (*27*, *28*, *24*) and remain difficult to reconcile with these levels of sublimation.

The latitudinal extent of the sub-Jupiter equatorial spot (Fig. 2, C to F) decreased by ~25% from 17 to 37 min after umbral ingress. Space Telescope Imaging Spectrograph (STIS) Io eclipse observations similarly hinted at FUV emissions more localized to the magnetic equator (*13*). In shadow, preferential closure of Io's electrodynamic current system was predicted to occur through local plume atmospheres (*29*, *30*). A combination of local dominance of the plume atmosphere over the sublimation source could explain this variation in the latitudinal extent of the sub-Jupiter equatorial spot with time in eclipse.

An emission feature between 200 km and 550 km above the limb and located near the bright, newly discovered "East Gish" volcano is seen in

Table 1. NH Io eclipse Alice observation summary. Supporting observations with the HST/SBC are also indicated. IEclipse02 was dropped from the plan and not performed.

Visit name	Date	Umbral ingress	Umbral egress	Instrument used	Number of exposures
IEclipse01	2/25/2007	19:53	21:58	Alice	16
IEclipse03	2/27/2007	14:21	16:27	Alice	2
				HST/SBC	8
IEclipse04	3/1/2007	8:50	10:56	Alice	20
IEclipse05	3/3/2007	3:18	5:25	Alice	12

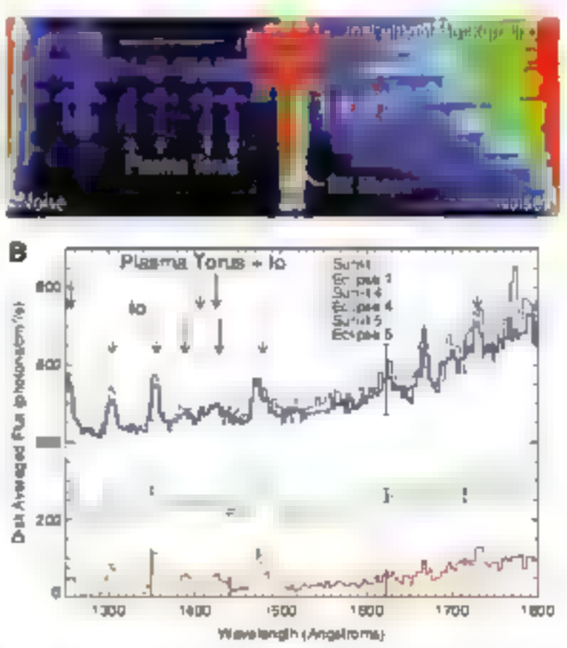

Fig. 1. (**A**) Alice spectral image, a combination of all IEclipse04 data. Features include Io in row 17, the Io plasma torus in rows 9 to 22, background interplanetary Lyman-α emissions in rows 7 to 26 (red rectangle/T-shaped slit; near this the sensitivity changes abruptly from a gap in the detector photocathode coverage), and increased detector noise at the left and right edges. Instrument-scattered Lyman-α from Jupiter and/or detector dark signal is ubiquitous at longer wavelengths in all rows and hint at row-to-row flat-field variations known from lab measurements. (**B**) Alice IEclipse01, IEclipse04, and IEclipse05 Io spectra combined into sunlit and eclipse averages. Spectra for each visit are offset by increments of 200 for clarity. Neutral and ionized atomic emissions are indicated with arrows ("Io" and "Plasma Torus + Io," respectively). The time variability is presented in Fig. 3, and integrated emission line brightnesses are listed in Table 2. Error bars are SDs of the variability. Adjacent rows are averaged for the background subtraction, which is incomplete at longer wavelengths.

[1]Southwest Research Institute, San Antonio, TX 78228, USA. [2]Southwest Research Institute, Boulder CO 80302, USA. [3]NASA Headquarters, Washington, DC 20546, USA. [4]University of Cologne, 50923 Koln, Germany. [5]The Johns Hopkins University, Baltimore, MD 21218, USA. [6]The Johns Hopkins University Applied Physics Laboratory, Laurel, MD 20723, USA. [7]University of Colorado, Boulder, CO 80302, USA. [8]Jet Propulsion Laboratory, Pasadena, CA 91109, USA. [9]NASA Goddard Spaceflight Center, Greenbelt, MD 20771, USA. [10]NASA Ames Research Center, Moffett Field, CA 94035, USA.

*To whom correspondence should be addressed. E-mail: KRetherford@swri.edu

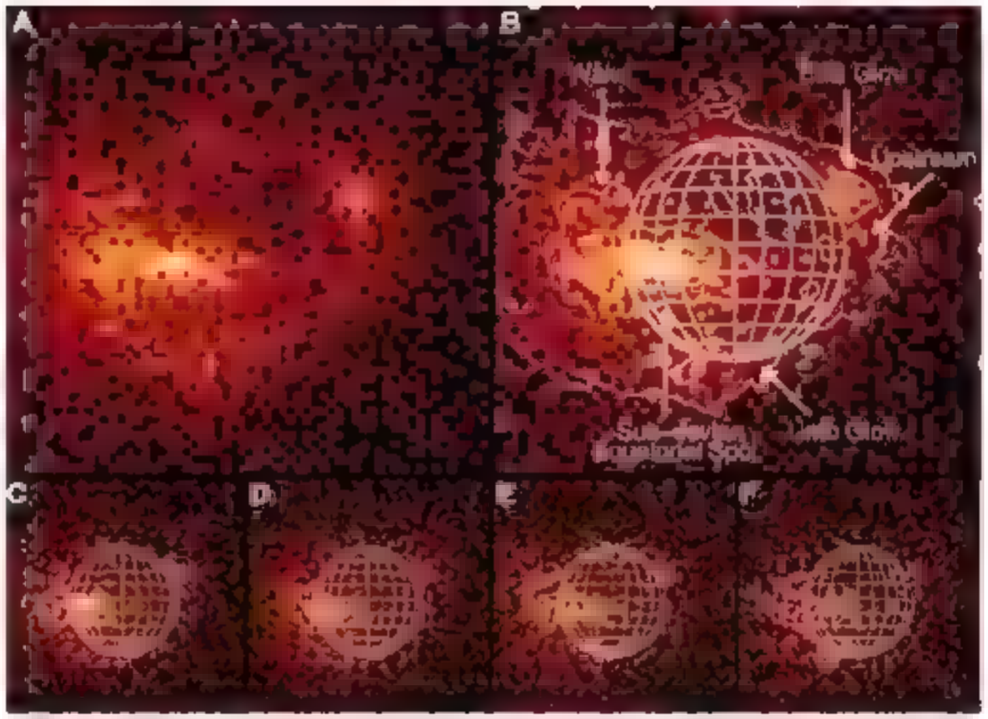

Fig. 2. HST/SBC FUV images of Io on 27 February 2007, concurrent with NH IEclipse03 observations. (**A**) Average of all eight 5-min HST exposures. (**B**) Same as (A), with labeled features. The sub-Earth longitude is 344°. The sub-jovian (0°) and orbital trailing (270°) longitudes are indicated with dashed and dotted meridians, respectively, with 15° gridding for the graticule. The view of Io from Earth is 33° from the concurrent NH view. Contours indicate 0.5 kilorayleigh (kR) increments in brightness levels. The aurora morphology is qualitatively consistent with previous FUV observations. The upstream-side auroral feature is nominally expected where the jovian magnetic field is tangent to the limb (shown with arrow). However, its location is ~15° North and likely influenced by the East Girru plume (*17*). The wake auroral feature is observed to extend >1 R_{Io} downstream relative to the plasma flow. The 1.4 ± 0.1 times brighter southern polar limb glow measured between 0.75 and 1.25 R_{Io} is consistent with Io being located "above" the plasma torus centrifugal equator (*23*). The nearby north, south, and west Masubi volcanoes known to be active at this time (*17*) may also enhance the southern limb glow brightness on the left (fig. S2). The F125LP filter includes FUV emissions in the 125-nm to 200-nm band-pass, which are primarily O I 130.4 nm, O I 135.6 nm, S I 138.9 nm, S I 147.9 nm, S I 166.7 nm, S I 181.2 nm, and S I 190.0 lines for atomic gas, with smaller contributions from ionized S II 125.6 nm, Si II 142.9 nm, and S I 172.9 nm (*20*). (**C** to **F**) HST/SBC time series of 10-min (two exposure) averages. The brightness contours (labeled in kilorayleighs) are scaled to match the ~50% brightness level in each image to better compare the equatorial spot shape and latitudinal extent as a function of time. The latitudinal extent decreases by ~25% from (C) to (F).

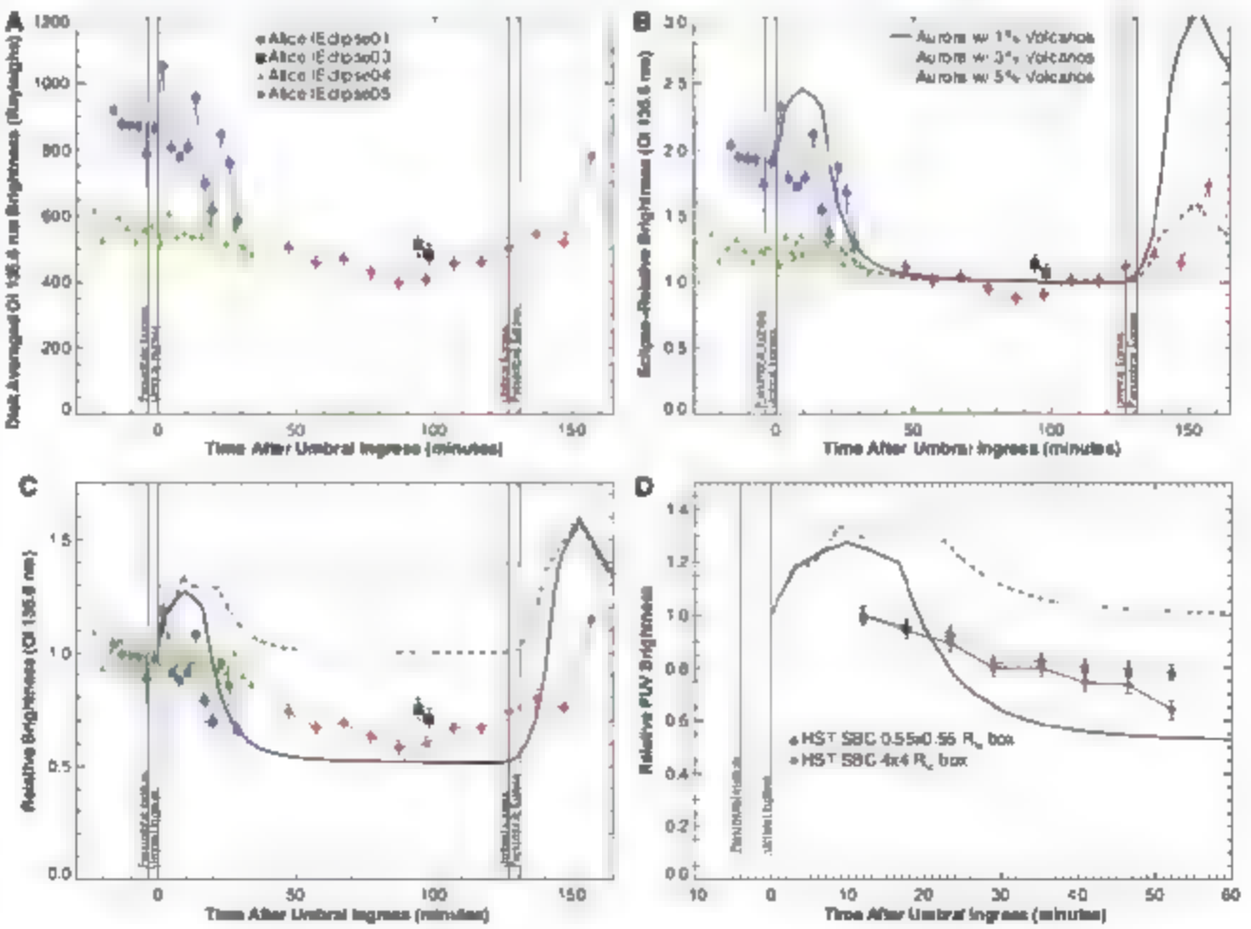

Fig. 3. Time series of Io's auroral emissions in Eclipse. (**A**) NH Alice IEclipse01, Eclipse03, IEclipse04, and IEclipse05 brightness measurements of O I 135.6 nm emissions are shown with time after umbral eclipse ingress. (**B**) Same as (A), but normalized to values in eclipse from 50 to 125 min after ingress and compared with aurora simulations (*14*) for three levels of volcanic contribution. (**C**) Same as (A) and (B), but normalized to pre-ingress, sunlit values. The last measurement in IEclipse05 supports the predicted posteclipse brightening. IEclipse01 views the dayside, whereas IEclipse04 views mostly the nightside and is dimmer. These diurnal (phase angle) variations indicate that the atmosphere in shadow (both on the nightside and in eclipse) is supplied primarily by volcanoes (see additional plots in fig. S1). Eclipse01, obtained at roughly twice the distance from NH as IEclipse04, has more statistical noise. (**D**) HST/ACS/SBC brightness measurements of regions within the limb and extending a few R_{Io} with time in eclipse, concurrent with the IEclipse03 event. The SBC brightnesses decreased by a factor of 1.3 during the period between 20 min and 50 min after ingress.

Table 2. Alice-measured emission line brightness averages and SDs in sunlight and eclipse.

Emission Line	Type	Disk-average brightness (rayleighs)		
		lEclipse01	lEclipse04	lEclipse05
OI 130.4 nm	Sunlight	706 ± 134	445 ± 27	347 ± 142
	Eclipse	597 ± 43	394 ± 14	254 ± 71
	Ratio S/E	1.18 ± 0.24	1.12 ± 0.08	1.37 ± 0.68
OI 135.6 nm	Sunlight	882 ± 177	577 ± 35	480 ± 188
	Eclipse	797 ± 57	536 ± 18	381 ± 94
	Ratio S/E	1.11 ± 0.24	1.08 ± 0.08	1.26 ± 0.58
SI 147.9 nm	Sunlight	1167 ± 271	986 ± 54	596 ± 288
	Eclipse	1205 ± 87	874 ± 28	429 ± 144
	Ratio S/E	0.97 ± 0.24	1.13 ± 0.07	1.39 ± 0.82

NH Long Range Reconnaissance Imager (LORRI) images (*17*). This same feature appears in the HST SBC image in Fig. 2B, obtained when East Giru was shifted just behind the limb. The auroral feature near East Giru in both LORRI and HST/SBC images is ~15° northward of Jupiter's field line tangent point at the limb, which suggests that ionospheric currents are diverted northward from this nominal position toward a region of higher gas density near the plume. Similar deviations of the ant-jovian FUV emissions from nominal tangent points observed with STIS are likely caused by the prevalence and distribution of plumes there (*21*). Volcanic plume auroras were not identified in previous lower-quality STIS FUV images, which caused an apparent discrepancy with visible images of plume auroras. The East Giru plume FUV auroral feature in Fig. 2 resolves this discrepancy and reveals the influence of plumes on Io's electrodynamic interaction. The upstream-side emission feature is more apparent when limb brightened at viewing geometries like those reported in Fig. 2. This feature was predicted by aurora image simulations (*22*) and is diagnostic of the divergence of the plasma flow upstream of Io, a primary trait of Io's interaction with the plasma torus.

References and Notes

1. F. Bagenal, *J. Atmos. Sol. Terres. Phys.* **69**, 387 (2007)
2. E. Lellouch, M. A. McGrath, K. L. Jessup, in *Io After Galileo* (Springer-Praxis, UK, 2006), pp. 231–264
3. J. Pearl *et al.*, *Nature* **280**, 755 (1979)
4. W. M. Sinton, C. Kaminski, *Icarus* **75**, 207 (1988)
5. J. R. Spencer *et al.*, *Science* **288**, 1198 (2000)
6. A. F. Cook *et al.*, *Science* **211**, 1419 (1981)
7. J. T. Clarke, J. Ajello, J. Luhmann, N. M. Schneider, I. Kanik, *J. Geophys. Res.* **99**, 8387 (1994)
8. P. E. Geissler *et al.*, *Science* **285**, 870 (1999)
9. A. H. Bouchez, M. E. Brown, N. M. Schneider, *Icarus* **148**, 316 (2000)
10. P. E. Geissler *et al.*, *J. Geophys. Res.* **106**, 26137 (2001)
11. P. E. Geissler *et al.*, *Icarus* **172**, 127 (2004)
12. I. DePater *et al.*, *Icarus* **156**, 296 (2002)
13. K. D. Retherford, thesis, The Johns Hopkins University (2002)
14. J. Saur, D. F. Strobel, *Icarus* **171**, 411 (2004)
15. S. A. Stern *et al.*, in *Astrobiology and Planetary Missions*, R. B. Hoover, G. V. Levin, A. Y. Rozanov, G. R. Gladstone, Eds. (Proc. SPIE Volume 5906, 2005), pp. 358–367
16. K. D. Retherford *et al.*, paper presented at the Magnetospheres of the Outer Planets Meeting, San Antonio, TX, 25 June, 2007
17. J. R. Spencer *et al.*, *Science* **318**, 240 (2007)
18. The angular size of Io varies with spacecraft distance but is smaller than the Alice slit width for these data. The spectral resolution varies between 0.3 nm and ~0.9 nm for emissions known to be located near the satellite disk (*22*); see, e.g., Fig. 2
19. H. C. Ford *et al.*, in *Future EUV/UV and Visible Space Astrophysics Missions and Instrumentation*, J. C. Blades, O. H. W. Siegmund, Eds. (Proc. SPIE Volume 4854, 2003), pp. 81–94
20. F. L. Roesler *et al.*, *Science* **283**, 353 (1999)
21. K. D. Retherford *et al.*, *J. Geophys. Res.* **105**, 27157 (2000)
22. J. Saur, F. M. Neubauer, D. F. Strobel, M. E. Summers, *Geophys. Res. Lett.* **27**, 2893 (2000)
23. K. D. Retherford, H. W. Moos, D. F. Strobel, *J. Geophys. Res.* **108**, 1333 (2003)
24. L. M. Feaga, thesis, The Johns Hopkins University (2005)
25. K. L. Jessup *et al.*, *Icarus* **169**, 197 (2004)
26. J. R. Spencer *et al.*, *Icarus* **176**, 283 (2005)
27. P. D. Feldman *et al.*, *Geophys. Res. Lett.* **27**, 1787 (2000)
28. D. F. Strobel, B. C. Wolven, *Astrophys. Space Sci.* **277**, 271 (2001)
29. F. Neubauer, *J. Geophys. Res.* **103**, 19843 (1998)
30. F. M. Neubauer, *J. Geophys. Res.* **104**, 3863 (1999).

31. We thank the New Horizons mission and science teams. New Horizons is funded by NASA. Support for this work was also provided by NASA through grant number GO-10871 from the Space Telescope Science Institute (STScI), which is operated by the Association of Universities for Research in Astronomy, Inc., under NASA contract NAS5-26555

Supporting Online Material

www.sciencemag.org/cgi/content/full/318/5848/232/DC1
Figs. S1 and S2
Tables S1 and S2

10 July 2007; accepted 19 September 2007
10.1126/science.1147594

REPORT

Io Volcanism Seen by New Horizons: A Major Eruption of the Tvashtar Volcano

J. R. Spencer,[1]* S. A. Stern,[2] A. F. Cheng,[2] H. A. Weaver,[3] D. C. Reuter,[4] K. Retherford,[5] A. Lunsford,[6] J. M. Moore,[6] O. Abramov,[1] R. M. C. Lopes,[7] J. E. Perry,[8] L. Kamp,[7] M. Showalter,[9] K. L. Jessup,[1] F. Marchis,[9] P. M. Schenk,[10] C. Dumas[11]

Jupiter's moon Io is known to host active volcanoes. In February and March 2007, the New Horizons spacecraft obtained a global snapshot of Io's volcanism. A 350-kilometer-high volcanic plume was seen to emanate from the Tvashtar volcano (62°N, 122°W), and its motion was observed. The plume's morphology and dynamics support nonballistic models of large Io plumes and also suggest that most visible plume particles condensed within the plume rather than being ejected from the source. In images taken in Jupiter eclipse, nonthermal visible-wavelength emission was seen from individual volcanoes near Io's sub-Jupiter and anti-Jupiter points. Near-infrared emission from the brightest volcanoes indicates minimum magma temperatures in the 1150- to 1335-kelvin range, consistent with basaltic composition.

The New Horizons (NH) Jupiter flyby provided the first close-up observations of the tidally driven volcanism of Jupiter's moon Io since the last Galileo orbiter observations of Io in late 2001 (*1*). The closest approach to Io occurred at 21:57 UT on 28 February 2007 at a range of 2.24 million km. Similar observations were made at solar phase angles from 5° to 159°, and four eclipses of Io by Jupiter were also observed. NH obtained 190 Io images with its 4.96 μrad per pixel panchromatic (400 to 900 nm) Long-Range Reconnaissance Imager (LORRI) and 17 color nighttime and eclipse images with the 20 μrad per pixel Multicolor Visible Imaging Camera (MVIC), although MVIC coverage of Io's day side was not possible because of detector saturation. NH also obtained seven 1.25- to 2.5-μm near-infrared image cubes at 62 μrad per pixel with the Linear Etalon Infrared Spectral Array instrument (LEISA) and numerous disk-integrated ultraviolet observations with the Alice instrument, discussed separately (*2*).

Eleven volcanic plumes were identified in the NH images (Fig. 1A and table S1). In addition to the single very large "Pele-type" plume at Tvashtar, which is described separately, NH observed 10 SO_2-rich "Prometheus-type" plumes (*3*–*5*). These smaller plumes averaged 80 km high and varied greatly in brightness. Plumes seen for the first time by NH include those at Zal and Kurdalagon and a large new plume, 150 km high, at north Lerna Regio, which has produced a large albedo change. Three of these plumes, north Lerna and north and south Masubi, are associated with recent large lava flows, supporting the idea that Prometheus-type plumes result from mobilization of surface volatiles by active lava flows. All active plumes that were on

the disk or near the limb were also visible in Jupiter eclipse images because of excitation of plume gases by the jovian magnetosphere (Fig. 2B), as also seen by Galileo (*6*).

[1]Southwest Research Institute, 1050 Walnut Street, Suite 300, Boulder, CO 80302, USA. [2]NASA Headquarters, Washington, DC 20546, USA. [3]Applied Physics Laboratory, Johns Hopkins University, 11100 Johns Hopkins Road, Laurel, MD 20723, USA. [4]NASA Goddard Space Flight Center, Greenbelt, MD 20771, USA. [5]Southwest Research Institute, Post Office Drawer 28510, San Antonio, TX 78228, USA. [6]NASA Ames Research Center, Moffett Field, CA 94035, USA. [7]Jet Propulsion Laboratory, 4800 Oak Grove Drive, Pasadena, CA 91109, USA. [8]Lunar and Planetary Laboratory, University of Arizona, Tucson, AZ 85721, USA. [9]Search for Extraterrestrial Intelligence (SETI) Institute, 515 North Whisman Road, Mountain View, CA 94043, USA. [10]Lunar and Planetary Institute, 3600 Bay Area Boulevard, Houston, TX 77058, USA. [11]European Southern Observatory, Casilla 19001, Santiago 19, Chile.

*To whom correspondence should be addressed. E-mail: spencer@boulder.swri.edu

LORRI imaged almost all of Io at relatively low phase angles with resolutions between 14 and 22 km per pixel, providing a surface albedo map suitable for comparison with previous maps (*7*) (Fig. 1A). There are at least 19 locations where surface changes have occurred since Galileo's last global images, taken between 1999 and 2001 (Fig. 1A). The number of surface changes detected is only one-fourth of those detected during the 5-year Galileo mission (*8*), perhaps because of NH's lower spatial resolution, the lack of a color data set with comparable resolution, and the possibility of surface changes that have faded since their formation.

The large plume at Tvashtar has renewed the large ring-shaped plume deposit seen at Tvashtar in 2000 (*1*), which had been obscured by other plume deposits by mid-2001. A two-lobed plume deposit surrounds a new, 240-km-long dark feature, probably a lava flow, at Masubi (Fig. 1, B to D) created by the two plumes observed by NH, "North Masubi" near the vent and "South Masubi" at the distal flow front. This flow is the longest new lava flow to be erupted on Io since the 1979 Voyager images. The North Lerna volcanic plume has produced a 700-km-wide concentric deposit (Fig. 1, E and F) surrounding a fresh, 130-km-long apparent dark lava flow. Other late-Galileo–era plume deposits, notably around Dazhbog and Thor (*8*), have faded to invisibility.

LEISA observed 1.25- to 2.5-μm volcanic thermal emission from Io's night side or in Jupiter eclipse at almost all longitudes at a spatial resolution of 140 to 170 km per pixel, producing a uniform global snapshot of Io's high-temperature volcanic thermal emission (Fig. 1A). Thermal emission from several volcanoes was also seen in 0.4- to 1.0-μm LORRI images in Jupiter eclipse or on the night side (Fig. 2A). At least 36 hot spots were detected. All correspond to previously known active volcanic centers

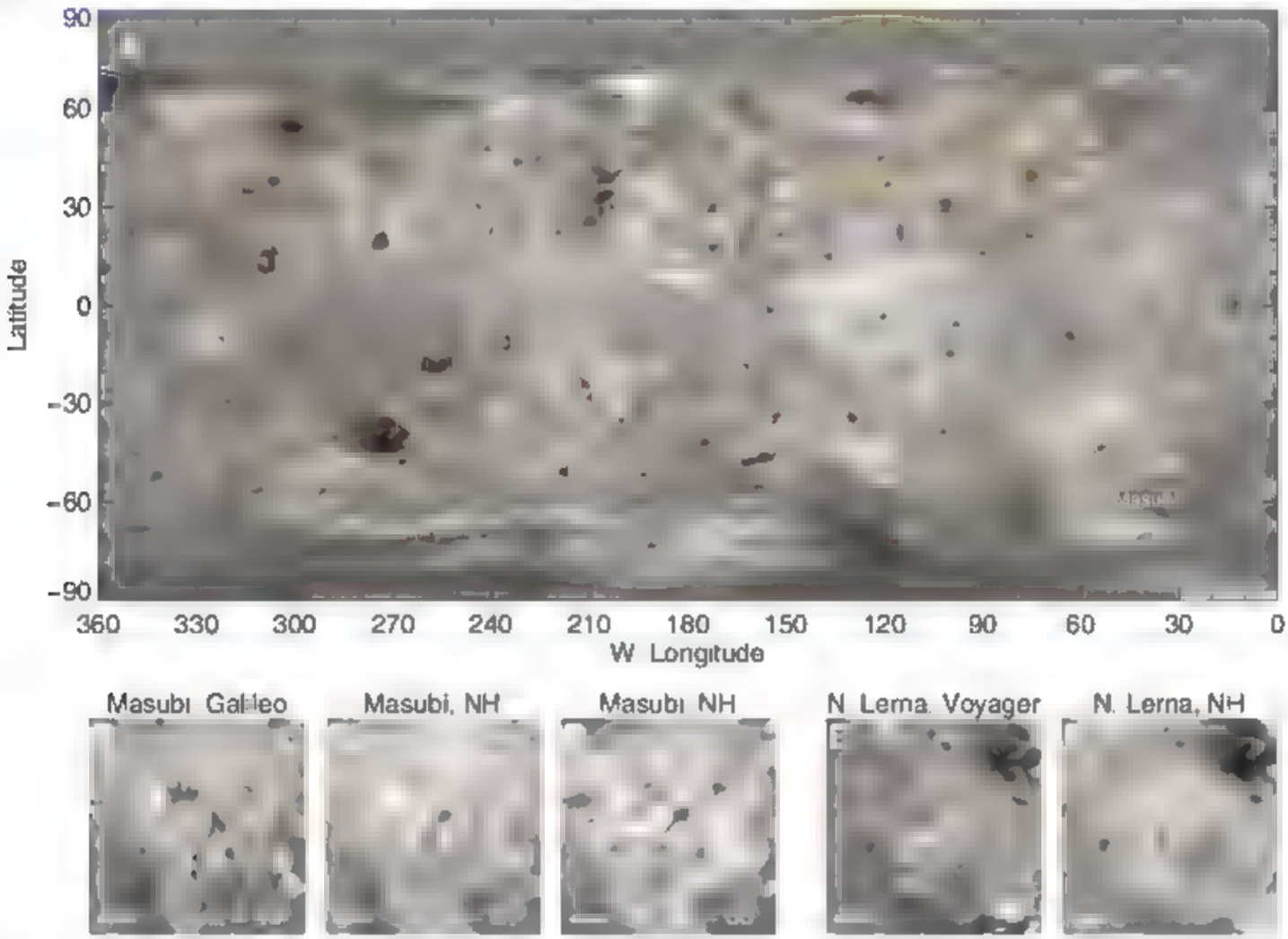

Fig. 1. (**A**) Global map of Io derived from eight LORRI images obtained at phase angles between 26° and 47°, showing volcanic activity detected by NH. See fig. S1 for an unannotated version. Yellow ovals denote areas with new, faded, or shifted plume or other volatile deposits since the last Galileo images in 2001. Green circles denote areas where probable new lava flows have occurred. Cyan diamonds indicate locations of active plumes (table S1), and orange hexagons are volcanic hot spots detected by LEISA. For plumes and hot spots, symbol size indicates the approximate relative size and brightness of the features. (**B** to **F**) Comparison of NH LORRI and earlier images (*7*) of major surface changes at Masubi (45°S, 57°W) and North Lerna (55°S, 290°W), reprojected to a consistent geometry. The scale bars are 200 km long, and α is the solar phase angle. At Masubi, old lava flows seen by Voyager and Galileo (B) have been obscured at low phase angles (C) by plume deposits associated with what is probably a new dark lava flow. The old flows are still seen by NH at high phase angles (D), suggesting the plume deposits are not thick enough to obscure the surface texture of the old flows. At North Lerna, a recent eruption has generated a 130-km-long dark feature (F), probably a lava flow, as well as an active plume that has produced a concentric pattern of deposits.

(9) except for a bright new hot spot that we call "East Gunu" at 22°N, 235°W, 130 km east of the known volcano Gunu. This hot spot location corresponds to an inconspicuous dark linear feature, possibly an old fissure eruption, in Galileo images. No associated albedo change is visible in sunlit LORRI images; perhaps East Gunu is a very young eruption that has not had time to produce observable albedo changes. No plume was seen in reflected light at East Gunu, but a detached glow 330 km directly above the hot spot was seen in eclipse images (Fig. 2A), suggesting some associated gas output.

LORRI eclipse images show numerous faint point sources of emission (Fig. 2A), particularly near the sub-jovian and anti-jovian points (on the equator at longitudes 0° and 180°W), with a typical brightness of ~100 kRayleigh assuming a 15-km-by-15-km source region. These were also seen in Galileo eclipse images (6). These spots all correspond to low-albedo volcanic centers (Fig. 2D), but because simultaneous LEISA images show no corresponding cluster of bright spots in the near-infrared (Fig. 2, E and F), where volcanic thermal emission dominates, it is likely that a non-thermal mechanism, probably plasma-related, creates the sub-jovian and anti-jovian clusters of point-source emission. Most of these spots are less than about 30 km in size, suggesting a near-surface origin.

A fortuitous major eruption of the Tvashtar volcano during the NH flyby provides a comprehensive view of a large, sulfur-rich Pele-class (3) volcanic plume on Io. Tvashtar, a series of calderas centered near 62°N, 122°W, has been one of Io's most active volcanos in recent years. An active period from late 1999 to early 2001 (10–12) produced a large infrared hot spot, plume, and orange pyroclastic deposits and was followed by quiescent conditions seen in late 2001 (1, 13) and early 2003 and 2004. Renewed thermal emission in April to May 2006 (14) may have been an earlier phase of the 2007 eruption seen by NH. Continued thermal emission from Tvashtar was seen by ground-based observations during and after the NH encounter from 18 January (15) to 27 May 2007.

The 2007 Tvashtar plume was first seen in back-scattered light in 260-nm wavelength images from the Hubble Space Telescope (HST) on 14 February 2007 (Fig. 3A) and again in absorption in Jupiter transit images on 21 February (Fig. 3B). Absorption in the 260-nm wavelength region suggests, by analogy with previous HST observations of the Pele plume, that the Tvashtar plume is rich in S_2 gas (16), as also inferred from the orange color of its plume deposits seen previously by Galileo (12, 17).

NH imaged the Tvashtar plume on 39 occasions over 7.8 days, at phase angles between 7° and 159° and LORRI resolutions between 12 and 38 km per pixel. The plume height was remarkably constant, varying between roughly 320 and 360 km, and full width was about 1100 km, consistent with the diameter of the pyroclastic deposits (Fig. 1). The plume had a bright top in all images (Fig. 3, C, D, and F to J), very similar to Voyager images of the Pele plume. This morphology is not consistent with simple ballistic models of plume particle flight, as noted for Pele (18), but is consistent with hydrodynamic models with entrained particles that include a gas shock front at the top of the plume (19). Most Tvashtar plume images show little evidence for a central upgoing column of particles (e.g., Fig. 3C), suggesting that the observed particles may condense out of the plume rather than being directly ejected from the vent.

The plume contains remarkable time-variable filamentary structures similar to those glimpsed in the single high-resolution Voyager 1 image of the Pele plume. This structure allows tracing of motion within the plume in a sequence of five images of the upper part of the plume obtained at 2-min intervals on 1 March (Fig. 3, F to J, and movie S1). Speeds projected on the plane of the sky are 0.4 to 0.7 km s^{-1} (Fig. 3E), comparable to expected ballistic ejection speeds for a 350-km-high plume (~1.0 km s^{-1}), and accelerate as plume features fall toward the surface. Features appear to slide down the upper surface of the plume rather than tracing ballistic trajectories originating at the vent.

The source of the Tvashtar plume is associated with by far the brightest hot spot seen by NH (Fig. 4).

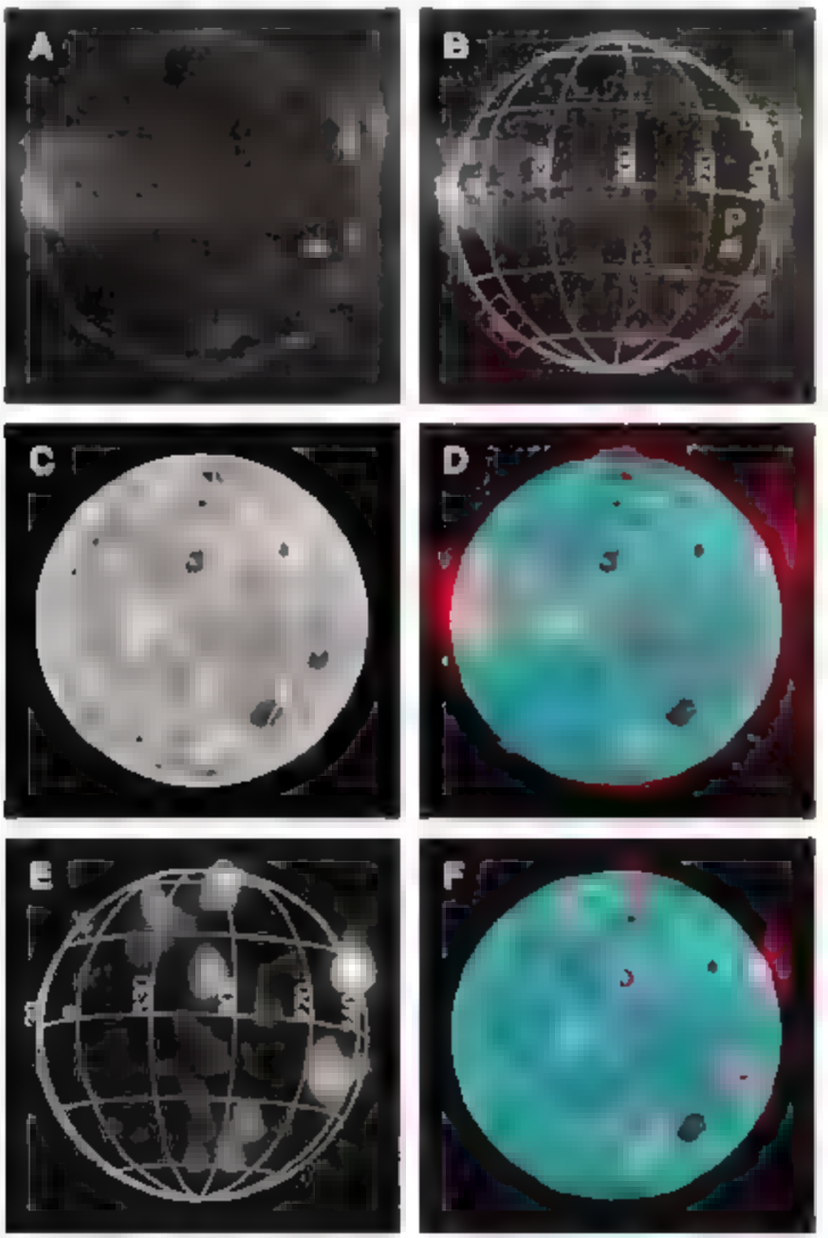

Fig. 2. Images of Io in Jupiter eclipse. (**A**) LORRI image taken at 27 February 14:37 UT with an effective exposure time of 16 s. Dark blotches and straight lines are artifacts. The brightest spots (P, Pele; EG, East Gunu) are thermal emission from active volcanoes, and more diffuse emission is from the plumes and atmosphere (6). (**B**) Same image with latitude/longitude grid showing glowing plumes (plume sources, table S1, indicated by red diamonds). (**C**) Simulated sunlit view with the same geometry, based on sunlit LORRI images (Fig. 1A). (**D**) Combined sunlit (cyan) and eclipse (red) image, showing that all pointlike sources of emission in the eclipse image correspond to low-albedo volcanic centers. (**E**) A ~2.3-μm LEISA eclipse image at 27 February 15:31 UT, showing thermal emission from active volcanoes. Elongation of the hot spots is an artifact. (**F**) Combined visible albedo (cyan) and LEISA thermal emission (red) image, showing the sources of the volcanic emission.

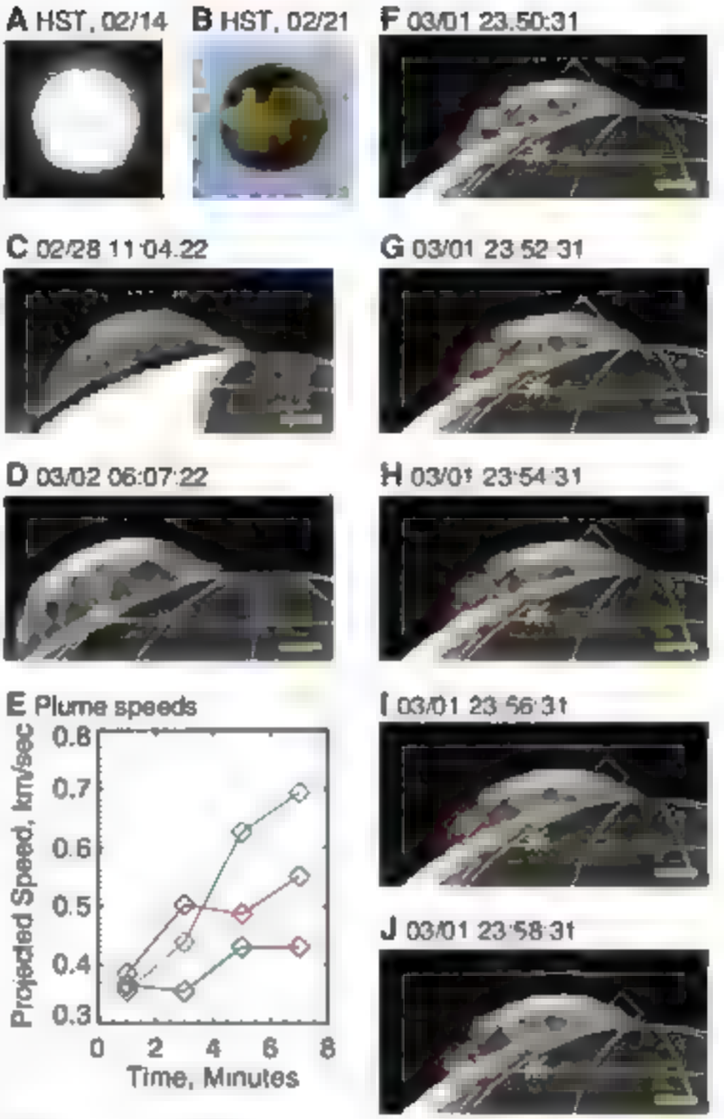

Fig. 3. The Tvashtar plume. (**A**) Discovery image by HST in backscattered light in the F255W filter (central wavelength = 260 nm). The red diamond indicates the plume source. (**B**) HST image of 260 nm absorption by the plume against Jupiter: 260 nm (blue) plus 330 nm (green) plus 410 nm (red) color composite. Other images are in visible light from NH LORRI. The scale bar is 200 km long, and the yellow star indicates the projected location of the hot spot at the plume source. The dashed line is the terminator. (**C**) Highest-resolution view of the full plume, at a resolution of 12.4 km per pixel and phase angle of 102°, showing the filamentary structure. Images are sharpened by unsharp masking; the dark line at the edge of the disk is an artifact of the sharpening. (**D**) Image at 145° phase angle at 22.4 km per pixel, showing the time variability of the details of the plume structure and the persistent bright top. (**F** to **J**) Sequence of frames at 2-min intervals showing dynamics in the upper part of the plume (the source is on the far side of Io). Colored diamonds track individual features whose speeds, projected on the plane of the sky, are shown in (**E**).

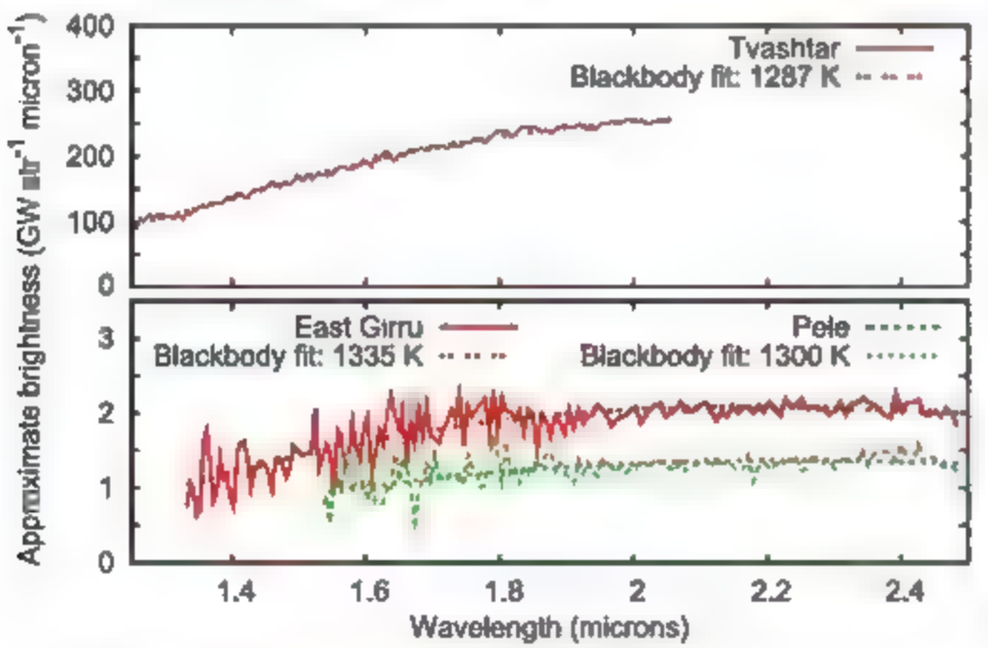

Fig. 4. LEISA spectra of volcanic thermal emission from Tvashtar, Pele, and East Girru, with best-fit blackbody curves superposed. Vertical axis units are GW steradian^{-1} μm^{-1}.

Thermal emission was observed on multiple occasions by LORRI, LEISA, and by MVIC at wavelengths from 2.5 to below 0.7 μm. The hot spot location, 62.5°N, 122.5°W, coincides with the fire fountains seen at Tvashtar by Galileo in November 1999. The spectrum can be fit with a single temperature blackbody at 1287 K from 1.25 to 2.04 μm, providing a lower limit to the magma temperature, comparable to Galileo estimates (*12*). Assuming a temperature of 1200 K for the Tvashtar hotspot, an area of 49 km^2 is derived from the brightness in LORRI images, comparable to the ~25 km^2 area of the incandescent fire fountain seen by Galileo at Tvashtar in November 1999 (*12*). The isothermal blackbody emission spectrum at close to magmatic temperatures is also consistent with an energetic eruption such as a fire fountain, rather than, for instance, spreading and cooling lava flows (*20*, *21*). Temperatures are consistent with basaltic lava composition. Exotic high temperature magmas, inferred from some Galileo observations (*22*), are not required either at Tvashtar or other hot spots seen by NH.

References and Notes

1. E. P. Turtle *et al.*, *Icarus* **169**, 3 (2004).
2. K. D. Retherford *et al.*, *Science* **318**, 237 (2007).
3. A. S. McEwen, L. Soderblom, *Icarus* **55**, 191 (1983).
4. P. Geissler, D. Goldstein, in *Io After Galileo*, R. M. C. Lopes, J. R. Spencer, Eds. (Praxis, Chichester, UK, 2007), pp. 163–192.
5. "Pele-type" plumes are thought to result from direct ejection of gas from a volcanic vent, whereas the smaller "Prometheus-type" plumes may result from remobilization of surface volatiles by lava flows.
6. P. E. Geissler *et al.*, *J. Geophys. Res.* **106**, 26137 (2001).
7. U.S. Geological Survey Astrogeology Research Program, http://astrogeology.usgs.gov/Projects/JupiterSatellites/io.html.
8. P. E. Geissler *et al.*, *Icarus* **172**, 127 (2004).
9. R. M. C. Lopes, J. Radebaugh, M. Malaska, J. Perry, F. Marchis, in *Io After Galileo*, R. M. C. Lopes, J. R. Spencer, Eds. (Praxis, Chichester, UK, 2007), pp. 307–323.
10. R. R. Howell *et al.*, *J. Geophys. Res.* **106**, 33129 (2001).
11. F. Marchis *et al.*, *Icarus* **160**, 124 (2002).
12. M. P. Milazzo *et al.*, *Icarus* **179**, 235 (2005).
13. F. Marchis *et al.*, *Icarus* **176**, 96 (2005).
14. C. Lavel, I. de Pater, F. Marchis, *Bull. Am. Astron. Soc.* **38**, 612 (2006).
15. J. A. Rathbun, J. R. Spencer, paper presented at the 39th annual American Astronomical Society, Division for Planetary Science meeting, Orlando, FL, 9 October 2007.
16. J. R. Spencer, K. L. Jessup, M. A. McGrath, G. E. Ballester, R. Yelle, *Science* **288**, 1208 (2000).
17. A. S. McEwen *et al.*, *Icarus* **135**, 181 (1998).
18. R. G. Strom, N. M. Schneider, in *Satellites of Jupiter*, D. Morrison, Ed. (Univ. of Arizona Press, Tucson, AZ, 1982), pp. 598–633.
19. J. Zhang *et al.*, *Icarus* **172**, 479 (2004).
20. J. A. Stansberry, J. R. Spencer, R. R. Howell, D. Vakil, *Geophys. Res. Lett.* **24**, 2455 (1997).
21. A. G. Davies *et al.*, *J. Geophys. Res.* **106**, 33079 (2001).
22. A. S. McEwen *et al.*, *Science* **281**, 87 (1998).

23. We thank the entire NH mission team, particularly D. Rose and E. Birath, and our colleagues on the NH science team. NH and the ancillary investigations described here are funded by NASA, whose financial support we gratefully acknowledge.

Supporting Online Material

www.sciencemag.org/cgi/content/full/318/5848/240/DC1
Fig. S1
Table S1

10 July 2007; accepted 19 September 2007
10.1126/science.1147621

Excitation of Lunar Eccentricity by Planetary Resonances

Matija Ćuk

The Moon is thought to have formed in a collision between Earth and another protoplanet (*1*), after which a circumterrestrial debris disk quickly accumulated into a satellite (*2*). Subsequent tidal interactions (*3*) expanded the lunar orbit from 3 to 60 Earth radii (R_E). The effects of tides on lunar eccentricity (e) are complex. Whereas tides raised on Earth increase e, solid body tides within the Moon damp it (*4*).

Goldreich (*4*) derived analytical estimates of the relative importance of the tides within Earth and the Moon and found that the lunar e should be increasing. Because currently lunar free eccentricity, e_{free}, is 0.053 (Materials and Methods), the two effects had to be close during much of the system's history if they were to prevent extreme damping or growth (*2*, *4*).

Lunar laser ranging (*5*) confirmed the recession but found the increase in e to be significantly larger than the theory predicts. The most plausible explanation for this is that the ocean tides, which are known to provide over 95% of the Earth's tidal dissipation, cannot be modeled by simple tidal bulges, which lead the Moon in longitude.

Both the system's age and ocean-tide models (*6*) suggest that Earth's tides have become more important over time, probably because the ocean dissipation depends on the forcing frequency (i.e., length of day). If they were weaker than lunar tides during the initial rapid orbital expansion, any primordial e would have been greatly reduced during this crucial epoch, contradicting Goldreich's hypothesis (*3*).

If not primordial, where does the present e come from? Kaula and Yoder (*7*) noted that an otherwise minor periodic perturbation known as jovian evection (governed by the geocentric angle between the lunar perigee and the position of Jupiter) becomes resonant at the Earth-Moon distance of about $53R_E$ and calculated that the resonance capture would have occurred if $e_{free} < 0.0076$ when entering the resonance.

To test this hypothesis, we constructed a numerical integrator by using a symplectic algorithm [explicitly separating Keplerian motion from small perturbations (*8*)]. The lunar orbit was integrated directly, whereas the orbits of Earth and Jupiter were considered unperturbed. Earth tides were included directly by using a quadrupole "bulge" leading the Moon by a constant angle, whereas the satellite tides were ignored.

The integration with a constant-e Earth's orbit (fig. S1) matched the analytical results (*7*). However, it is not a good model for the resonance passage because we have ignored the variation of lunar orbital precession, which mirrors the planet-induced oscillations in Earth's eccentricity. To avoid directly integrating all eight planets, we treat the Earth's orbit as Keplerian but with slowly varying eccentricity and longitude of pericenter following a secular theory (Materials and Methods). Thus, modified simulations (fig. S2 and Fig. 1) show that the present orbital e_{free} of the Moon can be generated by the resonance passage if $e_{free} > 0.005$ before the resonance.

We also considered other planetary resonances that the Moon must have encountered. The only other important resonance happens at $46.6R_E$ and involves Venus (table S1). With use of numerical simulations, we found that the preresonance e_{free} at $46.6R_E$ had to be larger than about 0.001 if the Moon was to enter jovian resonance at $53R_E$ with $e_{free} = 0.005$ (fig. S3).

A lunar $e_{free} \sim 10^{-3}$ could be a tidally damped remnant of a primordial e or a product of the lunar cataclysm (*9*) through basin-forming impacts or close encounters with massive (≥1000 km) objects. In either case, our results support the view that lunar tides were dominant over terrestrial ones during the first few 100 million years (My) of the system's history (*4*, *5*), which would make high-e lunar orbit (*10*) beyond $20R_E$ rather unlikely. Although our analysis cannot exclude solar resonances (*11*) inducing a high e closer to Earth, interactions with a circumterrestrial ring (*12*) likely made early lunar orbital evolution too fast for large eccentricity excitation (*11*).

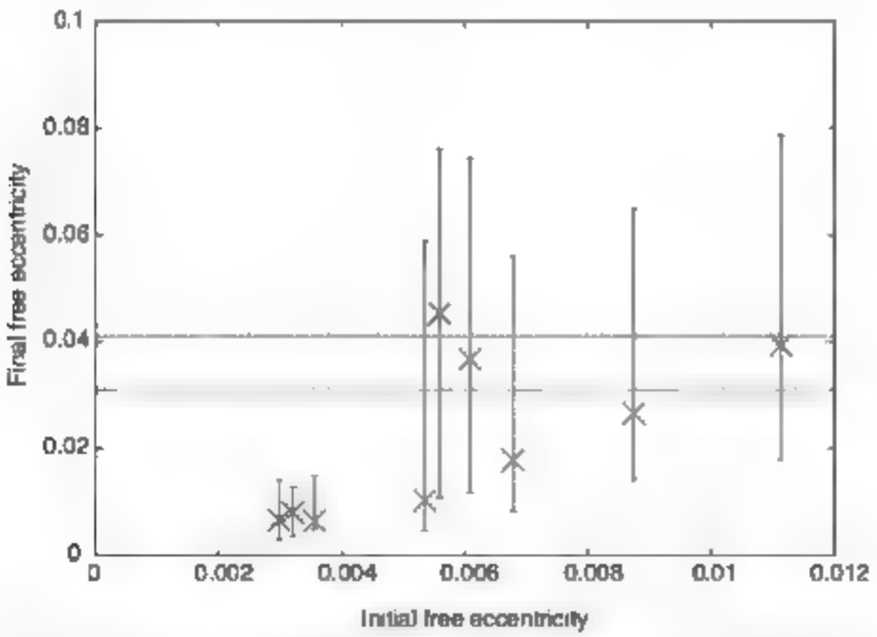

Fig. 1. Median postresonance e_{free} for nine sets of numerical simulations plotted against their initial e_{free}. Six sets of 30 runs with initial $e_{free} = 0.005$ to 0.015 lasted 50 My, and the three sets of 15 runs with lower initial e_{free} lasted 33 My. Each error bar plots the scatter of the 50% of the runs closest to the median. The two dashed lines show the free eccentricity of the Moon at $53R_E$ extrapolated back from the present, assuming Earth's tidal quality factor $Q_E = 12$ (bottom) or $Q_E = 35$ (top).

References and Notes

1. W. K. Hartmann, D. R. Davis, *Icarus* **24**, 504 (1975).
2. R. M. Canup, *Annu. Rev. Astron. Astrophys.* **42**, 441 (2004).
3. P. Goldreich, *Rev. Geophys.* **4**, 411 (1966).
4. P. Goldreich, *Mon. Not. R. Astron. Soc.* **126**, 257 (1963).
5. J. G. Williams, presentation at the 37th Meeting of the American Astronomical Society's Division of Dynamical Astronomy, Halifax, Nova Scotia, Canada, 25 to 29 June 2006, available at http://ddd.harvard.edu/browser_award/BrouwerAward_2006_Williams.pdf.
6. G. G. Bills, R. D. Ray, *Geophys. Res. Lett.* **26**, 3045 (1999).
7. W. M. Kaula, C. F. Yoder, *Lunar Planet. Sci. Conf. VII*, 440 (1976).
8. J. Wisdom, M. Holman, *Astron. J.* **102**, 1528 (1991).
9. F. Tera, A. A. Papanastassiou, G. J. Wasserburg, *Earth Planet. Sci. Lett.* **22**, 1 (1974).
10. L. Garrick-Bethell, J. Wisdom, M. T. Zuber, *Science* **313**, 652 (2006).
11. J. Touma, J. Wisdom, *Astron. J.* **115**, 1653 (1998).
12. W. R. Ward, R. M. Canup, *Nature* **403**, 741 (2000).

13. The author acknowledges support from the Canadian Institute for Theoretical Astrophysics and the Natural Sciences and Engineering Research Council of Canada and thanks B. Gladman for help on this project.

Supporting Online Material

www.sciencemag.org/cgi/content/full/318/5848/244/DC1
Materials and Methods
Figs. S1 to S3
Table S1
References

25 June 2007; accepted 7 September 2007
10.1126/science.1146994

Department of Physics and Astronomy, University of British Columbia, 6224 Agricultural Road, Vancouver, BC V6T 1Z1, Canada.

The *Chlamydomonas* Genome Reveals the Evolution of Key Animal and Plant Functions

Sabeeha S. Merchant,[1*] Simon E. Prochnik,[2*] Olivier Vallon,[3] Elizabeth H. Harris,[4] Steven J. Karpowicz,[1] George B. Witman,[5] Astrid Terry,[2] Asaf Salamov,[2] Lillian K. Fritz-Laylin,[6] Laurence Maréchal-Drouard,[7] Wallace F. Marshall,[8] Liang-Hu Qu,[9] David R. Nelson,[10] Anton A. Sanderfoot,[11] Martin H. Spalding,[12] Vladimir V. Kapitonov,[13] Qinghu Ren,[14] Patrick Ferris,[15] Erika Lindquist,[2] Harris Shapiro,[2] Susan M. Lucas,[2] Jane Grimwood,[16] Jeremy Schmutz,[16] *Chlamydomonas* Annotation Team,† JGI Annotation Team,† Igor V. Grigoriev,[2] Daniel S. Rokhsar,[2,6]‡ Arthur R. Grossman[17]‡

Chlamydomonas reinhardtii is a unicellular green alga whose lineage diverged from land plants over 1 billion years ago. It is a model system for studying chloroplast-based photosynthesis, as well as the structure, assembly, and function of eukaryotic flagella (cilia), which were inherited from the common ancestor of plants and animals, but lost in land plants. We sequenced the ~120-megabase nuclear genome of *Chlamydomonas* and performed comparative phylogenomic analyses, identifying genes encoding uncharacterized proteins that are likely associated with the function and biogenesis of chloroplasts or eukaryotic flagella. Analyses of the *Chlamydomonas* genome advance our understanding of the ancestral eukaryotic cell, reveal previously unknown genes associated with photosynthetic and flagellar functions, and establish links between ciliopathy and the composition and function of flagella.

Chlamydomonas reinhardtii is a ~10-μm, unicellular, soil-dwelling green alga with multiple mitochondria, two anterior flagella for motility and mating, and a chloroplast that houses the photosynthetic apparatus and critical metabolic pathways (Fig. 1 and fig. S1) (*1*). *Chlamydomonas* is used to study eukaryotic photosynthesis because, unlike angiosperms (flowering plants), it grows in the dark on an organic carbon source while maintaining a functional photosynthetic apparatus (*2*). It also is a model for elucidating eukaryotic flagella and basal body functions and the pathological effects of their dysfunction (*3*, *4*). More recently, *Chlamydomonas* research has been developed for bioremediation purposes and the generation of biofuels (*5*, *6*).

The Chlorophytes (green algae, including *Chlamydomonas* and *Ostreococcus*) diverged from the Streptophytes (land plants and their close relatives) (Fig. 2) over a billion years ago. These lineages are part of the green plant lineage (Viridiplantae), which previously diverged from opisthokonts (animals, fungi, and Choanozoa) (*7*). Many *Chlamydomonas* genes can be traced to the green plant or plant-animal common ancestor by comparative genomic analyses. Specifically, many *Chlamydomonas* and angiosperm genes are derived from ancestral green plant genes, including those associated with photosynthesis and plastid function; these are also present in *Ostreococcus* spp. and the moss *Physcomitrella patens* (Fig. 2). Genes shared by *Chlamydomonas* and animals are derived from the last plant-animal common ancestor and many of these have been lost in angiosperms, notably those encoding proteins of the eukaryotic flagellum (or cilium) and the associated basal body (or centriole) (*8*). *Chlamydomonas* also displays extensive metabolic flexibility under the control of regulatory genes that allow it to inhabit distinct environmental niches and to survive fluctuations in nutrient availability (*9*).

Genome sequencing and assembly. The 121-megabase (Mb) draft sequence (*10*) of the *Chlamydomonas* nuclear genome was generated at 13× coverage by whole-genome, shotgun end-sequencing of plasmid and fosmid libraries, followed by assembly into ~1500 scaffolds (*1*). Half of the assembled genome is contained in 25 scaffolds, each longer than 1.63 Mb. The genome is unusually GC-rich (64%) (Table 1), which required modification of standard sequencing protocols. Alignments of expressed sequence tags (ESTs) to the genome suggest that the draft assembly is 95% complete (*1*).

The *Chlamydomonas* nuclear genome comprises 17 linkage groups (figs. S2 to S18) presumably corresponding to 17 chromosomes, consistent with electron microscopy of meiotic synaptonemal complexes (*11*). Seventy-four scaffolds, representing 78% of the draft genome, have been aligned with linkage groups (Fig. 3 and figs. S2 to S18). Sequenced ESTs from a field isolate (*1*) of *Chlamydomonas*, fertile with the standard laboratory strain, identified 8775 polymorphisms, result-

[1]Department of Chemistry and Biochemistry, University of California at Los Angeles, Los Angeles, CA 90095, USA. [2]U.S. Department of Energy (DOE) Joint Genome Institute (JGI), Walnut Creek, CA 94598, USA. [3]CNRS, Université Paris 6, Institut de Biologie Physico-Chimique, 75005 Paris, France. [4]Department of Biology, Duke University, Durham, NC 27708, USA. [5]Department of Cell Biology, University of Massachusetts Medical School, Worcester, MA 01655, USA. [6]Department of Molecular and Cell Biology, University of California at Berkeley, Berkeley, CA 94720, USA. [7]Institut de Biologie Moléculaire des Plantes, CNRS, 67084 Strasbourg Cedex, France. [8]Department of Biochemistry and Biophysics, University of California at San Francisco, San Francisco, CA 94143, USA. [9]Biotechnology Research Center, Zhongshan University, Guangzhou 510275, China. [10]Department of Molecular Sciences and Center of Excellence in Genomics and Bioinformatics, University of Tennessee, Memphis, TN 38163, USA. [11]Department of Plant Biology, University of Minnesota, St. Paul, MN 55108, USA. [12]Department of Genetics, Development, and Cell Biology, Iowa State University, Ames, IA 50011, USA. [13]Genetic Information Research Institute, Mountain View, CA 94043, USA. [14]The Institute for Genomic Research, Rockville, MD 20850, USA. [15]Plant Biology Laboratory, Salk Institute, La Jolla, CA 92037, USA. [16]Stanford Human Genome Center, Stanford University School of Medicine, Palo Alto, CA 94304, USA. [17]Department of Plant Biology, Carnegie Institution, Stanford, CA 94305, USA.

*These authors contributed equally to this work.
†Full author list is included at the end of the manuscript.
‡To whom correspondence should be addressed. E-mail: dsrokhsar@lbl.gov (D.S.R.); arthurg@stanford.edu (A.R.G.)

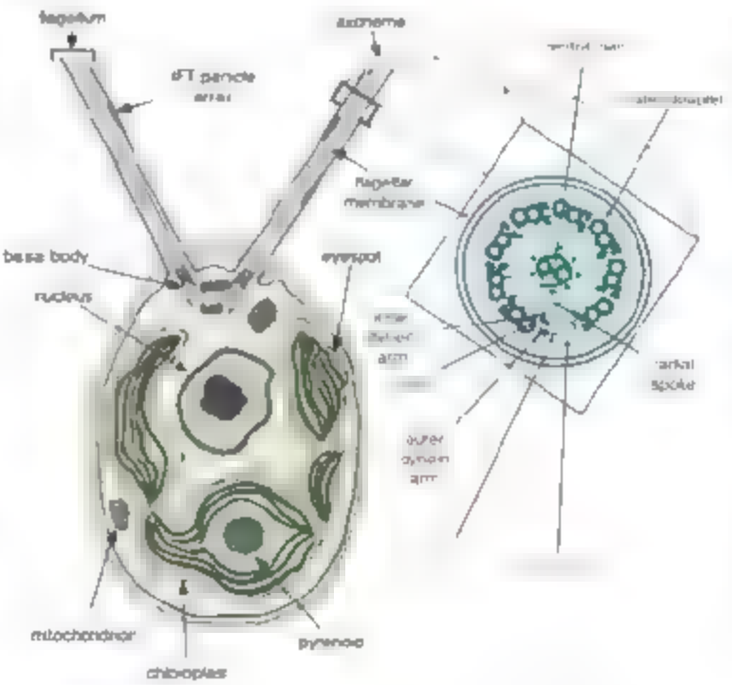

Fig. 1. A schematic of a *Chlamydomonas* cell (from transmission electron micrographs) showing the anterior flagella rooted in basal bodies, with intraflagellar transport (IFT) particle arrays between the axoneme and flagellar membrane, the basal cup-shaped chloroplast, central nucleus and other organelles. An expanded cross section of the flagellar axoneme, as redrawn from (*48*), shows the nine outer doublets and the central pair (9+2) microtubules; axoneme substructures are color-coded and labeled (see inset).

ing in a marker density of 1 per 13 kb (*12*, *13*). By comparing physical marker locations on scaffolds with genetic recombination distances, we estimated 100 kb per centimorgan (cM) on average.

The *Chlamydomonas* genome has approximately uniform densities of genes, simple sequence repeats, and transposable elements. Several AT-rich islands coincide with gene- and transposable element poor regions (figs. S2 to S18). As in most eukaryotes, the ribosomal RNA (rRNA) genes are arranged in tandem arrays. They are located on linkage groups I, VII, and XV, although assembly has only been completed on the outermost copies. We identified 259 transfer RNAs (tRNAs) (*1*) (table S1), 61 classes of simple repeats, ~100 families of transposable elements (*1*), and 64 tRNA-related short interspersed elements (SINEs) (tables S2 and S3), which is unusual for a microorganism. We also identified tRNAs clusters and a number of recent tRNA duplications (fig. S19), as well as clusters of genes associated with specific biological functions (fig. S20). Few chloroplast and mitochondrial genome fragments were detected in the nuclear genome ("cp" and "mito" in Fig. 3, and figs. S2 to S18).

Protein coding genes and structure. Ab initio and homology-based gene prediction, integrated with EST evidence, was used to create a reference set of 15,143 protein-coding gene predictions (*1*) (tables S4, S5, and S6). More than 300,000 ESTs were generated from diverse environmental conditions; 8631 gene models (56%) are supported by mRNA or EST evidence (*14*), and 35% have been edited for gene structure and/or annotated by manual curation, as of June 2007. Protein-coding genes have, on average, 8.3 exons per gene and are intron-rich relative to other unicellular eukaryotes and land plants (*15*) (fig. S21); only 8% lack introns (Table 1) (*1*). The average *Chlamydomonas* intron is longer (373 bp) than that of many eukaryotes (*16*), and the average intron number and size are more similar to those of multicellular organisms than those of protists (fig. S21) (*1*, *17*). Only 1.5% of the introns are short (<100 bp), and we did not observe the bimodal intron size distribution typical of most eukaryotes (fig. S21A). Furthermore, 30% of the intron length is due to repeat sequences (*1*), which suggests that *Chlamydomonas* introns are subject to creation or invasion by transposable elements.

Gene families. We identified 1226 gene families in *Chlamydomonas* encoding two or more proteins (*1*); of these, 26 families have 10 or more members (table S7). The genes of 317 of the 798 two-gene families are arranged in tandem, which suggests extensive tandem gene duplications. Gene families contain similar proportions of the total gene complement of *Chlamydomonas*, human, and *Arabidopsis*. As in *Arabidopsis*, *Chlamydomonas* has large families of kinases and cytochrome P-450s, but the largest one is the class III guanylyl and adenylyl cyclase family. With 51 members, the *Chlamydomonas* family is larger than that in any other organism (*18*). Although these cyclases are not found in plants, in animals they catalyze the synthesis of cGMP and cAMP (*18*), which serve as second messengers in various signal transduction pathways. Cyclic nucleotides are critical for mating processes, as well as flagellar function and regulation in *Chlamydomonas* (*19*–*21*), and may be vital for acclimation to changing nutrient conditions (*22*, *23*). *Chlamydomonas* also encodes diverse families of proteins critical for nutrient acquisition (*23*, *24*).

Transporters. The transporter complement in *Chlamydomonas* suggests that it has retained the diversity present in the common plant-animal ancestor. *Chlamydomonas* is predicted to have 486 membrane transporters (figs. S22 and S23) (*1*) that fall into the broad classes of 61 ion channels, 124 primary (active) adenosine triphosphate (ATP) dependent transporters and 293 secondary transporters; eight are unclassified. The 69-member ATP-binding cassette (ABC) and 26-member P-type adenosine triphosphatase (ATPase) families are large, as in *Arabidopsis*, and overall, the complement of transporters in *Chlamydomonas* resembles that of both *Ostreococcus* spp. and land plants (fig. S22). Furthermore, a number of plant transporters not found in animals are encoded on the *Chlamydomonas* genome (fig. S22 and table S8).

We also found copies of genes encoding animal-associated transporter classes, including some with activities related to flagellar function (e.g., the voltage-gated ion channel superfamily) (*25*) (fig. S22 and table S8). A number of these transporters redistribute intracellular Ca^{2+} in response to environmental signals such as light. Changing Ca^{2+} levels may modulate the activity of the flagella, which are structures found in animals but not in vascular plants (see below).

The *Chlamydomonas* genome also encodes a diversity of substrate-specific transporters that are important for acclimation of the organism to the fluctuating, often nutrient-poor, conditions of soil environments (*24*). Of the eight sulfate transporters, four are in the H^+/SO_4^{2-} family (characteristic of the plant lineage), three are in the Na^+/SO_4^{2-} family (not found in plants but present in opisthokonts), and one is a bacterial ABC-type SO_4^{2-} transporter (associated with the plastid envelope). The 12-

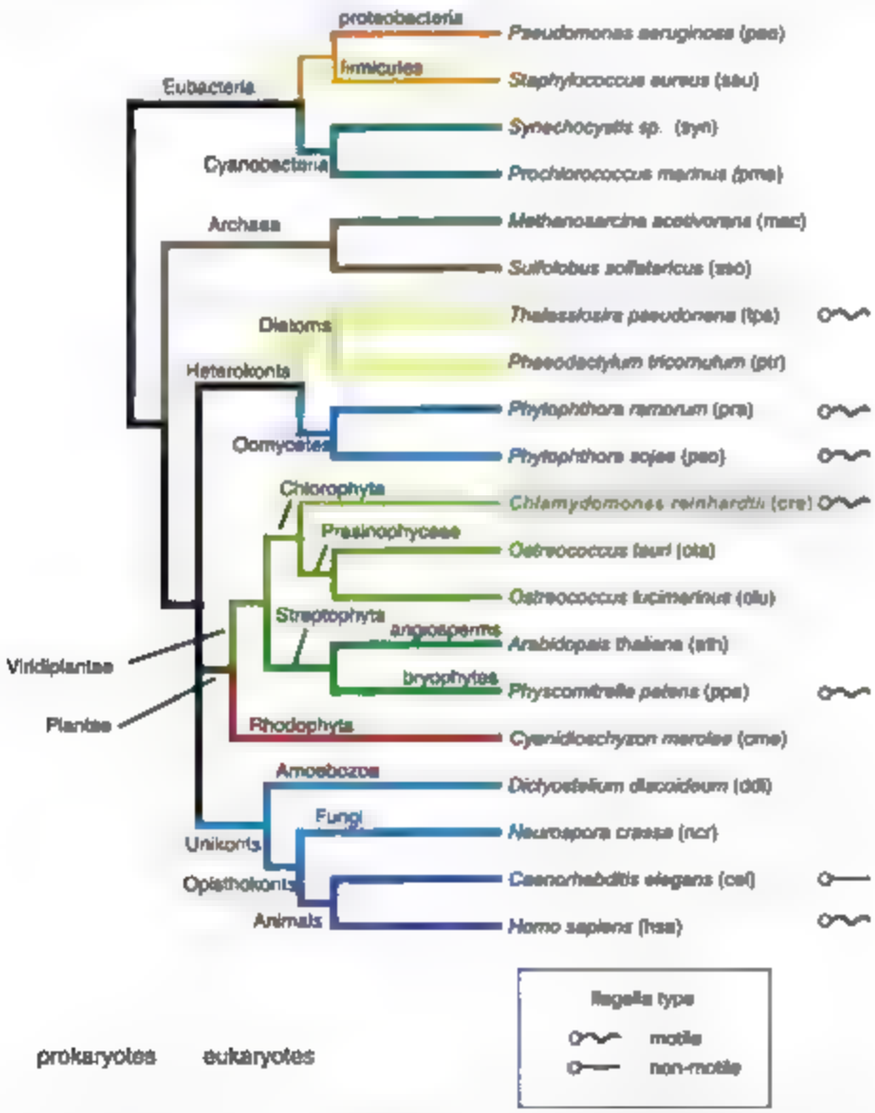

Fig. 2. Evolutionary relationships of 20 species with sequenced genomes (*54*, *55*) used for the comparative analyses in this study include cyanobacteria and nonphotosynthetic eubacteria, Archaea and eukaryotes from the oomycetes, diatoms, rhodophytes, plants, amoebae and opisthokonts. Endosymbiosis of a cyanobacterium by a eukaryotic protist gave rise to the green (green branches) and red (red branches) plant lineages, respectively. The presence of motile or nonmotile flagella is indicated at the right of the cladogram.

member PiT phosphate transporter and 6-member KUP potassium channel families are larger than in other unicellular eukaryotes, and the former underwent a lineage-specific expansion. *Chlamydomonas* has 11 AMT ammonium transporters, which is only surpassed by the number in rice.

Phylogenomics and the origins of *Chlamydomonas* genes. To explore the evolutionary history of *Chlamydomonas*, we initially compared the *Chlamydomonas* proteome to a representative animal (human) and angiosperm (*Arabidopsis*) proteome (*1*). We plotted the best matches, calculated on the basis of BLASTP (Basic Local Alignment Search Tool for searching protein collections) scores, of every *Chlamydomonas* protein to the *Arabidopsis* and human proteomes (Fig. 4A). Most *Chlamydomonas* proteins exhibit slightly more similarity to *Arabidopsis* than to human proteins. Many *Chlamydomonas* proteins with greater similarity to animal homologs are present in the flagellar and basal body proteomes (Fig. 4A and below). This is consistent with the maintenance of flagella and basal bodies as cilia and centrioles, respectively, in animals (*8*), and their loss in angiosperms.

A mutual best-hit analysis of *Chlamydomonas* proteins against proteins from organisms across the tree of life (*1*) identified 6968 protein families of orthologs, co-orthologs (in the case of recent gene duplications), and paralogs (*1*). Of the *Chlamydomonas* proteins, 2489 were homologous to proteins from both *Arabidopsis* and humans (Fig. 4B). *Chlamydomonas* and humans shared 706 protein families (774 and 806 proteins, respectively), but these were not shared with *Arabidopsis*. These genes were either lost or diverged beyond recognition in green plants (table S9), and are enriched for sequences encoding cilia and centriole proteins (*8*, *26*). Conversely, 1879 protein families are found in both *Chlamydomonas* and *Arabidopsis* (1968 and 2396 proteins, respectively), but lack human homologs. *Chlamydomonas* proteins with homology to plant, but not animal, proteins were either (i) present in the common plant-animal ancestor and retained in *Chlamydomonas* and angiosperms, but lost or diverged in animals, (ii) horizontally transferred into *Chlamydomonas*, or (iii) arose in the plant lineage after divergence of animals (but before the divergence of *Chlamydomonas*). This set is enriched for proteins that function in chloroplasts (table S9 and below).

The plastid and plant lineages. The plastids of green plants and red algae are primary plastids, i.e., direct descendants from the primary cyanobacterial endosymbiont (*27*). Diatoms, brown algae, and chlorophyll a– and c–containing algae are also photosynthetic, but their photosynthetic organelles were acquired via a secondary endo-

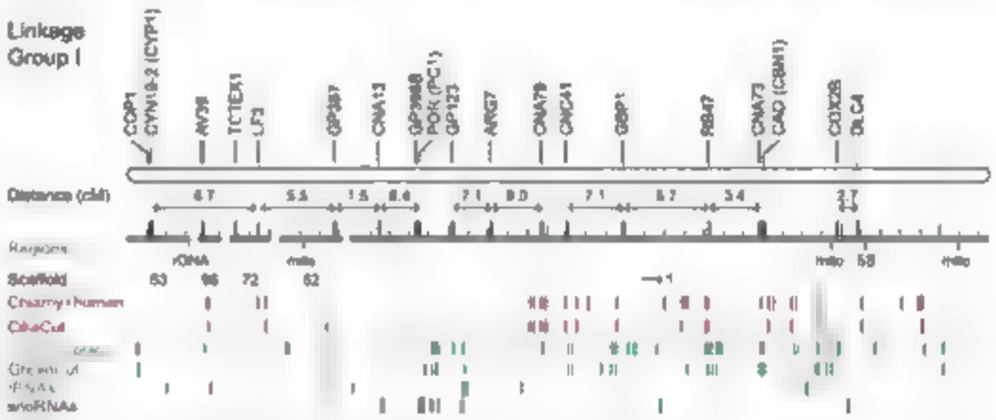

Fig. 3. Linkage group I depicted as a long horizontal rod, with genetically mapped scaffolds shown as open rectangles below (the scaffold number is under each scaffold, and arrows indicate the orientation of the scaffold where it is known; other scaffolds were placed in their most likely orientation on the basis of genetic map distances. The scale of each map is determined by molecular lengths of the mapped scaffolds. Short and long red ticks are drawn on scaffolds every 0.2 Mb and 1.0 Mb, respectively. We assumed small 50 kb gaps between scaffolds. Genetic distances between markers (centimorgans), where they are known, are shown by two-headed arrows above the scaffold, with the gene symbol and any synonyms in parentheses shown at the top. Genomic regions are labeled below the scaffolds: 5S, rDNA, mito (insertion of mitochondrial DNA). *Chlamydomonas* genes with homologs in other organisms/lineages ("Cuts" as defined in the text and Fig. 5) are shown as tracks of vertical bars: light red, genes shared between *Chlamydomonas* and humans, but not occurring in nonciliated organisms; dark red, genes in CiliaCut; light green, genes shared between *Chlamydomonas* and *Arabidopsis*, but not in nonphotosynthetic organisms; dark green, genes in GreenCut; magenta, predicted tRNAs, including those that represent SINE sequences; dark blue, small nucleolar RNAs (snoRNAs).

Table 1. Comparison of *Chlamydomonas* genome statistics to those of selected sequenced genomes. nd, Not determined. [Source for all but *Chlamydomonas* (*1*)]

	Chlamydomonas	*Ostreococcus tauri*	*Cyanidioschyzon*	*Arabidopsis*	Human
Assembly length (Mb)	121	12.6	16.5	140.1	2,851
Coverage	13×	6.7×	11×	nd	~8×
Chromosomes	17	20	20	5	23
G+C (%)	64	58	55	36	41
G+C (%) coding sequence	68	59	57	44	52
Gene number	15,143	8,166	5,331	26,341	~23,000
Genes with EST support (%)	63	36	86	60	nd
Gene density (per kb)	0.125	0.648	0.323	0.190	~0.0008
Average bp per gene	4312	nd	1553	2232	27,000
Average bp per transcript	1580	1257	1552	nd	nd
Average number of amino acids per polypeptide	444	387	518	413	491
Average number of exons per gene	8.33	1.57	1.005	5.2	8.8
Average exon length	190	750	1540	251	282*
Genes with introns (%)	92	39	0.5	79	85†
Mean length of intron	373	103	248	164	3,365
Coding sequence (%)	16.7	81.6	44.9	33.0	~1
Number of rDNA units (28S/18S/5.8S + 5S)	3 + 3	4 + 4	3 + 3‡	12 + 700	5 + nd
Number tRNAs	259§	nd	30	589	497
Selenocysteine (Sec) tRNAs	1	nd	nd	0	1

*National Center for Biotechnology Information (NCBI) NCBI 36 from Ensembl build 38. †[Source (*56*)]. ‡Three regions contain 5S rDNA exclusively, and three regions contain 28S-18S-5.8S rDNAs exclusively. §65 tRNAs that were included in SINE elements were removed from the tRNA-scanSE predictions.

symbiosis (*28*, *29*). Because of shared ancestry, nucleus-encoded plastid-localized proteins derived from the cyanobacterial endosymbiont are closely related to each other and to cyanobacterial proteins.

We searched the 6968 families that contain *Chlamydomonas* proteins for those that also contained proteins from *Ostreococcus*, *Arabidopsis* and moss, but that did not contain proteins from nonphotosynthetic organisms. The search identified 349 families, which we named the GreenCut (Fig. 5A, table S10 and table SA); each of these families has a single *Chlamydomonas* protein. On the basis of manual curation of GreenCut proteins of known function (*1*) (table S11), we estimated ~5 to 8% false-positives and ~4% false-negatives (*1*). By comparing GreenCut proteins to those of the red alga *Cyanidioschyzon merolae*, which diverged before the split of green algae from land plants (Fig. 2), we identified the subset of proteins present across the plant kingdom; we named this subset the PlantCut (Fig. 5A, table S10 and table SA). GreenCut protein families that also included representatives from the diatoms *Thalassiosira pseudonana* (*30*) or *Phaeodactylum tricornutum* (*31*) were placed in the DiatomCut (Fig. 5A and table S10 and table SA). Given the phylogenetic position of diatoms and their secondary endosymbiosis-derived plastids, we hypothesize that protein families present in both the PlantCut and DiatomCut should contain only those GreenCut proteins associated with plastid function. This subset is referred to as the PlastidCut (Fig. 5A).

The GreenCut contains proteins of the photosynthetic apparatus, including those involved in plastid and thylakoid membrane biogenesis, photosynthetic electron transport, carbon fixation, antioxidant generation, and a range of other primary metabolic processes (table S11 and table SA). Although light-harvesting chlorophyll-binding proteins are poorly represented (*1*), we identified specialized chlorophyll-binding proteins, as well as a photosynthesis-specific kinase, involved in state transitions. Numerous GreenCut entries are enzymes of plastid-localized metabolic pathways (lipid, amino acid, starch, nucleotide, and pigment biosynthesis) or are unique to plants or highly divergent from animal counterparts. Although tRNA synthetases are conserved between kingdoms, those in the GreenCut represent organellar isoforms that are often targeted to both plastids and mitochondria in plants (*32*). GreenCut proteins that do not function in the plastids tend to be green lineage–specific or highly diverged from animal counterparts. For example, the *Chlamydomonas* GreenCut protein TOM20 (*1*), an outer mitochondrial membrane receptor involved in protein import, evolved convergently from a different ancestral protein in plants than in fungi and animals (*33*).

Of the 214 proteins in the GreenCut without known function, 101 have no motifs or homologies from which function can be inferred, and we can predict only a general function for the others (table S12). Given that 85% of the known proteins in the GreenCut are localized to chloroplasts (table S13), we predict that the set of unknowns contains many novel, conserved proteins that function in chloroplast metabolism and regulation.

The most reducing and oxidizing biological molecules are generated in chloroplasts via the activity of photosystem I and photosystem II, respectively. The flow of electrons through the photosystems causes damage to cellular constituents as a consequence of the accumulation of reactive oxygen species. Therefore, regulation of these molecules is important. Accordingly, plastids house more redox regulators than do mitochondria. Thioredoxins are critical redox-state regulators, and we identified novel thioredoxins in the GreenCut (table S12). These novel thioredoxins have noncanonical active sites or are fused to domains of inferred function (e.g., a vitamin K binding domain) in plastid metabolism (fig. S1). These findings reveal the potential for identifying unique redox signaling pathways with selectivity and midpoint potentials associated with specific thioredoxin redox sensors (*1*).

Chlamydomonas has a structure called the eyespot (Fig. 1) which can sense light and trigger phototactic responses. The eyespot is composed of several layers of pigment granules, similar to plastoglobules in plants, and thylakoid membrane, which are directly apposed to the chloroplast envelope and a region of the plasma membrane carrying rhodopsin-family photoreceptors. The pigment granules or plastoglobules contain many proteins with unknown function, many of which are present in the GreenCut, and are likely critical to plastid metabolism; these include SOUL domain, AKC (see below), and PLAP (plastid- and lipid-associated protein) protein families (*34*–*36*). SOUL domain proteins of the GreenCut (SOUL4 and SOUL5) have homologs in the *Arabidopsis* plastoglobule proteome (*34*, *35*), and at least one (SOUL3) is associated with the eyespot. The SOUL domain, originally identified in proteins encoded by highly expressed genes in the retina and pineal gland, can bind heme (*37*, *38*). This domain may be important as a heme carrier and/or in maintaining heme in a bound, non-

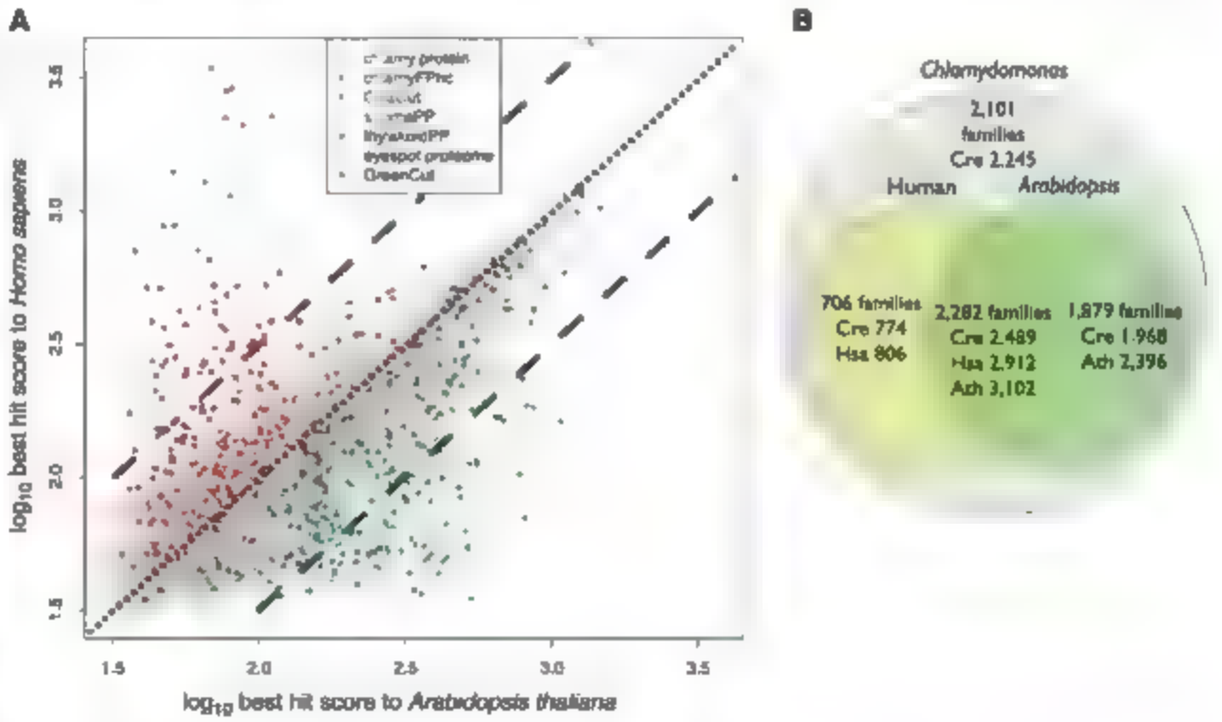

Fig. 4. (**A**) Scatter plot of best BLASTP hit score of *Chlamydomonas* proteins to *Arabidopsis* proteins versus best BLASTP hit score of *Chlamydomonas* proteins to human proteins. Functional or genomic groupings are colored [see inset key in (A)]: *Chlamydomonas* flagellar proteome (*42*) high confidence set (chlamyFPhc); CiliaCut; *Arabidopsis* stroma plastid proteome (stromaPP); *Arabidopsis* thylakoid plastid proteome (thylakoidPP); eyespot proteome; GreenCut; remaining proteins are gray. (**B**) *Chlamydomonas* protein paralogs were grouped into families together with their homologs from human and *Arabidopsis*. The outer circle represents the proteins in *Chlamydomonas*, 7476 (out of 15,143 total), that fall into 6968 families. Another 7937 proteins cannot be placed in families. Counts of families (and the numbers of proteins from each species in them) with proteins from *Chlamydomonas* and human only, *Chlamydomonas* and *Arabidopsis* only, and *Chlamydomonas* and human and *Arabidopsis*, are shown in the inner circles and the overlap between the two inner circles, respectively. Cre, *Chlamydomonas*; Hsa, human; Ath, *Arabidopsis*.

phototoxic form until it associates with proteins or may function in signaling circadian cues.

We also identified plant-specific AKCs (ABC1 kinase in the chloroplast, AKC1 to 4 in the GreenCut), one of which (designated EYE3) is required for eyespot assembly (*39*). These AKCs are distinct from the mitochondrial ABC1 kinase that regulates ubiquinone production (*40*). Protein phosphatases present in the GreenCut and plastoglobules may turn off signaling initiated by the AKCs.

The PLAPs (PLAP1 to 4 in the GreenCut), also called plastoglobulins, are also associated with the eyespot or plastoglobule. These proteins were originally identified by their abundance in carotenoid-rich fibrils and chromoplast plastoglobules and may be structural or organizational components of this plastid subcompartment. Other GreenCut proteins associated with plastoglobules (*34*, *36*) include short-chain dehydrogenases, an aldo-keto isomerase, various methyltransferases with unspecified substrates, esterases and lipases, and a protein with a pantothenate kinase motif.

In sum, the eyespot or plastoglobules contain proteins that likely function in the synthesis, degradation, trafficking, and integration of pigments and isoprenoid cofactors into the metabolic machinery of the cell and, most notably, into the photosynthetic apparatus, where they are in high demand. The numerous proteins in the GreenCut associated with the eyespot/plastoglobules may reflect the diverse repertoire of compounds, such as quinones, tocopherols, carotenoids, and tetrapyrroles (fig. S1B), required by photosynthetic organisms.

The 90 proteins in the PlastidCut (Fig. 5A) are likely to function in basic plastid processes because they are conserved in all plastid-containing eukaryotes. Sixty-one of these have unknown functions, with genes for most (except CPLD6 and CPLD29) expressed in chloroplast-containing cells, as assessed from EST representation in *Chlamydomonas* and *Physcomitrella*. For *Arabidopsis* homologs, expression (*41*) indicates that the genes represented in the PlastidCut tend to be expressed in leaves or all tissue, similar to genes that function in photosynthesis or primary chloroplast metabolism. Greater than 70% of previously unknown PlastidCut proteins have homologs in cyanobacteria, which suggests a critical, conserved, plastid-associated function.

Flagellar and basal body gene complement. *Chlamydomonas* uses a pair of anterior flagella to swim and sense environmental conditions (Fig. 1). Each flagellum is rooted in a basal body, which also functions as a centriole during cell division. The flagellar axoneme has the nine outer doublet microtubules plus a central pair (9+2) (Fig. 1) characteristic of motile cilia (cilia and eukaryotic flagella are essentially identical organelles). In addition to motile cilia, animals contain nonmotile cilia that function as a sensory organelle and typically lack outer and inner dynein arms, radial spokes, and central microtubules (Fig. 1), all of which are involved in the generation and regulation of motility. Both types of cilia have sensory functions and share conserved sensing and signaling components.

The loss of flagella in angiosperms, most fungi, and slime molds allowed us to identify cilia-specific genes through searches for proteins retained only in flagellate organisms (*8*, *26*). We searched the 6968 *Chlamydomonas* protein families (see above) for those that also contained proteins from human and a *Phytophthora* spp., but not from ciliates, and identified 186 protein families that we named the CiliaCut; these families contain 195 *Chlamydomonas* (Fig. 5B and table S8) and 194 human proteins. One hundred and sixteen of the *Chlamydomonas* proteins had been computationally identified (*8*, *26*), and 45 were identified in this study (*1*).

The *Chlamydomonas* CiliaCut proteins of unknown function that are missing from *Caenorhabditis*, which has only nonmotile sensory cilia (*26*), were designated MOT (motile flagella), whereas proteins of unknown function shared with *Caenorhabditis* were designated SSA (sensory, structural and assembly) (Fig. 5B). Thirty-five percent of CiliaCut proteins are in the *Chlamydomonas* flagellar proteome (*42*), double the number known from previous studies, and 27 of 101 previously identified flagellar proteins (*42*) are present in the CiliaCut. The CiliaCut contained δ-tubulin, which is required for basal body assembly (*43*), and a previously undescribed dynein light chain. Some flagellar proteins were not found by this analysis because they have orthologs in plants and fungi, whereas others are absent because they lack human orthologs. Most dynein heavy chains are missing, most likely due to the difficulty of identifying members of large gene families with a mutual best hit approach (*1*).

We manually curated 125 CiliaCut proteins (fig. S24) and identified large subsets as flagellar structural components (16%), mediating protein-protein interactions (26%), signaling (11%), GTP-binding (6%) and trafficking (6%). These results are consistent with proteomic

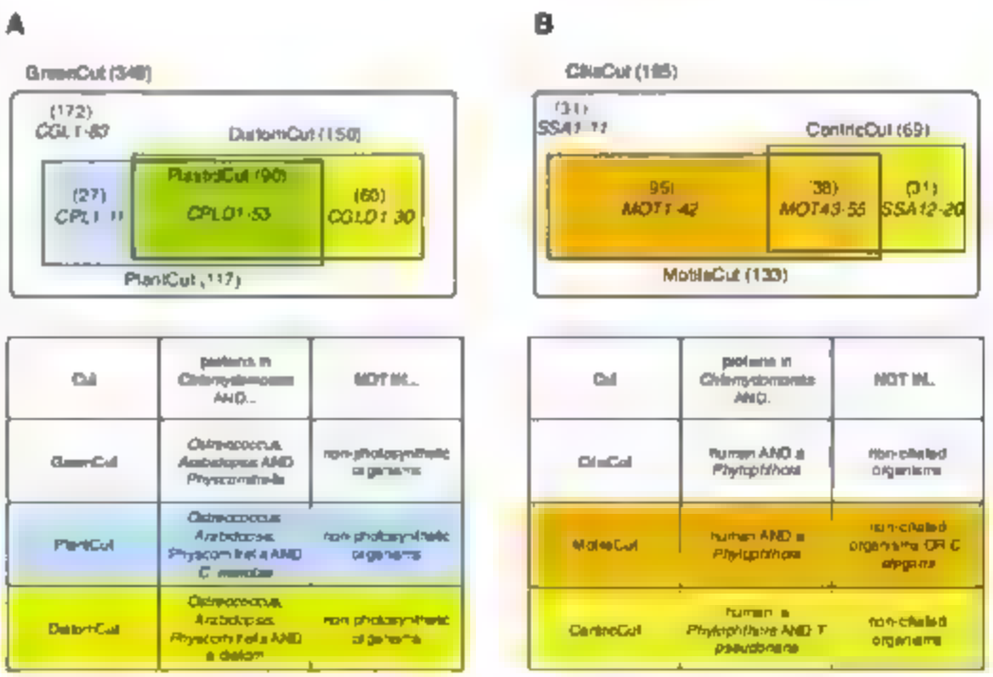

Cut	proteins in Chlamydomonas AND...	NOT in...
GreenCut	*Ostreococcus*, *Arabidopsis* AND *Physcomitrella*	non-photosynthetic organisms
PlantCut	*Ostreococcus*, *Arabidopsis*, *Physcomitrella* AND *C. merolae*	non-photosynthetic organisms
DiatomCut	*Ostreococcus*, *Arabidopsis*, *Physcomitrella* AND a diatom	non-photosynthetic organisms

Cut	proteins in Chlamydomonas AND...	NOT in...
CiliaCut	human AND a *Phytophthora*	non-ciliated organisms
MotileCut	human AND a *Phytophthora*	non-ciliated organisms OR *C. elegans*
CentricCut	human a *Phytophthora* AND *T. pseudonana*	non-ciliated organisms

Fig. 5. Summary of genomic comparisons to photosynthetic and ciliated organisms. (**A**) GreenCut: The GreenCut comprises 349 *Chlamydomonas* proteins with homologs in representatives of the green lineage of the Plantae (*Chlamydomonas*, *Physcomitrella*, and *Ostreococcus tauri* and *O. lucimarinus*), but not in nonphotosynthetic organisms. Genes encoding proteins of unknown function that were not previously annotated were given names on the basis of their occurrence in various cuts. CGL refers to conserved only in the green lineage. The GreenCut protein families, which also include members from the red alga *Cyanidioschyzon* within the Plantae, were assigned to the PlantCut (blue plus green rectangles). CPL refers to conserved in the Plantae. GreenCut proteins also present in at least one diatom (*Thalassiosira* and *Phaeodactylum*) were assigned to the DiatomCut (yellow plus green rectangle). CGLD refers to conserved in the green lineage and diatoms. Proteins present in all of the eukaryotic plastid-containing organisms in this analysis were assigned to the PlastidCut (green rectangle). CPLD refers to conserved in the Plantae and diatoms. The criteria used for the groupings associated with the GreenCut are given in the lower table. (**B**) CiliaCut: The CiliaCut contains 195 *Chlamydomonas* proteins with homologs in human and species of *Phytophthora*, but not in nonciliated organisms. This group was subdivided on the basis of whether or not a homolog was present in *Caenorhabditis*, which has only nonmotile sensory cilia. The 133 CiliaCut proteins without homologs in *Caenorhabditis* were designated the MotileCut (orange rectangle). Unnamed proteins in this group were named MOT (motility). Proteins with homologs in *Caenorhabditis* are associated with nonmotile cilia (white and yellow areas). Proteins in this group that were not already named were named SSA. The CentricCut (yellow plus light orange box) is made up of 69 CiliaCut homologs present in the centric diatom *Thalassiosira*. These proteins can be divided into those also in the MotileCut (38 proteins; light orange box) or those not present in the MotileCut (31 proteins; yellow box).

analysis of the flagellum (*42*) and highlight the importance of signaling even in motile flagella.

The 62 CiliaCut proteins that *Chlamydomonas* shares with *Caenorhabditis* are predicted to have structural, sensory, or assembly roles in the cilium. As expected, the 133 CiliaCut proteins missing from *Caenorhabditis* (Fig. 5B) (*1*), designated the MotileCut, include a number of proteins associated with motility (*42*) (table S14). This data set also contains 31 proteins of unknown function found in the flagellar and basal body proteomes, 36 known but uncharacterized proteins, and 55 novel proteins (designated MOT1 to MOT55); these flagellar proteins are all predicted to be involved specifically in motility.

A comparison of CiliaCut proteins with proteins encoded by the *Physcomitrella* genome indicates that *Physcomitrella* has lost five of the outer dynein arm proteins (Fig. 1, table S14). However, *Physcomitrella* contains inner dynein arm subunits IDA4 and DHC2, as well as subunits of the central microtubules, the radial spokes, and the dynein regulatory complex (table S14). From this we conclude that *Physcomitrella* sperm flagella have a "9+2" axoneme containing inner dynein arms, central microtubules, and radial spokes, but lack the outer dynein arms. Although the structure of the *Physcomitrella* sperm flagellum is not known, sperm flagella of the bryalean moss *Aulacomnium palustre* have just such an axoneme (*44*).

In contrast, the motile flagella of centric diatoms lack the central pair of microtubules (*45*, *46*). Orthologs of 69 of the 195 CiliaCut proteins (named CentruCut, Fig. 5B) were predicted to be present in the centric diatom *Thalassiosira*. As expected, *Thalassiosira* lacks all central pair proteins. However, it also lacks all radial spoke and inner dynein arm proteins, but has most of the outer dynein arm proteins. The contrasting patterns of loss of axonemal structures predicted for *Physcomitrella* and *Thalassiosira* suggest that the central pair and radial spokes function as a unit with the inner arms, but are dispensable for the generation of motility by the outer arms.

Intraflagellar transport (IFT), which is conserved in ciliated organisms except malaria parasites (*47*), is essential for flagellar growth (*48*). The IFT machinery consists of at least 16 proteins in two complexes (A and B) that are moved in anterograde and retrograde directions by the molecular motors kinesin-2 and cytoplasmic dynein 1b, respectively (Fig. 1). Our analysis of *Thalassiosira* reveals that it has components of the anterograde motor and complex B, but has lost the retrograde motor and complex A (table S14). This is intriguing, as retrograde IFT is essential for flagellar maintenance in *Chlamydomonas* (*49*) and is important for recycling IFT components (*50*). In addition, both *Physcomitrella* and *Thalassiosira* have lost the Bardet-Biedl syndrome (BBS) genes. BBS gene products are associated with the basal body in *Chlamydomonas* and mammals (*8*, *51*) and sensory cilia in *Caenorhabditis* (*52*), where they may be involved in IFT (*53*).

We searched the CiliaCut proteins for proteins shared with *Ostreococcus* spp., a green alga lacking a flagellate stage. The *Ostreococcus* spp. retain 46 (24%) of the 195 CiliaCut proteins but, consistent with loss of the flagellum, are missing genes encoding the IFT-particle proteins and motors, the inner and outer dynein arm proteins, the radial spoke and central pair proteins, and 32 out of 39 flagella-associated proteins (FAPs) (table S14). They have also lost many genes encoding basal body proteins, including all BBS proteins (table S14), which suggests that *Ostreococcus* also lack basal bodies. However, *Ostreococcus* spp. have retained many other CiliaCut proteins (table S14), which suggests either that they recently lost their flagella, or that they retained flagellar proteins for other cellular functions.

Conclusions. This analysis of the *Chlamydomonas* genome sheds light on the nature of the last common ancestor of plants and animals and identifies many cilia- and plastid-related genes. The gene complement also provides insights into life in the soil environment where extreme competition for nutrients likely drove expansion of transporter gene families, as well as sensory flagellar and eyespot functions (e.g., facilitating nutrient acquisition and optimization of the light environment). As more of the ecology and physiology of *Chlamydomonas* and other unicellular algae are explored, additional direct links between gene content and functions associated with the soil life-style will be unmasked with increased potential for biotechnological exploitation of these functions.

References and Notes

1. Materials and methods and supplemental online (SOM) text are available as supporting material on *Science* Online.
2. E. H. Harris, *Annu. Rev. Plant Physiol. Plant Mol. Biol.* **52**, 363 (2001).
3. L. C. Keller, E. P. Romijn, I. Zamora, J. R. Yates 3rd, W. F. Marshall, *Curr. Biol.* **15**, 1090 (2005).
4. G. J. Pazour, N. Agrin, B. L. Walker, G. B. Witman, *J. Med. Genet.* **43**, 62 (2006).
5. C. Vilchez, I. Garbayo, E. Markvicheva, F. Galvan, R. Leon, *Bioresour. Technol.* **78**, 55 (2001).
6. M. L. Ghirardi *et al.*, *Annu. Rev. Plant Biol.* **58**, 71 (2007).
7. H. S. Yoon, J. D. Hackett, C. Ciniglia, G. Pinto, D. Bhattacharya, *Mol. Biol. Evol.* **21**, 809 (2004).
8. J. B. Li *et al.*, *Cell* **117**, 541 (2004).
9. A. R. Grossman *et al.*, *Curr. Opin. Plant Biol.* **10**, 190 (2007).
10. *Chlamydomonas reinhardtii* v 3.0, DOE Joint Genome Institute, www.jgi.doe.gov/chlamy
11. R. Storms, P. J. Hastings, *Exp. Cell Res.* **104**, 39 (1977).
12. P. Kabir *et al.*, *Eukaryot. Cell* **2**, 362 (2003).
13. L. A. Rymarquis, J. M. Handley, M. Thomas, D. B. Stern, *Plant Physiol.* **137**, 557 (2005).
14. M. Jain *et al.*, *Nucleic Acids Res.* **35**, 2074 (2007).
15. Q. Yuan *et al.*, *Plant Physiol.* **138**, 18 (2005).
16. M. Yandell *et al.*, *PLoS Comput Biol* **2**, e15 (2006).
17. B. Palenik *et al.*, *Proc. Natl. Acad. Sci. U.S.A.* **104**, 7705 (2007).
18. P. Schaap, *Front. Biosci.* **10**, 1485 (2005).
19. E. Hasegawa, R. Hayashi, S. Asakura, R. Kamiya, *Cell Motil. Cytoskeleton* **8**, 302 (1987).
20. S. M. Pasquale, U. W. Goodenough, *J. Cell Biol.* **105**, 2279 (1987).
21. A. R. Gaillard, L. A. Fox, J. M. Rhea, B. Craige, W. S. Sale, *Mol. Biol. Cell* **17**, 2626 (2006).
22. D. Gonzalez-Ballester, A. de Montaigu, J. J. Higuera, A. Galvan, E. Fernandez, *Plant Physiol.* **137**, 522 (2005).
23. S. V. Pollock, W. Pootakham, H. Shibagaki, J. L. Moseley, A. R. Grossman, *Photosynth. Res.* **86**, 475 (2005).
24. A. Grossman, H. Takahashi, *Annu. Rev. Plant Physiol. Plant Mol. Biol.* **52**, 163 (2001).
25. S. Somlo, B. Ehrlich, *Curr. Biol.* **11**(9), R356 (2001).
26. T. Ando-Reis *et al.*, *Cell* **117**, 527 (2004).
27. M. W. Gray, *Curr. Opin. Genet. Dev.* **9**, 678 (1999).
28. D. Bhattacharya, H. S. Yoon, J. D. Hackett, *Bioessays* **26**, 50 (2004).
29. P. Keeling, *Protist* **155**, 3 (2004).
30. E. V. Armbrust *et al.*, *Science* **306**, 79 (2004).
31. *Phaeodactylum tricornutum*, v2.0, DOE Joint Genome Institute, www.jgi.doe.gov/phaeodactylum.
32. A. M. Duchêne *et al.*, *Proc. Natl. Acad. Sci. U.S.A.* **102**, 16484 (2005).
33. A. J. Perry, J. M. Hoxted, V. A. Jick, T. Lithgow, P. R. Gooley, *Curr. Biol.* **16**, 221 (2006).
34. A. J. Ytterberg, J. B. Peltier, K. J. van Wijk, *Plant Physiol.* **140**, 984 (2006).
35. M. Schmidt *et al.*, *Plant Cell* **18**, 1908 (2006).
36. P. A. Vidi *et al.*, *J. Biol. Chem.* **281**, 11225 (2006).
37. M. J. Zylka, S. M. Reppert, *Brain Res. Mol. Brain Res.* **74**, 175 (1999).
38. E. Sato *et al.*, *Biochemistry* **43**, 14489 (2004).
39. M. R. Lamb, S. K. Dutcher, C. K. Worley, C. L. Dieckmann, *Genetics* **153**, 721 (1999).
40. T. Q. Do, A. Y. Hsu, T. Jonassen, P. T. Lee, C. F. Clarke, *J. Biol. Chem.* **276**, 18161 (2001).
41. P. Zimmermann, M. Hirsch-Hoffmann, L. Hennig, W. Gruissem, *Plant Physiol.* **136**, 2621 (2004).
42. G. J. Pazour, N. Agrin, J. Leszyk, G. B. Witman, *J. Cell Biol.* **170**, 103 (2005).
43. E. T. O'Toole, T. H. Giddings, J. R. McIntosh, S. K. Dutcher, *Mol. Biol. Cell* **14**, 2999 (2003).
44. D. L. Bernhard, K. S. Renzaglia, *Bryologist* **98**, 52 (1995).
45. I. Manton, K. Kowallik, H. A. von Stosch, *J. Cell Sci.* **6**, 131 (1970).
46. I. B. Heath, W. M. Darley, *J. Phycol.* **10**, 51 (1972).
47. L. J. Briggs, J. A. Davidge, B. Wickstead, M. L. Ginger, K. Gull, *Curr. Biol.* **14**, R611 (2004).
48. J. L. Rosenbaum, G. B. Witman, *Nat. Rev. Mol. Cell Biol.* **3**, 813 (2002).
49. G. J. Pazour, B. L. Dickert, G. B. Witman, *J. Cell Biol.* **144**, 473 (1999).
50. H. Qin, D. R. Diener, S. Geimer, D. G. Cole, J. L. Rosenbaum, *J. Cell Biol.* **164**, 255 (2004).
51. S. J. Ansley *et al.*, *Nature* **425**, 628 (2003).
52. O. E. Blacque *et al.*, *Genes Dev.* **18**, 1630 (2004).
53. G. Ou *et al.*, *Mol. Biol. Cell* **18**, 1554 (2007).
54. F. D. Ciccarelli *et al.*, *Science* **311**, 1283 (2006).
55. P. J. Keeling *et al.*, *Trends Ecol. Evol.* **20**, 670 (2005).
56. L. Eichinger *et al.*, *Nature* **435**, 43 (2005).

57. We thank R. Howson for help with drawing figures, E. Begovic and S. Nicholls for comments on the manuscript. SM is supported by the grants NIH GM42143, DOE DE-FG02-04ER15529, USDA 2004-35318-1495. SP and DSR are funded by USDA and DOE Joint Genome Institute. ARG is supported by USDA 2003-35100-13235, DOE DE-AC36-99GO10337 and the NSF-funded *Chlamydomonas* Genome Project, MCB 0235878. SJK was supported in part by a Ruth L. Kirschstein National Research Service Award GM07185. The authors declare they have no conflicts of interest. Genome assembly together with predicted gene models and and annotations were deposited at DDBJ/EMBL/GenBank under the project accession ABCN00000000. Since manual curation continues, some models or annotations are changing and the latest set of gene models and annotations is available from www.jgi.doe.gov/Chlamy. The most recent set, which includes a number of changes compared with the frozen set used for this analysis, was submitted as the first version, ABCN01000000.

Full author list and affiliations

Sabeeha S. Merchant,[1]* Simon E. Prochnik,[2] Olivier Vallon,[3] Elizabeth H. Harris,[4] Steven J. Karpowicz,[1] George B. Witman,[5] Astrid Terry,[2] Asaf Salamov,[2] Lillian K. Fritz-Laylin,[6] Laurence Maréchal-Drouard,[7] Wallace F. Marshall,[8] Liang-Hu Qu,[9] David R. Nelson,[10] Anton A. Sanderfoot,[11] Martin H. Spalding,[12] Vladimir V. Kapitonov,[13] Qinghu Ren,[14] Patrick Ferris,[15] Erika Lindquist,[2] Harris Shapiro,[2] Susan M. Lucas,[2] Jane Grimwood,[16] Jeremy Schmutz,[16] Igor V. Grigoriev,[2] Daniel S. Rokhsar,[2,17] Arthur R. Grossman[12]

Chlamydomonas Annotation Team. Pierre Cardol,[3,18] Heriberto Cerutti,[19] Guillaume Chanfreau,[1] Chun-Long Chen,[9] Valérie Cognat,[7] Martin T. Croft,[20] Rachel Dent,[21] Susan

Dutcher,[34] Emilio Fernández,[41] Patrick Ferris,[35] Hideya Fukuzawa,[36] David González-Ballester,[37] Diego González-Halphen,[38] Armin Hallmann,[39] Marc Hanikenne,[18] Michael Hippler,[27] William Inwood,[21] Kamel Jabbari,[28] Ming Kalanon,[29] Richard Kuras,[3] Paul A. Lefebvre,[22] Stéphane D Lemaire,[30] Alexey V. Lobanov,[31] Martin Lohr,[32] Andrea Manuell,[33] Iris Meier,[34] Laurens Mets,[35] Maria Mittag,[36] Telsa Mittelmeier,[37] James V. Moroney,[38] Jeffrey Moseley,[17] Carolyn Napoli,[39] Aurora M. Nedelcu,[40] Krishna Niyogi,[41] Sergey V Novoselov,[31] Ian T. Paulsen,[14] Greg Pazour,[42] Saul Purton,[43] Jean-Philippe Ral,[43] Diego Mauricio Riaño-Pachón,[44] Wayne Riekhof,[45] Linda Rymarquis,[46] Michael Schroda,[47] David Stern,[48] James Umen,[15] Robert Willows,[49] Nedra Wilson,[50] Sara Lana Zimmer,[48] Jens Allmer,[51] Janneke Balk,[20] Katerina Bisova,[52] Chong-Jian Chen,[9] Marek Elias,[53] Karla Gendler,[54] Charles Hauser,[54] Mary Rose Lamb,[55] Heidi Ledford,[21] Joanne C. Long,[1] Jun Minagawa,[56] M. Dudley Page,[1] Jianmin Pan,[57] Wirulda Pootakham,[17] Sanja Roje,[58] Annkatrin Rose,[59] Eric Stahlberg,[28] Aimee M. Terauchi,[1] Pinfen Yang,[60] Steven Ball,[61] Chris Bowler,[20,62] Carol L. Dieckmann,[37] Vadim N. Gladyshev,[31] Pamela Green,[46] Richard Jorgensen,[30] Stephen Mayfield,[18] Bernd Mueller-Roeber,[44] Sathish Rajamani,[63] Richard T. Sayre[34]

JGI Annotation Team. Peter Brokstein,[7] Inna Dubchak,[7] David Goodstein,[7] Leila Hornick,[7] Y. Wayne Huang,[7] Jinal Jhaveri,[7] Yigong Luo,[7] Diego Martinez,[7] Wing Chi Abby Ngau,[7] Bobby Otillar,[7] Alexander Poliakov,[7] Aaron Porter,[7] Lukasz Szajkowski,[7] Gregory Werner,[7] Kemin Zhou[7]

[1]Department of Chemistry and Biochemistry, University of California Los Angeles, Los Angeles, CA 90095, USA. [2]U.S. Department of Energy, Joint Genome Institute, Walnut Creek, CA 94598, USA. [3]CNRS, UMR 7141, CNRS/Université Paris 6, Institut de Biologie Physico-Chimique, 75005 Paris, France. [4]Department of Biology, Duke University, Durham, North Carolina 27708, USA. [5]Department of Cell Biology, University of Massachusetts Medical School, Worcester, MA 01655, USA. [6]Department of Molecular and Cell Biology, University of California at Berkeley, Berkeley, CA 94720, USA. [7]Institut de Biologie Moléculaire des Plantes, CNRS, 67084 Strasbourg Cedex, France. [8]Department of Biochemistry and Biophysics, University of California at San Francisco, San Francisco, CA 94143, USA. [9]Biotechnology Research Center, Zhongshan University, Guangzhou 510275, China. [10]Department of Molecular Sciences and Center of Excellence in Genomics and Bioinformatics, University of Tennessee, Memphis, TN 38163, USA. [11]Department of Plant Biology, University of Minnesota, St. Paul, MN 55108, USA. [12]Department of Genetics, Development, and Cell Biology, Iowa State University, Ames, IA 50011, USA. [13]Genetic Information Research Institute, Mountain View, CA 94043, USA. [14]The Institute for Genomic Research, Rockville, MD 20850, USA. [15]Plant Biology Laboratory, Salk Institute, La Jolla, CA 92037, USA. [16]Stanford Human Genome Center, Stanford University School of Medicine, Palo Alto, CA 94304, USA. [17]Department of Plant Biology, Carnegie Institution, Stanford, CA 94305, USA. [18]Plant Biology Institute, Department of Life Sciences, University of Liège, B-4000 Liège, Belgium. [19]University of Nebraska-Lincoln, School of Biological Sciences—Plant Science Initiative, Lincoln, NE 68588, USA. [20]Department of Plant Sciences, University of Cambridge, Cambridge CB2 3EA, UK. [21]Department of Plant and Microbial Biology, University of California at Berkeley, Berkeley, CA 94720, USA. [22]Department of Genetics, Washington University School of Medicine, St. Louis, MO 63110, USA. [23]Departamento de Bioquímica y Biología Molecular, Facultad de Ciencias, Universidad de Córdoba, Campus de Rabanales, 14071 Córdoba, Spain. [24]Graduate School of Biostudies, Kyoto University, Kyoto 606-8502, Japan. [25]Departamento de Genética Molecular, Instituto de Fisiología Celular, Universidad Nacional Autónoma de México, México 04510 DF, México. [26]Department of Cellular and Developmental Biology of Plants, University of Bielefeld, D-33615 Bielefeld, Germany. [27]Department of Biology, Institute of Plant Biochemistry and Biotechnology, University of Münster, 48143 Münster, Germany. [28]CNRS UMR 8186, Département de Biologie, Ecole Normale Supérieure, 75230 Paris, France. [29]Plant Cell Biology Research Centre, The School of Botany, The University of Melbourne, Parkville, Melbourne, VIC 3010, Australia. [30]Institut de Biotechnologie des Plantes, UMR 8618, CNRS/Université Paris-Sud, Orsay, France. [31]Department of Biochemistry, N151 Beadle Center, University of Nebraska, Lincoln, NE 68588-0664, USA. [32]Institut für Allgemeine Botanik, Johannes Gutenberg-Universität, 55099 Mainz, Germany. [33]Department of Cell Biology and Skaggs Institute for Chemical Biology, Scripps Research Institute, La Jolla, CA 92037, USA. [34]PCMB and Plant Biotechnology Center, Ohio State University, Columbus, OH 43210, USA. [35]Molecular Genetics and Cell Biology, University of Chicago, Chicago, IL 60637, USA. [36]Institut für Allgemeine Botanik und Pflanzenphysiologie, Friedrich-Schiller-Universität Jena, 07743 Jena, Germany. [37]Department of Molecular and Cellular Biology, University of Arizona, Tucson, AZ 85721, USA. [38]Department of Biological Science, Louisiana State University, Baton Rouge, LA 70803, USA. [39]Department of Plant Sciences, University of Arizona, Tucson, AZ 85721, USA. [40]Department of Biology, University of New Brunswick, Fredericton, NB, Canada E3B 6E1. [41]Department of Physiology, University of Massachusetts Medical School, Worcester, MA 01605, USA. [42]Department of Biology, University College London, London WC1E 6BT, UK. [43]Unité de Glycobiologie Structurale et Fonctionnelle, UMR8576 CNRS/USTL, IFR 118, Université des Sciences et Technologies de Lille, Cedex, France. [44]Universität Potsdam, Institut für Biochemie und Biologie, D-14476 Golm, Germany. [45]Department of Medicine, National Jewish Medical and Research Center, Denver, CO 80206, USA. [46]Delaware Biotechnology Institute, University of Delaware, Newark, DE 19711, USA. [47]Institute of Biology II/Plant Biochemistry, 79104 Freiburg, Germany. [48]Boyce Thompson Institute for Plant Research at Cornell University, Ithaca, NY 14853, USA. [49]Department of Chemistry and Biomolecular Sciences, Macquarie University, Sydney 2109, Australia. [50]Department of Anatomy and Cell Biology, Oklahoma State University, Center for Health Sciences, Tulsa, OK 74107, USA. [51]Izmir Ekonomi Universitesi, 35330 Balcova-Izmir, Turkey. [52]Institute of Microbiology, Czech Academy of Sciences, Czech Republic. [53]Department of Plant Physiology, Faculty of Sciences, Charles University, 128 44 Prague 2, Czech Republic. [54]Bioinformatics Program, St. Edward's University, Austin, TX 78704, USA. [55]Department of Biology, University of Puget Sound, Tacoma, WA 98407, USA. [56]Institute of Low-Temperature Science, Hokkaido University, 060-0819, Japan. [57]Department of Biology, Tsinghua University, Beijing, China 100084. [58]Institute of Biological Chemistry, Washington State University, Pullman, WA 99164, USA. [59]Appalachian State University, Boone, NC 28608, USA. [60]Department of Biology, Marquette University, Milwaukee, WI 53233, USA. [61]UMR8576 CNRS, Laboratory of Biological Chemistry, 59655 Villeneuve d'Ascq, France. [62]Cell Signaling Laboratory, Stazione Zoologica, I 80121 Naples, Italy. [63]Graduate Program in Biophysics, Ohio State University, Columbus, OH 43210, USA.

Supporting Online Material

www.sciencemag.org/cgi/content/full/318/5848/245/DC1
Materials and Methods
SOM Text
Figs. S1 to S25
Tables S1 to S14
References and Notes

9 April 2007; accepted 5 September 2007
10.1126/science.1143609

REPORTS

Dislocation Avalanches, Strain Bursts, and the Problem of Plastic Forming at the Micrometer Scale

Ferenc F. Csikor,[1,2] Christian Motz,[3] Daniel Weygand,[3] Michael Zaiser,[2] Stefano Zapperi[4,5]*

Under stress, many crystalline materials exhibit irreversible plastic deformation caused by the motion of lattice dislocations. In plastically deformed microcrystals, internal dislocation avalanches lead to jumps in the stress-strain curves (strain bursts), whereas in macroscopic samples plasticity appears as a smooth process. By combining three-dimensional simulations of the dynamics of interacting dislocations with statistical analysis of the corresponding deformation behavior, we determined the distribution of strain changes during dislocation avalanches and established its dependence on microcrystal size. Our results suggest that for sample dimensions on the micrometer and submicrometer scale, large strain fluctuations may make it difficult to control the resulting shape in a plastic-forming process.

In recent years, experimental evidence has accumulated that indicates that plastic flow is—at least on the micrometer scale—characterized by intermittent strain bursts with scale-free (i.e., power-law) size distributions (*1*–*8*). The phenomenology of these strain bursts closely resembles that of macroscopic plastic instabilities: Stress-strain curves are characterized by serrated yielding under displacement control and assume a staircase shape under conditions of stress control. Temporal intermittency is associated with spatial localization because each strain burst corresponds to the formation of a narrow slip line or slip band (*9*). On the macroscopic scale, spatiotemporal localization of plastic deformation associated with plastic instabilities is well known to have a detrimental effect on formability. A classic example is the strain bursts discovered by Portevin and le Chatelier (PLC effect), which arise from the interaction between dislocations and diffusing solutes (*10*). The PLC effect limits the applicability of many aluminum alloys in sheet metal–forming processes, but only arises under specific deformation conditions. Thus, the instability can be circumvented by appropriately choosing the process path, avoiding those temperature and strain rate

regimes in which the dislocation and solute velocities are of the same order of magnitude.

Here, we demonstrate that the burstlike deformation of microcrystals represents a much more fundamental instability of plastic flow that could cause intrinsic problems in the plastic forming of micrometer-size crystals. Strain bursts in microcrystals arise from the collective, avalanche-like motion of dislocations. The constraints to their motion imposed by the crystal lattice structure give dislocations the ability to mutually trap each other into jammed configurations. The long-range mutual interactions between dislocations make the destruction of such jammed configurations a collective, avalanche-like process. Because their occurrence depends only on the most basic features of dislocation plasticity, dislocation avalanches are a universal feature that does not depend on specific materials properties and cannot be avoided by adjusting the deformation path as in the PLC effect. Similar to other crackling noise phenomena (*11*) observed in driven systems, such as the Barkhausen noise emitted along the hysteresis loop in ferromagnets (*12*) or ferroelectrics (*13*), the acoustic emission during fracture (*14*, *15*), or the seismic activity during earthquakes, dislocation avalanches are characterized by material-independent power-law size distributions. Although the existence of intermittent plastic strain bursts has been known for many years (*16*–*18*), a statistical characterization was performed only recently by acoustic emission (AE) experiments in single slip deformation of hexagonal ice (*3*) or hexagonal close-packed metals (*8*), as well as by direct observation of strain bursts during deformation of micropillars (*2*). AE experiments, in particular, record the acoustic energy released during a burst and find power-law distributions of AE energies that do not exhibit any apparent cut-off (*3*–*6*). These observations raise several intriguing questions. What are the minimum "ingredients" required to produce dislocation avalanches, and are the avalanche properties truly universal? If there is no intrinsic limit to the magnitude of dislocation avalanches, why do we not see them in deformation curves of macroscopic samples? Or, if there is an intrinsic limit, why do we not see such a limit in AE measurements on macroscopic samples?

To resolve these issues, we investigate the dynamic behavior of dislocation systems under various loading conditions. To this end, we simulate the deformation of monocrystalline specimens using three-dimensional discrete dislocation dynamics. The model, described in detail in (*19*), considers an assembly of dislocation lines in a block made of a face-centered cubic metal (we use materials parameters of Al). Most of our simulations consider uniaxial tension-compression of cube-shaped specimens. Deformation is driven either by controlling the axial displacement of the top face of the cube (displacement control) or by slowly increasing the total force acting on the top face (load control) (*20*, *21*). In addition, we simulate the compression of bicrystals and multicrystals of various sizes, as well as the bending of a monocrystalline beam (aspect ratio 3:1:1) that is cantilevered in a cube orientation and deformed by imposing a downward displacement on its free end. In the compression simulations, we record the plastic strain ε_{pl} as well as the average stress (force per unit area acting on the top surface of the block). In the case of bending, we record the maximum bending stress and surface strain, from which we deduce a "plastic" bending strain by subtracting the surface strain of a purely elastic beam under the same bending moment.

An example of a typical stress-strain curve recorded in a load-controlled compression test is shown in Fig. 1. The staircase character of the response is very similar to that of the experimental observations in micrometer-sized samples (*2*). By differentiating the plastic strain versus time signal, we obtain the strain rate shown in the inset of Fig. 1. This is a typical example of a crackling noise signal, consisting of intermittent bursts with widely fluctuating amplitudes (*11*). These bursts arise from the propagation of dislocation avalanches within the sample. Dislocation activity during an avalanche is usually dominated by a single-slip system, even if deformation proceeds, on average, in symmetrical multiple slip. Consequently, the avalanches exhibit a characteristic lamellar shape, as shown in Fig. 2.

To analyze the crackling noise signal, we first threshold it to eliminate effects coming from numerical noise, and then identify well-defined pulses. The area s under each pulse is equivalent to the plastic strain increment produced by a dislocation avalanche (the avalanche strain). In analogy with experimental measurements that use multiple samples, we determine avalanche strain distributions $P(s)$ from multiple simulations with different, but statistically equivalent, initial configurations. Avalanches in bending deformation are analyzed in an analogous manner by considering the evolution of the plastic bending strain. In either case, the avalanche strain distributions have the general form

$$P(s) = C\, s^{-\tau} \exp[-(s/s_0)^2] \qquad (1)$$

where C is a normalization constant, τ is a scaling exponent, and s_0 is the characteristic strain of the largest avalanches.

To test the robustness of Eq. 1 in various physical situations, we compare distributions of avalanche strains for compression simulations performed in load control and displacement control, with and without activation of cross slip, in single slip and in multiple slip conditions. The avalanche strain distributions are essentially insensitive to the slip geometry and to the presence or absence of cross slip (Fig. 3 and figs. S1 and S2). In either case, the distributions can be described by Eq. 1 with $\tau \cong 1.5$. The same is true for the bending simulations. A very similar exponent was also reported in the experiment (*2*). In addition, the mean-field value $\tau = 3/2$ was predicted to hold for single-slip conditions in general by the theory of the dislocation yielding transition (*22*, *23*). Our simulations demonstrate that the universality of the exponent extends also to multiple-slip conditions and to deformation modes such as bending, which impose strain gradients on the sample scale. The last finding is particularly interesting because it demonstrates that the accumulation of "geometrically necessary" excess dislocations that is characteristic of inhomogeneous deformation processes does not change the statistical characteristics of dislocation avalanches.

To elucidate the physical origin of the cut-off, we consider the proposition (*22*, *23*) that during the progress of an avalanche, two processes reduce the effective stress acting upon the dislocations: (i) Because of intrinsic hardening with strain hardening coefficient Θ, a higher driving stress is needed to sustain the avalanche, and (ii) in case of

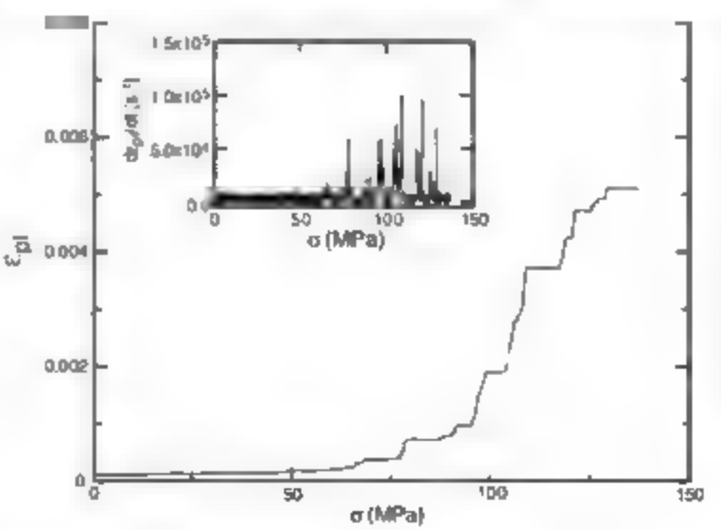

Fig. 1. A typical stress-strain curve obtained from simulation of the three-dimensional dislocation dynamics model in a load-controlled test in multiple-slip conditions. **(Inset)** The strain-rate signal displays the characteristics typical of crackling noise: bursts of activity of widely distributed amplitudes followed by more quiescent periods.

[1]Department of Materials Physics, Eötvös University, Post Office Box 32, H-1518 Budapest, Hungary. [2]Center for Materials Science and Engineering, University of Edinburgh, King's Buildings, Sanderson Building, Edinburgh EH93JL, UK. [3]Universität Karlsruhe, Institut für die Zuverlässigkeit von Bauteilen und Systemen, Kaiserstrasse 12, 76131 Karlsruhe, Germany. [4]Consiglio Nazionale delle Ricerche-Istituto Nazionale per la Fisica della Materia, Statistical Mechanics and Complexity, Dipartimento di Fisica, Sapienza–Università di Roma, P.le A. Moro 2, 00185 Roma, Italy. [5]Institute for Scientific Interchange Foundation, Viale S. Severo 65, 10133 Torino, Italy.

*To whom correspondence should be addressed. E-mail: stefano.zapperi@roma1.infn.it

displacement-controlled deformation, the driving stress decreases due to relaxation of the elastic strain. The total effective-stress drop caused by an avalanche of strain s is $(\Theta + \Gamma)s$, where Γ is the effective stiffness of the specimen-machine system (for a cubic compression specimen with rigid boundaries, Γ equals the elastic modulus E). This stress drop terminates the largest avalanches and, accordingly, we expect the cut-off to scale in inverse proportion with $(\Theta + \Gamma)$. A second scaling property can be motivated as follows: Large dislocation avalanches extend along a lamellar region across an entire specimen cross section. The total strain produced by such a "system-spanning" avalanche is proportional to the dislocation Burgers vector modulus b and inversely proportional to the characteristic specimen size L. Combining these relations, we find that (see also (*19*, *24*))

$$s_0 \propto \frac{bE}{L(\Theta + \Gamma)} \qquad (2)$$

To verify the validity of this scaling relation, we performed simulations of different system sizes in displacement control with a rigid constraint. As seen in Fig. 3, avalanche strain distributions obtained from specimens of different sizes fall on top of each other after rescaling $s \rightarrow S = sL(\Gamma + \Theta)/bE$ with $\Gamma = E$ and Θ deduced from the simulated stress strain curves (fig. S3). The same is true for the distribution we obtained under load control where $\Gamma = 0$, and we rescale by using the hardening coefficient Θ alone. The avalanche strain distributions obtained from our microbending simulations follow the same universal scaling curve if we identify L with the length of the bending beam and note that these simulations use displacement control.

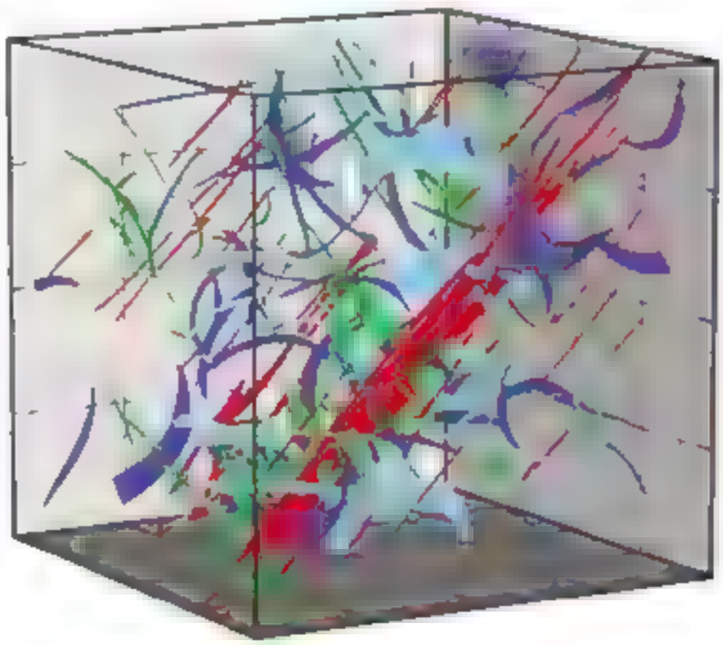

Fig. 2. Progress of a large dislocation avalanche in [010] symmetrical multiple slip for a specimen of size $L = 0.5$ μm. The graph shows an overlay of snapshots from every 10th global simulation timestep during a strain burst event. Red, green, blue, and cyan denote dislocations on the four {111} sets of crystal planes, yellow represents immobile Lomer locks created through dislocation reactions. Several geometrically separated dislocations become unpinned during the same event, which demonstrates the importance of long-range elastic interactions in strain burst initiation. The avalanche has a strongly anisotropic shape with more than 60% of the deformation occurring on one of the four equivalent sets of slip planes. Although a part of the deformation is taking place outside a single slip plane, the statistical analysis of the avalanche distribution suggests that the fractal dimension of the avalanches is close to two, indicating an effective lamellar shape.

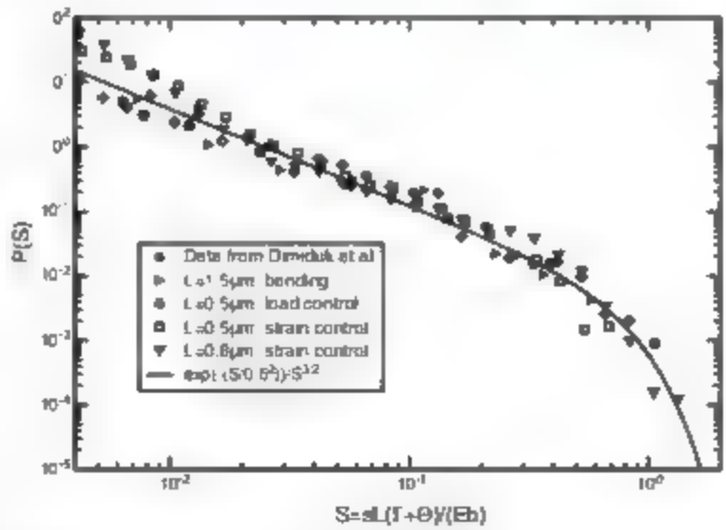

Fig. 3. Scaling collapse of avalanche size distributions. Open data points: data obtained from simulations of systems of different sizes in load and displacement control. Scaling parameters: $b = 2.8 \times 10^{-10}$ m (Al); $\Gamma = E$, $\Theta = E/10$ (displacement-controlled tension/compression and bending); $\Gamma = 0$, $\Theta = E/10$ (load-controlled tension/compression). Full data points: experimental data of Dimiduk *et al.* (*2*); scaling parameters: $b = 2.5 \times 10^{-10}$ m (Ni), $\Gamma = 0$, $\Theta = E/1000$ (load-controlled compression). Full line: scaling function $P(S) \propto S^{-3/2} \exp[-(S/0.6)^2]$.

It is instructive to apply the scaling (*2*) to the experimental data of (*2*) (solid circles in Fig. 3). In these experiments, the distribution of elongation increments $x = sL$ was determined during deformation in load control. Rescaling the experimental data points by setting $S = x\Theta/bE$ and using a hardening coefficient $\Theta = E/1000$ as deduced from the stress-strain curves in (*2*), we find that the scaled experimental data and simulation results are described by a single, universal scaling function, $P(S) \propto S^{-3/2} \exp[-(S/0.6)^2]$. In addition, the present theory can quantitatively explain high-resolution strain measurements that recorded strain bursts during stress-controlled torsion of tubular macroscopic samples of zinc, oriented for basal slip (*16*). Using the experimental parameters of (*16*), we estimate $s_0 \approx 2 \times 10^{-7}$, in agreement with the size of the largest strain jump reported in (*16*).

Our simulations demonstrate that intermittent dislocation avalanches are an intrinsic feature of crystal plasticity with properties that do not depend on the slip geometry, deformation mode, or details of the dynamical properties of dislocations. The avalanches are statistically characterized by a universal probability distribution whose characteristic parameter s_0 is determined by the specimen size, the hardening capacity of the material, and the response of the deformation "machine" to an avalanche. But what are the implications of these findings for deformation processes on the micrometer scale? To elucidate this aspect, we performed stochastic simulations of the bending of a long thin rod subjected to a bending moment that is constant along its length. The basic idea of these simulations (*19*) is that a long thin rod can be considered as a chain of segments that are similar to those we have simulated by discrete dislocation dynamics, and that behave in a statistically independent manner. The applied bending moment is increased until the total bending angle exceeds 2π, when the rod should assume an annular shape. As a consequence of the stochastic and intermittent nature of the deformation process, the deformation behavior of the individual segments can, however, no longer be predicted in a deterministic sense. As the maximum avalanche strain increases with decreasing system size, the stochastic heterogeneity of deformation becomes more and more pronounced. This leads to irregular shape distortions, as shown in Fig. 4. In the limit of very thin rods (illustrated by the bottom right shape in Fig. 4), the stochastic heterogeneity does not increase further. In very small specimens, the largest strain bursts that occur before the simulation is terminated remain below the intrinsic cut-off s_0 of the probability distribution.

Our findings demonstrate that it may be difficult, on the micrometer and submicrometer scale, to control the results of plastic-forming processes. Note, however, that micrometer-scale components such as bonding wires that are processed through plastic forming are polycrystals. We have studied the influence of grain boundaries on the propagation of dislocation avalanches by simulating bicrystalline and multicrystalline samples (*19*). The results suggest that in polycrystals, grain bounda-

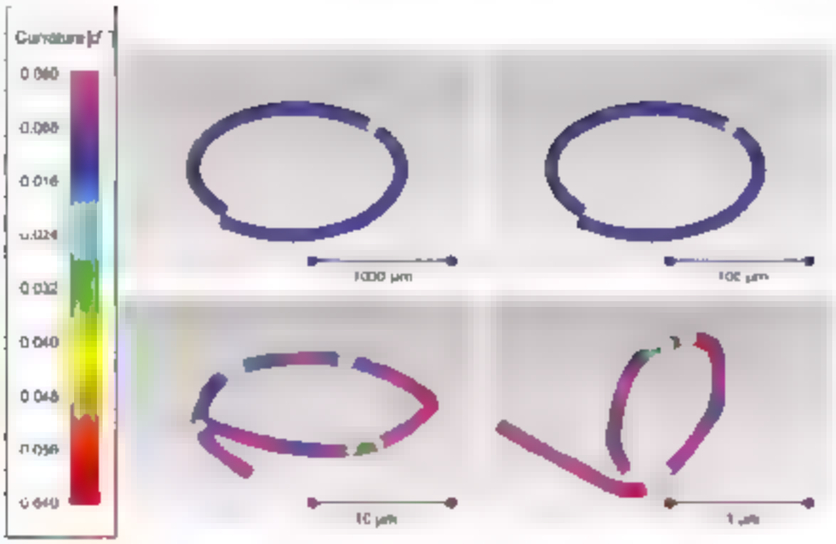

Fig. 4. Shapes of rods (aspect ratio 1:50) after simulated bending; rod thickness t from top left to bottom right: $t = 100$ μm, $t = 10$ μm, $t = 1$ μm, $t = 0.1$ μm; $b = 2.8 \times 10^{-10}$ m, $\Theta = E/1000$; the color code indicates the local bending angle over a segment of length t. In the last rod, the maximum avalanche size occurring in the simulations falls below the intrinsic cut-off of the distribution.

nes hinder avalanche propagation (fig. S4), and thus the size of strain bursts is reduced by a factor of $(\xi/L)^2$, where ξ is the grain size [see (*19*) for a more detailed discussion]. Accordingly, formability may be ensured even on the submicrometer scale if a correspondingly small grain size can be maintained throughout the processing.

Our results demonstrate the universality of avalanche behavior in plasticity and elucidate the crossover between intermittent and smooth plastic flow. That avalanche strains decrease in inverse proportion to sample size explains why it is difficult to observe strain bursts in macroscopic samples. In AE measurements, by contrast, the acoustic energy is recorded. The acoustic energy release during a dislocation avalanche may be assumed to be proportional to the dissipated energy e, which is related to the strain ε by $e \approx \sigma\varepsilon V$, where σ is the stress and V is the volume. Hence, the cutoff of the AE energy distribution is expected to increase with sample size as $e_0 \propto L^3$. This explains why acoustic emission avalanches are observed in macroscopic single crystals, whereas strain avalanches are not.

The picture that emerges from our analysis indicates that, even though the phenomenology of plastic deformation changes markedly with decreasing sample size, the fundamental physical processes are the same in macroscopic and micrometer-scale specimens. Dislocation avalanches on all scales arise from the most basic features of dislocation motion and can be described by a generic statistical distribution. In single crystals, the largest dislocation avalanches extend across an entire cross section of the specimen. Their extension is limited only by the sample size, and the stochastic nature of their occurrence may make it impossible to control the shapes resulting from a deformation process. In polycrystals, by contrast, dislocation avalanches are limited by grain boundaries. This may lead to an appreciable smoothing of deformation and improve the controllability of deformation processes.

References and Notes

1. M. D. Uchic, D. M. Dimiduk, J. N. Florando, W. D. Nix, *Science* **305**, 986 (2004)
2. D. M. Dimiduk, C. Woodward, R. LeSar, M. D. Uchic, *Science* **312**, 1188 (2006)
3. M. C. Miguel, A. Vespignani, S. Zapperi, J. Weiss, J. R. Grasso, *Nature* **410**, 667 (2001)
4. J. Weiss, J. R. Grasso, *J. Phys. Chem. B* **101**, 6113 (1997)
5. J. Weiss, F. Lahaie, J. R. Grasso, *J. Geophys. Res.* **105**, 433 (2000)
6. J. Weiss, D. Marsan, *Science* **299**, 89 (2003)
7. T. Richeton, J. Weiss, F. Louchet, *Nat. Mater.* **4**, 465 (2005)
8. T. Richeton, P. Dobron, F. Chmelik, J. Weiss, F. Louchet, *Mater. Sci. Eng. A* **424**, 190 (2006)
9. J. Schwerdtfeger *et al.*, *J. Stat. Mech.* L04001 (2007)
10. L. P. Kubin, C. Fressengeas, G. Ananthakrishna, in *Dislocations in Solids*, F. R. N. Nabarro, M. S. Duesbery, Eds. (North-Holland, Amsterdam, 2002) vol. 11, p. 101
11. J. P. Sethna, K. A. Dahmen, C. R. Myers, *Nature* **410**, 242 (2001)
12. G. Dunn, S. Zapperi, in *The Science of Hysteresis*, G. Bertotti, I. Mayergoyz, Eds. (Academic Press, New York, 2005), p. 181; also available at http://arxiv.org/abs/cond-mat/0404512.
13. E. V. Colla, L. K. Chao, M. B. Weissman, *Phys. Rev. Lett.* **88**, 017601 (2002).
14. A. Petri, G. Paparo, A. Vespignani, A. Alippi, M. Costantini, *Phys. Rev. Lett.* **73**, 3423 (1994)
15. L. I. Salminen, A. I. Tolvanen, M. J. Alava, *Phys. Rev. Lett.* **89**, 185503 (2002)
16. R. F. Tinder, J. P. Trzu, *Acta Metall.* **21**, 975 (1973)
17. H. H. Potthoff, *Phys. Stat. Sol. (a)* **77**, 215 (1983)
18. H. Godon, H. H. Potthoff, H. Neuhauser, *Cryst. Lattice Defects* **10**, 373 (1984)
19. See supporting material available on *Science* Online.
20. D. Weygand, L. H. Friedman, E. van der Giessen, A. Needleman, *Model. Simul. Mater. Sci. Eng.* **10**, 437 (2002)
21. O. Weygand, P. Gumbsch, *Mat. Sci. Eng. A* **400–401**, 158 (2005)
22. M. Zaiser, P. Moretti, *J. Stat. Mech.* P08004 (2005)
23. M. Zaiser, *Adv. Phys.* **55**, 185 (2006)
24. M. Zaiser, N. Nikitas, *J. Stat. Mech.* P04013 (2007).

25. Financial support of the European Commissions Human Potential Programme SizeDepEn (contract MRTN-CT-2003-504634) and the New and Emerging Science and Technologies (NEST) Pathfinder programme Triggering Instabilities in Materials and Geosystems (contract NEST 2005-PATH-COM-043386) as well as by the Engineering and Physical Science Research Council (grant EP/E029825/1) is gratefully acknowledged. Part of this work was performed on the PC cluster of the Department of Theoretical Physics at Eötvös University and at the High Performance Computing calculation facilities of the Rechenzentrum, University of Karlsruhe, within the HPC_DDD project. CM. acknowledges the financial support of the Austrian Fonds zur Förderung der wissenschaftlichen Forschung (FWF) through project J2646-N13. D.W. acknowledges the financial support of the European Union project NMP3-CT-2006-016710 (NANOMESO).

Supporting Online Material

www.sciencemag.org/cgi/content/full/318/5848/251/DC1
SOM Text
Figs. S1 to S4
References

12 April 2007; accepted 17 August 2007
10.1126/science.1143719

Polymers with Cavities Tuned for Fast Selective Transport of Small Molecules and Ions

Ho Bum Park,[1,2] Chul Ho Jung,[1] Young Moo Lee,[1]* Anita J. Hill,[3] Steven J. Pas,[3] Stephen T. Mudie,[3] Elizabeth Van Wagner,[2] Benny D. Freeman,[2] David J. Cookson[4]

Within a polymer film, free-volume elements such as pores and channels typically have a wide range of sizes and topologies. This broad range of free-volume element sizes compromises a polymer's ability to perform molecular separations. We demonstrated free-volume structures in dense vitreous polymers that enable outstanding molecular and ionic transport and separation performance that surpasses the limits of conventional polymers. The unusual microstructure in these materials can be systematically tailored by thermally driven segment rearrangement. Free-volume topologies can be tailored by controlling the degree of rearrangement, flexibility of the original chain, and judicious inclusion of small templating molecules. This rational tailoring of free-volume element architecture provides a route for preparing high-performance polymers for molecular-scale separations.

Small-molecule and ion diffusion through cavities (i.e., free-volume elements) in soft organic materials is an inherently subnano- or nanoscopic phenomenon. It has important implications for membrane separation processes in chemicals production as well as energy conver-

sion and storage applications [e.g., pharmaceutical separations (*1*), organic batteries (*2*), fuel cells (*3*), and gas separation (*4*)]. Transport of small gas molecules through polymers occurs by diffusion through transient free-volume elements or cavities formed by random, thermally stimulated motion of the flexible organic chains. Unlike pore sizes and shapes in rigid microporous inorganic materials such as zeolites (*5*) and carbon molecular sieve materials (*6*), cavity sizes and shapes are not uniform in amorphous polymers. The cavity radius (r) of the most selective polymers such as polyimides, polysulfones, and polycarbonates, as measured by positron annihilation lifetime spectroscopy (PALS), is 0.3 nm or less with a broad distribution of cavity sizes, and gas permeability is rather low (*7*).

Conversely, the most permeable polymer, poly(1-trimethylsilyl-1-propyne) (PTMSP), exhibits an approximately bimodal cavity size distribution centered at around r = 0.3 nm and r = 0.6 to 0.7 nm (*8*). The high concentration of large cavities and the high connectivity among cavities results in very high permeability for a polymer, but its ability to separate small molecules (kinetic diameter <0.45 nm) is too low to be useful, and the large cavities collapse over time due to physical aging (*8*). Thus, among known polymers, free-volume element size and distribution play a key role in determining permeability and separation characteristics. However, the broad size range of free-volume elements in such materials precludes the preparation of polymers having both high permeability and high selectivity.

We demonstrate that polymers with an intermediate cavity size, a narrow cavity size distribution, and a shape reminiscent of bottlenecks connecting adjacent chambers, such as those found elegantly in nature in the form of ion channels (*9*) and aquaporins (*10*), yield both high permeability and high selectivity. Central to our approach for preparing these intermediate-sized cavities is controlled free-volume element formation through spatial rearrangement of the rigid polymer chain segments in the glassy phase. It is known that a rearrangement, such as intramolecular cyclization, in glassy polymers could lead to changes in polymer structure for gas transport (*11*). For this purpose, aromatic polymers interconnected with heterocyclic rings (e.g., benzoxazole, benzothiazole, and benzimidazole) are of interest because phenylene-heterocyclic ring units in such materials have a flat, rigid-rod structure with high torsional energy barriers to rotation between two rings (*12*). The stiff, rigid ring units in such flat topologies pack efficiently, leaving very small penetrant-accessible free-volume elements. This tight packing is also promoted by intersegmental interactions such as charge-transfer complexes between heteroatoms containing lone electron pairs (e.g., O, S and N) (*13*). The genesis of these materials was the demand for highly thermally and chemically stable polymers. However, their application as gas separation membranes was frustrated by their lack of solubility in common solvents, which effectively prevents them from being prepared as thin membranes by solvent casting, which is the most widely practiced method for membrane preparation.

We circumvented this fabrication challenge by using postfabrication polymer-modifying reactions (*14*, *15*). Completely aromatic, insoluble, infusible polymers can be prepared from highly soluble precursors by irreversible molecular rearrangement at about 350° to 450°C for aromatic polyimides containing ortho-positioned functional groups (e.g., -OH and -SH) (Fig. 1). Two types of changes in chain structure occur during the rearrangement that alter chain packing: (i) random chain conformations resulting from the formation of meta- and para-linked chains (Fig. 1A); and (ii) relatively flexible, twisting pairs of short flat planes (α and β) that convert to single long flat planes (γ) (Fig. 1B) that are much more rigid than those of the parent moieties [e.g., the torsional angle (φ_2) of benzoxazole-phenylene ring is close to 0° at the energy-minimized state because the coplanar conformation is favored due to resonance stabilization]. The use of stiff, rigid chain elements (e.g., benzoxazole-phenylene ring or benzothiazole-phenylene ring) prevents large intrachain, indiscriminant torsional rotation, increases the efficiency of cavity formation, and inhibits rapid collapse of the created cavities. These materials are thermally stable, and the structural rearrangements occurring during this process do not correspond to partial burning (or carbonization) of the underlying polymer structure, a process that has been used in other cases to enhance gas separation properties of polymers.

If managed properly, these changes in chain conformation and topology create well-connected, narrow size distribution free-volume elements (i.e., cavities) appropriate for molecular separations. For example, PALS analysis of a precursor polymer [PIOFG-1, synthesized from 4,4′-(hexafluoroisopropylidene)-diphthalic anhydride (6FDA) and 2,2′-bis(3-amino-4-hydroxylphenyl) hexafluoropropane (bisAPAF) via thermal imidization up to 300°C] and its corresponding thermally rearranged samples (i.e., TR-1-350, TR-1-400, and TR-1-450, respectively) shows that the polymer undergoes microstructural change depending on the extent of rearrangement (*16*). Thermal degradation of the polymer chains is not observed within the heat-treatment temperature ranges, based on results from thermogravimetric analysis coupled with mass spectroscopy (fig. S1A) and elemental analysis (table S2). Spectroscopic analysis (i.e., Fourier transform infrared) provides convincing evidence that the conversion from imide to benzoxazole is achieved (fig. S1B).

Figure 2 shows that the cavity radius of PIOFG-1 polymer (which is centered at about 0.28 nm and is very broad) increases to ~0.4 nm, and the distribution of cavity sizes becomes narrow as the thermal rearrangement temperature increases to 450°C. PALS analysis reveals an increase in *o*-positronium (*o*-Ps) lifetime as rearrangement temperature increases from 300° to 450°C. In general, longer *o*-Ps lifetime indicates larger cavity sizes (*17*). The *o*-Ps intensity (%) increases by 700% as thermal rearrangement temperature is increased to 400°C, but decreases above this temperature. Notably, despite increasing *o*-Ps lifetime, the reduction of *o*-Ps intensity in the sample treated at 450°C indicates that an increase in mean cavity size is accompanied by a decrease in the number of cavities, suggesting coalescence of

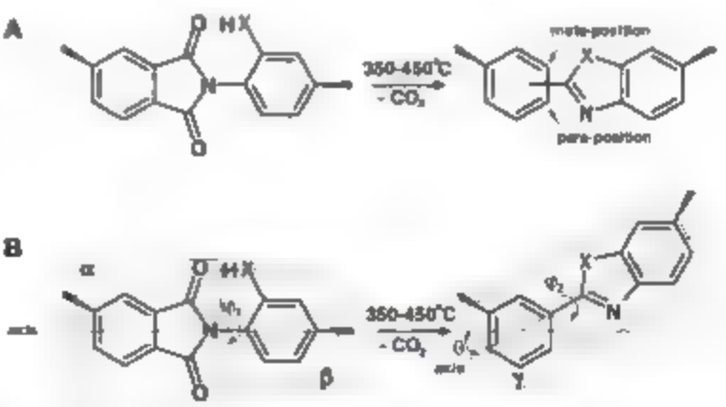

Fig. 1. Two major factors contributing to structural change during thermal chain rearrangement of polyimides containing ortho-positioned functional groups (X is O or S). (**A**) Change of chain conformation—polymer chains consisting of meta- and/or para-linked chain conformations can be created via rearrangement. (**B**) Spatial relocation due to chain rearrangement in confinement, which may lead to the generation of free-volume elements [α plane, phthalic imide ring; β plane, XH-containing phenylene ring; γ plane, newly created phenylene-heterocyclic ring (if X is O, benzoxazole-phenylene ring; if X is S, benzothiazole-phenylene ring); φ_1 and φ_2, dihedral angle; θ, tilting angle after transformation].

[1]School of Chemical Engineering, Hanyang University, Seoul 133-791, Korea. [2]Center for Energy and Environmental Resources and Department of Chemical Engineering, The University of Texas, Austin, TX 78758, USA. [3]The Commonwealth Scientific and Industrial Research Organization (CSIRO) Materials Science and Engineering, Private Bag 33, S Clayton, VIC 3169, Australia. [4]Australian Synchrotron Research Program, Building 434, 9700 South Cass Avenue, Argonne, IL 60439, USA.

*To whom correspondence should be addressed. E-mail: ymlee@hanyang.ac.kr

smaller cavities to form larger ones. Hourglass-shaped cavities, having narrow neck regions separating much larger adjacent chambers, are consistent with this scenario. To have excellent separation properties, the small neck regions must not be too large relative to the size of the molecules being separated, because large openings enable relatively nonselective flow mechanisms (e.g., Knudsen flow) (*7*). However, large cavities adjoining the necks will contribute to high rates of molecular transport. The large cavity size of the fully converted sample (TR-1-450) is smaller than that of PTMSP (0.675 nm) but substantially larger than that of common glassy polymers (e.g., 0.286 nm for polysulfone; 0.289 nm for polycarbonate) (*17*). Similar behavior is observed in other PIOFG samples prepared by a combination of other monomers based on the same methodology.

Synchrotron small-angle x-ray scattering (SAXS) measurements also indicate structural changes over the q-range 0.1 to 0.5 Å^{-1} ($q = 4\pi\sin\theta/\lambda$, where λ is the x-ray wavelength and 2θ is the scattering angle). Specifically, a peak is apparent in the SAXS profiles for samples processed at 400° and 450°C, but not in those processed at lower temperatures (Fig. 2). Furthermore, the peak in the 450°C sample is more pronounced and centered at a lower q than that of the 400°C sample. If we attribute this peak to scattering from cavities, these data suggest that cavities increase in size (i.e., the peak shifts to small q) at higher treatment temperatures.

To explore the separation properties of these polymers (hereafter referred to as TR polymers), we prepared dense membranes (thickness ~20 to 30 μm) for pure and mixed-gas permeability experiments. Figure 3 shows the gas separation performance of several families of polymers considered for CO_2/CH_4 separation at 35°C. Such separations are vital in natural gas processing, landfill gas recovery, and enhanced oil recovery (*18*).

TR polymers demonstrate excellent CO_2/CH_4 separation performance, surpassing the CO_2/CH_4 separation limitation (i.e., the "upper bound" line in Fig. 3A) (*19*) of typical polymer membranes (TR polymers also exceed the separation limit of other notable gas pairs such as O_2/N_2 and H_2/N_2). Counterintuitively, the CO_2 permeability and CO_2/CH_4 selectivity are both high, in contrast to the behavior of conventional strongly size-sieving polymer membranes, where high CO_2/CH_4 selectivity invariably leads to low CO_2 permeability (*20*). On the permeability-selectivity map, the separation performance of our polymer membranes is intermediate between the performance of common polymers and carbon molecular sieve membranes. As revealed by PALS and SAXS, the unusual microstructure of TR polymers (i.e., large cavities) provides an explanation for their high gas permeabilities, and the construction formed by cavity coalescence is presumably responsible for their precise discrimination among gas molecules such as CO_2 and CH_4. In addition, gas separation results (Fig. 3A) reveal that the cavity size in TR polymers can be tuned by adding small acidic dopants (e.g., HCl and H_3PO_4) because TR polymers include basic nitrogen atoms (-C=N-) on the heterocyclic rings (e.g., benzoxazole ring). After doping, the CO_2 permeability decreases but CO_2/CH_4 selectivity increases. However, after dedoping, the permeability and selectivity return to their original values, indicating that the cavity size and shape can be tailored.

In CO_2/CH_4 separation, CO_2 typically acts as a plasticizer, swelling the polymer matrix, causing the permeation of CH_4 to increase more than that of CO_2, which decreases selectivity (*21*). Glassy polymers such as polyimides and cellulose acetate exhibit substantial decreases in CO_2/CH_4 selectivity in mixed-gas experiments, particularly at high CO_2 fugacity. In contrast, TR polymer membranes do not exhibit substantially reduced selectivity, even at high CO_2 concentration (~80 mol%) and high CO_2 fugacity (~15 atm) (Fig. 3B). The small reduction in selectivity with increasing CO_2 fugacity is caused by a stronger decrease in CO_2 permeability as compared to CH_4 permeability, which is typical for glassy polymer membranes and is due to the effect of competitive sorption in mixtures (*22*, *23*). The CO_2 and CH_4 permeabilities slightly decrease with increasing CO_2 fugacity in all CO_2/CH_4 mixtures (fig. S4), and there is no evidence of plasticization. That is, TR polymer membranes show excellent resistance to plasticization at CO_2 partial pressures as high as 20 atm.

Gas permeabilities of TR polymers are often two orders of magnitude higher than those of the original PIOFG polymers but are still lower than those of PTMSP, the most permeable polymer. However, selectivities for important gas separations (e.g., O_2/N_2 and CO_2/CH_4) are much higher than in PTMSP (*24*) but comparable to or slightly lower than in carbon molecular sieve membranes (*25*). For TR polymers, the order of permeability is $CO_2 > H_2 > He > O_2 > N_2 > CH_4$, similar to that observed in ultrahigh free-volume polymers like PTMSP (*24*).

The outstanding performance results from largely unique cavity formation caused by random chain conformations during thermal molecular rearrangement. A few comparable studies are found in the literature. Barsema *et al.* (*26*) studied commercial polyimide membranes treated at different temperatures (300° to 525°C). They observed that the gas permeability of polyimide membranes treated below the thermal decomposition temperature (<450°C) did not change noticeably, but was slightly reduced due to polymer densification. At the decomposition temperature, the treated membranes exhibited a small increase in gas permeability.

A possible reason why these polymers have unique cavity sizes and shapes might be related to the role played by CO_2 molecules escaping from the original polymer matrix. Therefore, we designed a carboxylic acid group–containing polyimide film and performed the same thermal treatment. Here, the decarboxylation also occurs in a similar temperature range (T = 400° to 500°C). However, no outstanding change in gas permeability was apparent relative to that of the parent polyimide. From our model study, the evolution of CO_2 is not a decisive factor in the formation of gas-accessible free volume or cavities (fig. S5).

The polymers under investigation exhibit pseudo-microporous characteristics that can be probed by nitrogen adsorption/desorption, a technique usually applied to inorganic microporous materials rather than polymers. Conventional dense polymers are "nonporous" in that free-volume elements do not span the sample, so Brunauer-Emmett-Teller (BET) analysis is rarely used to characterize them (*27*). Nitrogen adsorption was used to study two PIOFG polymers [PIOFG-1 and PIOFG-2 (synthesized from 6FDA and 2,5-diamino-1,4-benzenedithiol (DABT)] and their

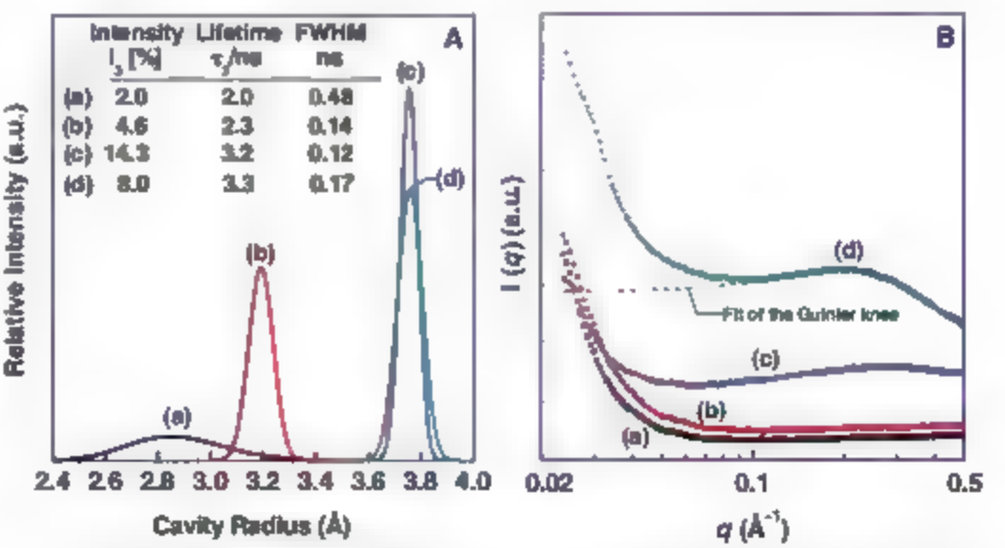

Fig. 2. (**A**) Change of cavity radius (Å) distribution, measured by PALS, of 6FDA + bisAPAF polyimide (PIOFG-1) as a function of thermal treatment temperature. (**B**) SAXS profiles of PIOFG-1 for all four processing temperatures and fit of the Guinier knee of TR-1-450 polymer (black dotted line). (a) PIOFG-1; (b) TR-1-350; (c) TR-1-400; (d) TR-1-450 (FWHM, full width at half maximum from the *o*-Ps lifetime τ_3 distribution).

thermally rearranged analogs at 450°C (TR-1-450 and TR-2-450) (Fig. 4). The PIOFG polymers exhibit an adsorption/desorption isotherm previously observed in glassy polymers (*27*). The nitrogen adsorption/desorption isotherms of TR-1-450 and TR-2-450 are of the irreversible Type I form with hysteresis. The BET surface areas are markedly large for polymers, 510 $m^2 g^{-1}$ (TR-1-450) and 410 $m^2 g^{-1}$ (TR-2-450), which indicates the presence of substantial amounts of free volume. The hysteresis loops for the TR polymers do not correspond to any of the IUPAC isotherms (*28*), but they are also observed in polymers of intrinsic microporosity (*29*). Materials showing similar isotherms are typically understood to possess "throat and cavity" type microporosity characteristic of activated carbons (*30*). These results further support the hypothesis from PALS of hourglass-shaped cavities.

There are two advantages to the materials described in this work. First, the original polyimides are soluble in common solvents; that is, they can be prepared in the form of hollow fibers and then continuously exposed to heat treatment because these TR polymers produce tough, ductile, robust films rather than brittle, fragile specimens such as zeolite or carbon membranes (table S3). This feature markedly enhances their potential utility and ultimate reduction to practice. Second, it is much easier and simpler to coat these polymers without any defects or cracks onto microporous ceramic support membranes than to coat zeolite, silica, and carbon membranes onto such supports. Recently, we observed that the separation performance of thin-layer coated composite membranes is comparable to that of thick, dense membranes and these membranes do not show permeability decay with time due to physical aging (fig. S5), as do high–free-volume glassy polymer membranes. These polymers with tailored porosity can also be applied as fuel cell membranes. When doped with acid molecules, these polymers exhibit high proton conductivity. For example, the proton conductivity of a H_3PO_4-doped TR-1-450 membrane reaches 0.15 S cm^{-1} at 130°C and low relative humidity (<30%). This value is higher than that of polybenzimidazole (PBI) (<0.1 S cm^{-1} at 200°C) (*31*), the most attractive proton-conducting polymer for high-temperature fuel cells. Currently we believe these polymers sequester water, bound acid, and free acid molecules in the cavity structure, and this phenomenon is responsible for the high conductivity. Most of all, the greatest benefit of these polymers is the ability to tune the cavity size and distribution for specific gas applications by using various templating molecules and heat treatments, with one starting material.

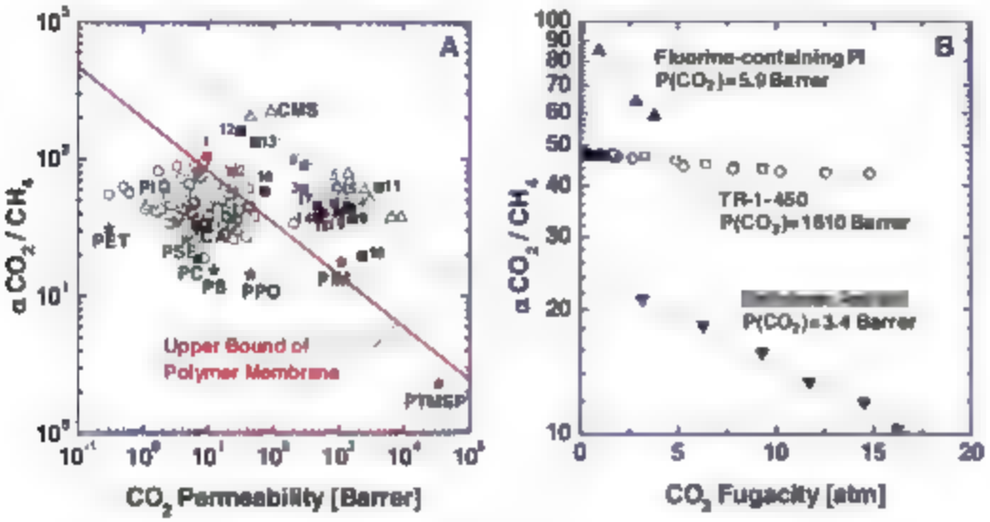

Fig. 3. (**A**) Relation between CO_2 permeability and CO_2/CH_4 selectivity of TR polymers (■) (1, PIOFG-1; 2, TR-1 350; 3, TR-1-400; 4, TR-1-450; 5, HCl-doped TR-1-450; 6, dedoped TR-1-450; 7, HCl-redoped TR-1-450; 8, H_3PO_4-doped TR-1-450; 9 to 19, other TR polymers prepared at 450°C from homopolyimides and copolyimides containing thermally convertible segment units (*26*)]. These data were obtained from pure gas experiments at 35°C. Gas separation performance data of polyimides (PI) reported in the literature (○) (*32*), other polymers (★) (*8*, *29*, *32*) [PET, poly(ethylene terephthalate); PSF, polysulfone; CA, cellulose acetate; PC, polycarbonate; PS, polystyrene; PPO, poly(phenylene oxide); PIM, polymer with intrinsic microporosity; PTMSP, poly(1-trimethylsilyl-1-propyne); CMS, carbon molecular sieve membranes (△) (*6*, *33*)] are included for comparison. The upper bound is from (*19*), and the dotted line is provided to guide the eye. (**B**) Effect of CO_2 partial pressure on mixed-gas CO_2/CH_4 selectivity in TR-1-450 at 35°C. Mixed-gas CO_2/CH_4 feed compositions (in mol% CO_2:mol% CH_4) were 10:90 (●), 50:50 (▲), and 80:20 (○). Mixed-gas data for a fluorine-containing polyimide (*32*) and cellulose acetate (*22*) are included for comparison. The CO_2 permeabilities of fluorine-containing polyimide, cellulose acetate, and TR-1-450 at 35°C and pressure = 10 atm are included for comparison. The dotted lines are provided to guide the eye.

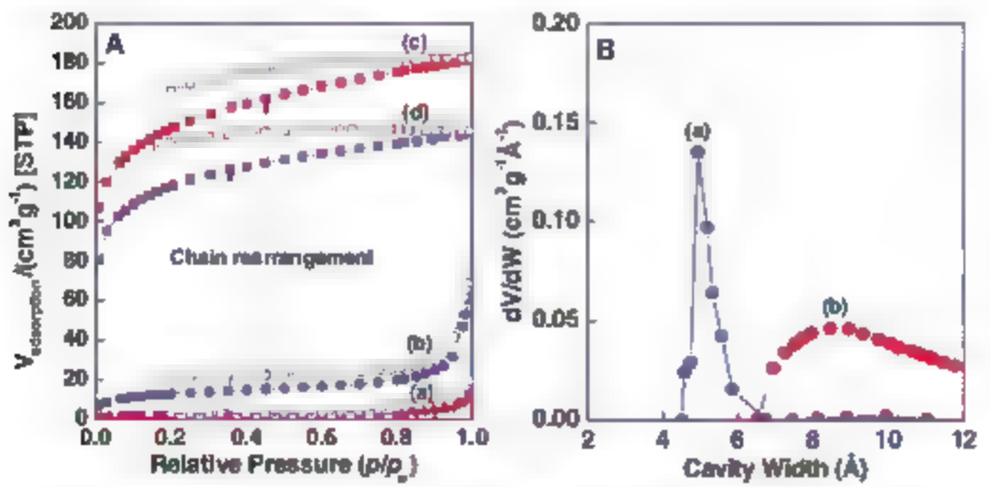

Fig. 4. (**A**) Nitrogen adsorption/desorption isotherms at 195°C for (a) PIOFG-1, (b) PIOFG-2, (c) TR-1-450, and (d) TR-2-450. p/p_0 is the ratio of gas pressure (p) to saturation pressure (p_0), with p_0 = 746 torr. (**B**) Apparent cavity size distributions of (a) TR-1-450, measured by BET, and (b) PTMSP (included for comparison).

References and Notes

1. B. Jeong, Y. H. Bae, D. S. Lee, S. W. Kim, *Nature* **388**, 860 (1997).
2. P. Tsiphtoori, M. A. Mehta, P. G. Bruce, *Science* **262**, 883 (1993).
3. M. A. Hickner, H. Ghassemi, Y. S. Kim, B. R. Einsla, J. E. McGrath, *Chem. Rev.* **104**, 4587 (2004).
4. H. Lin, E. Van Wagner, B. D. Freeman, L. G. Toy, R. P. Gupta, *Science* **311**, 639 (2006).
5. Z. Lai *et al.*, *Science* **300**, 456 (2003).
6. H. B. Park, Y. M. Lee, *Adv. Mater.* **17**, 477 (2005).
7. Y. Yampolskii, I. Pinnau, B. D. Freeman, *Materials Science of Membranes for Gas and Vapor Separation* (Wiley, London, 2006).
8. K. Nagai, T. Masuda, T. Nakagawa, B. D. Freeman, I. Pinnau, *Prog. Polym. Sci.* **26**, 721 (2001).
9. D. A. Doyle *et al.*, *Science* **280**, 69 (1998).
10. O. Kozono, M. Yasui, L. S. King, P. Agre, *J. Clin. Invest.* **109**, 1395 (2002).
11. L. K. Meyer, M. Langsam, H. C. Klotz, *J. Membr. Sci.* **94**, 195 (1994).
12. V. J. Vasudevan, J. E. McGrath, *Macromolecules* **29**, 637 (1996).
13. W. J. Welsh, D. Bhaumik, J. E. Mark, *Macromolecules* **14**, 947 (1981).
14. I. Ye. Kardash, A. N. Pravednikov, *Vysokomol. Soyed.* **B9**, 873 (1967).
15. G. L. Tullos, J. M. Powers, S. J. Jeskey, L. J. Mathias, *Macromolecules* **32**, 3598 (1999).
16. Materials and methods are available as supporting material on Science Online.
17. S. R. Wilks *et al.*, *J. Polym. Sci. Part B: Polym. Phys.* **41**, 2185 (2003).
18. H. Lin, E. Van Wagner, R. Raharjo, B. D. Freeman, I. Roman, *Adv. Mater.* **18**, 39 (2006).
19. L. M. Robeson, *J. Membr. Sci.* **62**, 165 (1991).
20. B. D. Freeman, *Macromolecules* **32**, 375 (1999).

21. A. Bos, I. G. M. Pünt, M. Wessling, H. Strathmann, *J. Membr. Sci.* **155**, 67 (1999).
22. T. Visser, N. Masetto, M. Wessling, *J. Membr. Sci.* 10.1016/j.memsci.2007.07.048 (2007).
23. W. R. Vieth, J. M. Howell, J. H. Hsieh, *J. Membr. Sci.* **1**, 177 (1976).
24. L. Pinnau, L. G. Toy, *J. Membr. Sci.* **116**, 199 (1996).
25. H. B. Park, I. Y. Suh, Y. M. Lee, *Chem. Mater.* **14**, 3034 (2002).
26. J. N. Barsema *et al.*, *J. Membr. Sci.* **238**, 93 (2004).
27. O. M. Ilinitch *et al.*, *Microporr Mesopor Mat.* **31**, 97 (1999).
28. K. S. W. Sing, R. T. Williams, *Adsorpt. Sci. Technol.* **22**, 773 (2004).
29. P. M. Budd, N. B. McKeown, D. Fritsch, *J. Mater. Chem.* **15**, 1977 (2005).
30. S. J. Gregg, K. S. W. Sing, *Adsorption, Surface Area and Porosity* (Academic Press, London, 1982).
31. J. A. Asensio, P. Gomez-Romero, *Fuel Cells* **5**, 336 (2005).
32. S. A. Stern, H. Kawakami, A. Y. Houde, G. Zhou, U.S. Patent 5 591 250 (1997).
33. K. M. Steel, W. J. Koros, *Carbon* **41**, 253 (2003).
34. This work was supported by the Carbon Dioxide Reduction and Sequestration Center, one of the 21st Century Frontier R&D Programs funded by the Ministry of Science and Technology in Korea. Positron experiments were performed within the framework of the ARC Centers of Excellence program through the Australian Research Council (ARC) Center for Electromaterials Science. CSIRO's Water for a Healthy Country Flagship and the Division of Materials Science and Engineering in CSIRO are acknowledged for their support of the internal membrane research program and this international collaboration. H.B.P. and B.D.F. acknowledge the support of the U.S. Department of Energy (DE-FG03-02ER15362) and the U.S. National Science Foundation (CTS-05-15425).

Supporting Online Material

www.sciencemag.org/cgi/content/full/318/5848/254/DC1
Materials and Methods
Figs. S1 to S6
Tables S1 to S3
References

19 June 2007; accepted 7 September 2007
10.1126/science.1146744

Microfluidic Adhesion Induced by Subsurface Microstructures

Abhijit Majumder, Animangsu Ghatak,* Ashutosh Sharma

Natural adhesives in the feet of different arthropods and vertebrates show strong adhesion as well as excellent reusability. Whereas the hierarchical structures on the surface are known to have a substantial effect on adhesion, the role of subsurface structures such as the network of microchannels has not been studied. Inspired by these bioadhesives, we generated elastomeric layers with embedded air- or oil-filled microchannels. These adhesives showed remarkable enhancement of adhesion (~30 times), which results from the crack-arresting properties of the microchannels, together with the surface stresses caused by the capillary force. The importance of the thickness of the adhesive layer, channel diameter, interchannel spacing, and vertical position within the adhesive has been examined for developing an optimal design of this microfluidic adhesive.

The feet of different arthropods and vertebrates show a remarkable ability to attach to almost any surface with varying surface properties and roughness (*1*–*6*). These biological adhesives not only show high adhesive strength, but they can also be detached rapidly and reused over and over. They are self-cleaning and do not leave any marks or footprints after they walk over a surface. Man-made pressure-sensitive adhesives lack these amazing qualities because their high adhesive strength is derived from their viscoelasticity. Although viscous dissipation increases the work or energy of adhesion, the failure occurs at the bulk of the adhesive rather than at the interface, which prevents a clean separation of the adhesive from the surface and also prevents its reusability. Viscoelastic adhesives are also susceptible to fouling by particulate contamination.

The extraordinary ability of naturally occurring adhesives of animals and insects, in particular, is in part related to the complex and hierarchal structural morphologies of their attachment pads (*2*, *8*), which use mechanisms of adhesion other than viscoelasticity (such as, friction, suction, and molecular interactions). Several studies on model textured surfaces (*9*–*14*) have shown that surface patterning can enhance adhesive strength remarkably. This is because the crack propagation is arrested when it encounters a surface discontinuity and has to be reinitiated thereafter. Crack initiation requires much higher stress than does propagation of the crack on a smooth surface (*10*, *11*).

Whereas the previous studies have focused on adhesion as an interfacial phenomenon and have thus employed surface-modified and -textured adhesive layers, we show that air and viscous domains or "patterns" buried within the subsurface or bulk phase can have equally important strong dissipative effects on the work of adhesion and, at the same time, offer a clean reversible separation. We embeded microchannels of different diameters at various vertical and spatial positions within cross-linked elastomeric adhesive layers bonded to a rigid substrate (*15*). A flexible microscope coverslip was then brought into complete contact with this adhesive and lifted vertically from its hanging edge at a constant rate, as shown in Fig. 1A. The flexibility of the adhering coverslip was chosen such that it underwent small bending during peeling. Small bending allows for a precise estimation of the interfacial adhesion strength directly from the force versus displacement measurements. A more general form of the experiment would be to peel an adhesive film bonded to a flexible backing off of another flexible plate. For small bending of the plates, the results for this general geometry are in fact equivalent to the experimental setup employed here by appropriately defining the rigidity of the peeled plate.

The peel experiments (Fig. 1A) on an elastic film (*16*) with air-filled microchannels shows that the contact line between the film and the plate or the crack does not propagate smoothly, but rather with intermittent arrests and initiations at the location of the channels (figs. S1 and S2). Thus, the channels act as a barrier for crack propagation on the surface of the film. This aspect is also captured in the plot of the peeling torque $M = F \cdot a$ against displacement Δ of the flexible plate (Fig. 1B), where a is the distance of the crack from the point of application of the load F. The plot shows the existence of several peaks, the first one corresponding to the formation of the cusp-shaped crack at the edge of the film (*10*, *11*) and the subsequent ones appearing because of the arresting effect of the buried channels. With an increase in Δ, the crack approaches an intermediate channel and remains arrested in its vicinity, whereas F continues to rise. The torque now increases linearly until it reaches a critical value at which the crack nucleates in the form of a cavity at the other side of the channel, and the torque increases sublinearly thereafter. Finally, the torque decreases sharply after a complete opening of the crack and its catastrophic propagation. The average maximum torque, $\overline{M}_{max}$, at which the cracks initiate is plotted in Fig. 1C, which shows that with an increase in the film thickness, $\overline{M}_{max}$ varies nonmonotonically, exhibiting very little influence of the channel for both a thick and a thin film. In essence, when the film thickness approaches the channel diameter, the influence is similar to that of adhesion on a fibrillar or patterned surface, whereas for very thick films, adhesion is similar to a smooth surface.

For the films thinner than the one with the maximum torque (~100 μm in Fig. 1C), the channels effectively partition the film into smaller portions, which enhances their compliance and consequent crack blunting, as is also seen in the context of adhesives with surface fibrils (*17*–*19*). To counter this effect of crack blunting, excess energy is required to initiate the crack, which eventually gets dissipated after its propagation. The effect of crack blunting is weaker for thin films but becomes more important with an increase in the film thickness, requiring larger crack-initiation torque. Hence, the maximum crack-initiation torque $\overline{M}_{max}$ increases initially with film thickness h, as shown in Fig. 1C. Beyond a threshold thickness (~100 μm in Fig. 1C), the volume fraction of the channels in the

Department of Chemical Engineering and Department of Science and Technology Unit on Nanoscience, Indian Institute of Technology, Kanpur 208016, India.

*To whom correspondence should be addressed. E-mail: aghatak@iitk.ac.in

film is too small to cause any effective partitioning of the film. Consequently, less torque is now required to initiate the crack from the vicinity of the channel. Finally, the effect of the channel becomes almost nonexistent for a very thick film. This situation prevails irrespective of the vertical position of the channel in the film (fig. S3).

The horizontal spacing s between the channels affects the $\bar{M}_{max}$. Figure 1D shows that for interchannel spacing $s = 3$ mm, the M versus Δ plot is characterized by the intermittent peaks corresponding to the arresting effect of the channels, but for $s = 0.5$ mm the channels are close enough that the effect of each individual channel is no longer felt. However, one sees a constant torque that is still substantially higher than is required to drive the crack over a smooth film. This result is in accordance with observations on surface-patterned adhesives where a constant torque is also observed (*10*, *11*) when the spatial dimensions of the patterns are decreased below a characteristic stress-decay length, $k^{-1} = \left(\frac{Eh}{12\mu}\right)^{\frac{1}{3}}$ (*20*). The later is a material length scale that signifies the distance from the contact line within which the stresses in the film remain concentrated. For the experiment corresponding to Fig. 1D, $D = 0.02$ Nm, $\mu = 1.0$ Mpa, and $h = 120$ μm (where D is the flexural rigidity of the adhering plate, and μ is the shear modulus of the film), and thus threshold distance $k^{-1} = 3.14$ mm. Therefore, the effect of individual channels is not felt when $s \sim k^{-1}$.

We now show that the adhesion is considerably enhanced when the channels are filled with liquids of appropriate surface tension and viscosity. Channels of diameter $d = 50$ to 1090 μm, embedded in elastic films of $h = 90$ to 1500 μm, were filled with silicone oils of viscosity $\eta = 5$ to 50,000 cP and surface tension $\gamma = 22$ mJ/m^2. Although these oils wet the surface of polydimethylsiloxane (PDMS), they do not diffuse into the network of PDMS in the time scale of the experiments (≈10 min). However, being a wetting liquid, the oil results in a negative capillary pressure of magnitude $\Delta p = 4(\gamma_s - \gamma_{sl})/d$ inside the channel and also in the vicinity of its elastic wall; away from the wall, the pressure in the film remains atmospheric. Here, γ_s (~22 mJ/m^2) and γ_{sl} (~0 mJ/m^2) are the surface energy of the PDMS elastomer and the interfacial energy of the elastomer and silicone oil, respectively. This stress field around the channel, resulting from the lateral and vertical asymmetries, effectively leads to a situation similar to that of an elastica under a compressive axial load. This leads to buckling and bulging out of the elastic wall of the channel. Figure 2B depicts the deformation profiles δ at the surface of the films obtained by optically scanning their surface in a direction perpendicular to the orientation of the channels. For thinner films (for example, those with $h = 90$ μm and $d = 50$ μm), the deformation bulges appear as spikes with narrow peaks that do not allow the plate to come in complete contact with the film. However, as h increases, the deformation flattens out, resulting in a complete contact with the contactor. For small deformations (i.e., $\delta/d \ll 1$), the elastic energy of the surface bulge scales as $\sim(\mu/2)(\delta/d)^2(h - d/2)Ld$, where L is the length of the channel. This increased elastic energy is supplied by a fraction of the reduction in the interfacial energy $\sim(\gamma_s - \gamma_{sl})\pi dL$ of the capillary. Equating the two energies yields the following scaling relation for the height of the bulge, $\delta \approx d\sqrt{2\pi\gamma_s/\mu(h - d/2)}$. When we plot the experimental data of δ obtained from various experiments against $d/(h - d/2)^{\frac{1}{2}}$, all of the data fall on a single straight line (Fig. 2C), with the result $\delta = 1.5 \times 10^{-3} d/\sqrt{(h - d/2)}$.

When a flexible plate is peeled off of these thicker films, as in Fig. 1A, we obtain the M versus Δ plots (Fig. 3A) consisting of intermittent peaks that correspond to crack initiations and arrests, similar to the observation shown in Fig. 1B with the use of air-filled channels. However, here the bulging induced compressive stress at the interface plays an important role in enhancing M. Whereas peeling causes tensile stress at the crack front (*10*), the compressive stress in the capillary diminishes it. Consequently, as compared with a film without channels, the plate now has to be lifted more in order to attain the necessary critical stress to drive the crack. Although it is natural to think that viscous dissipation inside the channel should also contribute to the additional torque needed to initiate the crack, experiments with oils show that $\bar{M}_{max}$ does not alter significantly (table S1) when the peeling rate is varied over two orders of magnitude (3 to 300 μm/s). Furthermore, when the liquid viscosity is varied systematically, both $\bar{M}_{max}$ and the adhesion energy increase until an optimum viscosity (100 to 1000 cP) is reached, beyond which they decrease.

The adhesion strength G is obtained by integrating the area under the F versus Δ curve (Fig. 3B). A decline in G for high-viscosity oils may occur because the relaxation time of the high-molecular weight oils can be substantially longer than the time scale in which the crack crosses the channel leading to lower viscous dissipation. Also, high-molecular weight oils would show elastic, rather than viscous, response at short time scales of crack propagation. These observations suggest that the enhancement of torque is mediated not so much by the viscosity of the liquid as by the pressure inside the capillary and the deformability of the film. Both of these aspects were investigated by systematically varying the h and d, while filling them with a viscous liquid. Figure 3C summarizes a typical

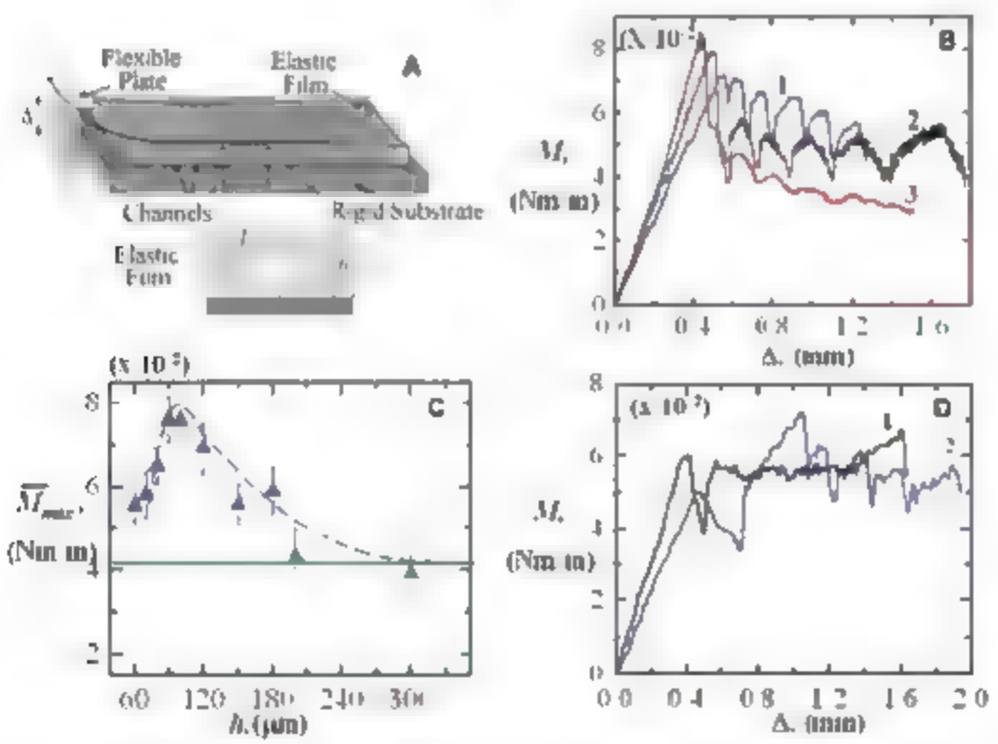

Fig. 1. (**A**) Schematic of the experimental setup where a flexible plate is lifted from its end off of an elastic adhesive layer with embedded microchannels. (**B**) $M = F \cdot a$ is plotted against Δ of the flexible plateCurves 1 to 3 correspond to $h = 80$, 150, and 200 μm, respectively; $\mu = 1.0$ MPa; and $D = 0.02$ Nm. Here, the first peak represents initiation at the sharp edge of the film, and the subsequent peaks capture the effect of each microchannel on peeling. (**C**) Variation of the $\bar{M}_{max}$ with h. The green horizontal line indicates the torque applied on a plate for peeling off of a smooth film, and the dashed line is a guide to the eye. Triangles represent the maximum torque at which the crack initiates, and error bars represent SD. (**D**) The effect of s between the channels on maximum M. Curves 1 and 2 correspond to peeling a flexible plate of $D = 0.02$ Nm off of films having multiple channels placed at $s = 0.5$ and 3 mm apart.

series in which d is kept constant while h is varied. G increases as the skin thickness $t = h - d$ is decreased, except for very small values of t for which G decreases. This implies that maximum enhancement of G is achieved at an intermediate thickness of the film dictated by the liquid pressure inside the channel. A similar set of experiments with channels of different diameters shows that G is optimally enhanced at intermediate ranges of channel diameter (700 to 800 μm) and liquid viscosity (100 to 1000 cP). Figure 3D illustrates a comparison of the optimal microfluidic adhesives with an unstructured adhesive and with a surface-textured adhesive. G increases by one order of magnitude to ~750 mJ/m^2 when the film is embedded with air-filled channels of $d = 710$ μm. This is similar to the performance of a surface-textured adhesive because in this case, d is nearly the same as h. G increases further to 1600 mJ/m^2 when these channels are filled with an oil of intermediate viscosity. This remarkable enhancement in G by about a factor of 25, compared to otherwise similar but smooth adhesives, is achieved without incorporating any viscoelasticity in the adhesive but by simply manipulating the pressure inside the subsurface channels.

We now show that the same elastic layer can be used both as a strong adhesive and an easy-release coating. In this context, the nonmonotonic dependence of G on t, as in Fig. 3C, motivated us to embed two layers of channel within the adhesive at two different vertical locations. When the channels of diameter $d = 50$ μm of the top layer ($t_1 = 120$ μm and $t_2 = 300$ μm) are filled with oil while those at the bottom layer contain air at atmospheric pressure, the deformations at the surface of the film (similar to $h = 90$ μm in Fig. 2B) do not allow the plate to come in contact with the film. The layer then behaves like a release coating. However, when the channels at the bottom layer are filled with oil of $\eta = 380$ cP while those at the top contain air, the peel experiment yields the M versus Δ plot with characteristic peaks at the location of the channels, as shown in Fig. 3E. This result shows that the same film can be used as a strong adhesive and a release coating without altering the intrinsic rheological or surface properties of the film.

In contrast to the known mechanisms of enhancing adhesion by surface patterning, hairy structures, and chemical modifications with sticky molecules, we have presented a mechanism for greatly enhancing and modulating adhesion by embedded subsurface liquid-filled microchannels in an adhesive layer. A spatial segregation of the elastic and viscous domains allows for a clean and reusable separation of the elastic surface, unlike the conventional viscoelastic adhesives. The confined liquid in the microchannels not only leads to viscous dissipation when a crack passes over it but, more importantly, exerts compressive stress on the flexible wall, which causes the formation of bumps on the film surface. These can either diminish or enhance the stress concentration and adhesive energy during separation. Our mecha-

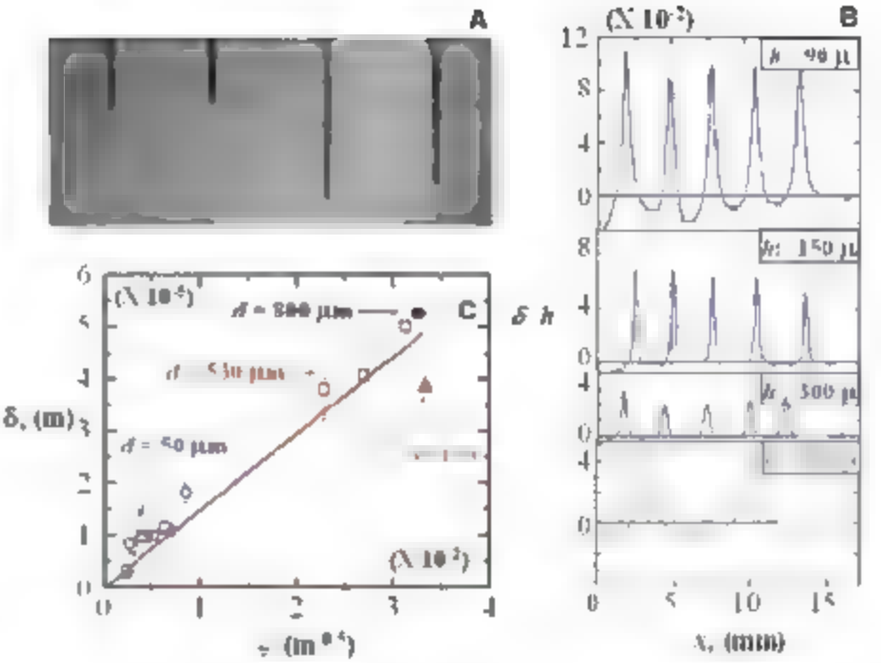

Fig. 2. Surface deformation of the film due to liquid pressure inside channel. **(A)** Top view of a typical adhesive film ($h = 120$ μm, $d = 50$ μm) with embedded channels partially filled with silicone oil of $\eta = 380$ cP. **(B)** Liquid pressure inside the channels deforms the film and creates microscopic ridges of height δ at the surface. The figure shows the dimensionless height δ/h along the direction of propagation of the contact line. **(C)** δ is plotted against the scaled diameter of the channels ζ, where $\zeta = d/(h - d/2)^{1/2}$. Error bars represent SD in δ.

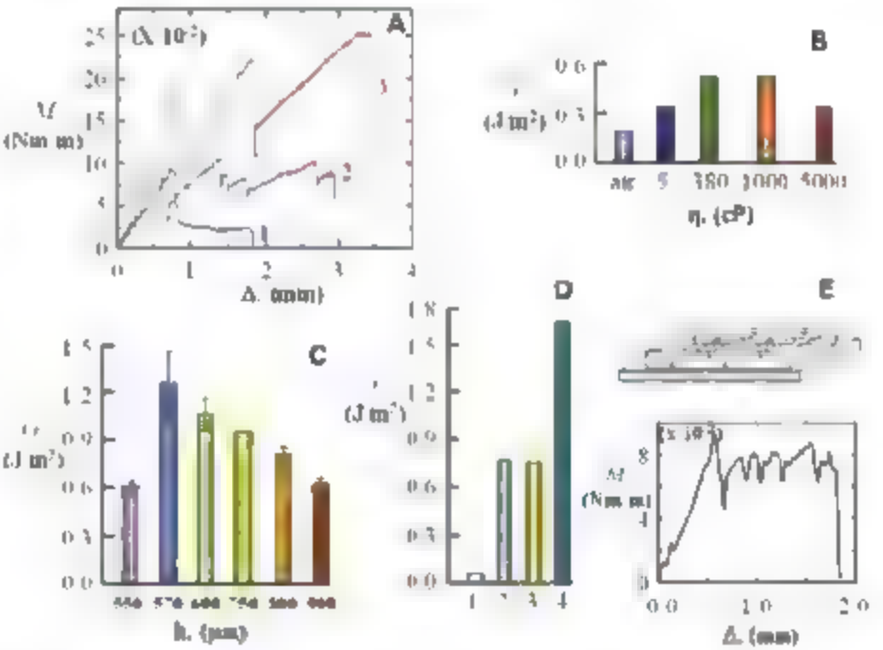

Fig. 3. Peeling off an elastic film with embedded microchannels filled with silicone oil of varying viscosity. **(A)** M versus Δ. Curve 1 corresponds to $h = 300$ mm and $d = 50$ mm for channels filled with air. Curves 2 and 3 correspond to $\eta = 380$ cP, $h = 570$ and 750 μm, and $d = 530$ and 710 μm, respectively. **(B)** Bar chart depicting G when the channels of diameter $d = 50$ μm embedded in film of thickness $h = 300$ μm are filled with air and liquids of different viscosities. **(C)** h is varied systematically while keeping $d = 530$ μm unaltered. The channels are filled with a liquid of $\eta = 380$ cP. Error bars represent SD. **(D)** While on a smooth film (1), the adhesion strength is estimated as $G = 60$ mJ/m^2 [similar to that obtained by Johnson *et al.* (21)]; on an incision-patterned film (2) and on a film of thickness $h = 750$ μm embedded with air-filled channels of diameter $d = 710$ μm (3), G is 750 mJ/m^2. G increases to ~1800 mJ/m^2 when these channels are filled with liquid (4). **(E)** Schematic of an adhesive film embedded with channels arranged in two different layers with skin thicknesses t_1 and t_2, respectively. When the peel experiment is done on this adhesive with the channels of the bottom layer filled with oil while those at the top contain air at atmospheric pressure, the M versus Δ plots are characteristic of crack arrests and initiations at the location of the channels.

nism suggests strategies for the design of more efficient, cleaner, and stimuli-responsive pressure-sensitive adhesives.

References and Notes

1. M. Scherge, S. N. Gorb, *Biological Micro- and Nanotribology: Nature's Solutions* (Springer, Heidelberg, Germany, 2001).
2. R. Spolenak, S. N. Gorb, H. Gao, E. Arzt, *Proc. R. Soc. London Ser. A* **461**, 305 (2005).
3. S. N. Gorb, Y. Jiao, M. J. Scherge, *Comp. Physiol. A* **186**, 821 (2000).
4. S. N. Gorb *et al.*, *Nature* **443**, 407 (2006).
5. C. Creton, S. N. Gorb, *MRS Bull.* **32**, 466 (2007).
6. J. M. Smith, W. J. P. Barnes, J. R. Downie, G. D. Ruxton, *J. Comp. Physiol. A* **192**, 1193 (2006).
7. K. Autumn *et al.*, *Nature* **405**, 681 (2000).
8. W. R. Hansen, K. Autumn, *Proc. Natl. Acad. Sci. U.S.A.* **102**, 385 (2005).
9. A. K. Geim *et al.*, *Nat. Mater.* **2**, 461 (2003).
10. A. Ghatak, L. Mahadevan, J. Chun, M. K. Chaudhury, V. Shenoy, *Proc. R. Soc. London Ser. A* **460**, 2725 (2004).
11. J. Y. Chung, M. K. Chaudhury, *J. R. Soc. Interface* **2**, 55 (2005).
12. T. Thomas, A. J. Crosby, *J. Adhes.* **82**, 311 (2006).
13. A. J. Crosby, M. Hageman, A. Duncan, *Langmuir* **21**, 11738 (2005).
14. H. Lee, B. P. Lee, P. B. Messersmith, *Nature* **448**, 338 (2007).
15. M. K. S. Verma, A. Majumder, A. Ghatak, *Langmuir* **22**, 10291 (2006).
16. Materials and methods are available as supporting material on *Science* Online.
17. A. Jagota, S. J. Bennison, *Int. Comp. Biol.* **42**, 1140 (2002).
18. M. J. Glassmaker, A. Jagota, C. Y. Hui, J. Kim, *J. R. Soc. Interface* **1**, 23 (2004).
19. M. J. Glassmaker, A. Jagota, C. Y. Hui, *Acta Biomater.* **1**, 367 (2005).
20. A. Ghatak, L. Mahadevan, M. K. Chaudhury, *Langmuir* **21**, 1277 (2005).
21. K. L. Johnson, K. Kendall, A. D. Roberts, *Proc. R. Soc. London Ser. A* **324**, 301 (1971).

22. A.G. acknowledges the research initiation grant of the Indian Institute of Technology, Kanpur (IITK/CHE/20040307) and the research grant of the Department of Science and Technology, India (DST/CHE/20050259) for this work.

Supporting Online Material

www.sciencemag.org/cgi/content/full/318/5848/258/DC1
Materials and Methods
SOM Text
Figs. S1 to S5
Table S1
References

30 May 2007; accepted 28 August 2007
10.1126/science.1145839

FKF1 and GIGANTEA Complex Formation Is Required for Day-Length Measurement in *Arabidopsis*

Mariko Sawa, Dmitri A. Nusinow, Steve A. Kay, Takato Imaizumi*

Precise timing of *CONSTANS* (*CO*) gene expression is necessary for day-length discrimination for photoperiodic flowering. The FLAVIN-BINDING, KELCH REPEAT, F-BOX 1 (FKF1), and GIGANTEA (GI) proteins regulate *CO* transcription in *Arabidopsis*. We demonstrate that FKF1 and GI proteins form a complex in a blue-light–dependent manner. The timing of this interaction regulates the timing of daytime *CO* expression. FKF1 function is dependent on GI, which interacts with a *CO* repressor, CYCLING DOF FACTOR 1 (CDF1), and controls CDF1 stability. GI, FKF1, and CDF1 proteins associate with *CO* chromatin. Thus, the FKF1-GI complex forms on the *CO* promoter in late afternoon to regulate *CO* expression, providing a mechanistic view of how the coincidence of light with circadian timing regulates photoperiodic flowering.

Many plants monitor seasonal changes in day length to regulate flowering time for successful reproduction (*1*). In *Arabidopsis*, regulation of daytime *CO* expression is the primary process of time measurement in the photoperiodic flowering pathway (*2*, *3*). FKF1 and GI proteins positively regulate *CO* transcription (*4*, *5*). *FKF1* and *GI* gene expression has similar diurnal patterns (*5*, *6*), which implies that these proteins may interact to regulate *CO*. We tested their direct interaction in yeast and found that FKF1 interacts with GI (Fig. 1A). Our results, obtained using truncated FKF1 proteins, suggest that this interaction occurs through the FKF1 LOV (Light, Oxygen, or Voltage) domain (Fig. 1A). In addition, the GI N terminus was sufficient to interact with FKF1 (fig. S1).

To assess whether this interaction occurs in vivo, and whether it is modulated by photoperiod or light conditions, we generated transgenic plants constitutively expressing both haemagglutinin (HA)–tagged FKF1 (HA-FKF1) and tandem affinity purification (TAP)–tagged GI (GI-TAP) proteins [*35S::HA-FKF1* / *35S::GI-TAP* lines (*7*)] for coimmunoprecipitation experiments. In the *35S::HA-FKF1* / *35S::GI-TAP* #18 / *fkf1* line, a similar amount of GI-TAP protein was precipitated at every time point in both long-day (16 hours light and 8 hours dark) and short-day (8 hours light and 16 hours dark) conditions (Fig. 1, B and C). HA-FKF1 protein was coimmunoprecipitated with GI-TAP protein (Fig. 1, B and C), demonstrating that GI-TAP and HA-FKF1 proteins form a complex in vivo. In both day-length conditions, the amount of coimmunoprecipitated HA-FKF1 protein increased until 4 hours after light onset, remained constant for the rest of day, and declined in the dark (Fig. 1, B and C), which suggests that light or the circadian clock modulate the FKF1 and GI interaction.

We therefore analyzed the interaction in dark-grown samples. A minimal amount of HA-FKF1 was coimmunoprecipitated with GI-TAP protein in the dark (Fig. 1D), indicating that this interaction is light dependent. In addition, as little as 10 min of light exposure resulted in a marked increase in the amount of FKF1 and GI interaction (fig. S2).

Next we analyzed how light quality (wavelength) affects this interaction. Similar amounts of FKF1 and GI interacted in blue-light irradiated samples (Fig. 1E) compared with white-light grown samples, but little interaction was observed in red-light irradiated samples (Fig. 1E), indicating that blue light induces this interaction. Further analysis revealed that the FKF1 and GI interaction is fluence rate dependent (Fig. 1F).

Because we have shown that the FKF1 LOV domain can absorb blue light (*5*), we postulated that the LOV domain may function as a blue-light-sensing domain for this interaction. We first tested whether FKF1 and GI proteins by themselves are sufficient to reconstitute the light-dependent interaction in vitro (*7*). FKF1-HA protein was copurified with the glutathione S-transferase–fused GI N terminus (GST-GI-N) protein incubated under light (Fig. 1G). We then analyzed the importance of the FKF1 LOV domain for light-induced interaction with GI by using FKF1 LOV variants containing three different photochemically blind mutations [C91A, R92D, and Q163L (*8*–*11*)]. All three blind mutations attenuated the light-dependent interaction (fig. S3). These results suggest that FKF1 controls the interaction with GI by absorbing blue light through the LOV domain.

To determine more accurately when this interaction occurs in vivo, we performed immunoprecipitation analysis using a transgenic line [*FKF1::HA-FKF1 GI::GI-TAP* / *fkf1 gi-2* (*7*)] in which both tagged *FKF1* and *GI* expression are regulated by endogenous promoters (fig. S4). Under long-day and short-day conditions, GI-TAP protein was expressed throughout the day with an afternoon peak, whereas HA-FKF1 expression largely occurred in the late afternoon (Fig. 2, A and B) (*5*, *12*). In long days, the peak expression of FKF1 and GI proteins coincided (Fig. 2A). The HA-FKF1 and GI-TAP interaction was observed in the late afternoon (Fig. 2A), when daytime *CO* expression occurs (Fig. 2E) (*4*, *13*). In short days, HA-FKF1 peaked about 3 hours later than the GI-TAP peak expression,

Department of Biochemistry, The Scripps Research Institute, 10550 North Torrey Pines Road, La Jolla, CA 92037, USA.

Present address: Division of Biological Sciences, University of California, San Diego, 9800 Gilman Drive #0130, La Jolla, CA 92093–0116, USA.

*To whom correspondence should be addressed. E-mail: timaizumi@ucsd.edu

and the FKF1 and GI interaction occurred only at the beginning of the FKF1 expression period (Fig. 2B).

When day-length shifts from short to long, daytime *CO* is immediately induced (*5*, *14*), and FKF1 is involved in this induction (*5*). We therefore examined the FKF1 and GI interaction under day-length shift conditions. On the day when conditions were switched from short to long, the expression patterns of HA-FKF1 and GI-TAP were similar to those on short days (Fig. 2C). However, the interaction between FKF1 and GI occurred throughout the extended light period (Fig. 2C). Our results show that the duration of the FKF1 and GI interaction seems to coincide with the pattern of daytime *CO* expression.

As our results indicate that FKF1 and GI may form a complex to regulate *CO* expression, we studied the importance of this interaction. We first examined whether FKF1 regulates GI protein stability, because FKF1 mediates protein degradation (*15*). The *fkf1* mutation did not alter the expression patterns of GI-TAP proteins (fig. S5), indicating that FKF1 does not regulate GI protein stability. We then studied the genetic relation between *FKF1* and *GI*. Both *fkf1* and *gi* mutants showed a late-flowering phenotype in long days, and the *gi* flowering phenotype was more severe (Fig. 2D). The flowering phenotype of the *fkf1 gi* double mutant in long days and short days resembled that of the *gi* mutant (Fig. 2D). Expression of *CO* in the *fkf1 gi* mutant in long days is also similar to that in the *gi* mutant (Fig. 2E). When the *gi* mutation was introduced into the *35S. HA-FKF1* #10 / *fkf1* line, the *gi-2 35S. HA-FKF1* #10 / *fkf1* line showed a strong late-flowering phenotype in long days, which is similar to the *gi* flowering phenotype (Fig. 2D). *CO* expression in the *gi-2 35S. HA-FKF1* #10 / *fkf1* line also resembled that in the *gi* mutant in long days (fig. S6). These results indicate that FKF1 function is largely dependent on GI function. In contrast, when the *fkf1* mutation was introduced in the *35S. GI-TAP / gi-2* line, the *fkf1 35S. GI-TAP / gi-2* plant flowered slightly later than the *35S. GI-TAP / gi-2* line but much earlier than the *fkf1* mutant (Fig. 2D), which indicates that GI function is not completely dependent on FKF1 function. This suggests that GI may regulate not only FKF1 activity but also the function of other proteins that play additional roles in the photoperiodic flowering pathway.

Timing of the circadian-regulated expression of FKF1 and/or GI is thought to be important for the timing of daytime *CO* expression (*5*, *16*). If this assumption were correct, then constitutive expression of either FKF1 or GI would abolish the day-length measurement ability of plants. However, at least in the Col wild-type accession, lines overexpressing either FKF1 or GI retained the ability to discriminate differences in day length (Fig. 2D) (*12*). This result suggests that, in the Col accession, FKF1 and GI expression alone may not be sufficient for regulating photoperiodic flowering responses. On the basis of our results that FKF1 and GI form a complex in vivo and that FKF1 function likely depends on GI function, we postulated that the timing of the FKF1-GI complex formation might constitute the time-measurement mechanism itself.

To test this hypothesis, we analyzed the flowering phenotype of two independent *35S. HA-FKF1 35S. GI-TAP / fkf1* lines (figs. S7 and S8) and the *35S. HA-FKF1 35S. HA-GI / fkf1 gi-2* line in long days and short days. All the *FKF1* and *GI* double overexpressing lines examined flowered at almost the same time in both day-length conditions (Fig. 2D and fig. S9). In the *35S. HA-FKF1 35S. GI-TAP / fkf1* lines, *CO* was expressed constantly during the day at a similar level to the daytime *CO* peak observed in wild-type plants in long days (Fig. 2F and fig. S8). In short days, *CO* expression in these lines was higher than that in wild-type plants in the daytime (Fig. 2G and fig. S8). These results indicate that FKF1-GI complex formation regulates the timing of daytime *CO* transcription.

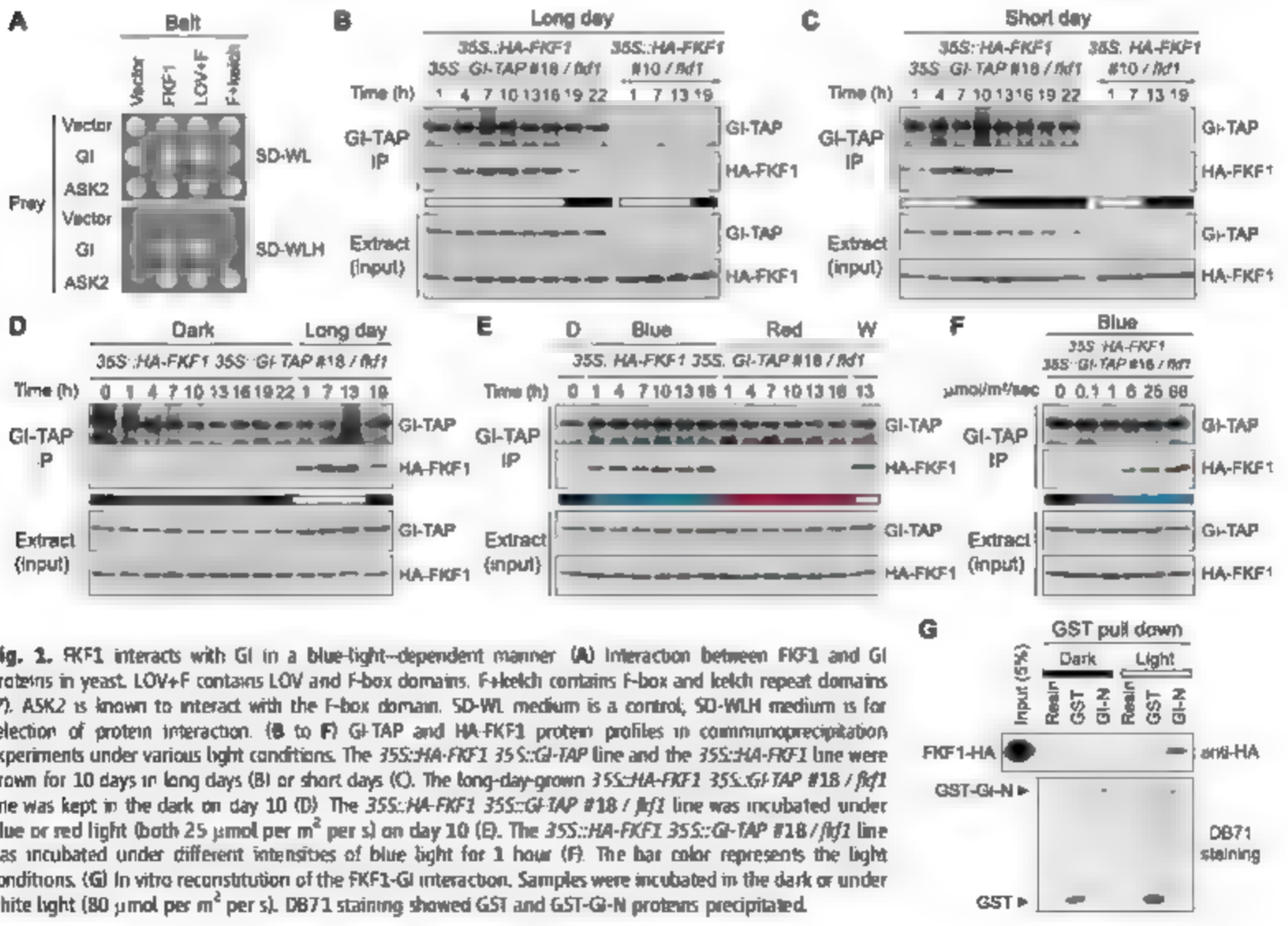

Fig. 1. FKF1 interacts with GI in a blue-light–dependent manner. (**A**) Interaction between FKF1 and GI proteins in yeast. LOV+F contains LOV and F-box domains. F+kelch contains F-box and kelch repeat domains (*7*). ASK2 is known to interact with the F-box domain. SD-WL medium is a control; SD-WLH medium is for selection of protein interaction. (**B** to **F**) GI-TAP and HA-FKF1 protein profiles in coimmunoprecipitation experiments under various light conditions. The *35S::HA-FKF1 35S::GI-TAP* line and the *35S::HA-FKF1* line were grown for 10 days in long days (B) or short days (C). The long-day-grown *35S::HA-FKF1 35S::GI-TAP #18 / fkf1* line was kept in the dark on day 10 (D). The *35S::HA-FKF1 35S::GI-TAP #18 / fkf1* line was incubated under blue or red light (both 25 µmol per m^2 per s) on day 10 (E). The *35S::HA-FKF1 35S::GI-TAP #18 / fkf1* line was incubated under different intensities of blue light for 1 hour (F). The bar color represents the light conditions. (**G**) In vitro reconstitution of the FKF1-GI interaction. Samples were incubated in the dark or under white light (80 µmol per m^2 per s). DB71 staining showed GST and GST-GI-N proteins precipitated.

Even though *CO* expression in these lines was constantly high in the daytime in both day-length conditions, *FT* expression was not constant (figs. S7 and S8). *FT* expression in the double overexpressors showed two distinct peaks in long days (figs. S7 and S8). This might be explained by the posttranscriptional regulation of CO protein (*17*). We observed daytime *FT* expression in the double overexpressors in short days (figs. S7 and S8). This may cause early flowering of these lines in short days.

Our results suggest that FKF1 function is mainly GI dependent and that the FKF1-GI complex regulates daytime *CO* gene expression. One of the mechanisms by which FKF1 regulates *CO* transcription is by degrading its repressor, CDF1 (*15*). We therefore explored the possibility that the FKF1-GI complex may be involved in this regulation. First, we tested whether the FKF1-GI complex contains CDF1. As the FKF1 and CDF1 interaction has been shown (*15*), we analyzed the possible interaction between CDF1 and GI. CDF1 interacted with the GI N terminus, the same fragment that interacted with FKF1, in yeast and in vitro (fig. S10). In plant materials harvested in the morning, HA-CDF1 was coimmunoprecipitated with GI-TAP (Fig. 3A).

Considering FKF1 functional dependence on GI, these data led us to predict that CDF1 protein may be stable in the *gi* mutant as a result of the loss of FKF1 activity. Therefore, we analyzed the CDF1 protein levels in *35S::HA-CDF1* lines (*15*) with or without the *gi* mutation. In the *35S::HA-CDF1* #17 line, the HA-CDF1 protein levels declined between 13 and 19 hours after light onset (Fig. 3B). In the *gi-2 35S::HA-CDF1* #17 line, HA-CDF1 expression did not change even at the end of the day (Fig. 3B), indicating that GI is involved in the regulation of FKF1-dependent CDF1 protein stability.

We also tested whether GI regulates CDF1 function using a transient expression system (*15*). The CDF1-VP64 (CDF1 fusion with transcriptional activation domains) increased the activity of luciferase regulated by the *CO* promoter in wild-type plants and *gi-2* mutants (fig. S11), suggesting that GI does not modulate the CDF1 DNA binding ability. This implies that in the *gi* mutants endogenous CDF1 may be stable even in late afternoon and participate in *CO* repression.

As GI binds to CDF1 in vivo, then GI might be present at the *CO* promoter. To investigate this possibility, we performed a chromatin immunoprecipitation (ChIP) analysis using *GI::GI-TAP / gi-2* plants. We analyzed the GI-TAP specific enrichment of 17 different amplicons with locations almost evenly distributed along the *CO* gene region (Fig. 3D) by quantitative polymerase chain reaction (Q-PCR) (*7*). In the *CO* promoter, the amplicon 4 region was the most highly enriched, and ampli-

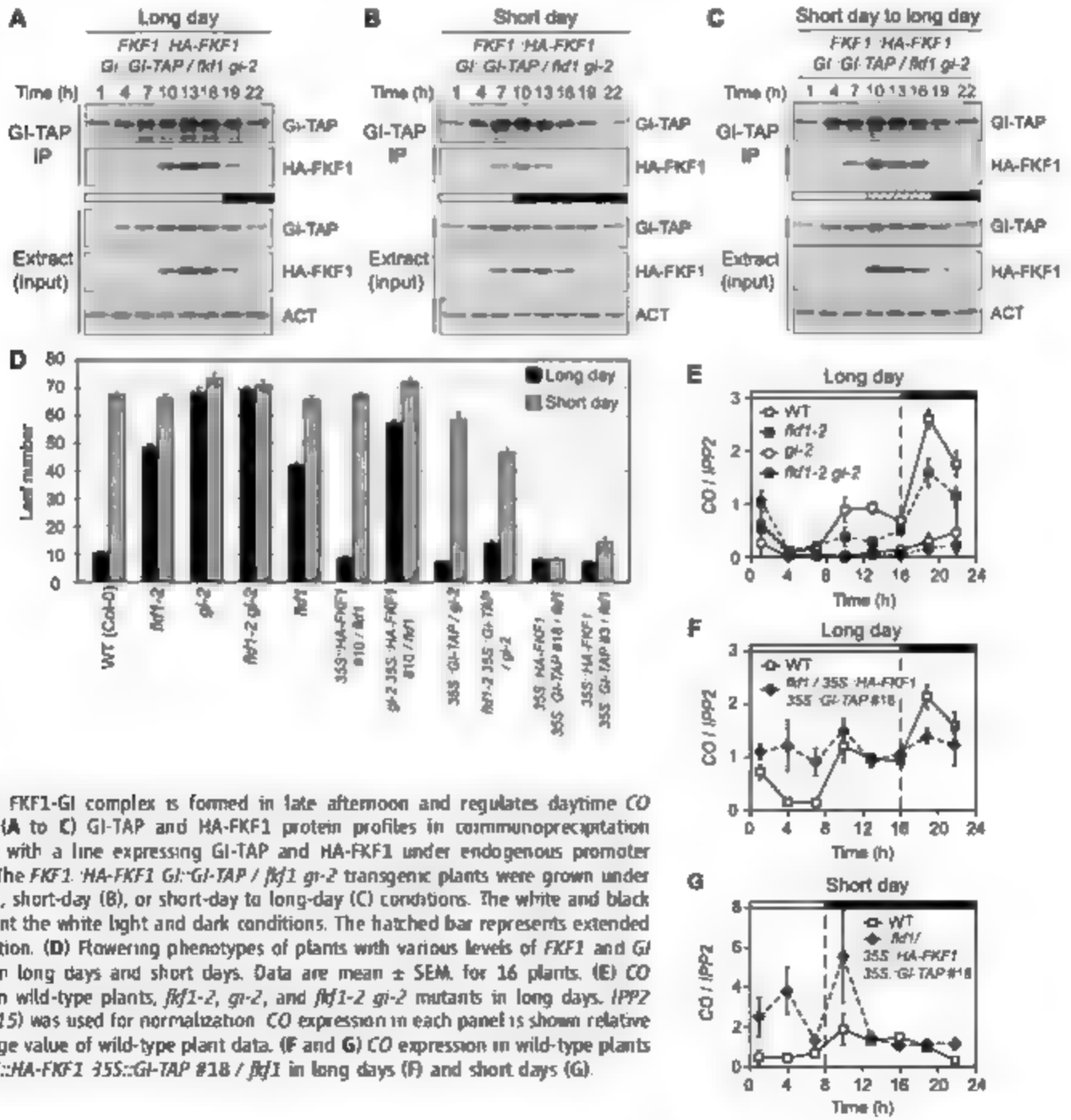

Fig. 2. The FKF1-GI complex is formed in late afternoon and regulates daytime *CO* expression. (**A** to **C**) GI-TAP and HA-FKF1 protein profiles in coimmunoprecipitation experiments with a line expressing GI-TAP and HA-FKF1 under endogenous promoter regulation. The *FKF1::HA-FKF1 GI::GI-TAP / fkf1 gi-2* transgenic plants were grown under long-day (A), short-day (B), or short-day to long-day (C) conditions. The white and black bars represent the white light and dark conditions. The hatched bar represents extended light incubation. (**D**) Flowering phenotypes of plants with various levels of *FKF1* and *GI* expression in long days and short days. Data are mean ± SEM. for 16 plants. (**E**) *CO* expression in wild-type plants, *fkf1-2*, *gi-2*, and *fkf1-2 gi-2* mutants in long days. *IPP2* expression (*15*) was used for normalization. *CO* expression in each panel is shown relative to the average value of wild-type plant data. (**F** and **G**) *CO* expression in wild-type plants and the *35S::HA-FKF1 35S::GI-TAP #18 / fkf1* in long days (F) and short days (G).

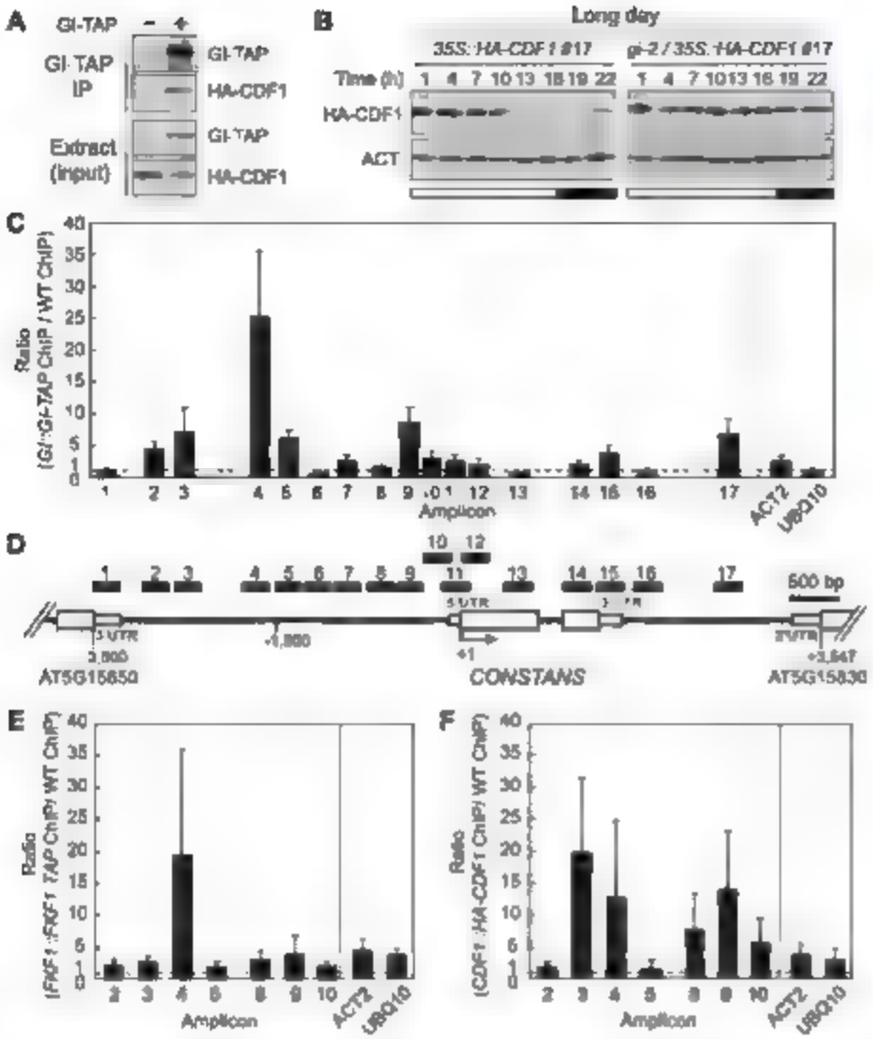

Fig. 3. GI-FKF1-CDF1 complex associates with *CO* promoter in vivo. **(A)** In vivo interaction between HA-CDF1 and GI-TAP. The *35S::HA-CDF1* #17 (GI-TAP-) and *35S::GI-TAP 35S::HA-CDF1* #17 (GI-TAP+) lines were grown in long days and harvested 4 hours after light onset on day 10, when coimmunoprecipitation assays were performed (*7*). **(B)** HA-CDF1 expression in the *35S::HA-CDF1* and *gi-2 35S::HA-CDF1* lines. Plants were harvested at day 10 in long days. Actin (ACT) was used as a loading control. **(C)** *CO* chromatin regions associated with GI-TAP protein. Plants were harvested 13 hours after light onset on day 10. The ratio between the specific enrichment value in the *GI::GI-TAP* sample and that in the wild-type sample on each amplicon was calculated from seven independent ChIP analyses (*7*). *ACT2* and *UBQ10* genes were used as controls. The dotted line indicates no enrichment. **(D)** Schematic drawing of the *CO* locus and the amplicon locations for ChIP analysis. The 17 amplicon locations are shown. White and light gray boxes represent exons and 5′- and 3′-untranslated regions (UTR). **(E** and **F)** *CO* promoter regions associated with FKF1-TAP and HA-CDF1 proteins. Plants were harvested 13 hours [FKF1-TAP (E)] and 4 hours [HA-CDF1 (F)] after light onset on day 10. Data were calculated from four independent analyses.

cons 3 and 9 also showed significant enrichment (Fig. 3C). This indicates that GI-TAP protein associates with these *CO* promoter regions.

We further investigated whether both FKF1 and CDF1 associate with the same *CO* regions where GI-TAP protein interacts. We used *FKF1 FKF1-TAP / fkf1* (*5*) and *CDF1 HA-CDF1* #19 (*15*) lines for the ChIP assays and analyzed the amounts of specific chromatin enrichment around amplicons 3, 4, and 9. Amplicon 4 was enriched in the *FKF1 FKF1-TAP / fkf1* samples harvested at the same time as the *GI::GI-TAP / gi-2* samples (Fig. 3E), indicating that both FKF1 and GI associate with this *CO* promoter region. Amplicons 3, 4, and 9 were all enriched in the *CDF1 HA-CDF1* samples harvested in the morning (Fig. 3F). Together with the in vivo GI and CDF1 interaction results, and because CDF1 peak expression occurs before the GI peak (*12*, *15*), GI might interact with CDF1 that has already bound to the *CO* promoter in the morning. Once FKF1 interacts with the GI-CDF1 complex in the afternoon, FKF1 might degrade CDF1 to release the repression of *CO*.

We have shown that FKF1 and GI form a complex in vivo, and that this interaction is induced by blue light absorbed by the LOV domain, verifying our previous proposal that FKF1 is a blue-light photoreceptor (*5*). In addition, our results indicate that the timing of FKF1-GI complex formation, which is controlled by both circadian regulation of FKF1 and GI expression and light induction of FKF1 and GI interaction, can regulate the timing of daytime *CO* expression (Fig. 4). Moreover, our results suggest that the FKF1-GI complex directly regulates CDF1 stability in the afternoon and that the FKF1-GI-CDF1 complex forms on the promoter region of the *CO* gene. This is likely to be a part of the molecular mechanism by which the FKF1-GI complex controls daytime *CO* transcription. Thus, we have uncovered the principal molecular mechanism that enables plants to distinguish seasonal differences in day length. In conjunction with posttranscriptional regulation of CO protein (*17*), this regulation could enable plants to select the most favorable season for successful flowering.

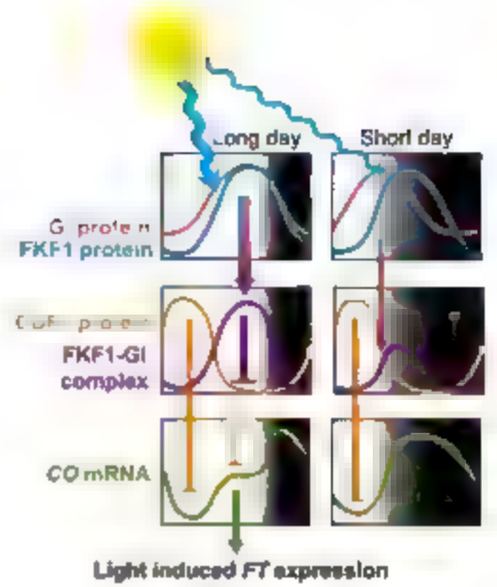

Fig. 4. A model of day-length–dependent *CO* transcriptional regulation. In long days, the circadian-regulated coincidence of FKF1 and GI peak expression and the light-induced FKF1 interaction with GI enable the formation of the FKF1-GI complex in late afternoon. When the complex is formed on the *CO* promoter, CDF1 associated with GI is degraded by FKF1 to facilitate the induction of daytime *CO* expression. Then CO protein is stabilized and activated by light to induce *FT* expression (*13*, *17*). In short days, FKF1 peaks in the dark at a different time than GI, thus, only a small quantity of the complex forms.

References and Notes

1. J. A. Zeevaart, *Plant Cell* **18**, 1783 (2006).
2. T. Imaizumi, S. A. Kay, *Trends Plant Sci.* **11**, 550 (2006).
3. L. Corbesier, G. Coupland, *J. Exp. Bot.* **57**, 3395 (2006).
4. P. Suárez-López *et al.*, *Nature* **410**, 1116 (2001).
5. T. Imaizumi, H. G. Tran, T. E. Swartz, W. R. Briggs, S. A. Kay, *Nature* **426**, 302 (2003).
6. S. Fowler *et al.*, *EMBO J.* **18**, 4679 (1999).
7. Materials and methods are available as supporting material on *Science* Online.
8. M. Salomon, J. M. Christie, E. Knieb, U. Lempert, W. R. Briggs, *Biochemistry* **39**, 9401 (2000).
9. S. Crosson, S. Rajagopal, K. Moffat, *Biochemistry* **42**, 2 (2003).
10. D. Nozaki *et al.*, *Biochemistry* **43**, 8373 (2004).
11. B. O. Zoltowski *et al.*, *Science* **316**, 1054 (2007).
12. K. M. David, U. Armbruster, N. Tama, J. Putterill, *FEBS Lett.* **580**, 1193 (2006).
13. M. J. Yanovsky, S. A. Kay, *Nature* **419**, 308 (2002).
14. A. Yamaguchi, Y. Kobayashi, K. Goto, M. Abe, T. Araki, *Plant Cell Physiol.* **46**, 1175 (2005).

15. T. Imaizumi, T. F. Schultz, F. G. Harmon, L. A. Ho, S. A. Kay, *Science* **309**, 293 (2005).
16. T. Mizoguchi *et al.*, *Plant Cell* **17**, 2255 (2005).
17. F. Valverde *et al.*, *Science* **303**, 1003 (2004).
18. We thank L. Pettigrew, E. Hamilton, E. Farré, G. Breton, S. Hazen, J. Pruneda-Paz, and D. Welsh for critical reading of the manuscript; M. Nakayama for pASGW-attR and pACEGW-attR plasmids; and J. Putterill for *35S::HA-GI*, *35S::GI-TAP*, and *GI::GI-TAP* lines and *GI* expression constructs. This work was supported by NIH grants to S.A.K. (GM056006 and GM067837) and T.I. (GM079721). This is manuscript number 18992 of the Scripps Research Institute.

Supporting Online Material
www.sciencemag.org/cgi/content/full/1146994/DC1
Materials and Methods
Figs. S1 to S11
References

25 June 2007; accepted 28 August 2007
Published online 13 September 2007;
10.1126/science.1146994
Include this information when citing this paper.

Lyso-Phosphatidylcholine Is a Signal in the Arbuscular Mycorrhizal Symbiosis

David Drissner,[1] Gernot Kunze,[1] Nico Callewaert,[2,3] Peter Gehrig,[4] M'Barek Tamasloukht,[1] Thomas Boller,[5] Georg Felix,[5] Nikolaus Amrhein,[6] Marcel Bucher[1,7]*

The arbuscular mycorrhizal (AM) symbiosis represents the most widely distributed mutualistic root symbiosis. We report that root extracts of mycorrhizal plants contain a lipophilic signal capable of inducing the phosphate transporter genes *StPT3* and *StPT4* of potato (*Solanum tuberosum* L.), genes that are specifically induced in roots colonized by AM fungi. The same signal caused rapid extracellular alkalinization in suspension-cultured tomato (*Solanum lycopersicum* L.) cells and induction of the mycorrhiza-specific phosphate transporter gene *LePT4* in these cells. The active principle was characterized as the lysolipid lyso-phosphatidylcholine (LPC) via a combination of gene expression studies, alkalinization assays in cell cultures, and chromatographic and mass spectrometric analyses. Our results highlight the importance of lysophospholipids as signals in plants and in particular in the AM symbiosis.

The AM symbiosis is thought to have facilitated plant colonization of land more than 400 million years ago, and today 80% of terrestrial plant species are colonized by AM fungi. In the AM symbiosis, fungal hyphae form coiled or ramified structures in root cortical cells of the host plant. Despite intracellular accommodation of the microsymbiont, the symbiotic partners remain separated by their plasma membranes, which thus demarcate the symbiotic interface, that is, the site of bidirectional exchange of compounds including signals and nutrients. Phosphorus (P) is taken up by plants as orthophosphate (Pi) via two pathways: the direct uptake pathway, at the level of the root-soil interface including root hair cells, as opposed to the mycorrhizal uptake pathway, extending from extraradical fungal hyphae to the cortical cells harboring fungal symbiotic structures. A detailed analysis of the contribution of the mycorrhizal Pi uptake pathway indicated that this pathway can dominate Pi supply to plants irrespective of whether plants forming AM symbioses exhibited improved growth and/or total P uptake (*1*). Mycorrhiza-inducible phosphate transporters have been found in several plant species and are likely to play a prominent role in growth and development of >200,000 plant species forming AM symbioses (*2*–*4*). A 5′ upstream untranslated region of 1.7 kb (herein referred to as *StPT3* promoter) of the gene encoding the mycorrhiza-inducible high-affinity Pi transporter StPT3 from potato (*5*) was recently shown to be activated in different plant species exclusively by fungi of the phylum Glomeromycota (*6*). This is consistent with a model in which the signaling pathway leading to the induction of mycorrhizal Pi transporters in the plant is evolutionarily conserved. To identify such signal compounds involved in *StPT3* gene regulation, we analyzed extracts from mycorrhized roots for their potential to trigger *StPT3* promoter activation

[1]Institute of Plant Sciences, Eidgenössische Technische Hochschule (ETH) Zurich, Experimental Station Eschikon 33, 8315 Lindau, Switzerland. [2]Zurich Glycomics Initiative, ETH Zurich, Wolfgang-Pauli-Strasse 10, 8093 Zurich, Switzerland. [3]Department for Molecular Biomedical Research, VIB, and Department for Biochemistry, Physiology, and Microbiology, Ghent University, B-9000 Ghent, Belgium. [4]Functional Genomics Center Zurich, University of Zurich, and ETH Zurich, CH-8057 Zurich, Switzerland. [5]Institute of Botany, University of Basel, Hebelstrasse 1, 4056 Basel, Switzerland. [6]Institute of Plant Sciences, ETH Zurich, Universitätstrasse 2, 8092 Zurich, Switzerland. [7]Institute of Botany, University of Cologne, Gyrhofstrasse 15, 50931 Cologne, Germany.
*To whom correspondence should be addressed. E-mail: m.bucher@uni-koeln.de

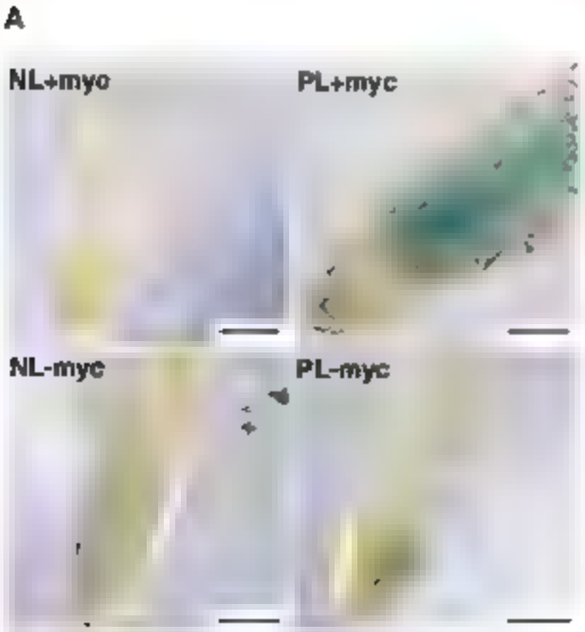

Fig. 1. Induction of phosphate transporter gene in roots treated with phospholipid extracts from mycorrhized roots. (**A**) Neutral lipids (NLs) and phospholipids (PLs) from mycorrhized (+myc) and nonmycorrhized (−myc) roots of plantain were applied to potato plants containing a chimeric gene consisting of a GUS reporter gene under the control of the *StPT3* promoter. Roots were stained for GUS after 3 hours of treatment with the lipids. Scale bars indicate 100 μm. (**B**) RT-PCR performed on RNA from potato roots after 3-hour treatment with PL−myc or PL+myc as indicated. RNA from untreated roots (N.T.) or roots treated with solvent (Solv.) were used as controls. Gene-specific primers for *StPT1*, *StPT3*, and *StPT4* were used. Non–reverse-transcribed RNA samples (−RT) did not give rise to amplification of cDNA, indicating absence of genomic DNA in the PCR templates. Shown is the inverted picture.

in a bioassay based on transgenic potato roots carrying the *StPT3* promoter-β-glucuronidase (GUS) reporter gene construct (*5*).

Infiltration of phospholipid (PL) extracts from mycorrhized roots (PL+myc) of plantain (*Plantago lanceolata* L.) caused *StPT3* promoter activation, as evident from positive GUS staining of transgenic roots; corresponding extracts from nonmycorrhized roots (PL−myc) failed to activate the *StPT3* promoter (Fig. 1A). GUS staining was absent on infiltration of neutral lipid fractions (NL+myc and NL−myc). Induction of GUS in transgenic potato roots was observed with PL+myc extracts from different plant species, including plantain, potato, and maize (*Zea mays* L.), but did not develop when PLs from nonmycorrhized roots of these species were applied (table S1). Moreover, PL extracts from AM fungal material, such as dormant spores, germinated mycelium, presymbiotic mycelium, or extraradical hyphae, were inactive (table S1). GUS staining was detected in roots treated with bioactive PL preparations, predominantly in the zone behind the root tip (Fig. 1A), which is the zone of AM fungal colonization. To verify induction of mycorrhiza-inducible phosphate transporter genes, we performed reverse transcription polymerase chain reaction (RT-PCR) with RNA from potato roots treated with PL−myc or PL+myc from plantain roots. Transcripts encoding the two inducible phosphate transporters StPT3 and non-orthologous StPT4 accumulated specifically after infiltration of PL+myc, whereas the level of constitutively expressed and AM-nonresponsive *StPT1* (*6*) transcripts remained constant (Fig. 1B). Overall, these results indicate the presence of signals in PL+myc extracts that can specifically activate mycorrhiza-specific transporter gene expression.

In previous work, undifferentiated suspension-cultured plant cells proved useful to identify and characterize signals derived from both plant pathogens and symbionts (*7*, *8*). The cells respond to these signals with rapid, characteristic changes in ion fluxes across their plasma membrane, which result in a change in the extracellular pH. We used suspension-cultured tomato cells to study their response to root lipid (L) and PL extracts. Rapid extracellular alkalinization was observed upon treatment of cells with L+myc and PL+myc extracts, whereas equivalent extracts from nonmycorrhized roots failed to evoke a rise in extracellular pH (fig. S1 and Fig. 2A). Alkalinization was dose-dependent and saturable (fig. S2) and resembled the response of these cells to microbial elicitors, as exemplified for the bacterial pathogen-associated molecular pattern (PAMP) flg22 (fig. S1 and Fig. 2A). However, the L+myc and PL+myc preparations did not induce Ca influx in these cells (fig. S3A), nor did the PL+myc and PL−myc preparations induce production of reactive oxygen species (ROS) in plant leaves (fig. S3B), two other responses typically observed after treatment with known elicitors like flg22. Instead, tomato cells responded with the accumulation of transcripts encoding LePT4 when treated with PL+myc but not with PL−myc (Fig. 2B). LePT4 is a phosphate transporter from tomato that is normally induced by AM fungal colonization of cortex cells and is orthologous to StPT4 (*9*). This induction of a normally mycorrhiza-specific gene prompted us to further use medium alkalinization in cultured tomato cells as a rapid and reliable assay

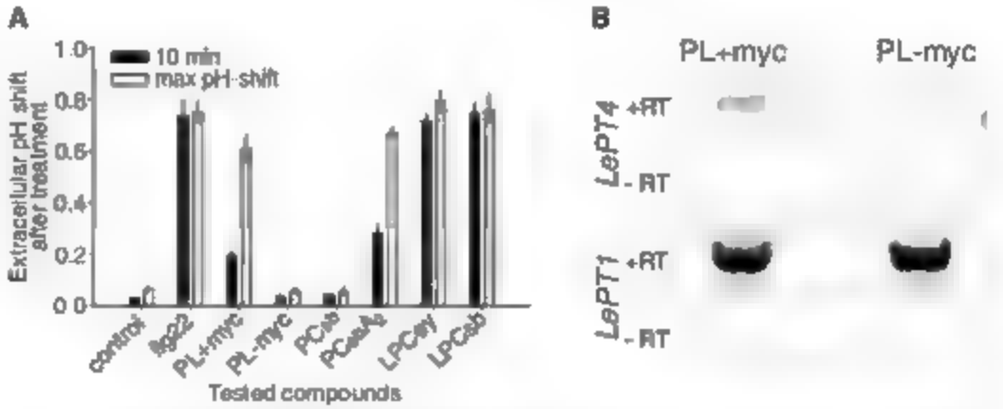

Fig. 2. Effects of lipid extracts on suspension-cultured tomato cells. (**A**) Shift in extracellular pH after 10 min of treatment or at the pH maximum reached within ~35 min of treatment with PL extracts from mycorrhized (PL+myc) or non-mycorrhized (PL−myc) roots, defined PLs or flg22 as indicated. PL extracts were applied at 15 μl/ml of suspension; defined PLs, at 100 μM; and flg22, at 1 μM. Results show means and standard deviations of three replicates. Controls label indicates treatment with solvent (methanol:water, 1:9); $PCsbA_2$, PCsb treated with PLA_2 (from bovine brain). (**B**) RT-PCR performed on RNA from tomato cell culture after application of PL−myc and PL+myc from plantain roots. Gene-specific primer pairs for *LePT1* and *LePT4* were used. Non–reverse-transcribed RNA samples (−RT) were used to test absence of genomic DNA in the RNA samples. Shown is the inverted picture.

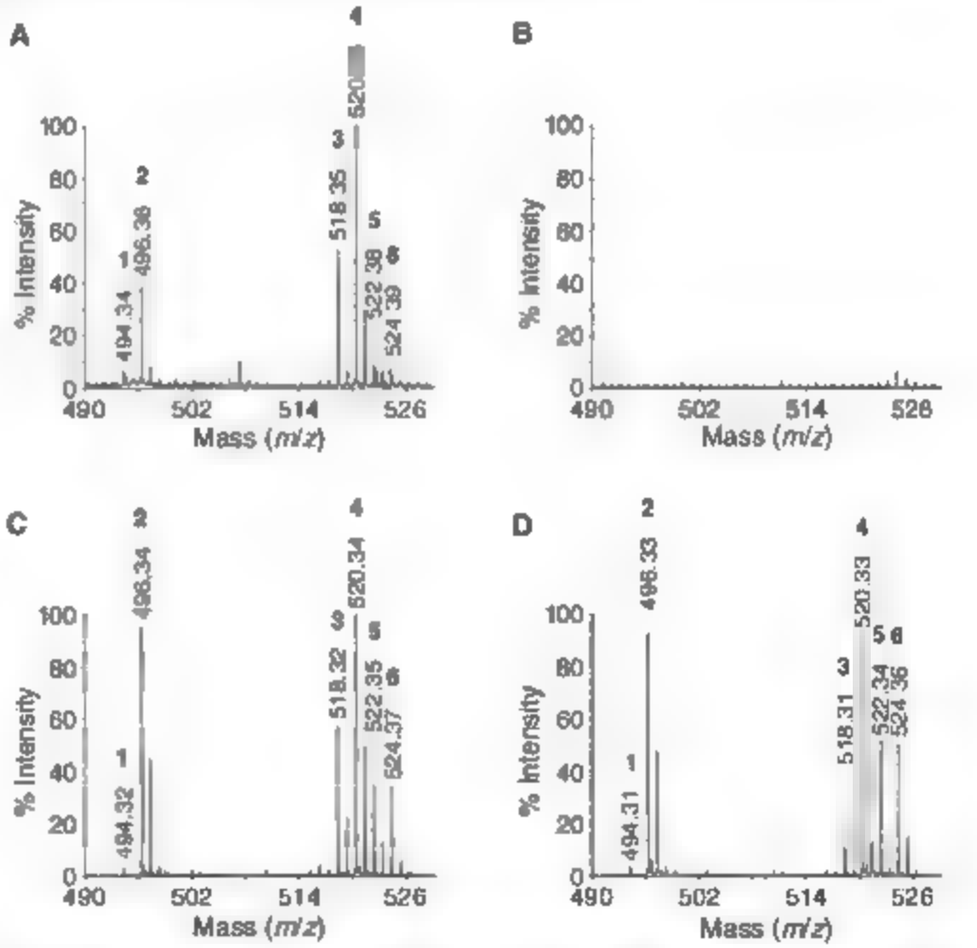

Fig. 3. Positive-ion MALDI-TOF mass spectra for LPC in PL fraction originating from mycorrhized (**A**) and nonmycorrhized (**B**) roots after chromatography. MALDI spectrum of $PCsbA_2$ (**C**) and of commercially available LPC (**D**). Numbers indicate the peak position (*m/z*) of the protonated form of different LPC molecular species. Species 1 is LPC 16:1, 2, LPC 16:0; 3, LPC 18:3; 4, LPC 18:2; 5, LPC 18:1, and 6, LPC 18:0.

toward the identification of the "signal" present in the PL+myc extract. By using various separation techniques coupled to mass spectrometry, we identified lyso-phosphatidylcholine (LPC) as a candidate bioactive compound. To prove the bioactivity of LPC directly, we tested commercially available phosphatidylcholine from soybean (PCsb). This preparation did not provoke any response in the cell culture (Fig. 2A). However, when PCsb was hydrolyzed with phospholipase A_2 (PLA_2) to release LPC, the preparation induced a strong alkalinization response (Fig. 2A), indicating that LPC might be the active signal. Indeed, commercially available LPC from egg yolk (LPCey) and soybean (LPCsb) induced alkalinization in a saturable and dose-dependent way (Fig. 2A and fig. S2B) but did not induce other responses typically observed after flg22 treatment, including production of ROS and ethylene in plant leaves (fig. S3, B and C).

Based on these findings, PLs from mycorrhized and nonmycorrhized roots were analyzed by matrix-assisted laser desorption ionization/time of flight mass spectrometry (MALDI-TOF-MS). This revealed the presence of distinct signals that specifically occurred in the PL+myc fractions. Molecular ions at m/z = 494.3, 496.3, 518.3, 520.3, 522.3, and 524.3, indicative of LPC containing C16:1, C16:0, C18:3, C18:2, C18:1, and C18:0 fatty acids at *sn*-1 position, were detected (Fig. 3, A and B). Moreover, after treatment of PC with PLA_2, releasing the fatty acid at position *sn*-2 of PC (*10*), molecular ions with the same masses were detected (Fig. 3C). This pattern of molecular ions was also observed in LPCsb (Fig. 3D). Nanoflow reverse-phase liquid chromatography (LC) separation and quantification of LPC revealed that the relative amounts of monounsaturated LPC species 16:1 and 18:1 in PL+myc extracts were higher than those present in LPCsb (fig. S4). LPC concentration in PL+myc was estimated to be 4 μM, whereas LPC amounts in PL-myc accounted for 0.5% of the amount in PL+myc. Thus, our analyses indicated that LPC might be the bioactive ingredient in PL+myc to induce mycorrhiza-specific phosphate transporter gene expression. Next, externally applied LPC was shown to be the signal inducing phosphate transporter genes in nonmycorrhized roots directly. As compared with solvent controls, *StPT3* and *StPT4* transcripts accumulated in potato roots that had been infiltrated with LPC (Fig. 4A). In contrast, transcript concentrations of the AM-nonresponsive *StPT1* gene (*9*) remained constant (Fig. 4A). We then looked at the GUS response in transgenic potato roots carrying the *StPT3* promoter–GUS chimeric gene. Similar to the activity seen in roots infiltrated with PL+myc (Fig. 1A), GUS activity in roots was stimulated by LPCsb and synthetic LPC with the fatty acid C18:1 (Fig. 4, B and C). In addition, no increase in GUS staining was observed when transgenic roots were treated with lyso-phosphatidylethanolamine (LPE) (Fig. 4C). This result suggested selectivity for the phosphocholine headgroup at *sn*-3 position.

Apparently, the signaling pathway to activate the mycorrhiza-specific phosphate transporters has its origin in the PL. PC, a major component of membranes of plants and, probably, also of the AM fungus. However, PC is not active in itself. It gains activity only after treatment with PLA_2 (Fig. 2A and Fig. 3C), suggesting an important role of this enzyme in the establishment of the mycorrhizal Pi uptake pathway. Whether the production of the LPC signal involves PLA_2 and PC from plants, fungus, or both remains to be explored further. Several PLA_2s have been identified in plants, and all are secretory proteins (*11*); their regulation and substrate specificities are unknown. This might hint at an extracellular production of the LPC signal. However, in the AM symbiosis, the phosphate transporter genes appear to be activated quite specifically in the arbuscule-containing cells (*5*, *6*). Therefore, the LPC signal might be generated more specifically in the arbuscule-containing cells. LPCs are highly mobile within intact cells, and LPC is therefore a good candidate for a cytoplasmic messenger that transduces signals to activate downstream processes and gene expression in the nucleus.

PLA_2-dependent activation of the defense responses involving LPC as a putative signal has been reported in plants (*12*, *13*). Interestingly, comparative transcriptomics in rice revealed a set of genes that was similarly expressed in associations with symbiotic and pathogenic fungi, revealing a conserved response to fungal colonization (*14*). Together with the findings of this report, this suggests commonalities between the signaling pathways in (i) wounding (*15*) and pathogen attack and (ii) cellular colonization of cortical cells with AM fungi. We observed similarities but also differences in the responses of tomato cells treated with mycorrhizal LPC and with the bacterial PAMP flg22. Further work is required to study the overlap between signaling pathways in response to AM fungi, to herbivore attack, and to PAMPs in plant innate immunity.

It is well documented that LPC is bioactive in mammals. An increasing amount of evidence has suggested that LPC is involved in the activation of inflammatory responses (*16*, *17*). Perception of LPC can occur through binding to G protein–coupled receptors (*18*). Furthermore, possible roles of LPC as functional vaccine (*17*) or second messenger have been discussed, underlining the functional importance of LPC in cellular responses.

In plants, PLA_2 and its lysolipid product LPC have been reported to be involved in numerous cellular processes (*19*), including cytoplasmic acidification, which is accompanied by extracellular medium alkalinization, with the latter leading to alterations in gene expression (*20*). So far, experimental evidence for a participation of PLs

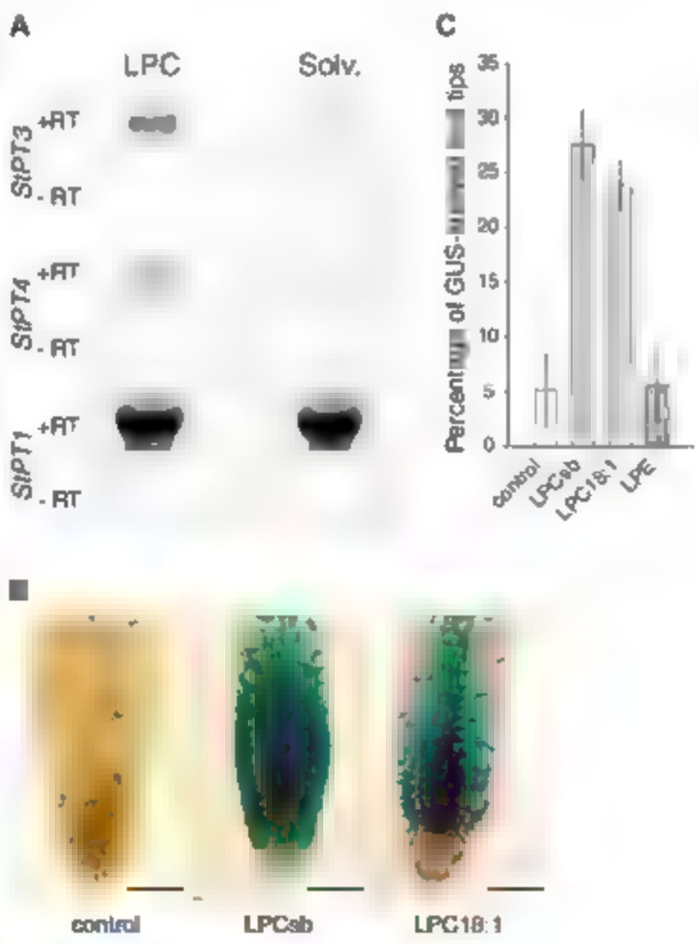

Fig. 4. Effect of LPC on phosphate transporters in potato roots. (**A**) RT-PCR with RNA from potato roots treated for 3 hours with LPCsb or the solvent as control. Gene-specific primers for *StPT1*, *StPT3*, and *StPT4* were used. Non–reverse-transcribed RNA samples (–RT) did not give rise to amplification of cDNA, indicating absence of genomic DNA in the PCR templates. Shown is the inverted picture. (**B**) *StPT3* promoter–driven expression of GUS reporter gene in transgenic potato roots after treatment with a solvent control (methanol:water, 1:9), LPCsb, or synthetic LPC with defined fatty acid 18:1, as indicated. Scale bars, 100 μm. (**C**) Percentage of root tips with GUS staining after 3 hours of treatment with a solvent control, LPCsb, LPC 18:1, and lyso-phosphatidylethanolamine (LPE). Compounds were applied at 100 μM. Bars show means of three independent experiments with each n > 20 root tips, and error bars indicate standard deviations of the three replicates.

in plant signaling and alteration of gene expression has only been demonstrated for phosphatidic acid, which is produced through the activity of phospholipase D (*21*). Therefore, further research on LPC generation and signaling can hopefully tell us more about the evolution of response regulation in plants and mammals, including that in the development of the AM symbiosis.

References and Notes

1. S. E. Smith, F. A. Smith, I. Jakobsen, *Plant Physiol.* **133**, 16 (2003)
2. H. Javot, R. V. Penmetsa, N. Terzaghi, D. R. Cook, M. J. Harrison, *Proc. Natl. Acad. Sci. U.S.A.* **104**, 1720 (2007)
3. V. Karandashov, M. Bucher, *Trends Plant Sci.* **10**, 22 (2005)
4. D. Maeda *et al.*, *Plant Cell Physiol.* **47**, 807 (2006)
5. C. Rausch *et al.*, *Nature* **414**, 462 (2001)
6. V. Karandashov, R. Nagy, S. Wegmüller, N. Amrhein, M. Bucher, *Proc. Natl. Acad. Sci. U.S.A.* **101**, 6285 (2004)
7. V. Tallboon *et al.*, *Plant Physiol.* **143**, 825 (2007)
8. C. Zipfel *et al.*, *Nature* **428**, 764 (2004)
9. R. Nagy *et al.*, *Plant J.* **42**, 236 (2005)
10. M. Petkovic *et al.*, *Anal. Biochem.* **308**, 61 (2002)
11. H. Y. Lee *et al.*, *Prog. Lipid Res.* **44**, 52 (2005)
12. J. Marsaez-Vasquez, J. Florin-Christensen, C. A. Ryan, *Plant Cell* **11**, 2249 (1999)
13. K. Viehweger, W. Schwartze, B. Schumann, W. Lein, W. Roos, *Plant Cell* **18**, 1510 (2006)
14. S. Gumil *et al.*, *Proc. Natl. Acad. Sci. U.S.A.* **102**, 8066 (2005)
15. I. T. Magel, C. P. Constabel, *New Phytol.* **172**, 617 (2006)
16. S. Bendel *et al.*, *Biochim. Biophys. Acta* **1761**, 1014 (2006)
17. L. Perrin-Cocon *et al.*, *Vaccine* **24**, 1254 (2006)
18. J. Qiao *et al.*, *Am. J. Physiol. Lung Cell. Mol. Physiol.* **291**, L91 (2006)
19. H. J. Meijer, T. Munnik, *Annu. Rev. Plant Biol.* **54**, 265 (2003)
20. J. Zhao, L. C. Davis, R. Verpoorte, *Biotechnol. Adv.* **23**, 283 (2005)
21. T. Munnik, H. J. Meijer, *FEBS Lett.* **498**, 172 (2001)

22. We thank V. Karandashov for initial support, E. Martinoia (University of Zurich) for helpful discussions, the Functional Genomics Center Zurich (FGCZ) for providing technology, and G. Neuhaus-Url (Syngenta, Basel) for the gift of aequorin-transformed MsK8 suspension-cultured cells. This work was supported by a Plant Science Center–Syngenta graduate research fellowship, by ETH research grant TH 5/05-1, and by the Zurich Glycomics Initiative (Glycoinit). D.D., G.K., N.C., N.A., and M.B. conceived the experiment. D.D., G.K. in part together with N.C., G.F., and M.T. carried it out. D.D., G.K., N.C., P.G., G.F., and M.B. designed and carried out the data analysis; and D.D., G.K., G.F., T.B., N.A., and M.B. co-wrote the paper.

Supporting Online Material

www.sciencemag.org/cgi/content/full/318/5848/265/DC1
Materials and Methods
Figs. S1 to S5
Table S1

14 June 2007; accepted 28 August 2007
10.1126/science.1146487

Functional Divergence of Former Alleles in an Ancient Asexual Invertebrate

Natalia N. Pouchkina-Stantcheva,[1]* Brian M. McGee,[2] Chiara Boschetti,[1] Dimitri Tolleter,[2] Sohini Chakrabortee,[1] Antoaneta V. Popova,[3]† Filip Meersman,[4]‡ David Macherel,[2] Dirk K. Hincha,[3] Alan Tunnacliffe[1]§

Theory suggests it should be difficult for asexual organisms to adapt to a changing environment because genetic diversity can only arise from mutations accumulating within direct antecedents and not through sexual exchange. In an asexual microinvertebrate, the bdelloid rotifer, we have observed a mechanism by which such organisms could acquire the diversity needed for adaptation. Gene copies most likely representing former alleles have diverged in function so that the proteins they encode play complementary roles in survival of dry conditions. One protein prevents desiccation-sensitive enzymes from aggregating during drying, whereas its counterpart does not have this activity, but is able to associate with phospholipid bilayers and is potentially involved in maintenance of membrane integrity. The functional divergence of former alleles observed here suggests that adoption of asexual reproduction could itself be an evolutionary mechanism for the generation of diversity.

Bdelloid rotifers (Rotifera, Bdelloidea) have survived for tens of millions of years without sexual reproduction and meiotic recombination (*1*–*4*). Male bdelloid rotifers have never been observed, and the genetic evidence is consistent with fully asexual reproduction by thelytoky. Long-lasting asexual lineages are thought to be rare because their apomictic nature does not allow the accumulation of favorable, or the elimination of detrimental, mutations through genetic exchange (*5*–*7*). However, one consequence of apomixis is that the sequence homogeneity of gene copies that previously were alleles in sexual ancestors is no longer maintained by recombination. This allows the former alleles to accumulate mutations and become divergent—a phenomenon referred to as the Meselson effect (*8*). Thus, in sexually reproducing monogonont rotifers (Rotifera, Monogononta) alleles differ very little from each other at synonymous sites (by up to 2.4% for *hspX2*), but corresponding gene copies in individual bdelloid clones can differ by as much as 49% (*1*). In principle, this effect should allow independent evolution of former alleles through which they can acquire different functions.

We looked for evidence of functional divergence among former alleles in a gene set associated with desiccation tolerance in bdelloid rotifers (*9*, *10*). cDNAs representing ~100 dehydration-induced genes from the bdelloid rotifer *Adineta ricciae* were identified, one of which encoded a polypeptide related to the group 3 late embryogenesis abundant (LEA) proteins characterized in plant seeds. LEA proteins are linked with desiccation tolerance in plants, invertebrates, and microorganisms (*11*). We identified two similar but distinct sequences and named them *Ar-lea-1A* and *Ar-lea-1B*. Both genes contain nine small introns (Fig. 1A), although there is a major structural difference in exon 2, which in *Ar-lea-1A* contains a 132–base pair (bp) segment with no counterpart in *Ar-lea-1B*. Aligned coding sequences show 13.5% synonymous site divergence (K_s) over the whole gene. This divergence is much greater than that observed between alleles of sexual animals, but is within the range of values observed in bdelloids for former allele pairs (*1*, *3*, *4*, *8*).

To confirm the presence of two *lea* gene copies in the *A. ricciae* genome, Southern hybridization experiments were performed with probes from both the 5′ and 3′ ends of *Ar-lea-1B*, which cross-hybridize to the corresponding regions of *Ar-lea-1A* (Fig. 1B). Both genes reside on ~5.0-kb Dra I genome fragments, but these could be distinguished by double digestion with either Eco RI or Nde I; a restriction map of each gene was constructed accordingly (Fig. 1, A and B). As further confirmation of *lea* gene copy number, fluorescence in situ hybridization (FISH) was carried out on *A. ricciae* embryo nuclei. Cytogenetic analysis shows 12 chromosomes in this species (Fig. 1C, left), as in the related species, *A. vaga* (*12*). Hybridization with a fluorescent probe corresponding to the whole of *Ar-lea-1A* produced two signals in interphase nuclei, consistent with detection of *lea* genes on two separate chromosomes (Fig. 1C, right). Our cloning and hybridization data show two related, but divergent, *lea* genes on different chromosomes in *A. ricciae*, and we interpret these to be former alleles that have diverged by the Meselson effect. Other interpretations are possible, for

[1]Institute of Biotechnology, University of Cambridge, Tennis Court Road, Cambridge CB2 1QT, UK. [2]UMR 1191 Physiologie Moléculaire des Semences, Université d'Angers/INH/INRA, 49045 Angers, France. [3]Max-Planck-Institute of Molecular Plant Physiology, Am Mühlenberg 1, D-14476 Potsdam, Germany. [4]Department of Chemistry, University of Cambridge, Lensfield Road, Cambridge CB2 1EW, UK.

*Present address: Department of Biology and Environmental Sciences, University of Sussex, Brighton BN1 9QG, UK.
†Present address: Institute of Biophysics, Bulgarian Academy of Sciences, 1113 Sofia, Bulgaria.
‡Present address: Department of Chemistry, Katholieke Universiteit Leuven, Celestijnenlaan 200 F, B-3001 Leuven, Belgium.
§To whom correspondence should be addressed. E-mail: at10004@biotech.cam.ac.uk

example, that the ancestral bdelloid was the result of a hybridization event between species with unusually similar *lea* genes, and that one copy of one *lea* gene from both parents was subsequently lost. However, the simplest interpretation, consistent with the current understanding of bdelloid genome structure and evolution (*1*, *4*, *8*), is that the two *lea* genes are divergent former alleles. Recent studies suggest that bdelloid rotifers have four copies of some genes located on separate chromosomes, which may indicate that they are ancestrally tetraploids (*1*, *2*), in which the four copies are two gene pairs that correspond to two pairs of former alleles (*3*). We have not obtained evidence to date for a second *lea* gene pair, although we cannot rule out that they are present in the genome but too divergent for us to detect with *Ar-lea-1A* sequences.

Expression of the *lea* genes was shown by quantitative polymerase chain reaction (PCR) to increase about sevenfold over 24 hours of drying (fig. S1 and table S1). A similar pattern of expression of *lea* genes during dehydration has been observed in other anhydrobiotic invertebrates (*11*) and is consistent with a role in desiccation tolerance.

The predicted protein sequences of ArLEA1A and ArLEA1B are very similar, differing only at 12 amino acid sites of 376 aligned positions; ArLEA1A is longer by 44 amino acids because of the 132-bp indel in exon 2 (Fig. 2A). Both sequences have at least four variants of the loosely conserved 11 amino acid motif characteristic of group 3 LEA proteins (*11*, *13*) (Fig. 2A and fig. S2A), although positions 4 and 5 are more likely to be apolar. The ArLEA1A and ArLEA1B proteins both have a 19-residue hydrophobic sequence at the N terminus, revealed by a hydropathy plot (*14*), and a putative variant endoplasmic reticulum (ER) retention signal, ATEL, at the C terminus (Fig. 2A and fig. S2). This suggests that these proteins are localized to or transported through the ER. Most group 3 LEA proteins are highly hydrophilic, with a mean hydropathy (GRAVY) score of −0.97 [SD 0.30; $n = 30$; dataset of (*15*)], but both bdelloid proteins score −0.46, similar to moderately hydrophilic proteins, such as bovine serum albumin (BSA) (GRAVY: −0.43). This reduced hydrophilicity of the bdelloid LEA proteins is unusual and may impact their structure.

Group 3 LEA proteins are largely unstructured in solution, probably because their extreme hydrophilicity favors interaction with water over intrachain binding, but they show increased folding when dried or associated with phospholipid bilayers (*11*, *16*). Secondary structures of recombinant forms of ArLEA1A and ArLEA1B, without putative N-terminal signal peptides, were examined by far-ultraviolet (far-UV) circular dichroism (CD) spectroscopy in hydrated and dry states. CD spectroscopy of ArLEA1A gave a solution spectrum with a single minimum at ~200 nm and low ellipticity at 222 nm, consistent with a disordered structure. However, when dried, its spectrum changed markedly, showing maxima near 208 nm and 222 nm, indicative of an α-helix (Fig. 2B). In contrast, ArLEA1B has an α-helical structure in the hydrated state, which does not change appreciably on drying (Fig. 2C). Secondary structure content calculated from CD spectra showed that in ArLEA1A the proportion of α-helix increased from 29 to 84% on drying, whereas ArLEA1B was 82% α-helix in solution, increasing slightly to 87% when dry. Protein denaturation analysis was performed by monitoring unfolding at 222 nm on exposure to urea at a range of concentrations from 0 to 6 M. For a typical globular protein, unfolding is cooperative and yields a sigmoidal curve. However, structure in ArLEA1B was lost linearly with increasing urea concentration (fig. S2E), which suggests that it exists as a premolten globule without significant tertiary structure in solution (*17*). The relatively small differences in primary structure of the bdelloid LEA proteins are therefore responsible for markedly different secondary structure.

We tested whether the structural differences between ArLEA1A and ArLEA1B are reflected in functional divergence. LEA proteins preserve the activity of desiccation-sensitive enzymes

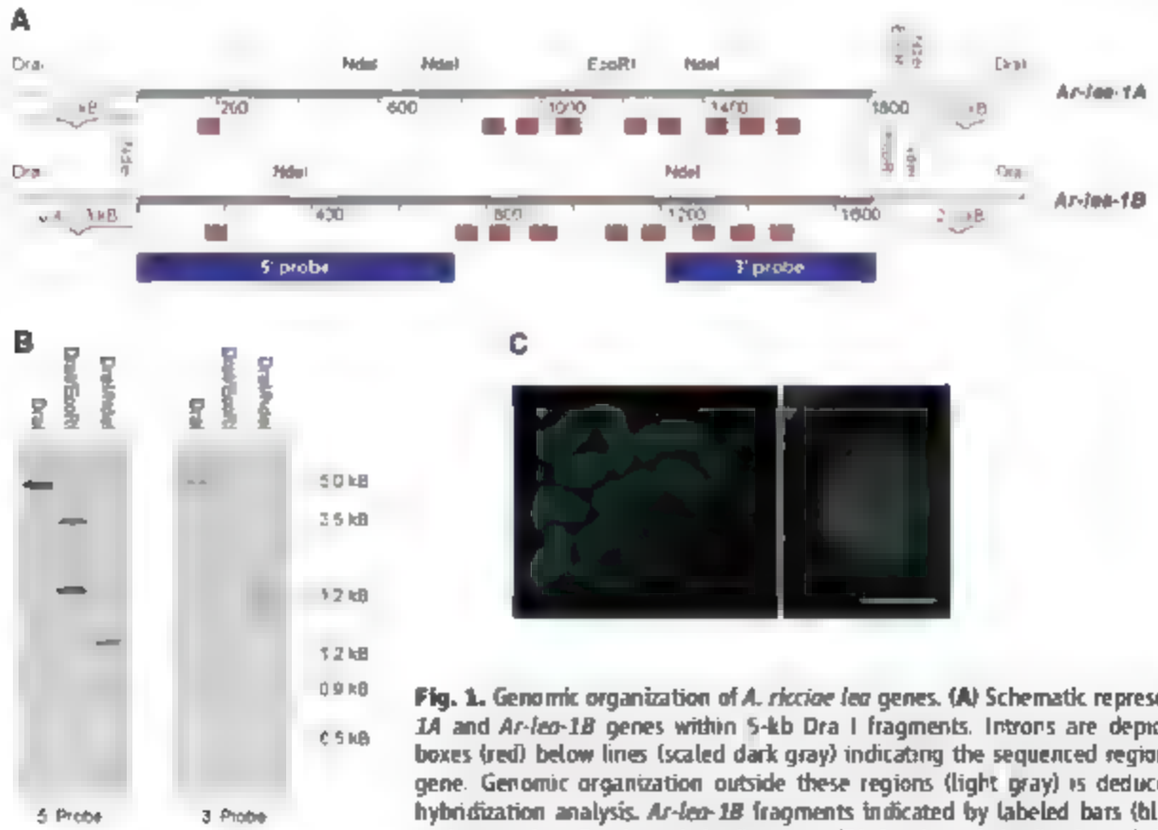

Fig. 1. Genomic organization of *A. ricciae lea* genes. **(A)** Schematic representation of *Ar-lea-1A* and *Ar-lea-1B* genes within 5-kb Dra I fragments. Introns are depicted as numbered boxes (red) below lines (scaled dark gray) indicating the sequenced region containing each gene. Genomic organization outside these regions (light gray) is deduced from Southern hybridization analysis. *Ar-lea-1B* fragments indicated by labeled bars (blue) correspond to probes used in Southern hybridizations. **(B)** Southern hybridization of *A. ricciae* genomic DNA with *lea* gene probes. Each panel contains genomic restriction digests with Dra I, Dra I/Eco RI, and Dra I/Nde I, respectively. Size marker positions are indicated. **(C)** *A. ricciae* karyotype and FISH with *lea* gene probe. (Left) The 12 chromosomes of *A. ricciae* in a single mitotic nucleus from an embryo stained with 4′,6′-diamidino-2-phenylindole (DAPI). (Right) Interphase nucleus hybridized at high stringency to *Ar-lea-1A* probe labeled with Alexa 488. Red (superimposed, false color): fluorescent signals; blue: DAPI-labeled DNA. Scale bar: 2 μm.

during drying (*18*, *20*), at least partly through prevention of aggregation, in what is called molecular shield activity (*21*). We investigated the ability of both bdelloid LEA proteins to behave as molecular shields by inhibiting desiccation-induced aggregation of citrate synthase (CS). When subjected to drying and rehydration, CS partially denatures and forms particulate aggregates; however, when dried in the presence of a group 3 LEA protein, such as AavLEA1 from the nematode *Aphelenchus avenae* (*22*), CS aggregation is suppressed (Fig. 3). Other proteins, such as BSA, are not effective. ArLEA1A was found to reduce CS aggregation as expected, although to a lesser extent than AavLEA1, perhaps because of the lower hydrophilicity of ArLEA1A compared with the nematode protein. However, ArLEA1B behaved differently, and drying of CS in its presence resulted in increased aggregation compared with CS dried alone. Indeed, ArLEA1B itself is prone to aggregation (Fig. 3), which ArLEA1A and AavLEA1 are not, possibly because of its more structured nature. Thus, ArLEA1A shows molecular shield activity in common with other group 3 LEA pro-

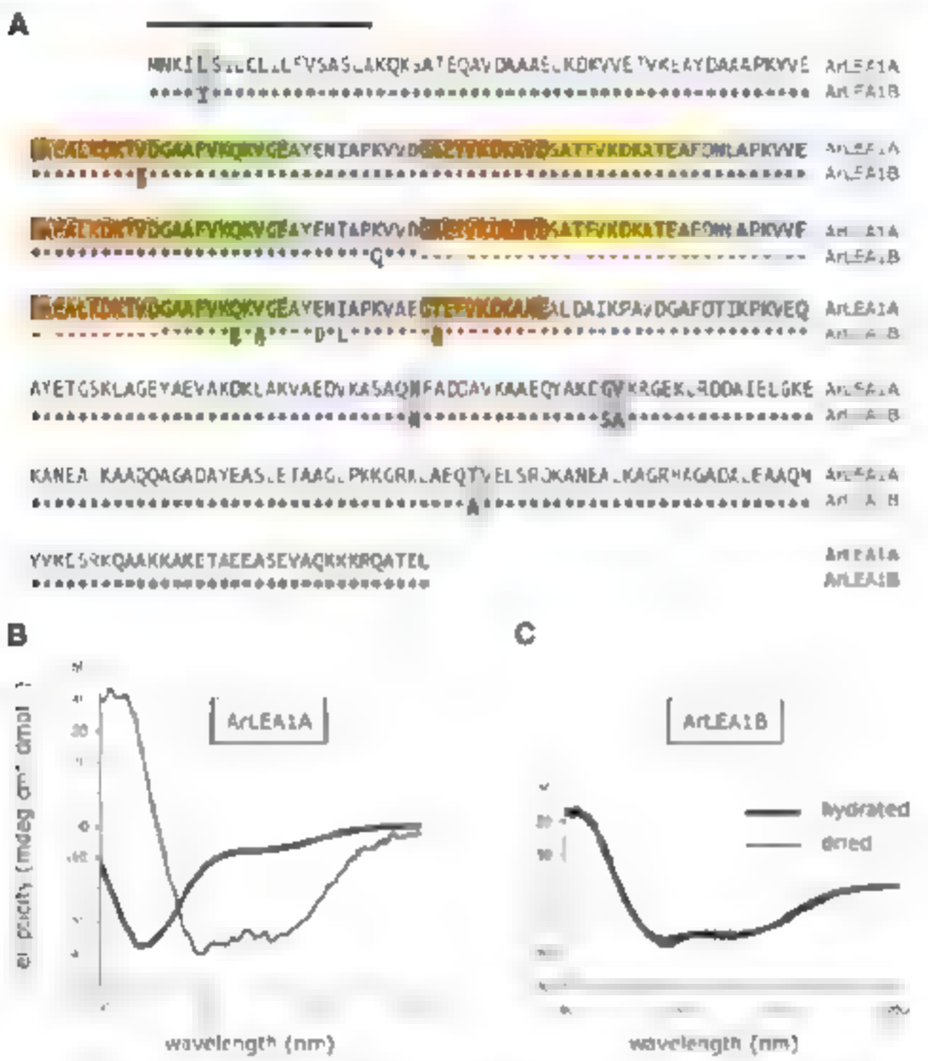

Fig. 2. Primary and secondary structure of *A. ricciae* LEA proteins. (**A**) Alignment of ArLEA1A and ArLEA1B protein sequences showing repeated 11-oligomer motifs. ArLEA1A is 420 residues long with a (predicted) molecular mass of 44.5 kD, whereas ArLEA1B extends for 376 residues with a (predicted) molecular mass of 39.8 kD. Near canonical motifs are orange, green, and yellow; degenerate motifs are gray; highlighted residues differ between the two proteins. The 44-residue indel, shown by dashes, is identical to a more N-terminal sequence whose 11-oligomer motifs are also highlighted orange-yellow-gray-orange. A putative signal peptide is overlined at the N terminus. (**B** and **C**) Far-UV CD spectroscopy of ArLEA1A and ArLEA1B in solution and dry state.

Fig. 3. Bdelloid LEA protein antiaggregation assay. Citrate synthase (CS), with or without LEA proteins or BSA, and the latter proteins alone where indicated, were subjected to two cycles of vacuum drying and rehydration. Light scattering by protein particulates was measured by apparent absorption at 340 nm in the spectrophotometer. Error bars show standard deviation ($n = 3$); ns, not significantly different ($P > 0.05$); significant values $^{*}P < 0.05$ or $^{**}P < 0.001$.

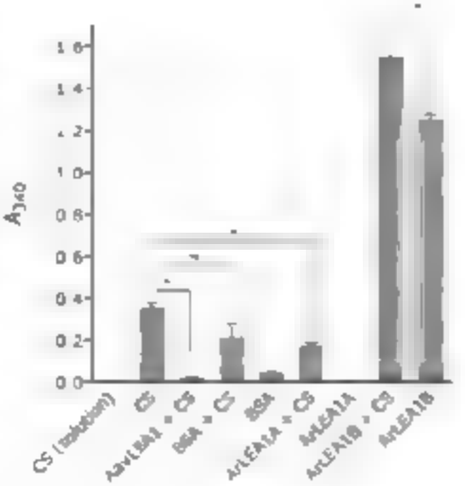

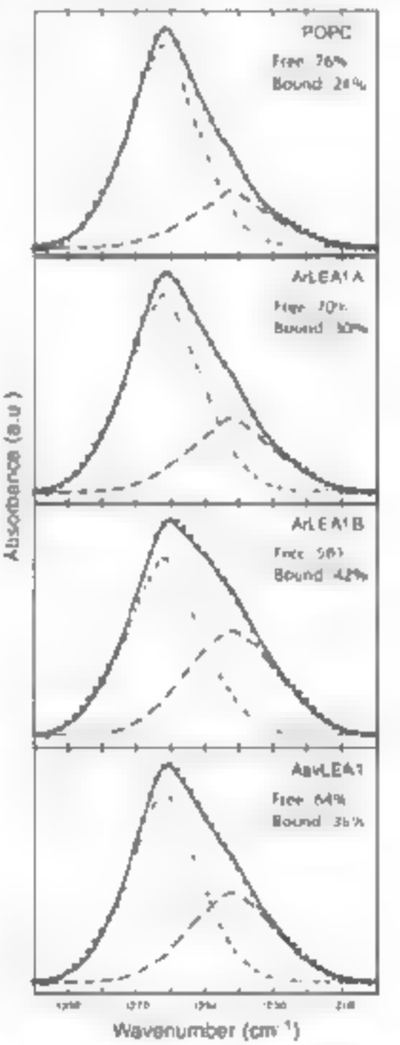

Fig. 4. Bdelloid LEA protein membrane association. Infrared spectra of the asymmetric phosphate stretching region of POPC liposomes dried alone or in the presence of ArLEA1A, ArLEA1B, or AavLEA1. Spectra were recorded at 78°C (liquid-crystalline phase). The solid curve comprises both the measured (dots) and fitted absorbance curves. Normalized peaks were fitted into two bands with maxima at 1262 and 1242 cm^{-1} corresponding respectively to $\nu P{=}O_{as_{free}}$ (short dashes) and $\nu P{=}O_{as_{bound}}$ (long dashes).

tents, but ArLEA1B does not and is itself sensitive to desiccation.

Some LEA proteins have a capacity to associate with and stabilize phospholipid bilayers on dehydration (*11*, *16*, *23*). Membrane interaction was assessed with Fourier transform infrared spectroscopy of liposomes dried in the presence of the bdelloid LEA proteins or AavLEA1. The gel-to-liquid crystalline phase-transition temperature (T_m) of dried palmitoyl oleoyl phosphatidylcholine (POPC) vesicles (59.8° ± 1.2°C) was not affected by the presence of ArLEA1A (58.2° ± 1.1°C) or AavLEA1 (61.9° ± 5.3°C). However, ArLEA1B significantly decreased T_m to 51.8° ± 2.9°C, which indicates that it interacts with lipids. Further examination of the spectra in the asymmetric phosphate-stretching region revealed a distinct effect of ArLEA1B with a marked shoulder at 1242 cm^{-1} (Fig. 4). The peaks were resolved into two components attributed to $\nu P{=}O_{free}$ (1262 cm^{-1}) and $\nu P{=}O$ H-bonded (1242 cm^{-1}) (*24*), similar to the effect of water and sugar (*25*). The correlation coefficients for the fitted curves were higher than 0.999. The small bonded P=O population in the absence of protein is because of interlipid charge-pair interactions between P=O and choline groups, whereas the separation of the two P=O populations is probably because ArLEA1B was only in contact with the outer monolayer of the liposomes (*26*). Clearly, a greater proportion of P=O groups are H-bonded in the presence of ArLEA1B compared with ArLEA1A (42% as opposed to 30%), whereas AavLEA1 has an intermediate value (36%). These results show that ArLEA1B has a stronger propensity to interact with dry phospholipid membranes than ArLEA1A and AavLEA1.

In summary, the bdelloid LEA proteins, encoded by gene copies representing former alleles, have different structures and functions. These functional differences are likely to be adaptive, because prevention of protein aggregation and protection of cellular membranes are essential for survival of desiccation (*10*, *27*). The presence of complementary activities in a single gene pair of a desiccation-tolerant bdelloid rotifer illustrates the potential for functional diversity resulting from divergence of former alleles. The process of abandoning sexual reproduction and meiosis, and the resulting sequence homogenization of homologous chromosomes, is similar to genomic duplication, which is a major evolutionary force (*28*, *29*) that results in orthologous genes evolving relatively independently. Similarly, apomixis could drive evolutionary change by allowing former alleles to diversify in function and may partly explain how bdelloid rotifers have, without genetic exchange, diversified into almost 400 taxonomic species (*30*, *31*).

References and Notes

1. O. Mark Welch, M. Meselson, *Science* **288**, 1211 (2000).
2. J. L. Mark Welch, D. B. Mark Welch, M. Meselson, *Proc. Natl. Acad. Sci. U.S.A.* **101**, 1618 (2004).
3. D. B. Mark Welch, M. P. Cummings, D. M. Hillis, M. Meselson, *Proc. Natl. Acad. Sci. U.S.A.* **101**, 1622 (2004).
4. C. W. Birky, *Proc. Natl. Acad. Sci. U.S.A.* **101**, 2651 (2004).
5. M. J. D. White, *Modes of Speciation* (Freeman, San Francisco, 1978).
6. A. Burt, *Evolution* **54**, 337 (2000).
7. M. R. Goddard, H. C. Godfray, A. Burt, *Nature* **434**, 636 (2005).
8. R. Butlin, *Nat. Rev. Genet.* **3**, 311 (2002).
9. C. Ricci, *Hydrobiologia* **387-388**, 321 (1998).
10. A. Tunnacliffe, J. Lapinski, *Philos. Trans. R. Soc. Lond. B Biol. Sci.* **358**, 1755 (2003).
11. A. Tunnacliffe, M. J. Wise, *Naturwissenschaften* **94**, 791 (2007).
12. J. L. Mark Welch, M. Meselson, *Hydrobiologia* **387-388**, 403 (1998).
13. J. A. Browne *et al.*, *Eukaryot. Cell* **3**, 966 (2004).
14. J. Kyte, R. F. Doolittle, *J. Mol. Biol.* **157**, 105 (1982).
15. M. J. Wise, *BMC Bioinform.* **4**, 52 (2003).
16. O. Tolleter *et al.*, *Plant Cell* **19**, 1580 (2007).
17. V. N. Uversky, *Protein Sci.* **11**, 739 (2002).
18. M. T. Sanchez-Ballesta, M. J. Rodrigo, M. T. Lafuente, A. Granell, L. Zacarias, *J. Agric. Food Chem.* **52**, 1950 (2004).
19. J. Gaviel *et al.*, *Plant Physiol.* **137**, 157 (2005).
20. J. L. Reyes *et al.*, *Plant Cell Environ.* **28**, 709 (2005).
21. K. Goyal, L. J. Walton, A. Tunnacliffe, *Biochem. J.* **388**, 151 (2005).
22. J. Browne, A. Tunnacliffe, A. Burnell, *Nature* **416**, 38 (2002).
23. P. L. Steponkus, M. Uemura, R. A. Joseph, S. J. Gilmour, M. F. Thomashow, *Proc. Natl. Acad. Sci. U.S.A.* **95**, 14570 (1998).
24. P. T. T. Wong, H. H. Mantsch, *Chem. Phys. Lipids* **46**, 213 (1988).
25. C. Caceta, D. K. Hincha, *Biophys. J.* **90**, 2831 (2006).
26. D. K. Hincha, E. M. Hellwege, A. G. Heyer, J. H. Crowe, *Eur. J. Biochem.* **267**, 535 (2000).
27. J. H. Crowe, F. A. Hoekstra, L. M. Crowe, *Annu. Rev. Physiol.* **54**, 579 (1992).
28. J. Spring, *Nat. Genet.* **31**, 128 (2002).
29. Y. Van de Peer, *Nat. Rev. Genet.* **5**, 752 (2004).
30. C. W. Birky Jr., C. Wolf, H. Maughan, L. Herbertson, E. Henry, *Hydrobiologia* **546**, 29 (2005).
31. D. Fontaneto *et al.*, *PLoS Biol.* **5**, e87 (2007).

32. We thank J. Mark Welch for advice on FISH and S. Batey for help with CD spectroscopy. Funded by the Biotechnology and Biological Sciences Research Council (S19912 98/D00130?1 and 02/A2/P08059), the Leverhulme Trust (F/09717/B), the Isaac Newton Trust (6.20), and Invitrogen Advanced Biosystems Ltd. A.V.P. would like to thank the Deutsche Forschungsgemeinschaft for a travel grant. Sequences are deposited into GenBank with accession numbers EF554863 through EF554866.

Supporting Online Material

www.sciencemag.org/cgi/content/full/318/5848/268/DC1
Materials and Methods
Figs. S1 and S2
Table S1
References and Notes

27 April 2007; accepted 17 August 2007
10.1126/science.1144363

Target Protectors Reveal Dampening and Balancing of Nodal Agonist and Antagonist by miR-430

Wen-Yee Choi,[1,2] Antonio J. Giraldez,[1,3]* Alexander F. Schier[1]*

MicroRNAs (miRNAs) repress hundreds of target messenger RNAs (mRNAs), but the physiological roles of specific mRNA-mRNA interactions remain largely elusive. We report that zebrafish microRNA-430 (miR-430) dampens and balances the expression of the transforming growth factor–β (TGF-β) Nodal agonist *squint* and the TGF-β Nodal antagonist *lefty*. To disrupt the interaction of specific miRNA-mRNA pairs, we developed target protector morpholinos complementary to miRNA binding sites in target mRNAs. Protection of *squint* or *lefty* mRNAs from miR-430 resulted in enhanced or reduced Nodal signaling, respectively. Simultaneous protection of *squint* and *lefty* or absence of miR-430 caused an imbalance and reduction in Nodal signaling. These findings establish an approach to analyze the in vivo roles of specific mRNA-mRNA pairs and reveal a requirement for miRNAs in dampening and balancing agonist/antagonist pairs.

MicroRNAs (miRNAs) are small RNA molecules ~22 nucleotides long and function to block the translation and enhance the decay of target mRNAs (*1*). Recent studies have uncovered activities of specific miRNA families and have identified hundreds of putative target mRNAs (*1*–*3*). However, the physiological roles of specific miRNA-mRNA pairs are largely unknown (*1*, *3*). To develop a method to disrupt specific miRNA-mRNA pairs, we focused on the zebrafish microRNA-430 (miR-430) family. This miRNA family is highly expressed during early zebrafish development, targets hundreds of mRNAs, and is required for embryonic morphogenesis and clearance of maternal mRNAs (*4*, *5*). Analysis of 3′ untranslated regions (3′UTRs) with sites complementary to miR-430 identified *squint* (*sqt*), a member of the Nodal family of transforming growth factor β (TGF-β) signals, and *lft1* and *lft2*, members of the Lefty family of TGF-β signals (fig. S1). Nodals are the key regulators of mesendoderm induction and left-right axis formation, whereas Lefties act as antagonists of Nodal signaling (*6*, *7*). The balance between Nodals and Lefties

[1]Department of Molecular and Cellular Biology, Harvard University, 16 Divinity Avenue, Cambridge, MA 02138, USA. [2]Developmental Genetics Program, New York University School of Medicine, New York, NY 10016, USA. [3]Department of Genetics, Yale University School of Medicine, New Haven, CT 06510, USA.

*To whom correspondence should be addressed. E-mail: schier@fas.harvard.edu; antonio.giraldez@yale.edu

determines the extent of mesendoderm formation (6–8) (fig. S1). Given their potent and concentration-dependent effects, we hypothesized that miR-430 might be required to dampen these signals.

Four lines of evidence indicate that *sqt*, *lft1*, and *lft2* are in vivo targets of miR-430. (i) Reporter mRNAs consisting of the green fluorescence protein (GFP) coding region and full-length *sqt*, *lft1*, or *lft2* 3′UTRs were repressed in the wild type but not in MZ*dicer* mutants, which lack all mature miRNAs including miR-430. Derepression of reporter genes was most pronounced for *lft2* and least marked for *lft1*, suggesting that *lft2* is more strongly repressed by miR-430 than *sqt* and *lft1* (Figs. 1A and 2D and figs. S2 and S5). (ii) Mutations of two nucleotides within the miR-430 target site (GCACUU to GGUCUU) abolished repression of reporter mRNAs (Fig. 1A and fig. S2). (iii) Endogenous expression of *sqt*, *lft1*, and *lft2* mRNAs was increased in MZ*dicer* mutants (Fig. 3, A and B, and fig. S2). (iv) Misexpression of *sqt*, *lft1*, or *lft2* mRNAs containing mutated miR-430 binding sites ($sqt^{mut\text{-}3'UTR}$, $lft1^{mut\text{-}3'UTR}$, $lft2^{mut\text{-}3'UTR}$) resulted in higher physiological activity (Fig. 1, B to F, and fig. S2). These results indicate that miR-430 represses *sqt*, *lft1*, and *lft2* expression and activity.

To study the physiological role of miR-430/*sqt* and miR-430/*lft* interactions, we developed a method to disrupt the interaction of miRNAs with target mRNAs. RNA-binding morpholino antisense oligonucleotides are commonly used in zebrafish to block the translation or splicing of target RNAs (9–11). We reasoned that morpholinos overlapping with mRNA target sites might inter-

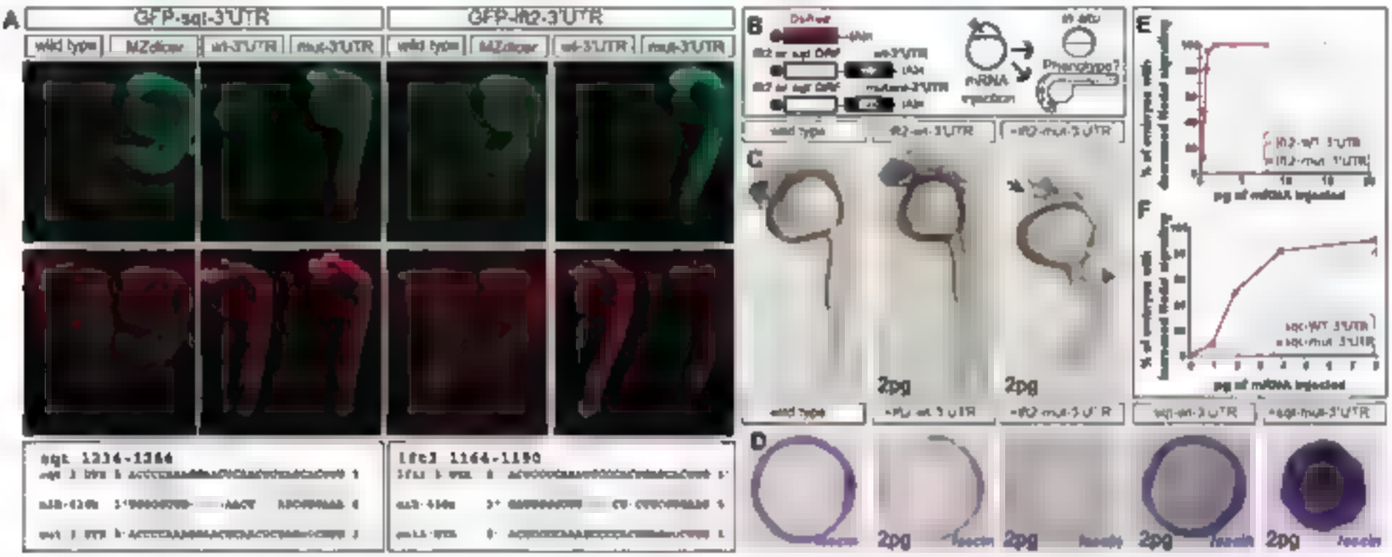

Fig. 1. miR-430 represses *sqt* and *lft2* expression and activity. (**A**) mRNAs for GFP reporters (green) containing the 3′UTRs of *sqt* or *lft2* are co-injected with control DsRed (red) mRNA. Expression is analyzed at 25 to 30 hours postfertilization (hpf). Wild-type (wt) reporters are repressed in wild-type embryos as compared to MZ*dicer* mutants. Repression is abolished by mutations in the predicted miR-430 target sites. Predicted pairings of the 3′ UTRs to miR-430 are shown. The *lft2* reporter appears more strongly repressed by miR-430 than the *sqt* reporter. (**B**) Outline of activity assays. *sqt* or *lft2* open reading frame (ORF) with either wild-type or mutated 3′UTR is injected at the one-cell stage. mRNA activity is assessed at 50% epiboly (~5 hpf) by RNA in situ hybridization or at 25 to 30 hpf by morphology. (**C**) Embryos injected with 2 pg of wild-type *lft2* mRNA appear similar to uninjected controls, whereas injection of 2 pg of $lft2^{mut\text{-}3'UTR}$ mRNA causes cyclopia (arrow) and loss of trunk mesoderm (arrowhead), hallmarks of reduced Nodal signaling. (**D**) Physiological activity of *sqt* or *lft2* mRNA assessed by *fascin* (*fas*) induction, a marker for Nodal signaling activity. $lft2^{mut\text{-}3'UTR}$ mRNA (2 pg) causes a stronger decrease in *fas* induction than wild-type *lft2*. $sqt^{mut\text{-}3'UTR}$ mRNA (2 pg) leads to greater ectopic induction of *fas* than wild-type *sqt*. (**E**) Percentage of embryos with decreased Nodal signaling (cyclopia and loss of trunk mesoderm) at increasing concentrations of wild-type *lft2* or $lft2^{mut\text{-}3'UTR}$ mRNA. (**F**) Percentage of embryos with increased Nodal signaling (ectopic *gsc* induction covering >50% of the animal pole) at increasing concentrations of wild-type *sqt* or $sqt^{mut\text{-}3'UTR}$ mRNA.

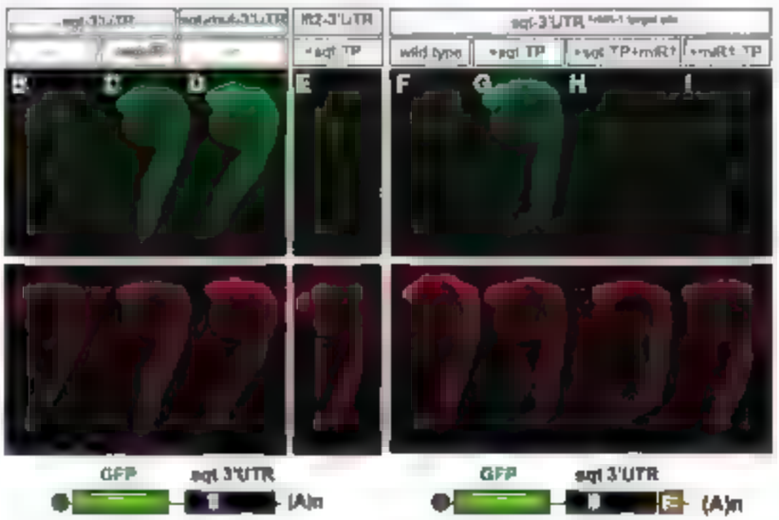

Fig. 2. miRNA target protectors (TPs) interfere with specific miRNA-mRNA interactions. (**A**) Experimental approach. Target protectors are co-injected with GFP-reporters (green) into wild-type embryos and prevent miR-430–induced target repression. Predicted pairings of sqt-$TP^{miR\text{-}430}$ and lft2-$TP^{miR\text{-}430}$ to *sqt* and *lft2* 3′UTRs are shown. DsRed mRNA (red) is injected as a control. (**B**) Wild-type reporter is repressed in wild-type embryos. (**C** and **D**) Co-injection of sqt-$TP^{miR\text{-}430}$ or mutation of miR-430 target site prevents GFP repression. (**E**) sqt-$TP^{miR\text{-}430}$ does not affect repression of *lft2*-GFP reporter. (**F**) *sqt*-GFP reporter with introduced miR-1 target site is repressed in wild-type embryos. miR-1 is not expressed during early zebrafish embryogenesis. (**G**) sqt-$TP^{miR\text{-}430}$ prevents GFP repression in the absence of miR-1. (**H**) sqt-$TP^{miR\text{-}430}$ does not interfere with activity of injected miR-1. (**I**) sqt-$TP^{miR\text{-}1}$ does not interfere with miR-430 activity.

fere with miRNA-mRNA interactions, thus protecting the target from the miRNA (target protector, TP) (Fig. 2A). Specificity would be attained by the sequences unique to the 3′UTR. To test this strategy, we analyzed the effect of morpholinos complementary to the region of the miR-430 target sites in the *sqt* or *lft* 3′UTRs. Four lines of evidence indicate that TPs interfere with miR-430–mediated repression of specific 3′UTRs. (i) Injection of sqt-TP$^{miR\text{-}430}$ blocked miR-430 induced repression of the *sqt*-GFP reporter (Fig. 2, B to D, and fig. S3). (ii) sqt-TP$^{miR\text{-}430}$ did not block repression of the *lft2*-GFP reporter, suggesting that TPs do not induce cross-protection (Fig. 2E). (iii) Control morpholinos complementary to other regions of the *sqt* 3′UTR did not prevent *sqt*-GFP repression by miR-430 (fig. S4). (iv) Injection of sqt-TPs into MZ*dicer* mutants did not affect the levels of *sqt* GFP reporter or *sqt* gene expression, suggesting that TPs do not cause nonspecific stabilization of mRNAs (Fig. 3A and fig. S5). Corresponding results were obtained with lft2-TP$^{miR\text{-}430}$ (Fig. 3B and figs. S2 to S5). To test whether TPs specifically block the interaction with one target site without affecting the interaction with other target sites in the same 3′UTR, we placed a miR-1 target site into the *sqt*–GFP reporter (Fig. 2, F to I). Protection of the miR-430 target site did not prevent miR-1–mediated GFP repression (Fig. 2H), and protection of the miR-1 target site did not interfere with miR-430 mediated repression (Fig. 2I). Taken together, these results indicate that target protection provides a powerful in vivo method to specifically investigate the role of individual miRNA-mRNA target site interactions.

To determine the role of miR-430 repression of *sqt*, we analyzed sqt-TP$^{miR\text{-}430}$ injected embryos. Similar to MZ*dicer* mutants, *sqt* expression was elevated (Fig. 3A). Protection of *sqt* increased the induction of mesodermal marker genes such as *goosecoid* (*gsc*), indicative of higher Nodal signaling during blastula stages (*6*, *8*, *12*) (Figs. 3C and 4B and fig. S6). The increased *gsc* induction resulted from the protection of zygotically transcribed but not maternally loaded *sqt* (fig. S7). Ectopic *gsc* induction in sqt-TP$^{miR\text{-}430}$ injected embryos was suppressed by a morpholino blocking *sqt* translation, indicating that sqt-TP$^{miR\text{-}430}$ specifically increased *sqt* activity (Fig. 3C and fig. S6). To quantify the effects of increased Nodal signaling, we analyzed the number of *sox17*-expressing endoderm progenitors and dorsal forerunner cells during gastrulation (*6*, *8*). Forerunner cells are induced by Nodal signaling at the dorsal margin and form Kupffer's vesicle, an embryonic organ that functions during left-right axis formation (*8*, *13*). Cell counting revealed an increase in the number of endoderm and forerunner cells in sqt-TP$^{miR\text{-}430}$ embryos (Fig. 4, C to E). These results suggest that miR-430 can dampen Nodal signaling by repressing *sqt*.

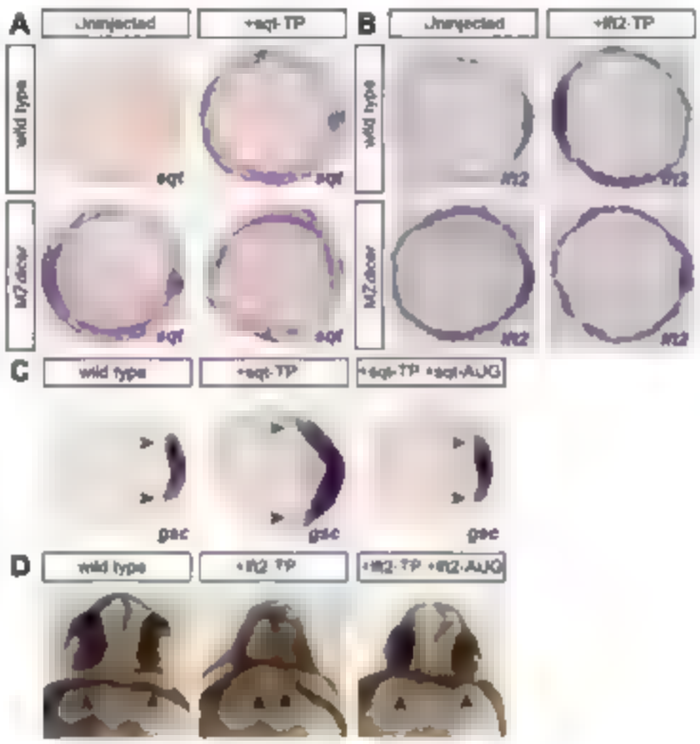

Fig. 3. Target protection results in increased *sqt* and *lft2* expression and activity. (**A**) sqt-TP$^{miR\text{-}430}$ injection results in elevated *sqt* expression, similar to the finding in MZ*dicer* mutants. sqt-TP$^{miR\text{-}430}$ does not increase *sqt* expression in MZ*dicer*. (**B**) lft2-TP$^{miR\text{-}430}$ injection results in elevated *lft2* expression, similar to the finding in MZ*dicer* mutants. (lft2-TP$^{miR\text{-}430}$ does not increase *lft2* expression in MZ*dicer*. (**C**) sqt-TP$^{miR\text{-}430}$–injected embryos exhibit increased *gsc* expression (arrowheads) that is suppressed by co-injection of a *sqt*-AUG morpholino. (**D**) lft2-TP$^{miR\text{-}430}$–injected embryos display cyclopia (arrowheads) that is suppressed by co-injection of a *lft2*-AUG morpholino.

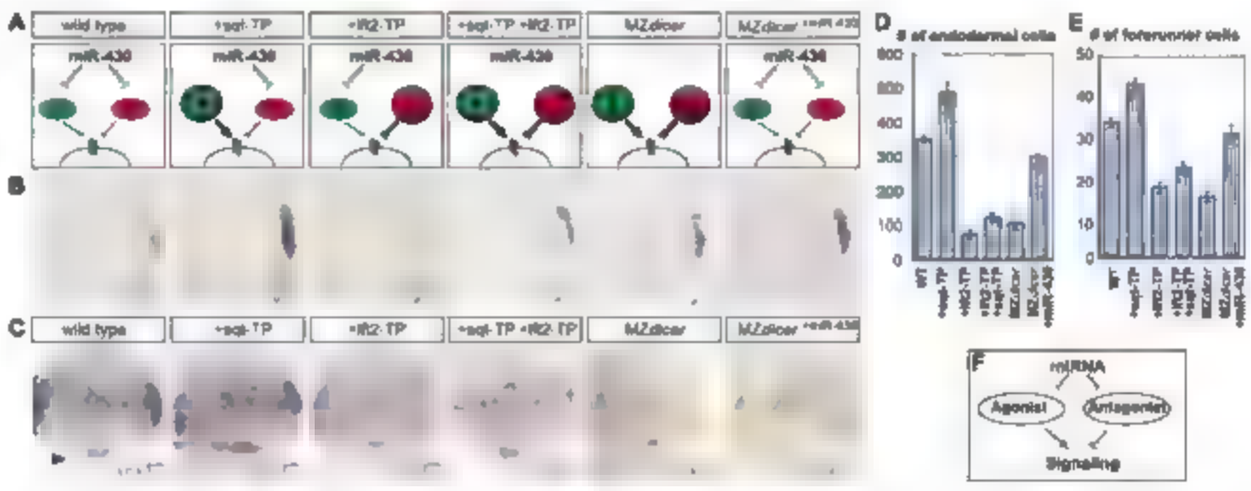

Fig. 4. miR-430 maintains the balance between *sqt* and *lft2*. (**A**) Schematics of miR-430 regulation of *sqt* (S) and *lft2* (L) in wild-type, wild-type + sqt-TP$^{miR\text{-}430}$, wild-type + lft2-TP$^{miR\text{-}430}$, wild-type + sqt-TP$^{miR\text{-}430}$ + lft2-TP$^{miR\text{-}430}$, MZ*dicer*, and MZ*dicer*$^{+miR\text{-}430}$ embryos. Removal of miR-430 regulation in each case results in increased *sqt* and/or *lft2* expression. (**B**) *gsc* expression is increased in sqt-TP$^{miR\text{-}430}$–injected embryos and decreased in lft2-TP$^{miR\text{-}430}$–injected embryos. *gsc* induction is similar in wild-type, wild-type + sqt-TP$^{miR\text{-}430}$ + lft2-TP$^{miR\text{-}430}$, MZ*dicer*, and MZ*dicer*$^{+miR\text{-}430}$ embryos at 50% epiboly. (**C**) *sox17* expression is reduced in wild-type + sqt-TP$^{miR\text{-}430}$ + lft2-TP$^{miR\text{-}430}$ and MZ*dicer* embryos as compared to uninjected wild types at 75% epiboly. *sox17* labels endodermal cells (bracket) and forerunner cells (arrowhead). (**D**) Quantification of *sox17*–expressing endodermal cells ($n = 5$ to 10 embryos for each genotype per injection). (**E**) Quantification of *sox17*–expressing forerunner cells ($n = 12$ to 35 embryos for each genotype per injection). (D and E) Endodermal and forerunner cell numbers vary from embryo to embryo. Bars represent mean ± SEM, which are significantly different between wild-type and wild-type + sqt-TP$^{miR\text{-}430}$ ($P < 0.0005$ by two-tailed Student's *t* test), wild-type and wild-type + lft2-TP$^{miR\text{-}430}$ ($P < 10^{-12}$), wild-type and wild-type + sqt-TP$^{miR\text{-}430}$ + lft2-TP$^{miR\text{-}430}$ ($P < 10^{-7}$), wild-type and MZ*dicer* ($P < 10^{-8}$), wild-type + lft2-TP$^{miR\text{-}430}$ and wild-type + sqt-TP$^{miR\text{-}430}$ + lft2-TP$^{miR\text{-}430}$ ($P < 0.02$), and MZ*dicer* and MZ*dicer*$^{+miR\text{-}430}$ ($P < 10^{-5}$) embryos. (**F**) Model for miRNA-mediated balancing of an agonist and an antagonist.

To determine the in vivo role of miR-430 repression of *lft*, we focused on *lft2* because the repression of *lft2* by miR-430 was more pronounced than it was for *lft1* (Fig. 1A and fig. S2). *lft2* target protection resulted in elevated *lft2* expression, similar to the finding in MZ*dicer* mutants (Fig. 3B). lft2-TP$^{miR-430}$–injected embryos displayed cyclopia, reduced *gsc* expression (Figs. 3D and 4B and fig. S6) (*6*, *8*, *12*), and fewer *sox17*-expressing endodermal and forerunner cells (Fig. 4, C to E). These results indicate that miR-430 can enhance Nodal signaling by dampening *lft2*.

To determine the role of miR-430 in simultaneously dampening both *sqt* and *lft2*, we coinjected sqt-TP$^{miR-430}$ and lft2-TP$^{miR-430}$. The induction of *gsc* was not strongly affected in sqt/lft2-TP$^{miR-430}$ embryos and MZ*dicer* mutants (Fig. 4B), but the expression of *sox17* revealed a reduced number of endodermal and dorsal forerunner cells in sqt/lft2-TP$^{miR-430}$ embryos and MZ*dicer* mutants (Fig. 4, C to E). These results indicate that loss of miR-430 regulation leads to an imbalance of *sqt* and *lft* inputs and reduces some outputs of Nodal signaling.

Our study of miR-430 and Nodal signaling provides two major insights. First, the regulation of *sqt* and *lft2* by miR-430 identifies a role for miRNAs as dampeners and balancers of agonist/antagonist pairs and reveals a previously unknown regulatory layer of Nodal signaling (Fig. 4, A and F, and fig. S1). miR-430 reduces the absolute levels of *sqt* and *lft2* expression (dampening) and regulates their relative levels to achieve optimal activity of the Nodal pathway (balancing). The protection of *sqt* and *lft2* from miR-430 does not appear to lead to major phenotypic changes during blastula stages (*gsc* expression) but reduces Nodal signaling during gastrulation (*sox17* expression). Because Nodal and Lefty signals have complex regulatory interactions (*6*, *7*), multiple mechanisms might contribute to this temporal difference. For example, stronger derepression (Figs. 1A and 3, A and B) and longer persistence of *lft2* after loss of miR-430 regulation could inhibit Sqt and the related Nodal signal Cyclops during gastrulation (*6*, *8*, *12*). The regulation of Nodal signaling by miR-430 is likely to be conserved, because miR-430 is found in other vertebrates (miR-302, miR-372, and miR-519) and predicted miR-430 target sites are present in other *Nodal* and *Lefty* genes (fig. S1) (*4*). More generally, our results reveal a regulatory interaction in which a repressor (miR-430) dampens the expression of both an agonist (*sqt*) and an antagonist (*lft*) (Fig. 4, A and F, and fig. S1). Dampening might not only allow balancing of counteracting inputs but also add robustness (*14*–*18*). For example, our overexpression experiments show that the embryo can tolerate increased expression of miR-430–regulated *sqt* or *lft* mRNA, whereas loss of miR-430–mediated regulation leads to gain-of-function phenotypes (Fig. 1C and fig. S2). mRNA-mediated balancing of agonist/antagonist pairs might also contribute to the evolution of phenotypic changes. The short region of sequence complementarity required for the recognition of miRNA target sites allows for the rapid acquisition, loss, or modulation of miRNA-mRNA target interactions (*19*–*21*). Our results raise the possibility that target sequence variations could change the balance of agonist/antagonist expression and induce phenotypic changes such as the expansion or reduction of progenitor fields.

Second, our study introduces a method to test the role of specific miRNA-mRNA pairs in vivo (fig. S8). Thousands of miRNA-mRNA interactions have been predicted, but less than a dozen have been shown to have an in vivo function (*2*, *3*). The sequence-selectivity of morpholino target protectors makes them excellent agents to disrupt specific miRNA-mRNA interactions. Other antisense oligonucleotides and small molecules that bind to miRNA target sites or their vicinities are also likely to serve as target protectors. Target protectors not only uncover the physiological role of miRNA-mRNA interactions, but also illustrate how miRNA phenotypes are a composite created by up-regulation of multiple targets (fig. S8). Additionally, target protectors might serve as therapeutic agents (fig. S8). More than 30% of all human genes are thought to be miRNA targets (*1*, *3*). By blocking the interaction of specific miRNA-mRNA pairs through the use of target protectors, the translation and stability of particular mRNAs could be increased and result in the suppression of hypomorphic mutations or the up-regulation of beneficial gene products such as tumor suppressors or peptide hormones (fig. S8).

References and Notes

1. M. Bushati, S. M. Cohen, *Annu. Rev. Cell Dev. Biol.* 10.1146/annurev.cellbio.23.090506.123406 (2007).
2. W. P. Kloosterman, R. H. Plasterk, *Dev. Cell* **11**, 441 [illegible].
3. N. Rajewsky, *Nat. Genet.* **38** (suppl.), S8 (2006).
4. A. J. Giraldez *et al.*, *Science* **308**, 833 (2005).
5. A. J. Giraldez *et al.*, *Science* **312**, 75 (2006).
6. A. F. Schier, *Annu. Rev. Cell Dev. Biol.* **19**, 589 (2003).
7. M. M. Shen, *Development* **134**, 1023 (2007).
8. A. F. Schier, W. S. Talbot, *Annu. Rev. Genet.* **39**, 561 (2005).
9. J. Summerton, *Biochim. Biophys. Acta* **1489**, 141 (1999).
10. A. Nasevicius, S. C. Ekker, *Nat. Genet.* **26**, 216 (2000).
11. B. W. Draper, P. A. Morcos, C. B. Kimmel, *Genesis* **30**, 154 (2001).
12. B. Feldman *et al.*, *Nature* **395**, 181 (1998).
13. J. J. Esner, J. D. Amack, M. K. Nyholm, E. B. Harris, M. J. Yost, *Development* **132**, 1247 (2005).
14. D. P. Bartel, C. Z. Chen, *Nat. Rev. Genet.* **5**, 396 [illegible].
15. E. Hornstein, N. Shomron, *Nat. Genet.* **38** (suppl.), S20 (2006).
16. A. Becker, B. B. Kaufmann, A. van Oudenaarden, *Nat. Genet.* **37**, 937 (2005).
17. E. M. Ozbudak, M. Thattai, I. Kurtser, A. D. Grossman, A. van Oudenaarden, *Nat. Genet.* **31**, 69 (2002).
18. J. M. Raser, E. K. O'Shea, *Science* **309**, 2010 (2005).
19. K. Chen, N. Rajewsky, *Nat. Rev. Genet.* **8**, 93 (2007).
20. K. Chen, N. Rajewsky, *Nat. Genet.* **38**, 1452 (2006).
21. A. Clop *et al.*, *Nat. Genet.* **38**, 813 (2006).

22. We thank S. Mango, D. Prober, J. Rihel, C. Stainier, A. Staton, and W. Talbot for helpful comments on the manuscript. A.J.G. was supported by European Molecular Biology Organization and Human Frontier Science Program fellowships. This research was also supported by grants from the NIH.

Supporting Online Material

[illegible]
Materials and Methods
Figs. S1 to S8
References

9 July 2007; accepted 21 August 2007
Published online 30 August 2007
10.1126/science.1147535
Include this information when citing this paper.

PKA Type IIα Holoenzyme Reveals a Combinatorial Strategy for Isoform Diversity

Jian Wu,[1] Simon H. J. Brown,[1] Sventja von Daake,[1] Susan S. Taylor[1,2]*

The catalytic (C) subunit of cyclic adenosine monophosphate (cAMP)–dependent protein kinase (PKA) is inhibited by two classes of regulatory subunits, RI and RII. The RII subunits are substrates as well as inhibitors and do not require adenosine triphosphate (ATP) to form holoenzyme, which distinguishes them from RI subunits. To understand the molecular basis for isoform diversity, we solved the crystal structure of an RIIα holoenzyme and compared it to the RIα holoenzyme. Unphosphorylated RIIα(90-400), a deletion mutant, undergoes major conformational changes as both of the cAMP-binding domains wrap around the C subunit's large lobe. The hallmark of this conformational reorganization is the helix switch in domain A. The C subunit is in an open conformation, and its carboxyl-terminal tail is disordered. This structure demonstrates the conserved and isoform-specific features of RI and RII and the importance of ATP, and also provides a new paradigm for designing isoform-specific activators or antagonists for PKA.

Cyclic adenosine monophosphate (cAMP) is a universal signal for environmental stress. In mammalian cells, major receptors for cAMP are the regulatory (R) subunits of cAMP-dependent protein kinase (PKA) (*1*, *2*). All R subunits share the same domain organiza-

tion that includes a dimerization/docking (D/D) domain at the N terminus and two tandem C-terminal cAMP-binding (CNB) domains (domains A and B). The linker joining the D/D and CNB domains is highly disordered in dissociated dimers (*3*) and contains an inhibitor site that resembles a peptide substrate and docks to the active site of the catalytic (C) subunit in the holoenzyme, thereby blocking its activity.

The two major classes of R subunit (I and II) each have α and β isoforms. The isoforms are functionally nonredundant, and isoform diversity is a primary mechanism for achieving specificity in PKA signaling (*4*). The inhibitor site is a distinguishing feature of the isoforms. RII subunits have a phosphorylation site in their inhibitor motif and thus are both substrates and inhibitors, whereas RI subunits with Ala or Gly at the P-site are pseudo-substrates. RI subunits require ATP and two Mg^{2+} ions to form a stable holoenzyme complex (binding affinity K_d = 0.1 nM) (*5*), whereas RII subunits do not (K_d = 0.1 nM).

Although the structures of the open and closed conformations of the C subunit (*6*, *7*) and the cAMP-bound structures of RIα and RIIβ (*8*, *9*) have been solved, they do not explain how C is inhibited by R, how the holoenzyme is activated by cAMP, and how the isoforms differ. To understand the molecular basis for differential regulation of type I and type II holoenzymes, we purified a deletion mutant of RIIα, RIIα(90–400), and cocrystallized it with the Cα subunit in the absence of ATP, then compared it to the RIα holoenzyme (*10*, *11*). In contrast to the C subunit's fully closed conformation in the type I holoenzyme, in the RIIα complex the C subunit is in an open conformation, the ATP binding pocket is empty, the αB/αC helix is distorted, and the C-terminal tail is disordered. Like RIα, RIIα undergoes major conformational changes as it wraps around the large lobe of the C subunit. The hallmarks of this conformational switch are changes associated with the helical subdomains of both cAMP-binding domains. Most striking is the helix switch in domain A, which snaps apart the two CNB domains. In the holoenzyme, domain B of RIIα docks onto the αH-αI loop of the C subunit.

This structure demonstrates the combinatorial diversity of the C subunit as it uses diverse sets of docking motifs to interact in unique ways with different inhibitors, and we presume that this diversity is also related to recognition of different protein substrates. The structure also demonstrates how ATP differentially regulates these two holoenzymes. ATP is essential for forming the type I holoenzyme, much as guanosine triphosphate (GTP) is essential for generating the active conformation of heterotrimeric GTP-binding proteins (G proteins), whereas in type II holoenzymes, ATP, through autophosphorylation, actually promotes dissociation.

A monomeric deletion mutant of RIIα was cocrystallized with the wild-type Cα subunit in the absence of Mg_2ATP (for statistics, see table S1). The structure reveals a large interface that engages the entire RIIα subunit but only the large lobe of the C subunit (Fig. 1). The C subunit, with the exception of a distorted αB-αC loop, assumes an open conformation. The active-site cleft is open and the C-terminal tail (residues 319 to 331) is disordered (Figs. 2 and 3). The inhibitor

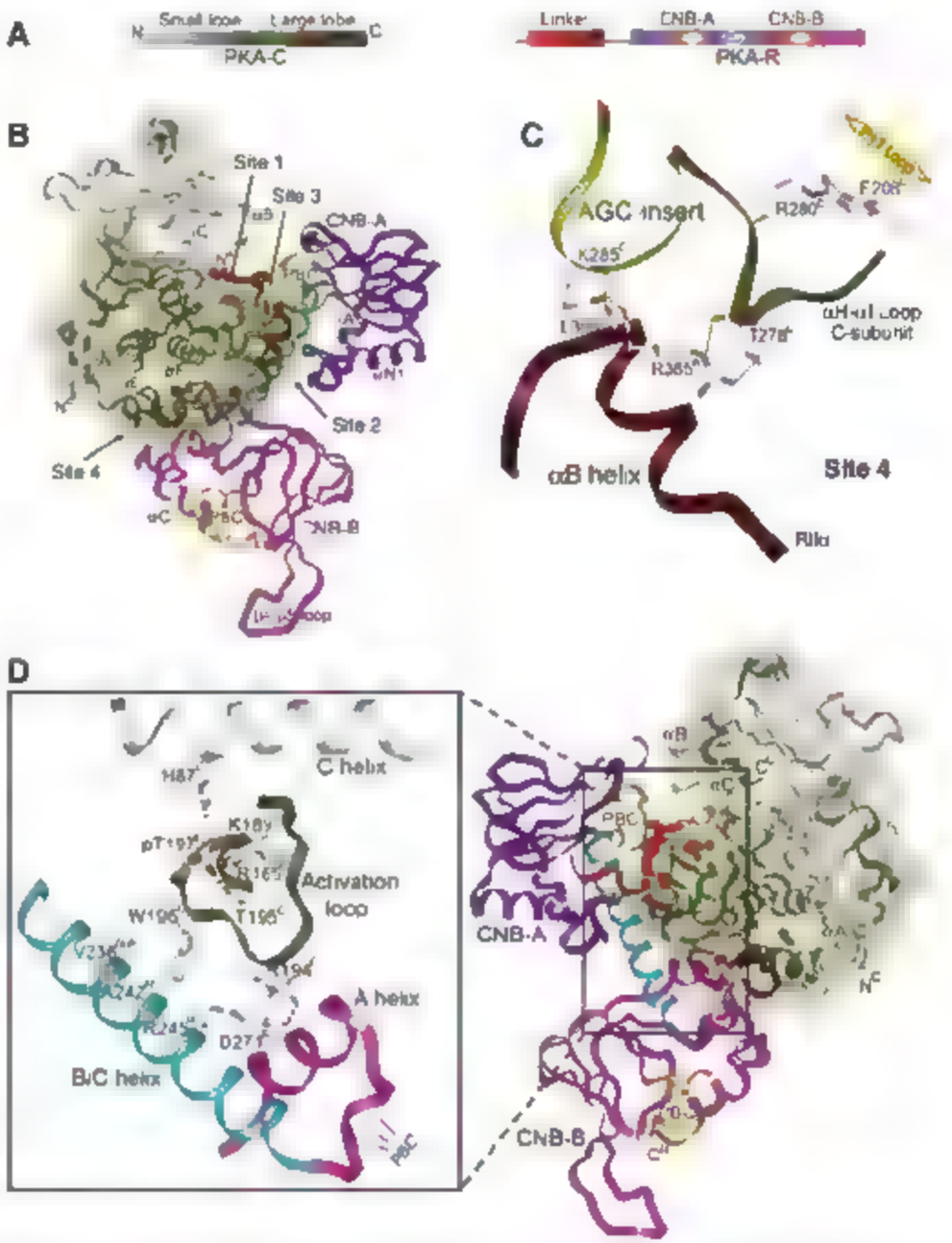

Fig. 1. Overall architecture of the RIIα(90-400)–C holoenzyme. (**A**) General domain organization and color coding for the R and C subunits. The small and large lobes of C are shown in gray and tan, respectively, with the position of the αG and αH-αI loops highlighted in dark red. The A and B domains of R are in purple and magenta, respectively, with the linker region in red, αB-αC in cyan, and the two PBCs in yellow. (**B**) The RIIα holoenzyme structure with the C subunit shown in its classic view with a shadowed space-filling surface. Site 1 (inhibitor site), site 2 (αG helix and P+1 loop), site 3 (activation loop and APE-αF loop), and site 4 (αH-αI loop) are indicated. Helices are labeled periodically to help track the Cα trace. (**C**) Essential features of site 4. The αB helix of RIIα (dark red) is shown docked to the αH-αI loop in C (tan). The AGC-specific insert is highlighted in yellow. The Arg^{280C}-Glu^{208C} ion pair connecting the αH-αI loop to the P+1 loop is also shown. (**D**) The 180° rotation of the complex, with the red and yellow circles indicating $pThr^{197C}$ and the P-site Ser of RIIα, respectively. Expanded at the left are the essential elements of the R-C interface: the αC helix and activation loop of C, as well as the αB/αC helix and the αA helix of domain B in RIIα.

[1]Department of Chemistry and Biochemistry, University of California, San Diego, La Jolla, CA 92093, USA. [2]Howard Hughes Medical Institute, University of California, San Diego, La Jolla, CA 92093, USA.

*To whom correspondence should be addressed. E-mail: staylor@ucsd.edu

site and linker region, which are disordered in the free RII subunit, become ordered in the holoenzyme. Docking of domain A onto the large lobe of the C subunit creates an extended interface, whereas domain B contributes a small, but essential docking motif that binds to the αH-αI loop on the C subunit (Fig. 1, B and C).

The large lobe of the C subunit functions as a stable scaffold for RIIα, with the binding interface extending from the common inhibitor binding site at the active-site cleft, over the activation loop and the P+1 loop, to the αH-αI loop (Fig. 1 and fig. S1). ATP is not required for this high-affinity binding (~1.0 nM). The C subunit is in an open conformation similar to that of the apoenzyme (*6*) (Fig. 2 and fig. S2). The small lobe is more dynamic than the large lobe, as indicated by the disorder of many side chains and the discontinuity of the C-terminal tail. Comparison of average temperature factors (*B* factors) for the RIIα and RIα holoenzymes reveals a striking isoform difference in dynamics (Fig. 3C). In both holoenzymes there is 70% water content, and crystal packing does not influence the small lobe.

In contrast to the C subunit, RIIα undergoes major conformational changes in almost its entire molecular architecture relative to the unbound structure. Each domain contains α and β subdomains. The β sandwich harbors the signature motif of the CNB, the phosphate-binding cassette (PBC), where the phosphate moiety of cAMP docks. The release of cAMP uncouples the α and β subdomains (*12*), thus allowing for global conformational changes in the helices that are induced and stabilized by binding of the C subunit. RIIα undergoes three major changes: (i) ordering of the inhibitor peptide and the following linker segment; (ii) reorganization of the helical subdomains of domain A, which leads to the separation of domains A and B; and (iii) reorganization of the helical subdomain of domain B to accommodate docking to the αH-αI loop in the C subunit. With this structure we can appreciate the conservation of the dynamic uncoupling of the A and B domains as they release cAMP and bind to the C subunit.

For simplicity, we divide the large R-C interface into four distinct sites on the C subunit (Fig. 1). Site 1, where the inhibitor peptide docks to the active-site cleft, most clearly distinguishes the R-subunit isoforms. Site 2 is dominated by the αG helix and the P+1 loop, site 3 includes the activation loop and the APE-αF loop, and site 4 is the αH-αI loop. The RII-specific features of sites 1 and 4 are described in detail below; sites 2 and 3 are discussed in (*13*).

Because RII subunits are substrates as well as inhibitors, they engage the active-site cleft differently from RIα subunits. RIIα(90–400) begins with Arg^{92R}-Arg-Val-Ser-Val^{96R}, where Ser^{95R} is the unphosphorylated P-site. (For clarity, we adopt a nomenclature where residues from the R and C subunits are respectively designated by superscripts R and C.) The positions of the backbone and side chains in this segment are nearly identical to those of the protein kinase inhibitor peptide PKI(5-24) and RIα, even though both PKI and RIα, with Ala at the P-site, are pseudosubstrates (Fig. 3). The C subunit in the RIIα holoenzyme structure assumes an open conformation, in contrast to the fully closed conformation found in the PKI(5-24)-C complex (*7*) and the RIα holoenzyme (*10*, *11*). Because the RIIα and C subunits were cocrystallized in the absence of MgATP, there is no phosphate on Ser^{95R}. In the presence of ATP the inhibitor site would undergo autophosphorylation, which reduces the affinity of RIIα for the C subunit (*14*).

A major isoform difference is that each residue from the five-residue peptide is docked firmly onto the large lobe, neither the small lobe nor the C-terminal tail is involved (Fig. 2C and fig. S2). In contrast, recruitment of the small lobe and the C-terminal tail are essential for RIα and PKI, where the γ-phosphate of ATP is trapped between the two lobes, as it is in the transition state during catalysis (*15*). Instead, in the RIIα holoenzyme, the P-site Ser forms hydrogen bonds with catalytic loop residues that are anchored to the P+1 loop (Fig. 2C).

The P+1 Val, disordered in the free RII subunit, docks onto the P+1 loop and nucleates the hydrophobic interface between RIIα and C by interacting with Tyr^{247C} in the αG helix of C and Tyr^{209R} in the PBC of RIIα (fig. S1). Although Tyr^{247C} does not change much relative to its position in the free C subunit, Tyr^{209R} is recruited because of the rearrangement of domain A. This hydrophobic docking surface, which is similar to RIα (*10*, *11*), is discussed in (*13*).

In addition to the P-site residue, the linker regions account for considerable variation in overall organization of full-length RI and RII subunits and their corresponding holoenzymes (*16*–*18*). In previous cAMP-bound structures of RIα and RIIβ, the linker region was always disordered (*8*, *9*). Figure 3 and fig. S3 highlight some of the RII-specific interactions in this region. Glu^{99R}, for example, causes a distortion of the αB-αC loop relative to all previous C-subunit structures (Fig. 2) and is essential for forming type II, but not type I, holoenzymes (*19*). The importance of other RII-specific sites in the linker is discussed in (*13*).

The αH-αI loop (Fig. 1, B and C) is an important docking site for domain B. This region contains a five-residue insert (residues 282^C to 287^C) that is unique to the AGC kinases (*20*). It also contains Arg^{280C}, the last highly conserved residue in the kinase core, which forms ion pairs with Glu^{230C} in the APE motif at the end of the P+1 loop. Recent genetic studies suggest that there is feedback between this region and the peptide recognition site (*21*). This site is thus likely to be a "hot spot" for allosteric regulation at several levels.

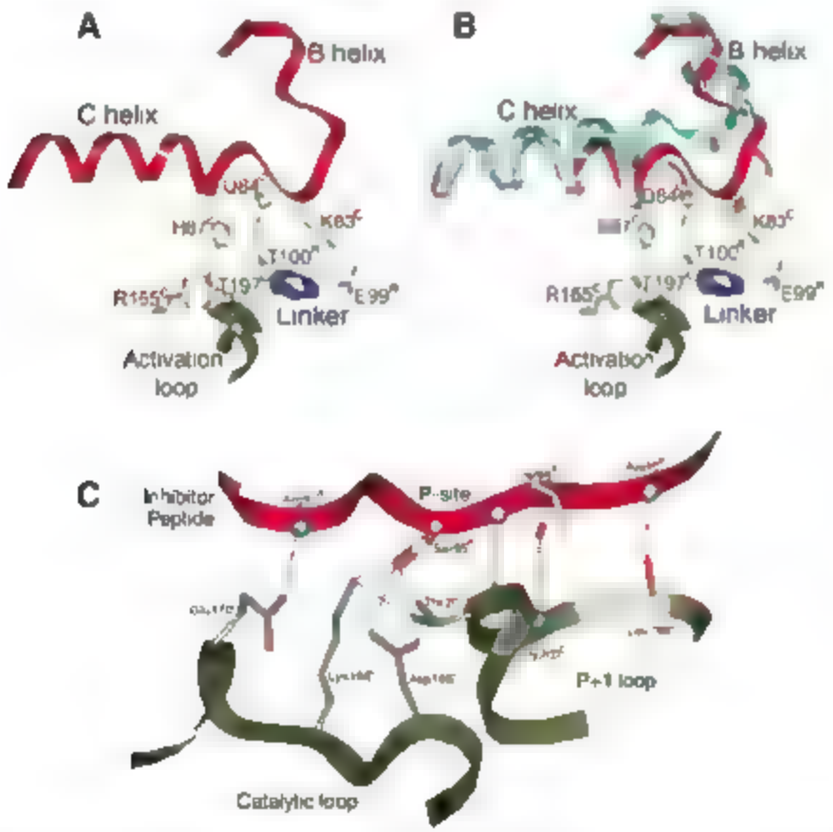

Fig. 2. The C subunit is in an open conformation. (**A**) The H-bond interactions between the αB and αC helices with activation loop and RI α linker are indicated in dashed lines. (**B**) Comparison of the αB-αC segment to the same region in the wild-type apoenzyme (in cyan) and a closed state of the C subunit (in white). (**C**) P-site Ser is centered on the preformed active site. In the absence of MgATP, Ser^{95R}, the P-site residue, forms hydrogen bonds with Asp^{166C} and Lys^{168C} from the catalytic loop. The peptide forms a short antiparallel β strand with a segment of the P+1 loop.

When holoenzyme forms, major changes take place in the CNB domains of RIIα. The global change in architecture that splays apart domains A and B is due to the long contiguous helix that is formed by the merging of the αB and αC helices in domain A (Fig. 4 and fig. S4). Changes in domain B are also substantial but different (figs. S4 and S5). Both hydrophobic capping residues for cAMP lie in domain B and are displaced by this movement. In contrast to the helical subdomains, both β subdomains are stable with the exception of the PBC.

Domain A provides the major isoform-independent docking surface for the C subunit and also mediates the global reorganization of the two CNBs. The most striking change is the "αB/αC switch" where the linked αB and αC helices of the cAMP-bound state snap into a fully extended single helix. This αB/αC switch, a conserved feature of both isoforms (Fig. 4 and fig. S4), not only separates the two CNB domains but also removes the capping residue for site A. The αB/αC motif provides a major interacting surface for docking to the C subunit (Fig. 1D) as well as to the linker region (fig. S3), with many residues previously exposed to solvent now serving to nucleate the RIIα-C interface (*13*).

In addition to being "flipped away" from domain A, domain B also undergoes major conformational changes within its helical subdomain. In domain B of RIIα the hydrophobic capping residue for cAMP is Tyr^{361R}, which is located within its own αC helix, similar to catabolite activator protein (CAP) (*22*); in the holoenzyme, Tyr^{361R} is no longer close to the PBC because of the conformational changes (Fig. 4). However, the αC helix does not fuse with the αB helix but forms a helix-turn-helix (αC′-αC″) motif (Fig. 4B and fig. S4). In the holoenzyme, Tyr^{361R} is exposed to solvent.

Although the cAMP-bound structures of RIα and RIIβ enabled the identification of residues essential for cAMP binding (*8*, *9*), the functions of other conserved residues were not explained. Their conserved functions are revealed only by the two holoenzyme structures. Arg^{376R} is an example. The electrostatic contact between Arg^{376R} in the αC helix and Glu^{260R} in the αA helix of domain B is a conserved feature of both holoenzymes, whereas in the cAMP-bound state both residues are exposed to solvent. This electrostatic interaction stabilizes the capping residues in both holoenzyme conformations, even though the location of the A-site capping residue is isoform-specific (Fig. 4B). Arg^{365R} in the αB helix is a conserved part of the R-C interface for both holoenzymes, where it forms essential multivalent interactions with Lys^{285C} in the AGC-specific insert that lies in the αH-αI loop (Fig. 1C). In RII subunits, however, Arg^{365R} is also the capping residue for cAMP bound to site A. Other residues such as Arg^{213R} and Glu^{204R} in the PBC play a conserved role in binding cAMP but are exposed to solvent in the holoenzymes. The roles of many key residues in each conformational state are summarized in table S2.

A tyrosine at the tip of the PBC is another highly conserved feature of A domains. In both holoenzyme structures this tyrosine is essential for docking to C (figs. S1 and S4). The environment of this tyrosine, however, is isoform-specific. In RIIα Tyr^{204R} is part of an extended hydrogen-bonding network, where it anchors the PBC of domain A to two essential elements in the helical subdomain of domain B. In RIα, Tyr^{205R} is exposed to solvent (fig. S4).

Comparison of the holoenzyme structures shows the wide dynamic range of the CNB domains (*23*). The A domains in both RI and RII are similar in their cAMP and holoenzyme conforma-

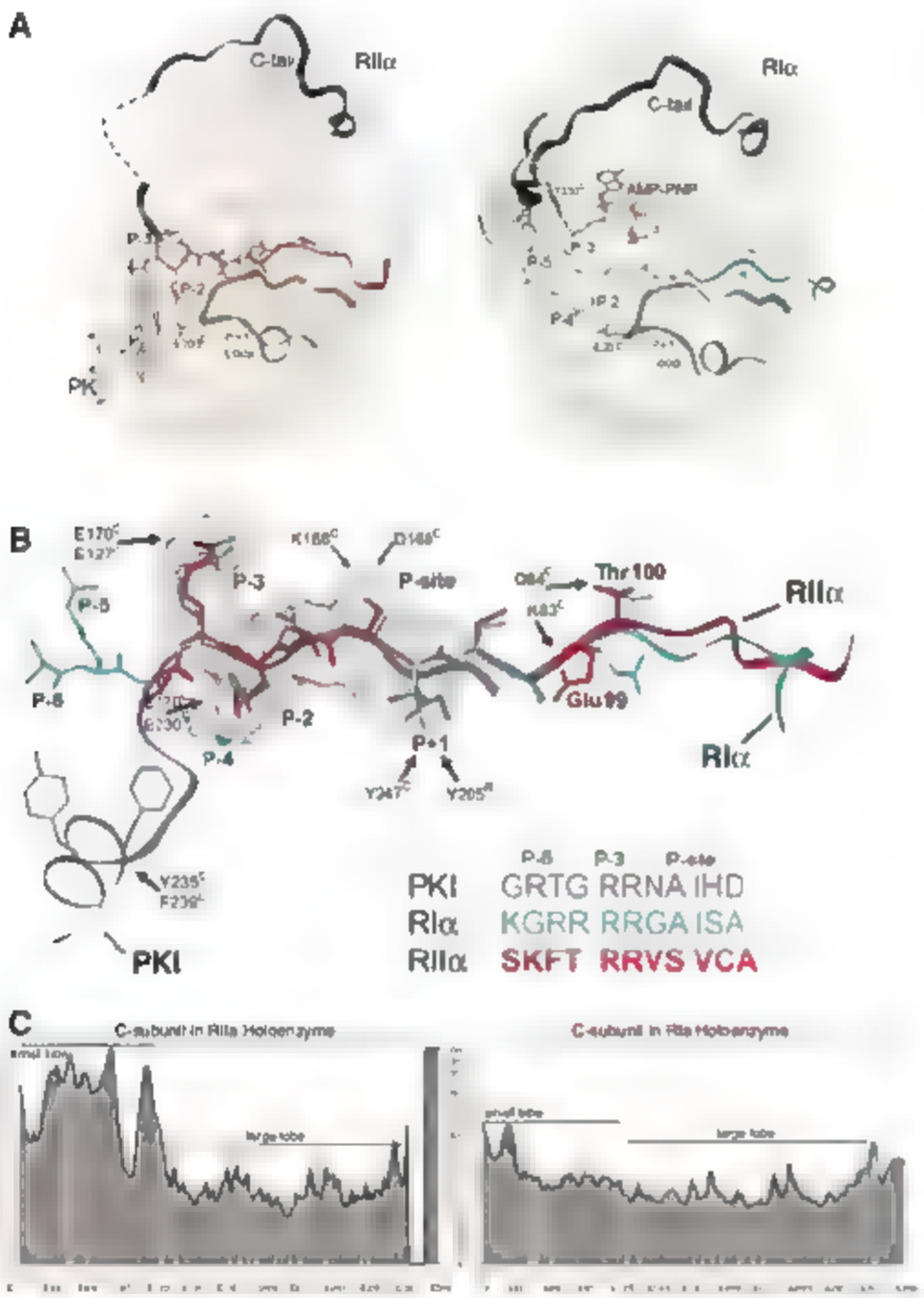

Fig. 3. Interactions of the inhibitor peptides with the active site. (**A**) The C subunits from RIIα and RIα holoenzymes, as shown in a space-filling format, with the small lobes in gray and the large lobes in tan. Both C-terminal tails are shown as a black ribbon, and a dashed link points to the disordered region in RIα. The inhibitor peptides, in red for RIIα and in cyan for RIα, are highlighted. We predict that the peptide of RIIα will continue interacting with the large lobe, in a manner similar to PKI. However, this region in the RIα holoenzyme structure further anchors the C-terminal tail (*21*). (**B**) Superimposition of RIIα peptide (in red) with those of RIα (in cyan) and PKI (in gray). The regions from P−3 to P+1 are very similar, whereas their N-termini use different docking surfaces on C. Their sequence comparison is also shown (*25*). (**C**) *B*-factor plots of C in the RIIα holoenzyme compared to the RIα holoenzyme. The *x* axis corresponds to the residue numbers, the *y* axis corresponds to the *B*-factor value scale.

tions. The B domains are also similar. However, the holoenzyme conformations of the A and B domains are different from each other (fig. S5). Thus, there is not a conserved mechanism for snapping open the αB-αC helix into a single fused helix.

To appreciate the versatility of the C subunit, one needs to consider it as a scaffold. Figure 4C and fig. S6 summarize the different parts of the C subunit that can be recruited to recognize its inhibitors (RI, RII, and PKI). Each inhibitor must accomplish two things: It must bind with high affinity and also must inhibit catalytic activity. A substrate-like inhibitor sequence is required for inhibition but is not sufficient for high-affinity binding. For both R subunits to achieve high-affinity binding, docking of domain A to the large lobe of the C subunit (sites 2/3) is essential; however, this is not sufficient. In addition to domain A, RI subunits require the N-lobe and C-tail coupled through Mg_2ATP to the inhibitor site (*24*), whereas RII subunits require site 4 coupled to domain B. Like RIα, PKI uses the N-lobe and C-tail, plus Mg_2ATP, but achieves high affinity by using another site entirely, the αF-αG loop (site 5) (*7*).

RI subunits and PKI both induce a fully closed conformation and require Mg_2ATP (*5*), where the γ-phosphate of ATP brings together both lobes (Fig. 4C). Because the inhibitor peptide is a pseudo-substrate and lacks a P-site acceptor, ATP traps the complex in an inactive state, much as GTP traps G proteins in an active state. Formation of RII holoenzyme does not require the N-lobe, the C-tail, or Mg_2ATP. Because the P-site is a Ser, RII subunits cannot trap the R-C complex in a stable transition state; instead, the P-site Ser is anchored to the large lobe (Fig. 4C). For RII holoenzymes, ATP facilitates dissociation through autophosphorylation of the P-site rather than stabilizing the inhibited state (*14*). A corollary for these two models is that RII holoenzymes depend exclusively on cAMP for activation, whereas RI holoenzymes can be regulated by Mg and ATP as well as by cAMP. These two holoenzymes provide a basis for designing novel isoform-specific activators and inhibitors of PKA.

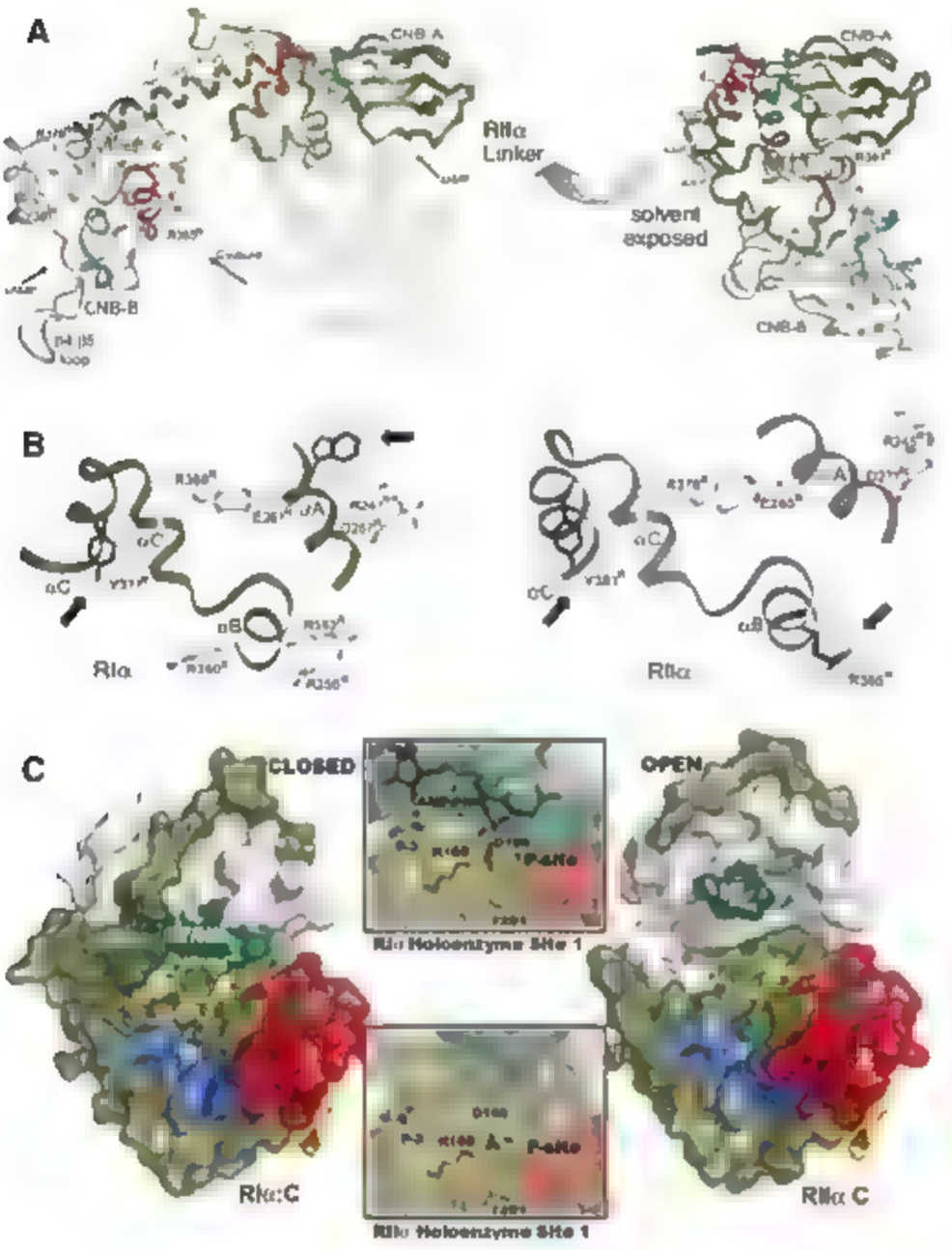

Fig. 4. Rearrangements of CNB domains. (**A**) Global change in domain B is due to the extension of the αB-αC helix into a single long helix. There is a ~120° flip from the cAMP-bound state (right) compared to its R-C complex state (left). The position of domain B in the cAMP-bound state is shown by a transparency on the left. The αB helices from both CNBs, shown in red, are essential docking motifs. The PBCs are shown in dark green. Also labeled are the capping residues (Arg^{365R} for site A and Tyr^{381R} for site B), a salt bridge pair (Arg^{376R}-Glu^{265R}), and four basic residues that dock to the RIIα linker. In the cAMP-bound state, these basic residues are exposed to solvent. (**B**) The capping residues (shaded and indicated by arrows) for RIα and RIIα in their holoenzyme conformation are far from their respective cAMP binding sites. A novel salt bridge (Arg^{366R}-Glu^{262R} for RIα, Arg^{376R}-Glu^{265R} for RIIα) is formed only upon holoenzyme formation. (**C**) The combinatorial diversity for the C subunit is demonstrated by shading the surface of the docking motifs that are used for binding different inhibitors (RI, RII, and PKI). Site 1, where the inhibitor peptide (yellow) docks, is essential for inhibition. Site 1 in each holoenzyme is expanded at the center of the panel. The other sites [N-lobe and C-tail in green, αG helix (site 2) in red, activation loop (site 3) in dark red, αH-αI loop (site 4) in yellow, and the αF-αG loop (site 5) in blue] are used in a combinatorial fashion to achieve high-affinity binding.

References and Notes

1. G. N. Gill, I. D. Garren, *Proc. Natl. Acad. Sci. U.S.A.* **68**, 786 (1971).
2. S. S. Taylor, J. A. Buechler, W. Yonemoto, *Annu. Rev. Biochem.* **59**, 971 (1990).
3. F. Li *et al.*, *Biochemistry* **39**, 15626 (2000).
4. P. S. Ameua, G. S. McKnight, *Ann. N.Y. Acad. Sci.* **968**, 75 (2002).
5. F. W. Herberg, S. S. Taylor, *Biochemistry* **32**, 14015 (1993).
6. P. Akamine *et al.*, *J. Mol. Biol.* **327**, 159 (2003).
7. J. Zheng *et al.*, *Acta Crystallogr. D* **49**, 362 (1993).
8. Y. Su *et al.*, *Science* **269**, 807 (1995).
9. T. C. Diller Madhusudan, N. H. Xuong, S. S. Taylor, *Structure* **9**, 73 (2001).
10. C. Kim, N. H. Xuong, S. S. Taylor, *Science* **307**, 690 (2005).
11. C. Kim, C. Y. Cheng, S. A. Saldanha, S. S. Taylor, *Cell* **130**, 1032 (2007).
12. R. Das *et al.*, *Proc. Natl. Acad. Sci. U.S.A.* **104**, 93 (2007).
13. See supporting material on *Science* Online.
14. J. Erlichman, R. Rosenfeld, O. M. Rosen, *J. Biol. Chem.* **249**, 5000 (1974).
15. Madhusudan *et al.*, *Nat. Struct. Biol.* **9**, 273 (2002).
16. D. Vigil *et al.*, *J. Mol. Biol.* **337**, 1183 (2004).
17. D. Vigil, O. K. Blumenthal, S. S. Taylor, J. Trewhella, *J. Biol. Chem.* **280**, 35521 (2005).
18. W. T. Heller *et al.*, *J. Biol. Chem.* **279**, 19084 (2004).
19. R. M. Gibson, Y. Ji-Buechler, S. S. Taylor, *J. Biol. Chem.* **272**, 16343 (1997).
20. M. Kannan, N. Haste, S. S. Taylor, A. F. Neuwald, *Proc. Natl. Acad. Sci. U.S.A.* **104**, 1272 (2007).

21. S. J. Deminoff, S. C. Howard, A. Hester, S. Warner, P. K. Herman, *Genetics* **173**, 1909 (2006)
22. N. M. Berman *et al.*, *Proc. Natl. Acad. Sci. U.S.A.* **102**, 45 (2005)
23. H. Rehmann, A. Wittinghofer, J. L. Bos, *Nat. Rev. Mol. Cell Biol.* **8**, 63 (2007)
24. L. J. Huang, S. S. Taylor, *J. Biol. Chem.* **273**, 26739 (1998)
25. Abbreviations for amino acid residues: A, Ala; C, Cys; D, Asp; E, Glu; F, Phe; G, Gly; H, His; I, Ile; K, Lys; L, Leu; M, Met; N, Asn; P, Pro; Q, Gln; R, Arg; S, Ser; T, Thr; V, Val; W, Trp; Y, Tyr
26. We thank the Advanced Light Source for assistance in data collection, E. Radzio-Andzelm for assistance in preparation of the figures, and M. Deal for purification of the C subunit. Supported by NIH grant GM34921 (S.S.T.) and NIH training grant T32-CA009524 (S.H.J.B.). The coordinate and structure factor are deposited with the Protein Data Bank (PDB accession code 2QVS).

Supporting Online Material
www.sciencemag.org/cgi/content/full/318/5848/274/DC1
Materials and Methods
Figs. S1 to S6
Tables S1 and S2
References

13 June 2007; accepted 11 September 2007
10.1126/science.1146447

Fluorescence-Force Spectroscopy Maps Two-Dimensional Reaction Landscape of the Holliday Junction

Sungchul Hohng,[1,2]* Ruobo Zhou,[1] Michelle K. Nahas,[1] Jin Yu,[1,4] Klaus Schulten,[1,3,4] David M. J. Lilley,[5] Taekjip Ha[1,2,3,4]†

Despite the recent advances in single-molecule manipulation techniques, purely mechanical approaches cannot detect subtle conformational changes in the biologically important regime of weak forces. We developed a hybrid scheme combining force and fluorescence that allowed us to examine the effect of subpiconewton forces on the nanometer scale motion of the Holliday junction (HJ) at 100-hertz bandwidth. The HJ is an exquisitely sensitive force sensor whose force response is amplified with an increase in its arm lengths, demonstrating a lever-arm effect at the nanometer-length scale. Mechanical interrogation of the HJ in three different directions helped elucidate the structures of the transient species populated during its conformational changes. This method of mapping two-dimensional reaction landscapes at low forces is readily applicable to other nucleic acid systems and their interactions with proteins and enzymes.

Many biological processes are dependent on tension. In recent years, single-molecule force measurements have shown directly that biochemical reactions can be influenced by applied force (*1*). Yet, purely mechanical tools cannot detect small-scale conformational changes unless strong and persistent force is applied. At weak forces, the flexible tether connecting the mechanical probe to the biological molecule is not stretched enough to transmit small movements. This is unfortunate because weak and transient forces are likely more prevalent in vivo, but the experimental limitations confine single-molecule mechanical studies to examining the effect of relatively large forces. We aimed to study the effect of weak external forces on the biomolecular conformational dynamics by combining single-molecule fluorescence resonance energy transfer (smFRET) (*2*–*4*) with manipulation using optical trap (*5*). smFRET has high spatial resolution [< 5 Å (*6*, *7*)] and can be measured at arbitrarily low forces. Previous attempts to combine FRET and optical trap using the DNA hairpin as a model system (*8*, *9*) did not reveal new information because the hairpin unzips at high forces (~15 pN), a regime that had been extensively investigated using force-based techniques (*10*, *11*). Here, we report an approach to detect nanometer-scale motion at sub-pN forces. We used the approach to gain insight into the reaction landscape of the Holliday junction (HJ) by gently stretching it along different directions.

The HJ is a four-stranded DNA structure that forms as an intermediate during recombination (*12*). To understand the mechanisms of cellular enzymes that function with the HJ, a detailed description of the static and dynamic structural properties of the HJ itself is needed. In the absence of added ions, the HJ adopts an open structure, where the four helical arms point toward the corners of a square (*13*, *14*) (Fig. 1A). In the presence of physiological concentrations of magnesium ions, the HJ becomes more compact by pairwise coaxial stacking of helical arms into a right-handed antiparallel stacked-X structure (*13*–*15*). There are two ways of forming this stacked structure that depend upon the choice of helical stacking partners (*isoI* and *isoII*) (Fig. 1B). For these studies, we have chosen a sequence with nearly equal population of stacking conformers *isoI* and *isoII* (*16*) (*17*) (fig. S1). smFRET studies showed that an HJ continually switches between the two stacking conformations (*18*). At present, there is no structural information on the transient species populated during these conformational changes.

To investigate the nature of such transient HJ structures and to understand how HJ conformational properties could depend on physiologically relevant forces, we built a hybrid instrument that combines smFRET with optical trapping via a long linker (bacteriophage λ DNA) (*17*). The trapping and fluorescence excitation beams in our confocal microscope are spatially separated (minimum 13 μm) (Fig. 1C), such that fluorescence and force processes can operate without mutual interference. The long linker acts as a loose spring that dampens the random forces generated by Brownian motion of the trapped bead and reduces force variations due to the nanometer-scale conformational change of the HJ. The effective stiffness of the λ DNA at 2 pN of force is about 0.002 pN/nm, such that a 5-nm movement of the HJ causes negligible force fluctuations (~0.01 pN) at the trapped bead. Therefore, the measurements can be performed under effectively constant force without the need for active force clamping. The relaxation time scales of the λ DNA under tension are faster than the time scale of conformational fluctuations we investigated (*19*). The trapping beam (1064 nm) was fixed along the optical axis of the microscope, and force was applied by moving the surface-tethered HJ using a piezoelectric sample scanner. The confocal excitation beam (532 nm) was programmed to follow the HJ using a piezo-controlled mirror to maintain uniform excitation and detection efficiencies regardless of the specimen location (and therefore force) (*17*).

To determine comprehensively the force response of the HJ, we used the following four constructs (Fig. 1A). The four helices composing the HJ are named B (red), H (green), R (dark gray), and X (gray). Helix R was labeled at its 5′ terminus with biotin for surface immobilization, and helices X, H, or B were extended by a 12-nt single-stranded DNA 5′ overhang to permit annealing to a cohesive end of λ DNA (named junctions *XR*, *HR*, and *BR*, respectively). The other end of the λ DNA was attached to a bead via digoxigenin/anti-digoxigenin coupling in order to pull on the DNA using optical tweezers in three different directions, between the X and R arms for junction *XR*, and so on. Junctions *XR* and *XR*-long differ in the length of the X and R arms [11 base pairs (bp) versus 21 bp]. Cy3 (FRET donor) was attached to the end of helix H, and Cy5 (acceptor) to the end of helix B. For

[1]Department of Physics, University of Illinois at Urbana-Champaign, Urbana, IL 61801, USA. [2]Howard Hughes Medical Institute, Urbana, IL 61801, USA. [3]Center for Biophysics and Computational Biology, University of Illinois at Urbana-Champaign, Urbana, IL 61801, USA. [4]Beckman Institute, University of Illinois at Urbana-Champaign, Urbana, IL 61801, USA. [5]Cancer Research UK Nucleic Acid Structure Research Group, MSI/WTB Complex, University of Dundee, Dundee DD1 5EH, UK.
*Present address: Department of Physics and Astronomy, Seoul National University, Seoul 151-742, Korea.
†To whom correspondence should be addressed. E-mail: tjha@uiuc.edu

junctions *XR* and *XR*-long, the stretching force should favor *isol* (low FRET), in which there is a larger separation between the two tether points, over *isoII* (high FRET) (Fig. 1D). Indeed, single-molecule FRET histograms as a function of force show that the low FRET state is significantly favored at forces exceeding 0.5 and 1.0 pN for junctions *XR*-long and *XR*, respectively (Fig. 1, E and F). Likewise, *isoII* (high FRET) would be favored at high forces for junction *HR*. In contrast, the two tether points would have similar distances for *isol* and *isoII* in the case of junction *BR*, and force-induced bias should be minimal.

Figure 2A shows smFRET time traces at five different forces (gray lines, 10 s duration each, with 10 ms integration time) obtained from a single molecule of junction *XR*. Enhanced photostability by means of the use of Trolox (*20*) allowed us to obtain one to five cycles of force data from a single molecule before photobleaching, corresponding to observation over 50 to 250 s. Idealized FRET trajectories generated by hidden Markov modeling (red lines) (*21*) are also shown. At the lowest force (0.3 pN), the junction switches between the high and low FRET states with similar populations. As the force exceeds 1 pN, the dynamics become clearly biased to the low FRET state. Figure 2B shows the transition rates determined from hidden Markov modeling as a function of force. The transition rate k_f for the forward reaction from the low FRET state (*isol*) to the high FRET state (*isoII*) decreases with increasing force (blue), whereas the transition rate for the backward reaction k_b (*isoII* to *isol*) increases with force (red) as expected. Both changes were linear in the log-linear scale but, interestingly, k_f had twice the slope of k_b. If the reaction is viewed as possessing a single transition state, the slope reflects the distance to the transition state (*1*). Therefore, the transition state lies closer to *isoII* than to *isol* when force is applied by the *XR* vector. Averaged over five molecules, the distance from *isoII* to the transition state ($\Delta x_b^{\ddagger}$) is 1.5 ± 0.3 nm, and the distance from *isol* to the transition state ($\Delta x_f^{\ddagger}$) is 2.9 ± 0.6 nm (Table 1).

We next studied junction *HR*, where the λ DNA tether has been transferred from the X to the H arm. In this construct, the force is expected to bias the HJ to the high-FRET *isoII* state, and indeed this was the result (Fig. 2C). k_b decreased and k_f increased with stronger forces, but with a slope twice as high for k_b as for k_f (Fig. 2D). Averaged over five molecules, $\Delta x_b^{\ddagger}$ = 2.4 ± 0.5 nm and $\Delta x_f^{\ddagger}$ = 1.3 ± 0.3 nm. In both junctions, ($\Delta x_b^{\ddagger}$ + $\Delta x_f^{\ddagger}$) is equal to the distance between *isol* and *isoII*, Δx_{eq}, calculated from equilibrium population versus force data (Table 1). Therefore, the distances between the ends of the pulled arms, d_{XR} for junction *XR* and d_{HR} for junction *HR*, are suitable reaction coordinates spanning the complete trajectory from *isol* to *isoII* (Fig. 3A).

In one pulling direction represented by d_{XR}, the transition state lies closer to *isoII* (Fig. 3A,

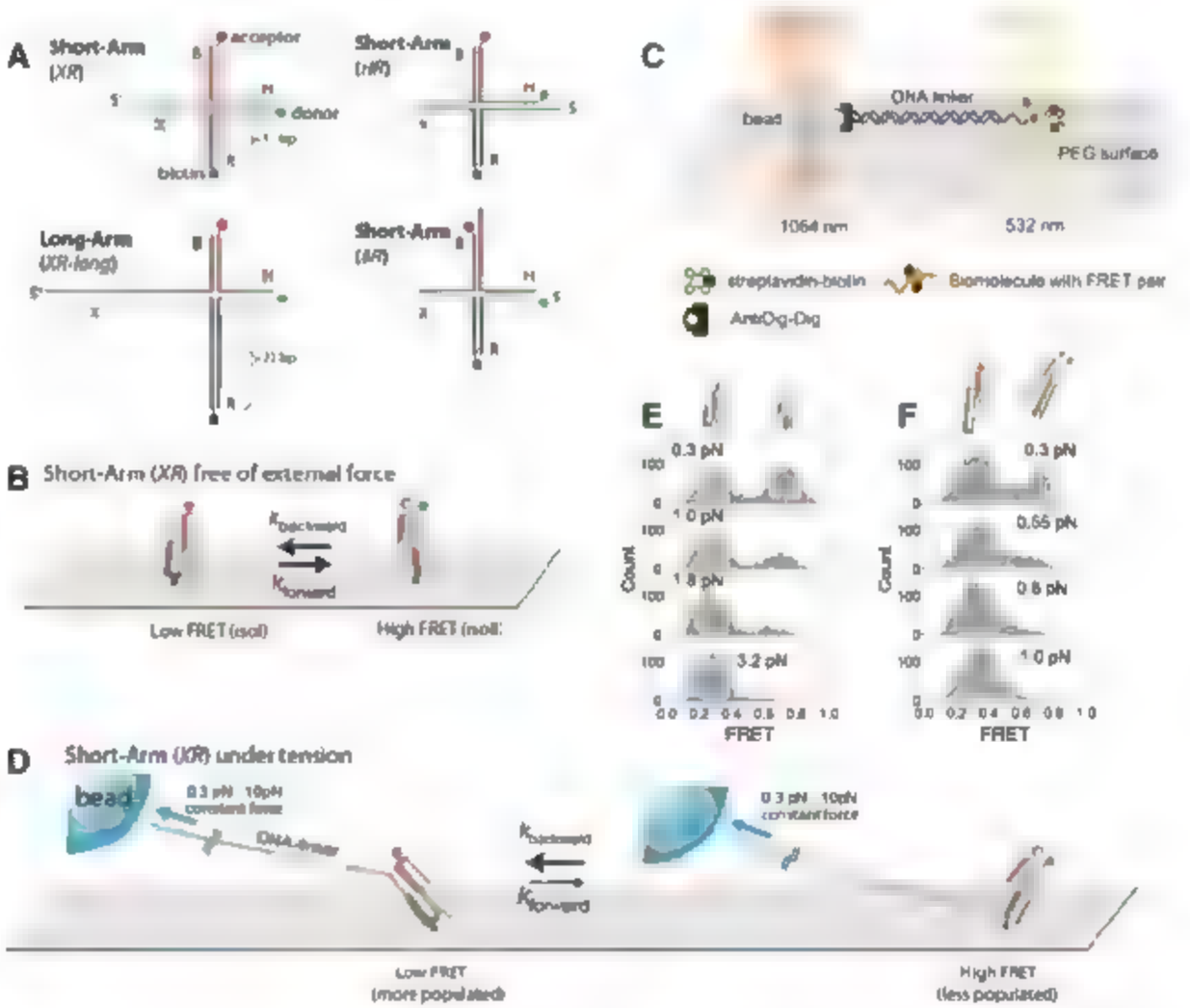

Fig. 1. Holliday junction constructs and experimental scheme. (**A**) The HJ species studied. Junction *XR* comprises four arms of 11 bp, termed B (red), H (green), R (dark gray), and X (gray). Cy3 and Cy5 fluorophores are terminally attached to H and B arms, respectively, and the molecule is tethered to the surface through biotin attached to the end of the R arm. Stretching force is applied through the λ DNA linker hybridized to the X arm. In junction *XR*-long, the lengths of arms R and X are increased to 21 bp. In junction *HR*, the λ DNA linker is hybridized to the H arm. In junctions *HR* and *BR*, the λ DNA linker is hybridized to the H and B arms, respectively. (**B**) Junction *XR* is known to alternate between two different stacking conformers, *isol* (low FRET) and *isoII* (high FRET), with similar populations in both states. (**C**) A surface-immobilized biomolecule with FRET labeling is connected to a trapped bead by a long DNA linker. The linker DNA spatially separates the confocal beam (532 nm) from the trapping beam (1064 nm), such that enhanced photobleaching and an overwhelming background signal induced by the intense trapping laser are avoided. To apply force, the surface-immobilized molecule was moved relative to the trapped bead. The confocal beam was programmed to follow the motion of the molecule using the mapping generated between sample scanning and beam scanning (fig. S6). (**D**) Force is expected to bias the junction *XR* to *isol*, which possesses a larger separation between the two tether points than *isoII*. (**E**) FRET histograms of a single-junction *XR* as a function of force. (**F**) FRET histograms of a single-junction *XR*-long as a function of force.

middle panel), whereas for the other pulling direction along d_{HR}, the transition state more closely resembles *isol* (Fig. 3A, bottom panel). These two transition states cannot represent a single structure because then both d_{XR} and d_{HR} must be relatively small, and by symmetry so must be d_{XB} and d_{HB}. Such a structure would have all four helices in the same hemisphere relative to the junction core, which is highly unlikely considering the symmetry of the HJ. Instead, we favor a model in which there are at least two different transition states, *ts1* and *ts11*, equal in energy but corresponding to different values of d_{XR} (or d_{HR}), such that force would elevate one of them into the single highest energy barrier by the tilting of the energy landscape (Fig. 3A).

The data presented so far show that the distance change upon stacking conformer transitions is about 4 nm. Because thermal energy is about 4 pN nm, a force on the order of 1 pN would consequently change the equilibrium between the two states by a factor of two or three. Such small-scale conformational fluctuations at these low forces are probably impossible to detect

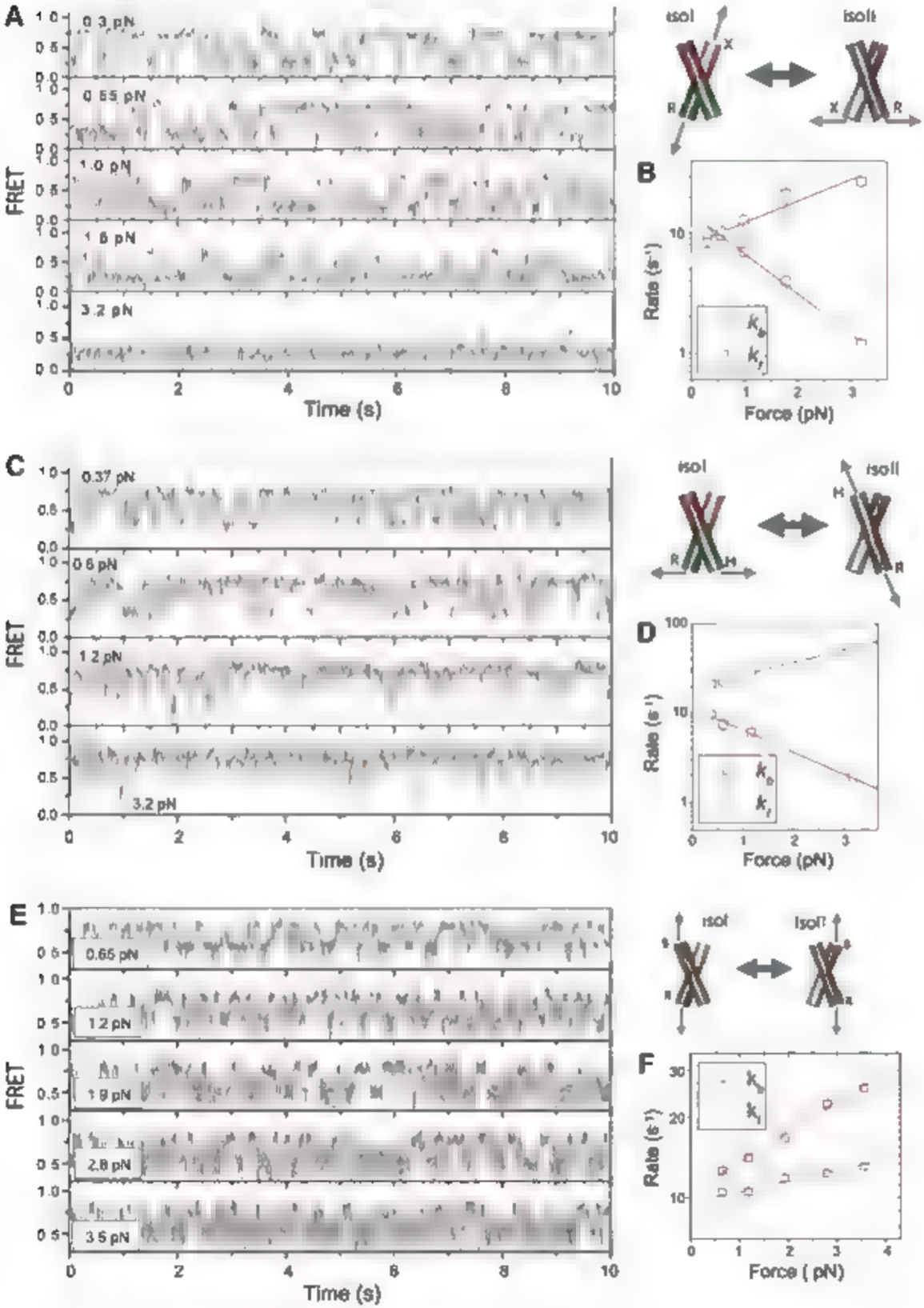

Fig. 2. Conformer exchange dynamics of the HJ as a function of applied force. **(A)** FRET time traces (gray lines) of a single-junction *XR* molecule at different forces. FRET efficiency is approximated by the acceptor intensity divided by the sum of the donor and acceptor intensities. Red lines are the most likely FRET trajectories generated by hidden Markov modeling. The imposed force (indicated on the top left of each plot) increases top to bottom. **(B)** Log-linear plot of rate constants of conformer exchange as a function of force. Rates of transition from states *isoII* to *isol* (k_b, red) and *isol* to *isoII* (k_f, blue) are differentiated by color. Error bars represent SDs obtained from repeated measurements of the same molecule. From linear fitting, we found that the transition state is closer to *isoII* (1.8 nm) than to *isol* (3.3 nm). **(C)** Same as (A) but for a single-junction *HR* molecule. **(D)** Same as (B) but for a single-junction *HR* molecule. **(E)** Same as (A) and (C) but for a single-junction *BR* molecule. **(F)** Same as (B) and (D) but for a single-junction *BR* molecule.

in a purely mechanical measurement, especially at our time resolution (10 ms).

What determines the force sensitivity of the junction? Is it an intrinsic property of the junction core or is it dependent on the length of helical arms on which the force is applied? Because the four arms of the HJ meet at its center, we may recast the experimental configuration as a torque being applied around the central pivot point. The torque is proportional to the product of the magnitude of force and the distance between the point of application of the force and the pivot point (i.e., the length of the arm). Therefore, it could be expected that increasing arm length would result in a greater torque for the same force. We tested such a lever-arm effect using junction *XR*-long, where the X and R arms are lengthened by about a factor of two (from 11 bp to 21 bp) compared to junction *XR*. FRET histograms as a function of applied force (Fig. 1E and Fig. 1F) show that increasing the lever arm length has magnified the force effect such that much lower force is needed for junction *XR*-long to achieve the same conformational bias. Fig. S4 compares the transition rates versus the force between five molecules each of junctions *XR* and *XR*-long and shows that junction XR-long exhibits much greater changes in rates for the same magnitude of force (also compare $\Delta x_f^{\ddagger}$ and $\Delta x_b^{\ddagger}$ in Table 1). Because the persistence length of double-stranded DNA is about 50 nm (~150 bp) (*22*), the lever-arm effect can probably be extended by another factor of five for arms of ≥100 bp. That is, forces as low as 0.1 pN would be enough to influence the junction conformations, illustrating the exquisite force sensitivity of the HJ.

Because the effect of force depends on the arm lengths, the most natural reaction coordinates are angular. The angles that define the global shape of the junction are ϕ, the interhelical angle between two stacked pairs of helices, and ψ, the angle that measures the degree of unstacking of stacked helices (*23*) (Fig. 3B). For example, for a stacked-X structure, ϕ is 40° and ψ is 0° (*15*), whereas for an open structure, ϕ is 0° and ψ is 90° (Fig. 3C). These two angles are well-defined within the angular space in which identities of stacking pairs are maintained. Our aim is to deduce the structure of the transition state by determining the ϕ and ψ values of the transition state using a geometrical analysis. The analysis below estimates the angles ($\phi_{\ddagger}$, $\psi_{\ddagger}$) of the transition state *ts*II in the *isoI*I half of the conformational reaction coordinate, but the same conclusions hold for *ts*I.

*ts*II lies a third of the way from *isoI*I to *isoI* along the d_{XR} coordinate (Table 1 and Fig. 3A). We can show that this condition is satisfied for a collection of ($\phi_{\ddagger}$, $\psi_{\ddagger}$) values, starting from (70°, 0°) at one extreme and arriving at (0°, 70°) at the other (Fig. 3C, gray zone) (*18*). To obtain an additional constraint, we performed an equiv-

Table 1. Distance to the transition state from *isoI* ($\Delta x_f^{\ddagger}$) and from *isoII* ($\Delta x_b^{\ddagger}$), measured from the force-dependent transition rates between *isoI* and *isoII* for four different junctions. Errors represent SD from five different molecules each. Also shown is Δx_{eq}, the distance between *isoI* and *isoII*, determined from force-dependent changes in the equilibrium constant. For junction *BR*, Δx_{eq} deviates significantly from ($\Delta x_b^{\ddagger}+\Delta x_f^{\ddagger}$) showing that d_{BR} is not a valid reaction coordinate connecting isoI and isoII. In contrast, $\Delta x_{eq} \approx \Delta x_b^{\ddagger} + \Delta x_f^{\ddagger}$ within error for junctions *XR* and *HR*, showing that d_{XR} and d_{HR} are reaction coordinates valid from isoI to isoII.

	XR	XR-long	HR	BR
$\Delta x_b^{\ddagger}$ (nm)	1.5 (±0.3)	2.6 (±0.6)	2.4 (±0.5)	1.1 (±0.2)
$\Delta x_f^{\ddagger}$ (nm)	2.9 (±0.6)	7.7 (±1.5)	1.3 (±0.3)	0.37 (±0.2)
Δx_{eq} (nm)	4.4 (±0.8)	9.9 (±2.6)	3.1 (±0.8)	0.7 (±0.2)
$\Delta x_b^{\ddagger} + \Delta x_f^{\ddagger}$ (nm)	4.4 (±0.8)	10.3 (±2.0)	3.6 (±0.5)	1.5 (±0.3)

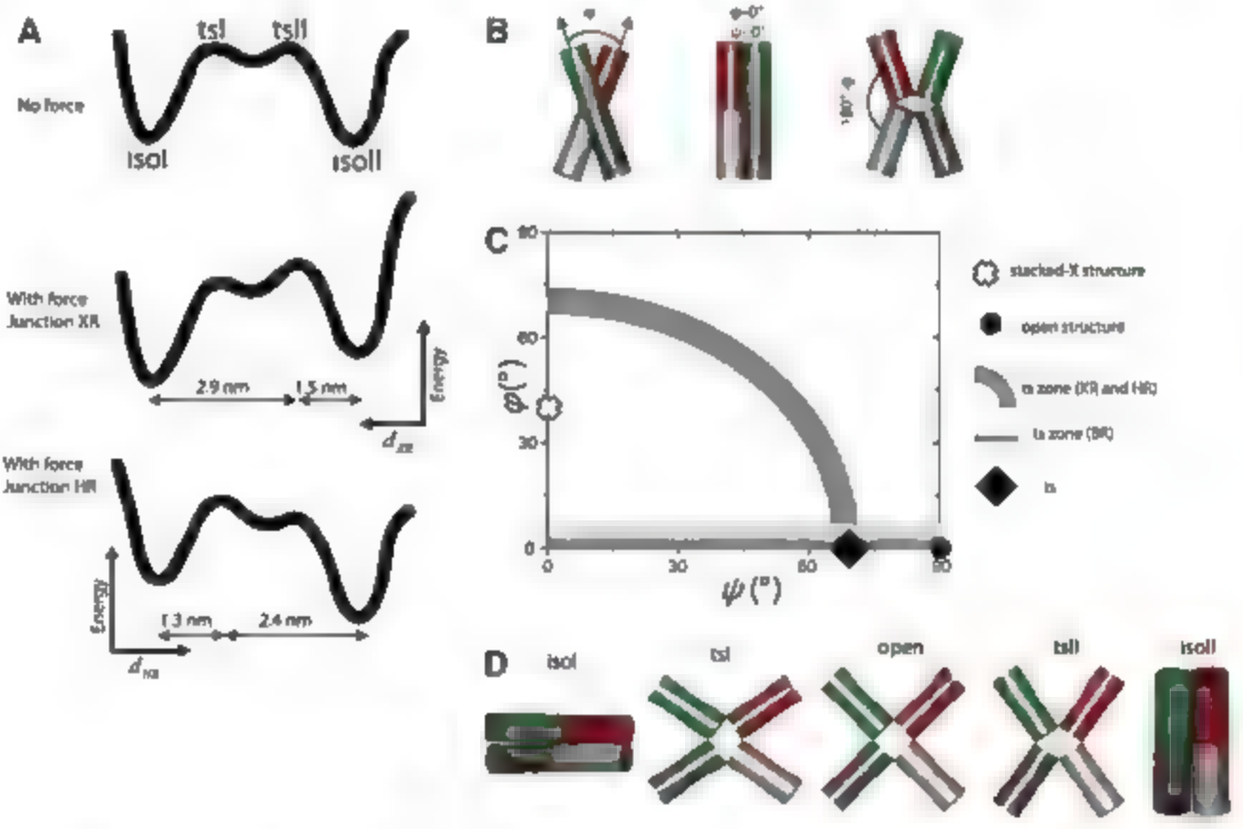

Fig. 3. Mapping the reaction landscape and determining the transition state structure. (**A**) A proposed reaction landscape with two distinct transition states with nearly identical energies (top). In junction *XR*, the applied force would tilt the energy landscape toward *isoI* so that the transition state, *ts*II, nearer to isoII would become the state of highest energy along the entire coordinate (middle). The reaction coordinate here is the distance between the ends of X and R arms, d_{XR}, which increases to the left as shown. Similarly, in junction *HR*, the transition state, *ts*I, nearer to *isoI* would become the single transition state upon application of force. The reaction coordinate here is the distance between the ends of H and R arms, d_{HR}, which increases to the right. (**B**) Two angular coordinates ϕ and ψ define the global conformation of the HJ. (**C**) A 2D conformational space of HJ conformations. The stacked-X structure and open structure are marked. The gray arc represents a zone that satisfies experimental constraints derived from *XR* and *HR* data, and the gradient zone is derived from *BR* data. The consensus location of the transition state is marked with a diamond. (**D**) Global structures of *isoI*, *isoII*, and two transition states, *ts*I and *ts*II, along with an open structure.

alent force analysis on junction *BR* (Fig. 2E, 2F, Table 1). Junction *BR* exhibited much reduced (by a factor of five or six) force dependence of the equilibrium populations compared with junctions *XR* and *HR* (compare Δx_{eq} values in Table 1). The residual force dependence of the equilibrium populations may be attributed to the finite diameter of the DNA duplex (*18*). In contrast to junctions *XR* and *HR*, application of force on junction *BR* accelerated both forward and backward transitions (Fig. 2F). Therefore, the distance between the ends of the B and R arms, d_{BR}, must be larger in the transition state than in the stacked-X structures. This condition is satisfied only if ϕ_{II} in the transition state is smaller than the 40° of the stacked-X structure. Furthermore, the distance to the transition state is 0.37 nm at minimum, which constrains ϕ_{II} to be essentially zero (*18*). In combination, our best estimate is $(\phi_{II}, \psi_{II})_{ts} = (0°, 70°)$ for *ts*II (Fig. 3C). Thus transition state is similar to the open state, but with arms deviating by about 20° from the ideal open state while displaying signatures on which pairs of helices are nearly stacked over each other (Fig. 3D). The structure bears a strong resemblance to the HJ structure bound to the Cre recombinase (*24*). Following the same argument, we can deduce that the transition state in the *ts*I-like conformational space, *ts*I, also has $(\phi_I, \psi_I)_{ts} = (0°, 70°)$.

By probing the HJ dynamics in response to pulling forces in three different directions, we mapped the location of the transition states in the two-dimensional (2D) reaction landscape and deduced the global structure of the transient species populated during the HJ conformational changes. Our simplest model envisions a shallow minimum between the two transition states, depicted as the open structure (Fig. 3A and 3D), but it is also possible that a continuum of conformations exist, spanning from *ts*I and *ts*II with nearly identical free energies, instead of having a single well-defined minimum.

The development reported here expands on the current arsenal of hybrid single-molecule techniques combining force and other observables (*8*, *25*–*27*). Unlike DNA or RNA hairpins, where forces on the order of 15 pN are necessary to induce mechanical unzipping (*10*, *11*), the conformations of HJs could be biased at 0.5 pN or lower. The lever-arm effect makes it unlikely that a purely mechanical tool could have probed the force effect on HJ conformations, because if the arms are lengthened to magnify the distance change, the force effect will occur at even lower forces. FRET can also report on vectors other than the end-to-end distances, which we exploited here by pulling on *XR*, *HR*, or *BR* arms while simultaneously measuring the same HB vector by FRET, which led to the 2D mapping of reaction landscapes. Our method is readily applicable to other nucleic acids systems and their interaction with proteins and enzymes, and with the advent of new orthogonal labeling techniques, should be extendable to proteins and protein complexes. The next technical challenge would be to obtain time evolution of the end-to-end distance by force, for example, due to the action of DNA processing enzymes (*28*), and correlate it with the enzyme conformational changes simultaneously measured by fluorescence.

References and Notes

1. C. Bustamante, Y. R. Chemla, N. R. Forde, D. Izhaky, *Annu. Rev. Biochem.* **73**, 705 (2004).
2. L. Stryer, R. P. Haugland, *Proc. Natl. Acad. Sci. U.S.A.* **58**, 719 (1967).
3. T. Ha *et al.*, *Proc. Natl. Acad. Sci. U.S.A.* **93**, 6264 (1996).
4. T. Ha, *Methods* **25**, 78 (2001).
5. A. Ashkin, J. M. Dziedzic, J. E. Bjorkholm, S. Chu, *Opt. Lett.* **11**, 288 (1986).
6. A. N. Kapanidis *et al.*, *Science* **314**, 1144 (2006).
7. S. C. Blanchard, R. L. Gonzalez, H. D. Kim, S. Chu, J. D. Puglisi, *Nat. Struct. Mol. Biol.* **11**, 1008 (2004).
8. M. J. Lang, P. M. Fordyce, S. M. Block, *J. Biol.* **2**, 6 (2003).
9. P. B. Tarsa *et al.*, *Angew. Chem. Int. Ed. Engl.* **46**, 1999 (2007).
10. J. Liphardt, B. Onoa, S. B. Smith, I. Tinoco, C. Bustamante, *Science* **292**, 733 (2001).
11. M. T. Woodside *et al.*, *Science* **314**, 1001 (2006).
12. R. Holliday, *Genet. Res.* **5**, 282 (1964).
13. D. R. Duckett *et al.*, *Cell* **55**, 79 (1988).
14. D. M. J. Lilley, *Q. Rev. Biophys.* **33**, 109 (2000).
15. B. F. Eichman, J. M. Vargason, B. H. M. Mooers, P. S. Ho, *Proc. Natl. Acad. Sci. U.S.A.* **97**, 3971 (2000).
16. R. J. Grainger, A. L. H. Murchie, D. M. J. Lilley, *Biochemistry* **37**, 23 (1998).
17. Materials and methods are available as supporting material on *Science* Online.
18. S. A. McKinney, A. C. Declais, D. M. J. Lilley, T. Ha, *Nat. Struct. Biol.* **10**, 93 (2003).
19. J. C. Meiners, S. R. Quake, *Phys. Rev. Lett.* **84**, 5014 (2000).
20. I. Rasnik, S. A. McKinney, T. Ha, *Nat. Methods* **3**, 891 (2006).
21. S. A. McKinney, C. Joo, T. Ha, *Biophys. J.* **91**, 1941 (2006).
22. C. Bustamante, J. F. Marko, E. D. Siggia, S. Smith, *Science* **265**, 1599 (1994).
23. J. Yu, T. Ha, K. Schulten, *Nucleic Acids Res.* **32**, 6683 (2004).
24. G. D. Van Duyne, *Annu. Rev. Biophys. Biomol. Struct.* **30**, 87 (2001).
25. A. Ishijima *et al.*, *Cell* **92**, 161 (1998).
26. H. Shroff *et al.*, *Nano Lett.* **5**, 1509 (2005).
27. J. Gore *et al.*, *Nature* **439**, 100 (2006).
28. J. B. Lee *et al.*, *Nature* **439**, 621 (2006).

29. We thank W. Cheng at University of California–Berkeley for providing the protocol for the preparation of anti-Dig coated bead, M. Wang at Cornell University for giving generous advice about building optical tweezers, Y. Chemla at University of Illinois for helpful discussion, and C. Joo for generous help in preparation of illustrations. Funding was provided by the National Sciences Foundation CAREER Award (PHY 0134916) and the National Institutes of Health (GM065367). T.H. is an investigator with the Howard Hughes Medical Institute.

5 June 2007; accepted 11 September 2007
10.1126/science.1146113

A Metagenomic Survey of Microbes in Honey Bee Colony Collapse Disorder

Diana L. Cox-Foster,[1] Sean Conlan,[2] Edward C. Holmes,[3,4] Gustavo Palacios,[2] Jay D. Evans,[5] Nancy A. Moran,[6] Phenix-Lan Quan,[2] Thomas Briese,[2] Mady Hornig,[2] David M. Geiser,[7] Vince Martinson,[8] Dennis vanEngelsdorp,[1,9] Abby L. Kalkstein,[1] Andrew Drysdale,[2] Jeffrey Hui,[2] Junhui Zhai,[2] Liwang Cui,[1] Stephen K. Hutchison,[10] Jan Fredrik Simons,[10] Michael Egholm,[10] Jeffery S. Pettis,[5] W. Ian Lipkin[2]*

In colony collapse disorder (CCD), honey bee colonies inexplicably lose their workers. CCD has resulted in a loss of 50 to 90% of colonies in beekeeping operations across the United States. The observation that irradiated combs from affected colonies can be repopulated with naive bees suggests that infection may contribute to CCD. We used an unbiased metagenomic approach to survey microflora in CCD hives, normal hives, and imported royal jelly. Candidate pathogens were screened for significance of association with CCD by the examination of samples collected from several sites over a period of 3 years. One organism, Israeli acute paralysis virus of bees, was strongly correlated with CCD.

Methods for cloning nucleic acids of microbial pathogens directly from clinical and environmental specimens afford unprecedented opportunities for pathogen discovery and surveillance. Subtractive cloning, polymerase chain reaction (PCR), and DNA microarrays have implicated previously unknown pathogens as the etiological agents of several acute and chronic diseases. Here, we describe the application of unbiased high-throughput pyrosequencing technology (*1*) in the characterization of the microflora associated with *Apis mellifera* in a search for the cause of colony collapse disorder (CCD).

CCD is characterized by the rapid loss from a colony of its adult bee population (*2*–*4*). No dead adult bees are found inside or in close proximity to the colony. At the final stages of collapse, a queen is attended only by a few newly emerged adult bees. Collapsed colonies often have considerable capped brood and food reserves. The phenomenon of CCD was first reported in 2006;

however, beekeepers noted unique colony declines consistent with CCD as early as 2004. An estimated 23% of beekeeping operations in the United States suffered from CCD over the winter of 2006–2007. These beekeepers lost an average of 45% of their operations (*5*). Since the introduction of the varroa mite in the late 1980s, colonies have experienced increased mortality. However, in contrast to CCD, these colony deaths are marked by dead bees in the hive, an incremental decline in worker population, and robbing and pest invasion. One hypothesis is that CCD is due to the introduction of a previously unrecognized infectious agent. This idea is supported by preliminary evidence that CCD is transmissible through the reuse of equipment from CCD colonies and that such transmission can be broken by irradiation of the equipment before use (*6*).

Bees were analyzed in a metagenomic survey of four widely separated operations across the United States that were affected by CCD. All of the operations were migratory, with wintering yards in either Florida or California in February 2007 (fig. S1) (*7*). Two non-CCD samples were collected from Hawaii and Pennsylvania. An additional sample of apparently healthy bees imported from Australia and four samples of imported royal jelly from China were also tested as potential sources of pathogens. Total RNA was extracted to capture RNA viruses as well as other pathogens. The RNA was pooled as presumed CCD-positive, presumed CCD-negative, and royal jelly for pyrosequencing. The raw sequencing reads were trimmed and assembled into contiguous sequences (contigs) (fig. S2). Analysis using nucleotide-nucleotide BLAST (BLASTN) and BLASTX (*8*) revealed the presence of bacteria, fungi, parasites, metazoa, and viruses (Table 1).

Sequences homologous to bacterial 16S ribosomal RNA (16S rRNA) were assembled into 48 contigs. The majority (87%) of the contigs aligned best to previously identified commensals of *A. mellifera* (Table 1). To obtain precision in typing the bacterial associates in the different samples, we obtained ~500-nucleotide (nt) fragments of the 16S rRNA gene, using conserved, near-universal PCR primers. A total of 536 clones from the entire range of samples were characterized by conventional sequencing. When these sequences were used as queries in BLASTN searches of GenBank, over 96% gave closest hits to the eight clusters isolated from *A. mellifera* in previous studies (*9*–*11*). These clusters included an abundant member of the Gammaproteobacteria and several less frequent but widespread organisms from the Betaproteobacteria, Alphaproteobacteria, Firmicutes, and Actinobacteria groups (Fig. 1). Only 20 bacterial 16S rRNA gene sequences were unidentified, and they were not concentrated in CCD samples. Sequences of *Paenibacillus larvae* and *Streptococcus pluton*, the causative agents of American and European foulbrood (diseases of bee larvae) were not detected.

Bacterial analysis indicated community composition (Table 1) similar to that in samples collected in Africa, Switzerland, and Germany (*9*–*11*), suggesting that *A. mellifera* has similar bacterial flora worldwide. Screens of the *A. mellifera* genome-sequence database revealed sequences corresponding to several of these bacterial groups, indicating that they are probably part of the normal flora. The *A. mellifera* database includes sequences for 926 genes with significant reciprocal best BLAST hits to genes from completely sequenced bacterial genomes. The most abundantly represented groups corresponded to taxa in our samples, including 299 (32%) with best hits to *Lactobacillus* species and 249 (27%) with best hits to *Neisseria* species (members of the Betaproteobacteria and closest relatives of *Simonsiella* for which screening was possible on the basis of the available full genome sequences). The gut lumen contains the majority of microorganisms in most insects. Because a similar profile of bacterial types was found in dissected intestines from *A. mellifera* (*9*, *11*), the bacterial species described here probably represent a characteristic gut-inhabiting community. Although we cannot exclude that a strain of a normally commensal bacterium has become pathogenic while retaining a near-identical 16S rRNA sequence, we observed no clear shift in abundance to suggest that this occurred in CCD. A trend toward increased abundance of one of the Gammaproteobacterial taxa in the CCD bees (Fig. 1) may reflect physiological changes accompanying CCD and affecting the commensal community. More sampling of individual colonies and age classes would be needed to determine the importance of this observation.

Metagenomic sequence data for a ~700-nt fragment of the 18S rRNA gene identified a trypanosomatid sequence. This sequence was identical across CCD and non-CCD samples. Phylogenetic analysis indicates that this parasite falls in the *Leptomonas-Leishmania-Crithidia* assemblage, but a precise taxonomic assignment is not possible because of the paucity of rRNA data in this region (fig. S3) (*12*–*14*).

Eighty-one distinct fungal 18S rRNA sequences were recovered from the pooled samples, primarily from four distinct lineages: Saccharomycotina, which includes a variety of presumed commensal yeasts; Microsporidia, including the important bee pathogens *Nosema apis* and *Nosema ceranae* (*15*); Entomophthorales/Entomophthoromycotina, a diverse group of insect pathogens; and Mucorales/Mucoromycotina, which includes *Mucor hiemalis*, a species known to kill honey bees under certain

Table 1. Closest sequenced relatives identified through BLAST analysis of the high-throughput sequence data.

Kingdom	Taxon (rank)	Organism
Bacteria	Firmicutes (phylum)	*Lactobacillus* sp.*†
		Uncultured Firmicutes†
Bacteria	Actinobacteria (class)	*Bifidobacterium* sp.*
Bacteria	Alphaproteobacteria (class)	*Bartonella* sp.*†
		Gluconacetobacter sp.*†
Bacteria	Betaproteobacteria (class)	*Simonsiella* sp.*†
Bacteria	Gammaproteobacteria (class)	Two uncultured species*†
Fungus	Entomophthorales (order)	*Pandora delphacis*
Fungus	Mucorales (order)	*Mucor* spp.
Fungus/microsporidian	Nosematidae (family)	*Nosema ceranae*
Fungus/microsporidian	Nosematidae (family)	*Nosema apis*
Eukaryota	Trypanosomatidae (family)	*Leishmania/Leptomonas* sp.
Metazoan	Varroidae (family)	*Varroa destructor*
Virus	(Unclassified)	CBPV‡
Virus	*Iflavirus* (genus)	SBV
Virus	*Iflavirus* (genus)	DWV‡
Virus	Dicistroviridae (family)	BQCV
Virus	Dicistroviridae (family)	KBV‡
Virus	Dicistroviridae (family)	ABPV
Virus	Dicistroviridae (family)	IAPV of bees‡

*Found by Jeyaprakash *et al.* (*10*) †Found by Babendreier *et al.* (*9*). ‡Indicates viruses not yet classified by the International Committee on the Taxonomy of Viruses but that exhibit the key features of the indicated taxon.

[1]Department of Entomology, Pennsylvania State University, University Park, PA 16802, USA. [2]Center for Infection and Immunity, Mailman School of Public Health, Columbia University, New York, NY 10032, USA. [3]Center for Infectious Disease Dynamics, Department of Biology, Pennsylvania State University, Mueller Laboratory, University Park, PA 16802, USA. [4]Fogarty International Center, National Institutes of Health, Bethesda, MD 20892, USA. [5]Bee Research Laboratory, U.S. Department of Agriculture–Agricultural Research Service, Beltsville, MD 20705, USA. [6]Department of Ecology and Evolutionary Biology, University of Arizona, Tucson, AZ 85721, USA. [7]Department of Plant Pathology, Pennsylvania State University, University Park, PA 16802, USA. [8]Center for Insect Science, University of Arizona, Tucson, AZ 85721, USA. [9]Pennsylvania Department of Agriculture, Bureau of Plant Industry–Apiculture, Harrisburg, PA 17110, USA. [10]454 Life Sciences, Branford, CT 06405, USA.

*To whom correspondence should be addressed. E-mail: wi2001@columbia.edu

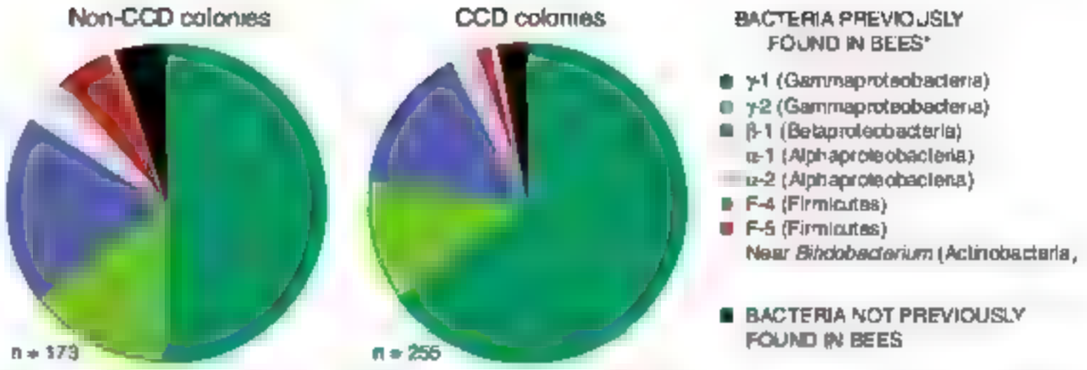

Fig. 1. Summary of bacterial groups from *A. mellifera* derived from colonies categorized as non-CCD and CCD. For both categories, the top BLAST hit for over 96% of sequences from 16S rRNA clones was a sequence obtained in previous studies on bacterial associates of *A. mellifera*. Asterisk indicates that the bacteria were categorized according to the cluster designations of Babendreier *et al.* (*9*) [except for the Bifidobacterium-like sequence of Jeyaprakash *et al.* (*10*)]. *n*, number of sequences. GenBank accession numbers corresponding to the categories are: γ-1 (AY370191-AY370192 and DQ837602-DQ837609), γ-2 (DQ837610-DQ837611), β-1 (AY370189-AY370190 and DQ837616-DQ837621), α-1 (AY370185-AY370187 and DQ837622-DQ837624), α-2 (AY370188 and DQ837625-DQ837626), F-4 (DQ837632-DQ837633), F-5 (AY370183 and DQ837634-DQ837637), near Bifidobacterium (AY370184).

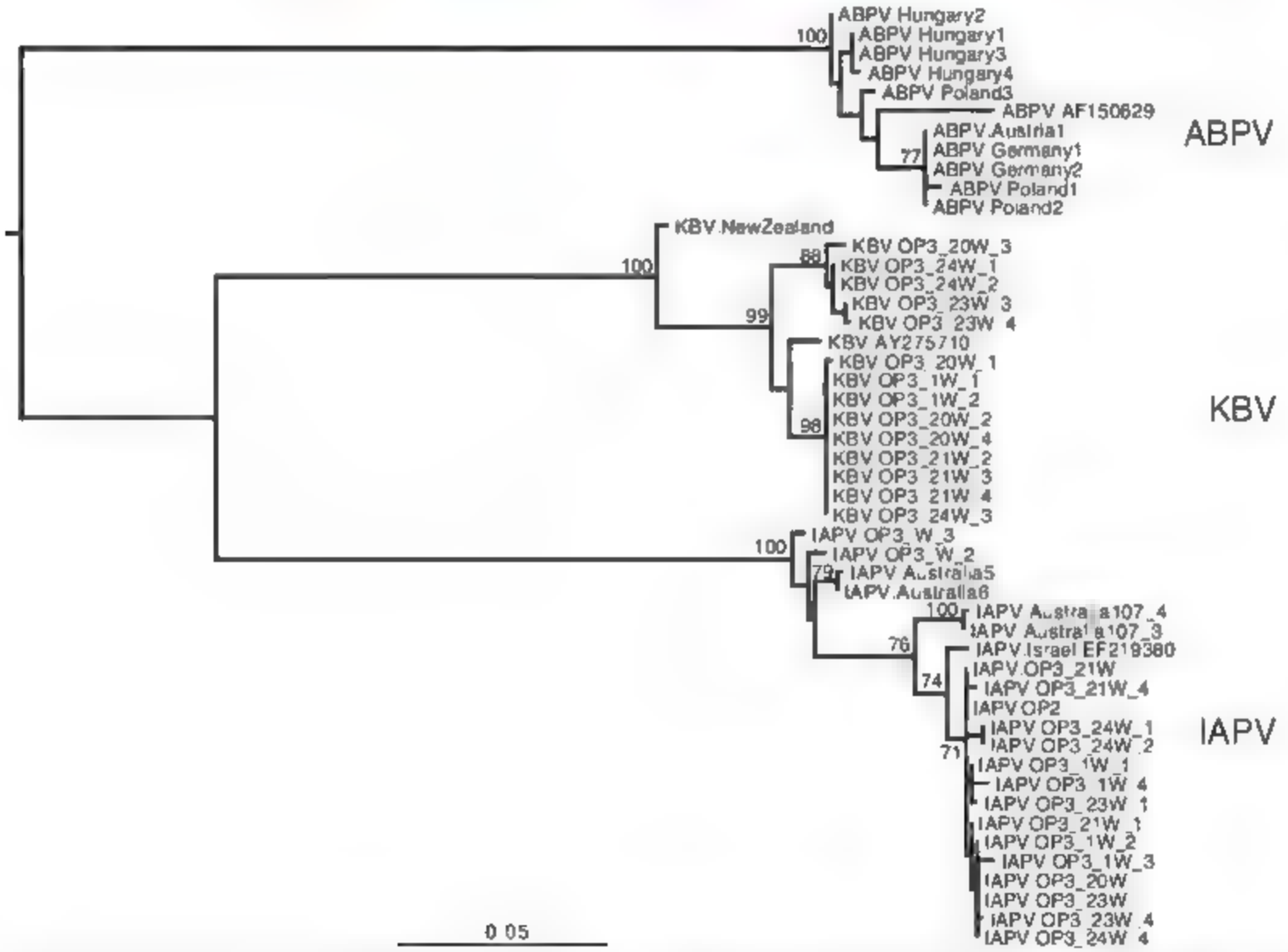

Fig. 2. Maximum likelihood phylogenetic tree of dicistroviruses, based on a 741-nt sequence including the IGR. All branches are drawn to a scale of substitutions per site, and bootstrap values are shown for key nodes. All KBV sequences (except KBV.NewZealand and KBV.AY275710) and all IAPV sequences (except IAPV.Israel.EF219380) were recovered in this study. 0.05 represents the number of nucleotide substitutions per site. GenBank accession numbers for the nucleotide sequences in file IAPVaug07IGR.sqn: IAPV.Australia107_4 EU122346, IAPV.Australia5 EU122347, IAPV.Australia6 EU122348, IAPV.Australia107_3 EU122349, IAPV.OP3_1W_1 EU122350, IAPV.OP3_1W_2 EU122351, IAPV.OP3_1W_3 EU122352, IAPV.OP3_1W_4 EU122353, IAPV.OP3_20W EU122354, IAPV.OP3_21W EU122355, IAPV.OP3_21W_1 EU122356, IAPV.OP3_W_2 EU122357, IAPV.OP3_W_3 EU122358, IAPV.OP3_21W_4 EU122359, IAPV.OP3_23W EU122360, IAPV.OP3_23W_1 EU122361, IAPV.OP3_23W_4 EU122362, IAPV.OP3_24W_1 EU122363, IAPV.OP3_24W_2 EU122364, IAPV.OP3_24W_4 EU122365, IAPV.OP2 EU122366, KBV.OP3_20W_1 EU122367, KBV.OP3_1W_1 EU122368, KBV.OP3_1W_2 EU122369, KBV.OP3_20W_2 EU122370, KBV.OP3_20W_3 EU122371, KBV.OP3_20W_4 EU122372, KBV.OP3_21W_2 EU122373, KBV.OP3_21W_3 EU122374, KBV.OP3_21W_4 EU122375, KBV.OP3_23W_3 EU122376, KBV.OP3_23W_4 EU122377, KBV.OP3_24W_1 EU122378, KBV.OP3_24W_2 EU122379, KBV.OP3_24W_3 EU122380.

conditions (*16*). We used 18S rRNA PCR primers designed to capture Entomophthorales and Mucorales (fig. S4). The occurrence of these fungi in our samples did not correlate with CCD (table S1). Although *N. ceranae* was detected by PCR in all operations affected by CCD, as well as in the Australian sample and two of the royal-jelly samples, it was also detected in non-CCD samples. A specific PCR assay for *N. apis* showed that it was present in all four CCD operations, as well as one non-CCD operation. *N. apis* was also found in the sample from Australia but not in the royal-jelly samples (table S1).

BLASTN analysis of the high-throughput sequencing data identified seven positive-sense single-stranded RNA viruses previously associated with disease in honey bees, including members of the family Dicistroviridae and the genus *Iflavirus*. The presence of the unclassified Chronic bee paralysis virus (CBPV) in only one out of four CCD operations (table S1) suggests that it is not a primary contributor to this syndrome. Recovered sequences were used to establish specific quantitative PCR assays for the remaining six insect viruses. Two iflaviruses, Sacbrood virus (SBV) and Deformed wing virus (DWV), as well as two dicistroviruses, Black queen cell virus (BQCV) and Acute bee paralysis virus (ABPV), were found in both CCD and non-CCD operations.

Two other dicistroviruses, Kashmir bee virus (KBV) and Israeli acute paralysis virus (IAPV) of bees—an unclassified virus that may reflect a distinct lineage of KBV or a previously unidentified species—were found only in CCD operations. IAPV sequence analysis in the intergenic region (IGR) (Fig. 2) indicated a close phylogenetic relation to both KBV and ABPV. IAPV was found in all four affected operations sampled, in two out of four royal-jelly samples, and in the Australian sample (table S1). KBV was present in three out of four CCD operations but not in the royal jelly. KBV was not found in the sample of Australian bees shown in table S1, however, KBV was subsequently found in five out of eleven individual bees from the same Australian source.

Both *N. ceranae* and an unspecified iflavirus were proposed to be associated with CCD in an earlier report (*17*). We found *Nosema* spp. by PCR and spore count in both CCD and non-CCD operations (tables S1 and S2) but no novel iflavirus. The overall prevalence of any *Nosema* species was 94.1% (100%, CCD; 85.7%, non-CCD). In contrast, the dicistroviruses KBV and IAPV correlated with CCD in our metagenomic survey. The prevalence of KBV, IAPV, *N. ceranae*, and *N. apis* was tested in 51 pools of bees (4 to 15 bees per pool) collected from 30 CCD colonies and 21 non-CCD colonies between 2004 and 2007 in Arizona, California, Florida, Georgia, Louisiana, and Pennsylvania. Individual CCD samples were more likely than samples from non-CCD operations to contain more than one of these four pathogens. The mean number of pathogen types (±1 SD) found in individual samples from each site was 3.7 ± 0.5 for CCD samples versus 2.1 ± 0.9 for non-CCD samples ($P < 0.0001$). The patterns of coinfection were complex and unevenly distributed throughout the sample set. All samples that were positive for IAPV also contained KBV. Although KBV was prevalent in both CCD and non-CCD samples (90.2% of all samples), IAPV was, with a single exception, confined to CCD samples, yielding a positive predictive value of 96.1% and a specificity of 95.2% (Table 2). Multinomial logistic regression was pursued to determine the contributions of the four pathogens, singly and in combination, to CCD outcomes. Models with the best explanatory power included IAPV as one of the independent variables. IAPV was found to increase the risk of CCD (odds ratio = 65, $P < 0.0001$) with a trend for increased CCD risk in samples positive for *N. apis* (odds ratio = 9, $P = 0.053$). Neither KBV nor *N. ceranae* contributed significantly to the risk for CCD, nor did they alter the influence of IAPV on CCD.

IAPV was first described in 2004 in Israel (*18*) where infected bees presented with shivering wings, progressed to paralysis, and then died just outside the hive. All of the CCD operations that were sampled used imported bees from Australia or were intermingled with operations that had done so. Importation to the United States of bees from Australia began in 2004, coinciding with early reports of unusual colony declines. Although the shivering phenotype is not reported in imported Australian bees or CCD, differences in IAPV pathogenicity may reflect strain variation, coinfection, or the presence of other stressors such as pesticides or poor nutrition. The varroa mite, for example, which is absent in Australia, immunosuppresses bees, making them more susceptible to infection by other organisms, including viruses (*19*, *20*). Other stressors may include chemical pesticides used on plants pollinated by bees and in hives to control pests. Crop pesticide use is similar in both the United States and Australia. Miticides are widely used in the United States but not in Australia and can have adverse effects on colony health (*21*); however, miticide use did not differ between CCD and non-CCD operations, as determined by detailed case histories (*22*).

We used CCD as a model to establish a strategy for investigating epidemics of unexplained infectious disease. Metagenomic sequencing enabled rapid assembly of a comprehensive inventory of microflora in CCD and non-CCD populations and provided the foundation needed to address the significance and provenance of candidate pathogens. We have not proven a causal relationship between any infectious agent and CCD; nonetheless, the prevalence of IAPV sequences in CCD operations, as well as the temporal and geographic overlap of CCD and the importation of IAPV-infected bees, indicate that IAPV is a significant marker for CCD.

Table 2. Analysis of pools of bees tested for candidate pathogens. Numbers in the CCD, Non-CCD, and Total columns represent the percentage of samples found to be positive among all samples tested in each category. The positive predictive value represents the probability that a positive result for a given agent is associated with CCD. The sensitivity is the probability that test results will be positive in all CCD cases. Specificity is defined as the probability that all non-CCD samples will be associated with negative test results.

Agent	CCD (n = 30)	Non-CCD (n = 21)	Total (n = 51)	Positive predictive value (%)	Sensitivity (%)	Specificity (%)
IAPV	25 (83.3%)	1 (4.8%)	26 (51.0%)	96.1	83.3	95.2
KBV	30 (100%)	16 (76.2%)	46 (90.2%)	65.2	100	23.8
N. apis	27 (90%)	10 (47.6%)	37 (72.5%)	73.0	90.0	52.4
N. ceranae	30 (100%)	17 (80.9%)	47 (92.1%)	63.8	100	19.0
All four agents	23 (76.7%)	0 (0%)	23 (45.0%)	100	76.7	100

References and Notes

1. M. Margulies *et al.*, *Nature* **437**, 376 (2005).
2. B. P. Oldroyd, *PLoS Biol.* **5**, e168 (2007).
3. A. Barrionuevo, "Bees vanish: Scientists race for reasons," *New York Times*, 24 April 2007, p. 1.
4. E. Stokstad, *Science* **316**, 970 (2007).
5. D. vanEngelsdorp, R. Underwood, D. Caron, J. Hayes Jr., *Am. Bee J.* **147**, 599 (2007).
6. J. Pettis, D. vanEngelsdorp, D. Cox-Foster, *Am. Bee J.* **147**, 595 (2007).
7. Materials and methods are available as supporting material on *Science* Online.
8. S. F. Altschul *et al.*, *Nucleic Acids Res.* **25**, 3389 (1997).
9. O. Saldarriaga, O. Joller, J. Romeis, F. Bigler, F. Widmer, *FEMS Microbiol. Ecol.* **59**, 600 (2007).
10. A. Jeyaprakash, M. A. Hoy, M. H. Allsopp, *J. Invertebr. Pathol.* **84**, 96 (2003).
11. K. J. Mohr, C. C. Tebbe, *Environ. Microbiol.* **8**, 258 (2006).
12. S. Podhajev, *Int. J. Parasitol.* **31**, 648 (2001).
13. S. A. Podhajev *et al.*, *J. Eukaryot. Microbiol.* **51**, 283 (2004).
14. A. L. Hughes, H. Piontkivska, *Mol. Biol. Evol.* **20**, 644 [illegible].
15. M. Higes, R. Martín, A. Meana, *J. Invertebr. Pathol.* **92**, 93 (2006).
16. C. E. Burnside, *Am. Bee J.* **25**, 75 (1935).
17. W. Ravven, "UCSF sleuths identify suspects in mystery of vanishing honeybees," *UCSF Today*, 25 April 2007; available at http://pub.ucsf.edu/today/cache/feature/20070425.html.
18. E. Maori, E. Tanne, I. Sela, *Virology* **362**, 342 (2007).
19. X. Yang, D. L. Cox-Foster, *Proc. Natl. Acad. Sci. U.S.A.* **102**, 7470 (2005).
20. P. G. Gregory, J. O. Evans, T. Rinderer, L. de Guzman, *J. Insect Sci.* **5**, 7 (2005).
21. J. Pettis, A. Collins, R. Wilbanks, M. F. Feldlaufer, *Apidologie* **35**, 605 (2004).
22. D. vanEngelsdorp, D. Cox-Foster, M. Frazier, N. Ostiguy, J. Hayes Jr., "Fall-Dwindle Disease: A preliminary report" (CCD Working Group, 2006); available at http://maarec.cas.psu.edu/ColonyCollapseDisorderInfo.html.

23 We thank M. Andree, A. V. Bassetti, J. Chen, D. Grove, M. Hamilton, V. Levi, H. Lin, D. Lopez, S. McDonald, N. Rice, K. Roccasecca, B. Smith, O. Thompson, A. Ulsamer, V. Williams, and the beekeepers who supplied the samples used in these analyses. The work reported here was supported by NIH awards 1R01AI070411 and 1U54AI57158 (Northeast Biodefense Center-Lipkin), the National Honey Board, and the Pennsylvania Department of Agriculture.

Supporting Online Material
www.sciencemag.org/cgi/content/full/1146498/DC1
Figs. S1 to S4
Tables S1 to S3
References

14 June 2007; accepted 30 August 2007
Published online 6 September 2007
10.1126/science.1146498
Include this information when citing this paper

Coactivation of Receptor Tyrosine Kinases Affects the Response of Tumor Cells to Targeted Therapies

Jayne M. Stommel,[1] Alec C. Kimmelman,[1,2] Haoqiang Ying,[1] Roustem Nabioullin,[3] Aditya H. Ponugoti,[3] Ruprecht Wiedemeyer,[1] Alexander H. Stegh,[1] James E. Bradner,[4] Keith L. Ligon,[1,5] Cameron Brennan,[6] Lynda Chin,[1,3,7] Ronald A. DePinho[1,3,8]*

Targeted therapies that inhibit receptor tyrosine kinases (RTKs) and the downstream phosphatidylinositol 3-kinase (PI3K) signaling pathway have shown promising anticancer activity, but their efficacy in the brain tumor glioblastoma multiforme (GBM) and other solid tumors has been modest. We hypothesized that multiple RTKs are coactivated in these tumors and that redundant inputs drive and maintain downstream signaling, thereby limiting the efficacy of therapies targeting single RTKs. Tumor cell lines, xenotransplants, and primary tumors indeed show multiple concomitantly activated RTKs. Combinations of RTK inhibitors and/or RNA interference, but not single agents, decreased signaling, cell survival, and anchorage-independent growth even in glioma cells deficient in PTEN, a frequently inactivated inhibitor of PI3K. Thus, effective GBM therapy may require combined regimens targeting multiple RTKs.

GBM, the most prevalent tumor in the central nervous system of human adults, is among the most lethal cancers, with a median survival of ~12 months (*1*). Aberrant activation of PI3K pathway components appears to be universal in human cancer, including GBM. PI3K is activated upon binding phosphorylated RTKs and/or adaptor proteins at the plasma membrane and signals to multiple downstream effectors, such as Akt (*2*). Over 80% of GBMs show robust Akt activation, and 40 to 50% have lost or mutated PTEN (*3*), underscoring the importance of the PI3K pathway in gliomagenesis (*4*). Activation of the RTK epidermal growth factor receptor (EGFR) is a critical pathogenetic event, with amplification, mutation, and rearrangement observed in more than 40% of cases, making it a compelling target for therapeutic inhibition (*5*, *6*). Other RTKs, such as the platelet-derived growth factor receptors α and β (PDGFRα and PDGFRβ) and MET (*1*, *7*), have been reported to be altered in GBM, albeit at lower frequencies. Notably, anti-PDGFR therapy has failed in GBM patients (*8*), and only 10 to 20% of patients benefit from EGFR inhibition (*9*), pointing to confounding factors that attenuate the response to RTK inhibition.

Coexpression of wild-type (WT) PTEN and a constitutively active EGFR (vIII mutant) in GBM correlates with clinical response to EGFR inhibitors, indicating that PTEN is a response biomarker for anti-EGFR therapy and that its loss renders these agents ineffective by dissociating EGFR inhibition from the abrogation of PI3K pathway activity (*10*). Alternatively, the activation state of critical survival pathways, such as PI3K and mitogen-activated protein kinase (MAPK), may be determined by the sum of multiple inputs, and multiple RTKs besides EGFR may be simultaneously or sequentially used by GBM cells to maintain signal flux through such pathways. In such a multiple-input system, single-agent anti-EGFR inhibition might be incapable of sufficiently suppressing PI3K signaling in the context of unopposed activation by PTEN loss, resulting in a lack of clinical efficacy. That is, the total signal flux through the PI3K pathway may dictate the response to upstream RTK inhibition, and multiple inputs to PI3K signaling would thus confer insensitivity to the inhibition of any single agent.

To evaluate this possibility, we sought evidence that multiple PI3K activators coexist in glioma cells (*11*). Because PI3K is activated by binding phosphorylated proteins to its regulatory subunit, p85α, we performed anti-p85α immunoprecipitations to identify PI3K-activating proteins. Multiple tyrosine-phosphorylated proteins were found to be in the PI3K complex (fig. S1A). Guided by Scansite [http://scansite.mit.edu (*12*)], which identifies potential p85α-binding proteins, we confirmed the endogenous PI3K interaction with specific RTKs by communoprecipitation assays. For example, 5 out of 14 cell lines showed activated ERBB3 (fig. S1B), which mediates the binding of EGFR and ERBB2 to PI3K (*13*), and 9 out of 20 cell lines had activated growth factor receptor–bound protein 2 (Grb2)–associated binder 1 (GAB1), a docking protein that binds activated RTKs directly or through Grb2 (*14*). In seven of these 20 cell lines, highly phosphorylated GAB1 communoprecipitated activated MET (fig. S2B) (*15*).

To define the compendium of coactivated RTKs in GBM, we used an antibody array that allows simultaneous assessment of the phosphorylation status of 45 RTKs. Consistent with figs. S1 and S2, three or more activated RTKs, including EGFR, ERBB3, PDGFRα, and MET, were detected in each of 19 out of 20 cell lines (Fig. 1A and table S1). Most activated RTKs remained phosphorylated under serum deprivation and in tumor cell xenografts (Fig. 1, B and C), indicating that the RTK activation in the transformed cells is not due to ligands in serum-containing culture media. Finally, RTK coactivation is not a distinctive feature of glioma cells, because similar patterns were detected in other solid tumor types such as lung and pancreatic adenocarcinoma cell lines (fig. S3).

To explore the therapeutic implications of RTK coactivation, we used U87MG glioma cells that constitutively express WT EGFR, EGFRvIII (EGFR*), or a kinase-dead EGFRvIII (EGFR*-KD) at levels comparable to those observed in primary GBMs (*16*). Although MET is phosphorylated and bound to GAB1 in U87MG cells (Fig. 2A and fig. S2B), activated MET was substantially displaced by EGFR in the GAB1/PI3K complex when WT EGFR and EGFR* are expressed. This outcome required the catalytic activity of EGFR, because EGFR*-KD only modestly displaced MET (lane 4 in Fig. 2A). Because EGFR*-KD was expressed at levels similar to those of WT EGFR and EGFR*, it is unlikely that the displacement was simply a consequence of ectopic overexpression. This apparent "swapping" of RTKs within the PI3K

[1]Department of Medical Oncology, Dana-Farber Cancer Institute and Harvard Medical School, Boston, MA 02115, USA. [2]Harvard Radiation Oncology Program, Harvard Medical School, Boston, MA 02115, USA. [3]Center for Applied Cancer Science, Belfer Institute for Innovative Cancer Science, Dana-Farber Cancer Institute, Boston, MA 02115, USA. [4]Division of Hematologic Neoplasia, Dana-Farber Cancer Institute and Harvard Medical School, Boston, MA 02115, USA. [5]Department of Pathology, Division of Neuropathology, Brigham and Women's Hospital, Boston, MA 02115, USA. [6]Departments of Neurosurgery, Memorial Sloan Kettering Cancer Center and Neurological Surgery, Weill Medical College of Cornell University, New York, NY 10021, USA. [7]Department of Dermatology, Brigham and Women's Hospital and Harvard Medical School, Boston, MA 02115, USA. [8]Departments of Medicine and Genetics, Harvard Medical School, Boston, MA 02115, USA.

*To whom correspondence should be addressed. E-mail: ron_depinho@dfci.harvard.edu

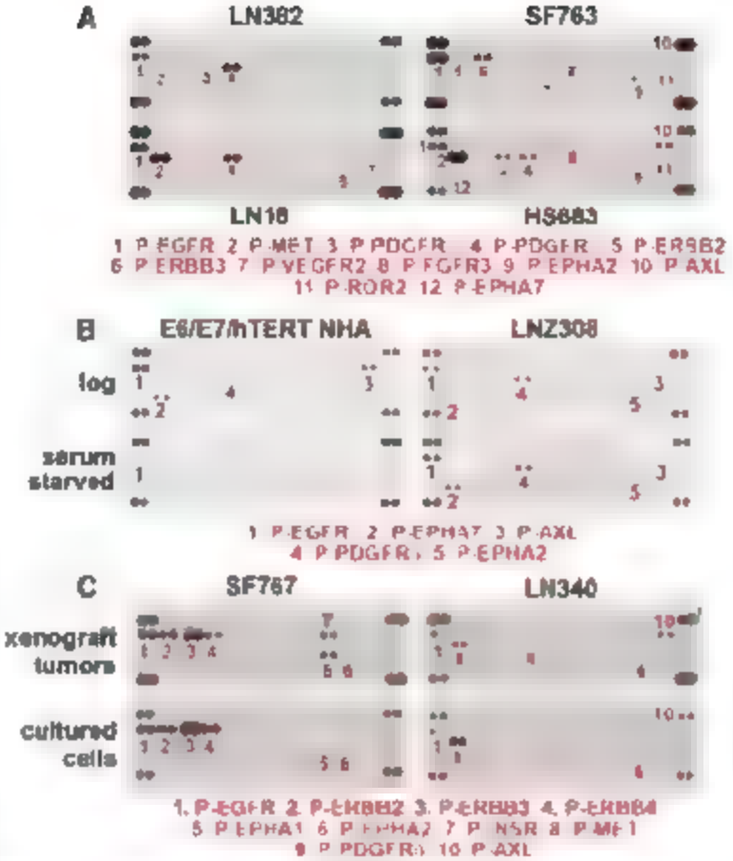

Fig. 1. Multiple RTKs are activated simultaneously in glioma cell lines. (**A**) Whole-cell extracts (WCEs) from the glioma cell lines LN382, SF763, LN18, and HS683 were incubated on RTK antibody arrays, and phosphorylation status was determined by subsequent incubation with anti-phosphotyrosine horseradish peroxidase. Each RTK is spotted in duplicate; the pairs of dots in each corner are positive controls. Each pair of positive RTK dots is denoted by a red numeral, with the identity of the corresponding RTKs listed below the arrays. These arrays are representative of various RTK coexpression patterns in the 20 glioma cell lines examined in table S1. (**B**) RTK antibody arrays were used as in (A) with WCEs from an immortalized human astrocyte cell line [E6/E7/hTERT NHA (*19*)] or the glioma line LNZ308 grown in 10% serum (log) or grown for 48 hours in 0.05% serum (serum starved). (**C**) RTK antibody arrays were used as in (A) to compare RTK activation in WCEs from xenograft tumors derived from the glioma cell lines SF767 or LN340 or from the corresponding in vitro cultured cells.

complex did not alter downstream signaling (right panel in Fig. 2A), indicating that MET and EGFR act as redundant but independent inputs to their signaling networks. Consequently, coactivated MET (or other RTKs) would be expected to render anti-EGFR inhibition ineffective in extinguishing downstream signaling by replacing activated EGFR in the PI3K complex.

To address whether coactivated RTKs confer resistance to single anti-RTK inhibition, we examined the consequences of single and combined inhibition of EGFR and MET in U87MG-EGFR* cells with these two coactivated RTKs, using P-Akt and P-S6 ribosomal protein as molecular surrogates of downstream RTK signaling. We first confirmed that treatment with either an EGFR inhibitor (erlotinib) or a MET inhibitor (SU11274) effectively blocked phosphorylation of their intended targets in U87MG-EGFR* cells (fig. S4A). Although treatment with either inhibitor alone had no discernible effect on PI3K association with GAB1, combined inhibition with both erlotinib and SU11274 resulted in the release of p85α from the RTK/GAB1 complex and faster migration of GAB1, which is consistent with a reduction in GAB1 phosphorylation. Accordingly, downstream signaling as measured by P-Akt and P-S6 was inhibited only when two inhibitors were combined (Fig. 2B). Moreover, combined RTK inhibition significantly decreased viability of cultured U87-EGFR* cells (Fig. 2C) and reduced the number and size of soft-agar colonies formed in a stringent

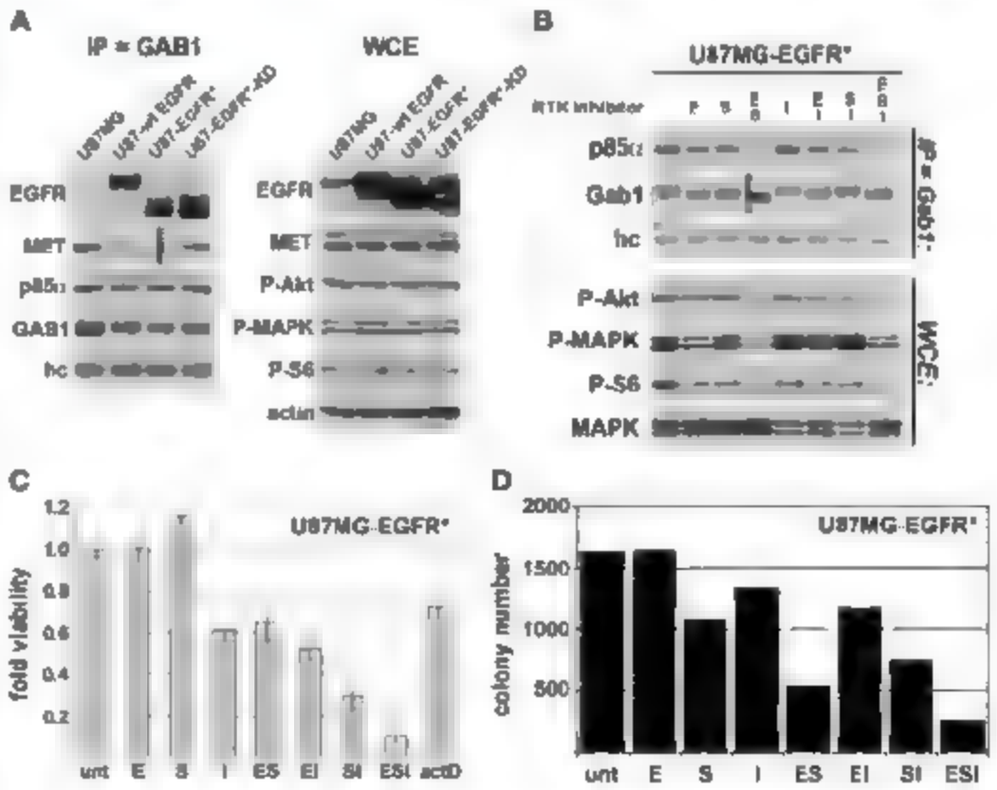

Fig. 2. Inhibition of multiple RTKs is necessary to abrogate PI3K and reduce cell survival. (**A**) The PI3K/GAB1 adaptor complex can readily switch between MET and EGFR binding with little discernable effect on downstream signaling. U87MG parental cells or cells constitutively expressing WT EGFR, the activating vIII deletion mutant (EGFR*), or the vIII mutant with an inactivating mutation in its kinase domain (EGFR*-KD) were immunoprecipitated (IP) with an antibody to the RTK/PI3K adaptor protein, GAB1 (left), and then immunoblots were probed with the indicated antibodies. Heavy chain (hc) is shown to demonstrate equal immunoprecipitation efficiency. WCEs from the same cells were immunoblotted with the indicated antibodies. (**B**) (Top) U87MG-EGFR* cells were treated with each of the RTK inhibitors [10 μM erlotinib (E), 10 μM SU11274 (S), and/or 10 μM imatinib (I)], and then WCEs were immunoprecipitated with an antibody to GAB1, eluted, and immunoblotted with antibodies to p85α or GAB1. Note the faster migration of GAB1 in lysates from RTK inhibitor–treated cells, which is consistent with a decrease in phosphorylation. (Bottom) WCEs were immunoblotted with the indicated antibodies. (**C**) Treatment with multiple RTK inhibitors decreases U87MG-EGFR* cell viability. Cells were treated for 72 hours with combinations of 10 μM E, 10 μM S, and 10 μM I, or with 100 nM actinomycin D (actD) in 0.05% serum-containing medium, and then cell viability was assayed by adenosine triphosphate quantitation. Error bars indicate SEM; n = four experiments. unt, untreated. (**D**) Impact of single and combination RTK-inhibitor treatments on soft-agar colony formation of U87MG-EGFR* cells. Cells were plated in 10% serum and 0.4% agarose-containing growth medium with 10 μM of each of the indicated RTK inhibitors. Colonies were counted after 18 days.

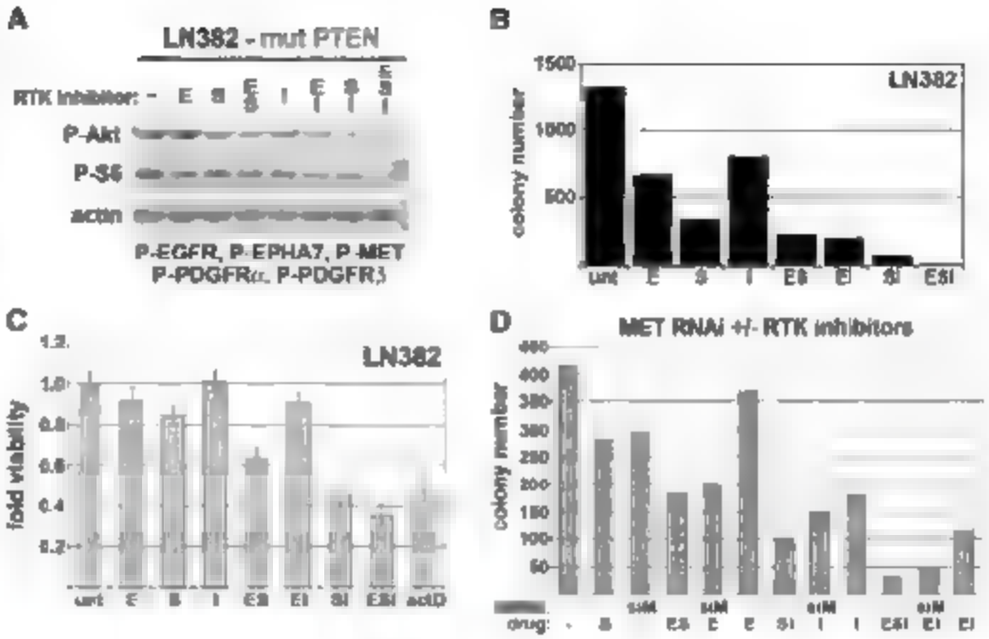

Fig. 3. Targeting multiple activated RTKs abrogates cell signaling, anchorage-independent growth, and viability. (**A**) The glioma cell line LN382 was treated with the indicated RTK inhibitors in 0.05% serum-containing medium and immunoblotted as in Fig. 2B. The activated RTKs detected in these cells on antibody arrays as in Fig. 1A are indicated beneath the blots. (**B**) Combined RTK-inhibitor treatments inhibit soft-agar colony formation in LN382 cells when plated and treated as in Fig. 2D. (**C**) The inhibition of multiple activated RTKs decreases cell viability. LN382 cells were treated with 10 μM E, 10 μM S, and/or 10 μM I, or with 100 nM actD, and then cell death was assayed as in Fig. 2C. Error bars indicate SEM; n = four experiments. (**D**) Soft-agar colony inhibition by MET siRNAs combined with RTK inhibitors. LN382 cells were transfected with MET siRNA (siM) or a scrambled negative control (–) and plated and treated with the indicated RTK inhibitors as in Fig. 2D.

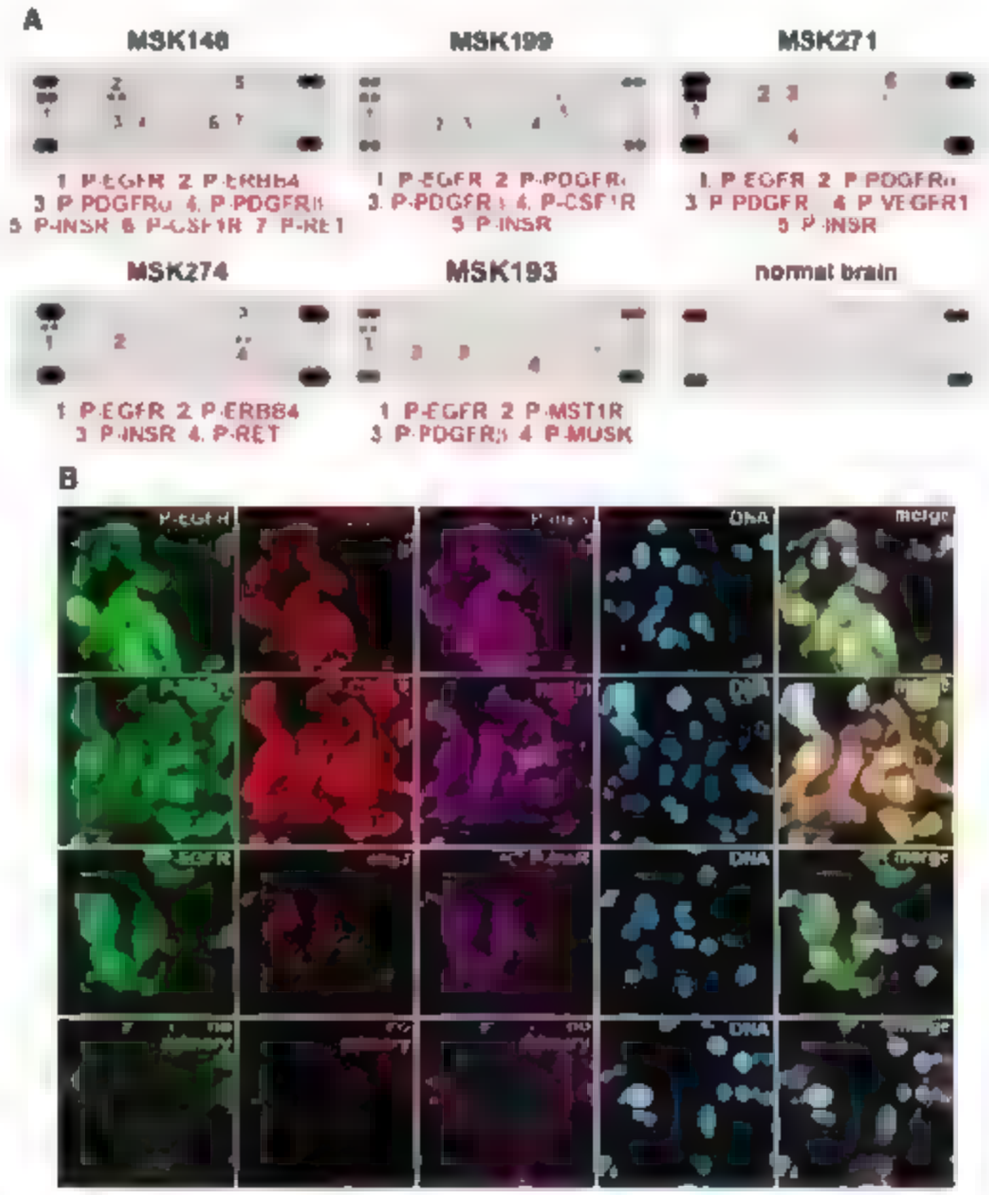

Fig. 4. Multiple RTKs are concomitantly activated in primary GBMs. (**A**) Antibody arrays were performed as in Fig. 1 on protein lysates extracted from snap-frozen primary human gliomas or normal brain autopsy material. (**B**) Coexpression of phospho-RTKs in cells dissociated from primary GBM MSK199. Individual tumor-derived cells were immunofluorescently stained with the phospho-RTK antibodies P-EGFR, P-PDGFRα, P-insR, or P-CSF1R. Each row depicts one field of cells from a slide simultaneously stained with the indicated antibodies. DNA is labeled with Hoechst 33342. Nestin is expressed in neural progenitor cells, tumor endothelial cells, and diffuse gliomas, including astrocytomas and GBMs (*20*), and olig2 is expressed in neural progenitors, normal oligodendroglia, and diffuse gliomas (*21*). The bottom row depicts cells stained only with secondary antibodies.

anchorage-independent growth assay (Fig. 2D and fig. S4B), whereas single inhibitors were less effective. In line with the lack of detectable phospho-PDGFR or c-KIT in U87MG-EGFR* cells (fig. S4A), treatment with the PDGFR/c-KIT/abl kinase inhibitor imatinib only slightly affected PI3K activation (Fig. 2B); however, when combined with erlotinib and SU11274, triple inhibitor treatment eliminated residual P-Akt and P-S6 activity (compare lanes 4 and 8 in Fig. 2B) and conferred the most dramatic inhibition on viability and anchorage-independent growth (Fig. 2, C and D), possibly reflecting the inhibitory activity of imatinib on other kinases in these cells (*17*).

Although it has been reported that PTEN loss abrogates the response of GBM to EGFR inhibitors (*10*), our finding that combination treatments significantly reduced P-Akt and P-S6 in PTEN-mutant U87MG-EGFR* cells (Fig. 2B) suggests that, even with PTEN deficiency, combined signaling from multiple RTKs is required to maintain downstream pathway activation, such as that of PI3K. To examine whether inhibition of coactivated RTKs via combination therapy mitigates PI3K activity in other PTEN-deficient glioma cells, we subjected multiple cell lines, either WT or mutant for PTEN, to single and combination treatment with erlotinib, SU11274, and imatinib. Consistently, PI3K signaling was reduced or completely abrogated with combined inhibition of coactivated RTKs irrespective of PTEN status (Fig. 3A and fig. S5A). Additionally, inhibition of PI3K activity via RTK inhibition abrogated anchorage-independent growth and cell viability (Fig. 3, B and C, and fig. S5, B and C). The decrease in cell viability was mediated in part by inhibition of PI3K signaling, because transient transfection of either myristoylated Akt or p110α-CAAX (C, cysteine; A, aliphatic amino acid; X, any amino acid) increased cell viability in drug-treated cells (fig. S6, $P < 0.001$). At the same time, the inability to completely rescue viability indicates that PI3K is not the sole mediator of functional RTK signaling. In these treatment studies, we are aware that (i) many kinase inhibitors exhibit activities against multiple kinases in addition to their primary targets (*17*) [e.g., SU11274 diminished P-PDGFRβ in LN382 cells (fig. S5D)] and (ii) a particular RTK may not be represented or be detected as activated on an antibody array. Nevertheless, in three different glioma cell lines, colony formation and cell viability were partially inhibited by single and dual treatment with RTK inhibitors but were most affected by combined treatment with all three inhibitors (Fig. 3, B and C, and fig. S5, B and C). Given the potential nonspecific actions of these agents, particularly SU11274 [the U.S. Food and Drug Administration (FDA)–unapproved MET inhibitor], we used RNA interference (RNAi) against MET to verify that genetic inhibition of MET can similarly confer enhanced anti-oncogenic activity of erlotinib and imatinib in LN382. Indeed, transfection of LN382 cells with MET small interfering RNAs (siRNAs), in combination with erlotinib and imatinib, resulted in a nearly similar level of inhibition in soft-agar colony formation in an anchorage-independent growth assay (Fig. 3D). Similar trends were observed with RNAi against PDGFR and EGFR (fig. S7). These results support the view that, even in PTEN mutant cells, more robust anti-oncogenic effects can be achieved through combined inhibition of relevant upstream signaling inputs.

Finally, we assayed untreated primary human GBM tumors from newly diagnosed patients for evidence of RTK coactivation. In contrast with a normal brain specimen that had no detectable RTK activation, each of the 14 GBM samples examined by antibody array profiling harbored multiple phosphorylated RTKs (Fig. 4A and table S2). These included known GBM RTKs, such as EGFR, PDGFRα, and MET, as well as RTKs not previously linked to GBM, such as RET, MST1R, and CSF1R. Given the well-known intratumoral heterogeneity in GBM, we performed immunofluorescence staining with phosphospecific antibodies against multiple RTKs and observed coexpression of activated RTKs in individual dissociated cells from a primary GBM (Fig. 4B). Together with the in vitro data above, this evidence of in vivo RTK coactivation supports our hypothesis that concomitant activation of multiple RTKs serves to reduce dependence on any single RTK for the maintenance of critical downstream signaling in a complex tumor microenvironment, thus rendering such tumors refractory to single-agent RTK inhibition.

The findings of this study provide a rational explanation for the feeble clinical responses to RTK-inhibitor monotherapy for many solid tumor types and anticipate more favorable outcomes by combinations of drugs against different activated RTKs or single drugs with inhibitory activities against multiple activated RTKs. Moreover, by demonstrating the capability to rapidly profile the activation status of most members of the RTKs in resected GBM specimens and the use of such profiles to tailor rational combination therapies, this study provides proof-of-concept for the eventual implementation of a "personalized" therapeutic paradigm in human cancer (*18*). Because FDA-approved RTK inhibitors are available and additional drugs are under development, this treatment paradigm could be readily implemented for cancers that are currently highly refractory to existing therapies.

References and Notes

1. E. A. Maher *et al.*, *Genes Dev.* **15**, 1311 (2001).
2. L. C. Cantley, *Science* **296**, 1655 (2002).
3. J. Li *et al.*, *Science* **275**, 1943 (1997).
4. H. Wang *et al.*, *Lab. Invest.* **84**, 941 (2004).
5. A. El-Obeid *et al.*, *Cancer Res.* **57**, 5598 (1997).
6. M. Nagane *et al.*, *Cancer Res.* **56**, 5079 (1996).
7. B. Wullich, H. P. Sattler, J. Fischer, E. Meese, *Anticancer Res.* **14**, 577 (1994).
8. P. Y. Wen *et al.*, *Clin. Cancer Res.* **12**, 4899 (2006).
9. J. N. Rich *et al.*, *J. Clin. Oncol.* **22**, 133 (2004).
10. I. K. Mellinghoff *et al.*, *N. Engl. J. Med.* **353**, 2012 (2005).
11. Materials and methods and supplementary figures are available as supporting material on *Science* Online.
12. J. C. Obenauer, L. C. Cantley, M. B. Yaffe, *Nucleic Acids Res.* **31**, 3635 (2003).
13. N. E. Hynes, H. A. Lane, *Nat. Rev. Cancer* **5**, 341 (2005).
14. H. Gu, B. G. Neel, *Trends Cell Biol.* **13**, 122 (2003).
15. K. M. Weidner *et al.*, *Nature* **384**, 173 (1996).
16. R. Nishikawa *et al.*, *Proc. Natl. Acad. Sci. U.S.A.* **91**, 7727 (1994).
17. M. A. Fabian *et al.*, *Nat. Biotechnol.* **23**, 329 (2005).
18. H. Varmus, *Science* **312**, 1162 (2006).
19. Y. Soneda *et al.*, *Cancer Res.* **61**, 4956 (2001).
20. K. Sugawara *et al.*, *Lab. Invest.* **82**, 345 (2002).
21. K. L. Ligon *et al.*, *J. Neuropathol. Exp. Neurol.* **63**, 499 (2004).

22. We thank W. Cavenee and F. Furnari for glioma cell lines, R. Pieper for the E6/E7/hTERT normal human fibroblasts, A. Chan for the myr-Akt construct, members of the DePinho and Chin laboratories, J. Engelman, and L. C. Cantley for helpful discussions, and Y.-H. Xiao, B. Feng, and J. Zhang for bioinformatics help. J.M.S. is funded by the American Brain Tumor Association and a Ruth L. Kirschstein National Research Service Award. H.Y. is funded by the American Brain Tumor Association. A.C.K. is a recipient of the Leonard B. Holman Research Pathway Fellowship. R.W. is supported by a Mildred Scheel Fellowship (Deutsche Krebshilfe). Grant support comes from The Claudia Adam Barr Foundation (A.H.S.), the Goldfarb Foundation (L.C.), and NIH grants RO1CA99041 (L.C.) and 5P01CA95616 (R.A.D., L.C., C.B., and K.L.L.). R.A.D. is an American Cancer Society Research Professor and an Ellison Medical Foundation Scholar and is supported by the Robert A. and Renee E. Belfer Foundation Institute for Innovative Cancer Science. This work was conducted solely at the Dana-Farber Cancer Institute and has no industrial connection or influence. R.A.D. is a member of the Senior Advisory Board of Abbott Pharmaceuticals and is a cofounder, scientific advisor, and director of Aveo Pharmaceuticals. L.C. is a cofounder and scientific advisor of Aveo Pharmaceuticals.

Supporting Online Material

www.sciencemag.org/cgi/content/full/1142946/DC1
Materials and Methods
Figs. S1 to S7
Tables S1 and S2

23 March 2007; accepted 31 August 2007
Published online 13 September 2007;
10.1126/science.1142946
Include this information when citing this paper.

X-Ray Detectors

The Saturn 944+ and Saturn 724+ are new high-performance charge-coupled device (CCD) based area x-ray detectors optimized for macromolecular and small molecule x-ray crystallography, respectively. With a four-fold increase in readout speed (to 8 MHz total) and improved signal-to-noise and dynamic range, the Saturn+ line of third generation CCD x-ray detectors is optimized for high-performance x-ray crystallography applications in which maximum productivity is essential. This new generation of CCD detectors delivers high readout speeds without any significant increase in read noise. Both detectors make use of the Kodak KAF-4320E CCD sensor, incorporating transparent indium tin oxide technology. A large-format, front-illuminated sensor, optimized for high dynamic range and superior spatial resolution, is coupled with a state-of-the-art, high-speed, 18-bit analog-to-digital converter and four-port parallel readout to deliver low noise, a true 17,500:1 dynamic range, and fast readout times.

Rigaku For information 281-362-2300 www.rigaku.com

Packaging Extracts

MaxPlax Lambda Packaging Extracts are a convenient, high-efficiency system designed for in vitro packaging of any vector containing cos sites. They are supplied as predispensed single-tube reactions that require no premixing of different components before use. The extracts are devoid of all known restriction activities and have been optimized for packaging of methylated and unmethylated DNA.

Epicentre Biotechnologies For information 800-284-8474 www.EpiBio.com

Isothermal Titration Calorimeter

The iTC200 isothermal Titration Calorimeter can achieve gold-standard binding affinities with only 200 µl of sample. The instrument determines all binding parameters label-free and without the need for immobilization, using as little as 5 µg to 10 µg of protein. Requiring no assay development, the unit is designed to address the needs of drug discovery and development in such applications as hit selection, lead optimization, and binding characterization. It is controlled by an intelligent user interface that assists in experimental design and processes data at the end of sample runs. Results are presented in an Excel format for further analysis or data transfer. It can be upgraded to a fully automated version capable of running up to 50 samples a day and 384 samples unattended.

MicroCal For information 800-633-3115 www.itc200.com

Polysorbate Analysis

Reverse-phase high-performance liquid chromatography can be used with the Corona CAD (charged aerosol detection) detector for sensitive and robust analysis of polysorbates. The system is suitable for both speciation of the various individual components of a non-ionic mixture and for batch-to-batch comparisons to measure variations in polysorbate composition from various sources or lots of material. Advantages of the system include low nanogram sensitivity, a dynamic range exceeding four orders of magnitude, and good precision response factors that are independent of structure.

ESA Analytical For information +44-1844-239381 www.esainc.com

Hydrogels for Stem Cell Applications

Extracel-LG hydrogel is a hyaluronan-based, synthetic extracellular matrix that can be easily customized for a specific stem cell type or application. For instance, researchers can add specific human growth factors and/or extracellular matrix proteins to the hydrogel to design the ideal formulation for their needs. Researchers can also adjust Extracel-LG's stiffness, allowing an additional level of experimental control.

Glycosan BioSystems For information 801-583-8212 www.glycosan.com

Mass Spectrometer

The apex ultra Fourier transform mass spectrometer (FT-MS) features outstanding dynamic range, resolving power, and mass accuracy. Its unique refrigerated superconducting magnet technology is available at 7, 9.4, 12, and 15 Tesla. It provides a powerful and flexible system for top-down proteomics and the analysis of complex mixtures in metabolomics. The apex ultra combines the power of FT-MS with the latest quadrupole technology (complete with linear ion trapping modes) and a multipole collision cell. It extends the power of FT-MS with improved mass accuracy and resolving power through the development of tailored, low-noise detection electronics. Features include exact MS analysis to sub-parts per million levels for unambiguous determination of elemental chemical composition and exact MS(n) capability for detailed structural analysis and peptide sequencing. Automated software confirms composition with m/z and isotopic pattern information.

Bruker Daltonics For information 978-667-9580 www.bdal.com

Grinding Resin

Designed for the extraction of proteins and DNA, EZ-Grind consists of grinding tubes containing a high-tensile microparticle grinding resin and matching pestles. The grinding resin is a neutral, abrasive material and does not bind protein or nucleic acids. The combination of the matching pestles and resin effectively disrupts tissues, cells, cell organelles, and nuclei.

Genotech/G-Biosciences For information 800-628-7730 www.GBiosciences.com

Cell Migration Assay

The sensitive and flexible Oris Cell Migration Assay provides key features that are critical to researchers performing cell-based assays. The assay is highly reproducible, allows for kinetic and endpoint studies, permits multiple approaches to cell labeling, makes use of readily available lab equipment, allows for morphological analysis of cells, and is available in a convenient, 96-well format. The assay is offered as a one-plate starter pack and as a five-plate refill pack. Cell migration is critical to a variety of bodily processes, including tumor cell metastasis, wound healing, development of new blood vessels, and tissue regeneration.

Platypus Technologies For information 608-237-1270 www.platypustech.com

Newly offered instrumentation, apparatus, and laboratory materials of interest to researchers in all disciplines in academic, industrial, and government organizations are featured in this space. Emphasis is given to purpose, chief characteristics, and availability of products and materials. Endorsement by Science or AAAS of any products or materials mentioned is not implied. Additional information may be obtained from the manufacturer or supplier.

POSITIONS OPEN

ASSISTANT PROFESSOR
Forage Breeder
Department of Agronomy

Appointment conditions: tenure track, nine months, full time. Proposed start date: August 16, 2008. The Raymond F. Baker Center for Plant Breeding and the Department of Agronomy invites applications for a faculty position in plant breeding. The successful candidate will develop and utilize contemporary breeding methods and emerging technologies to improve cultivars and germplasm of forages and bioenergy crops adapted to the upper midwestern United States. Crops include plant species that support livestock and/or bioenergy production systems. The individual will be able to participate in interdisciplinary research teams such as the sustainable agriculture and bioenergy programs. The appointee will be expected to attract extramural funding, release improved cultivars and germplasms, supervise the statewide forage variety testing program, and publish research in peer-reviewed journals. This position is seen as 75 percent research and 25 percent teaching. Teaching may include undergraduate and graduate classroom instruction, advising undergraduates, or directing undergraduate research. Supervision and advising of plant breeding graduate students, participation in curriculum development, outreach programs, and performance of University service are also expected. Iowa State University especially seeks candidates who will contribute to the diversity and excellence of the academic community through their research, teaching, and outreach. Iowa State University (ISU) is one of the country's leading agricultural research universities and is in one of the top agricultural states in the United States. Located in the city of Ames, ISU is in the heartland of U.S. culture and agriculture. Ames has abundant recreational and entertainment opportunities and an outstanding school system. This faculty position affords significant opportunities for the development of strong interdisciplinary research teams with departmental faculty, allied departments on the ISU campus, research organizations such as the USDA Agricultural Research Service, and other state and national partners.

Required qualifications: Ph.D. in plant breeding or related field with background in plant breeding field methods and laboratory analyses; experience that demonstrates statistical expertise; training in molecular technologies; and excellent written and oral communication skills.

Preferred qualifications: postdoctoral training in a field related to plant breeding and/or at least one year of experience in cultivar development. Skill in the application of emerging statistical and molecular technologies to plant breeding. Experience in one or more of the following: plant pathology, entomology, agronomic crop production, quantitative genetics, statistical genetics, or bioinformatics; documented ability to work collaboratively with researchers, industry, farmers, and consumers; documented evidence of professional interest, proficiency and experience in research and teaching; Salary: commensurate with qualifications. Application instructions: Please send a letter of application, curriculum vitae, credentials, descriptions of teaching and research interests and experience, and the name, address, and telephone numbers of three references to: **Dr. Kendall Lamkey, Chair, Department of Agronomy, 2101 Agronomy Hall, Iowa State University, Ames, IA 50011.** The application deadline is November 30, 2007, or until the position is filled.

Montana State University Department of Microbiology seeks an infectious disease **MICROBIOLOGIST** for a tenure-track position at the **ASSISTANT, ASSOCIATE, or FULL PROFESSOR** level. Responsibilities include teaching at the undergraduate and graduate levels and developing or maintaining an extramurally funded research program. Candidates for this position should have current extramural funding. Competitive salary and startup funds are available. For more information and to apply please see our website: http://www.montana.edu/cgi-bin/msuinfo/fpview/f/~4042. Screening of applications will begin October 15, 2007, and continue until the position is filled. *MSU Bozeman, is an AD A/Affirmative Action/Equal Opportunity/Females/ Preference Employer.*

POSITIONS OPEN

INSTITUT PASTEUR

POSTDOCTORAL FELLOWSHIPS
Institut Pasteur, Paris, France

Founded in 1887 by Louis Pasteur and located in the heart of Paris, the Institut Pasteur is a world renowned private research organization. The Pasteur Foundation of New York is seeking outstanding fellowship applicants. Candidates may apply to any laboratory within 10 Departments: Cell Biology and Infection, Developmental Biology, Genomes and Genetics, Immunology, Infection and Epidemiology, Microbiology, Neuroscience, Parasitology and Mycology, Structural Biology and Chemistry, and Virology. See website for details. Annual package is $70,000 for three years. This is a biannual call for applicants; see website for deadlines. EOE. *Interviews required.*

E-mail: pasteurus@aol.com Website: http://www.pasteurfoundation.org.

INTEGRATIVE VERTEBRATE PHYSIOLOGIST

The Department of Biology at Colorado State University invites applications for a full-time tenure-track faculty position in integrative vertebrate physiology, at the rank of **ASSISTANT PROFESSOR.** Competitive applicants will investigate physiological processes that integrate across complex systems in the laboratory and/or field, and address mechanistic questions at the cell, tissue, organ system, or organism level. Successful candidates will contribute to undergraduate and graduate teaching and education.

Candidates using molecular and/or biochemical approaches including but not limited to functional genomics, proteomics, or metabolomics are encouraged to apply. For full details see website: http://www.biology.colostate.edu/Jobs/.

Applicants must have a Ph.D. by the time of appointment; postdoctoral experience is preferred. To receive full consideration apply online by November 5, 2007 (website: http://www.natsci.colostate.edu/searches/Biology). Include curriculum vitae, statements of research/teaching interests, representative publications, and the names and contact information for three referees. Referees will receive instructions by e-mail for submitting letters online. Complete applications of semi-finalists will be available to all biology faculty. *Colorado State University is an Affirmative Action/Equal Opportunity Employer. Office of Equal Opportunity and Diversity, 101 Student Services.*

NATIONAL UNIVERSITY of SINGAPORE
Department of Chemical and Biomolecular Engineering

The Department of Chemical and Biomolecular Engineering at National University of Singapore invites applications for TENURE-TRACK FACULTY POSITIONS at all levels. The Department is one of the largest internationally with excellent in-house infrastructure for experimental and computational research. A Ph.D. in chemical engineering or related areas and a strong research record with excellent publications are required. Please refer to website: http://www.chbe.nus.edu.sg/ for more information on the areas of interest and for application details. Applicants should send full curriculum vitae (including key publications), a detailed research plan, a statement of teaching interest, and a list of names of at least three references to: **Professor Raj Rajagopalan, Head of Department (attention: Ms. Nancy Chia, e-mail nancychia@nus.edu.sg).**

THE INNOVATION IMPERATIVE

by Peter Gwynne

The 2007 version of Science's *annual survey of Top Employers features a tight race for first place among three companies. It also reveals the key ingredient for all successful employers a commitment to innovative thinking throughout the product pipeline, from the laboratory to the clinic or marketplace.*

For the first time in its six years of existence, *Science*'s survey of Top Employers in the biotechnology, biopharmaceutical, pharmaceutical, and related industries has produced a winner not named **Genentech**. In a desperately close contest, last year's No. 2, Germany-based **Boehringer Ingelheim**, just beat out Genentech and another California biopharma, **Amgen**. This year's survey also marked the arrival in the top 10 employers of two firms from beyond the traditional biotech/biopharma/pharmaceutical cluster: chemical giant **DuPont** and agricultural company **Monsanto**.

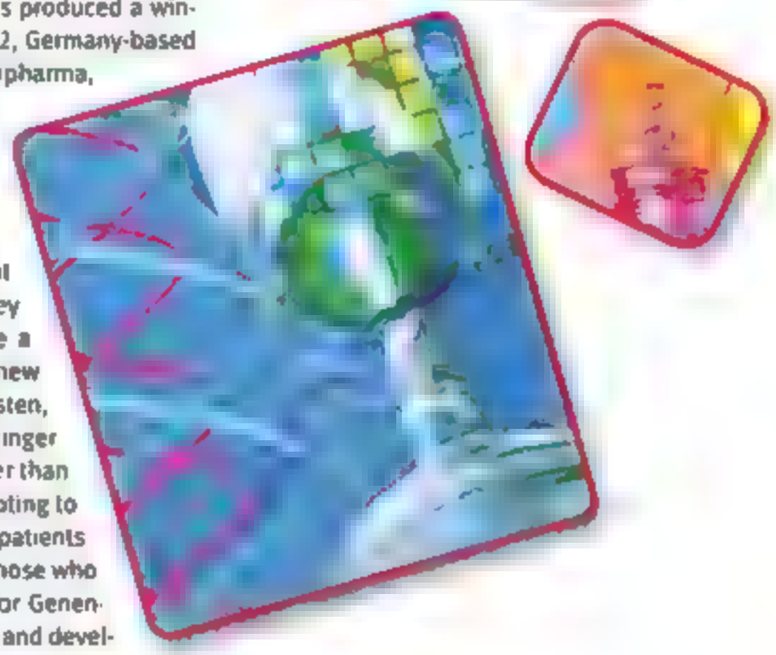

Constant Themes

The lineup of the top employers may have changed, but the themes that underpin their success remain largely constant. Respondents to the survey highlighted the critical importance of innovation. "It's important to have a strong commitment to research and innovation as a driver for producing new and better medicine for patients and for our own growth," says Mikael Dolsten, executive vice president, and head of worldwide pharma research, at Boehringer Ingelheim. Equally important is the ability to develop genuinely new—rather than me-too—drugs and other products. "With all our medications, we're attempting to develop an understanding of the mechanism of the disease and of which patients will respond, so that we can treat those patients who will respond and not those who won't," comments Richard Scheller, executive vice president of research for Genentech. Adds Roger Perlmutter, Amgen's executive vice president for research and development: "We use science and innovation to drive advances in medicine."

Survey takers—and representatives of top 10 companies—agree that the challenge of addressing unmet medical needs also plays a strong role in the perception of companies by potential employees and other outsiders. So does the flexibility and nimbleness that arrive when even the largest corporations encourage small-firm behavior. "We are succeeding by behaving like a small company with in a big company," explains Thomas Koestler, executive vice president at **Schering-Plough** (who placed fourth in the survey) and president of the Schering Plough Research Institute.

Respondents reported mixed feelings about their business. Issues such as drug recalls and failures of promising molecules in the late stages of clinical trials have continued to besmirch the industry's reputation. On the other hand, the emergence of new products such as drugs for cancer, HIV/AIDS, and rare diseases, as well as progress in stem cell research, are strong positives in the industry's favor. Nevertheless, almost a third of participants said that it was at least fairly likely that they would seek a new job within a year.

Two Groups of Respondents

Commissioned by *Science*'s Business Office, Senn-Delaney Culture Diagnostics & Measurement carried out the web-based survey between May 2 and June 6. This year the study involved an expanded group of respondents. In addition to AAAS members, registrants with ScienceCareers.org, and visitors to the *Science* website who had registered with AAAS, for the first time Senn-Delaney added a second tranche of survey takers, obtained continued »

> "It's important to have a strong commitment to research and innovation as a driver for producing new and better medicine for patients and for our own growth."

UPCOMING FEATURES

Careers in Neuroscience— October 26

Focus on Diversity 3— November 16

Interdisciplinary Research— November 23

Top Twenty Employers

2007 Rank	2006 Rank	Employer (Global Headquarters)	Three Top Characteristics		
1	2	Boehringer Ingelheim (Ingelheim, Germany)	Does important, quality research	Socially responsible	Loyal employees
2	1	Genentech, Inc. (South San Francisco, CA)	Innovative leader in the industry	Does important, quality research	Loyal employees
3	4	Amgen (Thousand Oaks, CA)	Does important, quality research	Innovative leader in the industry	Socially responsible
4	17	Schering-Plough Corp. (Kenilworth, NJ)	Does important, quality research	Socially responsible	Innovative leader in the industry
5	6	Genzyme Corp. (Cambridge, MA)	Does important, quality research	Innovative leader in the industry	Socially responsible
6	9	Novartis (Basel, Switzerland)	Does important, quality research	Innovative leader in the industry	Socially responsible
7	–	DuPont (Wilmington, DE)	Does important, quality research	Loyal employees	Socially responsible
8	–	Monsanto (Creve Coeur, MO)	Innovative leader in the industry	Does important, quality research	Loyal employees
9	5	AstraZeneca PLC (London, UK)	Does important, quality research	Innovative leader in the industry	Socially responsible
10	7	Johnson & Johnson (New Brunswick, NJ)	Socially responsible	Does important, quality research	Loyal employees
11	8	Eli Lily and Company (Indianapolis, IN)	Does important, quality research	Treats its employees with respect	Loyal employees
12	10	GlaxoSmithKline (London, UK)	Does important, quality research	Innovative leader in the industry	Socially responsible
13	–	Millennium Pharmaceuticals (Cambridge, MA)	Does important, quality research	Innovative leader in the industry	Treats its employees with respect
14	16	Merck & Co., Inc. (Whitehouse Station, NJ)	Does important, quality research	Innovative leader in the industry	Loyal employees
15	11	Wyeth Pharmaceuticals (Collegeville, PA)	Does important, quality research	Socially responsible	Loyal employees
16	–	Gilead (Foster City, CA)	Innovative leader in the industry	Does important, quality research	Treats its employees with respect
17	13	Biogen Idec (Cambridge, MA)	Does important, quality research	Treats its employees with respect	Innovative leader in the industry
18	3	Roche Pharmaceuticals (Basel, Switzerland)	Does important, quality research	Innovative leader in the industry	Loyal employees
19	18	Abbott (Abbott Park, IL)	Does important, quality research	Socially responsible	Loyal employees
20	20	Bristol-Myers Squibb Company (New York, NY)	Does important, quality research	Socially responsible	Treats its employees with respect

The 20 companies with the best reputations as employers, according to respondents in the 2007 survey undertaken for the *Science* Business Office.
The companies without a 2006 rank did not receive enough mentions to qualify during the 2006 survey.

via an e-mail blast to 968 human resources contacts in industry drawn from the AAAS sales database. The traditional list yielded 839 respondents, while the e-mail blast produced 2,318 more, for a total of 3,157. More details on the demographics of the respondents can be seen on page 296.

The survey asked each participant to list the companies that she or he regarded as the best, average, and worst employers in the biotechnology, biopharmaceutical, pharmaceutical, and related fields. Individuals were allowed to vote for their own companies; in fact 63 percent of participants work for the employers that they regarded as best. Respondents then rated the companies that they had chosen on 23 driving characteristics, such as financial strength, easy adaptation to change, and a research-driven environment. To categorize companies on the basis of that information, Senn-Delaney used a statistical process that included frequency analysis, stepwise regression, and discriminant analysis. That resulted in a unique ranking score for each company rated. Only those companies rated by at least 20 respondents qualified for inclusion in the survey.

Three Tiers in the Top 10

The top 10 companies occupy three tiers, based on their scores. In the top tier, separated by a hair's breadth with ranking scores between 90 and 100, are Boehringer Ingelheim, Genentech, and Amgen. Standing alone in the second tier, with a ranking score in the 80s, is fourth-placed Schering-Plough. And rounding out the top 10, scoring in the 70s, Genzyme, Novartis, DuPont, Monsanto, continued »

AstraZeneca, and **Johnson & Johnson** occupy the third tier.

The six most important driving characteristics, as judged by survey participants, changed from those of 2006 in only one respect. *Doing important quality research* replaced *having a clear vision toward the future* in sixth place. *Being an innovative leader in the industry* continued as the most important driver, followed by *treating employees with respect; having work culture values aligned with personal values; having loyal employees;* and *being socially responsible.*

Inevitably, the leading employers scored well on those key drivers. Respondents gave Boehringer Ingelheim and Amgen extremely high ratings on each of the six. Genentech scored top grades on innovative leadership, important quality research, and the loyalty of its employees. And Schering-Plough won plaudits for the quality of its research and social responsibility.

Demographics

Gender:
59% male, 41% female

Experience:
58% have more than 10 years work experience

Career Status:
3/4 report that they have not yet reached the peaks of their careers

Company Type.
31% biotech, 40% pharma, 17% biopharma; more than nine out of 10 work in private industry

Geography:
almost 1/4 in continental Europe; 71% from North America

No Overnight Success

The top employers haven't earned their reputations overnight. "Our process started in the early 1990s, when we developed a corporate vision of how we would establish an environment in which people would work well together," explains Hans-Joachim Geppert, head of corporate division human resources at Boehringer Ingelheim, which has improved from eighth place in 2005. "Then in 2004 we reloaded, with a concept that we call Lead & Learn. This outlines ways in which we can deliver our corporate vision of Value through Innovation.

Schering-Plough's Koestler attributes his company's rise from 17th place last year to a six- to eight-year plan laid out by newly arrived CEO Fred Hassan in 2003. A change in name and mission five years ago helped **Wyeth** to break into the top 20 in 2005 and to maintain its position there since. And the arrival of a new CEO helped **Millennium Pharmaceuticals** to regain the place in this year's top 20 that it had lost in 2006.

Maintaining high placement also requires a vision for the future. "It all starts with our mission, our aspiration, and our values, which are very clear to our employees and anyone who seeks a position here," says Amgen's Perlmutter. "We have a very strong commitment to getting the best people in the world and putting them into a system in which their performance is enhanced," says Jeffrey Elton, senior vice president of strategy and global chief operating officer of the Novartis Institutes for BioMedical Research.

Ideas and Initiatives

Recruiting the right people, inculcating them with the corporation's values, providing them with scientific challenges, and including them in discussion of the company's goals have played major roles in Boehringer Ingelheim's success. "We encourage everybody to come up with ideas and initiatives," Geppert explains. "To be successful, you need a long-term strategy; you have to convince people that you stay with your principles and your ethics."

Dolsten echoes those points. "We have been able to show over many years how we build on long-lasting core principles and deliver value by efficiently translating advances in basic science into new medicines," he says. "This continuity operates in a climate of continuous change in which we provide ourselves with challenges. We count on our people to contribute and grow together. In R&D we aim to have a dialogue with our associates as to where we are heading and what our key drivers are."

Trust in its employees earns the company a quid pro quo in terms of loyalty. "The average time our employees stay with us is almost 13 years," Geppert points out. "It's not unusual for some to celebrate their 25th and even their 40th year with us." Indeed, the company relies on internal promotions to fill 80 percent of its key positions worldwide. "This isn't a primary goal, but we feel very comfortable with it," Geppert says. "It shows that we want to give the majority of our people internal options while we like to bring in fresh blood."

That approach, combined with Lead & Learn principles, started three years ago, has paid dividends internally and externally. "Our emphasis on values through innovation has had a strong fingerprint," Dolsten notes. "Employees appreciate the company's commitment to provide drugs that make a true difference to patients." And in the past year, he continues, "candidates for jobs from other companies have been very interested in learning about Boehringer Ingelheim. People have actively contacted us to learn what we stand for and about our pipeline of new drugs. Senior scientists have even been prepared to make lateral moves to join us."

Continuing Success

Genentech continues to rely on the formulae that have made it so successful in the past. "We stick with the science," Scheller says. "We have not made any changes in our general philosophy of following scientific innovation in an attempt to develop novel, breakthrough medicines to improve and extend people's lives. Our approach produces new insights into basic biology. So much of what you learn depends on how you ask the questions; we are asking the questions a little differently from the academics who study mouse models."

The company challenges its scientists in both basic science and biomedical research. "People respond to our balance of basic and translational research," Scheller continues. "Our postdoctoral program continues to be strong, and to make fundamental discoveries that the postdocs can publish. We feel it's extremely important to contribute to the general knowledge of basic science."

Such knowledge led to a significant medical advance last year. It took the form of a molecule that might attack the wet form of macular degeneration—a major cause of blindness in older individuals—without causing unpleasant side effects. "We did a long series of studies with thousands of patients and showed that this medication, Lucentis, actually reduced wet macular continued

Driving Characteristics of Top Employers

2007	2006
1. Innovative leader in the industry	1. Innovative leader in the industry
2. Treats employees with respect	2. Treats employees with respect
3. Work and personal values are aligned	3. Work and personal values are aligned
4. Loyal employees	4. Loyal employees
5. Socially responsible	5. Socially responsible
6. Does important, quality research	6. Clear vision toward the future

Colored backgrounds indicate the characteristics in common for the two years

degeneration," Schelier recalls. "The company is really, really proud of this discovery. People work here because of things like that."

Encounters with Controversy

Not every good deed goes unpunished in the biopharmaceutical world, however. Ophthalmologists had found that Avastin, a Genentech cancer drug, could also modify wet macular degeneration when injected into the eye. Critics complained that the company priced Lucentis at a significantly higher rate than Avastin and prevented Avastin's use in the eye. However, Schelier says, "There have been no clinical studies to demonstrate that Avastin is safe for optical use. It's not manufactured to the standards that the US Food and Drug Administration requires for use in the eye."

Amgen had its own encounter with controversy during the past year. The company has faced challenges to its anemia franchise, including safety concerns that triggered regulatory changes to its Aranesp (darbepoetin alfa) and EPOGEN (Epoetin alfa) labels. Perlmutter sees plenty of positives in the fact that Amgen nevertheless maintained its position in the top five. "In the face of the challenges related to some of our products, we emphasize our commitment to patient safety and to scientific research," he says, "knowing that the truth will emerge despite economic and marketplace challenges."

Like Boehringer Ingelheim and Genentech, the number three company puts strong emphasis on innovation. "We are first and foremost science based," Perlmutter says. "We also try to provide an environment in which staff members feel empowered. In R&D, we encourage personal and scientific growth; we have a scientific career track for those who want to stay close to the lab and a managerial path for those who want to get more involved in those areas. We pay a lot of attention to leadership attributes. And we offer an enormously competitive benefits package."

Moving Up the Table

Echoing Boehringer Ingelheim, Schering-Plough has moved rapidly up the table as a result of a fresh management initiative and success in behaving like a small company within a large company. "A key component of our strategic plan has been to make long-term investments in science and technology, and to stress scientific excellence. This is demonstrated by our substantial growth in R&D investment between 2003 and 2007," Koestler says. "We are advancing and strengthening our pipeline. Across the organization we are delivering high performance, at a time when many of our industry peers are having issues and in some cases downsizing their work forces." The new emphasis has already led to the discovery of Zetia, which Koestler describes as "the first new class of cholesterol product in two decades."

Novartis, on the other hand, attributes its consistently high position in the annual surveys to a constant approach to drug discovery. "A couple of notions pop out more than others," Elton says. "As the first, Novartis overall and the Novartis Institutes for BioMedical Research have the commitment to focus on the unmet needs of patients, that's how we design our portfolio. The second area involves being an innovator—having unique insights, making them practical, and translating them into a therapeutic approach." Like other top companies, the firm believes in challenging its scientists. "There's a very strong emphasis on talent models," Elton continues, "and we take [into account] the opinions of all our associates."

Two Newcomers

Two of the newcomers to the top 10 focus on biotechnology beyond the pharmaceutical arena. "We have made a very strong commitment to the food and value chain—to green biotech," says Uma Chowdhry, senior vice president and chief science and technology officer for DuPont. "We're also committed to white biotech, the application of biotechnology to industrial production. We're now looking at the world of biology and asking how to use our tools to make a more sustainable world with a focus on biofuels and renewable materials, for example." Monsanto, meanwhile, "has been dedicated to being a leader in innovation, particularly in agriculture," says vice president of biotechnology Steve Padgette. "We invested heavily in biotechnology. Now we're delivering products to customers."

DuPont's basic principles mirror those of other members of the top 10 employers. "Because of our tradition of innovation via science," Chowdhry says, "we have successfully transformed our science into successful products for our customers." Staffers appreciate that. "Most employees in R&D stay here because of the caliber of our people and the quality of our science that is committed to improving peoples' lives," she continues.

Monsanto works on similar principles. "We're very much a technology-driven company," Padgette says. "We have a real commitment from our senior executives not only to support our R&D but also to make sure that we have a really great place for all our employees. We have this nice balance between long-term science investment and product focus."

The arrival of fresh blood in the corner office helped to reverse a decline in the perception of Millennium Pharmaceuticals. Last year, the biopharmaceutical company dropped out of the top 20 employers. This year, under new chief executive officer Deborah Dunsire, it has returned to 13th place. "She has overhauled the entire commercial situation and got it on track," says chief scientific officer Joseph Bolen. "And we have focused the entire R&D organi-

continued »

You can find an expanded version of this feature by going to: dx.doi.org/10.1126/science.opms.r0700045

zation —our most important asset. In research, the productivity is finally living up to what the expectations have been for a long time."

Wyeth has also benefited from an improved reputation that followed its change of name from American Home Products and its concentration on pharmaceuticals. "From the CEO downwards, there's a commitment to the belief that basic research will deliver the medicines of tomorrow," says Frank Walsh, vice president and head of discovery research. "Our drug discovery organization has been spectacularly successful over the past few years."

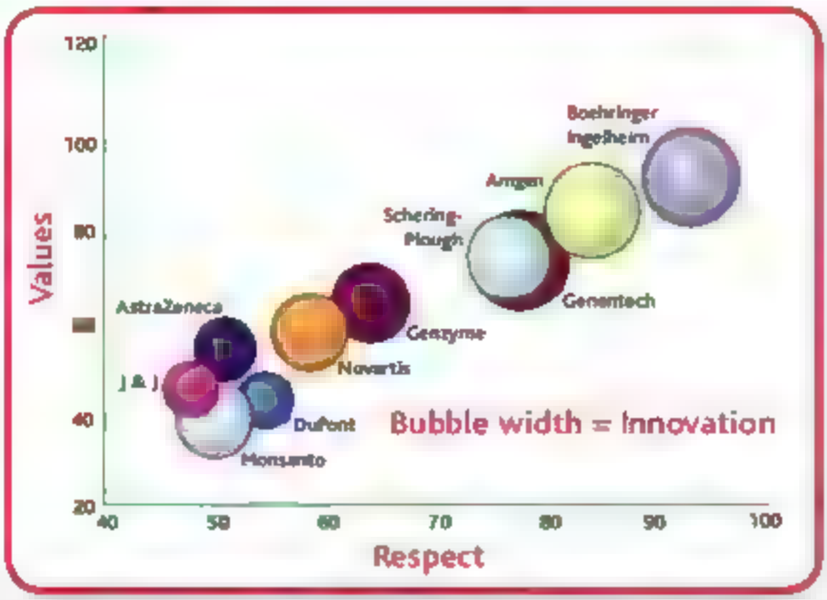

Comparison of the top 10 companies on the basis of the top 3 drivers (scored out of 100): *Innovative leader in the industry* (bubble width), *Treats employees with respect* (x-axis), and *Work and personal values are aligned* (y-axis).

says. "We also spend a lot of time monitoring the safety of our marketed products." Amgen offers its own assurances. "We're doing a lot of work to improve clinical trial design and to improve the way drugs are discovered and developed," Perlmutter says. "We've talked the talk and we also walk the walk." Schering-Plough's Koestler emphasizes a particular facet of improving corporate reputations. "It is very important that we maintain our sense of humility," he says, "while recognizing the importance of our contributions to improving the quality of human life."

Survey takers' ambivalence toward the biopharma/biotech industry extends to their personal places in it. The main advantages of working in the industry, they say, include the opportunity to have an impact on the world by developing life-saving drugs and helping patients to live better lives. On the other hand, respondents see the industry's negative public image as a major liability. That image, they say, has led to a loss of credibility, a low public opinion, and a perception that they are members of an untrustworthy industry.

The decline in the industry's reputation probably accounts for the fact that almost one-third of the respondents report that, within the next year, it's at least fairly likely that they will seek a different job. They give two main reasons: the desire for new challenges and experiences, sometimes in a new or different field, and a wish for career advancement, with the opportunity for professional growth. Other reasons include the impending end of a contract, the search for better salary and benefits, the ambition to take on a management role, distress at a change in corporate direction, stress in the workplace, and strictly personal issues such as location and family reasons.

Positive and Negative Perceptions

In addition to determining top employers, the survey gave respondents the opportunity to voice their thoughts about the industry as a whole and their places in it. It asked them to name recent events with the greatest impact on the industry's reputation, to suggest actions that could improve that reputation, and the advantages and disadvantages of working in the industry.

Like last year, respondents pinpointed two continuing controversies as the main causes of negative perceptions of the industry. First came drug recalls and the medical and legal issues surrounding drugs such as Vioxx that had been approved for sale and then had proved fallible. Failures in clinical trials, most notably the organ failures caused by the immunosuppressive drug candidate TGN1412, contributed their own negative sentiment. Other issues included the cost of medications and health care, and changes in the industry, such as acquisitions, mergers, downsizing, and outsourcing.

Again echoing last year's survey, respondents saw plenty of reasons to applaud the industry. New products and developments, such as new drugs for cancer, fresh therapies for rare diseases, progress in medications for HIV/AIDS, and advances in stem cell research had the greatest positive impact.

What should companies do to improve their own and the industry's reputation? Respondents' most common advice: Be honest, ethical, and more accountable, and educate and communicate with the public. That means admitting mistakes, answering tough questions, being forthcoming and open, increasing transparency, and earning the public's trust. Other actions recommended by respondents include showing social and environmental responsibility—by doing charity work, for example; fostering more collaborative research and funding more research; controlling costs and lowering drug prices; and demonstrating a commitment to safety.

Prescriptions for Improvement

Several companies have already taken actions in line with those recommendations. "We go to great lengths to ensure that patients who need our medications get our medications," Genentech's Scheller

Keep Them Smiling

The top employers report far lower levels of job seeking among their employees. That stems in large measure from their conscious efforts to keep their scientists and other staffers content. These include high salaries and benefits that range from stock options to child care help. But the main stimuli for a dedicated scientific workforce are challenging problems and top-notch colleagues. "As long as people believe that the options they have here and the teams they work with are the best, they'll stay to make Novartis a company that makes people proud to come to work for every day," Elton says. "We try to keep the challenges high and the understanding high," Monsanto's Padgette adds, "so that our people can be excited at the contributions they're making to the marketplace." Walsh of Wyeth summarizes the approach to retaining talent: "We have a very empowered scientific environment," he says, "in which scientists can make decisions and genuinely direct their science."

A former science editor of Newsweek, *Peter Gwynne writes about science and technology from his base on Cape Cod, Mass., U.S.A.*

TOP EMPLOYERS

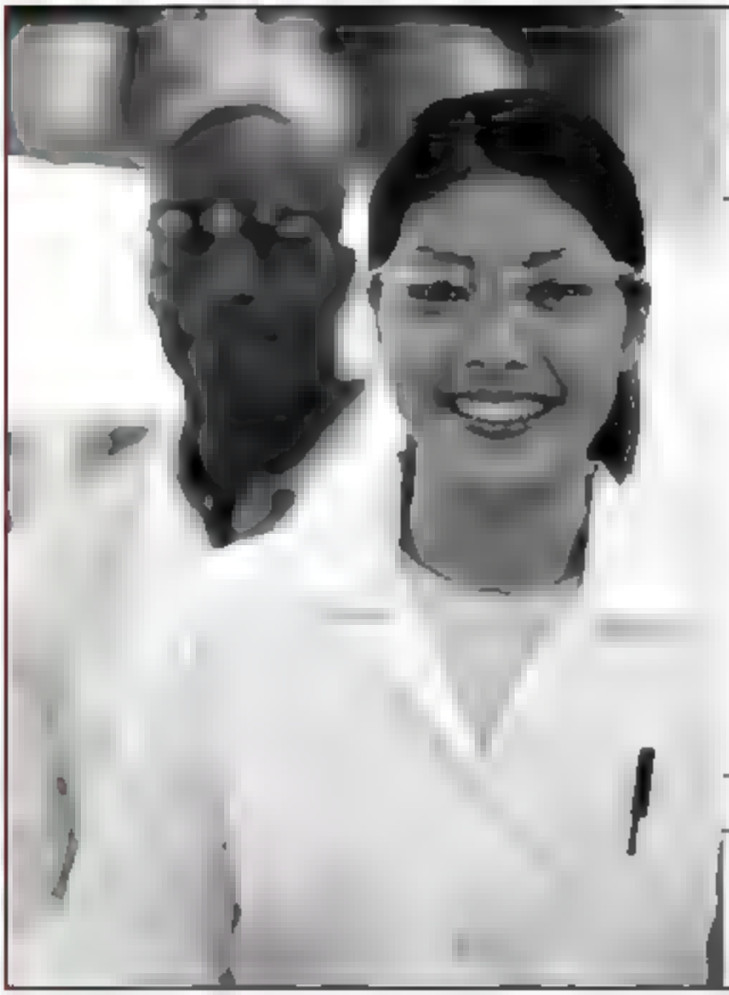

What will Lilly's robust product pipeline contribute to the pharma industry?

We impact lives by delivering answers to some of the world's toughest health care questions. And, with over a century of experience behind our name, there is no one better prepared than Eli Lilly and Company to tackle these questions and the challenges of our changing industry.

At Lilly, you will play an active role in the development of breakthrough science and the identification of high-potential drug candidates. Your career will benefit from working with a team that embraces new ideas and a creative thought process. Ultimately, your innovative work will provide powerful pharmaceutical solutions that will enhance the lives of patients throughout the world.

Lilly is proud to be recognized as one of the *Science* 2007 Top Biotech and Pharma Employers.

Today and in the future, Lilly will provide "Answers That Matter." Eli Lilly and Company is an equal opportunity employer.

www.lilly.com/careers

Lilly

Answers That Matter

POSITIONS OPEN

University of Pittsburgh School of Medicine
Department of Otolaryngology

Faculty Position In Auditory Neuroscience

The Department of Otolaryngology at the University of Pittsburgh School of Medicine is expanding its auditory research program by adding five faculty positions over the next years. The current position is intended to be filled at the level of Assistant Professor but qualified candidates at other levels will be considered. Individuals using electrophysiological and/or imaging techniques to address fundamental questions about function, development, or plasticity of auditory brainstem circuits in mammals are especially encouraged to apply. We offer a generous startup package, state-of-the-art core facilities, and a highly interactive research environment that provides ample opportunities for interactions on a basic science and translational level.

Applicants should have a Ph.D. and/or M.D. degree and several years of productive postdoctoral experience. Candidates will be expected to develop a successful, funded research program and participate in graduate and medical teaching training. Please submit, preferentially electronically, a curriculum vitae, statement of research interests (no longer than 3 pages), and the names of three references to **vallom@upmc.edu**. Applications can also be mailed to:

Karl Kandler, PhD
c/o Marykay Vallo
Department of Otolaryngology
Eye & Ear Institute, Room 127
203 Lothrop Street
Pittsburgh, PA 15213

The University of Pittsburgh is an Affirmative Action, Equal Opportunity Employer.

KIMMEL CANCER CENTER
JEFFERSON MEDICAL COLLEGE
An NCI-Designated Cancer Center
Thomas Jefferson University, Philadelphia, Pennsylvania

FACULTY POSITIONS IN CANCER RESEARCH

The Kimmel Cancer Center (KCC), an NCI-designated Cancer Center in Philadelphia, under the direction of Dr. Richard G. Pestell, is seeking outstanding, established investigators for several tenured/tenure-track positions at the rank of Associate [redacted]

Qualified candidates will have an advanced degree, a strong record of independent scientific accomplishments, and a solid extramural funding base. An active program in cancer research that integrates with existing KCC programs is also an important criterion for faculty candidates. Existing programs include cancer genetics and epigenetics, growth control, cellular signaling, tumor immunology and virology, apoptosis and angiogenesis. Additional information regarding the Cancer Center can be obtained at: **http://www.kimmelcancercenter.org**.

Successful applicants will be provided with a highly competitive package of laboratory space, start-up funding, and salary. As an NCI-designated Cancer Center, KCC provides extensive research support through multiple shared resources, including small molecule, genomic and proteomic platforms.

Applicants should submit a letter of application, curriculum vitae including current and past funding, a statement of research accomplishments and future directions, and the names of three references.

Applications will be evaluated on a rolling basis and should be submitted via email to: Dr. Steven McMahon, Chair, Committee for Faculty Recruitment, Kimmel Cancer Center, Thomas Jefferson University (**Faculty.Search@kimmelcancercenter.org**).

Thomas Jefferson University

Jefferson Medical College is located in Center City Philadelphia, a vibrant metropolitan center with rich cultural and historical traditions.

Affirmative Action/Equal Opportunity Employer

POSITIONS OPEN

USDA ARS Agricultural Research Service

www.ars.usda.gov

"The Nation's premier food and agricultural research agency"

CENTER DIRECTOR

U.S. Arid Land Agricultural Research Center (ALARC)
Maricopa, Arizona
Senior Scientific Research Service (SSRS) - Excepted Service
RA-0401-00/00. Salary Range of $140,000 to $165,000 with full potential to $186,000
Applications must be received by **November 26, 2007**

The USDA, Agricultural Research Service (ARS) is seeking a senior-level, outstanding research scientist for a permanent full-time SSRS position. This SSRS position is an opportunity for a highly qualified, talented, world-class research scientist to lead and conduct outstanding research in the field of arid land agriculture.

This position affords the opportunity to:

- Direct an exciting group of scientists working at the leading edge of agricultural science
- Work collaboratively with university and industry
- Oversee state-of-the art facilities with unique physical capabilities and pre-eminent scientific equipment
- Impact the Nation's leading issues of arid land agriculture including water management and conservation; pest management and biocontrol; and plant physiology and genetics.

Join us in enhancing the health and wealth of the Nation and its people solving problems, expanding knowledge, delivering answers.

To apply, print a copy of vacancy announcement **ARS:SSRS:07-07** from the ARS Careers Website at **http://www.ars.usda.gov/careers** and follow the application directions provided. To have a printed copy mailed or for questions about these positions, call **Deborah Crump** at **(301) 504-1448** or E-Mail **deborah.crump@ars.usda.gov**. U.S. citizenship is required.

USDA/ARS is an Equal Opportunity Employer and Provider

Tenure-track Faculty Positions
Institute of Physics, Academia Sinica, Taipei

The Institute of Physics (http://www.phys.sinica.edu.tw/), Academia Sinica (http://www.sinica.edu.tw/) invites applications for several tenure-track faculty positions in all ranks. The Institute of Physics, currently consisting of forty-two faculty members, conducts research in (1) Basic and applied research in nano-sciences, (2) Non-linear and complex systems, statistical computational and bio- physics, and (3) Intermediate and high energy physics. The position offers a free and superb research environment, an adequate startup research grant and good opportunities for interdisciplinary collaborations. Applicants should have an outstanding record of research achievements and will be expected to propose and pursue an independent research program. Interested applicants should send a Curriculum Vitae and a list of publications, copies of five major publications, a summary of research achievements, a plan for future research, and three letters of recommendation to Miss Ophelia Huang, Institute of Physics, Academia Sinica, Nankang, Taipei 11529, Taiwan; e-mail: ithuang@phys.sinica.edu.tw; phone: 886-2-27896718. Review of applications will begin as soon as they are received and will continue until the positions are filled. Academia Sinica in Taipei is the most prominent academic institution in Taiwan. While affiliated directly to the Presidential Office, Academia Sinica enjoys independence and autonomy in formulating its own research objectives. Its major tasks are to undertake in-depth academic research on various subjects in sciences and humanities. In recent years, under its superior leadership, Academia Sinica has transformed into a modern research institution. The Institute of Physics, being one of the institutes in Academia Sinica, vows to conduct leading-edge research projects and to pursue excellence in its research programs.

TOP EMPLOYERS

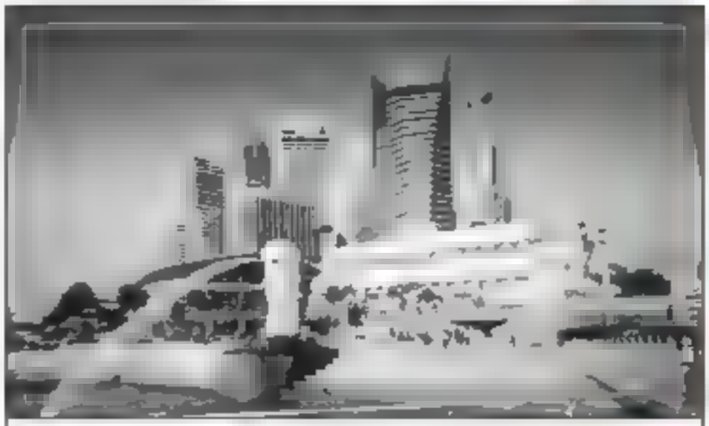

Lead the next generation of pharmaceutical science.

Eli Lilly and Company is a leading, innovation-driven pharmaceutical corporation with approximately 42,000 employees worldwide. Lilly is developing a growing portfolio of best-in-class, first-in-class pharmaceutical products. We achieve this by applying the latest research from our own worldwide laboratories, by collaborating with eminent scientific organisations and by making use of the most up-to-date technological tools.

Established in 2002, the Lilly-Singapore Centre for Drug Discovery (LSCDD) is now expanding its capability to discover and develop new medicines more productively, in the areas of cancer and metabolic disorders. We form a network of drug development partners, and through innovative data integration approaches, discover and apply biomarker and patient-tailoring solutions.

Located in the exciting Singapore Biopolis, LSCDD's multi-disciplinary and multi-cultural team is working to redefine the leading edge. We are looking for outstanding individuals to fill the following positions:

- **Director – Drug Discovery Research**
- **Director – Integrative Computational Sciences**
- **Senior Scientist – Assay Development**
- **Senior Scientist – Cancer Biology**
- **Senior Scientist – Diabetes**
- **Senior Scientist – Epigenetics**
- **Informatics Scientist**
- **Research Associate**
- **Software Engineer**
- **BioSafety Officer**

Log on to www.lscdd.lilly.com.sg to find out more about these positions and what a career at Eli Lilly and Company can offer you. Eli Lilly is an equal opportunity employer.

www.lscdd.lilly.com.sg

Lilly
Answers That Matter.

UMKC

UNIVERSITY OF MISSOURI KANSAS CITY
SCHOOL OF BIOLOGICAL SCIENCES

Professor and Head, Division of Cell Biology and Biophysics

Applications are invited for the Head of the Division of Cell Biology and Biophysics at the School of Biological Sciences, University of Missouri-Kansas City. The successful candidate should have a proven record of sustained externally funded research, scholarly activity, and leadership potential. The candidate will be expected to participate in graduate and/or undergraduate teaching, faculty mentorship, and work closely with the Dean on decision-making matters pertaining to the growth, development and direction of the School. The School of Biological Sciences is positioning itself to become a regional leader in the areas of structural biology and molecular cell biology and welcomes applications from qualified candidates in these research areas, however, outstanding scientists from all areas of basic life sciences research are encouraged to apply. The successful candidate will receive a competitive 12-month salary, renovated research space, a start-up package commensurate with rank, and the availability of excellent research support facilities within the School of Biological Sciences. Candidates should have a Ph.D. degree and currently be in a tenured academic position at the rank of Professor.

Please direct all inquiries or nominations to **Dr. Lawrence A. Dreyfus**, Dean, School of Biological Sciences (**dreyfusla@umkc.edu**). To apply please submit electronically (MS Word or pdf) a CV, a statement of present and future research interests, and the names and addresses of 3 references to **dreyfusla@umkc.edu**. All materials will be handled with strict confidentiality. The position will remain open until filled.

UMKC is an Affirmative Action Equal Opportunity Employer
Women, minorities, veterans, and individuals with disabilities are encouraged to apply

BENAROYA RESEARCH INSTITUTE

FACULTY POSITION AVAILABLE

The Benaroya Research Institute, a basic and translational medicine research center in Seattle WA, invites applications for a faculty position. Applications are particularly welcome in research areas that emphasize pathways that link innate and adaptive immune systems, interactions with extracellular matrix components, and regulation of inflammatory responses. Qualified candidates at all levels are welcome to apply.

The Benaroya Research Institute offers a competitive start-up package and newly renovated laboratory space. The Institute has 20 faculty with interests in immune tolerance and autoimmunity, lymphocyte trafficking, genetics, inflammation, extracellular matrix and matricellular proteins, tissue engineering, and vascular biology (see **www.benaroyaresearch.org** for details). The successful candidate will be eligible for an Affiliate faculty appointment at the University of Washington School of Medicine.

Please send *curriculum vitae*, brief description of future research interests, and names and contact information of 3 references to: **Gerald T Nepom, MD PhD, Director, Benaroya Research Institute, Attn: Faculty Search Committee, 1201 9th Avenue, Seattle, WA 98101**, or email **mwarren@benaroyaresearch.org**.

EEO/AA

ALBERT EINSTEIN COLLEGE OF MEDICINE OF YESHIVA UNIVERSITY

Faculty Positions
in The Diabetes Center of The Albert Einstein College of Medicine

The Diabetes Research Training Center at The Albert Einstein College of Medicine (**http://www.aecom.yu.edu/diabetes/page.aspx**) invites applications from outstanding candidates for **tenure-track** faculty positions at the levels of **Assistant or Associate Professor**.

Candidates should have an excellent record of research accomplishments, the ability to direct innovative independent research, and competitive funding potential in all areas of diabetes and obesity. We are particularly interested in individuals focused on immunology and inflammatory processes.

The positions offer generous start up packages, long-term salary support and newly renovated space in the Center for Genetics and Translational Medicine. Onsite support facilities include state-of-the-art imaging, transgenic, sequencing, proteomics, metabolomics, mouse physiology/phenotyping, microarray, cloning, protein expression, bioinformatics, and cell culture cores.

The review of applications will begin December 1, 2007 and will continue until the positions are filled. Applicants should forward a curriculum vitae, three letters of reference, selected reprints, and a brief summary of accomplishments and proposed future research program to: **DRTC Search Committee, c/o Aceleen Dizon, Dept of Endocrinology, 701 Belfer, Albert Einstein College of Medicine, Jack and Pearl Resnick Campus, 1300 Morris Park Avenue, Bronx, NY 10461; Email: adizon@aecom.yu.edu**

EOE

UCSF

University of California, San Francisco
Tenure Track Position at the Interface Between Physical Sciences and Biology

We are looking for an outstanding scientist at the interface between the physical and biological sciences, broadly defined. Of particular interest to us are single-molecule methods, microfluidics, synthetic biology, metabolic engineering, or in general, the development or application of technologies that can advance biological research, or the application of engineering approaches at the molecular or cellular level.

UCSF seeks candidates whose experience, teaching, research, or community service has prepared them to contribute to our commitment to diversity and excellence.

Please send a *curriculum vitae*, three letters of reference, a summary of current research (up to 2 pages), and a concise outline of future research (up to 2 pages) to the address listed below.

Applications will be considered beginning **December 1, 2007.**

Barbara Raymond
Physical Science and Biology Search Committee
Department of Pharmaceutical Chemistry
University of California, San Francisco
600 16th Street, MC 2280
Genentech Hall, Room 518
San Francisco, CA 94158-2517

UCSF is an Affirmative Action/Equal Opportunity Employer. The University undertakes affirmative action to assure equal employment opportunity for underutilized minorities and women, for persons with disabilities and for covered veterans.

Positions NIH

The National Institutes of Health

Tenure-Track Investigator
Clinical Neurogenetics
Division of Intramural Research

The Division of Intramural Research of the National Institute of Neurological Disorders and Stroke is recruiting an individual for a tenure-track position in the area of neurogenetics with a focus on clinical research. The applicant should have a special interest and experience in translational and clinical research relating to hereditary neurological disease. The individual would direct an independent research program in this area.

The work would be done in conjunction with the Neurogenetics Branch which was established to study the causes and treatment of hereditary diseases of the nervous system. The branch is led by Dr. Kenneth Fischbeck, a world renowned investigator and an experienced mentor. The Clinical Center at the NIH is the nation's largest hospital devoted entirely to clinical research. It is a national resource that makes it possible to rapidly translate scientific observations and laboratory discoveries into new approaches for treating neurogenetic diseases. The greater NIH community offers a uniquely rich collaborative environment to the tenure track investigator.

The individual should have a demonstrated background and knowledge in research focused on hereditary neurological disease with expertise in human genetics and/or the application of clinical trial methodology to testing new therapies. The candidate will have earned a US medical license and will have excellent scientific skills in structuring an original and productive research program using outstanding communication and collaborative abilities. Candidates for a tenured position will also be considered but this would require an international reputation and well-documented evidence of substantial independent accomplishments. An individual selected for a tenure-track position is expected to build a dynamic and productive research group.

Laboratory facilities, start-up and sustained research funds and salary will be competitive with premier academic institutions. Applicants should send curriculum vitae, bibliography, statement of research interests, and three names of references to **Dr. Alan Koretsky, Scientific Director, National Institute of Neurological Disorders and Stroke, c/o Peggy Rollins, Office of the Scientific Director, Division of Intramural Research, by email to Peggy_Rollins@NIH.gov or by mail to Building 35 Room GA908, NIH, Bethesda, MD 20892 (phone: 301-435-2232). Applications will be reviewed starting December 1, 2007.**

Postdoctoral Positions
National Institute of Child Health and Human Development

Molecular Mechanisms of Thyroid Hormone-dependent Frog Metamorphosis
Yun-Bo Shi, Ph.D., shiy@helix.nih.gov
http://eclipse.nichd.nih.gov/nichd/molecularmorphogenesis/index.htm

Vascular Development in the Zebrafish
Brant Weinstein, Ph.D., WeinsteB@mail.nih.gov
http://dir.nichd.nih.gov/lmg/sve/WEINS-AH.html

Embryonic and Adult Stem Cells
Heiner Westphal, M.D., hw@mail.nih.gov
http://www.westphal.nichd.nih.gov

Molecular Studies on HIV Replication
Judith G. Levin, Ph.D., levinj@mail.nih.gov
http://levinlab.nichd.nih.gov

Structure, Stability, and Interactions of Extracellular Matrix Proteins
Sergey Leikin, Ph.D., leikins@mail.nih.gov
http://www.training.nih.gov/webcams/postdoctoral/application/Addjobs.aspx?PodAdID=PD-3829

Eukaryotic Chromosome Biology
Alex Strunnikov, Ph.D., strunnik@mail.nih.gov
http://ycsf.nichd.nih.gov

TGFbeta Signaling in Drosophila melanogaster
Mihaela Serpe, Ph.D., serpe001@umn.edu
http://www.cbd.med.umn.edu/OConnor.cib.htm

Cell Biology of Genetic Bone Disease
Joan C. Marini, M.D., Ph.D., jmdocs@helix.nih.gov
http://eclipse.nichd.nih.gov/nichd/annualreport2006/scid.htm

Neurophysiology
Dax A. Hoffman, Ph.D., hoffmand@mail.nih.gov
http://neuroscience.nih.gov/Lab.asp?Org_ID=480

Applicants must have less than five years of postdoctoral experience

Chief, Visuomotor Disorders
Laboratory of Sensorimotor Research (LSR)
National Eye Institute

The National Eye Institute (NEI) seeks an outstanding clinician scientist for a tenured or tenure-track position as Chief, Visuomotor Disorders Section in the Laboratory of Sensorimotor Research (LSR) in the Division of Intramural Research. This recruitment is directed towards clinicians with expertise in central disorders that affect vision and/or eye movements (including disorders of binocular function). The post offers a unique opportunity for a talented individual to provide strong and stimulating leadership in an organization dedicated to uncovering new scientific knowledge, both laboratory and clinical. We welcome the full range of candidates at all levels.

The Laboratory of Sensorimotor Research is devoted to understanding the organization of the brain related to the control of eye movements, visual perception and their disorders. The Visuomotor Disorders Section Chief is expected to create a vigorous research program dedicated to elucidating the role played by these brain mechanisms in human disease, and to explore treatments. The Chief will develop broad investigational plans, independently and in collaboration with other NEI investigators and research scientists in the United States and abroad. The Chief will examine and treat patients, as well as design, implement and conduct research and clinical protocols. An opportunity exists for the Section Chief to recruit staff and supervise training.

The NEI provides an exceptional environment for clinical research including the infrastructure necessary for patient recruitment, a clinical protocol development group, and a Contract Research Organization that provides statistical and epidemiological expertise, data management and analysis, study monitoring, regulatory guidance, and overall operational support. The NIH Clinical Center provides additional access to exceptionally broad medical and diagnostic resources. In addition, the LSR provides exceptional support for more specialized needs, such as the measurement of eye movements and computational analysis/modeling. The position requires an ability to integrate basic, clinical and translational research, and create an intellectual synergy and an environment for state-of-the art patient care for those suffering from visual dysfunction.

At a minimum, candidates should have a Doctor of Medicine degree from a school in the U.S. or Canada approved by a recognized accrediting body in the year of the applicant's graduation, or a Doctor of Medicine or equivalent degree from a foreign medical school which provided education and medical knowledge substantially equivalent to accredited schools in the United States. Candidates should be Board-certified, have direct clinical experience in the pathophysiology of visuomotor disease from the perspective of relevant neurophysiological mechanisms, and be licensed to practice medicine in the USA.

Salary is commensurate with research experience and accomplishments. A full Federal package of benefits is available (including retirement, health, life and long term care insurance, Thrift Savings Plan etc).

Applicants should submit curriculum vitae, bibliography, copies of their five most significant publications, a summary of research accomplishments and three reference letters. Applicants should also submit a written statement with their perspective on the needs and opportunities necessary to move from the basic understanding of brain mechanisms supporting vision and eye movements to clinical therapeutic interventions and improved patient care. This statement should indicate how the applicant's particular expertise and background could contribute to this transition. The position will be open until filled. Applications should be sent to: **Mica Gordon, Executive Assistant, Office of the Scientific Director, National Eye Institute, Building 31, Room 6A22, 31 Center Drive, Bethesda, MD 20892; Tel: 301-451-6763, Email: gordonmi@nei.nih.gov**

NIH is dedicated to building a diverse community in its training and employment. NIH is a part of the U.S. Department of Health and Human Services.

STANFORD UNIVERSITY

Department of Biological Sciences
Evolutionary Developmental Biologist Faculty Position

The Department of Biological Sciences at Stanford University seeks applicants for a tenure track faculty appointment in Evolutionary Biology. We are primarily interested in making an appointment at the rank of Assistant or Associate Professor, but will also consider exceptional candidates at the rank of Professor. We seek applicants studying problems in any area of Evolutionary Biology: however those studying problems at the interface of Developmental and Evolutionary Biology are especially encouraged to apply. Applicants are expected to develop a vigorous research program and to participate in both undergraduate, graduate, and postdoctoral education and training. For information about the Department consult **http://biology.stanford.edu/**

Applicants are requested to provide a cover letter, a curriculum vitae including publication list, a statement of research accomplishments and future research plans, and a description of teaching experience. Junior candidates should arrange to have three letters of reference sent directly.

Applicant materials must be received by **December 3, 2007**. The appointment would begin September 1, 2008.

Interested candidates should apply online at
AcademicJobsOnline.Org

Stanford University is an Equal Opportunity Employer and is committed to increasing the diversity of its faculty. It welcomes nominations of and applications from women and minority groups, as well as others who would bring additional dimensions to the university's research, teaching and clinical mission.

INDIANA UNIVERSITY

Faculty Position in Meiosis and Eukaryotic Recombination

The Department of Biology invites applications for a **tenure-track faculty position at any rank in the area of meiosis and/or eukaryotic recombination**. Applicants working on any eukaryotic system and at any level of analysis (from biochemistry through evolution) are encouraged to apply. The successful candidate will be provided with a competitive startup package and salary, and will have access to outstanding research resources and core facilities.

Applicants should mail a curriculum vitae, a statement of research (past, present, and planned) and teaching interests, and representative publications and preprints to: **Meiosis/Recombination Search Committee, c/o Jeremy Bennett, Department of Biology, Indiana University Bloomington, 1001 E. Third St., Bloomington, IN 47405**. Please arrange to have at least four letters of recommendation sent by e-mail to: **jebennet@indiana.edu**. Questions should be addressed to **Mimi Zolan (mzolan@indiana.edu)**. Applications received by **December 1, 2007** will be assured of full consideration.

Indiana University is an Affirmative Action/Equal Opportunity Employer. Women and minority candidates are encouraged to apply.

Faculty Position
Developmental/Evolutionary Biology
University of Chicago

The Department of Organismal Biology and Anatomy is an integrative biology department with established strengths in developmental biology, evolutionary biology, neurobiology and functional morphology. We seek to hire a new tenure-track faculty member working in one of two areas, either (1) a developmental biologist with broad interests, which may include regeneration or comparative approaches, or (2) an evolutionary biologist using modern genomic tools to address key questions. We are particularly interested in individuals who can establish intellectual and research collaborations with existing faculty. Candidates must have a Ph.D., postdoctoral training, and outstanding potential in research and teaching. Appointment rank will be at a level commensurate with experience. Candidates will be expected to teach in their area of expertise at undergraduate and graduate levels.

Review of applications will begin **November 15, 2007** and continue until the position is filled. Applications should be submitted by e-mail to **evodevosearch@poodside.uchicago.edu** or by mail to: **Chair, Evodevo Search Committee, c/o H.A. Zayd, Department of Organismal Biology and Anatomy, 1027 E 57th St, Chicago IL 60637**. Applications should include a curriculum vitae, with a complete list of publications, and a statement of research and teaching interests. Three letters of recommendation should be sent to the same address. Electronic applications and letters, as PDF files, are strongly encouraged.

The University of Chicago

An Affirmative Action/Equal Opportunity Employer

Faculty Position in Chemical Biology

The Life Sciences Institute (LSI) at the University of Michigan invites applications for a position at the rank of Assistant or Associate Professor in the field of chemical biology. Chemical biology is broadly defined and the successful applicant will use chemical methods to address an important biological question.

The LSI is a scientific enterprise at the University of Michigan dedicated to opening new scientific paths by blending diverse research talents in a state-of-the-art collaborative physical space (www.lsi.umich.edu). The LSI is currently home to 26 interactive faculty in the areas of cell biology, genetics, bioinformatics, structural biology, signaling, and chemistry.

Candidates are expected to develop an internationally recognized program of scholarly research and to excel in teaching at undergraduate and graduate levels. The positions will remain open until filled but preference will be given to applicants who have submitted all requested materials prior to **October 15, 2007**. Applicants should send the following (in PDF format): a curriculum vitae, copies of up to three reprints, a one- to two-page summary of research plans, and arrange to have three letters of reference sent directly to: **lsichembio@umich.edu**.

The University of Michigan is supportive of the needs of dual career couples and is a non-discriminatory, Affirmative Action Employer. Women and minorities are encouraged to apply.

life sciences institute

RAMAPO COLLEGE OF NEW JERSEY

Ramapo College of New Jersey is located in the beautiful foothills of the Ramapo Mountains, approximately 25 miles northwest of New York City. Accredited by the Middle States Commission on Higher Education, Ramapo College is a comprehensive institution of higher education dedicated to the promotion of teaching and learning within strong liberal arts based curriculum, thus earning the designation "New Jersey's Public Liberal Arts College." Its curricular emphasis includes the liberal arts and sciences, social sciences, fine and performing arts, and the professional programs within a residential and sustainable living and learning environment. Organized into thematic learning communities, Ramapo College provides academic excellence through its interdisciplinary curriculum, international education, intercultural understanding and experiential learning opportunities.

ASSISTANT PROFESSOR of BIOLOGY

TENURE TRACK, COMMENCING FALL 2008

DESCRIPTION: Responsibilities include teaching microbiology for health sciences, introductory biology for majors and non-majors, in addition to developing a strong research program that involves undergraduate students. The successful candidate is also expected to develop specialty courses in his/her area of interest. Interdisciplinary collaborative opportunities are available in biochemistry, bioinformatics, ecology, environmental science, evolutionary biology and molecular biology.

REQUIREMENTS: Ph.D. is required and postdoctoral experience is preferred.

Faculty members are expected to maintain active participation in research, scholarship, college governance, service, academic advisement and professional development activities.

All applications must be completed online at: **http://www.ramapojobs.com.**

Applications should include a CV, reprints of recent publications, a statement of teaching philosophy and future research plans, and contact information for three references. Hard copies of resumes will not be accepted. Since its beginning, Ramapo College has had an intercultural/international mission. Please tell us how your background, interest and experience can contribute to this mission, as well as to the specific position for which you are applying.

Review of applications will begin immediately and continue until the position is filled. Position offers excellent state benefits. ***To request accommodations, call (201) 684-7734.*** Supportive materials in non-electronic format can be sent to Dr. Eta Rena Bacon, Search Committee Chair.

RAMAPO COLLEGE OF NEW JERSEY

Attention: Department 25
505 Ramapo Valley Road, Mahwah, NJ 07430
"New Jersey's Public Liberal Arts College"

Ramapo College is a member of the Council of Public Liberal Arts Colleges (COPLAC), a national alliance of leading liberal arts colleges in the public sector. EEO/AFFIRMATIVE ACTION

Johns Hopkins Medical Institutions Tenure-Track Positions

Influenza and Respiratory Virus Translational Research

Human Immunology, Vaccinology, Pharmacology

The Division of Infectious Diseases of the Johns Hopkins School of Medicine is recruiting 1-2 faculty at the Assistant or Associate Professor level to contribute to an emerging institutional Respiratory Viruses Program. Our focus is on persons with proven capabilities to conduct independent research on respiratory infections, especially investigations that contribute to the prevention or treatment of influenza in humans. This recruitment contributes to expanding programs in influenza virology, structural biology and vaccine testing. Emphasis will be given to researchers with complementary research such as in molecular biology of viral replication, host-virus interactions, and quantitative analysis of viral dynamics.

Candidates must have earned an MD and/or PhD degree and have a record of acquiring research funding and producing outstanding scholarship. Salary and resources will match experience.

Candidates should provide a curriculum vitae, a one-page statement of career interest, and 3 professional references to: **Dr. David Thomas, Chief Infectious Diseases, Johns Hopkins School of Medicine, Suite 437 1830 Monument Street, Baltimore, Maryland 21205** or by email care of Nadia Hay nhay@jhmi.edu. Application review will begin in Fall 2007.

Johns Hopkins is an Equal Opportunity Employer

STONY BROOK UNIVERSITY MEDICAL CENTER

Cancer Center Director

Stony Brook University Medical Center offers an exciting opportunity to join our senior executive team. As the only academic medical center on Long Island and the only tertiary care hospital in Suffolk County, SBUMC is an undisputed leader in Long Island health care. We were recently cited in the "America's Best Hospitals" issue of *U.S. News & World Report*. Located on Long Island's North Shore, Stony Brook University Medical Center is 60 miles east of New York City and minutes from the seashore. Stony Brook University Medical Center seeks a highly qualified physician scientist (Associate Professor/Professor) to serve as Cancer Center Director. This senior-level position will be directly involved in the strategic planning for clinical, academic and research programs; operations and fiscal oversight; faculty recruitments and appointments for the Cancer Center; as well as oversight of clinical and research resources and activities.

Required: An M.D. or M.D./Ph.D. The successful candidate must be board certified in his or her medical specialty and be eligible for a N.Y.S. license. We seek a qualified candidate with demonstrated leadership experience and scientific background as evidenced by a successful track record. We are looking for a seasoned professional who has a minimum of 10 years of relevant experience including the integration of research and clinical programs across schools and departments within a university setting. *Preferred:* Expertise integrating clinical research activities into inpatient and outpatient facilities to effectively link basic research to clinical care. *Salary:* Commensurate with experience.

To apply, send a cover letter including the following: qualifications for the position; curriculum vitae; names, telephone numbers, mailing and e-mail addresses for five references; and examples of written work to:
Wadie F. Bahou, M.D., Vice Dean for Scientific Affairs, Health Sciences Center, Level 4, Stony Brook University Medical Center, Stony Brook, NY 11794-8430. Fax: (631) 444-6148.

Review of applications will begin in September 2007 and will continue until the position is filled.

Stony Brook University/SUNY is an affirmative action, equal opportunity educator and employer.

POSTDOCTORAL POSITIONS in Plant Cell Wall Biosynthesis and Structure

The University of Georgia (UGA) Complex Carbohydrate Research Center (CCRC) BioEnergy Science Center (BESC)

The UGA CCRC (www.ccrc.uga.edu) is a component of BESC (www.bioenergycenter.org), a Department of Energy-funded Center whose mission is to understand and overcome the recalcitrance of lignocellulosic biomass to conversion to fermentable sugars and to enable cost-effective technologies for the production of biofuels. Postdoctoral positions are available for motivated individuals who wish to make fundamental contributions in:

- systems biology of wall biosynthetic pathways
- cell biology of plant cell walls
- hemicellulose and pectin synthesis
- identifying new wall biosynthetic enzymes
- utilizing polysaccharide-modifying enzymes
- wall structure and its relationship to recalcitrance
- high-resolution NMR spectroscopic analysis of walls
- characterizing lignin-polysaccharide complexes
- high-throughput analyses and data processing

A letter of interest, C.V. and contact information for at least three references should be addressed to **Regents Professor Alan Darvill, Director, CCRC, University of Georgia, Athens, GA, USA** and sent via email to **Sheilah Dixon (sheilah@ccrc.uga.edu)**.

EEO/AA

Cincinnati Children's Hospital Medical Center

Stem Cell Research

Faculty Positions in Stem Cell Research
Assistant, Associate and Full Professor

Applications are invited for several tenure track faculty positions in the area of stem cell biology to join a multidisciplinary research community with existing strengths in developmental and stem cell biology, cardiovascular biology, endocrinology, gastroenterology, genetics, hematopoiesis, immunology, neurobiology and pulmonary biology. Recruitment at the senior level could include a significant leadership role in the future direction of this program.

This interdisciplinary group of basic scientists and clinicians will study the fundamental properties of stem cells and the potential uses of adult and embryonic stem cells for therapy in childhood disease. Candidates must hold MD, PhD, or MD/PhD degrees. Applications of stem cell research to any organ system in the body, using a variety of animal models, are encouraged.

Faculty have access to high-quality graduate and MD/PhD programs and training programs for postdoctoral fellows, clinical fellows, residents and clinical faculty.

Applicants should submit their curriculum vitae, two-page research statement including past accomplishments and future goals, and contact information for three people who will provide letters of recommendation to DOSpositions@cchmc.org.

Cincinnati Children's Hospital Medical Center and the University of Cincinnati are Affirmative Action/Equal Opportunity employers. Qualified women and minority candidates are especially encouraged to apply.

DEPARTMENT OF BIOLOGICAL SCIENCE
TENURE-TRACK FACULTY POSITION
IN MICROBIOLOGY

The Department of Biological Science invites applications for a tenure-track position in Microbiology at the level of Assistant Professor. We are seeking candidates with notable research achievements, the ability to develop a well-funded independent research program, and a commitment to excellence in undergraduate and graduate education. Candidates should have a Ph.D. and postdoctoral experience.

Candidates should have a research program that involves the application of modern genetic, genomic, structural, or molecular approaches to the study of microorganisms, viruses, or the interaction of microbes with their host cells. The successful candidate's research is expected to complement the Department's existing strengths in **Virology, Genetics, Cell, Molecular, and Developmental Biology and in Ecology and Evolution**.

The Department has a newly constructed Life Science Research and Teaching Building and has established, well-equipped, and fully staffed core facilities. Opportunities for collaboration and access to additional instrumentation are available via affiliated programs in Structural Biology, Nanobiotechnology, Computational Science, and at the College of Medicine and the National High Field Magnetic Laboratory.

To apply, please submit electronic copies (PDF files preferred) of a cover letter, curriculum vitae, statement of research plans, and the names and email addresses of three references to: **Dr. Kenneth H. Roux**, Chair, Microbiology Search Committee, email: **microfacsearch@bio.fsu.edu**. Applications should be received by **December 7, 2007** for full consideration.

FSU is an AA/EO Employer. Applications from minority and female candidates are especially encouraged.

UNIVERSITY AT ALBANY
State University of New York

SENIOR FACULTY POSITION
RNA Sciences and Technology

The University at Albany, SUNY, invites applications for a tenured position at the rank of Associate or Full Professor in the broad area of RNA sciences and technology. Areas of interest include, but are not limited to, the structure and function of RNA and RNA-protein interactions.

The successful candidate will interact with a diverse group of research scientists already working in the RNA field. Recently, the Institute of RNA Sciences and Technology (IRNAST) has been created identifying this research theme as a focus of the University at Albany's $100 million life sciences research initiative [http://www.albany.edu/lifesciences/]. In the greater Albany area, RNA research also has a strong presence in institutions such as Wadsworth Center, Rensselaer Polytechnic Institute, Albany Medical College, and the Ordway Research Institute and thus, there is outstanding potential for research collaborations. The successful candidate will be offered a competitive start-up package and salary.

Qualifications: Candidates must qualify for a tenured appointment at the time of application, and must have internationally recognized, externally funded research programs in RNA sciences and technology. Degrees must be from a university accredited by a US Department of Education or an internationally recognized accrediting organization. Instructional responsibilities in the College of Arts and Sciences will be appropriate to the interests and funded research level of the candidate. Applications sent in PDF are preferable. All applicants must address in their applications their abilities to work with and instruct a culturally diverse population. Applicants should submit a CV, list of past and current grant support, and statement of research interests by e-mail to **Lifesciences@albany.edu**. Review of applications will begin on November 15, 2007 and continue until the position is filled.

TENURE-TRACK FACULTY POSITION
Bioorganic Chemistry/Nucleic Acid Chemistry

The Department of Chemistry is seeking an outstanding individual who can develop an externally funded, nationally recognized program in the area of organic synthesis relevant to nucleic acid chemistry. The successful candidate is also expected to teach courses in organic chemistry. Candidates must have a Ph.D. degree from a university accredited by a US Department of Education or an internationally recognized accrediting organization. Applications sent in PDF are preferable. All applicants must address in their applications their abilities to work with and instruct a culturally diverse population. Applicants should submit a CV, representative publications (PDFs), statements of teaching and research interests, and have three letters of reference sent, by e-mail, to **chemdept@albany.edu**. Review of applications will begin on November 15, 2007 and continue until the position is filled.

As the capital city of New York State, Albany provides outstanding cultural and recreational opportunities (**http://www.albany.org**). It maintains a vibrant small-city lifestyle while being within easy commuting distance (about 3 hours) of major metropolitan centers including New York City, Boston and Montreal.

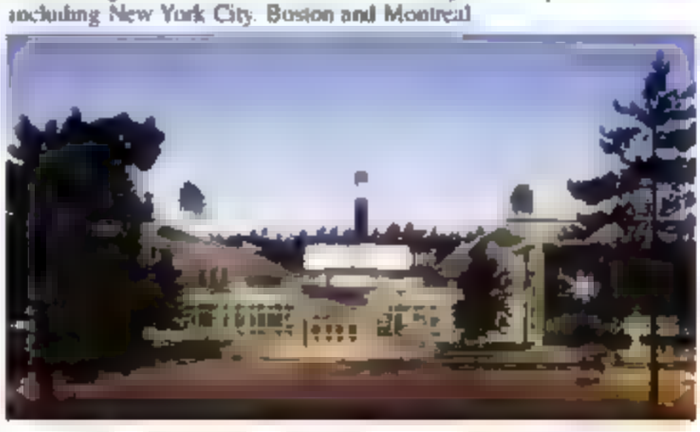

The University at Albany is an EO/AA/IRCA/ADA employer.

THE UNIVERSITY of NORTH CAROLINA
GREENSBORO

The College of Arts and Sciences at the University of North Carolina at Greensboro invites applications and nominations for a senior science educator who will be tenured as the Houston Professor in an appropriate science department in the College, with the possibility of a joint appointment in the School of Education. Candidates must have national recognition in the field and a strong record of external funding and accomplishments in science education. The successful candidate is expected to build on the interest and enthusiasm of UNCG's scientists and science educators seeking to enhance K-16 science education.

Review of applications will begin on **December 1, 2007**, and will continue until the position is filled. Applicants should submit a cover letter, detailed curriculum vitae, contact information for four professional references, and an articulation of her or his vision for the role of science education at a research campus. Electronic applications and inquiries (preferred): send to **Professor Jerry L. Walsh**, Chair of the Search Committee at JLWALSH@UNCG.EDU. Applications by mail: send to **Science Education Search Committee, College of Arts and Sciences, University of North Carolina at Greensboro, Greensboro, NC 27410**. Applications will be kept confidential on request.

UNCG has a diverse student body: 20% African-American, 6.5% other ethnic minorities, 68% females and is an EEO/AA Employer with a strong commitment to increasing faculty diversity.

DEPARTMENT OF BIOENGINEERING

Penn Engineering

FACULTY POSITIONS

The Department of Bioengineering in the School of Engineering and Applied Science at the University of Pennsylvania invites applications for both tenure track and tenured faculty positions at all professorial levels.

Bioengineering at Penn has collaborations and research connections spanning the medical school and hospitals, as well as many outstanding departments in the University's other schools, centers and institutions, (including, for example the Institute for Medicine and Engineering and Institute for Neurological Sciences). We are especially interested in energetic visionary faculty who are committed to developing a research enterprise in this environment.

Candidates should hold a doctoral degree in Bioengineering/Biomedical Engineering or a related field. At the assistant professor level, individuals should demonstrate superb academic credentials and promise for a career in bioengineering research. At higher professorial levels, an evident track record of research excellence including successful competitive research funding and academic standing is expected. Present areas of emphasis in our program are neuroengineering, nanobiotechnology, cellular, molecular and tissue engineering, and imaging. However we encourage applications from candidates in any emerging area of bioengineering. A commitment to teaching should also be apparent including development of undergraduate and graduate courses, supervision of doctoral students and academic advising of students at all levels.

To apply, please send a CV, a statement of research interests, a statement of teaching interests, three representative paper reprints, and a list of five references, in hard copy, to:

Faculty Search Committee
Department of Bioengineering, University of Pennsylvania
240 Skirkanich Hall, 210 South 33rd Street, Philadelphia, PA 19104

Applications will be considered beginning 10/01/07 and until positions are filled.

The University of Pennsylvania is an affirmative action, equal opportunity employer.

ASSISTANT AND ASSOCIATE PROFESSOR POSITIONS
in the Evolution of Human Intelligence
Indiana University-Bloomington

The College of Arts and Sciences at Indiana University seeks to fill two positions, **one associate professor** and **one tenure-track assistant professor**, both in the study of the evolution of human intelligence, to begin in fall 2008. Areas of special interest include hominid paleoneurology, brain imaging research pertinent to human evolutionary studies, evolutionary psychology, or molecular neuroscience directly relevant to human encephalization or language origins. Applicants must demonstrate a strong research history and publication record focusing on the evolution of human intelligence. Applicants should indicate whether their tenure home preference would be in the Department of Anthropology, Biology, or Psychological and Brain Sciences.

The successful candidates are expected to maintain close research relationships with the Center for Research into the Anthropological Foundations of Technology (CRAFT) and the Cognitive Science Program at Indiana University. For the associate professor position, the candidate should be recently tenured. For the assistant professor position, Ph.D. must be in hand before the beginning of the fall semester, 2008. Interested candidates should submit an electronic application or send a complete package by mail. A complete application should include: statement of research and teaching interests, curriculum vitae, and a list of at least three referees for the assistant professor position and six referees for the associate professor position, with the referees' full contact information including email addresses. Email complete applications to **humanevo@indiana.edu** or mail to: **Dr. Kathy Schick, Stone Age Institute, 1392 W. Dittemore Road, Gosport, IN 47433**. Please specify **"assistant professor position"** or **"associate professor position"** in the subject line or on the envelope. Formal review of applications will begin on **November 15, 2007** and continue until the positions are filled.

Indiana University is an Equal Opportunity/Affirmative Action Employer. Applications from women and minority candidates and international scholars are especially welcomed.

DEAN OF SCIENCE

FLSA Status: Exempt

Compensation: Commensurate with qualifications and experience

College Web Site: www.ccny.cuny.edu

Notice Number: EA1 9716

Closing Date: 01/09/07 An appointment effective January 1 or August 1, 2008 is anticipated.

POSITION DESCRIPTION AND DUTIES

The City College of New York invites applications and nominations for the position of Dean of the Division of Science. City College is the oldest senior college in the City University of New York system, and has been committed to the dual goals of accessibility and academic quality since its founding in 1847. It has an international reputation for its ability to promote scholarly excellence in students of diverse ethnic and cultural backgrounds and economic circumstances. The Division of Science, a unit of the College of Liberal Arts and Sciences at City College, comprises five academic departments (Biology, Chemistry, Earth and Atmospheric Sciences, Mathematics and Physics). The Division is a major center for research and scholarship, generating over $40,000,000 in research funding per year. The Division boasts nine Nobel laureates among its alumni.

The Dean will assume leadership in the management and administration of the Division: curriculum development, program planning, budgeting, and the acquisition of external funding. He or she will lead the expansion of the division which will include a comprehensive new science facility for the CCNY campus.

QUALIFICATION REQUIREMENTS

Candidates should possess distinguished records of scholarship and teaching, significant academic administrative experience, and strong leadership qualities and communication skills. Candidates should currently hold a tenured faculty position or equivalent, and have administrative experience at least at the level of Department Chair or equivalent. They should qualify for appointment at the rank of full professor in one of the departments of the Division through demonstrated excellence in teaching, scholarship and service. They should be responsive to the needs of faculty and the diverse student body, and committed to cultural and intellectual diversity. Candidates should be able to serve as effective and forceful advocates of the role of the sciences and have a demonstrated commitment to public education.

TO APPLY

Applicants should send a letter of interest, their curriculum vitae, and the names, telephone numbers, mailing and e-mail addresses of at least four (4) professional references postmarked by the closing date to: **Search Committee for the Dean of the Division of Science, Administration Building, Rm 218, The City College of New York, 160 Convent Avenue, New York, NY 10031.**

The City University of New York is an Equal Employment Opportunity, Affirmative Action/Immigration Reform and Control Act/ Americans with Disabilities Act Employer

CITY COLLEGE IS CUNY

VCU

Virginia Commonwealth University

SENIOR ASSOCIATE DEAN FOR RESEARCH

School of Engineering

Virginia Commonwealth University seeks a senior associate dean for research in its School of Engineering and invites applications/nominations for this position. The School of Engineering was founded in 1986 and stands as a remarkable example of public-private partnership. The School currently comprises five departments: biomedical engineering; chemical and life science engineering; computer science; electrical and computer engineering; and mechanical engineering. Its current enrollment is 1160 undergraduate and 530 graduate students with a faculty of 84.

The Position: Reporting to the dean of the School of Engineering, the senior associate dean will be responsible for providing vision and leadership in achieving the School's objectives for substantial growth in the size and scope of sponsored research. Over the next seven years, the School will increase its undergraduate enrollment by 20%, its graduate enrollment by 30%, and its faculty by 100%. The senior associate dean for research will develop and implement programs to enable the School to increase its annual external research funding from $5 million to $20 million over the same period. Working with the dean and faculty, the senior associate dean for research will assist in the recruitment and retention of outstanding junior faculty and senior faculty capable of achieving this objective. The School's strategic plan places particular emphasis on growth of basic and applied research related to clinical medicine. The senior associate dean for research will work closely with his/her counterparts in the VCU Schools of Medicine, Dentistry and Pharmacy to develop proposals for major grants in this area. The senior associate dean will be a member of the senior leadership team for the School and University and will represent the School in all matters related to its research mission.

Qualifications: An earned doctorate in engineering or a related discipline is required. The successful candidate will have outstanding management and leadership accomplishments in a progression of faculty and administrative roles and demonstrated success in leading interdisciplinary teams on major projects. She/he will have established an outstanding record of teaching and externally funded research sufficient for a tenured appointment in one of the School's academic departments. Strong skills in written and oral communication are essential. Experience in an industrial research and development setting is highly desirable.

Application, Nominations: Applicants should submit a statement of interest and curriculum vitae along with four references to: **Chair, Senior Associate Dean of Research Search Committee, Virginia Commonwealth University, School of Engineering, 601 West Main Street, P.O. Box 843068, Richmond, Virginia 23284.** Letters of nomination may be mailed to the same address. The search will continue until the position is filled.

VCU is an Equal Opportunity, Affirmative Action Employer
Women, minorities and persons with disabilities are strongly encouraged to apply

---

University of Florida
Biomedical Imaging Initiative

UF has a rich environment of federally funded investigators who conduct multidisciplinary and interdisciplinary basic, translational and clinical research using an array of state-of-the-art imaging resources. The Department of Radiology is now seeking an outstanding MD and/or PhD scientist to transform this program into a truly world-class enterprise. This position is at the rank of Assistant, Associate or Professor and is a tenure accruing, full-time position. Academic rank will depend on qualifications and experience. Minimum requirements include an M.D. and/or Ph.D. degree and candidate must be eligible for and obtain licensure in the State of Florida. Salary is negotiable. The ideal candidate will combine a track record of innovative research in biomedical imaging with the leadership skills required to contribute toward the organization of a wide variety of imaging initiatives and modalities. This effort will begin with creating a core MRI resource initially focused on fMRI and then expanding to guide the consolidation of other MR disciplines that are already largely in place. The range of responsibilities include managing the interface between studies directly applicable to many robust clinical programs, guiding seminal research activities involving the National High Field Magnet Laboratory and engaging the extraordinary resources for subcellular to organizational research at UF's McKnight Brain Institute.

A successful candidate will continue to advance the theory and practice of biomedical imaging by continuing a vibrant personal research agenda based on extramural funding. He or she will demonstrate (1) the commitment and interpersonal skills needed to foster collaborations across disciplinary, administrative and geographic boundaries, (2) a clear record of strong and successful organizational and administrative skills in advancing biomedical research projects, (3) a professional standing commensurate with a demonstrated track record of successful multidisciplinary collaborations in biomedical imaging research, based on publications, inventions and extramural funding and (4) credentials corresponding to an earned doctorate in a relevant research field, such as engineering and computing; the physical sciences; the medical sciences; or the behavioral sciences. Most importantly, the ideal candidate will have the drive, determination and vision to aid in the creation of a program where discovery, innovation and a fundamentally interdisciplinary environment in biomedical imaging is the norm rather than the exception.

Application deadline for this position is **March 30, 2008** with a starting date as soon as possible thereafter. If you are interested, please send a CV to: **A. Mancuso, MD, Professor and Chairman, Department of Radiology, PO Box 100374, Gainesville, FL 32610-0374 or email: mancusa@radiology.ufl.edu.**

AN EQUAL OPPORTUNITY INSTITUTION

The Ohio State University

Ohio Agricultural Research and Development Center- Wooster, Ohio

Assistant Professor of Entomology

Applied Landscape Ecology and Horticultural Food Crops
Department of Entomology

The successful candidate is expected to **conduct cutting edge, extramurally-funded research directed toward managing spatial heterogeneity in agricultural landscapes** in order to improve pest management, with special emphasis on horticultural food crops.

Examples of such research include but are not limited to: effects of crop and non-crop diversity and pattern on success of biological control; regional approaches to deployment of resistant host plants; pest management decision-making at whole farm or regional scales; spread and containment of exotic pest invasions in Ohio; area-wide management of highly mobile and migratory pests; pest phenology and insect distribution mapping; regional approaches to pesticide resistance management.

Expectations include collaboration with researchers in several disciplines, recruitment and training of graduate students, and participation in graduate level seminars and research colloquia. The candidate is expected to participate in interdisciplinary research and extension teams working toward sustainable crop production. It is expected that the successful candidate will provide high quality research information to growers of food crops and collaborate with industry in the development of ideas to improve insect pest management. The Ohio State University abounds in opportunities for collaboration on both Wooster and Columbus campuses. The position is 85% OARDC and 15% OSU Extension.

Minimum Qualifications: Ph. D. in Entomology or related field; excellent written and oral communication skills; willingness to travel and make personal contact with stakeholders throughout Ohio; demonstrated research expertise that compliments commodity responsibility; training and experience in spatial analysis and other research skills applicable to landscape-scale analysis of insect pest ecology and management; evidence of ability to secure extramural funding from industry and government sources; evidence of scholarly ability and productivity.

Desired Qualifications: Familiarity with horticultural food crops; demonstrated experience interacting with stakeholder groups; experience with interdisciplinary, inter-institutional and/or international collaborations; experience with integration of basic and applied research.

Applicants should submit: Cover letter describing interests, qualifications, philosophy and professional goals; Curriculum vitae and transcripts of academic work; Name, postal address, phone, fax and email addresses of 3 references to:

THE OHIO STATE UNIVERSITY

Dr. David J. Horn, Search Committee Chair
Department of Entomology
The Ohio State University
400 Aronoff Laboratories
[illegible]
Columbus, OH 43210

To build a diverse workforce, Ohio State encourages applications from individuals with disabilities, minorities, veterans and women. EEO/AA employer.

RUTGERS
THE STATE UNIVERSITY OF NEW JERSEY

Tenure Track Faculty Positions Computational Biology, Molecular Biophysics, and Systems Biology

The BioMaPS Institute for Quantitative Biology at Rutgers University invites applications for tenure track faculty positions at the junior or senior level in computational biology, molecular biophysics, and systems biology. The positions will be joint with an affiliated department in the School of Arts and Sciences or in Engineering. Areas of interest include but are not limited to the structure and function of molecular and cellular machines, biological networks, structural genomics and proteomics. Applicants should submit a cover letter, curriculum vitae, research summary and statement of future research goals, and a statement of teaching experience and interests and arrange for four letters of recommendation to be sent on their behalf. Materials should be submitted electronically as PDF files to **Dr. Paul Ehrlich**, Administrative Director BioMaPS Institute (email: **pehrlich@biomaps.rutgers.edu**). Currently BioMaPS Institute faculty hold joint appointments with the Departments of Chemistry, Mathematics, and Physics in the School of Arts and Sciences and the Department of Biomedical Engineering in the School of Engineering at Rutgers University, New Brunswick Campus. For more information about the BioMaPS Institute, the applicant is directed to: **http://www.biomaps.rutgers.edu**. The review of applications will begin on **December 1, 2007**. *Rutgers University is an Affirmative Action Equal Opportunity Employer. Women and minority candidates are especially encouraged to apply.*

HARVARD UNIVERSITY
DEPARTMENT OF CHEMISTRY AND CHEMICAL BIOLOGY
ASSISTANT PROFESSORSHIP IN CHEMISTRY

Applicants are invited to apply for tenure-track assistant professorships in all fields of chemistry. Applicants should arrange to have three letters of recommendation sent independently and should provide a curriculum vitae, a list of publications and an outline of their future research plans.

All applications and supporting materials must be submitted via:
http://www.lsdis.harvard.edu/cch/facultysearch/

The deadline date for receipt of applications and supporting materials is **November 1, 2007**.

Harvard University is an Affirmative Action, Equal Opportunity Employer. Applications from and nominations of women and minority candidates are strongly encouraged.

MRC Medical Research Council

MRC Laboratory of Molecular Biology, Cambridge

Group Leader Positions

The Protein and Nucleic Acid Chemistry Division of the MRC Laboratory of Molecular Biology is seeking applications from molecular biologists for two Group Leader positions.

The Division has broad expertise extending from X-ray crystallography, and nucleotide and protein chemistry through to transgenic animals. The Division also has an excellent record of innovative basic research leading to applications in medicine.

Group Leader in Synthetic/ Chemical Biology

Ref: 07/620

Existing groups of synthetic biologists within the Division (Winter, Holliger, Chin, http://www2.mrc-lmb.cam.ac.uk/PNAC) have mainly focused on the creation of novel polymers, but we would also welcome proposals to create small organic ligands to protein or nucleic acid targets.

Group Leader in Mammalian Molecular Biology

Ref: 07/621

Existing biological groups use cell-lines or transgenic mice to study signalling, cellular interactions, genomic stability and the regulation of immune responses (see http://www2.mrc-lmb.cam.ac.uk/PNAC). Applications will be welcomed from candidates whose research interests complement these activities.

Appointment would be at Programme-Leader Track level; these positions are permanent with a review in the fifth year. The successful applicants may expect to lead a group of 4 scientists by the fifth year.

Applicants should have a PhD in Molecular Biology with significant postdoctoral experience.

Further information about both positions is available at http://www2.mrc-lmb.cam.ac.uk/groupleaderinfo.html

These are permanent appointments with a salary range of £37,000 - £47,000 per annum, depending upon qualifications and experience. This is supported by a flexible pay and reward policy, 30 days annual leave entitlement, an optional MRC final salary pension scheme and excellent on site sports and social facilities.

Applications should include a covering letter and full CV, an outline of current research interests and a proposal for future research, along with the names and addresses of three professional referees who have agreed to be contacted prior to interview. Weight will be attached to the originality and nature of the project proposal, which should aim to tackle a problem of fundamental importance or utility. Enquiries are welcome at any time, but for this recruitment please reply by the date specified below.

For further information and to apply please visit our website: http://jobs.mrc.ac.uk or telephone 01793 201154 quoting reference LMB07/620 or LMB07/621.

Closing date: 19 November 2007.

For further information about the MRC visit www.mrc.ac.uk

The MRC is an Equal Opportunities Employer

'Leading science for better health'

BCM

Baylor College of Medicine

Tenure Track Faculty Position in Cognitive Neuroscience

The Department of Neuroscience at Baylor College of Medicine is continuing a major expansion of its program in cognitive neuroscience. This initiative includes hiring six new faculty members, the provision of five interactive 3.0 Tesla fMRIs dedicated exclusively to brain research and the development of the *Computational Psychiatry Unit* for the quantitative study of human behavioral brain disorders. The facilities and collaborative environment offer a unique opportunity for the study of individual and group behaviors, access to large and diverse populations of human subjects, outstanding computational expertise, one of the nation's leading programs in genetics and human genomics and a strong basic neuroscience research community. Candidates should have the Ph.D. and/or M.D. and postdoctoral training in an appropriate field. Research involving fMRI analysis of decision-making, social interaction or group dynamics utilizing computational or genomic approaches to study behavioral disorders is encouraged.

Send *curriculum vitae* and statement of research interests electronically as a single PDF to: friedlan@bcm.edu indicating cognitive position on the email header. Please have hard copies of at least three letters of reference sent to: **Cognitive Position, Michael J. Friedlander, Ph.D., Professor and Chair, Department of Neuroscience and Director of Neuroscience Initiatives, Baylor College of Medicine, One Baylor Plaza, Suite S740A, Houston, TX, 77030** by **October 25, 2007**. Please visit our departmental website at **http://neuro.bcm.edu** for more information.

Baylor College of Medicine is an Equal Opportunity Affirmative Action and Equal Access Employer.

University at Buffalo
The State University of New York

TENURE TRACK FACULTY POSITIONS IN ORAL BIOLOGY. The University at Buffalo's Strategic Planning Process - "UB 2020" - has identified several research areas for significant investment of resources over the next three years (see **http://www.buffalo.edu/ub2020/academic_planning/strategic_strengths/molecular.php**). The Department of Oral Biology invites applications for up to four full-time, tenure-track faculty positions at the Professor/Associate Professor/Assistant Professor level. We are seeking outstanding individuals capable of establishing and maintaining an independent research program, with an emphasis on molecular, cellular, genetic and/or computational biology approaches to:

- Host/immune response against oral pathogens
- Signaling networks
- Tissue engineering mineralized tissue (bone) biology
- Molecular/microbial pathogenesis of oral disease
- Craniofacial development
- Oral cancer

Candidates with research interests in bioinformatics, functional genomics, proteomics, or computational biology will have the opportunity to work as a member of the NYS Center of Excellence in Bioinformatics and Life Sciences. Additional collaborative opportunities are available through the UB School of Medicine and Biomedical Sciences, the UB School of Dental Medicine, Roswell Park Cancer Institute, and other affiliated organizations.

The successful candidate will be expected to contribute to the teaching mission of the department, including supervision of graduate students in Oral Biology and instruction in the undergraduate and graduate Dental School curricula. Candidates should hold DDS, DMD, MD, PhD or equivalent. Applications from individuals with dual degrees (e.g., DDS/PhD, DMD/PhD) are especially encouraged. Successful candidates will be expected to have or achieve significant grant funding, appropriate teaching experience, and for appointments at a higher rank, a national/international research reputation. Please apply through the UBJobs website at **www.ubjobs.buffalo.edu** (all applications MUST be submitted through this site).

The University at Buffalo is committed to increasing diversity within its faculty by seeking women and minority candidates.

UMBI
Shady Grove

TENURE TRACK FACULTY POSITION IN STRUCTURAL BIOLOGY

University of Maryland Biotechnology Institute – Shady Grove
Center for Advanced Research in Biotechnology
Center for Biosystems Research

As part of a major new expansion, the University of Maryland Biotechnology Institute (UMBI) invites applications for a tenure-track faculty position (Assistant Professor) in Structural Biology (X-ray crystallography or NMR spectroscopy). The successful candidate will be expected to develop a competitive and externally funded research program using structural biology approaches to address contemporary biological questions.

The Shady Grove Campus of UMBI includes scientists from the Center for Advanced Research in Biotechnology (CARB, **http://www.umbi.umd.edu/CARB**), the Center for Biosystems Research (CBR, **http://www.umbi.umd.edu/CBR**), and the National Institute of Standards and Technology (NIST). The campus is located in the heart of a major biotechnology community with easy access to the National Institutes of Health and NIST. The successful candidate will benefit from existing strengths in structural biology, biophysical chemistry, and computational biology at CARB, and from research into complex biological systems and pathobiology at CBR. State-of-the art facilities and support for X-ray crystallography and NMR are available at Shady Grove.

Qualifications: Ph.D. in Biochemistry or related field, postdoctoral experience and knowledge skills in structural biology. Applicants will be considered who have research interests in any area of contemporary structural biology including biomedical, plant or insect biology. Applicants should submit their curriculum vitae (referencing **position #300881**), a summary of research accomplishments and future research plans, and names of three references (**PDF file**) electronically to **carbsrch@umbi.umd.edu**. Review of candidates will begin **November 8, 2007** and continue until the position is filled.

UMBI is an EEO/ADA/AA Employer.

UMBI

Tenure Track Faculty Position in Metabolomics

University of Maryland Biotechnology Institute – Shady Grove
Center for Advanced Research in Biotechnology
Center for Biosystems Research

Applications are invited for a tenure-track faculty position at the Assistant, Associate, or Professor level. The successful candidate will be expected to develop a rigorous, externally funded research program in the field of metabolomics using advanced analytical methods.

The Shady Grove Campus of the University of Maryland Biotechnology Institute (UMBI) is developing an integrated research program in molecular systems biology, bridging the interests of the Center for Advanced Research in Biotechnology (CARB, **http://www.umbi.umd.edu/CARB**), a partnership with the National Institute of Standards and Technology (NIST)) and the Center for Biosystems Research (CBR, **http://www.umbi.umd.edu/CBR**). Research areas at the Shady Grove Campus include chemical biology, mass spectrometry, structural biology, bioinformatics, experimental and computational biophysics, systems modeling, plant and insect biology. Several new faculty hires are anticipated over the next two years, and a new 140,000 ft² research building equipped with state-of-the-art facilities has recently opened.

Qualifications: Ph.D. in Biochemistry or related field, postdoctoral experience and knowledge skills in metabolomics. Areas of interest include but are not limited to: metabolite changes in response to disease or environmental stress, applications in functional genomics, metabolic networks, medicinal plant metabolism; development of metabolomic databases. We are particularly interested in applicants who are seeking a highly collaborative research environment. Applicants should submit their curriculum vitae (referencing **position #300879**), a summary of future research plans, and names of three references (**PDF file**) electronically to **carbsrch@umbi.umd.edu**. Review of candidates will begin **November 8, 2007** and continue until the position is filled.

UMBI is an EEO/ADA/AA Employer.

國家衛生研究院
National Health Research Institutes

Immunology Research Center
National Health Research Institutes (NHRI), Taiwan

The newly established **Immunology Research Center** at the National Health Research Institutes (NHRI) in Taiwan invites applications for multiple tenure-track/tenured faculty positions at the rank of **Assistant, Associate or Full Investigator** (the equivalents of Assistant, Associate, and Full Professor in universities). Highly qualified candidates are sought with research interests in all areas of **Immunology and Signal Transduction**, especially in the areas of cell signaling, innate immunity, cytokines and chemokines, immune tolerance, autoimmunity, immunity to infection, and cancer immunology. Applicants should have a Ph.D. and/or M.D. degree as well as postdoctoral experience. Selection will be based on excellence in research and the potential to maintain an outstanding research program. Investigators also contribute to training graduate students from affiliated Ph.D. programs at several national universities as well as shaping Immunology research at NHRI in Taiwan. A generous annual intramural support will be provided. English is the official language for regular seminars and lectures at NHRI, and proficiency in the Chinese language is not required for application.

Applicants should send curriculum vitae, description of research accomplishments and future objectives, and three reference letters to:

Faculty Search Committee
Immunology Research Center
National Health Research Institutes
35 Keyan Road, Zhunan Town, Miaoli County 35053, Taiwan

Review of credentials is ongoing and will continue until the positions are filled. Further information can be obtained from **Ms. Shu-ling Su** at **sunlo@nhri.org.tw**

---

stem cell biology

The Life Sciences Institute and the University of Michigan Medical School invite applications for tenure track **ASSISTANT PROFESSOR** positions. We are seeking outstanding scholars, with Ph.D., M.D. or equivalent degrees and relevant postdoctoral experience, who show exceptional potential to develop an independent research program that will address fundamental issues in any aspect of stem cell biology. Applicants who have already established successful independent research programs will be considered for tenured **ASSOCIATE PROFESSOR** or **PROFESSOR** positions.

Applicants should send a curriculum vitae, copies of up to three reprints, a one- to two-page summary of research plans, and arrange to have three letters of reference sent directly by **November 1, 2007** to:

Stem Cell Search Committee
c/o Rebecca Fritts
Life Sciences Institute
University of Michigan
210 Washtenaw Avenue
Ann Arbor, Michigan, 48109-2216

The University of Michigan is an Affirmative Action/Equal Opportunity Employer

---

UNIVERSITY OF MARYLAND

Assistant/Associate or Professor(s)

The Fischell Department of Bioengineering, University of Maryland, College Park

The Fischell Department of Bioengineering is seeking highly talented individuals in the fields of bioengineering for two (2) tenure-track or tenured faculty positions.

The Department is a highly progressive unit catalyzed by a gift of $31 million from Robert E. Fischell and family. At the interface of engineering and life sciences, our Department seeks to build quantitative systems approaches that will define the multi-scale underpinnings of healthcare engineering for the next generation. The Department has over 55 graduate faculty mentors in cross-disciplinary areas of bioengineering including four colleges at College Park, the Schools of Pharmacy, Dentistry, and Medicine of the University of Baltimore, and the University of Maryland Biotechnology Institute. The undergraduate program is highly sought after by the most talented high school students in Maryland and elsewhere.

Located in the greater Washington DC area, the Department has access to vast research resources and facilities in the immediate vicinity, including those of the NIH, FDA, DOD, USDA, and NASA as well as over 600 Maryland biotech companies.

Qualifications: Open to all areas in bioengineering. Candidate must have Ph.D. in biomedical, biological, or closely related engineering field. Candidates with excellent communication skills and strong background in areas of, but not limited to, protein engineering, genomics, systems biology, biological engineering, or integrated medical devices are strongly encouraged to apply.

Application. To apply, please visit **http://apra.umd.edu/search.jsp?ID=BIOE0000103**. Applications received prior to **December 15, 2007** will receive earliest consideration.

The University of Maryland is an Equal Opportunity/Affirmative Action Employer. Women and minorities are encouraged to apply.

University of Minnesota

Stem Cell Institute and Department of Genetics, Cell Biology, and Development

Two Faculty Positions

Following appointment of its new director, **Dr Jonathan Slack**, the Stem Cell Institute at the University of Minnesota is conducting a search for faculty at the Assistant, Associate or Professor level working in the areas of stem cell biology, regenerative medicine or applied developmental biology. The University will devote competitive salaries, start up packages, and recently built laboratory space, with access to state-of the-art core facilities. The candidates must have a Ph.D. or M.D. with at least three years of postdoctoral experience, and evidence of high quality research productivity. Applicants are invited in any area with potential for interaction with existing research programs (see **http://www.stemcell.umn.edu**) and especially in the areas of (1) pancreatic beta cell generation, and (2) tissue, organ or appendage regeneration.

The persons selected will be expected to develop an independent, externally funded research program and participate in the teaching mission of the Department of Genetics, Cell Biology and Development (GCD).

Individuals interested in this position should apply online (**https://employment.umn.edu**). Search for Requisition Number **150879**. Attach a CV and a statement of current and future research. Three letters of reference should be mailed to: **Stem Cell Faculty Search, c/o Lauri Andersen, Stem Cell Institute, University of Minnesota, MTRF, 2001 6th Street SE, Minneapolis, 55455, USA.** For further details email **ander607@umn.edu**.

Closing date for application **31 December 2007**

The University of Minnesota is an Equal Opportunity Educator and Employer

Scientific Director at Fox Chase Cancer Center

FOX CHASE
CANCER CENTER

The Fox Chase Cancer Center (FCCC) is initiating a national search to identify the Scientific Director who will have the overall responsibility for directing, coordinating, and building the scientific portfolio within the FCCC, a NCI funded Comprehensive Cancer Center. The Center seeks to reduce the burden of human cancer through the pursuit of knowledge in basic biological research, the conduct of research specifically related to cancer etiology, treatment and prevention, and the application of new knowledge to the prevention of cancer and the compassionate care and treatment of cancer patients. In the next decade an emphasis will be placed on integrating emerging technologies to enhance team science to reduce the burden of cancer.

The Scientific Director will report to the president and will be appointed as senior vice president within the administrative structure of the institution. The individual in this new position will have oversight of all the scientific efforts in the Center and will work with other senior leadership of the institute to design future laboratory space and recruit individuals to fill new research space that will become available on the FCCC campus in the next several years. In addition, the individual will serve as the Deputy Director of the NCI funded Cancer Center Support Grant (CCSG) assuming significant responsibilities in the management of the CCSG grant which is current in its 45th year of continuous funding.

FCCC is one of seven free-standing National Cancer Institute-designated Comprehensive Cancer Centers. Research in the Basic, Medical and Population Science Divisions is structured around a number of focused programs that represent the Center's commitment to areas of investigation and interdisciplinary interaction that are critical to our mission of reducing the burden of cancer. Faculty members investigate problems that range from fundamental mechanisms about interesting and outstanding biological processes to the treatment of neoplastic diseases in the clinic. The juxtaposition of laboratory and clinical investigators with a broad range of interests and expertise opens the opportunity for cross-divisional interactions in which a variety of approaches are brought to bear. Such cross-divisional activities foster a uniquely collegial and interactive atmosphere that supports the mission of FCCC.

Major areas of research include: 1) structural biology; 2) cellular and developmental biology; 3) immunobiology; 4)tumor cell biology; 5) viral pathogenesis; 6) basic, translational and clinical research on ovarian, breast, colorectal and prostate cancers; radiation oncology; 7) diagnostic imaging, cancer prevention and control; 8) cancer epidemiology and etiology; 9) cancer genetics; behavioral and psychosocial research, and 10) health practices and outcomes research.

The ideal candidate will have an international reputation for innovative research and have a track record of productive peer reviewed funded science and have accumulated a series of professional experiences that demonstrated his or her leadership qualities. Experience within a comprehensive cancer center or academic medical center is highly desirable. In addition, important participation in large team-based science efforts in population science, genomics, translational research, bioengineering or molecular imaging is desirable but not required.

FCCC is an Equal Opportunity Employer and women and individuals from underrepresented groups are especially encouraged to apply. Letters of applications and resumes (electronic preferred) should be sent to: **nancy.cook@gyreinternational.com** or **Gyres International, PO Box 439, Oxford, MD 21654.**

IOWA STATE UNIVERSITY
College of Engineering

MAKING GLOBAL IMPACT

Discovery with purpose

Iowa State University, the nation's first land-grant institution, *is located in Ames, Iowa, a community of 50,000 residents located 35 minutes from Des Moines, our state capital. Iowa State has a long history of achievement in science and engineering; engineering was one of the institution's original divisions. The university enrolls 26,000 students with 4,600 undergraduate and nearly 1,000 graduate students in the College of Engineering. Iowa State is a Carnegie Foundation Doctoral/Research-Extensive University recognized by U. S. News & World Report as one of the nation's top 50 public universities; the magazine ranks the engineering graduate program among the nation's top 20 percent.*

The College of Engineering at Iowa State University has an aggressive mission to advance our global impact by addressing the challenges that will define our worldwide quality of life in the coming decades. To that end, the college will continue to fill 50 new faculty positions with faculty who possess the talent and passion to positively impact our students, nation, and world. To help focus our efforts in pursuit of this mission, these new faculty will be members of the following interdisciplinary research and education clusters.

- Biosciences and Engineering
- Energy Sciences and Technology
- Engineering for Extreme Events
- Information and Decision Sciences
- Engineering for Sustainability

For background information on the cluster areas and the desired qualities of our new faculty, see ***www.engineering.iastate.edu/clusters.***

Applications for faculty positions at all levels (assistant, associate, and full professors) in all departments are welcome.

- Aerospace Engineering
- Agricultural and Biosystems Engineering
- Chemical and Biological Engineering
- Civil, Construction, and Environmental Engineering
- Electrical and Computer Engineering
- Industrial and Manufacturing Systems Engineering
- Materials Science and Engineering
- Mechanical Engineering

Additional information on the missions of our college and departments is available at ***www.engineering.iastate.edu.***

To be considered for a position, you must submit your application materials via our Web site http://www.engineering.iastate.edu/clusters/application-process.html. Your packet must include a cover letter indicating your department(s) of interest, vita, publication list, research and teaching plans, and at least three references. Questions can be directed to ***clusterhires@engineering.iastate.edu.*** *We particularly encourage women and underrepresented minorities to apply. Iowa State University is an Equal Opportunity/Affirmative Action Employer and an NSF ADVANCE grantee with the goal of enhancing the success of women faculty in STEM fields.*

An Equal Opportunity Employer

www.engineering.iastate.edu

United Nations Educational, Scientific and Cultural Organization

Intergovernmental Oceanographic Commission

Position of Chief of Ocean Sciences
Intergovernmental Oceanographic Commission of UNESCO
Paris, France

Duty station: Paris, France
Grade: P-5
Post number: SC-314
Closing date: 19 November 2007

In 2010, the Intergovernmental Oceanographic Commission of UNESCO will celebrate five decades as the only inter-governmental organisation with a remit for ocean science in the UN system. The Commission has served its 136 Member States with distinction. Beginning with the establishment of the Committee on Climate Change and the Ocean, of which Roger Revelle was the founding Chairman, its work continued through the establishment of the Global Ocean Observing System, and today it leads the UN Global Marine Assessment effort.

As it adapts to new ways of delivering on its mandate of promoting the best ocean science that feeds into policies, an opportunity presents itself in the recruitment of a new Chief of the Ocean Sciences Section.

The Commission is looking for an established oceanographer with (i) excellent scientific credentials to facilitate interactions within the oceanographic community, and (ii) experience in leading an institute active in marine sciences or large national or international marine research programs. This profile will allow the candidate to interface between scientists and policy makers, as well as appreciate what works in implementing science plans at the international level.

The Commission is looking for a candidate with (i) foresight and enthusiasm to coordinate today's new areas of enquiry for the ocean science issues of tomorrow, (ii) plans and a vision to include all member states to participate and benefit from the ocean, and (iii) patience and skills to translate science information into forms suitable for policy makers. The full post description is available at http://recruitweb.unesco.org/pdf/SC_314.PDF

Conditions of employment: UNESCO's salaries are calculated in US dollars but mainly paid in local currency. They consist of a basic salary and a post adjustment which reflects the cost of living in a particular duty station and exchange rates. For this post, the annual remuneration in local currency will start from around €95,600 (€88,800 if without dependants), exempt from income tax. In addition, UNESCO offers an attractive benefits package including 30 days annual vacation, home travel, education grant for dependent children, pension plan and medical insurance. The initial appointment, which is for two years, includes a probationary period of 12 months and is renewable subject to satisfactory service. Worldwide mobility is required as staff members have to serve in other duty stations according to UNESCO's job rotation policy. UNESCO is a non-smoking Organization.

How to apply: Candidates wishing to apply for this post should use the UNESCO on-line recruitment system at the following website: http://www.unesco.org/employment

---

Founding Chair, Department of Basic Sciences

The Commonwealth Medical College, a new independent medical school in Pennsylvania is searching for a founding basic sciences department Chair who wants to build an integrated and collaborative basic sciences department, help develop a state of the art curriculum, and foster research in a collaborative setting. This is a chance to help shape the future of a new, innovative mode of medical education. The Commonwealth Medical College will train in a community based, distributive model working with clinical faculty throughout north central and northeastern Pennsylvania, linked by state of the art technology. We are in the accreditation process with LCME and the Pennsylvania Department of Education and hope to accept our first class in 2009. We are funded by state dollars and a generous grant from Blue Cross. The school enjoys tremendous regional support for its mission of education, research and service and has developed relationships with outstanding local colleges, universities, hospitals and physicians to create a new model of medical education.

The Department of Basic Sciences within The Commonwealth Medical College seeks an outstanding scientist for the position of Founding Chair of the Department of Basic Sciences. The Commonwealth Medical College has identified strategic research interests which include genomics, pharmacogenomics, pharmokinetics and pharmacodynamics that are relevant to cancer and epidemiologically important infections and diseases. It is anticipated that the successful candidate will have research interests in one of these "signature" programs. Cancer, diabetes, and heart disease are the leading issues of concern, but other areas of expertise are also welcomed.

Minimum requirements include a MD, PhD, or MD/PhD with a minimum of five years of experience as an Associate Professor or equivalent. A record of sustained accomplishments and evidence of leadership in his/her field, relevant administrative experience, and evidence of effective interpersonal, collaborative and communication skills is required. The successful candidate is expected to have a distinguished record of scholarly activity, a continuous history of extramural funding and requisite recruitment experience in a medical graduate curriculum. A legacy of building interdisciplinary programs and experience with successfully mentoring medical students is also highly desirable.

Please submit your curriculum vitae to: Robert M. D'Alessandri, MD, Dean, The Commonwealth Medical College, 150 North Washington Avenue, Scranton, PA 18503 or electronically to RMD@nepamedc.org.

thecommonwealthmedical.com | The link to the Dean's blog is newmedicalschool.blogspot.com

**This school is proposed and in development phase. Has yet granted degree granting authority from the Pennsylvania Department of Education*

ASSISTANT PROFESSOR
Environmental Soil Scientist
Department of Agronomy

Appointment conditions: tenure track, nine months, full time, proposed start date August 16, 2008. The Department of Agronomy invites applications for a faculty position in environmental soil science. The successful candidate will conduct research in environmental soil science related to the fate and transport of nutrients used in Iowa agricultural production systems. The appointee is expected to develop leadership in integrating the application of soil chemical, microbiological, and physical principles to agriculture and natural resource challenges that span spatial scales from the root zone to the landscape. The appointee will engage in interdisciplinary research on topics such as biogeochemical aspects of nutrient management and nitrogen processes along the soil/plant/groundwater/surface water continuum. The appointee will teach an undergraduate course in the environmental science major as well as a graduate course related to agrichemicals in the environment. The appointee may also advise undergraduates and direct undergraduate research. Supervision and advising of soil science graduate students, participation in curriculum development and outreach programs, and performance of University service are also expected. This position is seen as 75 percent research and 25 percent teaching. Iowa State University especially seeks candidates who will contribute to the diversity and excellence of the academic community through their research, teaching, and outreach. Iowa State University (ISU) is one of the country's leading agricultural research universities and is in one of the top agricultural states in the United States. Located in the city of Ames, ISU is in the heartland of U.S. culture and agriculture. Ames has abundant recreational and entertainment opportunities and an outstanding school system. This faculty position affords significant opportunities for the development of strong interdisciplinary research teams with departmental faculty, allied departments on the ISU campus, research organizations such as the USDA Agricultural Research Service National Soil Tilth Laboratory, and other state and national partners.

Required qualifications: Ph.D. in soil science, environmental science, or a closely related field. Demonstrated evidence of research and teaching proficiency, including experience in studying the fate and transport of nutrients and agrichemicals in the environment. Excellent written and oral communication skills.

Preferred qualifications: teaching, research, and outreach experience beyond the Ph.D. degree; background in using modeling tools and geographic information systems; demonstrated success in grant writing and administration of external research; and experience working collaboratively with researchers, extension staff, industry, and agency personnel.

Salary: commensurate with qualifications.

Application instructions: Please send a letter of application, curriculum vitae, credentials, descriptions of teaching and research (including methods and equipment that will be used), interests and experience, and the name, address, and telephone number of three references to: **Dr. Kendall Lamkey, Chair, Department of Agronomy, 2101 Agronomy Hall, Iowa State University, Ames, IA 50011.** The application deadline is November 30, 2007, or until the position is filled.

ASSISTANT PROFESSOR, BIOLOGY
Framingham State College

The Biology Department at Framingham State College seeks applications for a tenure-track position starting in September 2008. The successful applicant will be a broadly trained Biologist with expertise in molecular biology, genetics, and cell biology, a Ph.D. in biology, and a passion for teaching undergraduates. For a full job description and how to apply, please refer to website: **http://www.framingham.edu/humanresources.**

Framingham State College is an Equal Opportunity/Affirmative Action Employer.

POSITIONS OPEN

EMORY

EMORY UNIVERSITY
Department of Environmental Studies

The Department of Environmental Studies at Emory University invites applications for two positions at the **ASSISTANT or ASSOCIATE** level to begin fall 2008. We seek candidates who will actively engage with a faculty that is committed to teaching and research that integrates the natural and social sciences in the study of the environment. Thematic areas of particular interest to the Department include, but are not limited to, global health and environment, sustainability, and urban ecology, with a focus on either terrestrial or aquatic environments. We welcome applicants already holding a faculty position or with Ph.D. completed by August 2008, in a relevant discipline such as earth and atmospheric sciences, ecology, economics, geography, public health, public policy, or urban studies. Successful candidates should be prepared to establish a vigorous research program and be committed to excellence in the training of undergraduate and graduate students. The position provides an opportunity to join a growing Department in collaborative research, teaching, and training programs that are consistent with the University's newly launched Strategic Initiatives (**website: http://www.emory.edu/univ_planning.cfm**) in state-of-the-art facilities within a metropolitan urban forest setting. For additional information about the Department and links to Atlanta and Emory University, please visit the departmental **website: http://www.envs.emory.edu.** Applications should include curriculum vitae, a statement of research interests and teaching philosophy, representative publications, and the names of three references. Materials should be submitted electronically to e-mail: **jbyrd01@emory.edu.** The review will begin December 14, 2007. General inquiries may be directed to **Dr. William Szar, e-mail: wszar@emory.edu.** *Emory University is an Equal Opportunity, Affirmative Action Employer. Women and minority candidates are encouraged to apply for this position.*

PLANT PHYSIOLOGICAL/ECOSYSTEM ECOLOGIST
Rutgers University, Newark

Applications are invited for a tenure track **ASSISTANT PROFESSOR** position in the Department of Biological Sciences (**website: http://newarkbiosci.rutgers.edu/**), particularly strong candidates at the advanced Assistant or Associate Professor level will also be considered. We are interested in hiring a **PLANT ECOPHYSIOLOGIST** whose research links organisms to their surrounding ecosystem. The successful candidate will join the Ecology and Evolution Research Group that currently encompasses large scale ecology, community ecology, marine ecology, and theoretical ecology. Ability to interact with colleagues in the Department of Earth and Environmental Science, the mathematical biology group at New Jersey Institute of Technology, and the Meadowlands Environmental Research Institute is also desirable. Applicants must have a Ph.D. degree or equivalent, postdoctoral training, a record of research accomplishment, and the ability to develop an externally funded program of research. Applications will be reviewed starting November 15, 2007, and will be accepted until the position is filled. Curriculum vitae, statements of research and teaching interests, and three letters of recommendation should be sent to: **Ecology Search Committee, Dr. Edward Bender, Chairman, Department of Biological Sciences, Rutgers University, University Heights, 195 University Avenue Newark, NJ 07102-1811 U.S.A.** Electronic submissions via PDF files are strongly encouraged, **e-mail: biosci@newark.rutgers.edu**

Rutgers University is an Affirmative Action/Equal Opportunity Employer.

POSITIONS OPEN

DIRECTOR of BASIC SCIENCE RESEARCH
SimmonsCooper Cancer Institute
Southern Illinois University

The SimmonsCooper Cancer Institute (SCCI) at the Southern Illinois University School of Medicine in Springfield is recruiting a scientific leader to provide vision and administrative oversight to its basic science research program. This is an exciting opportunity to influence how basic science research faculty work in collaboration with clinical cancer specialists to develop innovative translational research programs. A new Cancer Institute building with state-of-the-art facilities is currently under construction and is slated to open in July 2008. This will enhance existing facilities committed to cancer research which include more than 25,000 square feet of laboratory space.

The successful candidate for this leadership position will possess a Ph.D. and/or M.D., significant experience in research, mentoring, and administration, and external funding for basic science research relevant to oncology. Teaching opportunities with medical and graduate student education programs are available. The appointment will be a tenure-track position at the level of **ASSOCIATE/FULL PROFESSOR** in an appropriate academic department, with a cross appointment to the Institute. A competitive salary, benefit, and laboratory facility package is provided by the Southern Illinois University School of Medicine.

Applicants should submit a letter of interest, curriculum vitae with a history of external funding, a description of research accomplishments and plans, and the names and contact information for three professional references to:

Mr. Garrison C. Vecht
Administrator, SimmonsCooper Cancer Institute at Southern Illinois University
P.O. Box 19677
Springfield, IL 62794-9677

This position has been designated security-sensitive and employment is contingent upon the results of a criminal background investigation. SIU is an Equal Opportunity Employer. Women and minorities are encouraged to apply.

TENURE TRACK ASSISTANT PROFESSOR
University of Michigan
Biophysics

Biophysics at the University of Michigan anticipates that one or two tenure track faculty positions will be available with a September 2008 starting date. The position is a tenure-track Assistant Professorship with a University year appointment. We are considering applications in all areas of biophysics, especially those areas focused on problems of biological interest that use and develop modern biophysical methodologies. We are primarily interested in experimental work to compliment the theoretical and numerical modeling efforts that currently exist in the area of structural dynamics. Information about our research areas can be found at **website: http://www.umich.edu/~biophys/.** Candidates are required to have a doctoral degree in biophysics or a related field such as chemistry, biological chemistry, physics, et cetera. The successful candidate is expected to establish an independent research program and to contribute effectively to the Department's undergraduate and graduate teaching programs. Applicants should submit curriculum vitae, a brief statement of present and future research plans, a statement of teaching experience and interests, at least three letters of recommendation, and evidence of teaching excellence, if any. The deadline for applications is December 10, 2007. Applications and signed letters of recommendation in PDF format can be e-mailed to e-mail **biophysics.search@umich.edu** or can be mailed to **Ms. Ann Titus, Biophysics, 930 N. University Avenue, 4028 Chemistry Building, University of Michigan, Ann Arbor, MI 48109-1055.** *Women and minorities are encouraged to apply. The University of Michigan is supportive of the needs of dual-career couples and is an Equal Opportunity/Affirmative Action Employer.*

Bioinformaticist

The Howard Hughes Medical Institute, a national and international philanthropy devoted to biomedical research and science education, is seeking a Bioinformaticist to join our new Science Education Alliance (SEA) program located in **Ashburn, VA**.

The SEA program is an exciting new initiative that promises to become a national resource for science education. The SEA's first major project will be to develop a national genomics experience implemented as a research-based laboratory course for undergraduate freshmen and sophomores, infusing undergraduate curricula with authentic discovery science.

As a key contributor to the successful development and implementation of this and future initiatives, the **Bioinformaticist** will identify and customize a suite of bioinformatics tools for genome assembly, annotation, and analyses, a role set in a diverse community of scientists, educators and students. Additionally, you will provide strategic direction toward the development and implementation of workshops to train users, and serve as the primary liaison between the SEA and IT support staff.

To excel in this position, you must possess an MS or PhD in Bioinformatics or Computer Science, at least 2 years of direct experience with bioinformatics tools, and an in-depth knowledge of molecular biology as it relates to genomics. You must demonstrate a mastery of UNIX/Linux operating systems as well as demonstrated proficiency in the following software applications: Phred; Phrap; Consed; Sequencher; Lasergene; and BLAST. Strong service-oriented attitude coupled with exceptional interpersonal and communication skills is also required.

HHMI is an intellectually demanding, results-oriented organization with excellent salaries and benefits. Responses should include your present position, and a brief summary of your scientific accomplishments. Please send your resume to HHMI via e-mail at **jobs@hhmi.org**. Please include the job title in the subject line. To learn more about HHMI and this position, visit our website at **www.hhmi.org**.

The Howard Hughes Medical Institute is an Equal Opportunity Employer.

HHMI
HOWARD HUGHES MEDICAL INSTITUTE

University of Pittsburgh
Faculty Positions
Center for Vaccine Research

The Center for Vaccine Research (CVR) of the University of Pittsburgh is seeking outstanding scientists involved in emerging pathogens and biodefense research for several tenure and tenure-track positions at the Assistant, Associate, or Professor levels. Established investigators with expertise or interest in pathogenesis or immunology of infectious diseases with special emphasis on influenza or flaviviruses are strongly encouraged to apply. Appointments are available in the School of Medicine, the Graduate School of Public Health, or one of the other schools of the health sciences.

The CVR is housed in the new, state-of-the-art, 300,000 sq. ft. Biomedical Research Tower (BSTV) which is located on the main campus of the University of Pittsburgh-one of the nation's leading research institutions. The CVR is composed of two components-the Vaccine Research Lab (VRL) and the Regional Biocontainment Lab (RBL), offering comprehensive BSL2 and BSL3 laboratory and animal facilities.

Applicants must demonstrate academic accomplishments that meet the standards for a tenure-track appointment, including an advanced degree (MD, PhD or equivalent). Successful candidates will have a sound publication record, be active contributors to the vaccine research field, and have a demonstrated ability to obtain extramural research funding. Salary, rank, and academic appointment will be commensurate with qualifications and experience.

Review of applications will begin immediately and continue until all positions are filled. Interested individuals should submit a letter of application, curriculum vitae, a statement of research accomplishments and goals, and the names, mailing addresses, e-mail addresses and telephone numbers of three professional references. Electronic applications are preferred and should be sent to **CVRInfo@pitt.edu** (subject line: CVR Faculty Search). Applications submitted by [illegible] to:

University of Pittsburgh

CVR Search Committee, c/o Donald S. Burke, MD
Director, Center for Vaccine Research, University of Pittsburgh
9014 Biomedical Science Tower 3, 3501 Fifth Avenue, Pittsburgh, PA 15261, USA

Inquiries: e-mail CVRInfo@pitt.edu or telephone 412-624-4488.

The University of Pittsburgh is an equal opportunity, affirmative action employer. Women and minority candidates are strongly encouraged to apply.

For more information about the CVR, please visit our web site at:

http://www.cvr.pitt.edu

Chair of Mechanical Engineering.

The Faculty of Engineering

The University of Melbourne is a leading international university with a tradition of excellence in teaching and research. It is the only Australian university to take a new approach to tertiary education with the launch of the Melbourne Model, a major higher education reform which will align the University's curriculum with international standards and provide an outstanding and distinctive experience for all students.

The Chair of Mechanical Engineering will lead the development of world-class research, scholarships and education with a focus on Dynamic Systems and Control.

This Chair is expected to make a major contribution to the research activities in at least one of the Faculty's research themes: Information and Communications Technology, Bioengineering, Sustainable Systems and Structured Matter. Leadership and vision that enhances the relevance of dynamic systems and control research and its application in one or more of the faculty's research themes will be sought from this Chair. The appointee must be able to make a strong contribution to the Department's undergraduate and graduate teaching programs, particularly in the area of mechatronics.

It will be essential that the Chair can combine action on some of the urgent contemporary problems of industrial society with fundamental investigations of physical and human-related phenomena in engineering settings.

Salary: An attractive, highly competitive remuneration package will be negotiated including employer superannuation of 17%.

Employment Type: Full time (continuing) position.

Advice to applicants: Applicants must address the selection criteria, quote job number 0017840 and include the contact details of three referees.

Applications can be forwarded to one of the following:

Email: select@ckh.com.au

Fax: +61 3 9620 2811

Post: Sarah Hunter, Partner, Corrsner King,
Level 44, Rialto, 525 Collins Street,
Melbourne VIC 3000 Australia

Closing date: 4 December 2007

For further information, obtain the position description and selection criteria at www.jobs.unimelb.edu.au and search under the job title or job no. 0017840.

An Equal Opportunity employer.

THE UNIVERSITY OF MELBOURNE

POSITIONS OPEN

ECOLOGISTS

The Department of Biology at Appalachian State University (website: **http://www.biology.appstate.edu**) seeks to fill two tenure-track positions. Although appointment at the rank of **ASSISTANT PROFESSOR** is anticipated, one position may be filled by an outstanding candidate at the **ASSOCIATE PROFESSOR** rank. We seek Teacher Scholars who will combine excellence in undergraduate and graduate (Master's) teaching with an active research program. Applicants must have a Ph.D. and should have postdoctoral research experience and complement existing faculty. Successful candidates are expected to teach courses in their specialty and may teach in the general Biology Program. The positions are **MICROBIAL ECOLOGIST.** We are seeking an individual who investigates the role of prokaryotes in ecosystem processes, e.g. nutrient cycling, energetics, soils, or interactions with plants, fungi, or insects. The ability to teach general microbiology and expertise in molecular ecological techniques are required. **Search Chair: Dr. John F. Walker (e-mail: walkerjf@appstate.edu).**

ECOSYSTEM ECOLOGIST. We are seeking an individual who applies experimental approaches to ecosystem processes, e.g. ecosystem energetics, biogeochemistry, organic matter processing, and/or the effect of biodiversity on ecosystem functioning. Research experience at the terrestrial-aquatic interface and/or with global change biology is desirable. Teaching responsibilities may include ecosystem ecology and global change biology. **Search Chair: Dr. Howard S. Neufeld (e-mail: neufeldhs@appstate.edu).**

Appalachian State University, located in the southern Appalachian Mountains, is a highly ranked comprehensive university and a member institution of the 16 campus University of North Carolina System, enrolling over 15,600 students. Appalachian State University seeks to maintain its reputation for excellence in teaching while continuing to enhance its research reputation.

To apply, send a cover letter, curriculum vitae, separate statements of research and teaching interests/philosophy, and contact information for at least three references (name, address, telephone, e-mail address) to: **Chair, Ecologist Search** (specify which position), **Department of Biology, 572 Rivers Street, Appalachian State University, Boone, NC 28608.** Electronic applications accepted only in (PDF format). Positions will remain open until filled; review of applications begins November 12, 2007. *Appalachian State University is an Affirmative Action/Equal Opportunity Employer. Women and minorities are encouraged to apply. The University and Department are committed to increasing diversity and welcome applications from members of minorities and underrepresented groups.*

CELL/MOLECULAR BIOLOGIST
Fordham University

Individuals are invited to apply for a tenure-track position at the **ASSOCIATE PROFESSOR** level. The Department has an active research program and provides excellent physical facilities, state of the art equipment, a stimulating research environment, startup funds, and competitive salaries and benefits. Preference will be given to candidates who possess expertise in the area of cell/molecular biology, and have an ongoing grant-supported research effort underway. Candidates with research interests in molecular biology, stem cells, cancer, development, or genetic diseases are particularly encouraged to apply. The appointee will be expected to establish an active research program and participate in teaching at the graduate and undergraduate levels. Please submit curriculum vitae, two reprints, and the names and addresses of three references by January 3, 2008, to: **Dr. William B. Thornhill, Chair, Department of Biological Sciences, Fordham University, Bronx, NY 10458.** *Fordham is an independent, Catholic university in the Jesuit tradition that welcomes applications from men and women of diverse backgrounds. Fordham is an Affirmative Action/Equal Opportunity Employer.*

POSITIONS OPEN

ASSISTANT/ASSOCIATE PROFESSOR
Department of Biomedical Engineering
The University of Michigan

The Department of Biomedical Engineering at the University of Michigan College of Engineering is searching for new faculty positions in biomechanics, biomedical optics, neural engineering, in vivo imaging, and stem cell engineering. Applications in these areas are of particular interest but applications in all areas within biomedical engineering will be considered. Successful candidates will join a vibrant bioengineering community with strengths in biomaterials, biosensors, tissue engineering, biofluid mechanics, microfluidics, biomolecular engineering, biomolecular devices, bioprocess technology, biomedical imaging and optics, neural engineering, bioMEMS, and micro/nano biotechnology. Qualifications include an earned Ph.D. in engineering or a physical science related discipline and demonstrated excellence in and commitment to teaching, research, and scholarship. We seek candidates who will provide inspiration and leadership in research and contribute actively to teaching, and are especially interested in candidates who can contribute, through their research, teaching, and/or service, to the diversity and excellence of the academic community. The University of Michigan is responsive to the needs of dual-career families.

Applicants should send a letter of interest with curriculum vitae and a list of references to:

Biomedical Engineering Search Committee
Biomedical Engineering
The University of Michigan
1107 Carl A. Gerstacker Building
2200 Bonisteel Boulevard
Ann Arbor, MI 48109-2099
E-mail: bausch@umich.edu

An Equal Opportunity/Affirmative Action Employer

TENURE-TRACK FACULTY POSITION
University of Maryland, Baltimore
Department of Biomedical Sciences

The Department of Biomedical Sciences, University of Maryland, Baltimore, invites applications for a tenure track position in molecular and cellular biology. Applications for a position at the **ASSISTANT PROFESSOR** level are encouraged; however, we will also consider applications from more senior investigators. Applicants must have a Ph.D. degree (or equivalent) with training and postdoctoral experience in molecular and cell biology. Successful applicants will have a record of outstanding research accomplishment and an active research program. Preference will be given to applicants with an interest in molecular cancer and cancer biology including metastasis. Applicants are expected to develop an independent extramurally funded research program that will contribute to the Department's research focus in cancer development, progression, and metastasis. The individual filling this position will also be expected to participate in professional and graduate student educational training programs. The successful applicant will have research space in a new state-of-the-art facility with access to animal facilities and resources for small animal tumorigenicity studies. Members of the Department may become members of the Greenebaum Cancer Center at the University and interact with basic and clinical cancer researchers throughout the campus. Applications will be accepted until the position is filled. Send curriculum vitae, statement of career objectives, and the names of at least three references by mail or e-mail to Judy Pennington, e-mail: jpennington@umaryland.edu, **Coordinator, Molecular and Cell Biology Search Committee, Department of Biomedical Sciences, University of Maryland, Baltimore, 650 W. Baltimore Street, Baltimore, MD 21201.**

POSITIONS OPEN

ASSOCIATE/FULL PROFESSOR
Immunology and/or Infectious Disease

An accomplished scientist who studies infectious disease, particularly zoonoses, or host response to infectious agents is sought for a tenure-track position (90 percent research, ten percent instruction) in the Department of Veterinary Molecular Biology (VMB) at Montana State University (MSU). MSU is a land-grant university located in a community of 35,000 people, with a high quality of life, excellent public schools, and close proximity to outstanding recreational opportunities. VMB currently has annual grants and contracts expenditures exceeding $12.5 million per 11 faculty members, which represents the largest research effort on campus. VMB has a dynamic research and teaching environment, with state-of-the-art facilities for biochemistry, genomics, immunology, and cell biology. VMB is housed in a new research building occupied in 2003, with state-of-the-art facilities for flow cytometry, cell biology, molecular sciences, and newly constructed pathogen containment BSL-3 and large animal small animal ABL 2 facilities. We are seeking an individual to complement or expand existing VMB expertise in the study of viral, protozoan, fungal, prion, and bacterial pathogens of major livestock and wildlife, as well as host responses against these pathogens. This position is funded by a competitive international salary, nine months with excellent institutional support and a generous startup package. Candidates must have a doctoral degree in a biomedical discipline and an established competitive, funded, independent research program is required. An **ASSOCIATE** or **FULL PROFESSOR** position will be offered commensurate with qualifications.

To apply: No fax applications. To complete the application, please consult the complete job description (see website: http://vmb.montana.edu) and submit applications to: **Chair, Veterinary Molecular Biology Associate/Full Professor Faculty Search, Montana State University.** Screening will begin December 3, 2007, and continue until a suitable candidate is identified. For questions contact **David W. Pascual (e-mail: dpascual@montana.edu, telephone: 406-994-4706).** *MSU is an Equal Opportunity/Affirmative Action Employer. Veterans' Preference.*

ASSISTANT PROFESSOR/ASSISTANT CURATOR (ICHTHYOLOGIST/TENURE TRACK)

Department of Biological Sciences/Museum of Natural Science, the Department of Biological Sciences, and the Museum of Natural Science at Louisiana State University (LSU) invite applications for an Assistant Professor/Assistant Curator (Ichthyologist/Tenure-track) position. Required Qualifications: Ph.D. or equivalent in biological sciences or a related field, curatorial experience in a research collection. Additional qualifications desired: research focus on the evolutionary biology of fish; postdoctoral experience; strong background in the development, management, and use of museum collections. Responsibilities: develops a strong, competitively funded research program; teaches one course per year; directs graduate students, curates LSU's ichthyology collection. Visit websites: **http://www.biology.lsu.edu** and **http://www.lsu.edu/museum** for additional information. *An offer of employment is contingent on a satisfactory pre-employment background check.* Application deadline is November 30, 2007, or until a candidate is selected. Send curriculum vitae (including e-mail address), statements of research and teaching interests, and the names and contact information for three references to:

Ichthyologist Search
c/o Mark Hafner
Department of Biological Sciences
202 Life Sciences Building
Louisiana State University
Ref: #002406
Baton Rouge, LA 70803

LSU is an Equal Opportunity/Equal Access Employer.

John Innes Centre

Tenure Track or Tenured Project Leader in Biomathematical Modelling/Biological Physics

The John Innes Centre (JIC) is one of the world's leading not-for-profit research institutes (http://www.jic.ac.uk) focusing on plant and microbial science. The institute presently has a thriving department of computational and systems biology, consisting of six groups in modelling and genome-based informatics. The department is an ideal location for biomathematical modelling, offering close links to JIC's world-leading plant/microbial experimentalists. As part of the department's ongoing expansion, we are now looking to make an additional appointment in the general area of biomathematical modelling/biological physics. The open position is a pure research appointment with no teaching and with very limited administrative duties. The successful candidate will be a creative, high-level researcher in an area of theoretical systems biology/biological physics relevant to JIC's overall programme and with demonstrated ability to provide scientific leadership. The post holder will be expected to build his/her own research group through external funding. Depending on the candidate, appointment is possible at either tenure track or tenured levels, at up to the equivalent of full professor level.

A strong start up package including salary for a permanent Research Assistant and an allocation for consumables, equipment and travel is offered, together with a continuing programme of professional development.

Starting salary will be in the range £36,500 to £41,800 per annum depending on qualifications and experience. A higher pay band may be offered to an exceptional candidate.

For more information and to apply, please visit our web site http://jobs.jic.ac.uk or contact Human Resources, The Operations Centre, Norwich BioScience Institutes, Norwich, NR4 7UH, UK, 01603 450462, quoting post reference 1001664. Further information can be obtained from Susie Death (susie.death@bbsrc.ac.uk). When applying, please include statements of current and future research plans (no more than 2 sides A4 for each) as part of your application.

The closing date for applications will be 9th November 2007.

The John Innes Centre is a registered charity (No223852) grant-aided by the Biotechnology and Biological Sciences Research Council and is an Equal Opportunities Employer.

Postdoctoral and Research Scientist Positions

Postdoctoral and Research Scientist Positions are available at Texas A&M University, College Station, for NIH funded projects to study intracellular lipid trafficking, nuclear regulation (PPARs) by dietary lipids and lipid binding proteins, and/or the role of lipid binding proteins in fatty acid and cholesterol trafficking through membrane domains rafts caveolae. The projects will employ recombinant proteins, overexpressing cell lines, and mutant mice overexpressing or ablated in fatty acid, fatty acyl CoA, or cholesterol binding proteins. The lab is equipped with state-of-the-art instrumentation for elucidating protein structure as well as ligand or protein interactions in vitro (CD, fluorescence, stopped-flow FRET) and in living or fixed cells (confocal, multiphoton, and lifetime imaging, FCS, FRET). The ideal candidates should be self driven and motivated researchers with experience in biochemistry, molecular biology, or other biological discipline.

Qualified candidates should send their curriculum vitae, including contact information for three references, to e-mail fschroeder@cvm.tamu.edu or to

Dr. Friedhelm (Fred) Schroeder
Department Physiology and Pharmacology
MI-4466
Texas A&M University
College Station, TX 77843-4466

VCU

Virginia Commonwealth University

TENURE-TRACK FACULTY POSITION

Chemical and Life Science Engineering

The Department of Chemical and Life Science Engineering (CLSE) in the School of Engineering at Virginia Commonwealth University (VCU) has a tenure-track faculty opening at the Associate level starting in the Fall of 2008. Chemical and Life Science Engineering at VCU represents the broad, formal interaction of the disciplines of chemical engineering with life and health sciences to create a forward-looking, nationally distinct program. Many of the Life Science areas at VCU enjoy national rankings, including those in the medical sciences, biological sciences and environmental life sciences. The new School of Engineering formed in 1996 has embarked on a "25 in 25" initiative to become a top 25 program in 25 years. Notable facilities include the new 120,000 sq ft School of Engineering building, the new Tissue Center for Life Sciences, the Rice Institute for Environmental Life Sciences located along the coastal plain region of the James River, and VCU's Medical School and Hospitals. Current research areas in CLSE include stem cell and stem-cell derived tissue engineering, cellular engineering and signal pathway analysis, biological systems engineering, bioinformatics and biocomputing, genetic and protein molecular engineering, small molecule and cellular based therapeutics, reaction engineering and molecular transport, advanced polymeric materials and processing methods. A new research Institute for Health and Life Science Engineering and a new Phase II Engineering building expansion will be open in 2007-2008 that will greatly expand and enhance research and education capabilities in the life science engineering areas. Candidates must have earned a Ph.D. and at least one degree in Chemical Engineering or Bioengineering or closely related discipline.

Outstanding candidates should submit a complete curriculum vitae, statement of research and teaching interests, and a list of four references to **Dr. Michael H. Peters, Chair, Chemical and Life Science Engineering, Virginia Commonwealth University, 601 West Main St., Room 403A, P.O. Box 843028, Richmond, VA 23284-3028.** Electronic submissions are acceptable by *.pdf files only please to: **jhschrei@vcu.edu**

Candidates must be eligible for employment in the United States by indicating their citizenship or visa status. Review of applications will continue until the position is filled.

VCU is an Equal Opportunity/Affirmative Action Employer
Women, minorities and persons with disabilities are strongly encouraged to apply

POSITIONS OPEN

TENURE-TRACK HARD TISSUE BIOLOGIST/ANATOMIST

The Purdue University, School of Veterinary Medicine's Department of Basic Medical Sciences seeks to fill a position for a full-time ten-month tenure track **ASSISTANT or ASSOCIATE PROFESSOR.** Preference will be given to a person who has a D.V.M., M.D., or equivalent professional degree, and a Ph.D. Postdoctoral experience is desired. Preference will be given to individuals with experience in using research animal models large enough to scale to humans and which have been used to study biological and pathobiological processes involving hard tissue biology. The individual should be capable of developing an extramurally funded research program and of collaborating with individuals in diverse disciplines including surgeons, radiologists, and biomedical engineers. The individual will be encouraged to employ the most up to date techniques in morphometry/histology relevant to the fields of prosthetic and orthobiology, tissue engineering, regenerative medicine and or medical device biocompatibility. The Department participates in campus-wide interdisciplinary programs such as the Clinical Discovery Laboratory which includes investigative surgery, the Purdue Histology and Phenotyping Laboratory, the National Cancer Institute recognized Purdue Cancer Center, Purdue University Nanoscience Program, Biomedical Engineering, and Purdue's Discovery Park. The individual will be expected to participate with others to teach veterinary gross anatomy to D.V.M. students. Further information is available at **website: http://www.vet.purdue.edu/bms/**. Applicants should submit a letter of intent, statement of professional goals, curriculum vitae, and the names and contact information of three references to: **Dr. Kevin Hannon, Department of Basic Medical Sciences, Purdue University, 625 Harrison Street, West Lafayette, IN 47907-2026.** Electronic submissions to e-mail: **hannonk@purdue.edu** in PDF or M.S. Word format are encouraged. Review of applications will begin 1 October 2007, and will continue until 1 January 2008, or until the position is filled. *The School is an Equal Opportunity/Equal [illegible] Affirmative Action Employer. Minorities and females are especially encouraged to apply.*

TENURE-TRACK FACULTY POSITION in CANCER
Faculty Excellence Initiative

The Department of Pathology, Microbiology, and Immunology at the School of Medicine at the University of South Carolina, in partnership with the recently established Center for Colon Cancer Research, is undergoing major expansion, and invites applications for a tenure-track **ASSISTANT/ASSOCIATE/PROFESSOR** position in cancer research. Preference will be given to candidates with expertise in colon cancer. Candidates must have a Ph.D. or M.D. or equivalent with postdoctoral research experience. Candidates for Associate/Professor positions should have current extramural funding. Competitive salary and startup funds are available. Candidates are expected to develop a strong, extramurally funded research program, to participate in the teaching mission of the Department, and to be jointly appointed to the Center for Colon Cancer Research. Information on the Department of Pathology, Microbiology and Immunology can be found at **website: https://pathmicro.med.sc.edu**, while that for the Center for Colon Cancer Research, is at **website: https://www.ccr.sc.edu**. Interested applicants should submit curriculum vitae, a statement of research plans, and three letters of recommendation to the **Chair, Search Committee, Department of Pathology, Microbiology and Immunology, University of South Carolina School of Medicine, Columbia, SC 29208, or e-mail: feicancer@gw.med.sc.edu.** *The search will start immediately and continue till the position is filled. The University of South Carolina is an Equal Opportunity/Affirmative Action Employer, encourages applications from women and minorities, and is responsive to the needs of dual-career couples.*

POSITIONS OPEN

University of Central Florida

FACULTY POSITIONS in
[redacted]

The Burnett School of Biomedical Sciences and the School of Electrical Engineering and Computer Science seek outstanding new faculty in the area of bioinformatics relevant to biomedical sciences for joint appointment. Successful candidates should have an active research program related to bioinformatics and experience in some aspect of this field such as computational genomics, regulatory genomics, nucleic acid sequence analysis algorithms, population genetics, computational proteomics, biological pathways, structural genomics, or biological data mining. Successful applicants are expected to establish a well-funded research program and contribute to graduate education. Faculty at any rank will be considered and exceptional candidates can be considered for a Provost's Research Excellence Professorship. Competitive salaries and startup funds as well as modern research facilities will be provided; collaborations between the various departments are actively encouraged.

The University of Central Florida is committed to building a bioinformatics research and graduate education program involving collaboration between the College of Medicine, the College of Science, and the College of Engineering and Computer Science.

The University of Central Florida has over 48,000 students and an outstanding technology based infrastructure. It is located in Orlando, a dynamic and progressive metropolitan region, and a major player in high tech industry, adjacent to a top-ranked research park and a great place to live and work.

Review of candidates will begin on November 30, 2007. Please send curriculum vitae, a two-page summary of research plans, and the names and contact information of three or more references to: **Chair, Bioinformatics Search (e-mail: biomed@mail.ucf.edu) 4000 Central Florida Boulevard, HPAH, 335, University of Central Florida, Orlando, FL 32816-2360.**

The University of Central Florida is an Equal Opportunity/Equal Access, and Affirmative Action Employer. As a member of the Florida State University System, all application materials and selection procedures are available for public review.

ASSISTANT/ASSOCIATE PROFESSOR
Molecular and Cellular Biology

The Department of Biological Sciences in Dedman College at Southern Methodist University invites applications for a tenure-track faculty position at the **ASSISTANT or ASSOCIATE PROFESSOR** levels. The position is in molecular and cellular biology (MCB). Individuals investigating aspects of neurobiology, development, stem cell biology, or host pathogen interactions are particularly encouraged to apply.

Candidates will be expected to develop strong extramurally funded research programs and teach in their area of expertise. Competitive startup funds and generous laboratory space in the new Dedman Life Sciences Building will be offered. For a more complete description of our program and facilities please see our **website: https://www.smu.edu/biology/.**

Candidates should forward curriculum vitae, a statement of research plans, and three letters of recommendation to: **Molecular and Cellular Biology Search, Department of Biological Sciences, Southern Methodist University, Dallas, TX 75275-0376.** Position begins fall semester 2008. To ensure full consideration for the position, the application must be postmarked by November 15, 2007, but the Committee will continue to accept applications until the position is filled. The Committee will notify applicants of its employment decision after the position is filled. *SMU will not discriminate on the basis of race, color, religion, national origin, sex, age, disability, or veteran status. SMU is committed to nondiscrimination on the basis of sexual orientation.*

POSITIONS OPEN

FACULTY POSITION in ATMOSPHERIC and SPACE SCIENCES
Department of Atmospheric, Oceanic, and Space Sciences
College of Engineering, University of Michigan

The Department of Atmospheric, Oceanic and Space Sciences (AOSS) at the University of Michigan is seeking applications for a tenured or tenure-track faculty position. The position is to be filled with a candidate focusing on scientific instrumentation, in particular space flight hardware development, in either space science (including planetary science) or earth system science and engineering (ESSE).

Research interests of our space science faculty include: solar heliospheric physics, magnetospheric physics (including planetary magnetospheres), magnetosphere-ionosphere coupling, aeronomy and planetary atmospheres (including atmospheres of small bodies and planetary satellites). AOSS faculty members are engaged in observational, theoretical, and computer simulation studies. Over the last six decades faculty and staff of AOSS and its Space Physics Research Laboratory have designed, built, flown, and analyzed more than 100 rocket experiments and nearly 40 space instruments. AOSS/SPRL instruments are on the way to, or have visited, all planets of the solar system except Pluto.

We seek candidates who will provide inspiration and leadership in research and contribute actively to teaching, and are especially interested in candidates who can contribute, through their research, teaching, and/or service, to the diversity and excellence of the academic community. The University of Michigan is responsive to the needs of dual-career couples.

To apply, please send an electronic copy of your curriculum vitae, statement of research accomplishments and goals, and the names and contact information of five references to **Ms. Susan Griffin (e-mail: sgriffin@umich.edu).** For further information about AOSS, please go to **website: http://aoss.engin.umich.edu/**. Informal inquiries may be directed to **Prof. Michael W. Liemohn, Chair, Faculty Search Committee, Atmospheric, Oceanic, and Space Sciences, e-mail: liemohn@umich.edu.**

Reviews of applications will begin November 1, 2007 and will continue until the position is filled.

A nondiscriminatory, Affirmative Action Employer.

TENURE TRACK FACULTY POSITION
DEPARTMENT of NEUROSCIENCE
School of Arts and Sciences
University of Pittsburgh

Applications are invited for a tenure track position at the level of **ASSISTANT PROFESSOR** starting September 2008, pending budgetary approval. Individuals whose research is in the area of molecular and cellular neuroscience are especially encouraged to apply. Collegial interactions and collaborative research are widespread within the Department of Neuroscience (**website: http://www.neuroscience.pitt.edu/**), and across the extensive neuroscience community found in Pittsburgh. Our integrative research environment is exemplified by the Center for Neuroscience at the University of Pittsburgh (CNUP, **website http://cnup.neurobio.pitt.edu/**) and the Center for the Neural Basis of Cognition (CNBC, **website http://www.cnbc.cmu.edu/**), which bridges the University of Pittsburgh and Carnegie Mellon University. The successful candidate will be expected to establish an independent research program and participate in teaching of neuroscience to undergraduate and graduate students.

Applicants should send electronic copies of curriculum vitae, a brief statement of research accomplishments and goals, and the names and contact information of the three references via e-mail: **neurosci@pitt.edu**. For full consideration, application materials must be received by December 1, 2007. Review of applications will continue until the position is filled. *The University of Pittsburgh is an affirmative action/equal opportunity employer. Women and members of minority groups underrepresented in academia are especially encouraged to apply.*

CBR

CENTER FOR BIOSYSTEMS RESEARCH

Tenure-Track Faculty Position Pathobiology

The **Center for Biosystems Research** (CBR) invites applications for a tenure-track faculty position at the **Assistant Professor** level in pathobiology of multicellular animal systems. The center's interests in pathobiology include causes, symptoms, or progression of disease, as well as response and repair mechanisms. The position will be available by Fall 2008. Applicants should have strong research programs that address fundamental problems related to biotechnology. Attractive areas of research include but are not limited to the study of regeneration, wound healing, stem cells, neural degeneration, aging, cellular trafficking, model systems for human diseases, and host-pathogen interactions.

CBR is one of four research centers of the University of Maryland Biotechnology Institute (**http://www.umbi.umd.edu/~cbr/**) and is located on the campus of the University of Maryland, College Park, which is inside the Washington, D.C. beltway and in close proximity to the NIH, FDA, USDA and the I-270 technology corridor.

The investigator is expected to establish an extramurally funded, independent research program within the setting of an interdisciplinary research institute on a large university campus. For full consideration submit current curriculum vitae, summary of research activities and future plans (all in pdf format) and arrange for three letters of recommendation to be sent to: **Pathobiology Faculty Search Committee – Position # 300037 cbrsrch@umbi.umd.edu**

Review of applications will begin **November 16, 2007** and continue until the position is filled.

UMBI is committed to Affirmative Action and Equal Opportunity Employment. As required by the 1986 Immigration Act, applicants should be prepared to present acceptable documentation showing their identities, their U.S. citizenship or alien status, and their authorization to work in the United States.

OFFICE OF AIDS RESEARCH

Department of Health and Human Services National Institutes of Health Office of AIDS Research Health Scientist Administrator, GS-15

The Office of AIDS Research (OAR), a component of the Office of the Director of the National Institutes of Health (NIH), is expanding and restructuring its coordination of scientific programs in microbicide research and development. The OAR is seeking applications from exceptional scientists to join a dedicated and dynamic staff to help guide NIH efforts in this critical area of HIV prevention research. OAR has the responsibility for a broad range of scientific, planning, budgetary, legislative, and public policy matters relevant to the conduct and future development of AIDS research at the NIH, including its programs, policies, and operations.

The individual will serve as the principal advisor to the OAR Director on microbicide research and will also serve as the Chair of the Trans-NIH Microbicide Research Coordinating Committee. This new position will be responsible for the direction and management of OAR's Microbicide research planning, budget, evaluation, and policy activities through the establishment and maintenance of working relationships with other government and non-government organizations.

Applicants must be a U.S. citizens, and have an advanced degree (M.D., Ph.D. or equivalent) in an academic field of the health or pertinent sciences (i.e. biochemistry, molecular biology, physiology, etc.) allied to health or health-related research. This position is located in Bethesda, Maryland. The salary range is $110,363 - $143,471 and a full package of benefits is included.

A detailed vacancy announcement with the mandatory qualifications and application procedures can be obtained on USAJOBS at **www.usajobs.gov** (announcement number **OD-07-205530**) and the NIH Web Site at **http://www.jobs.nih.gov**. Questions on the applications procedures may be addressed to **Nneka Ukpabi, 301-594-5331**. Applications must be received by midnight eastern time on **November 1, 2007**.

The NIH is an Equal Opportunity Employer.

Skirball Institute of Biomolecular Medicine

NEW YORK UNIVERSITY SCHOOL OF MEDICINE

Faculty Positions

The Skirball Institute and the Kimmel Center of Biology and Medicine at New York University School of Medicine invite applicants for tenure-track positions at the assistant, associate or full professor level. We seek applicants with an exceptional record of achievement to join our existing programs in Molecular Neurobiology, Developmental Genetics, Structural Biology and Molecular Pathogenesis. These programs are interdisciplinary and reflect strengths at NYU's School of Medicine and College of Arts and Sciences. Special priority will be given to applicants with broad interests working at the cutting edge of mammalian genetics, stem cell research, neurobiology or molecular cell biology.

NYU School of Medicine offers excellent resources to support new faculty, including generous start-up packages and core facilities for cell sorting, imaging, proteomics, mouse molecular genetics, genomics and structural biology.

Successful candidates are expected to initiate and maintain vigorous independent research programs that will enrich and be enriched by the highly collaborative environment at the Skirball Institute and throughout the NYU research community.

This is an electronic application process. No mail applications will be accepted. Create your application packet by formatting it as a single PDF document. Use the following page order: (1) Cover Letter - **indicating Program preference**, (2) Curriculum Vitae, (3) Research Statement.

Email application packet to **skirballsearch@saturn.med.nyu.edu**.

Three letters of reference should be sent independently to: **skirballsearch@saturn.med.nyu.edu**

New York University School of Medicine was founded in 1841 and is an equal opportunity affirmative action employer. Women and minority candidates are encouraged to apply.

http://saturn.med.nyu.edu

POSITIONS OPEN

ASSISTANT PROFESSOR TENURE-TRACK POSITION in BIOPHYSICS
Integrative Molecular Life Sciences and Biophysics Program
Department of Physics and Astronomy
University of Denver

The Departments of Biological Sciences, Chemistry and Biochemistry, and Physics and Astronomy, are forming the Integrated Molecular Life Sciences and Biophysics (IMLSB) Program which will include a multidepartmental graduate program with emphases in neuroscience, biochemistry, biophysics, and bioinformatics. At the current time five tenure-track positions are allocated for this initiative with two of those positions already filled in spring 2007.

As part of this initiative, the Department of Physics and Astronomy at the University of Denver invites applications for a tenure-track Assistant Professorship beginning September 1, 2008, in areas of computational or experimental biophysics. A special emphasis will be given to candidates with research interests in cell signaling, transport phenomena associated with proteins and membranes, protein conformational dynamics and folding, neural physics and biological complexity, network system dynamics.

The successful candidate will have a B.S. in physics and Ph.D. in biophysics or related discipline, will develop an extramurally funded research program, will supervise undergraduate and graduate research, and will teach undergraduate and graduate courses. Applicants will primarily be expected to support our medical physics minor and other interdisciplinary programs. The Department offers degrees through the Ph.D. Individuals with postdoctoral experience are particularly encouraged to apply.

Applicants must apply through **website: https://www.dujobs.org.** The application should include a cover letter, curriculum vitae, and statements of teaching philosophy and research interests. Under separate covers please send two recent publications and arrange for three letters of recommendation to be sent to **Integrative Molecular Life Sciences and Biophysics Faculty Search, University of Denver, Department of Physics and Astronomy, Denver, CO 80208.** The selection process will begin on November 16, 2007 and will continue until the position is filled. *The University of Denver is committed to enhancing the diversity of its faculty and staff and encourages applications from women, minorities, people with disabilities, and veterans. DU is an Equal Employment Opportunity/ Affirmative Action Employer.*

THREE ASSOCIATE/FULL PROFESSORS
Cancer Biology
Indiana University, Bloomington

As part of an overall expansion in life sciences (**website: http://lifesciences.iu.edu**), Indiana University Bloomington is pleased to announce the development of a Cancer Biology Research Program in partnership with the Indiana University (IU) School of Medicine. We seek to fill three tenured positions at the Associate or Full Professor level. Successful applicants must have a Ph.D., M.D. or M.D./Ph.D. and demonstrate a strong record of research endeavors that will strengthen existing ties with the National Cancer Institute designated Cancer Research Center of the IU School of Medicine. Successful applicants will have a well-established, federally funded research program in basic or translational research. Candidates will be associated with biochemistry, biology, or chemistry within the College of Arts and Sciences and/or with Medical Sciences within the IU School of Medicine. Full review of applications will commence October 15, 2007, and continue until the three positions are filled. Inquiries can be sent to **Search Committee** at e-mail: **cancerbi@indiana.edu.** Applicants should send curriculum vitae and research and teaching statements as a single PDF file to e-mail: **cancerbi@indiana.edu.** Additional materials may be mailed to: **Cancer Biology Search Committee, Myers Hall, Indiana University, Bloomington, IN 47405.**

Indiana University is an Equal Opportunity/ Affirmative Action Employer. Women and minorities are encouraged to apply.

POSITIONS OPEN

UNIVERSITY OF CALIFORNIA
UCRIVERSIDE

FACULTY POSITIONS
Department of Bioengineering
Bourns College of Engineering

The Department of Bioengineering invites applications for tenure track and senior level positions in molecular and cellular bioengineering, tissue engineering, systems biology, human physiology, drug design and delivery, bioimaging, and biocomputation. Successful applicants should have a doctoral degree and are expected to complement the highly motivated spirit of the bioengineering faculty by establishing a leading, interdisciplinary innovative research effort while providing significant contributions to teaching, and professional service. Joint appointments with the Material Science and Engineering (MSE) Program and other departments are possible and encouraged. The MSE Program is innovative and interdisciplinary, comprised of 20 internationally recognized participating faculty members who currently emphasize nanotechnology, energy, and biomaterials, see **website: http:www.engr.ucr.edu/mse.** Salary levels will be competitive and commensurate with qualifications and experience. For more information please visit **website: http ://www.bioeng.ucr.edu.** Application review will start on December 15, 2007, and will continue until the positions are filled. To apply please register and submit the requested PDF files at **website: http://www.engr.ucr.edu/facultysearch.** For inquiries please e-mail as at e-mail: **facultysearch@engr.ucr.edu.**

The University of California, Riverside is an Equal Opportunity/ Affirmative Action Employer.

GEORGE GAYLORD SIMPSON POSTDOCTORAL FELLOWSHIPS in VERTEBRATE SYSTEMATICS and EVOLUTION
University of Arizona

The Department of Ecology and Evolutionary Biology (EEB) announces three Postdoctoral Fellowship positions for fall 2008, named in honor of **G.G. Simpson's** long tenure at the University of Arizona. Simpson Fellows are expected to conduct an active research program that is facilitated and complemented by the Department's extensive natural history collections in ichthyology, herpetology, ornithology, and mammalogy. The EEB collections have a strong taxonomic focus on the fauna of the southwest United States, northwest Mexico, the Gulf of California and the Eastern Pacific. The positions are part of a renewed commitment to natural history collections on the University of Arizona campus and a new initiative in biodiversity informatics, and Postdoctoral Fellows are encouraged to establish research collaborations with faculty in the Department of Ecology and Evolutionary Biology. Responsibilities of the positions include teaching one course per year in the Fellow's taxonomic specialty. Salary is $37,500 (depending on experience) plus benefits. A research stipend of $5,000 will also be included. The positions are renewable for at least two years based on satisfactory performance.

Applicants should submit application materials online at the University of Arizona Human Resources **website: https://www.uacareertrack.com**, look for job **#30500**, and upload a curriculum vitae, statement of research and teaching interests and experience, and two letters of reference. Position is open until filled, but we anticipate reviewing applications beginning on November 15, 2007.

Contact **Dr. Peter Reinthal (e-mail: por@e-mail.arizona.edu), Dr. Alex Badyaev (e-mail: abadyaev@e-mail.arizona.edu),** or **Dr. Michael Sanderson (e-mail: sanderm@e-mail.arizona.edu)** for further information.

POSITIONS OPEN

ASSOCIATE/FULL PROFESSOR (SHELL ENDOWED CHAIR in OCEANOGRAPHY/WETLANDS STUDIES/TENURE TRACK)
School of the Coast and Environment

Louisiana State University's School of the Coast and Environment is seeking external candidates for the Associate/Full Professor (Shell Endowed Chair in Oceanography/Wetlands Studies/tenure track) position. Required qualifications: Ph.D. in oceanography, wetland science, ecosystem studies, or related fields; strong research background, established record in coastal systems science with an emphasis on interactions between natural and human influences. Additional qualifications desired: strong publication record and federal funding, recent experience mentoring doctoral students. Responsibilities: develops and maintains a rigorous, externally funded research program with relevance to wetland restoration and the sustainable management of coastal ecosystems; collaborates in multidisciplinary projects with coastal/wetland scientists; mentors graduate students; provides advice to state and federal agencies and service to the University. The School of the Coast and Environment has strong biological, physical, chemical, geological, ecological, and wetland biogeochemistry programs in continental shelf, estuarine, wetland environments, and a strong environmental studies academic program. For more information, contact **Robert P. Gambrell, Chair, Department of Oceanography and Coastal Sciences (telephone: 225-578-6426).** Additional information about the University and School can be found at **website: http://www.sce.lsu.edu.** An offer of employment is contingent on a satisfactory pre-employment background check. Application deadline is December 10, 2007, or until a candidate is selected. Complete applications will include curriculum vitae (including e-mail address) and contact information for five letters of reference, and should be sent to:

Chair
Department of Oceanography and Coastal Sciences
Louisiana State University
Reference: Log #1052
Baton Rouge, LA 70803

LSU is an Equal Opportunity/ Equal Access Employer.

FACULTY POSITION, ENERGY SCIENCE and TECHNOLOGY, MIT. The Department of Mechanical Engineering is seeking outstanding candidates for a tenure track **ASSISTANT PROFESSOR** position in the field of energy, energy technology and energy systems. The Department is looking for individuals who will contribute to the engineering and engineering science of modern energy conversion systems and processes. Topics of interest include, but are not limited to, carbon capture in power generation, alternative engines, alternative fuel utilization, hybrid power trains, large-scale energy storage, and integrated power systems. Energy related engineering science topics include, but are not limited to, multiphysics simulation of transport-chemistry interactions, fundamentals of complex multiphase and reactive flows, interfacial processes, energy conversion under extreme conditions and large scale energy storage. Candidates must have an earned Ph.D. in their field at the time of appointment. The successful candidate is expected to teach at the undergraduate and graduate levels in mechanical engineering courses including energy conversion subjects. The candidate will also be expected to develop an outstanding research program.

Applicants should send curriculum vitae, a research statement, a teaching statement, and copies of not more than three publications. They should also arrange for four individuals to submit letters of recommendation on their behalf. This information must be entered electronically at the following **website: http://search-meche.mit.edu.**

Applications received before December 15, 2007 will be given full consideration.

MIT is an Equal Opportunity/ Affirmative Action Employer. Women and underrepresented minorities are especially encouraged to apply.

Gladstone/UCSF Faculty Positions

The **Gladstone Institute of Cardiovascular Disease (GICD)** is a renowned center of excellence focused on applying basic science to the problem of heart disease. The Institute is closely affiliated with the **University of California San Francisco (UCSF)** and located in the rapidly expanding Mission Bay area of UCSF. The GICD shares a new building with the Gladstone Institute of Neurological Disease and the Gladstone Institute of Immunology and Virology, together providing a rich and diverse basic science community.

GICD, in conjunction with relevant programs at UCSF, seeks to expand in two distinct areas in order to capitalize on the emerging opportunities in cardiovascular science. We invite applications from scientists with Ph.D. and/or M.D. degrees who are potential or established leaders in the following areas:

Cardiac Stem Cell and Development Biology

Applicant should have an interest in developing and leveraging knowledge of cardiac differentiation using a diverse array of technologies including use of stem cell biology. The applicant may have a background in cardiogenesis or in stem cell biology. Interests in general areas of cardiac cell biology or metabolism will also be considered. The successful applicant will also be a member of the new Program in Developmental and Stem Cell Biology and the Cardiovascular Research Institute at UCSF.

Cardiovascular Genetics

Applicant should have the skills to apply modern tools of human genetics toward an understanding of cardiovascular disease. Scientists studying genetics of complex traits including, but not limited to, atherosclerosis, hypertension, heart failure, metabolic disorders or congenital diseases will be considered. An established genomics core is present at Gladstone and extensive core facilities for genomics and human genetics exist at UCSF. The successful applicant will be a part of the UCSF Center for Human Genetics and the Cardiovascular Research Institute.

Candidates may be at the Assistant, Associate or Full Professor level. Interested candidates should send a curriculum vitae and a brief description of research interests to the following address:

Deepak Srivastava, M.D.
Professor and Director
Gladstone Institute of
Cardiovascular Disease
University of California San Francisco
1650 Owens Street
San Francisco, CA 94158
dsrivastava@gladstone.ucsf.edu

The J. David Gladstone Institutes and UCSF are Affirmative Action/Equal Opportunity Employers. Gladstone and the University undertake affirmative action to assure equal employment opportunity for underutilized minorities and women, for persons with disabilities, and for Vietnam-era veterans and special disabled veterans. We seek candidates whose experience, teaching, research, or community service has prepared them to contribute to our commitment to diversity and excellence.

Max-Planck-Institut für Molekulare Pflanzenphysiologie

The Max-Planck-Institute of Molecular Plant Physiology at the Science Center Golm in Potsdam has a opening for a position as a

Group Leader

in the Department of Organelle Biology, Biotechnology, and Molecular Ecophysiology.

The Department strives to investigate fundamental questions in plant molecular biology and promotes integrated research approaches bridging genetics, molecular physiology, biochemistry, and evolutionary biology using higher plant and algal model systems. Applications are invited from individuals with a strong interest in establishing an innovative and multidisciplinary research program in molecular plant science, preferentially with a focus on organelle biology, organelle-nuclear interactions or molecular ecophysiology. The successful applicant will be provided with funds equivalent to a technician position, a post-doctoral grant, and a budget for consumables, equipment, and travel.

Applicants should have a proven track record in plant physiology, molecular genetics, and/or biochemistry, ideally with at least two years of postdoctoral experience. The salary will be according to the German public service scale (TVöD) including fringe benefits.

The Max Planck Institute provides an excellent infrastructure for modern cross-disciplinary training. With three Max Planck Institutes, two Fraunhofer Institutes, and a new center for start-up companies, the Science Center Golm is the largest research Center in the state of Brandenburg. It is located in close proximity to the University of Potsdam and also offers fast access to the many research and educational facilities in Berlin. Further information about the institute can be found at www.mpimp-golm.mpg.de.

Applications including a curriculum vitae, a full list of publications, names of three referees, and a three-page summary of current and future research interests should be submitted as an e-mail attachment to pflo@mpimp-golm.mpg.de or sent by mail to reach the institute by 30 November 2007 and should be addressed to:

Max Planck Institut für Molekulare Pflanzenphysiologie
Personalverwaltung, Wissenschaftspark Golm
Am Mühlenberg 1, 14476 Potsdam

MAX PLANCK GESELLSCHAFT

CHAIR, DEPARTMENT OF BIOCHEMISTRY AND MOLECULAR GENETICS UNIVERSITY OF COLORADO SCHOOL OF MEDICINE

The University of Colorado School of Medicine seeks applicants for Chair of the Department of Biochemistry and Molecular Genetics. The Department consists of 17 primary faculty as well as more than 20 secondary faculty members. The Department currently occupies over 35 000 square feet of state-of-the-art research and office space, primarily on the 9th and 10th floors of the newly occupied Research Complex at the new UCHSC Fitzsimons campus. Details are available at the departmental web site: **http://www.uchsc.edu/sm/bbgn/**

Research programs include chromatin structure, gene transcription and translation, RNA structure and enzymatic activity, protein structure, protein degradation, signal transduction, cell cycle regulation, bioinformatics and cell fate determination. Department faculty, currently with over eight million dollars in federal funding, houses the Molecular Biology, Biomolecular Structure, Biomedical Sciences and Biochemistry graduate programs. In addition, department faculty draw graduate students from several other programs including: MSTP, Bioinformatics, and Neuroscience.

The Chair of the Department of Biochemistry and Molecular Genetics reports to the Dean of the School of Medicine and participates with his staff and other departmental chairs in program development, administration, and budgetary planning and implementation. The position requires excellence in teaching, demonstrated administrative leadership and ability, and, in particular, leadership in research and scholarly activity.

The University of Colorado is committed to the recruitment and employment of a diverse faculty. We encourage applications from women and minorities. Review of applications will continue until the position is filled. Applicants should respond by sending a letter of interest and curriculum vitae to:

John C. Cambier, Ph.D.
Ida and Cecil Green Professor and Chairman of the Department of Immunology,
Chair, Department of Biochemistry and Molecular Genetics Search Committee
University of Colorado School of Medicine and
National Jewish Medical and Research Center
Room K803
1400 Jackson Street, Denver CO 80206
FAX: (303) 270-2325
Email: Duranskik@NJC.org

The University of Colorado is committed to diversity and equality in education and employment.

POSITIONS OPEN

FACULTY POSITIONS in TERRESTRIAL BIOGEOCHEMISTRY and CLIMATE CHANGE

The Appalachian Laboratory (AL) of the University of Maryland Center for Environmental Science (UMCES) seeks two individuals for full time faculty positions at either the **ASSISTANT or ASSOCIATE PROFESSOR** level to enhance our strengths in terrestrial and aquatic ecology, landscape and watershed ecology, and remote sensing. Excellent research and computing facilities are available at AL, including plant, soil, and water analysis laboratories with state-of-the-art analytical instrumentation, growth chambers, and a greenhouse. The main responsibility of these positions is research, but UMCES faculty also participate in graduate education, outreach, and application of basic science to regional (e.g., restoration of Chesapeake Bay) and global (e.g., land use and climate change) environmental problems. We will interview candidates who are interested in collaborative research, are published in top scientific journals, and can acquire external funding to support their research.

We are particularly interested in (1) effects of climate change on terrestrial and/or aquatic ecosystems. We seek an **ECOLOGIST** who applies climate change data and forecasts to address the problem of ecosystem change, including issues such as invasive species, mitigation of ecosystem impacts, ecosystem restoration, adaptation of land and aquatic resource management, and ecosystem/climate feedback processes. (2) terrestrial biogeochemistry in multi-use landscapes. We seek an outstanding researcher who may address topics such as carbon sequestration by soils, forest nutrient transformations, and effects of land use change and ecosystem disturbances on elemental cycles.

Applicants should send curriculum vitae, statement of research interests, brief discussion of how the applicant's research would complement ongoing research at AL/UMCES; selected reprints; and list of four references (name, title, mailing address, telephone, fax, and e-mail address) to either the **Climate Change** or **Terrestrial Biogeochemistry Search Committee, Appalachian Laboratory, UMCES, 301 Braddock Road, Frostburg, MD 21532.** Review of applications will begin on December 1, 2007. Information about AL and UMCES can be found at **websites: http://www.al.umces.edu/** and **http://www.umces.edu/**. *UMCES is an Affirmative Action/Equal Opportunity Employer. Women and minorities are strongly encouraged to apply.*

ASSISTANT PROFESSOR
Center for Neurobehavioral Genetics
Department of Psychiatry and Biobehavioral Sciences
Semel Institute for Neuroscience and Human Behavior
The David Geffen School of Medicine at UCLA

The Center for Neurobehavioral Genetics is seeking applications for an Assistant Professor, tenure track, in any area of neurogenetics or behavioral genetics including human genetics and model genetic organisms.

Both **PHYSICIAN SCIENTISTS** and **BASIC SCIENTISTS** are encouraged to apply.

More advanced candidates may be considered under special circumstances. The new faculty member will be expected to develop a strong and creative research program and to participate in training activities within the highly collaborative Center for Neurobehavioral Genetics.

Candidate selection will begin December 15, 2007, and continue until the position is filled. Applicants should send curriculum vitae, a summary of research interests, and arrange for three letters of reference to be sent to:

Kelsey C. Martin
Chair, Search Committee
c/o Margaret Chu
Center for Neurobehavioral Genetics
Gonda 3506
695 Charles Young Drive S.
Los Angeles, CA 90095-1761

POSITIONS OPEN

ROOSEVELT UNIVERSITY

Roosevelt University, a national leader in educating socially conscious citizens, is a private, student-centered University with more than 7,000 students. Founded on the principles of inclusion and social justice, Roosevelt offers academic programs in arts and sciences, business, performing arts and education.

Roosevelt University is seeking an **ASSISTANT PROFESSOR of BIOLOGY** for a newly created tenure-track position to begin August 2008. The specialty is open, but organismic, population, or community-level biology, physiology, or immunology would complement existing strengths.

We offer degrees in biology, chemistry, biotechnology and Pre-Professional Programs: Pre-Medicine, Pre-Dentistry, Pre-Pharmacy and Pre-Veterinary Medicine.

Applicants must have a Ph.D. and a commitment to teaching and undergraduate research.

To apply, visit our **website: http://www.roosevelt.edu/hr/careers/default.htm** and submit your curriculum vitae and three professional references before December 1, 2007.

Roosevelt University welcomes female, lesbian, gay, bisexual, transsexual, disabled, international, and minority-identified individuals to applicants for all positions.

ASSISTANT PROFESSORS
Microbiology and Molecular Genetics
Section of Microbiology
University of California, Davis

The Section of Microbiology, College of Biological Sciences, University of California, Davis, invites applications for two tenure track positions at the level of Assistant Professor. This is a broadly based search for candidates working on bacterial, archaeal, or eukaryotic systems (microbial and nonmicrobial). Candidates must have an outstanding record of achievement in research and will be expected to develop a strong, externally funded research program in microbiology and/or molecular genetics. Successful candidates will be expected to participate in normal undergraduate and graduate teaching responsibilities. Department faculty members use microbial and nonmicrobial systems to study diverse research subjects ranging from environmental microbiology and bacterial gene regulation to single molecule studies of protein-DNA interaction and transcriptional control in mammalian cells. See **website: http://microbiology.ucdavis.edu/ugfaculty.htm** for descriptions of faculty research. Due to limits on laboratory space availability, one of the two positions must commence on or after January 1, 2009.

Applicants should submit (1) curriculum vitae, (2) a statement of current and proposed research, (3) copies of no more than two key publications, (4) a statement of teaching interests, and (5) arrange to have at least three letters of recommendation submitted.

Applications will only be accepted online at **website: http://microbiology.ucdavis.edu/**. Please see the website for details.

While applications will be reviewed until the positions are filled, only applications completed by November 16, 2007, can be assured of full consideration.

The University of California is an Equal Opportunity/Affirmative Action Employer with a strong institutional commitment to the development of a climate that supports equality of opportunity and a respect for differences.

POSTDOCTORAL POSITIONS available at the Dana Farber Cancer Institute, Boston, to study DNA repair. Positions will focus on chromatin remodeling and microRNAs in the repair of DNA breaks. Published expertise with chromatin structure, histone modification, chromatin immunoprecipitation assays, micro RNAs or protein purification is required. Applications to **Dr. D. Chowdhury** or **Dr. B.D. Price, Department of Radiation Oncology,** by e-mail: **dipanjan_chowdhury@dfci.harvard.edu** or e-mail: **brendan_price@dfci.harvard.edu.** *Equal opportunity Employer.*

POSITIONS OPEN

DIRECTOR
Institute of Arctic and Alpine Research
University of Colorado, Boulder

The University of Colorado, Boulder, seeks applications for Director of the Institute of Arctic and Alpine Research (INSTAAR). The successful candidate will also be a tenured **PROFESSOR** in an appropriate academic department. INSTAAR research spans geochronology, human and ecosystem ecology, hydrology, glaciology, oceanography, landscape evolution, biogeochemistry, and climate in a range of Quaternary and modern environments. The Institute is connected to seven departments, administers the Mountain Research Station, and maintains ties with federal labs including the U.S. Geological Survey, National Oceanic and Atmospheric Administration, and National Center for Atmospheric Research. The Director has primary responsibility for INSTAAR's management, and reports to the Vice Chancellor for Research and Dean of the Graduate School. Applicants should have an outstanding record of scientific achievement and leadership, and be able to balance INSTAAR's management with a vigorous research program and a commitment to graduate education. All correspondence including applications should be sent to **e-mail: aardir@colorado.edu.** Applications should include a letter of interest, current curriculum vitae, and the names of four references. Review of applications will begin on October 22, 2007, and continue until the position is filled. See **website: http://instaar.colorado.edu/director** for more information on the position and INSTAAR.

FACULTY POSITION in MATERIALS CHEMISTRY
University of California, Irvine

The Department of Chemistry of the University of California, Irvine, is establishing a new Area of Excellence in Materials Chemistry with the addition of multiple faculty positions over the next three years. We thus invite applications for a tenure track position at the **ASSISTANT PROFESSOR** level in materials chemistry. We are seeking a Ph.D.-level scientist who will establish a vigorous research program whose central aim is in the design and synthesis of materials and the characterization of their properties. The candidates should also be committed to teach chemistry at the undergraduate and graduate levels. Applicants should send their curriculum vitae, a list of publications, and a description of their proposed research program, to the **Materials Search Committee, Department of Chemistry, University of California, Irvine, CA 92697-2025.** Application may also be submitted electronically via the web at **website: https://recruit.ap.uci.edu/.** Web applications should include a cover letter and the information requested above. Applicants should also arrange to have three letters of recommendation submitted on their behalf. To insure full consideration, applications and supporting materials should be received by November 15, 2007. *The University of California is an Equal Opportunity/Affirmative Action Employer committed to excellence through diversity, and it CE has an ADVANCE program dedicated to gender and ethnic equity.*

Burnham Institute for Medical Research, in La Jolla, California, has a **POSTDOCTORAL ASSOCIATE POSITION** available in the Laboratory of **Dr. Jeff Smith.** The successful candidate will be trained in the basic mechanisms connecting central carbon metabolism in tumor genesis. Previous experience in metabolic modeling, computation and experimental flux analysis, metabolic labeling, and metabolite analysis by mass spectrometry and/or nuclear magnetic resonance is required. Interested, qualified applicants should e-mail their curriculum vitae including a brief description of research experience in three to four sentences, and names and contact information of three references to **e-mail: jamesleet@burnham.org.**

UNC CHARLOTTE

TENURE-TRACK FACULTY POSITION
BIOINFORMATICS RESEARCH CENTER

The University of North Carolina at Charlotte invites applications for a tenure-track faculty position (all levels) in environmental microbial genomics and metagenomics in the Bioinformatics Research Center. The Center is engaged in a multi-year expansion program encompassing two major sites, with a state-of-the-art campus building and a leading role at the NCRC -Kannapolis (http://www.ncresearchcampus).

Preference will be given to applicants with interests in the study of complex microbial communities, using either novel computational methods or an integrated approach with experimental and computational techniques. Research areas of interest include the study of symbiotic microbial communities with direct impacts on human health (e.g. mammalian gut), the ecology of microbial communities, and the development of new microbial technologies such as biofuels. Applicants with method development interests in any area of microbial genomics, however, are encouraged to apply. Our Center offers ample opportunities for collaborations with and access to wet-labs within the department, University or nearby clinical and biotechnology centers. The successful applicant will be expected to develop a program of original research supported by external funding, and to develop and teach graduate core courses in Statistical Methods, Population Genetics or Numerical Methods. Successful candidates must hold a Ph.D. in Biology, Bioinformatics, Genetics, Statistics, or a related field.

Applications must be submitted online (https://jobs.uncc.edu, position #1913) and should include vitae, at least three references, and a letter of interest. We are unable to consider applications submitted only by mail or e-mail. For full consideration, your application should be received by **November 30, 2007** although the position will remain open until filled. Informal inquiries can be made to the Search Committee Chair, **Dr. Cynthia Gibas** (cgibas@uncc.edu). For additional information, please visit our website at **www.bioinformatics.uncc.edu**

The University of North Carolina at Charlotte is an EO/AA Employer and an ADVANCE Institution

Discover the many small-company environments
behind the big-company impact
of the Johnson & Johnson companies.

find more
jnj.com/careers

Director
Vacancy #46701
Institute for Interdisciplinary Coastal Science and Policy

East Carolina University seeks an individual to oversee the development and management of the new Institute for Interdisciplinary Coastal Science and Policy (ICSP). The new institute combines the Institute for Coastal Marine Resources (ICMR), the PhD Program in Coastal Resources Management (CRM) and the Office of Diving and Water Safety with an annual permanent budget exceeding $1.6 million, including 13 faculty (7.5 FTE, 3 expansion positions currently vacant), 9 office and support staff, a fleet of 10+ research vessels, $311,000/yr in graduate assistantship funds, and operating funds of about $150,000/yr. The new institute will serve as a multidisciplinary focal point, drawing broad support from over 70 faculty members in 8 core departments from 3 colleges and large interactions with other institutes and universities, including the UNC Coastal Studies Institute (http://csi.northcarolina.edu/).

The goal of the new institute is to enhance understanding of the complex interactions between human behavior and coastal/marine environmental resources and to draw on this understanding to develop sound public policy. The institute will focus its research at the interface between 4 areas: coastal & estuarine ecology, coastal geosciences, social science & coastal policy, and maritime studies. The new director will guide a planned expansion that will add at least 3 new faculty positions to further the institute's goal of fostering an interdisciplinary environment focused on coastal issues. Salary will be commensurate with qualifications.

Minimum Qualifications: Candidates must have the credentials, experience, and achievements appropriate for the appointment at the Full or Associate Professor level, including a PhD in an area closely related to the scope of the institute, experience in the development and administration of multidisciplinary programs, and an established record of externally supported research and publications.

Screening will begin October 21, 2007, and continue until the position is filled. Please submit a candidate profile, letter of interest, current curriculum vita, and the names and contact information of three references to:

East Carolina University
Department of Human Resources at
www.jobs.ecu.edu.

Equal Opportunity / Affirmative Action Employer

View complete job description/requirements at
https://ecu.peopleadmin.com/applicants/Central?quickFind=54629

RUSH UNIVERSITY MEDICAL CENTER

The Department of Dermatology at Rush University Medical Center is seeking two nationally recognized senior research scientists with interest in skin cancer. Applicants should be accomplished investigators (Ph.D., M.D. or M.D./Ph.D.) with current federal grants and a proven track record in basic and/or translational research. The successful candidates will join an expanding faculty within a large academic healthcare system. The researcher will play a critical role in directing and expanding research activities in the Department of Dermatology and have an opportunity to collaborate with other national, and internationally recognized investigators in cell biology, genomics, and proteomics at Rush.

Rush University Medical Center serves a large clinical base throughout Chicago land. There are outstanding clinical practice and laboratory facilities on campus that perform state of the art molecular and cellular biology techniques, flow cytometry, proteomics and genomics as well as biostatistical support services. Animal laboratory facilities include areas to perform medical and surgical procedures. Laboratory space and appropriate start-up package for the researcher will be provided. Rush University Medical Center is the primary clinical and hospital teaching campus for the Rush University Medical College. Academic appointments will be commensurate with qualifications and experience.

Interested candidates should send a copy of their curriculum vitae, letter addressing their qualifications and a list of 3 individuals who can provide references to: **Michael D. Tharp, M.D., The Clark W. Finnerud, M.D., Professor and Chairman, The Department of Dermatology, Rush University Medical Center, 1653 W. Congress Parkway, 220 Annex Building, Chicago, Illinois 60612**

FACULTY POSITIONS
ASSISTANT/ASSOCIATE PROFESSOR
Pharmacology or Physiology

The College of Veterinary Medicine at the University of Georgia is seeking **PHARMACOLOGISTS or PHYSIOLOGISTS** for multiple tenure-track positions in the Department of Physiology and Pharmacology. The successful candidates will be expected to develop and maintain externally funded research programs and participate in teaching pharmacology or physiology to students in our professional and graduate programs. Qualifications for positions include a Ph.D., M.D., D.V.M., or equivalent degree. Evidence of research excellence will be given priority over specific area of study. Current departmental strengths include neuroscience, toxicology, molecular cellular physiology, vascular physiology, pharmacology, and endocrinology. See website: **http://www.vet.uga.edu/vph/** for more information. Interested applicants should submit a letter of application including a statement of research plans, a statement of teaching interests, curriculum vitae, and four letters of reference to: **Dr. Julie Coffield, Chair of the Search Committee, College of Veterinary Medicine, University of Georgia, 501 D.W. Brooks Drive, Athens, GA 30602** or electronically to e-mail: **physphen@uga.edu**. Applications received by November 10, 2007, are assured full consideration. *The University of Georgia is an Equal Opportunity/Affirmative Action Employer.*

The American Chemistry Council (ACC), a national trade association representing the world's leading chemical and plastics manufacturers, currently has an opportunity for a **DIRECTOR** within our Long Range Research Initiative (LRI) Department in the Washington DC metro area. This position directs the research management process for the LRI, additionally providing the focal point for the chemical risk assessment/health effects component of the research program. The LRI is a major program of the ACC that sponsors an independent research program ($17 million in 2007) that advances the science of risk assessment of the health effects of chemicals to enhance decision making by government, industry, and the public. The primary duties are to (1) serve as the lead for several Request for Proposal (RFP) Teams, which develop and implement RFPs via a competitive process; (2) perform senior level administrative functions related to research and research contracts; and (3) provide outreach and communication about the program. To learn minimum qualifications, more details about the position, and application instructions, visit our website: **http://www.americanchemistry.com/jobs**. To learn more about the LRI, please visit **website http://www.americanchemistry.com/lri**. ACC offers a salary commensurate with experience and excellent benefits.

The Department of Medicine in the School of Medicine at the University of California, San Diego (UCSD) is actively recruiting a **TENURE TRACK or TENURED FACULTY POSITION in PHYSIOLOGY.** Successful applicants will be expected to teach in organ physiology for medical students and maintain a vigorous program of high-quality federally funded research in physiological sciences. Applicants should have an appropriate doctoral degree. Appointment level will be commensurate with experience and qualifications; compensation is based on established UCSD salary scales. Review of applications will begin November 5, 2007, and will continue until the position is filled. Applicants should submit curriculum vitae, list of publications, a statement of research interests and teaching experience including leadership activities and contributions to diversity, teaching evaluations, and the names and addresses of five references to: **Physiology Search Committee, University of California, Department of Medicine - 0623A, 9500 Gilman Drive, La Jolla, CA 92093-0623,** or e-mail: **physiology@ucsd.edu.**

Affirmative Action/Equal Opportunity Employer

POSITIONS OPEN

CBES

TWO POSTDOCTORAL POSTIONS
at the University of North Carolina at Charlotte

(1) A dynamic and self-motivated Postdoctoral Fellow is invited to join the Engineering of Biological Devices and Materials Laboratory within the Center for Biomedical Engineering Systems (website: http://www.CBES.uncc.edu) in Charlotte, North Carolina in the area of oxygen transport within liver tissue equivalents. The successful candidate will be able to integrate knowledge of tissue culture, flow device design, and computational modeling (for transport analysis and property prediction) into research on improving liver function through media and ethanol concentration manipulations. A Ph.D. in biomedical engineering, mechanical engineering, or chemical engineering is required, with demonstrated experience in transport and bioreactor performance analyses. Candidate must be able to design and conduct independent experiments with a strong commitment towards goals. Excellent oral and written communication skills and an ability to work well in a collaborative research atmosphere are essential. The position is for one year, available immediately, with the possibility of extension based on performance and funding availability. Applications (full curriculum vitae, research summary, and the contact information of three references) should be sent to e-mail: **cbes@uncc.edu.**

(2) An enthusiastic Postdoctoral Fellow is invited to join the Orthopedic Tissue Engineering and Biomaterials Laboratory within the Center for Biomedical Engineering Systems to conduct studies on coating orthopedic metal implants with a newly designed bioceramic. The successful candidate must have strong interests in bioceramic, metal coating, and surface analyses. A Ph.D. in materials science, chemical engineering, mechanical engineering, or bioengineering is required with demonstrating experience in coating ceramic on metals by electrophoretic deposition or other techniques, evaluation of ceramic-metal adhesion strength, and/or ceramic preparation by sol-gel are essential. The position is available immediately, supported by a two-year renewal grant. We offer competitive compensation, exciting research projects, and dynamic interdisciplinary research environment in Charlotte, North Carolina. Applications (full curriculum vitae, research summary, and the contact information of three references) should be sent to e-mail: **zrelgah@uncc.edu.** *The University of North Carolina at Charlotte is an Equal Opportunity Employer.*

ASSISTANT or ASSOCIATE PROFESSOR
Developmental Biology
University of California, Irvine

The Department of Developmental and Cell Biology invites applications for a faculty appointment in the area of developmental biology. We are particularly seeking candidates that take genetic and/or cell biological approaches to study vertebrate embryonic patterning and organogenesis. The successful applicant is expected to conduct a strong research program and to contribute to the teaching of undergraduate and graduate students.

Applicants should send a letter of application, curriculum vitae, three letters of reference, and statements of research and teaching interests using the following online recruitment URL, website: **http://jobs.bio.uci.edu/showopenjobs_tenure.cfm** for applications/instructions under Department of Developmental and Cell Biology.

To receive full consideration, material should be received December 1, 2007.

The University of California, Irvine is an Equal Opportunity Employer committed to a diverse workforce and actively encourages applications from all qualified applicants, including women and minorities.

POSITIONS OPEN

TENURE-TRACK or TENURED FACULTY POSITION. The Division of Pulmonary and Critical Care Medicine, Feinberg School of Medicine at Northwestern University in Chicago invites applications for a full-time tenure-track or tenured faculty position at the **ASSISTANT, ASSOCIATE, or PROFESSOR** level. Applicant should have a Ph.D. and/or M.D. degree/s, be Board-certified in pulmonary and critical care medicine, and preferably have an independent NIH-funded lung biology research program. The Division wishes to add to its strengths in lung injury biology, signaling, and receptor function. Expertise in transgenic/knockout technology as an integral component of the research program is desirable. The position comes with a competitive start-up package and research space. Salaries will commensurate experience. Please send complete curriculum vitae, a brief statement of research interest, and names of three references to: **Jacob I. Sznajder, M.D., Division of Pulmonary and Critical Care Medicine, Northwestern University, 240 East Huron, McGaw 2300, Chicago, IL 60611.** Or e-mail: **scanan@northwestern.edu.** Applications must be received by October 1, 2007. Start date will be from February 1, 2008. *Northwestern University is an Affirmative Action/Equal Opportunity Employer. Hiring is contingent upon eligibility to work in the United States. Women and minorities are encouraged to apply. (Research # P-128-08)*

California State University, Fresno, is searching for a tenure track **ASSISTANT PROFESSOR in MICROBIOLOGY.** The successful candidate is expected to develop a research program in a current area of microbiology that involves both undergraduate and graduate students, and to pursue the external funding necessary to maintain a successful research effort. Additionally, the successful candidate will be expected to teach an upper division majors/service course in Microbiology on a rotational basis, and an undergraduate and a graduate course in their areas of expertise. An earned Doctorate (Ph.D.) in microbiology or related field is required. Strong preference will be given to candidates with postdoctoral experience. Send completed application, including form available at website: **http://www.csufresno.edu/aps/vacancy/acf.pdf**, a cover letter, curriculum vitae, statements of teaching and research philosophy, and three current letters of reference (dated within the last 12 months) to: **Dr. Paul R. Crosble, Committee Chair, Department of Biology, California State University, Fresno, 2555 E. San Ramon Avenue, M/S SB73, Fresno, CA 93740-8034,** or to e-mail: **perosble@csufresno.edu, telephone: 559-278-2074, fax: 559-278-3963.** For full consideration, all materials must be received by 5 November 2007. *California State University, Fresno is an Equal Opportunity Employer.*

ASSISTANT/ASSOCIATE PROFESSOR, IMMUNOLOGY (TENURE TRACK), School of Veterinary Medicine, University of California, Davis. Ph.D. required with advanced training in immunology as it pertains to host-pathogen interaction. D.V.M.s encouraged to apply. Demonstrated aptitude/experience or potential in teaching. Documented research record or potential to develop an independent research program in immunology. Demonstrated ability or potential in acquisition of extramural funding. Must possess excellent interpersonal and communication skills and a demonstrated ability to work with others in a collegial team atmosphere. To receive fullest consideration, applications must be received by December 7, 2007; position opened until filled. Expanded position description at **website: http://www.vetmed.ucdavis.edu/pmu/PMIpage.cfm.** Submit letter of interest stating special interest in the position, overall qualifications, experience and career goals, curriculum vitae, and names, addresses, and e-mail addresses of three professional references to: **Dennis W. Wilson, Chairman, Department of Pathology, Microbiology and Immunology, School of Veterinary Medicine, University of California, Davis, Davis, CA 95616, Attn: Donna Roggenkamp.** *Affirmative Action/Equal Opportunity Employer.*

POSITIONS OPEN

GENOMICS STAFF SCIENTIST

The Center for Genomics and Bioinformatics (**website: http://cgb.indiana.edu**) at Indiana University (Bloomington) seeks B.S-level candidates (or M.S.) for the position of Genomics Staff Scientist to join our team. We recently acquired high throughput pyrosequencing technology from 454/Roche. The ideal candidates will mainly work on pyrosequencing, including library construction, sequencing run, and data analysis. Requisite skills include molecular biology, biochemistry, or bioinformatics. Appointments will be at the rank of **RESEARCH ASSOCIATE** and salary will be based on a candidate's preparation and prior experience. Inquiries about all openings should be directed to **e-mail: jobs@cgb.indiana.edu.** Applications will be accepted until positions are filled. Those received by November 12, 2007, will be assured full consideration. Please submit curriculum vitae and a description of your background and interests, and have three letters of recommendation sent directly to the address below. Refer to Genomics Staff Scientist - CGB-012 in your cover letter.

Position #CGB-012
Attn: Genomics Staff Scientist
Center for Genomics and Bioinformatics
Indiana University
1001 E. 3rd Street
Bloomington IN 47405-3700

Indiana University is an Affirmative Action Equal Opportunity Employer.

ASSISTANT PROFESSOR/CURATOR, GENETIC RESOURCES. The University of Washington is seeking applications for a full-time, tenure-track faculty position to serve as Academic Curator of Genetic Resources at the Burke Museum (**website: http://www.burkemuseum.org**) and as a faculty member in the Biology Department. Appointment is anticipated at the Assistant Professor rank. In exceptional circumstances, appointment at the Associate or Full Professor level may be considered for candidates who have demonstrated a commitment to mentoring underrepresented students in the sciences. Ph.D. required by date of appointment. University of Washington faculty engage in teaching, research, and service. The successful candidate should conduct externally funded research in such areas as molecular systematics, evolution, or ecology at the population or phylogenetic level, curate, and contribute to the growth of tissue and DNA collections, as well as organismal collections in the taxon of the candidate's specialty, and guide student research based on those collections. Responsibilities also include undergraduate and graduate teaching. Submit curriculum vitae, descriptions of research/teaching interests, three letters of reference, and reprints (PDF) of three recent publications at **website: http://www.burkemuseum.org/curator.** Priority will be given to applications received before November 15, 2007. *The University of Washington is building a culturally diverse faculty and strongly encourages applications from women and minority candidates. UW is an Affirmative Action, Equal Opportunity Employer.*

Spelman College seeks Ph.D. **BIOLOGISTS in PHYSIOLOGY** for a tenure track **ASSISTANT PROFESSORSHIP** starting fall 2008. Successful candidate is expected to teach introductory and elective courses in specialty area and establish a research program with undergraduate students. Spelman College is the oldest predominantly black college for women in the United States. Spelman's Biology Department is nationally recognized for training women of color for graduate/professional studies in the sciences. Applicants must have a Ph.D. or equivalent and be committed to teaching and mentoring science students in a liberal arts environment. Competitive salary and startup funds are available. Send application materials by December 3, 2007, to: **Provost's Office, Attn: Biology Search Committee Chair, Spelman College, 350 Spelman Lane S.W., Atlanta, GA 30314.** For more information see **website: http://www.spelman.edu/academics/programs/biology/index.shtml.**

POSITIONS OPEN

ASSISTANT PROFESSOR
University of California, Irvine
Department of Pharmaceutical Sciences

The Department of Pharmaceutical Sciences and the Department of Computer Science at University of California (UC), Irvine invite applications for a tenure-track faculty position in the area of computational biology. The appointment will be made at the **ASSISTANT, ASSOCIATE, or FULL PROFESSOR** level, as supported by the qualifications and experience of the successful applicant. The successful candidate will be expected to establish an active research program using computational methods to address fundamental problems in structural biology, enzyme function, molecular modeling, structure-based drug design, chemoinformatics, or other areas of computational biology or chemistry relevant to the pharmaceutical sciences.

Interested applicants should submit curriculum vitae, at least three letters of reference, and a brief outline of future research plans. Application instructions can be found at **website: https://recruit.ap.uci.edu.** Review of applications will begin November 30, 2007. To ensure full consideration, applications and all supporting materials should be received by this time. The position will remain open until filled. *UCI is an Equal Opportunity Employer committed to excellence through diversity and strongly encourages applications from all qualified applicants, including women and minorities.*

CLAIRE BOOTH LUCE PROFESSORSHIP CELL/MOLECULAR BIOLOGIST
Fordham University

Individuals are invited to apply for a tenure-track position at the **ASSISTANT PROFESSOR** level for the Claire Booth Luce Professorship. The Department has an active research program and provides excellent physical facilities, state-of-the art equipment, a stimulating research environment, startup funds, and competitive salaries and benefits. Preference will be given to candidates who possess expertise in the area of cell/molecular biology and candidates with research interests in molecular biology, stem cells, cancer, development, or genetic diseases are particularly encouraged to apply. The appointee will be expected to establish an active research program and participate in teaching at the graduate and undergraduate levels. Please submit curriculum vitae, two reprints, and the names and addresses of three references by January 3, 2008, to: **Dr. William B. Thornhill, Chair, Department of Biological Sciences, Fordham University, Bronx, NY 10458.** *Fordham is an independent, Catholic university in the Jesuit tradition that welcomes applications from women of diverse backgrounds. Fordham is an Affirmative Action/Equal Opportunity Employer.*

WILDLIFE ECOLOGIST ASSISTANT/ ASSOCIATE PROFESSOR
Department of Natural Resources and Environmental Science, University of Nevada, Reno

We seek candidates to fill a key position in the Wildlife Ecology and Conservation Program in our Department. We will consider candidates with a broad range of skills and an interest in wildlife ecology and management issues relevant to the state of Nevada. Candidates must possess strong writing and oral communication skills and the ability to develop an externally funded research program, and they should have a documented commitment to excellence in undergraduate/graduate teaching and advisement. Applications must be submitted electronically, **website: https://www.unrcareers.com/applicants/Central?quickFind=52536.**

Contact: **Dr. Kurt S. Pregitzer, Department Head, e-mail: ksp@cabnr.unr.edu, telephone: 775-784-4000,** for additional information about the position. Application questions: **Heidi McConnell, telephone: 775-784-4020, e-mail: hmc@cabnr.unr.edu.**

POSITIONS OPEN

FACULTY POSITION in INTEGRATIVE ANIMAL PHYSIOLOGY

The Department of Biological Sciences at Clemson University invites applications for a tenure-track faculty position in integrative animal physiology at the **ASSISTANT PROFESSOR** level, to begin August 2008. Postdoctoral experience is required. We are seeking a broadly trained **BIOLOGIST** whose research utilizes multidisciplinary approaches to improve understanding of organismal function and adaptation. Specific areas of research are open but should emphasize comparative, experimental, or evolutionary approaches; preference will be given to candidates with expertise in vertebrate systems. The successful candidate will be expected to interact with faculty having diverse interests ranging from organismal biology, ecology, and evolution to cell, developmental, and molecular biology, thereby supporting University emphasis areas in sustainable environment and biomedicine and biotechnology. The successful candidate will also be expected to establish innovative, externally funded research programs of national distinction, and to be an excellent teacher. Teaching responsibilities include one upper-level undergraduate course in comparative physiology or vertebrate biology and graduate course(s) in one's specialty. Applications should include curriculum vitae, no more than three reprints, a statement of current and planned research, a statement of teaching philosophy and interests, and names and contact information for three references. Review of applications will begin November 9, 2007, and will continue until the position is filled. Please send application materials by e-mail as Word or PDF files to **e-mail: sallyb@clemson.edu.** Further information about this position, departmental resources, programs, and faculty research interests are available at **website: http://www.clemson.edu/biosci.**

Clemson University is an Affirmative Action/Equal Opportunity Employer. Clemson University does not discriminate against any person on the basis of age, color, disability, gender, national origin, race, religion, sexual orientation, or veteran's status.

FACULTY POSITIONS in BIOLOGY
The University of Washington

The University of Washington's Department of Biology has two open tenure-track faculty positions. We welcome applicants in both core and interdisciplinary areas of biology but have particular interest in areas of cellular, molecular, and physiological levels of organization in plants or animals. A record of outstanding achievement, a promising research program, and a commitment to teaching are more important than the specific research area. Our consolidation of Botany, Zoology and Undergraduate Biology Programs into a single unit expands opportunities for new projects and interdisciplinary initiatives. Information about the Department is available at **website: http://www.biology.washington.edu.**

Appointments at the **ASSISTANT PROFESSOR** rank are anticipated. Appointments at the **ASSOCIATE or FULL PROFESSOR** rank may be considered for candidates who have demonstrated a commitment to mentoring underrepresented students in the sciences. Applicants must have earned a Doctorate by the date of appointment.

Please apply online at **website: http://www.biology.washington.edu/fachires/** and submit a cover letter, curriculum vitae, sample reprints, statements of research and of teaching interests, and names of at least three references. Applications received by November 1, 2007, will be given priority.

University of Washington faculty engage in teaching, research, and service. The University of Washington, a recipient of the 2006 Alfred P. Sloan award for Faculty Career Flexibility, is committed to supporting the work-life balance of its faculty. *The University is building a culturally diverse faculty and staff and strongly encourages applications from women, minorities, individuals with disabilities, and covered veterans. The University of Washington is an Affirmative Action, Equal Opportunity Employer.*

POSITIONS OPEN

FACULTY POSITIONS IN MOLECULAR, CELLULAR AND DEVELOPMENTAL BIOLOGY

UNIVERSITY OF ARIZONA

The Departments of Molecular and Cellular Biology, UA College of Science (**www.mcb.arizona.edu**) and Cell Biology and Anatomy, UA College of Medicine (**www.cba.arizona.edu**) have formed a joint department and are seeking to fill 3-4 tenure-track faculty positions for appointment in 2008. Although an appointment at the assistant professor level is preferred, outstanding candidates at all levels will be considered. Applicants with research interests in any area of molecular, cellular, or developmental biology, including those pursuing mathematical and statistical approaches to biological problems, will be considered. Opportunities for interaction and collaboration are particularly strong in areas of basic research related to cancer, cardiovascular biology, diabetes, neurobiology, functional genomics and imaging. Successful candidates will be expected to establish a competitive research program and to contribute to undergraduate, graduate, and/or medical education.

To apply, submit an on-line faculty application for job number **39300** at **www.uacareertrack.com**. Applicants should be prepared to attach a curriculum vitae and a 1-2 page statement of research and teaching interests at the time of application. Separately, have at least three supporting letters sent directly to: **Denise Slay, Search Coordinator, University of Arizona, Department of Molecular and Cellular Biology, 1007 E Lowell, Life Sciences South Bldg, Tucson, AZ 85721, USA**, or send via email to **medb@email.arizona.edu**. Review of applications will begin **November 1, 2007** and continue until positions are filled.

The University of Arizona is an EEO/AA Employer/M/W/D/V and is seeking individuals who are able to work with diverse students or colleagues, and who have experience with a variety of teaching methods and curricular perspectives.

COURSE

NINTH ADVANCED VACCINOLOGY COURSE
ADVAC 9

Les Pensières, Veyrier-du-Lac (near Annecy, French Alps)
19 - 31 May 2008

Organized by Fondation Mérieux and University of Geneva
co-sponsorship of European Commission, Gates Foundation, NIAID, Johns Hopkins, ESPID, NFID, NVPO, Vaccine Industry.

Objective of the course: To facilitate critical decision-making in vaccinology. English language.

Who should apply?: Scientists and decision-makers from the public and private sectors.

Application deadline: 15 November 2007

www.advac.org
advac@medecine.unige.ch
katia.mielczarek@fondation-merieux.org

Programme Fees
1- Standard registration fee, incl. full attendance EUR 3 500, VAT incl.; Reduced fee for academic sector, NGOs : EUR 1400, VAT incl.
2- Accommodation fee : EUR 2 050, VAT incl.

Fellowships available for participants from Developing Countries & new EU members. Also offered to selected ESPID members whereas NFID provides fellowships to young American vaccinologists.

POSITIONS OPEN

FACULTY POSITION IN PHARMACOLOGY UNIVERSITY OF CALIFORNIA, IRVINE

The Department of Pharmacology at the University of California, Irvine (UCI) invites applications for a tenure-track faculty position at the level of Assistant Professor. We seek scholars with a proven record of research accomplishments and specific interest in one of the following areas:

1. Regulation of gene expression
2. Molecular mechanisms of signal transduction
3. Drug discovery

Applicants must indicate which research area they are applying for. Applicants must have an M.D. and/or Ph.D. in pharmacology or a related field, a strong drive to pursue a dynamic research program and an interest in and talent for graduate teaching. Curriculum vitae, names of three references, and a summary of research interests should be sent to: **Kimberly Kich, Academic Personnel Coordinator, Department of Pharmacology, School of Medicine, University of California, Irvine, Irvine, CA 92697-4625.**

The University of California, Irvine has an active career partner program and an NSF ADVANCE Program for Gender Equity and is an Equal Opportunity Employer committed to excellence through diversity.

ANNOUNCEMENTS

JDRF Juvenile Diabetes Research Foundation International

dedicated to finding a cure

Identify, Develop or Evaluate Therapeutics for Type 1 Diabetes Complications

JDRF is requesting expressions of interest for identification, development or pre-clinical testing of novel therapeutic approaches designed to prevent, treat, reverse or ameliorate the following complications of type 1 diabetes: retinopathy, with a higher priority on non-proliferative retinopathy or progression from nonproliferative to proliferative stages, and all stages of diabetic neuropathy or nephropathy.

JDRF seeks projects aimed at identifying compounds for a specific drug target via library screening, developing novel compounds for pre-clinical testing or implementation of pilot and feasibility studies in animal model systems of clinical relevance. This request seeks to provide support towards the pre-clinical translation of novel or existing therapeutic compounds.

Expressions of interest should be submitted to JDRF no later than **November 21, 2007.**

For details, please see:
www.jdrftherapeutics.org

JDRF Juvenile Diabetes Research Foundation International

dedicated to finding a cure

Identify or Validate Targets for Therapeutics against Type 1 Diabetes Complications

JDRF requests expressions of interest for innovative projects aimed at identification or validation of new targets for therapeutic intervention to prevent, treat, reverse or ameliorate the following complications of type 1 diabetes: retinopathy, neuropathy or nephropathy.

Target identification signifies the identification of a specific gene or protein whose expression level or concentration can be demonstrated to have disease modifying qualities. Target validation is defined as the experimental confirmation of the role of a given gene or protein involved in pathways relevant to these complications of type 1 diabetes. Proposed projects should have the potential of demonstrating the targets' ability to modulate such a pathway in a manner that could be therapeutically useful. Through this request JDRF seeks to identify projects to support towards the identification or validation of novel therapeutic targets.

Expressions of interest should be submitted to JDRF no later than **November 21, 2007.**

For details, please see: **www.jdrftarget.org**

POSITIONS OPEN

The BUSINESS of MARINE BIOTECHNOLOGY FELLOWSHIPS

The Center for Marine Science at the University of North Carolina, Wilmington is offering three exceptional **RESEARCH FELLOWS** in marine biotechnology. Candidates must have a Ph.D. in a biotechnology-related area and are expected to conduct research in marine science laboratories at the University while pursuing a professional M.B.A. degree in the University's Cameron School of Business. The goal of this 24 month program is to produce individuals with a solid science background as well as the business skills needed to prosper in a modern competitive business environment. Students in the M.B.A. portion of the Program will master the core functions of business, develop analytical and quantitative business skills, and study current and future business issues through real world experiences with regional companies involved in marine biotechnology. Excellent verbal and written skills are required.

The research portion of the Program generally involves working in one of three focus areas: (1.) Bioassay technique development focusing on novel sensing methods with particular application in the marine environment; (2.) Finfish mariculture which may include reproduction, genetics and selective breeding, larval physiology, nutrition, health and disease management, recirculating aquaculture technology, and commercial demonstration; and (3.) Marine pharmaceuticals and nutraceuticals from cultured organisms, bioengineered natural products, novel enzymes and biosynthetic pathways. Candidates should clearly identify their interests in one of the three focus areas in their cover letters. Candidates with interests in other biotechnology related area will be considered based on the strength of their application. Selected candidates would receive salary and benefits including health insurance and retirement contributions for 24 months. Position title will be **VISITING RESEARCH ASSISTANT PROFESSOR.** Tuition for the coursework necessary to obtain the MBA is also provided.

Screening of the applicants will begin December 15, 2007 and applicants will be invited to join the program April 1, 2008 and will be required to start May 1, 2008. All degree requirements must be met by May 1, 2008, to qualify for the Fellowship. Letter of application, curriculum vitae, summary of research plans, and names and addresses of three references should be sent via the online application process available on the web at **website: http://consensus.uncw.edu;** not e-mailed or mailed. M.S. Word or Adobe PDF attachments are strongly preferred. For questions regarding the online applications process, contact **Jody Smith** at **telephone: 910-962-2330.** For questions regarding the positions or the Center contact **Dr. Ronald K. Sizemore** at **e-mail: sizemorer@uncw.edu** or visit our **website: http://www.uncw.edu/cmsr.** *UNCW conducts criminal background checks on finalists prior to offers of employment. UNCW is an Equal Opportunity, Affirmative Action Employer. Minorities and women are encouraged to apply.*

INSTRUCTOR/ADVANCED POSTDOCTORAL FELLOW in NEUROINFORMATICS

Expertise and demonstrated successful R&D projects in: biomedical informatics, semantic web, description logics, biomedical ontologies, and advanced webcentric software engineering. Substantial experience in developing semantic knowledge bases for use by clinicians and researchers.

Our group provides outstanding opportunities to collaborate with other world-class informaticians and biomedical researchers. Ph.D. in bioinformatics, biomedical informatics, bioengineering, or a closely related field required. Send cv e-mail curriculum vitae, a letter of interest, and three references to: **Tim Clark, Director of Informatics, Massachusetts General Institute for Neurodegenerative Disease, 114 16th Street, CNY 114-2012, Charlestown, MA 02129; e-mail: tim_clark@harvard.edu.**

POSITIONS OPEN

ASSISTANT and/or ASSOCIATE PROFESSOR of HUMAN GENETICS

The Department of Human Genetics at the University of Utah School of Medicine is continuing a new major expansion, recruiting three new investigators over the next three years to build upon existing strengths in human genetics and developmental biology.

We are seeking outstanding applicants at the level of **ASSISTANT and/or ASSOCIATE PROFESSOR** in the broad fields of genetics and functional genomics, including but not limited to human genetics, genetic approaches to complex disease, population genetics, behavioral genetics, regenerative medicine, developmental genetics, and animal models of human disease and development. Our Department has a strong history in human genetics and resources, such as the Utah Population Data Base, that are unique in the world. These resources have created a highly productive and collaborative environment between researchers, clinicians, and the community.

Creative scientists with a record of achievement and commitment to excellence in both research and teaching are encouraged to apply. Successful candidates will receive a substantial startup package and enjoy a stimulating and supportive research environment.

Applicants should submit curriculum vitae, a summary of research plans, relevant reprints and/or preprints, and three letters of reference to:

Dr. Mario R. Capecchi
Co-Chair, Department of Human Genetics
Howard Hughes Medical Institute
University of Utah School of Medicine
15 North 2030 East, Room 2130
Salt Lake City, UT 84112-5330

Application materials, including letters of reference, should be submitted by November 9, 2007.

The University of Utah is an Equal Opportunity/Affirmative Action Employer, encourages nominations and applications from women and minorities, and provides reasonable accommodation to the known disabilities of applicants and employees.

POSTDOCTORAL FELLOWSHIPS Reproductive Biology at Vanderbilt

Applications are now being accepted for Postdoctoral Fellowships in a National Institute of Child Health and Human Development-funded Reproductive Biology Training Program. The candidates must have Ph.D., M.D., or M.D./Ph.D. degrees and be interested in pursuing research in reproduction. Preceptors in this program use various model systems including humans, mice, *C.elegans*, *Xenopus* and *Drosophila*. The goal of this Program is to produce a future cadre of independent investigators in reproduction research. The trainees will have access to contemporary technologies. *Applicants must be U.S. citizens or must hold permanent residency status in the United States.* Send resume, statement of interest, and three letters of support to: **S.K. Dey, Ph.D., Director, Division of Reproductive and Developmental Biology, Departments of Pediatrics, Cell and Developmental Biology and Pharmacology, Vanderbilt University Medical Center, D-4100 Medical Center North, Nashville, TN 37232-2678; or via e-mail:sk.dey@vanderbilt.edu.**

DISTINGUISHED BIOETHICS PROFESSOR Wake Forest University

The College of Arts and Sciences seeks a Distinguished Scholar in Bioethics for a **FULL PROFESSOR,** and possibly a Chaired, position beginning fall 2008. The successful candidate will play a leading role in developing an interdisciplinary, campus-wide Bioethics Center of national prominence. The area of specialization within bioethics is open, though expertise in biotechnology or bioscience issues is especially welcome. Wake Forest is a private university whose academic programs are consistently ranked in the top tiers nationally. Those interested should consult **website: http://www.wfu.edu/hr/careers/undergraduate/** for more information.

POSITIONS OPEN

NEUROSCIENCE FACULTY POSITIONS

The Department of Biomedical Sciences at Marquette University invites applications for up to two tenure-track faculty positions at the level of **ASSISTANT PROFESSOR,** pending funding. Successful candidates will be expected to develop independent, extramurally funded research programs. We are particularly interested in applicants that utilize molecular techniques with a research focus that would complement the current areas of strength in the Department, including the neurobiology of motivated behavior, stress-related disorders, and neurodegeneration. Teaching responsibilities for these positions will include participation in a graduate neuroscience course and an undergraduate histology or anatomy course. The Department of Biomedical Sciences (**website: http://www.marquette.edu/chs/bisc/**) provides a highly collaborative work environment that is experiencing rapid growth. Interested individuals with a Ph.D. in a neuroscience-related field and at least two years of postdoctoral training should apply online by submitting curriculum vitae and statement of research interests at **website: http://careers.marquette.edu/applicants/Central?quickFind=50954.** Review of applications will begin on November 16, 2007, and continue until the positions are filled. Inquiries regarding this position can be addressed to **David A. Baker, Ph.D., Department of Biomedical Sciences, Marquette University, P.O. Box 1881, Milwaukee, WI 53201-1881 (e-mail: david.baker@mu.edu).** *Marquette University is an Affirmative Action/Equal Opportunity Employer.*

FACULTY POSITION in ECOLOGY or CONSERVATION BIOLOGY

Biology Department of Indiana University Southeast seeks qualified Ph.D. applicants for **TENURE-TRACK ASSISTANT PROFESSOR** beginning August 2008. Postdoctoral experience preferred. Teaching duties includes ecology, field biology, introductory biology, and related courses; candidate is expected to pursue a research program. For more information and how to apply go to **website: http://www.ius.edu/hr/employment_opportunities.cfm.** Deadline is November 16, 2007. *IUS is an Affirmative Action/Equal Opportunity Employer.*

POSTDOCTORAL POSITIONS are available to study the mechanisms underlying chronic pain. Strong background in pain research and experience in pain behavioral testing, neuropathic pain animal models, and immunocytochemistry are required. Preference will be given to applicants seeking first postdoctoral position. Please e-mail/send curriculum vitae to: **Dr. Yuan-Xiang Tao, Department of Anesthesiology, Johns Hopkins University School of Medicine, 355 Ross, 720 Rutland Avenue, Baltimore, MD 21205; e-mail: ytao1@jhmi.edu.** *Equal Opportunity Employer.*

MARKETPLACE

CALL FOR ENTRIES

AAAS Student Poster Competition

Colella Photography ™

Put yourself in the picture.

American Association for the Advancement of Science

2008 Annual Meeting • 14–18 February in Boston

"Science and Technology from a Global Perspective"

Put yourself in the picture by entering the 2008 AAAS Student Poster Competition. Winners receive a cash prize, framed award certificate, and a one-year AAAS membership—including a subscription to *Science!*

Don't miss out on this opportunity to put your research in the spotlight and discuss your work with leading scientists and engineers from across the country and around the world.

All submissions will be peer reviewed. Accepted posters will be listed in the 2008 Annual Meeting Poster Book. A complete list of winners will be published in *Science* and at **www.aaasmeeting.org**. *The competition is open to college undergraduate and graduate students only.*

To learn more, including how you can volunteer and attend the Annual Meeting for free, visit **www.aaasmeeting.org**.

Submission Deadline:
Thursday, 1 November 2007.

AAAS
ADVANCING SCIENCE, SERVING SOCIETY